

Vol. 18, No. 1, March, 2019

ISSN (Print): 0972-6268; ISSN (Online) : 2395-3454

NATURE ENVIRONMENT & POLLUTION TECHNOLOGY



Technoscience Publications

website : www.neptjournal.com

A Multidisciplinary, International Journal on all Aspects of Environment



Technoscience Publications

A-504, Bliss Avenue, Balewadi,
Opp. SKP Campus, Pune-411 045
Maharashtra, India

www.neptjournal.com

Nature Environment and Pollution Technology

(An International Quarterly Scientific Research Journal)

EDITORS

Dr. P. K. Goel

Former Head, Deptt. of Pollution Studies
Y. C. College of Science, Vidyanaagar
Karad-415 124, Maharashtra, India

Dr. K. P. Sharma

Former Professor, Deptt. of Botany
University of Rajasthan
Jaipur-302 004, India

Published by : Mrs. T. P. Goel, B-34, Dev Nagar, Tonk Road, Jaipur-302 018
Rajasthan, India

Managing Office : Technoscience Publications, A-504, Bliss Avenue, Balewadi,
Pune-411 045, Maharashtra, India

E-mail : contact@neptjournal.com; journalnept@gmail.com

INSTRUCTIONS TO AUTHORS

Scope of the Journal

The Journal publishes original research/review papers covering almost all aspects of environment like monitoring, control and management of air, water, soil and noise pollution; solid waste management; industrial hygiene and occupational health hazards; biomedical aspects of pollution; conservation and management of resources; environmental laws and legal aspects of pollution; toxicology; radiation and recycling etc. Reports of important events, environmental news, environmental highlights and book reviews are also published in the journal.

Format of Manuscript

- The manuscript (*mss*) should be typed in double space leaving wide margins on both the sides.
- First page of *mss* should contain only the title of the paper, name(s) of author(s) and name and address of Organization(s) where the work has been carried out along with the affiliation of the authors.

Continued on back inner cover...

Nature Environment and Pollution Technology

Vol. 18, No. (1), March, 2019

CONTENTS

1. **Miguel Ángel López-Ramírez, Olaya Pirene Castellanos-Onorio, Manuel Alberto Susunaga-Miranda, Fabiola Lango-Reynoso, María del Refugio Castañeda-Chávez and Jesús Montoya-Mendoza,** Treatment of Leachates of a Controlled Landfill in Veracruz by Using the Fenton Method 1-8
2. **Neha Sharma, Sreemoyee Chatterjee and Pradeep Bhatnagar,** Degradation of Direct Red 28 by *Alcaligenes* sp. TEX S6 Isolated from Aeration Tank of Common Effluent Treatment Plant (CETP), Pali, Rajasthan 9-20
3. **Siti Asmaniyah Mardiyani, Soemardi Hadi Sumarlan, Bambang Dwi Argo and Amin Setyo Leksono,** Design of Eco-friendly Fixed Bed Dryer Based on a Combination of Solar Collector and Photovoltaic Module 21-30
4. **Dewi Hidayati, Norela Sulaiman, B. S. Ismail, Nurul Jadid and Lutfi Surya Muchamad,** Volcanic Mud Contamination in the River Ecosystem: The Case Study of Lusi Mud Volcano, Indonesia 31-40
5. **Demian Fang,** Composite System for the Coupling Degree of Tourism Industry and Regional Ecological Environment: A Case Study of Henan Province, China 41-48
6. **Arunkumar Mani and Sheik Abdulla Shahul Hameed,** Improved Bacterial-Fungal Consortium as an Alternative Approach for Enhanced Decolourisation and Degradation of Azo Dyes: A Review 49-64
7. **Mingtao Zhou, Tianqi Li, Jiazhen Gao and Wennian Xu,** Erosion Resistance and Aggregate Distribution Characteristics of Vegetation Concrete 65-72
8. **Prashanth Gururaja, Nittaya McNeil and Bright Emmanuel Owusu,** Statistical Modelling of 4-hourly Wind Patterns in Calcutta, India 73-80
9. **Yuan Gao, Zi-Ni Lai, Guang-Jun Wang, Qian-Fu Liu and Er-Meng Yu,** Distribution of Zooplankton Population in Different Culture Ponds from South China 81-88
10. **Kehui Cheng and Fang Lv,** Environmental Pollution Status Quo and Legal System of Third-Party Governance in Hebei Province, China 89-96
11. **Radhika Birmole, Azza Parkar and K. Aruna,** Biodegradation of Reactive Red 195 By a Novel Strain *Enterococcus casseliflavus* RDB_4 Isolated from Textile Effluent 97-109
12. **Gang Ding, Xiajing He and Ling Ye,** Inter-regional Differences in Environmental Regulation Intensity Among Chinese Provincial Governments and the Overall Planning Countermeasures 111-118
13. **Yue liu, Laiqun Zhao, Yanyan Dou, Weijin Gong, Haifang Liu, Jingjing Lv, Zizhen Zhou and Fuwang Zhao,** Iron-Manganese Silicate Polymerization (IMSP) Catalytic Ozonation for Removal of *p*-Chloronitrobenzene in Aqueous Solution 119-124
14. **C.I.C. Anyadiiegwu, A.C. Igbojionu, N.P. Ohia and R.C. Eluagu,** The Role of Advanced Technologies in the Remediation of Oil-Spilled Environment: A Decision-Matrix Approach 125-132
15. **Mengxi Gao,** Interaction Between Foreign Trade and Environmental Pollution: A Case Study of Guizhou Province, China 133-140
16. **H. Joga Rao, P. King and Y. Prasanna Kumar,** Effect of Process Parameters on Adsorption of Cadmium from Aqueous Solutions by Activated Carbon Prepared from *Bauhinia purpurea* Leaves 141-148
17. **Dharna Tiwari, Lakshmi Raghupathy, Ambrina Sardar Khan and Nidhi Gauba Dhawan,** A Study on the E-waste Collection Systems in some Asian Countries with Special Reference to India 149-156
18. **Fida Rachmadiarti, Tarzan Purnomo, Diana Nur Azizah and Ayudhiniar Fascavetri,** *Syzigium oleina* and *Wedelia trilobata* for Phytoremediation of Lead Pollution in the Atmosphere 157-162
19. **Euis Nurul Hidayah, Muhammad Firdaus Kamal, Fauzul Rizqa and Mukhamad Rifki Hendianto,** Pretreatment Comparison Between Preoxidation and Prechlorination on the Changing of Natural Organic Matter 163-166
20. **Musthofa Lutfi, Wahyunanto A. Nugroho, Winny P. Fridayestu, Bambang Susilo, Chusak Pulmar and Sandra Sandra,** Bioflocculation of Two Species of Microalgae by Exopolysaccharide of *Bacillus subtilis* 167-173
21. **Junjie Cao,** Regional Environmental Performance Evaluation and Its Influencing Factors: A Case Study of Shandong Province, China 175-182

22. **R. Chandramohan, T.E. Kanchanabhan and N. Siva Vignesh**, Identification of Artificial Recharges Structures Using Remote Sensing and GIS for Arid and Semi-arid Areas 183-189
23. **Anti Kolonial Prodjosantoso and Cahyorini Kusumawardani**, The Use of Cobalt-Doped Tin(IV) Oxide as Catalysts for the Photodegradation of Methyl Orange 191-196
24. **Muqing Qiu**, Degradation of Azo Dye Acid Orange 7 by Zero Valent Iron Activated with Potassium Persulphate 197-201
25. **Syeda Amber Fatima and Tayyaba Ishaq**, Prevalence of Skin and Respiratory Diseases in the Workers of Bird Markets 203-209
26. **Lulu Hao and Jing Gao**, Influence of Environmental Pollution on Residents' Health: Evidence from Hubei, China 211-216
27. **Zhifei Li, Deguang Yu, Gong Wangbao, Wang Guangjun, Yu Ermeng and Xie Jun**, Aquatic Ecotoxicology and Water Quality Criteria of Three Organotin Compounds: A Review 217-224
28. **Chunxia Hu and Muqing Qiu**, Characterization of the Biochar Derived from Peanut Shell and Adsorption of Pb(II) from Aqueous Solutions 225-230
29. **Seema Maheshwari, Ajay Singh Jethoo, Vinod Kumar Vishvakarma, Meena Khwairakpam and Prashant Kriplani**, Biodegradation of Sludge Produced from Common Effluent Treatment Plant (CETP) Using Drum Composting Technique 231-236
30. **Chandrasekhar Matli, Bhaskar Challa and Rakesh Kadaverugu**, Co-firing Municipal Solid Waste with Coal - A Case Study of Warangal City, India 237-245
31. **Soleha Mohamat Yusuff, Ong Keat Khim, Wan Md Zin Wan Yunus, Mansor Ahmad, Nor Azowa Ibrahim, Anwar Fitrianto, Syed Mohd Shafiq Syed Ahmad and Chin Chuang Teoh**, Isotherms and Thermodynamics of CO₂ Adsorption on Thermally Treated Alum Sludge 247-250
32. **Lili Zhang and Gang Zong**, Functional Mechanism and Cointegration Relation of Environmental Regulations on Industrial Structure Upgrading in Beijing, China 251-259
33. **Manar Fawzi Bani Mfarrej**, Climate Change Patterns in the UAE: A Qualitative Research and Review 261-268
34. **Jigan Zhang and Muqing Qiu**, Adsorption Kinetics and Isotherms of Copper Ion in Aqueous Solution by Bentonite Supported Nanoscale Zero Valent Iron 269-274
35. **Binguo Zheng, Zhenmin Wan, Lizhen Liang, Qingzhao Li and Chunguang Li**, Effect of Solution pH and Coexisting Ions on Cefradine Adsorption onto Wheat Straw 275-280
36. **J. S. Chauhan and J. P. N. Rai**, Assessment of the Efficiency of Fly Ash Amended Soil for Distillery Effluent Treatment 281-284
37. **V. Hariram, R. Prakash, S. Seralathan and T. Micha Premkumar**, Exhaust Emission Reduction in a Single Cylinder Compression Ignition Engine Fuelled With Optimized Biodiesel Blends of *Eucalyptus teriticornis* 285-291
38. **Ming Zhong**, The Impact of Regional Economic Structural Changes on Smog Control: Empirical Evidence from Hubei, China 293-298
39. **V. Kunhambu, D. S. Sureshbabu and N. Vinayachandran**, Hydrogeo-Stratigraphic Model of Coastal Sediments in Kuttanad Area of Kerala, India 299-305
40. **Teodoro A. Amatoso, Jr., Michael E. Loretero, Romeo B. Santos and Marnie B. Giduquio**, Analysis of Sea-water Treated Laminated Bamboo Composite for Structural Application 307-312
41. **Muhammad Fakhri, Arning Wilujeng Ekawati, Nasrullah Bai Arifin, Ating Yuniarti and Anik Martinah Hariati**, Effect of Probiotics on Survival Rate and Growth Performance of *Clarias gariepinus* 313-316
42. **Jianmian Deng, Zufeng Zhai, Qinying Yuan and Guoting Li**, Effect of Solution pH on Adsorption of Cefradine by Wheat Straw and Thermodynamic Analysis 317-321
43. **Wenjie Yao**, Macroscopic Factor Decomposition of Non-Point Source Pollution of Chemical Fertilizer: Scale, Structure and Constraint 323-327
44. **Ya Tang, Youping Li, Hong Zhou and Jialing Guo**, Source Apportionment and Elemental Composition of PM_{2.5} in Chengdu, China 329-334
45. **Lei Wang, Yunna Jia, Yunlong Yao and Dawei Xu**, Accuracy Assessment of Land Use Classification Using Support Vector Machine and Neural Network for Coal Mining Area of Hegang City, China 335-341
46. **Yang Fang and Jinling Wang**, Interactive Relations Among Environmental Pollution, Energy Consumption and Economic Growth in Jilin Province, China 343-348

**The Journal
is
Currently
Abstracted
and
Indexed
in:**

International Scientific Indexing with Impact Factor 2.236 (2018)

NAAS Rating of the Journal (2019) = 3.85

Scopus®, SJR (0.193) 2017

Index Copernicus (2016) = 109.45

El Compendex of Elsevier

Indian Science Abstracts,
New Delhi, India

Chemical Abstracts, U.S.A.

Elsevier Bibliographic
Databases

Pollution Abstracts, U.S.A.

Zoological Records

Paryavaran Abstract,
New Delhi, India

Indian Citation Index (ICI)

Electronic Social and Science
Citation Index (ESSCI)

EBSCO: Environment Index™

Zetoc

Google Scholar

ProQuest, U.K.

J-Gate

Environment Abstract, U.S.A.

British Library

Centre for Research Libraries

WorldCat (OCLC)

JournalSeek

Connect Journals (India)

CSA: Environmental Sciences and Pollution Management

Research Bible (Japan)

Indian Science

Geobase

Elektronische
Zeitschriftenbibliothek (EZB)

SHERPA/RoMEO

Directory of Science

CNKI Scholar (China National
Knowledge Infrastructure)

Access to Global Online Research in Agriculture (AGORA)

AGRIS (UN-FAO)

Full papers are available on the Journal's Website:
www.neptjournal.com

UDL-EDGE (Malaysia) Products like *i*-Journals, *i*-Focus and *i*-Future

The journal is also included in the UGC approved list of journals in India

www.neptjournal.com

Nature Environment and Pollution Technology

EDITORS

Dr. P. K. Goel

Former Head, Deptt. of Pollution Studies
Yashwantrao Chavan College of Science
Vidyanagar, Karad-415 124
Maharashtra, India

Dr. K. P. Sharma

Former Professor, Ecology Lab, Deptt. of Botany
University of Rajasthan
Jaipur-302 004, India
Rajasthan, India

Marketing Manager: Mrs. Apurva Goel Garg, C-102, Building No. 12, Swarna CGHS, Beverly Park, Kanakia, Mira Road (E)-401107, Distt. Thane, Maharashtra, India (**E-mail: journalnept@gmail.com**)

Business Manager: Mrs. Tara P. Goel, Technoscience Publications, A-504, Bliss Avenue, Balewadi, Pune-411 045, Maharashtra, India (**E-mail: contact@neptjournal.com**)

Managing Editor at Jaipur: Dr. Subhashini Sharma, Department of Zoology, Rajasthan University, Jaipur, Rajasthan, India

All correspondence regarding publication of papers in the journal must be made only by e-mail (contact@neptjournal.com) to the Editor

EDITORIAL ADVISORY BOARD

1. **Dr. Prof. Malay Chaudhury**, Department of Civil Engineering, Universiti Teknologi PETRONAS, Malaysia
2. **Dr. Saikat Kumar Basu**, University of Lethbridge, Lethbridge AB, Canada
3. **Dr. Sudip Datta Banik**, Department of Human Ecology, Cinvestav-IPN Merida, Yucatan, Mexico
4. **Dr. Elsayed Elsayed Hafez**, Deptt. of Molecular Plant Pathology, Arid Land Institute, Egypt
5. **Dr. Dilip Nandwani**, College of Agriculture, Human & Natural Sciences, Tennessee State Univ., Nashville, TN, USA
6. **Dr. Ibrahim Umaru**, Department of Economics, Nasarawa State University, Keffi, Nigeria
7. **Dr. Prof. D.S. Mitchell**, Albury, Australia
8. **Dr. Prof. Alan Heritage**, Sydney, Australia
9. **Mr. Shun-Chung Lee**, Deptt. of Resources Engineering, National Cheng Kung University, Tainan City, Taiwan
10. **Samir Kumar Khanal**, Deptt. of Molecular Biosciences & Bioengineering, University of Hawaii, Honolulu, Hawaii
11. **Dr. Prof. P.K. Bhattacharya**, Dept. of Chemical Engineering, IIT, Kanpur, U.P., India
12. **Dr. Zawawi Bin Daud**, Faculty of Civil and Environmental Engg., Universiti Tun Hussein Onn Malaysia, Johor, Malaysia
13. **Dr. Srijan Aggarwal**, Civil and Environmental Engg. University of Alaska, Fairbanks, USA
14. **Dr. M. I. Zuberi**, Department of Environmental Science, Ambo University, Ambo, Ethiopia
15. **Dr. Prof. A.B. Gupta**, Dept. of Civil Engineering, MREC, Jaipur, India
16. **Dr. Kiran Tota-Maharaj**, Faculty of Engineering & Science, University of Greenwich, Kent, ME4 4TB, United Kingdom
17. **Dr. Bing Jie Ni**, Advanced Water Management Centre, The University of Queensland, Australia
18. **Dr. Prof. S. Krishnamoorthy**, National Institute of Technology, Tiruchirappally, India
19. **Dr. Prof. (Mrs.) Madhoolika Agarwal**, Dept. of Botany, B.H.U., Varanasi, India
20. **Dr. Anthony Horton**, Envirocarb Pty Ltd., Australia
21. **Dr. Riccardo Buccolieri**, University of Salento-DISTEBA S.P. 6 Lecce-Monteroni - 73100 Lecce, Italy
22. **Dr. Prof. A.M. Deshmukh**, Dept. of Microbiology, Dr. B.A. Marathwada University Sub-Centre, Osmanabad, India
23. **Dr. Prof. M.P. Sinha**, Vinoba Bhave University, Hazaribagh, India
24. **Dr. G.R. Pathade**, H.V. Desai College, Pune, Maharashtra, India
25. **Dr. Hossam Adel Zaqoot**, Ministry of Environmental Affairs, Ramallah, Palestine
26. **Dr. T.S. Anirudhan**, Dept. of Chemistry, University of Kerala, Trivandrum, Kerala, India
27. **Dr. James J. Newton**, Environmental Program Manager, 701 S. Walnut St. Milford, DE 19963, USA
28. **Dr. M.G. Bodhankar**, Dept. of Microbiology, Yashwantrao Mohite College, Pune, India
29. **Dr. Murat Eyvaz**, Department of Environmental Engg. Gebze Inst. of Technology, Gebze-Kocaeli, Turkey
30. **Dr. Zhihui Liu**, School of Resources and Environment Science, Xinjiang University, Urumqi, China
31. **Dr. Sandeep Y. Bodkhe**, NEERI, Nagpur, India
32. **Dr. D. R. Khanna**, Gurukul Kangri Vishwavidyalaya, Haridwar, India
33. **Dr. S. Dawood Sharief**, Dept. of Zoology, The New College, Chennai, T. N., India
34. **Dr. B. N. Pandey**, Dept. of Zoology, Purnia College, Purnia, Bihar, India
35. **Dr. Xianyong Meng**, Xinjiang Inst. of Ecology and Geography, Chinese Academy of Sciences, Urumqi, China
36. **Dr. Ms. Shaheen Taj**, Dept. of Chemistry, Al-Ameen Arts, Science & Commerce College, Bangalore, India
37. **Dr. Nirmal Kumar, J. I.**, ISTAR, Vallabh Vidyanagar, Gujarat, India
38. **Dr. Wen Zhang**, Deptt. of Civil and Environmental Engineering, New Jersey Institute of Technology, USA



Treatment of Leachates of a Controlled Landfill in Veracruz By Using the Fenton Method

Miguel Ángel López-Ramírez*, Olaya Pirene Castellanos-Onorio**, Manuel Alberto Susunaga-Miranda**, Fabiola Lango-Reynoso*†, María del Refugio Castañeda-Chávez* and Jesús Montoya-Mendoza*

*Tecnológico Nacional de México/Instituto Tecnológico de Boca del Río, Carretera Veracruz-Córdoba 12, 94290 Boca del Río, Veracruz, México

**Tecnológico Nacional de México/Instituto Tecnológico de Veracruz. Av. Miguel Ángel de Quevedo 2779, Formando Hogar, 91897 Veracruz, Veracruz, México

†Corresponding author: Fabiola Lango-Reynoso

Nat. Env. & Poll. Tech.
Website: www.neptjournal.com

Received: 28-05-2018
Accepted: 02-08-2018

Key Words:

Controlled landfill
Leachate
Fenton Method
Chemical treatment
Contamination

ABSTRACT

Leachates are formed by the decomposition of solid waste contained in the final disposal site from liquids formed by precipitation or humidity in the area. Which, when filtered through waste, entrain substances in dissolved form and/or in suspension, creating a dark coloured liquid of variable characteristics and difficult to degrade, leading to contamination of soil and water bodies. Due to its variable characteristics, typical treatments such as evaporation, U.V. or recirculation are not suitable as chemical treatments. The Fenton process, being an advanced oxidation technique, has shown optimal performance in the treatment of young and mature leachates. Different parameters were tested during the Fenton oxidation-reduction process, which is consisted of treating the leachate with different combinations of hydrogen peroxide (H_2O_2) and ferrous sulphate ($FeSO_4$) under different acidic conditions, determining the optimal pH values, and doses of the Fenton reagent. Optimal conditions of the oxidation process were: contact time 1 hour, a pH value equal to 2, H_2O_2 concentrations of 250 mg/L and 75 mg/L of Fe^{2+} . The percentage of removal measured as BOD was of 96% at a final pH of 1.8.

INTRODUCTION

Leachate is the result of percolation of liquids through solid wastes in a stabilization process. That is, they are generated from the biochemical decomposition of waste or as a result of water infiltration from external sources, such as surface drainage, rain, groundwater and water from underground springs. Or, through waste in degradation processes, extracting dissolved or suspended materials generating a highly variable and toxic liquid. The organic matter load of leachate varies depending on the age of the landfill, from 2,000 to 3,000 mg/L in young fillings and from 100 to 200 mg/L in fillings considered as mature. Similarly, with the level of acidity that goes from 4.5 to 7.0 in young leachates and from 6.6 to 7.5 in mature leachates (Tchobanoglous 2000). Leachates, due to their physico-chemical characteristics, strongly variable in quantity and quality, are classified as one of the most polluting and difficult to treat waste, as indicated in Table 1.

The leachate, in terms of quality, contains heavy load of organic matter (high BOD), in addition to inorganic substances such as heavy metals (with its potential effect on aquatic ecosystems), high content of total and dissolved solids, presence of nitrogen in ammoniacal form, high con-

centration of chlorides, diverse organic compounds, as well as great pH variability. This depends on the nature of the waste (pH, age, temperature) and the stabilization phase in which they are located (Borzacconi et al. 1996a, El-Fadel et al. 2002).

Leachates are eventually removed from the landfills to be treated by physico-chemical and/or biological methods, thus avoiding soil, aquifers or surface water contamination through leaching, due to the runoff they generate. Treatment options include the reuse of leachates to maintain the moisture content of the landfills, on-site treatment (aerobic, anaerobic or physico-chemical), discharge to municipal treatment plants, or a combination of the above.

Several researchers have studied landfill leachate treatments obtaining promising results through different processes. These results indicate that the efficiencies of contaminant removal, obtained in a given leachate, are influenced by their chemical composition, which in turn is related to the characteristics and degree of sludge stabilization or the landfill age (Borzacconi et al. 1996b, Enzminger et al. 1997).

The controlled landfill of the city of Veracruz contains a type of sandy soil with particle sizes greater than 0.125 mm

and smaller than 1.0 mm. In addition, it contains an average alkaline pH of 7.40, with an average conductivity of 1.40 dS/cm, resulting in a very slightly saline characteristic throughout the year. The fact that this landfill has a sandy soil, shows that it is not suitable because it retains less water than others; resulting in a leachate with an average BOD₅ of 74.140 mg/L and an average COD of 340.35 mg/L implying a biodegradability of 0.217. When the index of biodegradability is higher than 0.3, the leachate is considered biodegradable and is known as young leachate (typically less than two years old) (Deng 2007). For this reason, the first stage of treatment, always recommendable for young leachates, is the application of biological treatments; whereas physico-chemical processes are the best option for old leachates, as is the case of the one produced in the controlled filling of the city of Veracruz (Kurniawan et al. 2009).

One of the most promising physico-chemical treatments for leachates is the Fenton oxidation, which consists of the oxidation of the contaminant load with a combination of hydrogen peroxide and ferrous sulphate (Fenton reagent), typically at atmospheric pressure and temperature between 20°C and 40°C. This type of treatment is used generally in leachates considered old, in which the biodegradability index (BOD₅/COD) is low; therefore, biological treatments, whether aerobic or anaerobic, would be inefficient.

The optimal conditions of the Fenton reagent are obtained at acid pH values and with them, high removals of organic contaminants can be achieved. The Fenton process involves:

- A structural change of organic compounds that make possible a later biological treatment.
- A partial oxidation that results in a decrease in the toxicity of the effluent, and/or a total oxidation of the organic compounds in harmless substances that enable a safe discharge of the effluent without the need for further treatment.

The agent responsible for oxidation in the Fenton process is the hydroxyl radical ($\bullet\text{OH}$), $\text{Fe}^{2+} + \text{H}_2\text{O}_2 + \text{H}^+ \rightarrow \text{Fe}^{3+} + \text{H}_2\text{O} + \bullet\text{OH}$. This free radical is extremely reactive and is formed by the catalytic decomposition of hydrogen peroxide in an acidic medium (Kitis et al. 1999, Yoo et al. 2001, Lu et al. 2001). There is a wide variety of organic compounds that are possible to degrade with the Fenton reagent; some compounds are more refractory than others, requiring higher temperatures for oxidation. For example, benzene or phenol are oxidized relatively easily, while chlorinated derivatives are less reactive and require longer time or higher temperatures for their treatment. In many cases, an organic substrate, apparently refractory to the treatment can be oxidized by altering the conditions of temperature, pH

or catalyst concentration.

There are numerous studies on the effect of the Fenton reagent on the removal of leachate contaminants from landfills. When a ratio of $[\text{Fe}^{2+}]/[\text{H}_2\text{O}_2]$ equal to or greater than 1.25 is used, the Fenton reaction can be divided into two processes. The first consists of an initial oxidation at low pH values, around 3. The second process, which follows the oxidation, is the coagulation-flocculation at high pH values (between 7-8). It was interpreted that the coagulation step in the Fenton process had a primary role in selective removal of contaminants, though the Fenton reaction is not coagulation. However, since the efficiency of organic removal in the Fenton reaction was higher than coagulation, the Fenton process in the landfill leachate treatment process may be called “a type of enhanced coagulation” (Yoo et al. 2001).

MATERIALS AND METHODS

Characterization of leachates: Samples were taken between the months of June 2017 and February 2018, where the following parameters were determined as per APHA-AWWA-WPCF (1998): pH, chemical oxygen demand (COD), ammoniacal nitrogen ($\text{NH}_3\text{-N}$), total Kjeldahl nitrogen (TKN), organic nitrogen (org-N), total phosphorus (TP), fats and oils, settleable solids (SS) and total suspended solids (TSS). The samples were collected in a temporary oxidation lagoon located inside the controlled landfill of the city of Veracruz, where the leachates of different ages are mixed.

The leachate samples were homogenized with a Thermolyne Cimarec® 2 stirrer, at 600 r.p.m. In order to determine the optimum pH, concentration and dose conditions of Fenton reagent (peroxide and Fe^{2+}), and a contact time of one hour was proposed.

Determination of the pH: To this effect, the pH value of the leachates was adjusted to 2, 4 and 6, using concentrated H_2SO_4 (97% w/w oxidation tests, and a dose of 30% Fenton reagent (500 mg/L of hydrogen peroxide and 150 mg/L of ferrous sulphate) occupying a volumetric proportion of 25% according to the volume of the leachate to be treated.

Determination of concentration: The determination of the optimal concentration was obtained from the adjusted pH, with a concentration of 25%, according to the volume of the sample and with the concentrations of 30% Fenton reagent (500 mg/L of hydrogen peroxide and 150 mg/L of ferrous sulphate), 60% (500 mg/L of hydrogen peroxide and 300 mg/L of ferrous sulphate) and 90% (500 mg/L of hydrogen peroxide and 450 mg/L of ferrous sulphate).

Determination of optimal volume: The optimal dose is determined, based on the results obtained from the pH and the concentration of the Fenton reagent, by volume per-

centages of 25%, 50% and 75%.

Determination of the biochemical oxygen demand: To determine the biochemical oxygen demand (BOD) of the treated leachate, the procedures established in the Mexican standard NMX-AA-028-SCFI-2001 were followed. This standard establishes the determination of the biochemical oxygen demand in natural, residual waters (BOD₅) and treated wastewater - test method; the pH is then reduced to 8 with potassium permanganate so that the residual or residual peroxide does not affect the BOD readings.

RESULTS

Table 2 shows the results of the characterization of leachates, and Table 3 presents the treatments performed for the determination of the optimum pH, whereas Fig. 1 shows their respective results in the form of a removal percentage of organic matter measured as BOD.

Table 4 gives the treatments carried out to determine the concentration of the Fenton reagent and Fig. 2 shows the percentage results of the organic matter degradation obtained.

Table 5 shows the experimentation to determine the effective dose of the Fenton reagent in the leachates, and Fig. 3 shows the results measured in percentage of degradation of organic matter.

The controlled landfill of the city of Veracruz has a sandy soil, which is most prone to erosion by water and wind, as well as being the most porous. This is due to the large amount of water that filters out allowing larger particles to go through, thus maintaining a constant biochemical oxygen demand, since it does not act as a retention filter.

The pH of the leachate is alkaline, even though it does not come into direct contact with carbonates, calcium or magnesium bicarbonates, as reported by Méndez Novelo (2010) in the leachates of the landfill of the city of Mérida, being more similar to the value obtained in Hong Kong by Lau (2001).

Fig. 1 shows the removal percentages obtained in the different pHs treated in the sample, showing that pH 2 in treatments 1, 2 and 3 got better degradation results similar to those by Zhang et al. (2005), which was 2.5 units.

The results obtained, using a concentration of Fenton at 30% in treatments 10, 11 and 12, showed an 84% removal of organic matter (Fig. 2) that was higher than that reported by Cortez et al. (2011) in Portugal, with Fenton at 33% and a maximum efficiency of 44%. In addition, the coagulation-flocculation process was presented, in which several authors have reported high removals of organic matter as reported by Duran et al. (2002) with a maximum efficiency of

Table 1: Characteristics of young and mature leachate.

Characteristics	Units	Young leachate	Mature leachate
BOD ₅	mg/L	2000-3000	100-200
COD	mg/L	3000-60000	100-500
Nitrates	mg/L	5-40	5-10
TSS	mg/L	200-2000	100-400
Ammoniacal nitrogen	mg/L	10-800	20-40
Total organic nitrogen	mg/L	10-800	80-120
pH	-	4.5-7.5	6.6-7.5
Total phosphorus	mg/L	5-100	5-10

Table 2: Characterization of the leachates of the controlled landfill of the Veracruz city.

Parameters	Units	Value
pH	-	8.500
COD	mg/L	340.35
BOD ₅	mg/L	74.140
Ammoniacal nitrogen	mg/L	1.944
Total nitrogen	mg/L	3.058
Organic nitrogen	mg/L	1.112
Total phosphorus	mg/L	0.519
Fat and oil	mg/L	5.000
Sedimentable solids	mg/L	0.100
Total suspended solids	mg/L	15.000

Table 3: Treatments to determine the optimum pH.

Treatment	pH	Fenton	
		H ₂ O ₂ (mg/L)	Fe(mg/L)
1	2	500	150
2	2	500	150
3	2	500	150
4	4	500	150
5	4	500	150
6	4	500	150
7	6	500	150
8	6	500	150
9	6	500	150

Table 4: Treatments for determining the concentration of the Fenton reagent.

Treatment	pH	Fenton	
		H ₂ O ₂ (mg/L)	Fe(mg/L)
10	2	500	150
11	2	500	150
12	2	500	150
13	2	500	300
14	2	500	300
15	2	500	300
16	2	500	450
17	2	500	450
18	2	500	450

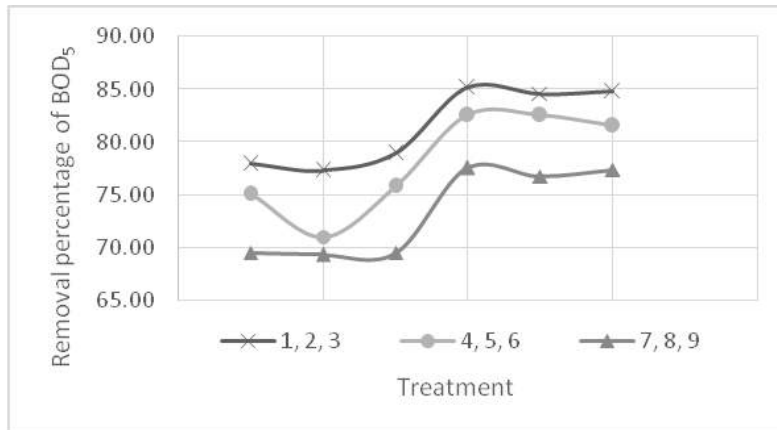


Fig. 1: Percentage of organic matter removal according to pH.

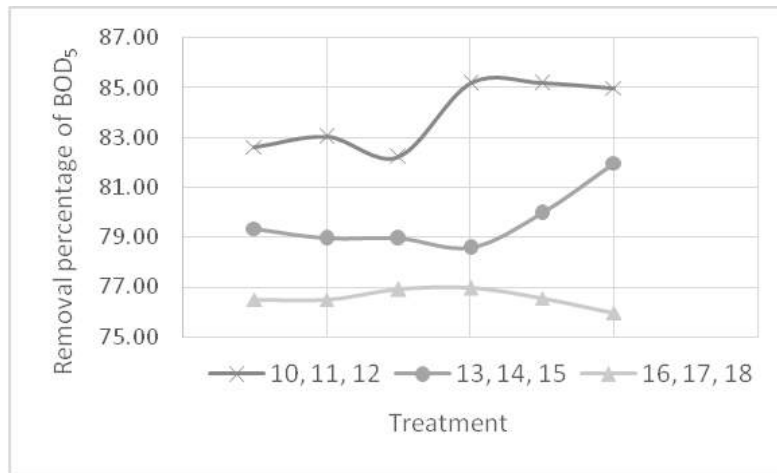


Fig. 2: Percentage of organic matter removal according to the concentration.

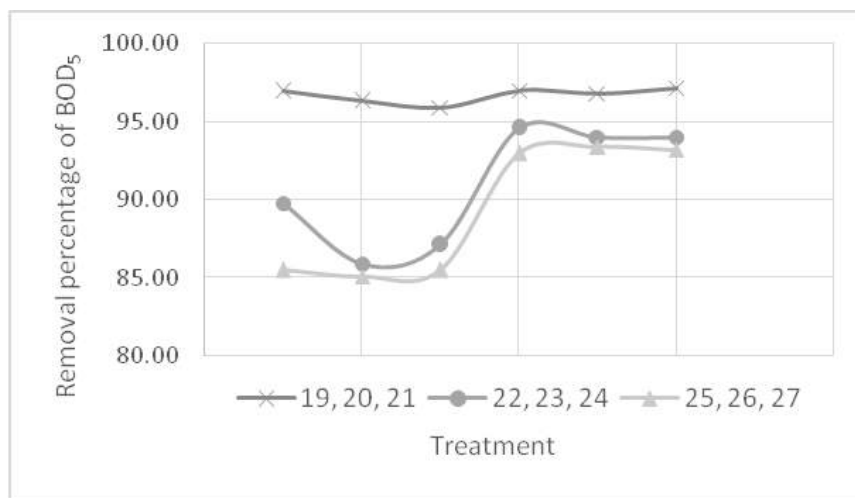


Fig. 3: Percentage of organic matter removal according to the optimal dose.

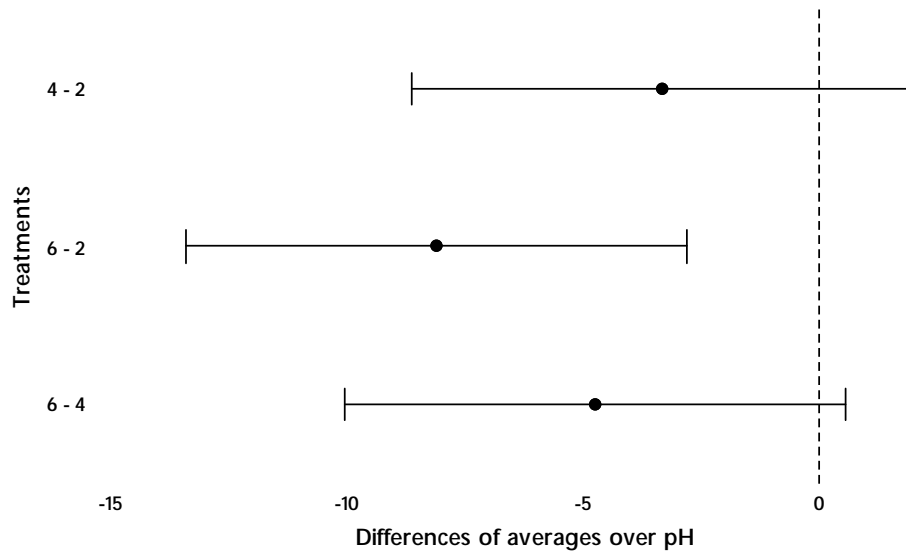


Fig. 4: A 95% ANOVA analysis for pH during the Fenton oxidation process.

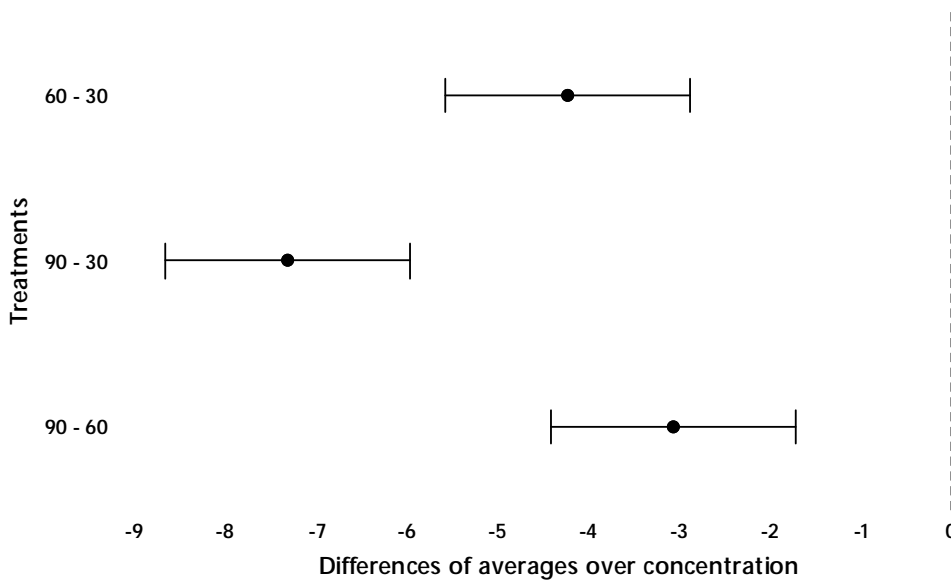


Fig. 5. A 95% confidence level ANOVA analysis for the effect of concentration.

78% and Ahn et al. (2002) of 83%, eliminating colloidal particles of small size that infer in the colour of the leachate.

Fig. 3 presents the removal results obtained from the dose of the Fenton reagent, according to the amount of effluent to be treated, with treatments 19, 20 and 21 showing the best results using a dose of 25% v/v .

As seen in Table 6, the efficiency of the Fenton reagent varies depending on the concentration of Fe^{+2} , because it acts as a catalyst in the oxidation reaction, ranging from

275 mg/L to 2792 mg/L. Due to the low presence of organic matter in the leachates, the concentration of the catalyst is 150 mg/L, in the same way, the hydrogen peroxide is 500 mg/L, while in the literature it varies between 200 mg/L and 34 000 mg/L, as given in Table 6.

DISCUSSION

The percentages of efficiency between the optimization treatments of pH and concentration, show characteristics, which differ among them, because the first results obtained

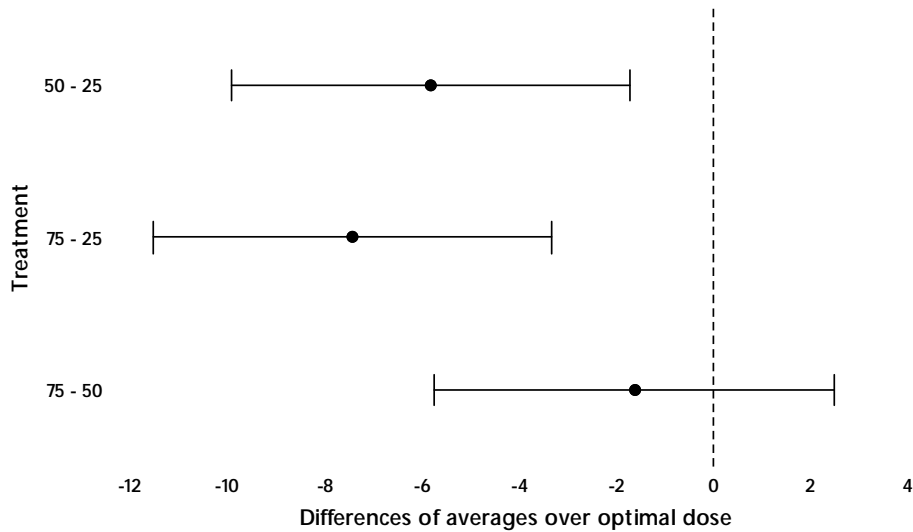


Fig. 6: A 95% ANOVA analysis regarding the optimal dose.

were collected during the rainy season and the following set of results during the North winds season, which can be noted by observing the valleys and crests formed in Figs. 1 and 2.

A 95% confidence level ANOVA analysis was carried out for the pH treatments during the Fenton oxidation process (Fig. 4) and it is concluded that the efficiency achieved in the use of the pH 2 and 6 is significantly different at the 95% confidence level. However, treatments with a pH 2 and 4 do not present a significant difference, as do treatments with a pH 4 and 6. Therefore, pH 2 is proposed as optimal, since it showed greater degradation of organic material.

According to the ANOVA analysis (Fig. 5), it was determined that the concentration of the Fenton reagent influences the efficiency in the degradation of organic matter, besides that it does not present similarities to each other.

According to the optimal dose, the ANOVA analysis (Fig. 6) showed that the optimal doses of 50% v/v and 75% v/v do not present significant statistical differences, whereas the 25% dose is different, besides that it presented a higher efficiency of BOD removal.

At the levels of optimum treatment for the degradation of organic matter, defined as Fenton 30% (500 mg/L of hydrogen peroxide and 150 mg/L of ferrous sulphate), with a volumetric concentration of 25% v/v and pH 2; the analysis does not present significant statistical differences between the seasons (rainy and north winds) (Fig. 7) previously described in the Fisher tests at 95% confidence.

Table 5: Determination of the effective dose of Fenton reagent.

Treatment	pH	Fenton	Volume (%v/v)
19	2	30%	25%
20	2	30%	25%
21	2	30%	25%
22	2	30%	50%
23	2	30%	50%
24	2	30%	50%
25	2	30%	75%
26	2	30%	75%
27	2	30%	75%

According to the characteristics of leachates from the controlled landfill of the city of Veracruz, which present low chemical and biochemical oxygen demands, they are classified as old leachates. Therefore, the use of the Fenton reagent as treatment in the degradation of organic matter is adequate.

The leachate collected in the controlled landfill of the city of Veracruz has a biodegradability index of less than 0.3; therefore, it is not susceptible to biological processes.

The optimum removal of organic matter measured as BOD reached percentages higher than the averages reported in Table 4 and similar to those obtained in Spain by Trujillo et al. (2006).

By decreasing the pH of leachates, the decrease in organic matter produces a greater efficiency in the degradation of organic matter.

By demonstrating average efficiencies of organic mat-

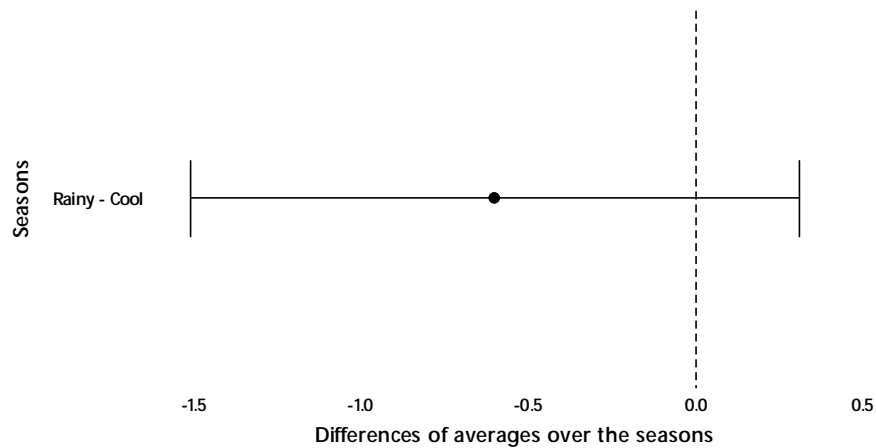


Fig. 7: A 95% confidence level ANOVA analysis for the efficiency between seasons.

Table 6: Comparison of leachate oxidation works by Fenton method.

Parameter	Unit	Veracruz a	Mérida b	Italia c	USA d	Hong Kong e	España 1 f	España 2 g	Estambul h			
pH	pH units	8.5	8.57	8.2	6.67	8.5	-	7.1	7.3			
Conductivity	mS/cm	10.7	21.83	45.35	-	-	-	47.1	-			
Alkalinity	mg/L	-	6115.96	21470	4050	-	-	-	9850			
BOD ₅	mg/L	74.14	647	2300	0	75	475	3510	1220			
COD	mg/L	340.35	9080	10540	8596	1500	8100	6500	20700			
TOC	mg/L	-	2266	3900	2124	470	-	-	-			
BOD ₅ /COD	-	0.218	0.071	0.218	-	0.05	0.059	0.54	0.589			
Optimal values												
Reaction time	Minutes	60	20	120	120	30	40	-	60	5		
pH	pH units	2	4	3	3	2.5	6	3.5	3	3.5-4.0		
H ₂ O ₂	mg/L	500	600	3300	10000	2550	200	34000	6500	2000		
Fe ⁺²	mg/L	150	1000	275	830	2792	300	558	650	1000		
Efficiency achieved												
COD	%	71	77	-	60	61	49	38	70	80	85	75
BOD ₅	%	96.67	44	-	-	-	-	-	-	-	98	-
DBO ₅ /COD	-	-	0.100	0.5	-	-	-	-	-	-	-	-

a. Present study; b. Novelo et al. (2010); c. Lopez et al. (2003); d. Zhang et al. (2005); e. Lau et al. (2001); f. Rivas et al. (2004); g. Trujillo et al. (2006); h. Calli et al. (2005)

Total Organic Carbon (TOC)

ter removal of 96%, the Fenton reagent has shown to be an effective chemical procedure in the treatment of leachates from the controlled landfill of the city of Veracruz.

REFERENCES

- Ahn, D.H., Chung, Y.C. and Chang, W.S. 2002 Use of coagulant and zeolita to enhance the biological treatment efficiency of high ammonia leachate. *Journal of Environmental Science Health, A37(2)*: 163-173.
- APHA-AWWA-WPCF 1998. *Standards Methods for the Examination of Water and Wastewater*. 20th Edition, USA.
- Borzacconi, L., López, I. and Anido, C. 1996a. Metodología para la estimación de la producción y concentración de lixiviado de un relleno sanitario. In: XXV Congreso Interamericano de Ingeniería Sanitaria y Ambiental. México DF, Vol. 31.
- Borzacconi, L., López, I., Arcia, E., Cardelino, L., Castagna, A. and Vinas, M. 1996b. Comparación de tratamientos aerobios y anaerobios aplicados a un lixiviado de relleno sanitario. In: XXV Congreso Interamericano de Ingeniería Sanitaria y Ambiental, 25: 1-8, AIDIS.
- Calli, B., Mertoglu, B. and Inanc, B. 2005. Landfill leachate management in Istanbul: Applications and alternatives. *Chemosphere*, 59: 819-829.
- Cortez, S., Teixeira, P., Oliveira, R. and Mota, M. 2011. Evaluation of Fenton and ozone-based advanced oxidation processes as mature landfill leachate pre-treatments. *Journal of Environmental Management*, 92: 749-755.

- Deng, Y. and Englehardt, J. 2007. Electrochemical oxidation for landfill leachate treatment. *Waste Management*, 27: 380-388.
- Durán, P., Ramírez, Z.Y. and Durán, M. 2002. Bioadsorción de lixiviados viejosclarificados. Memorias del XIII Congreso Nacional de laFEMISCA, Morelia, pp. 455-460.
- El-Fadel, M., Bou-Zeid, E., Chahine, W. and Alayli, B. 2002. Temporal variation of leachate quality from pre-sorted and baled municipal solid waste with high organic and moisture content. *Waste Manage.*, 22: 269-282.
- Enzinger, J.D., Robertson, D., Ahlert, R.C. and Kosson, D.S. 1997. Treatment of landfill leachates. *J. Hazard. Mater.*, 14: 83-101.
- Kitis, M., Adams, C.D. and Daigger, G.T. 1999. The effects of Fenton's reagent pretreatment on the biodegradability of non-ionic surfactants. *Wat. Res.*, 33(11): 2561-2568.
- Kurniawan, T.A., Wai-Hung, L. and Chan, G.Y.S. 2006. Physico-chemical treatments for removal of recalcitrant contaminants from landfill leachate. *J. Hazard. Mater.*, B129: 80-100.
- Lau, I.W.C., Wang, P. and Fang, H.H.P. 2001. Organic removal of anaerobically treated leachate by Fenton coagulation. *Journal of Environmental Engineering*, 127(7): 666-669.
- Lopez, A., Pagano, M., Volpe, A. and Di Pinto, A. 2003. Fenton's pre-treatment of mature landfill leachate. *Chemosphere*, 54: 1005-1010.
- Lu, M.C., Lin, C.J., Liao, C.H., Ting, W.P. and Huang, R.Y. 2001. Influence of pH on the dewatering of activated sludge by Fenton's reagent. *Wat. Sci. Technol.*, 44(10): 327-332.
- Méndez Novelo, R.I., Pietrogiovanna Bronca, J.A., Santos Ocampo, B., Sauri Riancho, M.R., Giacomán Vallejos, G. and Castillo Borges, E.R. 2010. Determinación de la dosis óptima del reactivo Fenton en un tratamiento de lixiviados por Fenton-Adsorción. *Investigación and Contaminación Ambiental*, 26(3): 211-220.
- NMX-AA-028-SCFI-2001. que establece la determinación de la demanda bioquímica de oxígeno en aguas naturales, residuales (DBO5) y residuales tratadas - Método de prueba. México, D.F., a 6 de abril de 2001.
- Rivas, F.J., Beltrán, F., Carvalho, F., Gimeno, O. and Frades, J. 2005. Study of different integrated physical-chemical+adsorption processes for landfill leachate remediation. *Industrial Engineering Chemical Research*, 44: 2871-2878.
- Tchobanoglous, G., Theisen, H. and Vigil, S.A. 2000. *Gestión Integral de Residuos Sólidos. Volumen I*. Editorial Mc Graw Hill, pp. 469.
- Trujillo, D., Font, X. and Sánchez, A. 2006. Use of Fenton reaction for the treatment of leachate from composting of different wastes. *Journal of Hazardous Materials*, B138: 201-204.
- Yoo, H.C., Cho, S.H. and Ko, S.O. 2001. Modification of coagulation and Fenton oxidation processes for cost-effective leachate treatment. *Journal of Environmental Science and Health*, 36(1): 39-48.
- Yoon, J., Lee, Y. and Kim, S. 2001. Investigation of the reaction pathway of OH radicals produced by Fenton oxidation in the conditions of wastewater treatment. *Wat. Sci. Technol.*, 44(5): 15-21.
- Zhang, H., Choi, H.J. and Huang, C.P. 2005. Optimization of Fenton process for the treatment of landfill leachate. *Journal of Hazardous Materials*, B125: 166-174.



Degradation of Direct Red 28 by *Alcaligenes* sp. TEX S6 Isolated from Aeration Tank of Common Effluent Treatment Plant (CETP), Pali, Rajasthan

Neha Sharma*†, Sreemoyee Chatterjee** and Pradeep Bhatnagar**

*Department of Zoology, Poddar International College, Sector 7, Shipra Path, Mansarovar, Jaipur-302020, India

**Department of Biotechnology, The IIS University, SFS, Gurukul Marg, Mansarovar, Jaipur-302020, India

†Corresponding author: Neha Sharma

Nat. Env. & Poll. Tech.
Website: www.neptjournal.com

Received: 24-12-2016
Accepted: 18-07-2018

Key Words:

Alcaligenes sp. TEX S6
Biodegradation
Direct red 28
Process optimization
Textile effluent

ABSTRACT

Pali city in Rajasthan has been a major environmental concern in the terms of extensive water pollution caused by the textile industries. The textile effluents are characterized by remarkably strong colour, high pH, BOD and COD. The major culprits are the direct diazo dyes and one such dye is Direct Red 28. To develop an effective bioprocess for dye degradation, bacteria were screened from different stages of the common effluent treatment plant situated in Mandia Road, Pali. The most potential bacteria was an isolate from aeration tank and characterized as *Alcaligenes* sp. TEX S6 by 16S rDNA sequencing. The dye removal efficacy of the strain was expressed as a reduction in absorbance maxima of the dye. The strain removed the dye (0.15 g/L) up to 86% within 48 hours of static incubation utilizing fructose and peptone at 37°C and pH 7. The inoculum concentration had no effect on the decolourisation process. A significant increase in bioefficacy of the strain was observed with respect to abiotic control. TLC chromatogram and FTIR spectra of the pure dye compound and the decolourised dye was suggestive of enzymatic degradation in accordance with biodecolourisation.

INTRODUCTION

Rapid industrialization has undoubtedly led to tremendous growth of economy, but at the same time has proved to be catastrophic for environment. Textile industry is the major consumer of synthetic dyes and utilizes enormous volumes of water for its different processes (Shah 2014a) and likewise generates huge volumes of wastewater (Saranraj et al. 2010), which in most cases is discharged directly into the adjoining surface waters (Rajendran et al. 2011, Ponraj et al. 2011). Pali, a district headquarters located in the south western Rajasthan, is known for its textile dyeing and printing work. Approximately, 800 textile dyeing and printing units situated at Pali discharge about 49 million litres per day (MLD) effluents in the Bandi River which owes its origin in Luni basin (Rathore 2012). The untreated effluents flow regularly in the dry bed of river about 45 km downstream Pali city (Khandelwal & Chauhan 2005). Dyes are widely used in the textile, rubber, paper, printing, colour photography, pharmaceuticals, cosmetics and many other industries. Amongst these, azo dyes represent the largest and most versatile class of synthetic dyes (Keharia et al. 2004). Dyes usually have a synthetic origin and complex aromatic molecular structures contribute to their stability and impart recalcitrance to them. Azo dyes have found widespread use in textile industries because of the ease in synthesizing them as compared to their natural counterparts and are designated as major environmental contaminants (Shah et al. 2013).

Azo dyes are difficult to treat by conventional wastewater treatment. Existing treatment strategy for textile effluent utilizes neutralization of alkaline pH, coagulation, flocculation followed by aerobic biological treatment, but complete removal of recalcitrant dyes from effluents is not attainable, which may be attributed to the colour fastness and stability of dyes to degradation (Anjaneyulu et al. 2005). Biotreatment, most popularly known as bioremediation is the microbial clean up approach which leads to biomineralization and biotransformation of toxic chemicals to less harmful forms by using microorganisms. In addition to being cost-effective, the most satisfactory aspect of biotreatment is its being environmental friendly with minimal sludge generation (Chen et al. 2003). The process of bioremediation gains momentum if the microbes used in the bioprocess are adapted to the system rather than using the non adapted forms. Screening of potential microorganisms based on their specificity and adaptability which governs the microbial activity is a critical step in devising an effective bioprocess.

A number of bacterial isolates *Pseudomonas* sp. (Isik & Sponza 2003, Perumal et al. 2012, Soundararajan et al. 2012, Raja et al. 2013, Shah 2014b), *Proteus* sp., *Salmonella* sp., *Klebsiella* sp. (Saranraj et al. 2010, Perumal et al. 2012), *Aeromonas hydrophila* (Chen et al. 2003, Bumpus 2004), have been reported for their role in dye decolourisation process. The present study is aimed at optimizing decolourisa-

tion of azo dye, which forms the main constituent of textile wastewater generated by textile industries located at Pali, by indigenous bacterial species to attain an accelerated bioprocess.

MATERIALS AND METHODS

Chemicals and Dye Used

All chemicals and reagents used in the study were of analytical grade. The dye used in the study was of commercial grade and procured from the local market with the specifications mentioned in Table 1.

Screening and Characterisation of Indigenous Bacteria

Indigenous bacterial strains were isolated from textile effluent and qualitatively screened by plate assay (Shah 2014b). For plate assay a thin layer of cotton was wrapped onto a match stick and sterilised at 121°C for 15 minutes. A single colony was picked from the pure culture and aseptically transferred onto the plates as single spots containing BHA and incubated at 37°C for 24 to 48 hours. Following incubation, clear zones around spots were observed and diameter around spots was measured in mm and compared with uninoculated plates which served as negative or abiotic controls. Identification of strain was carried out by 16S rDNA sequencing. Upon isolation of DNA, fragments of 16S rDNA gene were amplified by PCR. Forward (27F) and reverse (1542R) DNA sequencing reaction of PCR amplicon was carried out with forward and reverse primers using BDT v3.1 Cycle sequencing kit on ABI 3730xl Genetic Analyser. The 16S rDNA gene sequence was used to carry out BLAST.

Acclimatization of Screened Isolate

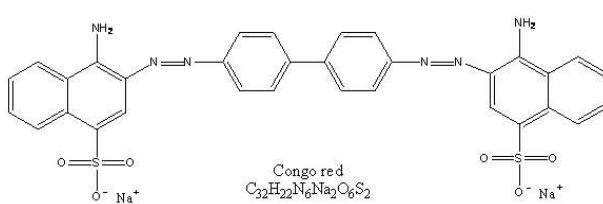
Inoculum preparation: The screened isolate was initially grown in nutrient broth (NB) with composition (g/L): Beef extract-3g, NaCl-5g, Peptone-5g and incubated at 37°C for 24 to 48 hours under agitated conditions (120 rpm) till a desired ($O.D_{660} = 0.6$) has attained (Suizhou et al. 2006).

Growth curve of isolate: The actively growing strain ($O.D_{660} = 0.6$) in nutrient broth was inoculated as monoculture 1% v/v in a 250 mL Erlenmeyer flasks containing 100 mL of Bushnell & Haas Broth (BHB) with the following composition (g/L): Magnesium sulphate = 0.2; Calcium chloride = 0.02; Monopotassium phosphate = 1.0; Dipotassium phosphate = 1.0; Ammonium nitrate = 1.0; Ferric chloride = 0.05; pH = 7.0, supplemented with diazo dye in a minimum concentration (0.1g/L) and were incubated at 37°C for 24 to 48 hours under agitated conditions (120 rpm). Negative biotic controls were also maintained which were devoid of dye under study. $O.D_{660}$ for both the set of experiments was monitored at regular intervals.

Dye Decolourisation by Optimization of Process Parameters by OFAT Approach

Decolourisation of diazo dye by bacteria was studied in a cell free extract (CFE). Aliquots of 1.5 mL were withdrawn in 2 mL vials from the monocultures of acclimatized bacterial strains. The aliquots were then centrifuged at 10,000 rpm for 15 minutes. The decolourisation activity was monitored spectrophotometrically in cell free extract at the absorption maxima of the dye ($\lambda_{max} = 495.5$ nm) and measured as % decolourisation of dye:

Table 1: Physico-chemical properties of Direct Red 28 (Shinde & Thorat 2013)

S.No	Specification	Properties
1	CAS number	573-58-0
2	Molecular mass	696.66g/mol
3	Molecular formula	$C_{32}H_{22}N_6Na_2O_6S_2$
4	IUPAC name	Disodium 4-amino-3-[4[4-(1-amino-4-sulfonato-naphthalen-2-yl) diazenylphenyl]diazenyl-naphthalene-1-sulphonate
4	Molar extinction-coefficient	45,000[L]/[mol].[cm]
5	Absorption maxima	490-495 nm
6	Chromopheric group	(Azo)-N=N-
7	Chemical structure	 <p style="text-align: center;">Congo red $C_{32}H_{22}N_6Na_2O_6S_2$</p>

$$\% \text{ decolourisation} = \frac{\text{Initial } O.D. - \text{final } O.D.}{\text{initial } O.D.} * 100$$

For optimizing the process, one factor at a time (OFAT) approach was used in which one parameter under consideration was varied keeping other factors constant (Fig. 1). The parameter under consideration was fixed in a decolourisation assay and expressed as percent decolourisation as explained earlier. The process was repeated until all the parameters were optimized (Moharrery et al. 2012).

Incubation hour: Actively growing strain ($O.D._{660} = 0.6$) was inoculated in 100 mL BHB in 250 mL Erlenmeyer flasks amended with dye in the concentration (0.1 g/L) and incubated for 24, 48, 72 and 96 hours.

Temperature: Different temperatures, psychrophilic (4°C), mesophilic (27°C, 37°C) and thermophilic (60°C) were selected to study their effect on decolourisation whilst keeping other factors constant.

pH: The effect of pH on dye decolourisation was considered by varying the pH in the range from 2-10.

Carbon sources: Different carbon sources were used like starch, dextrose, sucrose, fructose, mannitol, glucose+fructose. These carbon sources were amended into the medium in the concentration of 0.1% w/v prior to sterilisation.

Nitrogen sources: Different nitrogen sources were used like yeast extract, tryptone, peptone, beef extract and urea. These nitrogen sources were amended into the medium in the concentration of 0.1% w/v prior to sterilisation.

Inoculum percent: Different inoculum concentrations of 0.1%, 0.5 %, 1%, 1.5%, 2% and 2.5% v/v were used in the medium.

Dye concentration: To study the effect of dye concentration on decolourisation, different concentrations of the dye were used in the range (100-400) mg/L.

Incubation condition: To study the effect of incubation condition on the process of decolourisation, two variations in incubation conditions were studied, static and shaking.

DYE DEGRADATION STUDIES

Thin Layer Chromatography

For initial conformational change in the di azo moiety after the treatment, thin layer chromatography (TLC) was performed with decolourised broth. The bacterial isolate was allowed to grow till the maximum decolourisation has attained. 5 mL samples were withdrawn from the decolourised broth culture in a sterile 10 mL vial. The sample was centrifuged at 10,000 g or 10,258 rpm for 15 min-

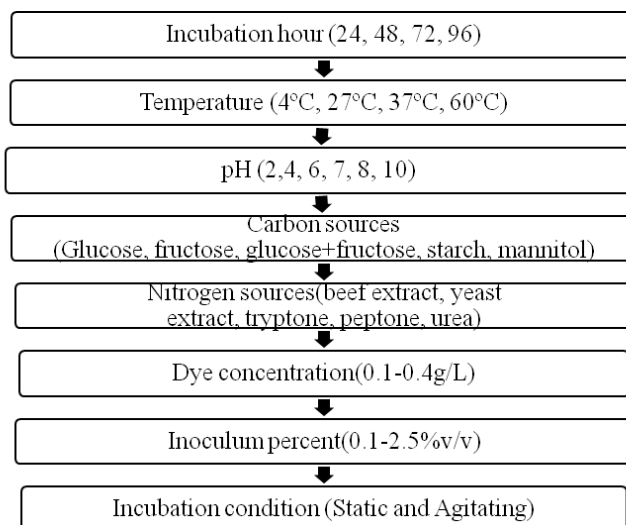


Fig. 1: Different process parameters for OFAT approach for optimisation of decolourisation process.

utes at 4°C and Cell Free Decolourised Supernatant (CFDS) was extracted with equal volume of ethyl acetate. A pinch of sodium sulphate (Na_2SO_4) was added to the extract. The extracts were evaporated to dryness and further dissolved in 1 mL of methanol. The control sample, which was only devoid of inoculum, was processed in a similar manner. 100 μ L of samples were loaded as spots using micropipette on commercially available TLC plates coated with silica gel 60F 254 on aluminium foil having dimensions 1-0 cm \times 5 cm \times 0.25 mm (Merck, Germany). The solvent system used was water: ethanol: acetone (4:4:1) for Direct Red 28. Upon drying, the plates were observed under UV transilluminator (365 nm) (Mali et al. 2000).

FTIR Spectroscopy

Biodegradation of Direct Red 28 was finally monitored by FTIR spectroscopy. For this 100 mL sample was procured after decolourisation. Centrifugation was carried out at 10,000 rpm for 15 minutes and the metabolites were extracted from CFDS using equal volume of ethyl acetate. The extract was dried over anhydrous Na_2SO_4 and evaporated to dryness in a rotary vacuum flash evaporator. The treated Congo Red dye was characterized by Fourier Transform Infrared Spectrometer (Perkin Elmer Spectrum 65) and compared with abiotic control and reference dye. The samples were mixed with spectroscopically pure KBr in the ratio of 1:100 and pressed to obtain IR-transparent pellet. The pellet was placed in sample holder and the analysis was carried out in the mid IR region of 500-4000 cm^{-1} with 16 scan speed (Shinde & Thorat 2013).

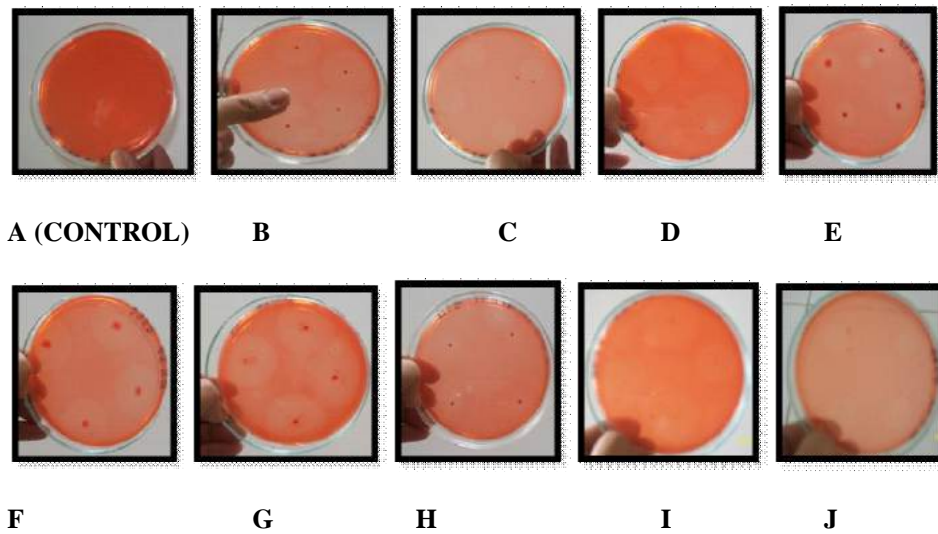


Fig. 2A: Abiotic control B-J:Plate assay of different strains representing clear zone around colonies (mm).

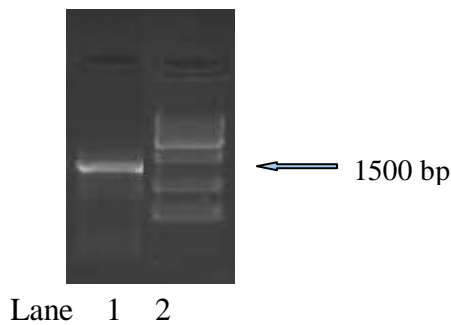


Fig. 3: Gel Image of 16S rDNA amplicon (Lane 1: 16S rDNA amplicon and; Lane 2: DNA marker).

Statistical Analysis

Data were analysed by one-way analysis of variance (ANOVA) with the Tukey-Kramer multiple comparisons test.

RESULTS

Screening of Indigenous Bacteria

A total of 9 bacterial isolates were screened at different stages of CETP for their dye decolourising potential which was expressed in terms of appearance of clear zones around colonies (Fig. 2A-J).

Strain G, encoded as Tex S6, exhibited maximum zone of clearance (0.6 mm) around colonies as compared with abiotic control, and was selected for further dye degradation studies.

Identification of Strain Tex S6

Molecular characterization of strain G revealed a single discrete PCR amplicon band of 1500 bp on agarose gel (Fig. 3). Based on the nucleotide homology and phylogenetic analysis, the strain was identified as *Alcaligenes* sp. TEXS6 (GenBank Accession Number: KF534470.1) (Fig. 4).

Acclimatization and Growth Curve Analysis of the Isolate

The effect of dye on bacterial growth profile indicated that in the presence of dye bacteria, growth was accelerated significantly ($p < 0.01$), presumably utilizing dye as the sole source of energy when compared with the negative biotic control (Fig. 5). The blue line indicates growth in presence of dye and red line depicts bacterial growth in absence of dye. A significant increase in bacterial growth was observed with increase in duration of incubation.

Dye Decolourisation Studies by Process Optimization

Effect of incubation hour on decolourisation process: The duration of incubation plays a significant role in a microbially mediated decolourisation process, which may be attributed to optimal growth of the species in concern. A significant increase ($p < 0.01$) in decolourisation was observed with increase in duration of incubation from 24 hours to 96 hours (Fig. 6) with 1% v/v inoculum size under static conditions with an initial dye concentration of 0.1 g/L, with no additional carbon and nitrogen sources and pH of the medium was fixed to 7 and temperature 37°C. The acclimatized strain had attained growth exponentially after 48 hours

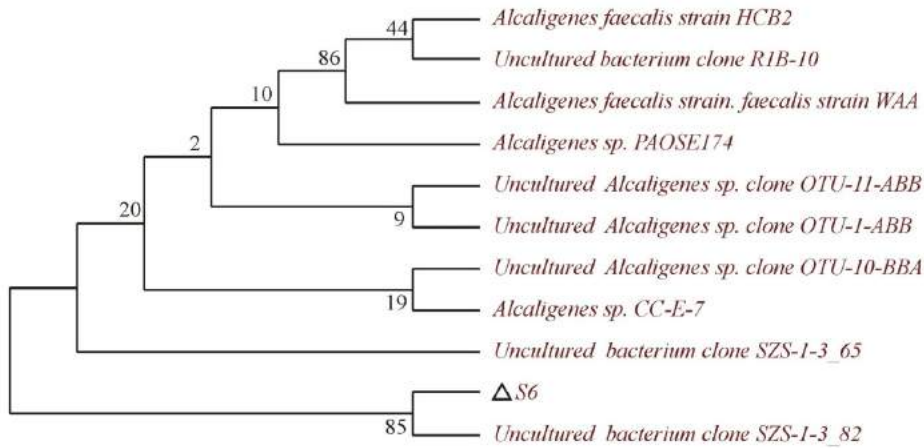


Fig. 4: Phylogenetic tree of Strain Tex S6.

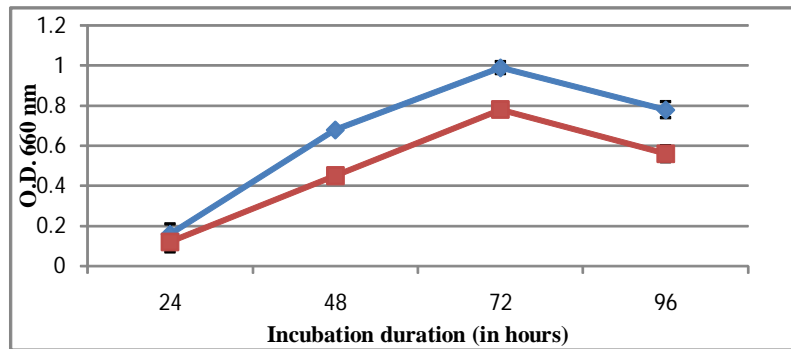


Fig. 5: Effect of Direct Red 28 on growth of *Alcaligenes* sp. TEX S6.

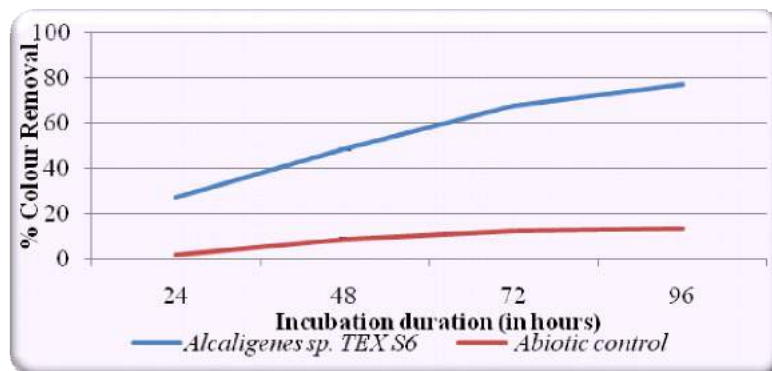


Fig. 6: Effect of incubation duration on decolourisation by *Alcaligenes* sp. TEX S6.

of incubation as elucidated earlier and dye removal efficiency was related to the growth profile of *Alcaligenes* sp. TEX S6. After 24 hours, the dye removal efficiency of the strain was found to be 26.78% which was continuously increased up to 67.41% after 72 hours. Although, a decline in growth was observed after 96 hours of incubation, but a

significant increase in dye removal efficiency of the strain (77.03%) was attainable, which may be attributed to biosorption of the dye by biomass during the early stationary phase of growth. The abiotic control had witnessed minimal decolourisation in the range of 1.78%-13.48% after 96 hours of incubation.

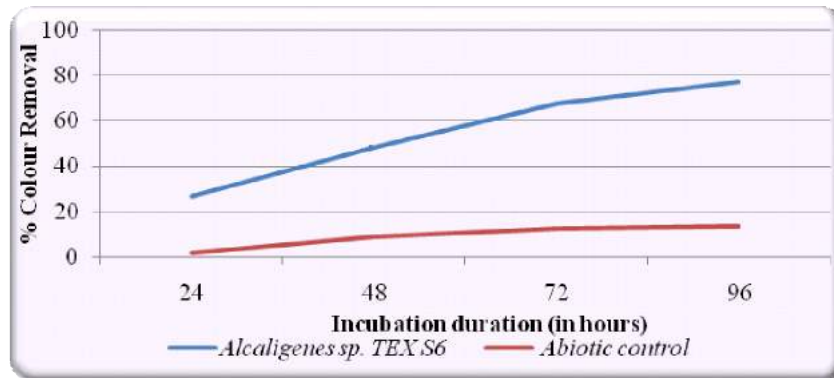


Fig. 7: Effect of temperature on decolourisation by *Alcaligenes* sp. TEX S6.

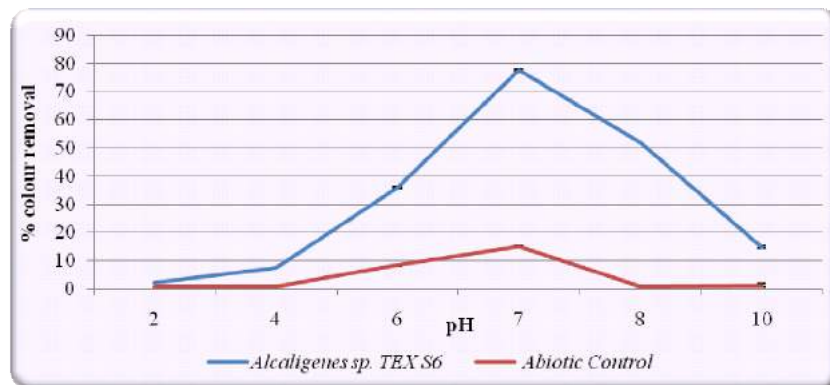


Fig. 8: Effect of pH on decolourisation by *Alcaligenes* sp. TEX S6.

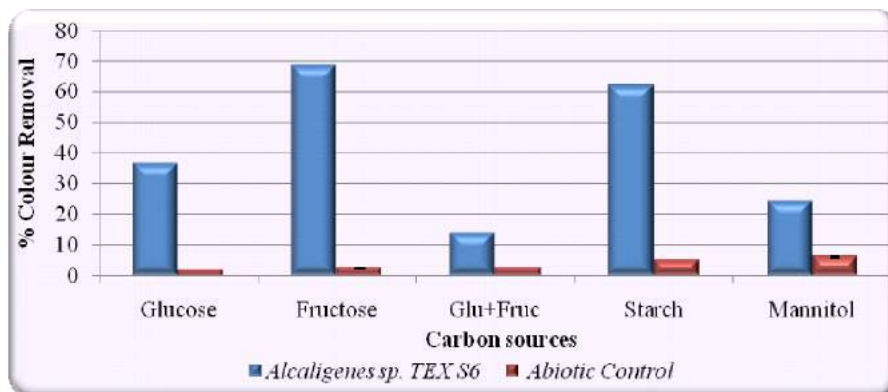


Fig. 9: Effect of different carbon sources on decolourisation by *Alcaligenes* sp. TEX S6

Effect of temperature on decolourisation process: Temperature is the quintessential factor which governs the microbial growth and enzymatic activity. The most pronounced bacterial activity is observed in mesophilic range (25°C-40°C). In our study, the best temperature for optimum de-

colourisation (72%) was found to be 37°C attained after 72 hours for *Alcaligenes* sp. TEX S6 with 1% v/v inoculum size under static conditions with an initial dye concentration of 0.1 g/L, with no additional carbon and nitrogen sources and pH of the medium at 7, followed by 63.9%

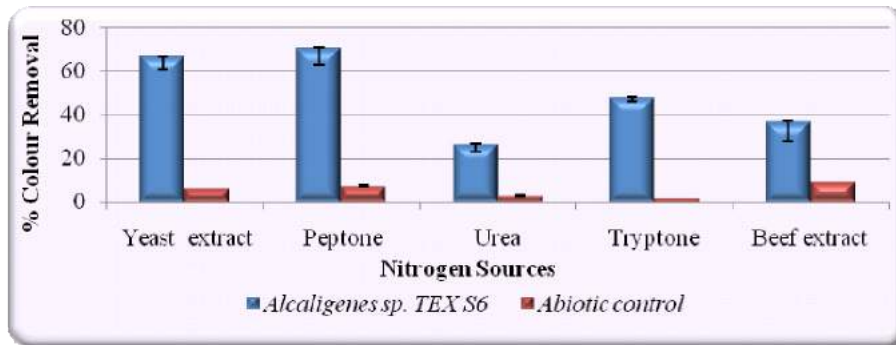


Fig. 10: Effect of different nitrogen sources on decolourisation by *Alcaligenes* sp. TEX S6.

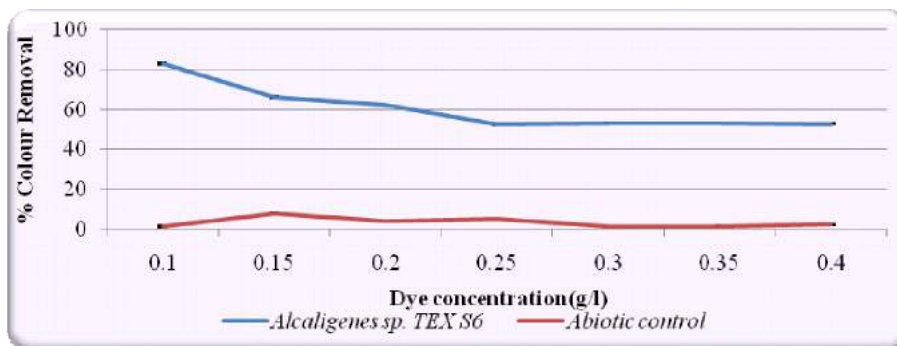


Fig. 11: Effect of dye concentration on decolourisation by *Alcaligenes* sp. TEX S6.

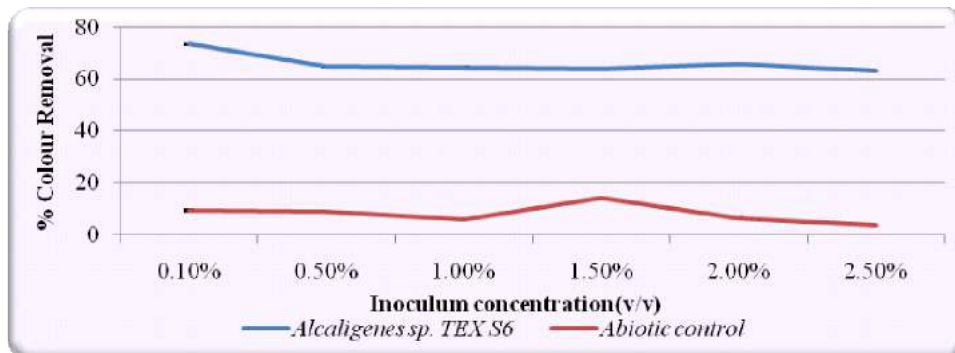


Fig. 12: Effect of inoculum size (v/v) on decolourisation by *Alcaligenes* sp. TEX S6.

(27°C) and negligible decolourisation was attained at both psychrophilic (4.63%) and thermophilic (14.06%) range under same physiological conditions which was found to be statistically different from abiotic control group (Fig. 7).

Effect of pH on decolourisation process: The variation in pH of the growth medium results in change in activity of bacteria, and hence the bacterial growth rate as well as decolourisation also gets affected. Bacteria are active over

certain range of pH. The optimum pH for the growth is the same for the dye decolourising activity as it is mainly the metabolic process. A significant difference in colour removal efficacy of *Alcaligenes* sp. TEX S6 was observed at different pH values (Fig. 8). The maximum colour removing efficiency of 65.5% was observed at pH 7 at 37°C and after 72 hours of static incubation with no additional carbon and nitrogen wherein the concentration of dye was 0.1 g/L. It

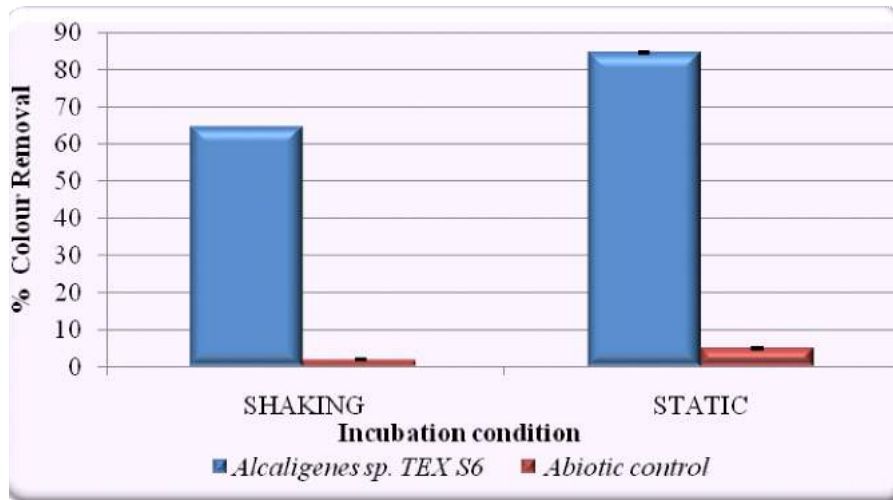


Fig. 13: Effect of incubation condition on decolourisation by *Alcaligenes sp. TEX S6*.



Fig. 14: Colour removal by *Alcaligenes sp. TEX S6* with respect to abiotic control.

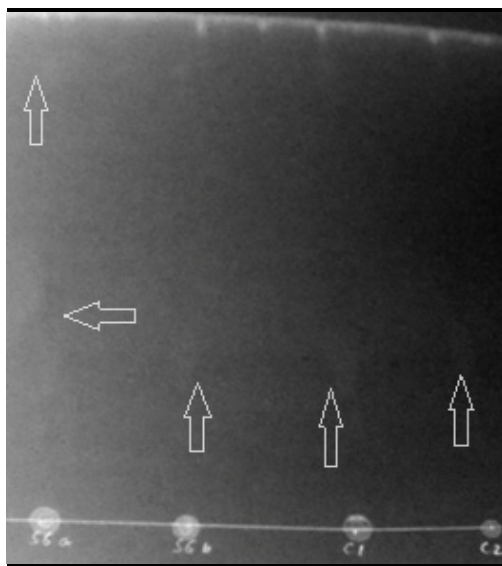


Fig. 15: TLC chromatogram representing degradation of Direct Red 28 by *Alcaligenes sp. TEX S6* (Lane 1 and Lane 2: Decolourised medium; Lane 3 and Lane 4: Abiotic control).

was followed by 51.95% at pH 8; 35.97% at pH 6; 14.8% at pH 10; 7.4% at pH 4 and 2.34% at pH 2.

Effect of different carbon sources on the process of decolourisation: Textile effluent is usually considered as being deficient in carbon (Bhatt et al. 2012). The decolourisation process was optimized for effective biodecolourisation in presence of wide range of carbon sources like glucose, fructose, glucose and fructose in combination, starch, mannitol and lactose. Significant changes in decolourisation

on utilization of different carbon sources by *Alcaligenes sp. TEX S6* was observed. Maximum decolourisation of 68.6% at concentration of 0.1 g/L of the dye was attained within 72 hours of static incubation wherein the pH of the medium was 7, incubation temperature 37°C, and inoculum size 1% v/v in presence of fructose (1% w/v) as a co-substrate. This was followed by starch (61.9%), glucose (36.6%), mannitol (24.34%), glucose and fructose in combination (14.15%) under similar culture conditions. Very less decolourisation (1.8–6%) was observed for abiotic controls under similar culture conditions (Fig. 9).

Effect of nitrogen sources on the process of decolourisation: Nitrogen is an important factor which governs the microbial growth and henceforth the process of decolourisation which is directly or indirectly linked to microbial growth. Amongst various nitrogen sources like yeast extract, beef extract, tryptone, peptone and urea; maximum decolourisation (70.41%) by utilization of peptone and dye (0.1g/L) was attained within 72 hours of static incubation, wherein the pH of the medium was 7, incubation temperature 37°C, inoculum size 1% v/v and fructose as a co-substrate. It was followed by yeast extract (64.98%), tryptone (48%), beef extract (37%), urea (26.33%) under similar culture conditions. Statistically significant differences in decolourisation were found between abiotic control (2–9%) and different nitrogen substrates (Fig. 10).

Effect of dye concentration on the process of decolourisation: The effect of dye concentration on the decolourisation of dye by *Alcaligenes sp. TEX S6* was studied over a range of 0.1 g/L to 0.4 g/L. A significant decrease in decolourisation was observed with increase in dye concentra-

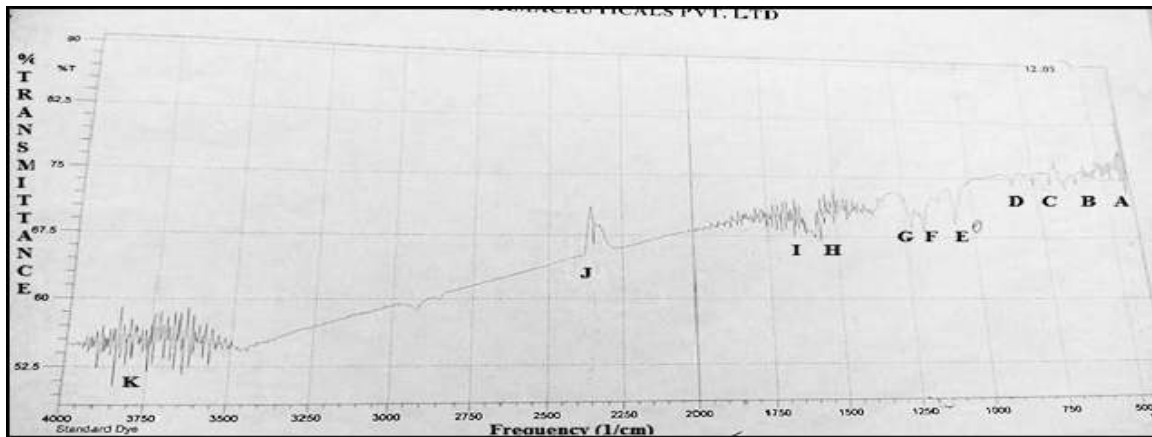


Fig. 16a: Interferogram of standard dye compound (DR 28).

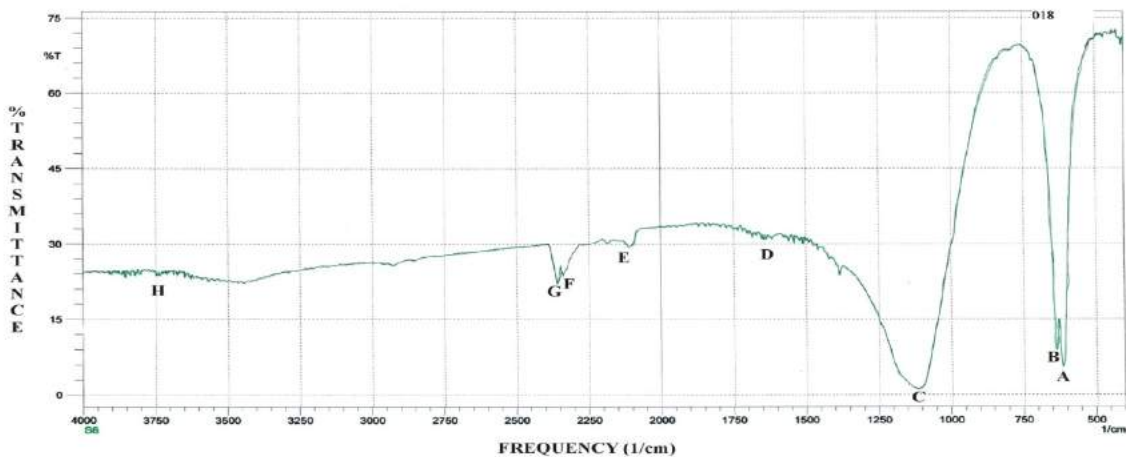


Fig. 16b: Interferogram of DR 28 treated by *Alcaligenes* sp. TEX S6.

tion from 0.1 g/L to 0.25 g/L. Further, the decolourisation attained for the dye concentration in the range from 0.25 g/L to 0.4 g/L was found to be nonsignificant and almost steady. Maximum decolourisation of 83.1% of dye at 0.1 g/L was attained after 72 hours of static incubation, wherein the pH of the medium was 7, incubation temperature 37°C, inoculum size 2.5% v/v with fructose and peptone as co-substrates. Under similar conditions of incubation, decolourisation attained with 0.15 g/L (66.09%); with 0.2 g/L (62.4%); with 0.25 g/L (52.37%); with 0.3 mg/L (53.1%); with 0.35 g/L (52.76%) and with 0.4 g/L (52.62%). Significant differences in decolourisation with respect to abiotic control (1.2-7.9%) were appreciable (Fig. 11).

Effect of inoculum size on the process of decolourisation:

The inoculum size is also an important factor upon which the decolourisation is dependent. With increase in inocu-

lum size from 0.1% v/v to 2.5% v/v, the decolourisation efficiency of *Alcaligenes* sp. TEX S6 marginally increased. After 72 hours of incubation under static conditions at 37°C, pH 7, fructose and peptone (both 1% w/v) with 0.1% v/v, the decolourisation of dye (0.1 gm/L) was found to be 63.31% which was non significantly increased to 67.98% at 2.5% inoculum size; although significant difference in decolourisation by abiotic controls (4-14.4%) was observed (Fig. 12).

Effect of incubation condition on the process of decolourisation:

A significant difference in the decolourisation potential of *Alcaligenes* sp. TEX S6 was observed when incubation conditions were varied from static to agitating. After 72 hrs of incubation under static conditions at 37°C, pH 7, fructose and peptone (both 1% w/v) with 2.5% v/v inoculum concentration, the decolourisation of dye (0.1 g/L) was

found to be 84.7%, whereas keeping all the culture conditions same with a variation in incubation condition from static to agitating, decolourisation was found to be 64.66% (Table 13 & 14).

Dye Degradation Studies

Thin layer chromatography: The dye decolourisation study of *Alcaligenes* sp. TEX S6 was further supported by thin layer chromatography (TLC) analysis. Upon observation under UV light (365 nm), TLC chromatogram comprised of four lanes (Fig. 15). Lane 1 and Lane 2 comprised of treatment group which represented biotic decolourised medium, whereas Lane 3 and Lane 4 comprised the abiotic control which was devoid of the strain. The spot corresponding to R_f value of Direct Red 28 = 0.35 (Table 2) was observed in abiotic control and no spot corresponding to this R_f value was observed in the decolourised medium indicating that decolourisation was due to its degradation into unidentified intermediates. Additionally, in Lane 1 and Lane 2, two spots corresponding to R_f values 0.87 and 0.51 (Table 2) were observed, possibly indicating the degradation of dye by induced enzymes like plausibly azoreductases.

Fourier Transform Infra Red (FTIR) spectroscopy: FTIR spectrum of the parent dye compound essentially revealed peaks at 515-690 cm^{-1} (A- alkyl halides); 610-700 cm^{-1} (B- alkynes); 720-725 cm^{-1} (C- alkanes); 1050 cm^{-1} (D- aliphatic amines); 1150 cm^{-1} (E- alkyl halides); 1200 cm^{-1} (F- aliphatic amines); 1250 cm^{-1} (G- aromatic amines); 1550 cm^{-1} (H- nitro compounds) which is characteristic feature of an azo group (-N=N-); 1600 cm^{-1} (I- aromatics); 2250-2500 cm^{-1} (J- nitriles and alkynes) (Fig. 16 a). The FTIR spectrum of metabolites obtained after decolourisation of Direct Red 28 by *Alcaligenes* sp. TEX S6 showed complete disappearance of peaks at 1550 cm^{-1} (C) characteristic of -N=N- group indicates that the dye has been degraded by bacteria and possibly the azo bond has been cleaved by its enzymatic activity. Additional peaks at 2050 cm^{-1} (D), indicative of C=C for acetylinic compounds stretching vibration, indicates formation of an additional product or metabolite of bacterial activity (Fig. 16b).

DISCUSSION

The bacterial strain *Alcaligenes* sp. TEX S6 isolated from activated sludge of CETP exhibited a tremendous potential in degrading the dye (84.7%) under optimized process parameters like incubation conditions and effect of co substrates. Previously, *Aeromonas hydrophila* strain DN322 was isolated from activated sludge of textile printing wastewater treatment plant, Guangzhou, China, and found to decolourise a wide variety of synthetic dyes including

Table 2: Summary of TLC chromatogram indicating presence of additional spots in biotic group.

Groups	Solvent(cm)	Spots(cm)	R_f value
Biotic (Lane 1 and 2)	13.4	11.7, 6.9	0.87, 0.51
Abiotic (Lane 3 and 4)	13.4	4.8	0.35

azo, anthroquinone and triphenylmethane (Suizhou et al. 2006). A multitude of reports pertaining to decolourisation of textile dyes by *Alcaligenes* sp. isolated from textile effluent and soil contaminated with dyes are widely available hence suggesting *Alcaligenes* sp. to be a promising isolate for dye decolourisation studies (Pandey & Dubey 2012, Sethi et al. 2012, Palani Velan et al. 2012, Vivekanandan et al. 2013). Our study revealed that *Alcaligenes* sp. TEX S6 decolourised dye within 72 hours of incubation. The duration of incubation is an important factor which governs the process of decolourisation, which is a catabolic process carried out by enzymes or biosorption as the process is found to be growth linked (Sridevi & Rao 2013). Complete degradation of Congo Red had been attained by *Bacillus megaterium* DMZ 32 (X60629) in 16 hours of incubation, isolated from sugarcane industrial wastewater (Pradhan et al. 2011). In our study, the optimum temperature for effective decolourisation by *Alcaligenes* sp. TEX S6 was found to be 37°C which supports the findings of previous studies conducted. Maximum decolourisation of Remazol Black B by *Bacillus* ETL-2012 was observed at 37°C (Shah 2013). The hydrogen ion concentration has a profound effect on the efficacy of the decolourisation process and the optimal pH for obliteration of colour from the system usually ranges from 6-10 (Kilic et al. 2007). The optimum pH in our study was in accordance with previous studies where optimum pH for removal of Congo Red by *Pseudomonas stutzeri* ETL-4 has been found to be 7 (Shah 2014b). The azo dye reduction and the rate is dependent upon the presence and availability of a co-substrate because it acts as an electron donor (Derle et al. 2012). The rate of azo reduction process also depends on the type of co-substrate used and chemical structure of azo dye. In our study, the best co-substrates were found to be fructose (70.41%) and peptone (68.6%). 100% decolourisation of Reactive Red R195 was attained by *Micrococcus glutamicus* NCIM 2168 in the presence of sucrose followed by 90.05% in presence of glucose while 88-89% of decolourisation was shown in presence of yeast extract and peptone (Leelangkrangsak & Borisut 2012). The dye concentration in which 83.1% decolourisation was attained by *Alcaligenes* sp. TEX S6 was 0.1 g/L (Verma & Madamwar 2003) which suggests that decolourisation decelerates with increase in dye concentration, which may be attributed to stronger inhibition at high concentration. In-

oculum size also plays an important role in decolourisation activity as the process is growth linked. In our study, the inoculum size, which yielded 67.98% decolourisation by *Alcaligenes* sp. TEX S6, was found to be 2.5% v/v. A 4% v/v inoculum has been used to attain decolourisation of textile effluent by *Bacillus subtilis* and *Streptococcus faecalis* isolated from activated sludge (Rajeshwari et al. 2012). The literature suggests that the process of decolourisation is more favoured in static conditions as opposed to agitating conditions, because under aerobic conditions azo dyes are generally resistant to attack by bacteria (Hu 1994), and our study was also in accordance with decolourisation being on a higher side under static incubation conditions. *Bacillus boro-niphilus* showed about 100% decolourisation of Reactive Yellow 145 within 9 hours under static conditions (Derle et al. 2012). Whereas as opposed to our findings, Shah (2014b) reported 61.8% of Congo Red under agitating conditions as opposed to 57% under static conditions.

Thin layer chromatography preliminarily investigates the degradation of dyes which may be associated with expression of enzymes. Our TLC chromatogram was suggestive of dye degradation as the R_f value of abiotic control sample was 0.35, whereas that of decolourised dye was found to be 0.57 and 0.81. Previous study on degradation of Reactive Red 195 by *Micrococcus glutamicus* NCIM 2168 suggested R_f value of pure dye as 0.9, whereas the degraded product showed R_f value 0.6 (Sahasrabudhe et al. 2012).

FTIR studies conducted to confirm the degradative properties of indigenous microbes have been phenomenal in suggesting the role of inducible enzymes, which carry out the metabolic process of dye degradation. Our study revealed that the dye was degraded as the peak at 1587.66 cm^{-1} for N=N stretching vibrations, is characteristic of the diazo bond and its complete disappearance suggests the degradation into acetylinic components exhibiting stretching vibration at 2050 cm^{-1} which was in accordance with the study conducted previously aimed at establishing the bioefficacy of *Fusarium* sp. to degrade Congo Red dye (Shinde & Thorat 2013).

CONCLUSION

This work was carried out to screen, characterize the isolated bacteria from activated sludge of a common effluent treatment plant. The most potential strain was found to be *Alcaligenes* sp. TEX S6 identified by 16S rDNA sequencing. The strain removed 86.7% of Direct Red 28 dye which finds its common usage in textile industry. FTIR analysis revealed that the dye had been removed from the culture medium which was expressed as reduction in absorption maxima of

dye. The process of decolourisation was attributed to degradation of dye.

Hence, there is an urgent need for simple and cost-effective treatment methods for this problem of water pollution caused by untreated or partially treated textile effluents released in surface waters. Microbial degradation with decolourisation of dyes gives us a hope to circumvent this problem as it is environment friendly, cost-effective and produce no harmful intermediates.

REFERENCES

- Anjaneyulu, Y., Sreedhara, N.C. and Suman Raj, D.S. 2005. Decolourization of industrial effluents- available methods and emerging technologies- a review. *Reviews in Environmental Science and Biotechnology*, 4: 245-273.
- Bumpus, J.A. 2004. Biodegradation of azo dyes by fungi. In: Arora, D.K. (Ed.), *Fungal Biotechnology in Agricultural, Food and Environment Applications*. Marcel Dekker: New York, pp. 457-480
- Chen, K.C., Wu, J.Y., Liou, D.J. and Huang, S.C.J. 2003. Decolourization of textile dyes by newly isolated bacterial strains. *Journal of Biotechnology*, 101: 57-68.
- Derle, S.G., Patil, N.P. and Gaikwad, V.B. 2012. Eco-friendly biodegradation of reactive yellow 145 by newly isolated *Bacillus boroniphilus* from industrial effluent. *Journal of Environmental Research and Development*, 7(1A): 303-311.
- Hu, T.L. 1994. Decolorization of reactive azo dyes by transformation with *Pseudomonas luteola*. *Bioresource Technology*, 49: 47-51.
- Isik, M. and Sponza, T.D. 2003. Effect of oxygen on decolorization of azo dyes by *Escherichia coli* and *Pseudomonas* sp. and fate of aromatic amines. *Process Biochemistry*, 38(8): 1183-1192.
- Keharia, H., Patel, H. and Madamwar, D. 2004. Decolorization screening of synthetic dyes by anaerobic methanogenic sludge using a batch decolorization assay. *World Journal of Microbiology and Biotechnology*, 20(4): 365-370.
- Khandelwal, M.K. and Chauhan, M.L. 2005. *Dyeing, Printing and Textile*. Ritu Publications, Jaipur.
- Kilic, N.K., Nielsen, J., Yuce, L. and Donmez, G. 2007. Characterization of a simple bacterial consortium for effective treatment of wastewaters with reactive dyes and Cr(VI). *Chemosphere*, 67: 826-831.
- Leelakriangsak, M. and Borisut, S. 2012. Characterization of the decolorizing activity of azo dyes by *Bacillus subtilis* azoreductase Azo R1. *Songklanakarin Journal of Science and Technology*, 34(5): 509-516.
- Mali, P.L., Mahajan, M.M., Patil, D.P. and Kulkarni, M.V. 2000. Biodecolourization of members of triphenylmethane and azo groups of dyes. *Journal of Scientific and Industrial Research*, 59: 221-224.
- Moharrery, L., Otadi, M.A., Safekordi, A., Amiri, R. and Ardjmand, M. 2012. Biodegradation of Toluidine Red, an oil soluble azo dye, with *Halomonas Strain D2*. *World Applied Sciences Journal*, 18(8): 1065-1072.
- PalaniVelan, R., Rajkumar, S. and Ayyasamy, P.M. 2012. Exploring the promising dye decolourising strains obtained from Erode and Tirrupur textile wastes. *International Journal of Environmental Sciences*, 2(4): 2470-2481.
- Pandey, A.K. and Dubey, V. 2012. Biodegradation of azo dye Reactive Red BL by *Alcaligenes* sp. AA09. *International Journal of Engineering and Science*, 1(12): 54-60.

- Perumal, K.R., Malleswari, B., Catherin, A. and Moorthy, T.A.S. 2012. Decolourization of Congo Red dye by bacterial consortium isolated from contaminated soil, Paramakudi, Tamil Nadu. *Journal of Microbiology and Biotechnology Research*, 2(3): 475-480.
- Ponraj, M., Gokila, K. and Zambare, V. 2011. Bacterial decolorization of textile dye-ORANGE 3R. *International Journal of Advanced Biotechnology and Research*, 1: 168-177.
- Pradhan, P., Kumar, H.D. and Gireesh, B.K. 2011. Degradation of Azo and Triphenylmethane dye by bacteria isolated from local industrial waste. *International Journal of Current Research and Reviews*, 4(20): 39-49.
- Raja, P., Chellaram, C., Jebasingh, S.E.J., Maheshwari, N., Chandrika, M. and Gladis, C. 2013. Bio-degradation of harmful textile dyes by marine bacteria from Tuticorin coastal waters southeastern India. *Journal of Chemical and Pharmaceutical Research*, 5(7): 146-151.
- Rajendran, R., Sundaram, K.S. and Maheshwari, U.K. 2011. Aerobic biodecolorization of a mixture of azo dyes containing industrial textile effluent using adapted microbial strains. *Journal of Environmental Science and Technology*, 1: 1-11.
- Rajeshwari, S., Agnes, C., Dorthy, M. and Venkatesh, R. 2011. Isolation, characterization and growth kinetics of bacteria metabolising textile effluent. *Journal of Bioscience and Technology*, 2(4): 324-330.
- Rathore, J. 2012. Studies on pollution load induced by dyeing and printing units in River Bandi at Pali, Rajasthan, India. *International Journal of Environmental Sciences*, 3(2): 735-742.
- Sahasrabudhe, M., Bhattacharya, A., Pathade, A. and Pathade, G. 2012. Detoxification of Reactive Red 195 by *Micrococcus glutamicus* NCIM 2168. *Journal of Environmental Research and Development*, 9(1): 120-128.
- Saranraj, P., Sumathi, V., Reetha, D. and Stella, D. 2010. Decolourization and degradation of direct azo dyes and biodegradation of textile dye effluent by using bacteria isolated from textile dye effluent. *Journal of Ecobiotechnology*, 2(7): 07-11.
- Sethi, S., Malviya, M.M., Sharma, N. and Gupta, S. 2012. Biodecolorization of azo dye by microbial isolates from textile effluent and sludge. *Universal Journal of Environmental Research and Technology*, 2(6): 582-590.
- Shah, M.P., Patel, K.A., Nair, S.S. and Darji, A.M. 2013. Microbial decolorization of textile dye by *Bacillus* sp. ETL-79: an innovative biotechnological aspect to combat textile effluents. *American Journal of Microbiological Research*, 1(3): 57-61.
- Shah, M.P. 2014a. An application of bioaugmentation strategy to decolorize and degrade Reactive Black dye by *Pseudomonas* spp. *International Journal of Environmental Bioremediation & Biodegradation*, 2(2), 50-54.
- Shah, M.P. 2014b. Exploited application of *Pseudomonas stutzeri* ETL-4 in microbial degradation of Congo red. *Open Access Biotechnology*, 10: 1-19.
- Shah, M.P. 2013. Microbial degradation of textile dye (Remazol Black B) by *Bacillus* spp. ETL-2012. *Journal of Applied and Environmental Microbiology*, 1(1): 6-11.
- Shinde, K.P., and Thorat, P.R. 2013. Biodecolorization of diazo direct dye congo red by *Fusarium* sp. TSF-01. *Review of Research*, 2(8): 1-7.
- Soundararajan, N., Gopi, V., Ugrade, A. and Begam, N. 2012. Bioremediation ability of individual and consortium of non-immobilized and immobilized bacterial strains on industrial azo textile effluent. *Annals of Biological Research*, 3(4): 1773-1778.
- Sridevi, N. and Rao, J.C.S. 2013. Biodegradation studies on selected textile dye by using bacterial isolates. *Asian Journal of Experimental Biology and Science*, 4(2): 288-292.
- Suizhou, R., Jun, G., Guoqu, Z. and Guoping, S. 2006. Decolorization of triphenylmethane, azo and anthraquinone dyes by a newly isolated *Aeromonas hydrophila* strain. *Applied Microbiology and Biotechnology*, 72: 1316-1321.
- Verma, P. and Madamwar, D. 2003. Decolorization of synthetic dyes by a newly isolated strain of *Serratia marcescens*. *World Journal of Microbiology and Biotechnology*, 19: 615.
- Vivekanandan, N., Vishwanathan, M., Shanmugam, V. and Thangavel, B. 2012. Degradation and detoxification of reactive azo dyes by native bacterial communities. *African Journal of Microbiology Research*, 2(20): 2274-2282.



Design of Eco-friendly Fixed Bed Dryer Based on A Combination of Solar Collector and Photovoltaic Module

Siti Asmaniyah Mardiyani^(**)†, Sumardi Hadi Sumarlan^{***}, Bambang Dwi Argo^{***} and Amin Setyo Leksono^{****}

^{*}Doctoral Program of Environmental Studies, Brawijaya University, Jl. Veteran, Malang, 6514, Indonesia

^{**}Department of Agrotechnology, Faculty of Agriculture, University of Islam Malang, Jl. MT. Haryono 193 Malang, 65144, Indonesia

^{***}Department of Agricultural Engineering, Faculty of Agricultural Technology, Brawijaya University, Jl. Veteran, Malang, 65145, Indonesia

^{****}Department of Biology, Faculty of Mathematic and Natural Science, Brawijaya University, Jl. Veteran, Malang, 65145, Indonesia

†Corresponding author: Siti Asmaniyah Mardiyani

Nat. Env. & Poll. Tech.
Website: www.neptjournal.com

Received: 07-05-2018
Accepted: 02-08-2018

Key Words:

Eco-friendly fixed bed dryer
Solar collector
Solar photovoltaic module

ABSTRACT

A study to develop a convective eco-friendly fixed-bed solar dryer is presented in this article. The aim of this study was to design an efficient eco-friendly fixed bed dryer using solar collector and solar photovoltaic panel with a forced convective system. The design consists of a V-corrugated solar collector, a centrifugal fan, a solar photovoltaic module (100 WP) and a drying unit in the mini-silo model with five layers. The dryer performance test was conducted in September, October, and November 2017 in Malang, East Java, Indonesia. The observation showed that the temperature of the solar collector and the first layer of the drying unit could reach 40-70°C on a sunny day and 30-50°C in cloudy/rainy conditions. The efficiency of the daily collector varied from 20% to 50%. Based on a multiple regression analysis, it showed that some variables (solar intensity, voltage of photovoltaic panel, air speed around the blower, air collector velocity, collector relative humidity, ambient temperature and relative humidity temperature) significantly influenced the collector temperature. The result of drying simulation using red pepper showed that the design has a potential to be used as an eco-friendly fixed bed convective drying. Based on the empirical model, the drying time needed to reach 12% of moisture content (wet basis), respectively, was 5-6 days for the first tray, 8-9 days for the second tray and 9-10 days for the third tray in rainy season.

INTRODUCTION

Drying activities in agricultural products have been carried out for centuries as an alternative processing for enhancing shelf life, reducing volume, minimizing microbial activities, improving flavour and increasing economic value (Prakash & Kumar 2014, Agrawal & Savriya 2016, Naderinezhad et al. 2016). In general, drying is defined as a water removal process through complex and simultaneous concepts of heat and mass transfer with a high energy demand (Sebaili & Shalaby 2012, Mujumdar 2010). It is a complicated process that requires the highest energy consumption compared to other food processing technology. A drying consumes 55% of energy in total energy needed for food preparation, while harvesting process needs 15%, cultivation consumes 10%, sowing needs 10% and transportation consumes 6% (Jerald 2013). Strumillo (2006) estimated 12% on average of energy utilized in the manufacturing process is consumed by industrial drying.

Rural farmers in Indonesia usually use direct sunlight in open areas to dry agricultural products. This method is slow, labour-intensive, time-consuming and requires a large open space. It also depends to a large extent on the availability of sunlight (Bennamoun & Belhamri 2003, Fudholi et al. 2014, Aghbashlo et al. 2015). This process produces low quality and quantity of dry products due to contamination by dust and dirt. The products also have a high risk of spoiling due to rain, wind, and moisture imbalance, so they cannot meet the international standard quality demand (Mustayen et al. 2014). The total amount of dry products can also be reduced during the drying process due to the attack possibility by birds, rodents, and insects (Prakash & Kumar 2013). Choucia et al. (2014) said that the main problem in an open air-sun drying method is the limitation in the control of some factors that influence the drying process.

Therefore, research was carried out to innovate and optimize the use of solar energy to solve problems in the

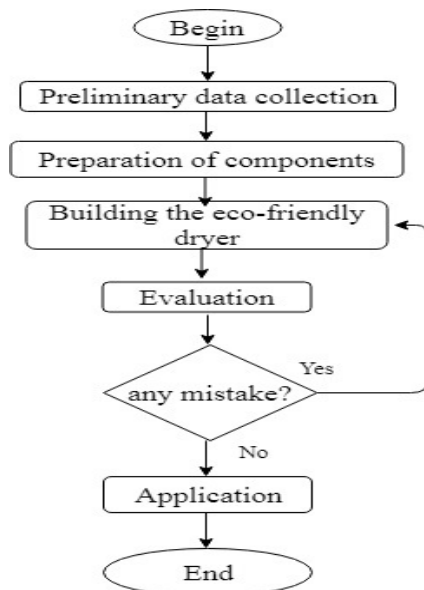


Fig. 1: Flow diagram of the dryer design process.

natural solar drying method (Mustayen et al. 2014). A properly designed solar dryer can reduce the disadvantage of sun drying and improve the quality of drying products (Hossain & Bala 2005). Kaewkiew et al. (2012) made an observation about drying models in the greenhouse for the drying of red peppers on a large scale (with room dimensions of $8 \times 20 \times 3.5 \text{ m}^3$). It used 9 volt DC fans that operated with electrical energy derived from a photovoltaic module. This method resulted in a significant reduction in drying time as compared to drying under the sun. The colour of the red peppers was also better than the natural samples dried in the sun. The design disseminated to the small-scale agriculture drying industries in Thailand.

Some researchers worked with photovoltaic solar technology dryers. They proposed ideas to drive the fan in the forced convection drying system. The model will allow a convective dryer to be used in remote areas that have no connection to the electricity grid. The result showed that greenhouse drying under forced convection using photovoltaics were more suitable for crops with high moisture content (e.g. vegetables and fruits) and greenhouse drying under natural convection was better for crops with low moisture content (Prakash & Kumar 2014, Hossain & Bala 2005, Banout et al. 2011, Bala 2005, Chen et al. 2010). Chouicha et al. (2013) using a hybrid photovoltaic and solar thermal dryer to support a better drying system. The electrical energy generated from the photovoltaic modules used to turn on the heaters when the solar intensity decreases.

Due to our knowledge, the design of a fixed bed dryer model for horticultural products with a forced convective

system that uses a solar collector and a photovoltaic panel to produce good quality dry products with an efficient drying time is not popular yet. Aghbashlo et al. (2015) stated that a deep/fixed bed drying technology is one of the most used for the drying of the heterogeneous biological material. This technique places the materials in a fixed bed of more than 20 cm thick.

A research development based on a combination of solar and photovoltaic collectors on agricultural products is important to do, to support solar energy development in Indonesia mainly to solve the high damage of horticultural products problem and the difficulty of electricity and fuel access in some remote areas of Indonesia. As a tropical country, Indonesia receives abundant solar radiation (16 MJ/day) (Batubara et al. 2017). Handayani & Ariyanti (2012) said that the average daily radiation in most areas in Indonesia is about 4 KWH/m². Optimizing the use of solar energy is a good option to solve post-harvest problems, mainly for perishable crops.

Small farmers need adequate information on the use of solar energy such as heat and energy resources to get high quality dry agricultural products. The aim of this study was to design an efficient and eco-friendly fixed bed dryer using solar collector and solar photovoltaic panel with a forced convective system. This work will support the development and strengthen the use of solar energy as an environmentally friendly resource of renewable energy for farmers in rural areas.

MATERIALS AND METHODS

Design consideration: The design concept developed in this study is based on an eco-friendly fixed bed dryer on a combination of solar collectors and photovoltaic solar panels. The dryer is expected to produce high quality dry agricultural products. The developed technology is a forced convective fixed bed dryer which uses solar collectors and

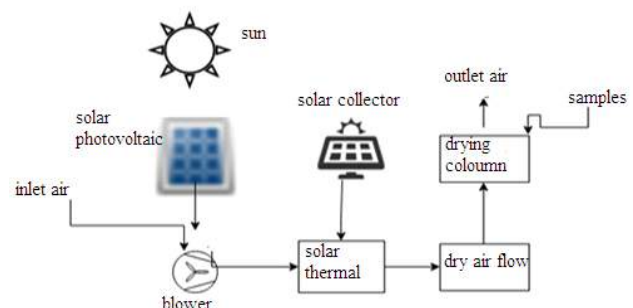


Fig. 2: Concept and principle of operation of the fixed bed respectful with the environment through solar collector solar photovoltaic (adopted and modified by Akpinar & Bicer 2008).

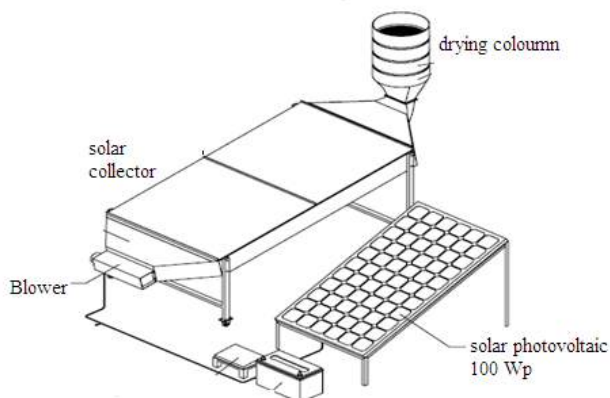
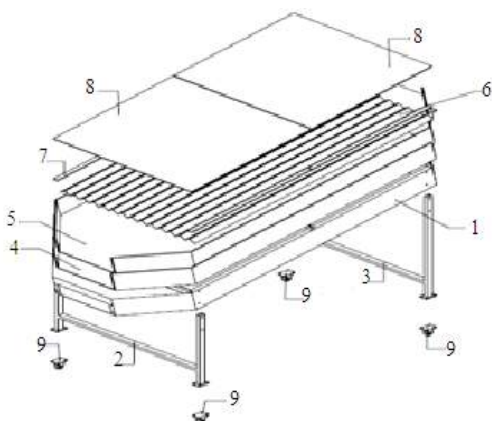


Fig. 3: Schematic view of eco-friendly forced convective fixed bed dryer using solar collector and solar photovoltaic.



Part No.	Part Name	QTY	Material
1	Chamber	1	Stainless steel
2	Feet A	1	Steel
3	Feet B	1	Steel
4	Glasswool isolator	1	Glasswool
5	Sheet Isolator	1	Aluminium Sheet
6	Heat Absorber	1	Iron Sheet
7	Rubber protector	4	Rubber
8	Glass panel	2	Glass
9	Polley Trolley	4	

Fig. 4: Schematic view of solar collector.

photovoltaic modules. The design process was carried out through some steps, as shown in Fig. 1.

The variables measured to figure the dryer function are ambient temperature, relative humidity of the environment, collector temperature, relative humidity of the collector, inlet temperature of drying, relative humidity of the drying inlet, solar intensity, electrical energy generated

by the photovoltaic and air drying speed. Fig. 2 shows the concept and operating principle of the dryer designed in this study.

Fig. 2 shows that the basic principle of the dryer is a process of heating the air in the collector, moved by a blower supported by the electricity resulted from the photovoltaic panel. The heated air with a certain speed will pass the layers of the product in the drying column with a fixed bed concept.

Instrumentation: The dryer consists of four parts: a collector, a solar photovoltaic panel, a drying unit in a silo model and a blower. The measuring tools used in this study were a thermometer, hygrometer, lux meter, wind meter, and digital balance.

Solar collector: A solar collector is the most important part of an active solar drying system (Fig. 4). The solar collector will gather solar energy, transform its radiation into heat and transfer heat through the fluid inside the collector (Hematian et al. 2012). In this investigation, the solar absorber collector was a V-groove iron plate (0.55 mm thick), painted in black and mounted in a box made in the same area. The lower part of the absorber was insulated with 19 mm thick glass wool. To create a greenhouse effect, a transparent glass sheet of a 4 mm thick layer was placed on the absorber. The total length, width, and height of the solar collector are 1500, 800 and 200 mm, respectively. According to Sebaili & Shalaby (2012), the V-groove collector had an efficiency of 7-12% higher than a flat plate collector.

Solar photovoltaic module: The photovoltaic solar module used in this study was polycrystalline with 72 cells equal to 100 WP. It converts solar energy into electricity to support the centrifugal fan. The dimension of the photovoltaic panel is 1020 mm × 670 mm × 30 mm. The photovoltaic panel produces 16-18 volts, respectively, according to the solar intensity. The photovoltaic module has been certified by the Agency for the Evaluation and Application of Technology, Republic of Indonesia (certificate number: 2016079).

Blower: The centrifugal blower (ORIX-FO107) used in this study has the following specification: motor diameter: 7.7 cm, length: 30.5, blower diameter: 7.3 cm, total fan wings: 26, maximum voltage: 24 volts and maximum speed: 5 m/s.

The drying unit: The drying unit adopted a silo model, with 30 cm in diameter and 7 cm in height for each layer/tray (Fig. 5). It consists of 5 trays. The total volume of each tray is 537.075 cm³, it is equal to 1-1.5 kg of red pepper. The drying trays were constructed with fine mesh for the drying air that passes through the elements of the material. Hot air

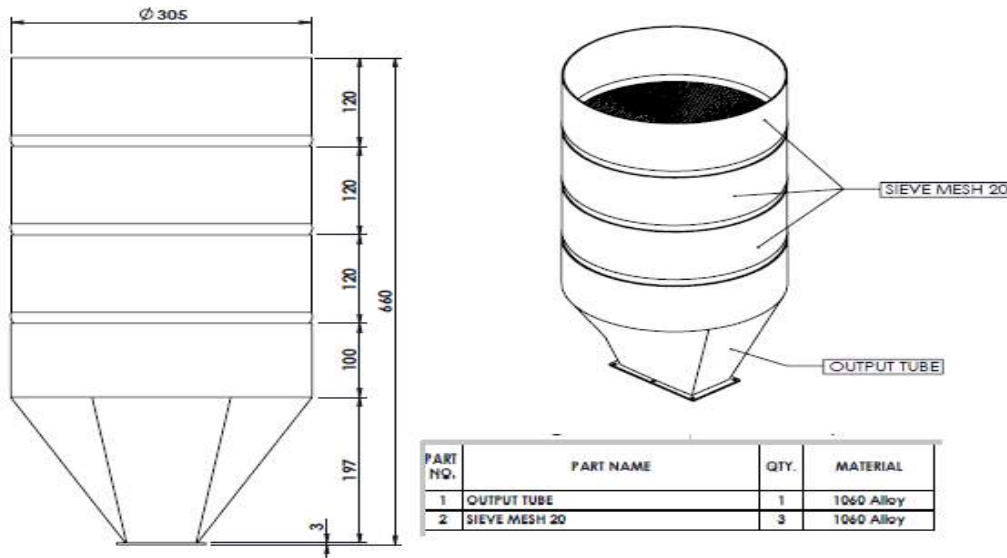


Fig. 5: Schematic view of drying coloumn.

passes through the trays directly from the solar collector.

Performance evaluation of the solar dryer: The principle that governs the transfer of heat within a solar collector is the greenhouse effect. It occurred when solar radiation passes the transparent cover of the collector and is absorbed by the V-shaped plate inside. The plate will return the radiation to the inner side of the cover, where it will return to the plate. During this process, the fluid between the plate and the cover will absorb the energy. Almiron & Lara (2016) said that the thermal efficiency of the solar collector is affected by solar intensity, fluid density, heat capacity and fluid velocity. In order to determine the performance of the dryer, including the thermal efficiency of the collector, an experimental study was conducted in September, October and November 2017.

During the performance test process, the temperature and relative humidity of the environment, internal collector and air inlet to the drying unit were measured with a standard digital thermometer and hygrometer. The device was calibrated using a wet mercury bulb laboratory thermometer. The solar intensity was measured with a lux meter, with a one-hour interval between 07:00 a.m. and 16. 00 p.m. at the local time. The airspeed around the blower and the outlet collector area/inlet drying unit were measured by a wind meter. The data were collected in September, October and November 2017. It was the beginning of the rainy season in September and peak season in November.

The efficiency of the solar collector is the ratio of useful energy in the solar collector to the solar energy arrived on the surface of the solar collector (Hematian et al. 2012).

Referred from Bennamoun (2012), collector efficiency in this convective solar drying system supported by solar thermal collector and solar photovoltaic panel was determined by the following equation:

$$\eta = \frac{Q_{useful}}{Q_{sc} + Q_{pv}} \times 100 \quad \dots(1)$$

Where, Q_{sc} is the energy gained by solar collector and Q_{pv} is the energy gained by solar photovoltaic panel. The useful energy is determined by the following equation:

$$Q_{useful} = m \cdot C_p \cdot (T_c - T_a) \quad (\text{Watt}) \quad \dots(2)$$

Where, C_p is the specific heat capacity of the air at constant pressure ($J/kg/^\circ C$) and $(T_c - T_a)$ is the temperature difference of ambient and solar collector output. m is the mass of the air flow, and is determined by the following equation:

$$m = \rho \cdot A \cdot V \quad (\text{kg/s}) \quad \dots(3)$$

Where, ρ is the fluid density/moist air density, A is the collector absorber surface and V is the air velocity.

Q_{sc} is determined by the following equation :

$$Q_{sc} = I \cdot A_c \quad (\text{Watt}) \quad \dots(4)$$

Where, I is the global solar intensity (W/m^2) and A_c is solar collector width, Q_{pv} is determined by:

$$Q_{pv} = V_{pv} \cdot i_{current} \quad (\text{Watt}) \quad \dots(5)$$

According to the photovoltaic guidance information the rates of I current is 5.69 Ampere. The lost energy in the collector and photovoltaic panel was ignored.

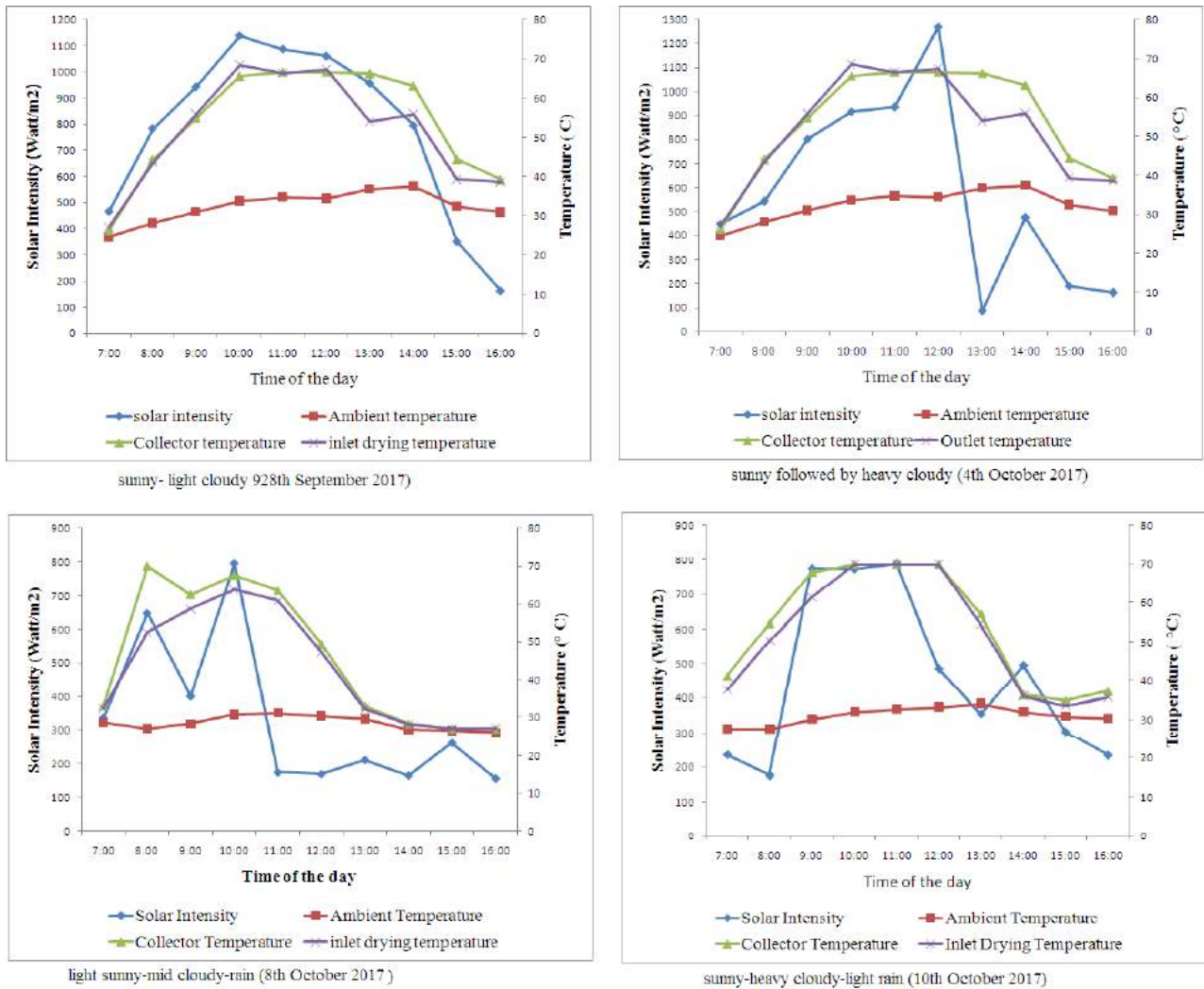


Fig. 6: Drier temperature performance rates in various weather condition.

To predict the fitted model and the most influential factor of the dryer performance, a multiple regression analysis was done. The solar collector temperature was the dependent variable and solar intensity, voltage photovoltaic, air-speed around the blower, air collector velocity, collector relative humidity, ambient temperature and relative humidity temperature were independent variables. Zhu & Chen (2013) reported the using of regression analysis based on experimental data as a simplified method for thermal responsive performance of passive solar house in China. Kicsiny (2014) proposed a multiple linear regression based model for solar collectors. The result of the study showed that MLR based model has a good precision and can be easily applied to many collectors in practice.

The data in this study were tested by collinearity, heteroscedasticity, autocorrelation, and residual normality

test to make sure that they fit to be analysed by multiple regressions.

Drying implementation: Drying implementation was done on red pepper on 8-10 October 2017. The drying time was 6 hours/day (between 7.00-14.00), two hours shorter than the targeted time due to the inappropriate weather in the afternoon. Fresh red peppers from the local market were used as the simulation drying product. The main parameter observed was the decrease of moisture content.

RESULTS AND DISCUSSION

The schematic view: The schematic view of the dryer can be seen in Fig. 3. It shows that the dryer has some important parts : solar collector, solar photovoltaic panel, blower and drying column. The solar dryer was designed and produced

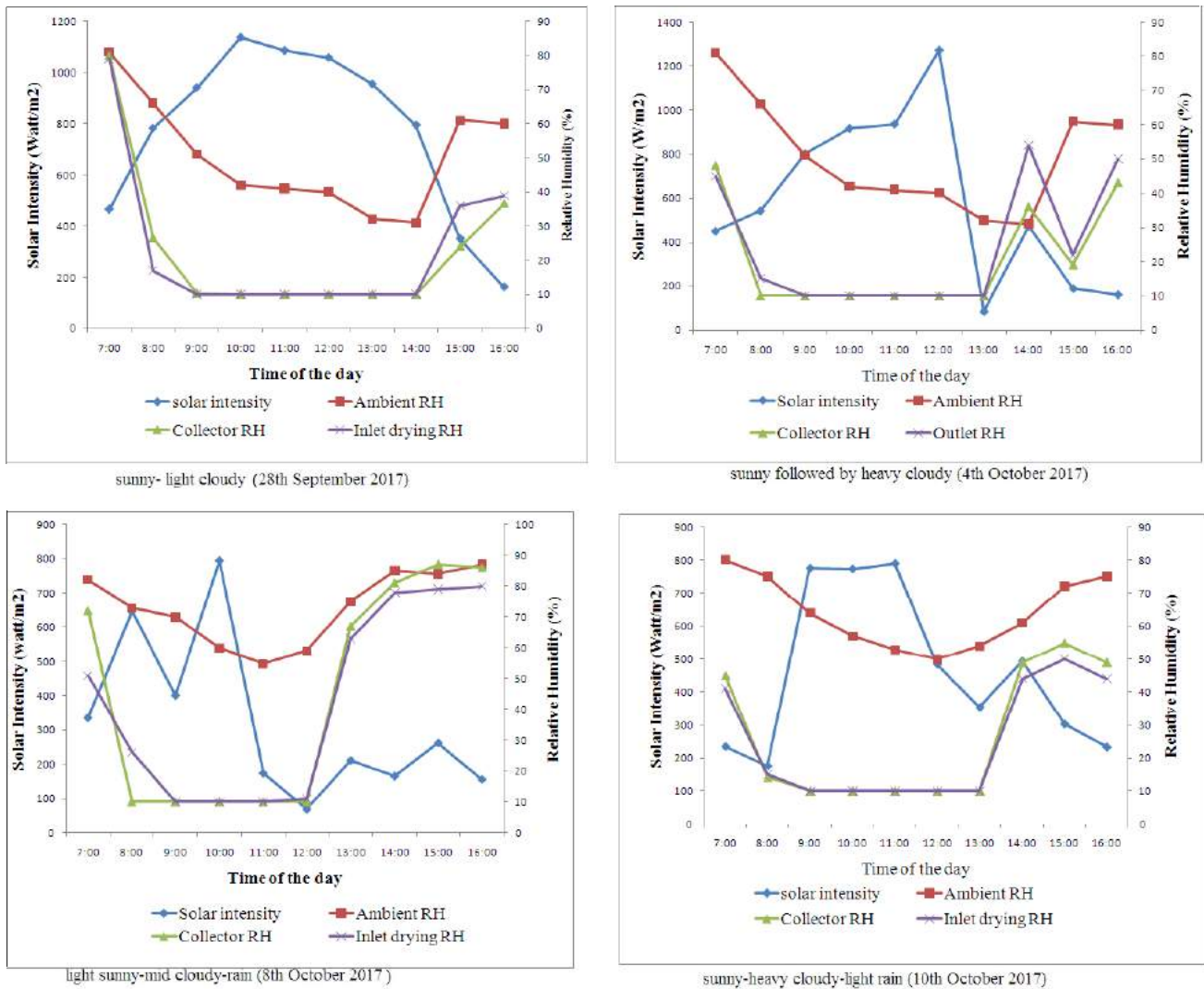


Fig. 7: Relative humidity of solar dryers in various weather condition.

in the Agricultural Engineering Laboratory of Brawijaya Malang, Indonesia. It is an ecological solar dryer that converts solar energy into thermal energy through a solar collector and electricity through a polycrystalline photovoltaic module to support the blower. The designing and building process was taken 4 months from May to August 2017. The air was moved by a centrifugal fan (DC 24 V) and air passed the surface of the solar collector to the drying column. The air was forced to move using the fan powered by photovoltaic electricity, to accelerate the drying process.

Solar Dryer Performance

Temperature: The outlet air temperature of the collector and the inlet air temperature of the drying unit were relatively higher than the ambient temperature. On sunny days,

the temperature of the first tray can reach 70°C. It happened at 10.00-12.00 when the solar intensity was > 1000 W/m². The solar intensity gradually increased from 465.6 W/m² in the morning to 1131 W/m² at 10.00-12.00. It gradually decreased to 161.99 W/m² at 16.00 p.m.

The performance test of the solar dryer was also conducted in rainy/cloudy circumstances, occurred in the afternoon. The temperature of the solar collector and the inlet air temperature to drying unit decreased along with the decrease of solar intensity due to the cloud and the rain condition. Fig 6 shows that, in general, temperature of the solar collector and inlet drying area was relatively higher than environmental temperature both in sunny day or hostile condition. According to Sharma et al. (1993) and Mustayen et al. (2014), an indirect-type solar dryer using

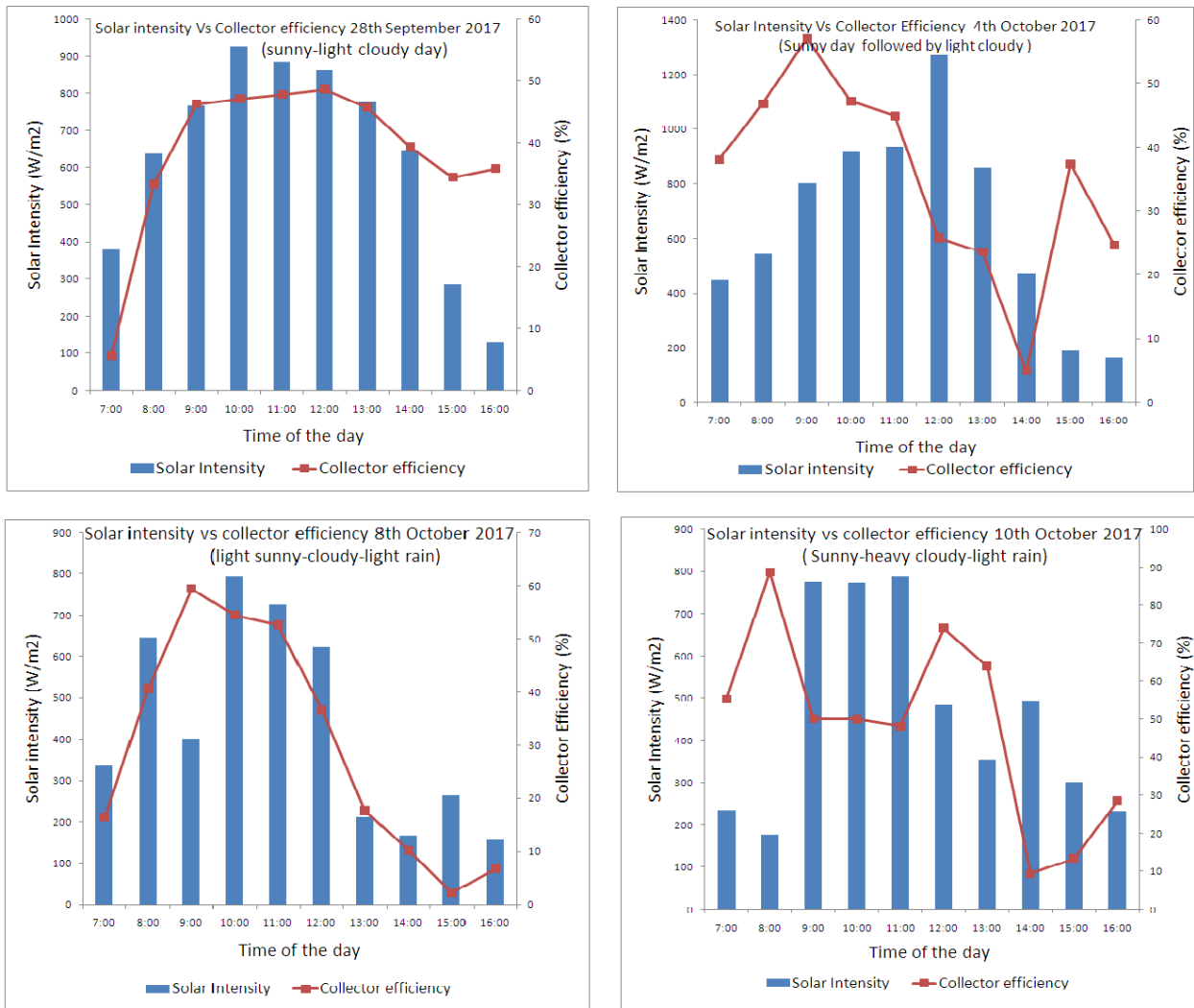


Fig. 8: Daily solar radiation and solar collector efficiency in various weather conditions.

active solar collector is still capable of giving good output under bad weather condition. Wulandani and Oscar (2009) justified that the drying of the solar-powered greenhouse with forced convection system has a more stable temperature performance than the greenhouse drying system with natural convection.

Relative humidity: Fig. 7 showed that relative humidity of the solar collector and air inlet in clear sky day was stable at 10%, after one-hour drying in sunny days condition. It remained stable for 5.5 hours forward. The relative humidity began to increase in the afternoon (after 15.00 pm). Low relative humidity (10%) is the best condition in a drying process. It can be said that this dryer had sufficient relative humidity to support a drying process. In cloudy/rainy condition, relative humidity in inlet drying seemed unsta-

ble. It seemed that, although it is possible to carry out a drying process on cloudy days according to the inlet drying temperature, which was higher than ambient temperature, it was not supported by the relative humidity of the collector and the drying unit.

Solar collector efficiency: Thermal collector efficiency depends on the type of collector absorber, covered material, air velocity and collector width (Hematian et al. 2012). Based on the data which were taken on 28 September, 4 October, 8-12 October 2017 and equations 1-6, solar collector efficiency is shown in Fig. 8. The efficiency in cloudy/rainy days was higher than the efficiency in the sunny days. It can happen because the collector has a good function as an energy saving, so while the solar intensity decreases, it still keeps the energy gained before the cloudy/

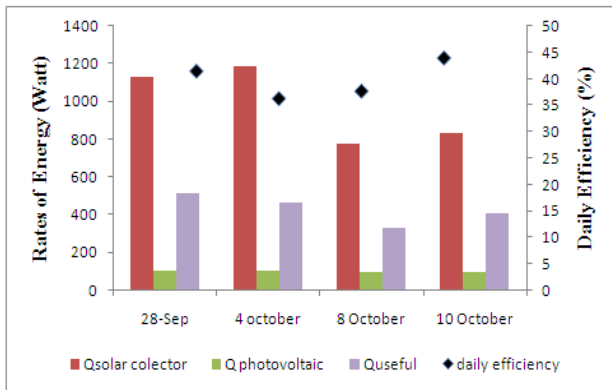


Fig. 9: Daily rates of energy gained by solar collector and solar photovoltaic, useful energy and collector efficiency.

rainy conditions. Hermatian et al. (2012) in his study showed that the efficiency of convective solar collector has ascending tendency until the evening (the research was done from 09.00-20.00). It is similar with the result of this study, where the ascending tendency happened in 28th September 2017 when the weather is in a good condition (clear sky with a light cloudy). Hii & Law (2012) and Batubara et al. (2017) stated that the higher the intensity of solar energy received in the solar collector, the solar collector efficiency also will be higher in a normal weather condition. In the days of unstable weather (4th October, 8th October and 10th October 2017), the trend of efficiency cannot be predicted properly.

Rates of daily energy collected from the solar collector and solar photovoltaic panel compared with useful energy are shown in Fig. 9. Rates of daily efficiency of the collector varied from 36-44%, depending on solar intensity rates and the weather. Total energy gained in clear sky days is higher than that in unstable weather days.

Regression and correlation of solar intensity, photovoltaic voltage, air flow, temperature and relative humidity:

Based on the data taken on 12-15 November 2017 a multivariate regression analysis was done. It aimed to find

the most influenced variables for collector performance. The residual normality test that was done using Anderson-Darling Statistic Test (Razali & Wah 2011) showed a normal result. The weather on the observation days was mid cloudy before noon, and heavy cloudy followed by rain after mid-noon. Solar intensity observed was 75-790 W/m², ambient humidity was 44%-77%, the ambient temperature was 27.1-34.10, collector humidity variation was 11-54% and collector temperature variation was 31-57°C. Dependent variable determined in the analysis was the collector temperature. The independent variables were solar intensity, voltage photovoltaic panel, airspeed around the blower, air collector velocity, collector relative humidity, ambient temperature and relative humidity.

The heteroscedasticity test showed an appropriate result for the data of variables to be analysed by multivariate regression. The data were also non-multicollinear and non-autocorrelation. The regression statistic result is given in Table 1.

Based on the information from Table 1, the linear model to simplify the relationship of a dependent variable (collector temperature) and independent variables is described in the following equation :

$$Y = 138.54 + 0.011x_1 - 1.81x_2 - 2.273x_3 + 7.45x_4 - 0.44x_5 - 1.13x_6 - 0.34x_7$$

Where, Y: collector temperature, x1: solar intensity, x2: voltage photovoltaic, x3: velocity around the blower, x4: collector velocity, x5: collector relative humidity, x6: ambient temperature, and x7 is ambient relative humidity. The model is fitted with the data, shown by the value of adjusted R² (0,93). This value means that 93% of the variations in the collector temperature changes can be explained by dependent variables in this investigation (x₁-x₇) and the other 7% depends on the other variables excluded in this investigation.

The probability value showed that solar intensity, voltage photovoltaic panel, air collector velocity, collector

Table 1: Regression statistical result.

Regression statistic		Coefficient	P-value
Multiple R	0,9764	Intercept	138.54
R Square	0,953357	Solar Intensity (watt/cm2)	0.011
Adjusted R Square	0,930036	Voltage Photovoltaic	-1.81
Standard Error	1,969358	Velocity around the blower	-2.27
Observations	22	Air collector velocity	7.45
Significance F model	2,92815E-08	collector humidity	-0.44
Significance F heteroscesdasticity	2,62E-16	Ambient Temperature	-1.12
		Ambient Humidity	-0.34

*significant (p<0.05)

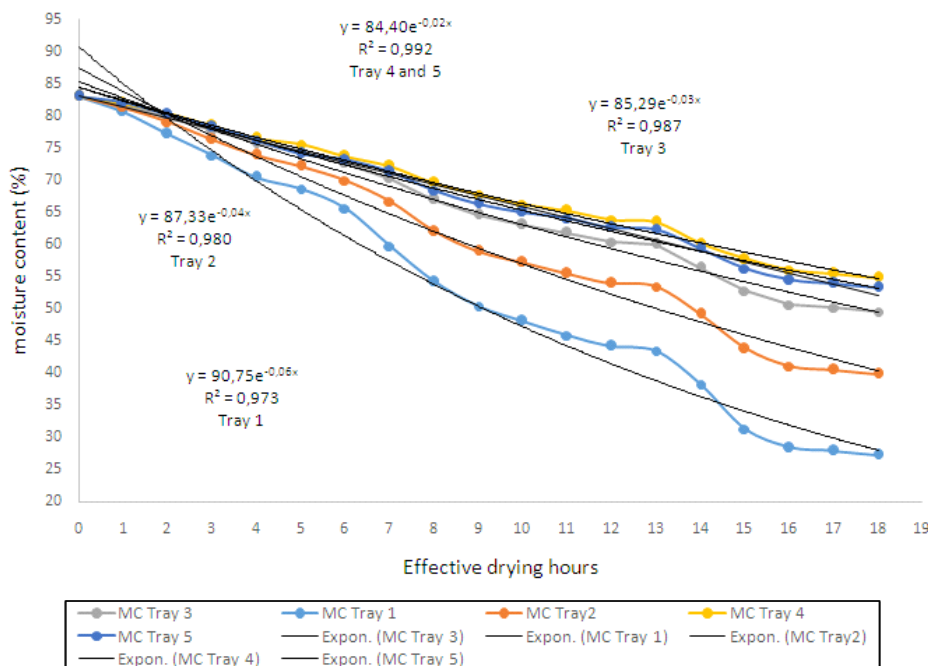


Fig. 10: Drying rates of red pepper using eco-friendly fixed bed dryer based on a combination of solar collector and solar photovoltaic panel (8-10 October 2017).

humidity and ambient humidity gave a significant influence to the solar collector temperature ($p < 0,05$). In rainy condition, it seems that ambient temperature did not give a significant influence on the rates of collector temperature. Afriyie et al. (2013) reported that the relative humidity of the environment greatly affects the drying process with solar energy. Batubara et al. (2017) said that the inside collector temperature is strongly influenced by solar intensity.

Drying implementation: In a fixed bed drying process, the product is filled in thick layers so that the drying column can be supposed as porous media (Bennamoun 2012). Fig. 10 showed that drying rates of the red pepper in the first trays were the fastest, and the drying rates of the fourth and fifth trays were the lowest.

Statistically, there is no significant difference on drying rates based on ANOVA test ($p < 0,05$). The drying rates were varied between 2.96 % moisture content/hour and 1.51 % moisture content/hour. Although the final moisture content of the pepper was not adequate yet, the model can be used to predict the time needed to dry hot pepper in a rainy season using the eco-friendly fixed bed dryer based on a combination of solar collector and solar photovoltaic panel.

Based on the exponential empirical model, the drying time needed to reach 12% of moisture content (wet basis),

respectively, was 33,72 hours (5-6 days) for the first tray (0-7 cm thick), 49.61 (6-7 days) hours for the second tray (7-14 cm thick) and 65.37 hours for the third tray. It seems that in the rainy seasons, the drying is only possible to do in the first and second tray. It is not suggested using the higher trays due to the longer drying time.

CONCLUSIONS

This research developed a design of an eco-friendly convective fixed bed dryer with a combination of solar collector and solar photovoltaic panel. Collector efficiency was measured as a representative of the dryer performance. A multiple regression analysis was done to decide the most important variables influencing the performance. The result showed that the collector temperature can reach 70°C in sunny days and 50°C in cloudy/rainy conditions, the efficiency of solar collector varied from 30-50%, and the collector has a relatively stable performance in cloudy/rainy conditions. The multiple regression analysis showed that solar intensity, voltage of photovoltaic panel, air collector velocity, collector humidity and ambient humidity significantly influence the solar collector temperature in the drying system. The result of drying implementation using red pepper as the drying product showed that the drying time needed to reach 12% of moisture content (wet basis), respectively, was 5-6 days for the first tray (0-7 cm thick), 8-9

days for the second trays (7-14 cm thick) and 9-10 days for the third tray in rainy season.

ACKNOWLEDGEMENTS

This article is a piecework of the dissertation research of the first author, as a doctorate student of post graduate program, Brawijaya University. This research was funded by the Ministry of Research, Technology and Higher Education of the Republic of Indonesia.

REFERENCES

- Afriyie, J.K., Rajakaruna, H., Nazha, M.A. and Forson, F.K. 2013. Mathematical modelling and validation of the drying process in a chimney-dependent solar crop dryer. *Energy Conversion and Management*, 67: 103-116.
- Aghbashlo, M., Müller, J., Mobli, H., Madadlou, A. and Rafiee, S. 2015. Modeling and simulation of deep-bed solar greenhouse drying of chamomile flowers. *Drying Technology*, 33(6): 684-695.
- Agrawal, A. and Sarviya, R. M. 2016. A review of research and development work on solar dryers with heat storage. *International Journal of Sustainable Energy*, 35(6): 583-605.
- Almirón, J.O. and Lara, M.A. 2016. Experimental development of solar collector of unconventional air. *Sustainable Energy*, 4(1): 17-27.
- Akpinar, E.K. and Bicer, Y. 2008. Mathematical modelling of thin layer drying process of long green pepper in solar dryer and under open sun. *Energy Conversion and Management*, 49(6): 1367-1375.
- Bala, B.K., Ashraf, M.A., Uddin, M.A. and Janjai, S. 2005. Experimental and neural network prediction of the performance of a solar tunnel drier for drying jackfruit bulbs and leather. *Journal of Food Process Engineering*, 28(6): 552-566.
- Banout, J., Ehl, P., Havlik, J., Lojka, B., Polesny, Z. and Verner, V. 2011. Design and performance evaluation of a double-pass solar drier for drying of red chilli (*Capsicum annum*). *Solar Energy*, 85(3): 506-515.
- Batubara, F., Dina, S. F., Turmuzi, M., Siregar, F. and Panjaitan, N. 2017. Effect of openings collectors and solar irradiance on the thermal efficiency of flat plate-finned collector for indirect-type passive solar dryer. In: *AIP Conference Proceedings*, 1855(1): 070001.
- Bennamoun, L. and Belhamri, A. 2003. Design and simulation of a solar dryer for agriculture products. *Journal of Food Engineering*, 59(2-3): 259-266.
- Bennamoun, L. 2012. An overview on application of exergy and energy for determination of solar drying efficiency. *International Journal of Energy Engineering*, 2(5): 184-194
- Chen, Z., Gu, M., Peng, D., Peng, C. and Wu, Z., 2010. A numerical study on heat transfer of high efficient solar flat-plate collectors with energy storage. *International Journal of Green Energy*, 7(3): 326-336
- Chouicha, S., Boubekri, A., Mennouche, D. and Berrbeuh, M. H. 2013. Solar drying of sliced potatoes - An experimental investigation. *Energy Procedia*, 36: 1276-1285.
- Fudholi A., Sopian K., Yazdi M.H., Ruslan M.H., Gabbana M. and Kazem H.A. 2014. Performance analysis of solar drying system for red chillies. *Solar Energy*, 99: 47-54.
- Handayani, N.A. and Ariyanti, D. 2012. Potency of solar energy applications in Indonesia. *International Journal of Renewable Energy Development*, 1(2): 33-38.
- Hematian, A., Ajabshirchi, Y. and Bakhtiari, A.A. 2012. Experimental analysis of flat plate solar air collector efficiency. *Indian Journal of Science and Technology*, 5(8): 3183-3187.
- Hii, C. L. and Law, C. L. 2012. Solar drying of major commodity products. In: Hii, C.L., Ong, S.P., Jangam, S.V. and Mujumdar, A.S. (Eds.) *Solar Drying: Fundamentals, Applications and Innovations*, pp. 73-94.
- Hossain, MA., Woods, J.L. and Bala, B.K. 2005. Simulation of solar drying of chilli in solar tunnel dryer. *International Journal of Sustainable Energy*, 24(3): 143-153.
- Jerald, A.L. 2013. Life cycle assesment for food processing. *International Journal Of Emerging Technology and Advance Engineering*, 3: 677-680.
- Kaewkiew, J., Nabnean, S. and Janjai, S. 2012. Experimental investigation of the performance of a large-scale greenhouse type solar dryer for drying chilli in Thailand. *Procedia Engineering*, 32: 433-439.
- Kicsiny, R. 2014. Multiple linear regression based model for solar collectors. *Solar Energy*, 110: 496-506.
- Mujumdar, A. S. 2010. *Handbook of Industrial Drying*. CRC Press.
- Mustayen, A.G.M.B., Mekhilef, S. and Saidur, R. 2014. Performance study of different solar dryer: A review. *Renewable and Sustainable Energy Review*, 34: 463-470.
- Naderinezhad, S., Etesami, N., Poormalek Najafabady, A. and Ghasemi Falavarjani, M. 2016. Mathematical modeling of drying of potato slices in a forced convective dryer based on important parameters. *Food Science & Nutrition*, 4(1): 110-118.
- Prakash, O. and Kumar, A. 2013. Historical review and recent trends in solar drying systems. *International Journal of Green Energy*, 10(7): 690-738.
- Prakash, O. and Kumar, A. 2014. Solar greenhouse drying: A review. *Renewable and Sustainable Energy Reviews*, 29: 905-910.
- Razali, N.M. and Wah, Y.B. 2011. Power comparison of Shapiro-Wilk, Kolmogorov-Smirnov, Lilliefors and Anderson-Darling test. *Journal of Statistical Modelling and Analysis*, 2(1): 21-33.
- Sebaili, A.A. and Shalaby, S.M. 2012. Solar drying of agricultural product: A review. *Renewable and Sustainable Energy Reviews*, 16: 37-43.
- Sharma, V.K., Colangelo, A. and Spagna, G. 1993. Experimental performance of an indirect type solar fruit and vegetable dryer. *Energy Conversion and Management*, 34(4): 293-308.
- Strumillo, C. 2006. Perspectives on developments in drying. *Drying Technology*, 24(9): 1059-1068.
- Wulandani, D. and Oscar Nelwan, L. 2009. Design of solar flat plate collector and concentrator as heater of dryer for agricultural product. *Proceeding of Research Results of Bogor Agricultural University. IPB Bogor (in Bahasa Indonesia with English Abstract)*.
- Zhu, J. and Chen, B. 2013. Simplified analysis methods for thermal responsive performance of passive solarhouse in cold area of China. *Energy and Buildings*, 67: 445-452.



Volcanic Mud Contamination in the River Ecosystem: The Case Study of Lusi Mud Volcano, Indonesia

Dewi Hidayati*†, Norela Sulaiman**, B. S. Ismail**, Nurul Jadid* and Lutfi Surya Muchamad*

*Biology Department, Faculty of Science, Institut Teknologi Sepuluh Nopember, Surabaya, Indonesia

**Faculty of Science and Technology, Universiti Kebangsaan Malaysia, Selangor, Malaysia

†Corresponding author: Dewi Hidayati

Nat. Env. & Poll. Tech.
Website: www.neptjournal.com

Received: 30-06-2018
Accepted: 21-09-2018

Key Words:

Mud volcano
Lusi mud
Fish biotic integrity
Water quality
Habitat quality

ABSTRACT

The assessment of the impact of volcanic mud discharge into a river based on several quality indices including habitat quality index (HQI), water quality index (WQI) and fish biotic integrity (FIBI) using the case study of Lusi in Sidoarjo-Indonesia, was undertaken from January 2011 to February 2012. Compared to the data collected at the control station (HQI= 21; WQI= 59-75; FIBI=75), the siltation caused by the Lusi discharge adversely affected several factors. Firstly, the declining value of stream covers and aesthetics resulted in lower HQI (10-13); secondly, the increasing concentration of total suspended solids (TSS), biochemical and chemical oxygen demand (BOD and COD) resulted in low WQI, primarily in the dry season (22.3-49.3); and thirdly, the limited supporting habitat for cyprinids and the mud-intolerant native fish species lowered the FIBI score (60-65). The abundance of mud-tolerant species revealed that the downstream aquatic communities have the ability to adjust to the volcanic mud contamination. However, since there was a strong positive correlation between HQI and FIBI, the expected long term exposure to Lusi will be followed by more habitat degradation, thus limiting the life of fishes that are not tolerant to the mud and lowering of the quality indices permanently. Further investigations using *Mystus gulio* as the bioindicator for Lusi mud contamination is proposed, as follow-up research.

INTRODUCTION

The Sidoarjo mud volcano in Indonesia, also known as Lusi has been emitting mud nearly 90,000 m³/day since 2006 (Istadi et al. 2009), and as estimated will continue for 26 more years (Davies et al. 2011). Lusi contains a high portion of very fine clay particles, which contain major metal Al, organic matter and a wide range of symbiotic bacteria (UNDAC 2006, Plumlee et al. 2008, Niemann & Boetius 2010, Jennerjahn et al. 2013, Hidayati et al. 2014). Lusi mud particle size of less than 10 µm (USGS 2008) could possibly have direct effect to the fishes by clogging onto the gill surfaces, and adhering to the spaces between the gill filaments (Muraoka et al. 2011). Previously, toxicity test in the laboratory found that Lusi lead the physical damage to gills (Hidayati 2010).

Lusi has been channeled to the adjacent river namely Porong river (the downstream of the biggest river in East Java, Brantas river). Porong river has an average depth of 1.6 m (Damar 2012) with average flow of 600 m³s⁻¹ during wet season, while in dry season the flow commonly reduces to almost zero (Van der Linden 1989). The endurance of Lusi mud into Porong river, may result in the extreme suspended solids and increasing organic matter which is

declining the water quality, as well as the siltation that buried the physical structure in river bed such as rocks, coarse woody debris (CWD) and macrophytes that are important to improve fish habitat quality (Kennedy & Johnston 1986, Roni & Quinn 2001, Thomaz & Ribeiro da Cunha 2010). Habitat quality is an essential measurement in any biological survey (Barbour et al. 1999). Zhang et al. (2014) reported that water quality and sediment pollution significantly affect the biotic integrity through direct effects on the fish community.

Hypothetically, the discharge of the Lusi effluent into the river for long periods will cause a decrease in the quality of water and habitat as well as adversely affect the life of aquatic organisms, included fish. Despite Indonesian freshwater has higher fish diversity than any other country (Dudgeon 2006), the environmental monitoring tools are not well developed in Indonesia (Pearce & Butler 2005). Generally, the study of environmental factors to the local riverine fish assemblages is carried out in temperate zones (compared to tropical ones), hence more studies in tropical rivers are required (Tejerina-Garro et al. 2005). Moreover, Boulton et al. (2008) reported that ecological process variables in the temperate region are similar to the tropical one. Ecological assessments using the physical and biotic indices had de-

rived in temperate region, e.g. in western USA (Bryce et al. 2010), Texas (Pollack et al. 2009), Iowa (Wilton 2004) and North China (Zhang et al. 2014) as well as in tropical region, such as in West African river (Kamdem-Toham & Teugels 1999). This Lusi case study can be used to determine the impact of volcanic mud discharge on the river ecosystem from physical and biological indices (WQI, HQI and FIBI).

MATERIALS AND METHODS

Sampling sites: Description and duration: The Lusi mud volcano is located in the Sidoarjo district, East Java, Indonesia. To prevent the mud from flooding a nearby human settlement, the watery mud is collected initially in a settling pond from which it is channeled to the Porong River (Table 1 and Fig. 1).

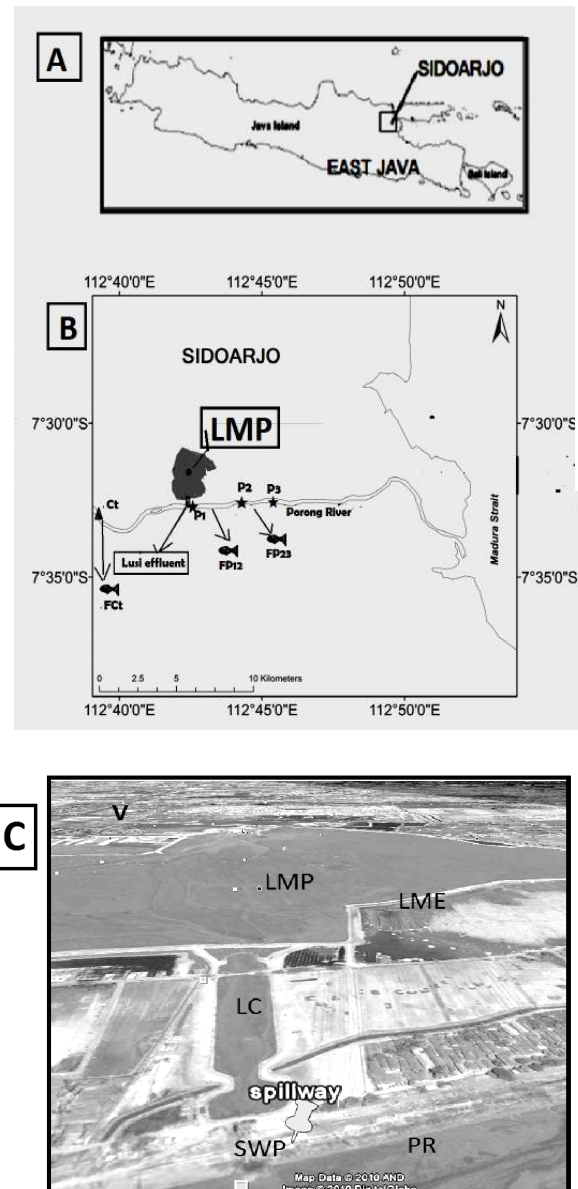
Water sampling during the survey period was carried out from January 2011 to February 2012, and coded S1, S4 and S5 for the wet season, while S2 and S3 represented the dry season. Meanwhile, the HQI observations and fish sampling activities were undertaken in the intermediate season between the wet and dry seasons (S1 - S2).

Water quality was analysed according to the WQI of DOE Malaysia, which has been successfully applied to measure water quality for rivers in Malaysia as well as Indonesia (Susilo & Febrina 2011). The WQI serves as the basis for environmental assessment of a water course in relation to pollution load using the following variables: DO (Dissolved Oxygen), BOD (Biochemical Oxygen Demand), COD (Chemical Oxygen Demand), AN (Ammonium Nitrogen), TSS (Total Suspended Solids) and pH. Then, all variables are combined into a single number which is used for categorization and designation of classes of beneficial uses (DOE Malaysia 2010, Susilo & Febrina 2011, Abassi & Abassi 2012).

The parameters namely DO, temperature, pH and ammonium nitrogen were measured at the sampling sites using the water quality tester, TROLL ® 9500. Platinum sensors were cleaned with a swab dipped in alcohol and gently rubbed (Geotech 2009). Salinity was measured by placing a drop of water sample onto the refractometer and reading the value.

Water samples were preserved in an icebox for 24 hours prior to analysis of TSS, BOD and COD in the laboratory in accordance to the methodology of the USEPA (1971, 1974, 1978). After analysis, classification of the water quality based on the WQI of the DOE Malaysia was as follows: Class I (< 92); Class II (76.5-92.7); Class III (51.9-76.5); Class IV (31.0-51.9); Class V (<31.0).

Assessment of the physical habitat quality was done in accordance to the standards of the Texas Commission on



LMP= Lusi Mud Pond; LME=Lusi Mud Embankment; V=Village; LC=Lusi Channel; SWP=Spillway pipe (effluent pipe); PR=Porong river

Fig. 1: Map showing the sampling stations. Note: (A) The Lusi mud volcano is located in the Sidoarjo district-East Java Province. (B); (C): The mud flow is collected in the Lusi Mud Pond (LMP) from which it is channelled to the Porong River (Source of Lusi's satellite image, CRISP (2010)).

Environmental Quality (TCEQ 2004), which included parameters such as availability of in-stream cover, bottom substrate stability, number of riffles, dimensions of the largest pool and channel flow status, bank stability, channel sinuosity and aesthetics of reach (Table 2). Most of the physi-

Table 1: Description of sampling stations.

Parameter	Station	Site description and coordination
Water and habitat	P1	Located at the area of initial discharge (closest to the Lusi Effluent quality Pipe (LEP), coordinates: 7°32'41.8'S; 112°42' 31.67'E
	P2	At an area about 3 km from the LEP, coordinates: 7°32'42.91'S; 112°43'49.53'E
	P3	At an area about 4 km from the LEP, coordinates: 7°32'36.57'S; 112°44' 35.06'E
	Ct	Located about 6 km upstream, and it represented a Lusi-free station, coordinates: 7°33' 10.42'S; 112°39' 30.32'E
Fish integrity	F12	Located between P1 and P2
	F23	Located between P1 and P2
	FCt	Located at Ct station area

cal habitat data were obtained by visual observations, which were supported by photographs and when necessary enhanced with online satellite imaging. In addition, sediments and cover types on the riverbed such as cobbles, undercut banks and coarse woody debris, which were used to identify the substrates and in stream covers, were collected using a sediment grab sampler. Classification of substrates based on particle size was determined based on the Wentworth Grade Scale by sieving sediment samples through a series of sieve sizes ranging from 1.25 mm up to 63 mm (UNEP/WHO 1996).

The fish sampling methods adopted were of the Wilton (2004) and ARI (2011). Both the methods have several similarities with current research, i.e. sampling location of river, fish sampling technique that combines fishing gear and electric shock; measurement of biological integrity and physical habitat. Moreover, Wilton (2004) sampling methods are well proven and widely used across Iowa State since 1994. Fish were captured using fishing gear combined with electric shock. The fishing gear was a net with 2 mm mesh size, 2.5 m deep and 46 m length. The pulsed direct current (DC) was delivered in waveform to the water, by which the fish gets stunned and is easily collected with a gear. The fishing gear was hauled from a boat as well as walked onto the banks at approximate length area of 350 m passed through downstream to upstream.

The collected fish were placed in tanks of water, and then most fish species were identified in the field according to the reference of Fischer & Bianchi (1984) and Froese & Pauly (2011). Their total and standard length were measured prior to returning them to the water. However, unidentified fish species were preserved in 10% formalin solution prior to be identification in laboratory. In addition, the Fish Index for Biotic Integrity (FIBI) was calculated using the scoring system of component metrics (Table 3) from Moyle & Marchetty (1999). FIBI is a combination of several individual measures or metrics (Table 3), which have an ecologically relevant and quantifiable attribute of the aquatic

biological community. The metrics response may be used to predict the environmental disturbances (Wilton 2004). Categories of fish metrics, whether they are native, carnivore or tolerant, were determined referring to the fish database that is listed by Froese & Pauly (2011).

RESULTS AND DISCUSSION

The bottom substrate analysis is important to determine the score of physical habitat quality (HQI) parameters such as in-stream cover and substrate stability. The substrate composition in the Lusi-receiving stations, i.e. P1, P2 and P3 lacked gravels (0%). The highest percentage of clay (77%) was found in the P1 stations, which were located at the initial discharge area of the Lusi effluent.

Substrate composition in the Lusi-receiving stations possibly occurred due to sedimentation and siltation, which were affected by the long period of the Lusi discharge that was rich in clay (particle size of 0.004-0.00024 mm) and dominated by fine particles less than approximately 10 micrometers (Plumlee et al. 2008). During the research, measured discharge of Porong river was in level of 16.7-81.4 m³ s⁻¹ in dry season and 128-316.7 m³ s⁻¹ in wet season. Volume of Lusi that moved to the Porong River was reported about 30.5-41.9 million m³/year, while the density of particles was 2.19 × 10³ kg/m³ (BPLS 2011, Hidayati et al. 2014, Yanuar et al. 2009). This meant that the values of several habitat parameters including those available in the stream cover (HQI score=1-2), bottom stability (HQI score=1) and dimensions of the river pool (HQI score=1-3) in the Lusi-receiving stations, primarily at P1, were lower than those of the control station which was free from Lusi (Table 4).

Moreover, the fine particles in the Lusi discharge were considered the main factor for the high levels of TSS in the Lusi-receiving stations (Fig. 3) as they affected the water clarity and lowered the score of aesthetics parameter (HQI score=1). The HQI of the Lusi-receiving stations (P1=10; P2=12; P3= 13) was lower than that of the control station (Fig. 2). According to the results obtained for HQI, the sta-

Table 2: Scoring method for Habitat Quality Index (HQI) based on the method of the Texas Commission on Environmental Quality (TCEQ 2004)

Habitat Parameter	Scoring Category		
Available In-stream Cover	Abundant (score: 4) >50% of substrate favourable for colonization and fish cover; good mix of several stable (not new fall or transient) cover types such as snags, cobble, undercut banks, macrophytes	Common (score: 3) 30-50% of substrate supports stable habitat; adequate habitat for maintenance of populations; may be limited in the number of different habitat types	Rare (score: 2) 10-29.9% of substrate supports stable habitat; habitat availability less than desirable; substrate frequently disturbed or removed
Bottom Substrate Stability	Stable (score: 4) >50% gravel or larger substrate; gravel, cobble, boulders; dominant substrate type is gravel or larger substrate.	Moderately Stable (score 3) 30-50% gravel or larger substrate; dominant substrate type is a mix of gravel with some finer sediments	Moderately Unstable (score:2) 10-29.9% gravel or larger substrate; dominant substrate type is finer than gravel, but may still be a mix of sizes
Number of Riffls	Abundant (score: 4) > 5 riffls	Common (score: 3) 2-4 riffls	Rare (score: 2) 1 riffl
Dimensions of Largest Pool	Large (score: 3) Pool covers more than 50% of the channel width; maximum depth is > 1 m	Moderate (score: 2) Pool covers approximately 50% or slightly less of the channel width; maximum depth is 0.5-1 m	Small (score: 1) Pool covers approximately 25% of the channel width; maximum depth is <0.5 m
Channel Flow Status	High (score: 3) Water reaches the base of both lower banks; < 5% of channel substrate is exposed	Moderate (score: 2) Water fills >75% of the channel; or <25% of channel substrate is exposed	Low (score: 1) Water fills 25-75% of the available channel and/or riffl substrates are mostly exposed
Bank Stability	Stable (score: 3) Little evidence (<10%) of erosion or bank failure; bank angles average <30°	Moderately Stable (score: 2) Some evidence (10-29.9%) of erosion or bank failure; small areas of erosion mostly healed over; bank angles average 30-39.9	Moderately Unstable (score: 1) Evidence of erosion or bank failure is common (30-50%); high potential of erosion during flooding; bank angles average 40-60°
Channel Sinuosity	High (score: 3) > 2 well-defined bends with deep outside areas (cut banks) and shallow inside areas (point bars) present	Moderate (score: 2) 1 well-defined bend or > 3 moderately defined bends present	Low (score: 1) <3 moderately defined bends or only poorly-defined bends present
Riparian Buffer Vegetation	Extensive (score: 3) Width of natural buffer is >20 m	Wide (score: 2) Width of natural buffer is 10.1-20m	Moderate (score: 1) Width of natural buffer is 5-10 m
Aesthetics of Reach	Wilderness (score: 3) Outstanding natural beauty; usually wooded or unpastured area; water clarity is usually exceptional	Natural Area (score: 2) Trees and/or native vegetation are common; some development evident (from fields, pastures, dwellings); water clarity may be slightly turbid	Common (score: 1) Settling Not offensive; area is developed, but uncluttered such as in an urban park; water clarity may be turbid or discolored
			Offensive (score: 0) Stream does not enhance the aesthetics of the area; cluttered highly developed; may be a dumping area; water clarity is usually turbid or discolored

Note: Status of Habitat Quality based on Total Score of HQI: 26 – 31 (Exceptional); 20 – 25 (High); 14 - 19 (Intermediate) and < 13 Limited

Table 3: Component metrics and scoring methods for the Index of Fish Biotic Integrity (FIBI) adopted from Moyle & Marchetty (1999).

Component Metrics		Score		
		1	3	5
I	Percentage native fish species	<20%	20-80%	>80%
II	Number of native species present	0-1	2-4	>4
III	Number of age classes, cyprinids	0-1	2	3+
IV	Total number of fish species	<5	5-7	>7
V	Total fish abundance	low number present	common, small numbers captured without difficulty	abundant, easy to capture in large numbers
VI	Percentage top carnivores	<1%	1-5%	>5%
VII	Percentage tolerant species	>20%	5-20%	<5%
VIII	Percentage introduced species	>40%	10-40%	<10%

Notes: IBI Score = [Total points/Number of metrics] × 20

Status of aquatic communities

80-100 Aquatic communities in very good to excellent condition

60-79 Aquatic communities in good condition

40-59 Aquatic communities in fair condition

<40 Aquatic communities in poor condition

Table 4: Habitat Quality Index (HQI) in the control area and in Lusi-receiving stations.

Station	Score of HQI parameter									HQI	Status
	I	II	III	IV	V	VI	VII	VIII	IX		
Ct	3	3	1	4	3	1	2	2	2	21	High
P1	1	1	2	1	1	3	0	0	1	10	Limited
P2	1	1	1	3	2	3	0	0	1	12	Limited
P3	2	1	1	3	2	3	0	0	1	13	Limited

Notes: I = available in stream cover; II = bottom substrate stability; III = number of riffles; IV = dimensions of largest pool; V = channel flow status; VI = bank stability; VII = channel sinuosity; VIII = riparian buffer vegetation; IX = aesthetics of reach

tus of habitat quality at the Lusi-receiving stations was rated as “limited”, while at the control station the rating was “high”.

As previously described, the Lusi discharge was responsible for the high concentration of TSS in the Lusi-receiving stations ([P1=676-4176]; [P2=459-1146]; [P3= 493-1013] mg/L). These concentrations were found to be significantly higher ($p<0.05$) than the TSS concentration at the control station (Ct=40-380.5 mg/L) primarily in the dry season. Furthermore, the Pearson analysis indicated that the TSS was positively correlated to the BOD ($r=0.80$) and this explains why the highest concentrations of TSS (4176 mg/L) as well as BOD (120.5 mg/L) occurred at the same station and time as seen at P1, S2 (Fig. 3). Hydrocarbon content in the sediments of the mud volcano supports chemosynthesis in various bacteria (Niemann & Boetius 2010, Yang et al. 2012). Moreover, Jennerjahn et al. (2013) reported that the Lusi input increased the concentration of suspended matter and the load of particulate organic carbon (POC), which have the potential to increase BOD as well as COD levels (Quayle 2009). Consequently, the high levels of TSS, BOD and COD contributed to the low WQI level (Fig. 4).

The multivariate and Tukey test indicated that WQI at all stations receiving Lusi were significantly lower ($p<0.05$) than that of the control stations. Compared to the range of the WQI in the control site (59-75), the station P1, located at the site of the initial discharge of Lusi exhibited the lowest WQI (19-63) and was most often categorized in class IV. Meanwhile, the WQI at P2 (35-69) and P3 (31-62), generally categorized in Class III, was significantly higher ($p<0.05$) than that of P1. Overall the WQI at the Lusi-receiving stations, during the dry season was significantly lower than wet season ($p<0.05$). This declining trend in WQI (22.3-49.3) resulted in the lowering of the water class (Fig. 4).

The presence of rocks and coarse woody debris (CWD) in the river bed increases the riffle areas that increase the dissolved oxygen, enhancement of habitat diversity, hence improving fish habitat quality primarily for juvenile and followed by increasing the fish communities (Kennedy & Johnston 1986, Roni & Quinn 2001). Macrophytes provide the physical structure for fish nursery, improve the complexity and diversity of habitats that can increase the diversity of life for animals such as invertebrates, fish and water birds (Thomaz & Ribeiro da Cunha 2010) as well as in-

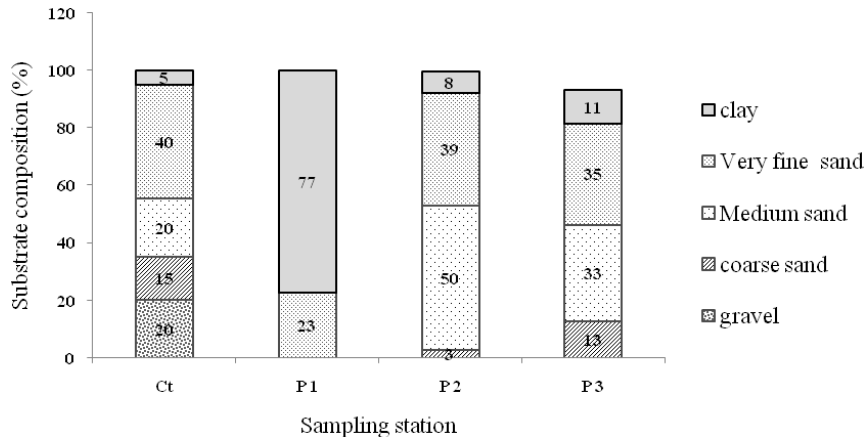


Fig. 2: Comparison of the substrate composition in the Lusi-receiving stations (P1, P2 and P3) and the Control (Ct) station.

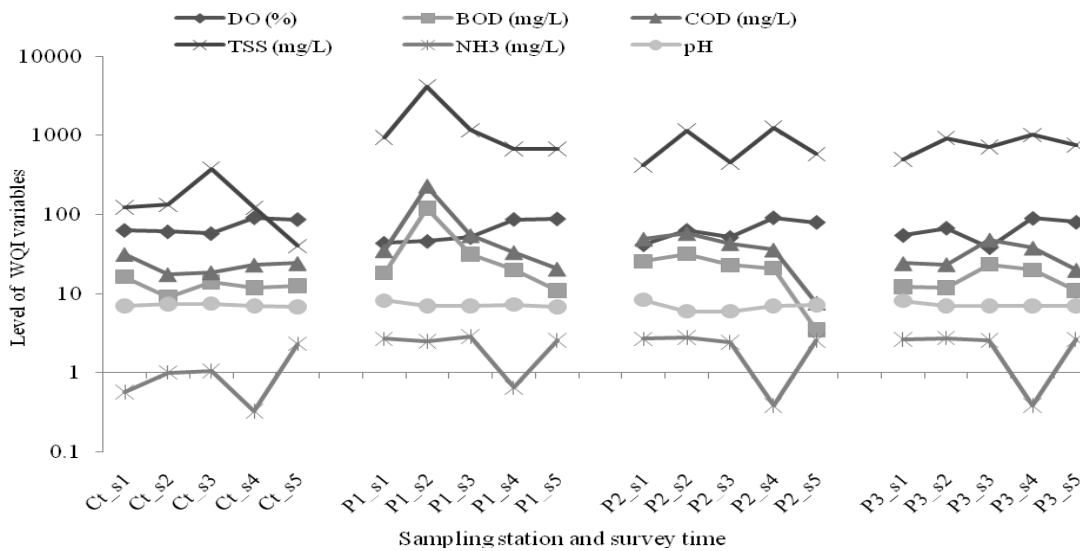


Fig. 3: Comparison of the values of the WQI-variables (TSS, DO, BOD, COD, NH₃ and pH) among sampling stations and time of survey (S1, S2, S3, S4 and S5).

crease the level of dissolved oxygen (Hunt & Christiansen 2000). The siltation of the Porong river by the Lusi discharge contributed to the lack of in-stream covers (Fig. 2 and Table 4) including gravel, buried CWD and aquatic macrophytes (Chen et al. 2014) thus causing adverse effects on the fish population.

With reference to the composition of fish species (Table 6), it was observed that the percentage of the fish species *Mystus gulio* (Hamilton) at (44%) and *Saurida tumbil* (Bloch) at (39%) occurred in abundance at the Lusi-receiving stations (FP12 and FP23) despite being exposed to Lusi contamination. The study on effect of Lusi exposure to the milkfish (Hidayati 2010) indicated that Lusi caused gill alteration. The fine Lusi particles were possibly attached to

the surface of the gills and filled the space between the gill filaments that causes the oxygen deficiency as a result of changes in gill respiratory surface area (Plumlee et al. 2008, Muraoka et al. 2011). Visually, the gill surface of *M. Gulio*, which caught in Lusi effluent area (P1), was physically covered by mud (Fig. 5). The survival of *M. gulio* is likely to be related to its behavioural characteristic of facultative air breathing (Veerasamy 2012). Concentrations of Al and Fe in all sediment samples of Lusi-receiving stations (Hidayati 2014) did not exceed the reference level of soil and clay (UNDAC 2006, Hidayati 2014). The observed pH level in all sampling stations was in safe level (pH=7-7.24) according to the National Recommended Water Quality Criteria (USEPA WQC 2009), that is stipulated in the range of 6.5-

9.0. The AI toxicity relatively depended on the ambient pH (Jeziarska & Witeska 2006); since the water showed near-neutral pH, Lusi effect to the fish might be related to its particle size rather than AI as the major metal.

Rusch & Oesterheld (1997) suggested that it is important to use the dominant species as the bioindicator of water pollution. *M. gulo* is the potential candidate for use as the bioindicator of the Lusi contaminated river due to its dominance at the Lusi-receiving stations. In addition, its presence in a previous investigation by Herlina et al. (2005) suggested that *M. gulo* could adapt to extreme changes in the concentration of suspended solids and through modification of substrates. Moreover, its body size range of 5.2 to 20.4 cm, indicated that all growth phases of *M. gulo* may have adapted well to the Lusi exposure.

The finding, based on the composition and identification of fish biotic integrity (FIBI) criteria (Table 5 and Table 6), resulted in the FIBI order, of FCt (75) > FP23 (65) > FP12 (60). The lowest FIBI score was that exhibited at station FP12 and this was seemingly attributed to the absence of cyprinids (Table 3 and Table 4), which were limited because of the low HQI and WQI scores (Beamish et al. 2006).

Table 7 shows that the FIBI showed positive strong correlation with the HQI ($r=0.99$) and was moderately corre-

lated to the WQI ($r=0.62$). A previous investigation by Herlina et al. (2005) recorded that Cyprinidae (genus *Barbodes/Puntius*) were present in the study area. Cyprinids possibly live in fast flowing rivers that are supported by gravel and rock substrates (Rachmatika et al. 2005). Lack of gravel in FP12 lowered the HQI score due to changes in the bottom substrates ability (Table 2), could possibly be responsible for the absence of cyprinids (Table 3).

With reference to the status of aquatic community (Table 6), it was indicated that integrity of the fish community at the Lusi-receiving stations was in a good condition as that found at the control station. Results revealed that the river was able to adjust the extreme mud contamination and maintain its community by the survival of mud-tolerant native species such as *M. gulo* and *S. tumbil* (Table 5). However, reference to Table 4 indicated that the volcanic mud caused decrease in habitat quality that could support cyprinids and mud-intolerant native fish species. Further adverse impact on fish assemblage could possibly occur due to the predicted long period of the mud volcano eruptions (Davies et al. 2011), and this could probably cause the lowering of the indices permanently. Further investigations using *M. gulo* as the bioindicator for Lusi mud contamination is proposed, as a follow up research.

Table 6: FIBI scoring according to Moyle & Marchetty (1999).

Metrics No.	Percentage (%) or number of species			FCt	Score (1-3-5)		
	FCt	FP12	FP23		FCt	FP12	FP23
I	100%	100%	71%	5	5	3	
II	5	3	5	5	3	5	
III	2	0	2	3	1	3	
IV	5	3	7	3	1	3	
V	Common	Common	Common	3	3	3	
VI	20%	67%	43%	5	5	5	
VII	40%	100%	86%	1	1	1	
VIII	0%	0%	29%	5	5	3	
Total Score				30	24	26	
IBI				75	60	65	
Status of Aquatic Communities				Good	Good	Good	

Table 7: The Pearson correlation analysis between quality assessment indexes.

	Station	Correlations		
		IBI	HQI	WQI
Station	Pearson Correlation	1.00	0.92**	0.91**
	Sig. (2-tailed)		0.00	0.00
IBI	Pearson Correlation	1.00	0.99**	0.62**
	Sig. (2-tailed)		0.00	0.00
HQI	Pearson Correlation		1.00	0.59**
	Sig. (2-tailed)			0.00
WQI	Pearson Correlation			1.00

** Correlation is significant at the 0.01 level (2-tailed), N=60

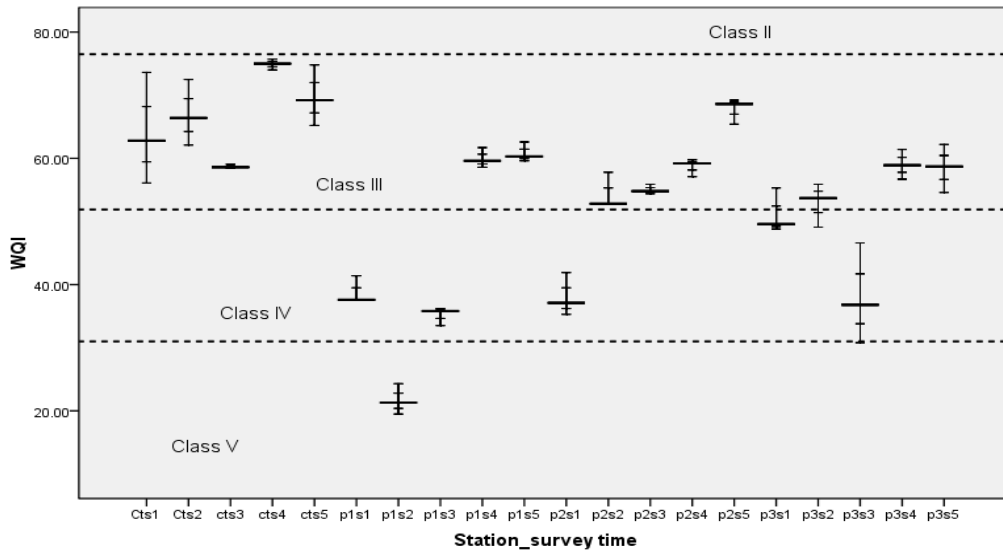


Fig. 4: Comparison of the levels of WQI and water classification among sampling stations and time of survey (S1, S2, S3, S4 and S5).

Table 5: Composition and identification of fish biotic integrity criteria

Station	Name of Species	Family	Carnivore No. of Caught	Native or Intermediate	Tolerance	Feeding habit	Total species	Number of native species	Number of cyprinids	Number of tolerant species	Number of Carnivores
FCt	<i>Anabas testudineus</i>	Anabantidae	3	Nat	v	Om					
	<i>Barbonymus altus</i>	Cyprinidae	3	Nat	X	Om					
	<i>Lutjanus griseus</i>	Lutjanidae	1	Nat	v	Car	5	5	2	3	1
	<i>Puntius binotatus</i>	Cyprinidae	2	Nat	X	Om					
	<i>Trichopodus trichopterus</i>	Osphronemidae	1	Nat	v	Om					
FP12	<i>Mugil cephalus</i>	Mugilidae	8	Nat	v	Om					
	<i>Mystus gulio</i>	Bagridae	25	Nat	v	Car	3	3	0	3	2
	<i>Saurida tumbil</i>	Synodontidae	8	Nat	v	Car					
FP23	<i>Barbonymus altus</i>	Cyprinidae	2	Nat	X	Om					
	<i>Mugil cephalus</i>	Mugilidae	4	Nat	v	Om					
	<i>Mystus gulio</i>	Bagridae	20	Nat	v	Car					
	<i>Oreochromis niloticus</i>	Cichlidae	2	Int	v	Om					
	<i>Rasbora argyrotaenia</i>	Cyprinidae	1	Int	v	Her	7	5	2	6	3
	<i>Saurida tumbil</i>	Synodontidae	32	Nat	v	Car					
	<i>Terapon theraps</i>	Terapontidae	1	Nat	v	Car					

Notes: Nat = Native; Om = omnivore; Car = carnivore; Her = herbivore

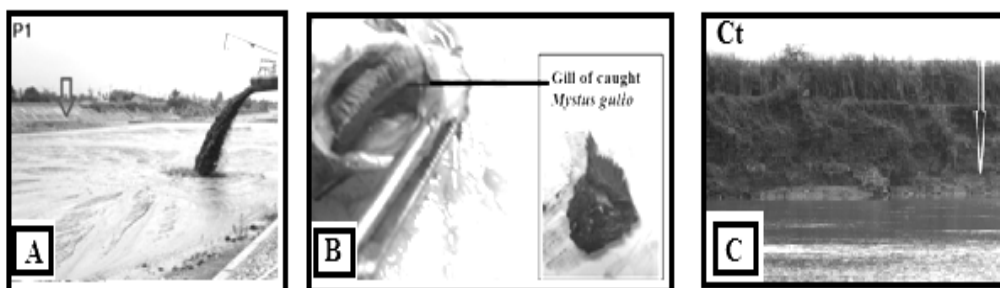


Fig. 5: Site sampling condition: A. Lusi-receiving station (P1); B. Performance of *M. gulo* gill that caught in P1; C. Control station (Ct). Arrow shows water body performance, where Lusi-receiving station exhibit highly siltation.

CONCLUSION

Based on the Lusi case, there has been an indication that the volcanic mud discharge into the river has resulted in the degradation of the habitat and water quality, resulting in the lowering of the class of water, and subsequently lower FIBI scores. However, the river has adjusted to the volcanic mud contamination and with the survival of mud-tolerant species.

ACKNOWLEDGEMENTS

This work was supported by “Dirjen Pendidikan Tinggi” National Education Ministry (Indonesia) for the doctoral program scholarship and the School of Environmental and Natural Resource Sciences, Faculty of Science and Technology, Universiti Kebangsaan Malaysia (UKM), while physical, chemical and biological analyses were conducted at Institut Teknologi Sepuluh Nopember Surabaya (ITS), Indonesia.

REFERENCES

- Abassi, T. and Abassi, S.A. 2012. Water Quality Indices. Elsevier, Oxford UK, pp. 384.
- ARI 2011. Documenting fish assemblages in the Anglesea river estuary following acidification events. Anglesea River Fish Survey Report. The Arthur Rylah Institutes, DSE.
- Barbour, M.T., Gerritsen, J., Snyder, B.D. and Stribling, J.B. 1999. Rapid Bioassessment Protocols for Use in Streams and Wadeable Rivers: Periphyton, Benthic Macroinvertebrates, and Fish. 2nd edition, EPA/841-B-99-002. U.S., Environmental Protection Agency, Office of Water, Assessment and Watershed Protection Division, Washington D.C.
- Beamish, F.W.H., Saardrit, P. and Tongnunui, S. 2006. Habitat characteristics of the Cyprinidae in small rivers in central Thailand. Environmental Biology of Fishes, 76: 237-253.
- Boulton, A.J., Boyero, L., Covich, A.P., Dobson, M., Lake, S. and Pearson, R. 2008. Are tropical streams ecologically different from temperate streams? In: Tropical Stream Ecology. Elsevier Inc. 256-257.
- BPLS 2011. Badan Penanggulangan Lumpur Sidoarjo Review Rencana-strategis 2010-2014. Badan Pelaksana BPLS (Strategic plan Review of Sidoarjo Mud Management Agency) <http://www.bpls.go.id/penanganan-luapan-ke-kali-porong>. Accessed 14th of July 2014.
- Bryce, S.A., Lomnický G.A. and Kaufmann, P.R. 2010. Protecting sediment-sensitive aquatic species in mountain streams through the application of biologically based streambed sediment criteria. Journal of the North American Benthological Society, 29(2): 657-672.
- Chen, X., Deng, Z., Xie, Y., Feng, Li., Hou, Z., Xu, L. and Li, Y.F. 2014. Effects of sediment burial disturbance on the vegetative propagation of *Phalaris arundinacea* with different shoot statuses. Aquatic Ecology, 48(4): 409-416.
- CRISP 2010. Centre for Remote Imaging, Sensing and Processing National University of Singapore. <https://crisp.nus.edu.sg/coverages/EJmudflow/index20101117.html>. Accessed on 7th December 2010.
- Damar, A. 2012. Net phytoplankton community structure and biomass dynamics in the Brantas River estuary, Java, Indonesia. In: Subramanian. V. (Ed.) Coastal Environment Focus Asian Coastal Region, pp. 173
- Davies, R.J., Mathias, S.A., Swarbrick, R.E. and Tingay, M.J. 2011. Probabilistic longevity estimate for the LUSI mud volcano, East Java. Journal of the Geological Society, 168: 517-523.
- DOE (Department of Environment) Malaysia. 2010. Malaysia Environmental Quality Report. Edited by Publication Section Strategic Communications Division Department of Environment Malaysia. Kuala Lumpur: Ministry of Natural Resources and Environment Malaysia, pp. 78.
- Dudgeon, D., Arthington, A.H., Gessner, M.O., Kawataba, Z.I., Knowler, D.J., Leveque, C., Naiman, R.J. et al. 2006. Freshwater biodiversity: Importance, threats, status and conservation challenges. Biological Reviews, 81: 163-182.
- Fischer, W. and Bianchi, G. 1984. FAO Species Identification Sheets for Fishery Purposes. Western Indian Ocean (Fishing Area 51). Prepared and printed with the support of the Danish International Development Agency (DANIDA). Rome, Food and Agricultural Organization of the United Nations, Vol. I.
- Froese, R. and Pauly, D. 2011. Fish Base. World Wide Web Electronic Publication. www.fishbase.org.
- Geotech 2009. Multi Parameter TROLL 9500 Operator's Manual. www.geotechenv.com.
- Herlina, E., Kusumaningrum, N.S., Rahmawati, N.Z. 2005. Ancaman penurunan kualitas air Sungai Brantas terhadap kelestarian diversitas dan perilaku makan ikan lokal. Laporan Program Kreativitas Mahasiswa Penelitian. Direktorat P2M Dikti, LPPM Universitas Brawijaya Malang, Indonesia.
- Hidayati, D. 2010. An evaluative study on Sidoarjo mud flow after phytoremediation treatment in milk fish (*Chanoschanos*) liver. IPTEK- The Journal for Technology and Science, 21: 28-31.
- Hidayati, D., Norela, S., Ismail, B.S. and Shuhaimi-Othman, M. 2014.

- Impact of mud volcano lava to the aquatic life using the fish biological study case in Lusumud volcano Indonesia. *Research Journal of Environmental Toxicology*, 8: 1-24.
- Hunt, R.J. and Christiansen, I.H. 2000. Dissolved Oxygen Information Kit. A CRC Sugar Technical Publication, CRC for Sustainable Sugar Production, Townsville, pp. 27.
- Istadi, B., Pramono, G.H., Sumintadireja, P. and Alam, S. 2009. Modeling study of growth and potential geohazard for Lusi mud volcano East Java, Indonesia. *Marine and Petroleum Geology*, 26: 1724-1739.
- Jennerjahn, T.C., Janen, I., Propp, C., Adi, S. and Nugroho, S.P. 2013. Environmental impact of mud volcano inputs on the anthropogenically altered Porong River and Madura Strait coastal waters, Java, Indonesia. *Estuarine, Coastal and Shelf Science*, 130: 152-160.
- Jezierska, B. and Witeska, M. 2006. The metal uptake and accumulation in fish living in polluted waters. In: Twardowska, I., Allen, H.E., M.M., Haggblom, M.M. and Stefaniak, S. (Eds.) *Soil and Water Pollution Monitoring. Protection and Remediation*, Springer, New York, pp. 107-114.
- Kandem-Toham, A. and Teugels, G.G. 1999. First data on an index of biotic integrity (IBI) based on fish assemblages for the assessment of the impact of deforestation in a tropical West African river system. *Hydrobiologia*, 397: 29-38.
- Kennedy, G.J.A. and Johnston, P.M.A. 1986. Review of salmon (*Salmosalar* L.) research on the river Bush. In: Crozier, W.W., Johnson, P.M. (eds.) *Proceedings of the 17th Annual Study Course*, Institute of Fisheries, pp. 49-69.
- Moyle, P.B. and Marchetti, M. 1999. Application of indices of biotic integrity to California streams and watersheds. In: Simon, T.P. (ed.) *Assessing the Sustainability and Biological Integrity of Water Resources Using Fish Communities*. CRC Press, Boca Raton, Florida, pp. 367-379.
- Muraoka, K., Amano, K. and Miwa, J. 2011. Effects of suspended solids concentration and particle size on survival and gill structure in fish. *Proceedings of the 34th World Congress of the International Association for Hydro-Environment Engineering and Research*, June 26-July 1, 2011, Brisbane Convention and Exhibition Centre, Brisbane, Australia, pp. 2893-2900.
- Niemann, H. and Boetius, A. 2010. Mud volcanoes. In: Timmis K.N. (ed.) *Handbook of Hydrocarbon and Lipid Microbiology*, Springer-Verlag, Berlin Heidelberg, pp. 205-214.
- Pearce, D.G. and Butler, R.W. 2005. *Contemporary Issues in Tourism Development*. Taylor and Francis E-library, pp. 249.
- Plumlee, G.S., Casadevall, T.J., Wibowo, H.T., Rosenbauer, R.J., Johnson, C.A., Breit, G.N. and Lowers, H.A. et al. 2008. Preliminary analytical results for a mud sample collected from the Lusi mud volcano, Sidoarjo, East Java, Indonesia. U.S. Geological Survey Open-File Report.
- Pollack, J.B., Kinsey, A.P. and Montagna, A. 2009. Freshwater inflow biotic index (FIBI) for the Lavaca-Colorado Estuary Texas. *Environmental Bioindicator*, (4): 153-169.
- Quayle, W.C., Fattore, A., Zandona, R., Christen, E.W. and Arienzo, M. 2009. Evaluation of organic matter concentration in winery wastewater: a case study from Australia. *Water Science and Technology*, 60(10): 2521-2528.
- Rachmatika, I., Nasi, R., Sheil, D. and Wan, M.A. 2005. First look at the fish species of the middle Malinau. Center for International Forestry Research (CIFOR), Bogor, Indonesia, pp. 34-35.
- Roni, P. and Quinn, T.P. 2001. Density and size of juvenile salmonids in response to placement of large woody debris in western Oregon and Washington streams. *Canadian Journal of Fisheries and Aquatic Sciences*, 58(2): 282-292.
- Rusch, G.M. and Oosterheld, M. 1997. Relationship between productivity and species and functional group diversity in grazed and non-grazed pampas grassland. *Oikos*, 78: 519-526.
- Susilo, G.E. and Febrina, R. 2011. The simplification of DOE water quality index calculation procedures using graphical analysis. *Australian Journal of Basic and Applied Sciences*, 5(2): 207-214.
- TCEQ 2004. Texas Commission on Environmental Quality TCEQ-20156-C (Rev. 04-15-2004). Surface water quality monitoring program. Habitat Assessment Worksheet-Part III Habitat Quality Index.
- Tejerina-Garro, F.L., Maldonado, M., Ibañez, C., Pont, D., Roset, N. and Oberdorff, T. 2005. Effects of natural and anthropogenic environmental changes on riverine fish assemblages: A framework for ecological assessment of rivers. *Brazilian Archives of Biology and Technology*, (48): 1.
- Thomaz, S.M. and Ribeiro da Cunha, E. 2010. The role of macrophytes in habitat structuring in aquatic ecosystems: methods of measurement, causes and consequences on animal assemblages composition and biodiversity. *Acta Limnologica Brasiliensia*, 22(2): 218-236.
- USGS (U.S. Geological Survey) 2008. Volcano Hazards Program (VHP) Photo Glossary: Mud Volcano. <http://volcanoes.usgs.gov/about/pglossary/MudVolcano.php>.
- UNDAC (United Nation Disaster Assessment and Coordination) 2006. Environmental assessment hot mud flow East Java Indonesia. Published in Switzerland by the Joint UNEP/OCHA Environment Unit, 1-56, Final Technical Report, July 2006.
- UNEP/WHO 1996. Water quality monitoring: A practical guide to the design and implementation of freshwater quality studies and monitoring programmes. In: Bartram J. and R. Ballance (eds.) *Sediment Measurements*, UNESCO, WHO and UNEP, London, UK, pp. 1-15.
- USEPA 1971. Method 160.2, Residue, Non-filterable (gravimetric, dried at 103-105°C).
- USEPA 1974. Method 405.1. Biochemical Oxygen Demand (5 Days, 20°C).
- USEPA 1978. Method 410.1. Chemical Oxygen Demand (Titrimetric, Mid-Level). Approved for National Pollutant Discharge Elimination System (NPDES). Editorial Revision.
- USEPA, WQC 2009. National Recommended Water Quality Criteria. <https://www.epa.gov/wqc/national-recommended-water-quality-criteria-aquatic-life-criteria-table>
- Van der Linden, W.J.M., Cloetingh, S.A.P.L., Kaasschieter, J.P.H., Jef Vandenberghe, Van de Graaff, W.J.E. and Van der Gun, J.A.M. 1989. *Coastal Lowlands: Geology and Geotechnolgy*. Kluwer Academic Publishers. Springer.
- Veerasamy, M.A. 2012. Study of impact distillery waste on the catfish *Mystus gulio* (Hamilton). Department Zoology, Barathidasan University, India.
- Wilton, T. F. 2004. Iowa Biological Assessment of Iowa's Wadeable Stream. Iowa Department of Natural Resources.
- Yang, H.M., Lou, K., Sun, J., Zhang, T. and Ma, X.L. 2012. Prokaryotic diversity of an active mud volcano in the Usu City of Xinjiang, China. *Journal of Basic Microbiology*, 52(1): 79-85.
- Yanuar, R., Budiarso and Koestoer, R.A. 2009. Hydraulics convances of mud slurry by a spiral pipe. *Journal of Mechanical Science and Technology*, 23(7): 1835-1839.
- Zhang, H., Shan, B. and Liang, A.O. 2014. Application of fish index of biological integrity (FIBI) in the Sanmenxia Wetland with water quality implications. *Journal of Environmental Sciences*, 26(8): 1597-1603.



Composite System for the Coupling Degree of Tourism Industry and Regional Ecological Environment: A Case Study of Henan Province, China

Demian Fang

Xinyang Vocational and Technical College, Xinyang, Henan, 464000, China

Nat. Env. & Poll. Tech.
Website: www.neptjournal.com

Received: 10-01-2019
Accepted: 11-02-2019

Key Words:

Coupling degree
Tourism industry
Environment

ABSTRACT

Tourism is a worldwide industry, but the per capita share of tourism resources in China is relatively small, and the capacity of the tourism environment is limited. Achieving economic growth in tourism and preserving tourism resources and the ecological environment are the premise and guarantee of tourism's sustainable development under the constraints of tourism resources and ecological environment. By calculating the coupling degree of the tourism industry and regional ecological environment, the coupling degree of the regional economy and environment in a particular area can be effectively determined, and a basis for promoting the coordinated development of tourism and ecological environment can be provided. Taking Henan Province as an example, this study establishes a comprehensive evaluation system of the coupling degree between the tourism industry and regional ecological environment system, and uses the coupling model to analyse the coupling status of the two subsystems in Henan Province, and proposes policy suggestions to promote the coupling development of the two subsystems. Results show that the tourism subsystem of Henan Province increased from 0.024 in 2010 to 0.862 in 2016, and the order degree of the ecological subsystem rose from 0.070 in 2010 to 0.770 in 2016. The orderliness of the eco-environment subsystem is less than that of the tourism subsystem, indicating that further improvement of the eco-environment in Henan Province is still possible. The coupling degree of the tourism industry and regional ecological environment showed an increasing trend annually from 0.169 in 2011 to 0.766 in 2016 and exhibited a particularly large increase in 2013. This study's results can provide a theoretical reference for understanding the coordinated development between the tourism industry and regional ecological environment, promoting the coupling between them, and enhancing the sustainable tourism industry of Henan Province.

INTRODUCTION

With the rapid advancement of social progress and the tourism industry, the eco-environmental problems of tourist destinations have become an endogenous obstacle to the promotion of the tourism industry. Various countries and regions have gradually realized the relationship between the development of tourism and the ecological environment. Tourism is a comprehensive industry. The industrial status and economic role of tourism in the development of the national economy have been gradually strengthened. Tourism also plays an increasingly important role in stimulating the national economy, driving social employment, and promoting the utilization of resources and the environment. China is currently in a process of rapid industrialization and urbanization. The increasing demand for mass and diversified consumption has opened up possibilities for tourism development. The rapid development of tourism has not only produced positive effects, but also changed the ecological environment on which human beings depend to survive. This has caused destructive damages to the environment and affected the sustainable development of tourism.

Tourism is a resource-based industry. From the perspective of tourism developers, the development and utilization of tourism resources inevitably change or destroy the original ecological resources. From the perspective of tourists, water pollution, vegetation destruction, and noise pollution caused by excessive tourism activities affect the local ecological environment.

Henan, an important province in central China, has an excellent history and culture and contains numerous tourist attractions. The long history and profound cultural connotations of this province attract Chinese and international tourists. As shown in Fig. 1, the tourism industry in Henan Province has developed rapidly in recent years; particularly, the number of star-rated hotels and the total number of tourist agencies have increased. Although the tourism industry of Henan Province has achieved remarkable progress, compared with the tourism products of other developed tourism provinces, those of Henan Province are not outstanding and fail to form a system and a unique tourism brand. The level of tourism industrialization is low, and the construction of the tourism service infrastructure is imperfect, and

the quality of tourism practitioners does not meet the current demands of high-end tourism. The phenomena of occupying cultivated land, destroying grasslands, and deforestation are also prominent due to the construction of houses, roads, and cableways in several tourist areas in Henan Province. These phenomena destroy the local environment and ecology to a considerable extent and cause a decline in the overall environmental quality of tourist destinations and the deterioration of the life quality of residents in tourist destinations.

EARLIER STUDIES

Since the beginning of the 20th century, foreign scholars have been conducting preliminary explorations of the relationship between the tourism economy and the ecological environment. They focused on the impact of tourism on the environment, eco-tourism, sustainable tourism development, and tourism and ecological environment coupling. Coupled development of tourism ecology is a new product of the integration of ecological theory and tourism theory. Scholars and experts generally accept the viewpoint that the degree of tourism ecology coupling can represent the dynamic relationship between tourism and the regional ecological environment system. Butler (1991) believed that with the increasing popularity of sustainable development, tourism was regarded as an activity that could easily develop along appropriate routes. However, the lack of understanding of the complexity of tourism results in the disregard for the pollution caused by tourism to the environment. Morrison et al. (1991) believed that although tourism has been widely promoted as a tool for economic development, it may have adverse social and environmental impacts on host communities. Bithas (1997) calculated and studied an ecosystem and its environmental-economic interaction. Sun et al. (1998) examined the relationship between tourism and the environment and between tourism activities and environmental factors and investigated the mechanism of their interaction. Madan et al. (2000) posited that due to the influx of tourists, a huge demand for accommodation, hotels, and other related infrastructure and facilities emerged in tourist destinations, and this demand placed considerable pressure on the natural environment. Hunter (2002) stated that tourism was one of the largest industries in the world. The development of tourism may have an extensive impact on the local environment; therefore, sustainable development of tourism destinations is an important issue. Mbaiwa (2003) believed that tourism in the Okavango Delta provided employment opportunities for local communities, but tourism had begun to exert negative impacts on the region, such as the destruction of the region's ecology due to driving beyond the prescribed lanes, noise pollution, and poor

waste management. Li et al. (2012) proved that in an urban centre, a certain spatial coupling existed between the areas with high ecological vulnerability and those with intensive tourism activities. The impact of tourism activities on the reservoir ecological environment cannot be ignored. Yuan et al. (2014) analysed the interactive relationship among tourism, the ecosystem, and the regional economy in the process of development and concluded that this interactive relationship was mutually influential and restrictive. Zhao et al. (2014) reported that the impact of tourism on the water environment had become a popular topic in ecotourism research. The relationship between tourism activities and the water environment in Liupanshan Ecotourism Area in China was analysed. Amir et al. (2015) believed that the tourism industry had a negative impact on the regional environment; however, if tourism could develop harmoniously with the environment to a certain extent, then the tourism industry would achieve sustainable development. Budeanu et al. (2016) discussed the relationship between tourism development and environmental coupling development to achieve sustainability. Law et al. (2016) constructed the concept of green economy from the perspective of tourism and proposed a model for transforming the concept of green economy into the participation process of tourism stakeholders; the model was validated in a case study of Bali, Indonesia. Dvarkas (2017) believed that although the development of tourism could provide economic benefits to a region, the increasing number of tourists had a long-term impact on the ecological situation. Carrillo et al. (2017) studied the sustainability of Spanish regional tourism by building a comprehensive index and using multi-criteria decision-making technology to synthesize and weigh the simple indexes considered. Fadafan et al. (2018) stated that ecosystems are sensitive and vulnerable. He developed and applied a non-compensatory framework to analyse the impact of tourism development on land use. Tamayo et al. (2018) analysed the impact of tourism development on the ecological environment of Philippine coral reefs.

Existing literature shows that the impact of tourism on the ecological environment is a controversial issue. The positive and negative impacts of tourism on the environment are closely related to the research and evaluation system of the ecological environment and the evaluation methods of the tourism environment. Therefore, taking Henan Province as an example, this study calculates the coupling value of tourism and the regional ecological environment composite system in 2010-2016 by using the coupling model then proposes concrete measures to change the situation wherein tourism economic growth lags behind that of the ecological environment. Therefore, protection of the tourism environment can be promoted, and ecology can be

actively developed in the process of tourism development. Suggestions for tourism and other aspects are also provided in this study.

BRIEF INTRODUCTION TO THE TOURISM-ECOLOGY COUPLING MODEL

Coupling is a concept in physics in which two or more systems or motion forms influence each other through various interactions. From the perspective of coupling, coupling and its effect and the degree of coupling refer to the dynamic evolution process of multiple systems and their coupling elements from disorder to order on the basis of a virtuous cycle. The degree of coupling shows the movement of the order and structure of the system when it reaches a critical region, which determines the trend of the system from disorder to order. The key to the mechanism of the system from disorder to order is the coupling between the order parameters in the system, and the coupling degree is a measure that reflects the coupling effect. Therefore, this study defines the tourism-ecological coupling degree as the degree of interaction between the tourism industry and the ecological environment system through its own coupling factors, which can be used as an index to reflect the strength of the role of the tourism industry and regional ecological environment system.

Determination of order parameters: Considering scientific and practical principles, the selected order parameter must be able to represent the variables of tourism industry status to serve as the order parameter index. In consideration of data availability, we choose four indicators to evaluate the tourism system. These four indicators are the numbers of Chinese tourists, international tourists, star-rated hotels, and employees of the hotel and catering industry. The index system of the ecological environment includes six indicators, namely, industrial wastewater discharge, industrial smoke and dust discharge, forest coverage, industrial solid waste production, comprehensive utilization rate of industrial solid waste, and investment in environmental pollution control. The data used in this study are from Henan Statistical Yearbook, China Environmental Statistical Yearbook, and China Tourism Statistical Yearbook. The investigation period is from 2010 to 2016.

Order degree of the system: Considering subsystems $S_j, j \in [1, k]$, we set the order parameter variables in the development process as $e_j = (e_{j1}, e_{j2}, \dots, e_{jn})$ and $n \geq 1, \beta_{ji} \leq e_{ji} \leq \alpha_{ji}, i \in [1, n]$. For generality, we assume that $e_{j1}, e_{j2}, \dots, e_{jn}$ increases. The higher the order degree of the system is, the smaller the value is. The larger the value of $e_{j1+1}, e_{j1+2}, \dots, e_{jn}$ is, the lower the order degree of

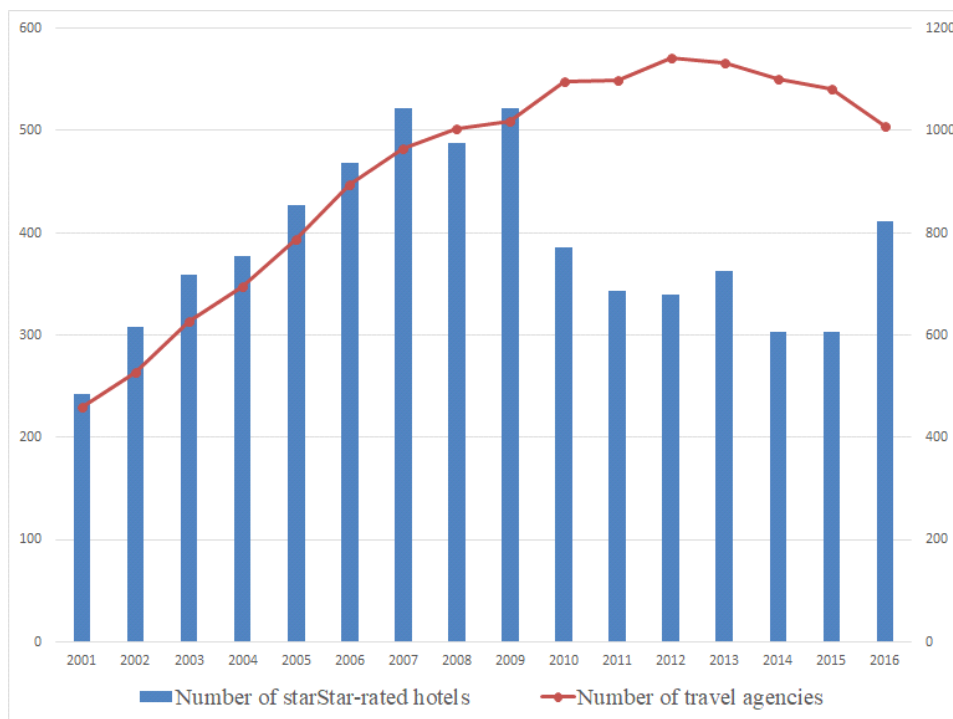


Fig. 1: Number of star-rated hotels and travel agencies in Henan Province from 2001-2016. (Data from the China Tourism Statistics Yearbook)

the system is. The smaller the value is, the higher the order degree of the system is. The complex system of the tourism industry and regional ecological environment includes tourism and regional ecological environment systems, and the order parameter in the development process of the tourism system is $e_1 = (e_{11}, e_{12}, \dots, e_{1n})$. According to the concept of system order degree, we define the order degree of order parameter e_{1j} components as follows:

$$u_1(e_{1i}) = \begin{cases} \frac{e_{1i} - \beta_{1i}}{\alpha_{1i} - \beta_{1i}} & (i = 1, 2, \dots, l) \\ \frac{\alpha_{1i} - e_{1i}}{\alpha_{1i} - \beta_{1i}} & (i = l + 1, l + 2, \dots, n) \end{cases} \quad \dots(1)$$

Where, α_{1i} and β_{1i} belong to the maximum and minimum of the first index of the tourism industry system, respectively. According to this definition, after normalization treatment, $u_1(e_{1i}) \in [0, 1]$. When the value is large, the contribution of e_{1i} to the orderly tourism industry system is also large. The total contribution of ordinal parameters to the orderliness of the tourism system can generally be achieved by an integrated method $u_1(e_{1i})$. The commonly used methods are geometric average and linear weighted. The geometric average method is expressed as:

$$u_1(e_1) = \sqrt[n]{\prod_{i=1}^n u_1(e_{1i})} \quad \dots(2)$$

The linear weighting method proceeds as:

$$u_1(e_1) = \sum_{i=1}^n \omega_{u1}(e_{1i}), \quad (\omega \geq 0, \sum_{i=1}^n \omega = 1) \quad \dots(3)$$

Where, ω is the weight of each index.

In the order degree of the tourism system $u_1(e_1) \in [0, 1]$, when $u_1(e_1)$ is large, the contribution of the order parameters e_1 to the order of the tourism system and the order degree of the tourism system are high and vice versa. The order parameters are set in the development process of the regional ecological environment system as $e_2 = (e_{21}, e_{22}, \dots, e_{2i})$. According to the calculation method of the order degree of the tourism system, the order degree of the component of regional ecological environment parameters e_{2i} can be obtained as $u_2(e_{2i}), u_2(e_{2i}) \in [0, 1]$.

Coupling degree of the system: At initial time t_0 , the order degree of the tourism system is set as $u_1^0(e_1)$ and that of the regional ecological environment system is set as $u_2^0(e_2)$. When the system evolves to time t_1 , the order degree of the tourism system is set as $u_1^1(e_1)$ and that of the regional ecological environment system is $u_2^1(e_2)$. If $u_1^1(e_1) \geq u_1^0(e_1), u_2^1(e_2) \geq u_2^0(e_2)$ can be true at the same time, then the tourism and regional ecological environment systems can be regarded as coupled development, and the cou-

pling degree model is as follows:

$$c = sig(\bullet) \sqrt{|u_1^1(e_1) - u_1^0(e_1)| |u_2^1(e_2) - u_2^0(e_2)|} \quad \dots(4)$$

In which:

$$sig(\bullet) = \begin{cases} 1, u_1^1(e_1) \geq u_1^0(e_1) \text{ and } u_2^1(e_2) \geq u_2^0(e_2) \\ -1, u_1^1(e_1) < u_1^0(e_1) \text{ or } u_2^1(e_2) < u_2^0(e_2) \end{cases} \quad \dots(5)$$

As indicated in Formulas (4) and (5), a high degree of coupling can only be realized when the tourism and regional ecological environment systems are in an orderly state. If the orderly degree of one subsystem considerably increases but that of the other subsystem slightly increases or decreases, then the entire tourism industry-regional ecological environment will be affected. Achieving a good coupling state is impossible for a composite system.

EMPIRICAL RESEARCH

Through the standardization of the original data, the calculation is conducted according to Formulas (1) to (4), and the settlement results are shown in Fig. 2. As shown in the figure, the subsystems of tourism and the ecological environment in Henan Province from 2010 to 2016 showed an overall steady upward trend. Among the subsystems, the rising trend was evident (from 0.024 in 2010 to 0.862 in 2016). In recent years, cities in Henan Province have focused on strengthening the development of the tourism industry, using the regional economy to drive the development of tourism-related industries, conducting in-depth excavations, and developing local tourism resources to increase the attractiveness of tourism. This can effectively promote the orderly development of the tourism subsystem itself. The orderliness of the ecological environment subsystem in Henan Province increased from 0.070 in 2010 to 0.770 in 2016, and the environment was effectively improved. However, the orderliness of the ecological environment subsystem in 2016 was lower than that of the tourism subsystem, which indicates that further improvement of the ecological environment in Henan Province is still needed, and it cannot effectively support Henan Province. The gradual improvement of the orderliness of eco-environmental subsystems shows that Henan Province has attached great importance to the eco-environment in recent years and strengthened the protection of the eco-environment, which has produced good results. The eco-environment has been effectively protected through the continuous improvement and maintenance of eco-environment development. With the acceleration of the urban process, sustained and rapid development of tourism economy, and change in tourism consumer demand, the pressure on

the ecological environment increases. Henan Province should further formulate policies for the development of tourism, and protect the ecological environment well, and promote the further improvement of the orderliness of the ecological environment subsystem.

On the basis of the order degree of tourism and eco-environment subsystems, the coupling degree of tourism-regional eco-environment complex system is calculated according to Formula (5), as shown in Table 1.

As shown in Table 1, the coupling degree of tourism and ecological environment in Henan Province from 2011 to 2016 showed an upward trend from 0.169 in 2011 to 0.766 in 2016. A particularly large increase was noted in 2013. In recent years, Henan Province has increased the protection and improvement of the ecological environment and focused on building an environment-friendly eco-tourism system while enhancing the economic growth of tourism and the ecological environment. By planning, integrating, and modifying the natural landscape and beautifying the ecological environment, Henan Province has produced various tourism products and designed distinctive tourism projects to reduce the destruction of the ecological environment, and beautify the natural landscape, and promote the quality of the tourist ecological environment and tourism.

POLICY RECOMMENDATIONS

Strengthen the assessment of the tourism environment and conduct real-time monitoring of the tourism environment:

The assessment of the environmental effects of tourism development should be strengthened, and protection of the ecological environment should be controlled at the source. Understanding the development of tourism projects is necessary to protect the ecological environment of tourist cities and scenic spots. In addition, the evaluation of the positive and negative effects and the extent of development projects on natural and man-made environments must be strengthened from all aspects; then, it can be used as an important basis for departmental decision making to strictly prohibit the development of projects that seriously damage the ecological environment. Simultaneously, the carrying capacity of the tourism ecological environment should be scientifically determined, and the development plan of tourism resources should be rationally formulated, and the eco-

logical protection of tourism resources should be reinforced, thereby avoiding human-caused damage to tourism resources. Moreover, a monitoring mechanism of the tourism environment should be established to control pollution in time. It is necessary to establish and improve the ecological management and monitor institutions of tourist cities and scenic spots, and formulate a scientific index system for ecological protection, and improve the professional and technical team for ecological protection. Lastly, advanced technical means should be used for monitoring and governance, and the ecological environment monitoring of tourist cities and scenic spots should be strengthened.

Strengthen the government's leading role in tourism development and comprehensively improve the level of tourism management:

The government should give full play to the function of macro-control, and formulate proper and feasible policies, and improve the corresponding laws and regulations. The advantages of the government should be utilized to conduct considerable market research, and forecast the tourism demand situation of various places, and adopt reasonable diversion measures to balance the tourism demand of hot and cold spots. Therefore, the occurrence of events that will damage the tourism image of Henan Province, when the tourism booms burst, can be avoided. When the demand for tourism is predicted to exceed the supply of tourism, the price can be raised, and additional fees other than the usual can be charged to effectively control the consumption of resources. Illegal operators who damage the image of the tourism market must be punished according to the law to ensure the orderly development of the tourism industry. Tourism is a highly cooperative development industry that requires government departments to play a good coupling function, do a good job of coupling between various relevant departments, and comprehensively improve the management level, thereby ensuring the smooth development of tourism, reducing unnecessary resource consumption, and promoting the sustainable development of tourism.

Implement taxing on the tourism environment and focus on the long-term benefits of tourism development:

The increasingly serious environmental problems appear to be caused by limited environmental capacity and accumulation of environmental pollution. However, these problems are in fact caused by people's obsession to satisfy immedi-

Table 1: Coupling degree of tourism and regional eco-environmental composite system in Henan Province from 2011-2016.

Year	2011	2012	2013	2014	2015	2016
Coupling degree of tourism and regional eco-environmental composite system	0.169	0.250	0.408	0.504	0.636	0.766

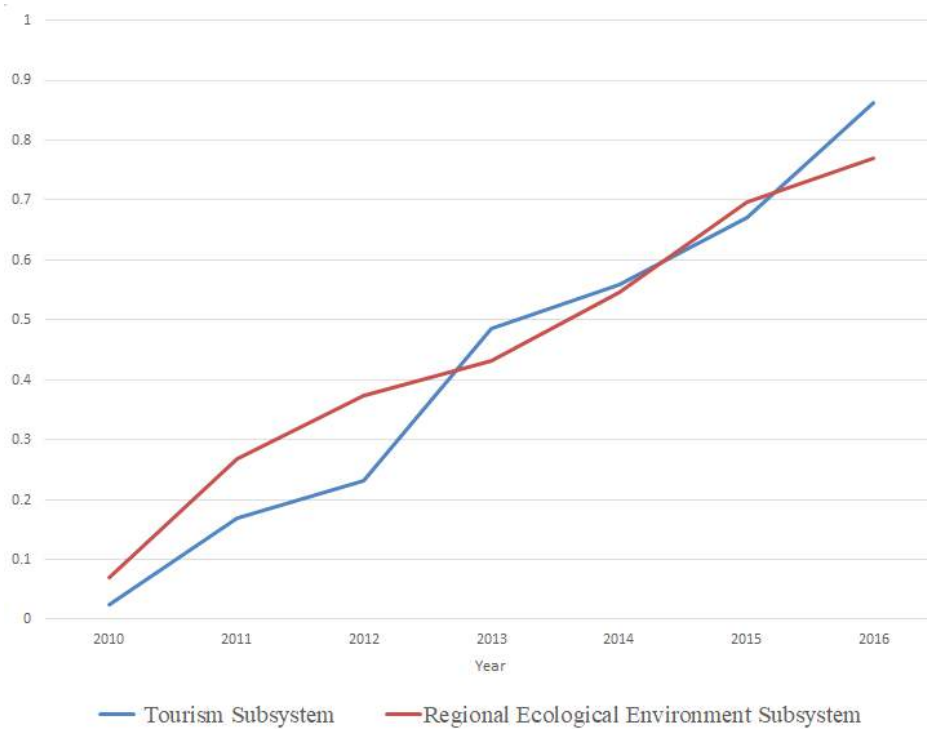


Fig. 2: Orderliness of tourism and eco-environment subsystems.

ate vested interests while ignoring the future development potential and the advancement of contemporary and future generations. Therefore, when environmental tax is used as a means to solve environmental problems, we can not only focus on the present, short-term, and contemporary efficiency and fairness, but also realize that the environmental resources we have do not belong to the contemporary people but are borrowed from future generations. Therefore, time factor, discounting time, and compound interest should be respectively considered when allocating environmental resources, and measuring the value of environmental resources, and calculating the benefits of environmental protection to realize the intergenerational equity of environmental benefits. Environmental tax may slow down economic development in the short run, but the intergenerational equity of the environment helps promote the long-term stability of economic benefits. The implementation of environmental tax is particularly important and focuses on the principle of long-term interests.

Strengthen the legislation of the tourism environment and raise public awareness of tourism environmental protection: Local governments should formulate local laws and regulations to protect the tourism ecological environment. According to relevant laws and regulations, tourism administration departments should formulate local laws and regu-

lations on tourism development and ecological environment protection, and gradually set up ecological law enforcement teams, and publicize the ecological legal system. These departments should also punish acts of destroying the ecological environment to promote ecological protection into the track of the legal system. Furthermore, the government should improve people's understanding of eco-environmental protection in tourist cities and scenic spots. The government should also use new and traditional media to disseminate knowledge on human beings, the environment, and development to the public as well as legal and technological knowledge on environmental protection so as to increase public awareness of environmental protection. Tourist environmental protection education in tourism can enhance tourists' awareness of environmental protection. Moreover, it can reduce the damage to the ecological environment by tourists by setting up corresponding explanations of the ecological environment landscape, and reminding tourists to focus on environmental hygiene signs, and facilitating an environment-coupled waste collection system.

Speed up the transformation and upgrading of the tourism industry and improve the mechanism of tourism ecological compensation: The supply of tourism products should be optimized (changed from sightseeing to experi-

ential tourism) to realize the transformation and upgrading of tourism, and tourism products with minimal pollution and improved experience, such as rural, agricultural, ecological, cultural, and medical tourism, should be vigorously developed. Well-known tourist attractions are cultivated and diverted during holidays to prevent a large number of tourists from pouring into the same scenic area and exceeding the carrying capacity of the scenic area. Henan Province has rich cultural connotations in the development of tourism derivatives. We should fully tap this culture and develop cultural derivatives, such as tourism performances and tourist souvenirs. The effective development of tourism activities cannot be separated from the guidance of tourism policies and the norms of tourism laws and regulations. Tourism is a comprehensive industry involving various industries; therefore, additional laws and regulations are needed to clarify the responsibilities of all parties. In addition, the construction of the tourism legal system should be perfected, and acts that destroy the ecological environment in the process of tourism development and tourism management should be punished, and the behaviours of people should be effectively standardized to create a good tourism environment. Lessons should also be drawn from the ecological compensation experience of other provinces, and the eco-environmental defenders of tourism should be compensated by means of taxation, financial subsidies, and policy support. Only in this way can the tourism industry consider ecological, social, and economic benefits and achieve sustainable development.

CONCLUSIONS

With the rapid development of the tourism industry of China in recent years, tourism has become an important part of national life and one of the basic driving points of national economic development. However, the development of tourism activities cannot be separated from the dependence on resources. The unbalanced level of energy consumption and environmental protection in the tourism industry has become an important factor that affects the coordinated development of tourism and the ecosystem. Taking Henan Province as an example, this study constructs a comprehensive evaluation system for the coupling degree between the tourism industry and regional ecological environment system and uses the coupling model to analyse the coupling status of the tourism industry and regional ecological environment system in Henan Province. The results show that the orderliness of the eco-environment subsystem in Henan Province is less than that of the tourism subsystem, indicating that further improvement of the eco-environment is still required. The coupling degree between tourism and the ecological environment increased from 0.169 in 2011 to 0.766 in 2016, and a particularly large increase occurred in 2013.

This study also proposes policy suggestions, such as strengthening tourism environment assessment, reinforcing the leading role of the government in tourism development, implementing tourism environment tax collection, strengthening tourism environment legislation, and accelerating the transformation and upgrading of the tourism industry. In the future, we can continue to study the determination of the factors that affect the tourism ecological environment, the construction of an index system for the carrying capacity of the ecotourism environment, and the establishment of a sustainable development model for the ecotourism area. Quality evaluation of the tourism ecological environment and application of high technology in the management of the tourism environment are also worth investigating.

REFERENCES

- Amir, S., Osman, M.M. and Bachok, S. 2015. Sustaining local community economy through tourism: Melaka UNESCO World Heritage City. *Procedia Environmental Sciences*, 443-452.
- Budeanu, A., Miller, G. and Moscardo, G. 2016. Sustainable tourism, progress, challenges and opportunities: An introduction. *Journal of Cleaner Production*, 285-294.
- Butler, R.W. 1991. Tourism, environment, and sustainable development. *Environmental Conservation*, 18(3): 201-209.
- Carrillo, M. and Jorge, J.M. 2017. Multidimensional analysis of regional tourism sustainability in Spain. *Ecological Economics*, 140: 89-98.
- Dvarskas, A. 2017. Dynamically linking economic models to ecological condition for coastal zone management: Application to sustainable tourism planning. *Journal of Environmental Management*, 188: 163-172.
- Fadafan, F.K., Danehkar, A. and Pourebrahim, S. 2018. Developing a non-compensatory approach to identify suitable zones for intensive tourism in an environmentally sensitive landscape. *Ecological Indicators*, 87: 152-166.
- Hunter, C. 2002. Sustainable tourism and the touristic ecological footprint. *Environment, Development and Sustainability*, 4(1): 7-20.
- Bithas, Kostas, Peter Nijkamp and Anastasios Tassopoulos 1997. Environmental impact assessment by experts in cases of factual uncertainty. *Project Appraisal*, 12(2): 70-77.
- Law, A., De Lacy, T. and Lipman, G. 2016. Transitioning to a green economy: The case of tourism in Bali, Indonesia. *Journal of Cleaner Production*, 295-305.
- Li, H.Q. and Hou, L.C. 2021. Vulnerability evaluation of tourism eco-environment in reservoir area: case study on Danjinagkou in Hubei Province. *Environmental Science & Technology*, 35(7): 191-196.
- Madan, S. and Rawat L. 2000. The impacts of tourism on the environment of Mussoorie, Garhwal Himalaya, India. *The Environmentalist*, 20(3): 249-255.
- Mbaiwa, J.E. 2003. The socio-economic and environmental impacts of tourism development on the Okavango Delta, north-western Botswana. *Journal of Arid Environments*, 54(2): 0-467.
- Morrison, P. and Selman, P. 1991. Tourism and the environment: A case study from Turkey. *Environmentalist*, 11(2): 113-129.
- Sun, D. and Walsh, D. 1998. Review of studies on environmental impacts of recreation and tourism in Australia. *Journal of Environmental Management*, 53(4): 323-338.

- Tamayo, N.C.A., Anticamara, J.A. and Acosta-Michlik, L. 2018. National estimates of values of Philippine Reefs' ecosystem services. *Ecological Economics*, 146: 633-644.
- Yuan, Y.Q., Jin, M.Z. and Ren, J.F. 2014. The dynamic coordinated development of a regional environment-tourism-economy system: A case study from western Hunan Province, China. *Sustainability*, 6(8): 5231-5251.
- Zhao, M.F., Xi, J.C. and Liu, S.H. 2014. Simulating the saturation threshold of a water environment's response to tourist activities: A case study in the Liupan mountain eco-tourism area. *Journal of Mountain Science*, 11(1): 156-166.



Improved Bacterial-Fungal Consortium as an Alternative Approach for Enhanced Decolourisation and Degradation of Azo Dyes: A Review

Arunkumar Mani† and Sheik Abdulla Shahul Hameed

Department of Chemistry & Biosciences, Srinivasa Ramanujan Centre, SASTRA Deemed University, Kumbakonam, Tamil Nadu-612001, India

†Corresponding author: Arunkumar Mani

Nat. Env. & Poll. Tech.
Website: www.neptjournal.com

Received: 22-06-2018
Accepted: 02-08-2018

Key Words:

Bacterial-fungal consortium
Strain development
Biodecolorization
Biodegradation
Azo dyes
Oxidoreductive enzymes

ABSTRACT

Over the past five decades, the Indian textile industries have increasingly become a major user of azo dyes due to their wide range of applications. India is considered as one of the second largest producers of textiles in the world. Due to the rapid increase in the production rate of fabrics, the textile industry generates a huge amount of dyestuff and dyes in the environment. Continuous discharge of wastewater into the environment creates various types of pollution and also health impact on human beings. Azo dyes are toxic aromatic man-made compounds, which cannot be easily degraded by the indigenous microbes, and thus persist in ecosystems over a long period of time. In the current scenario, most wastewater treatment plants are obsolete and especially physico-chemical methods failed to achieve the satisfactory result because they are more expensive and produce a huge amount of sludge which again causes the secondary disposal problems. So, there is an urgent need to develop an alternative method to improve the degradation of azo dyes in an eco-friendly manner with low cost. In order to achieve the higher degradation efficiency in bioremediation technology, the present review mainly focuses on three important factors such as strain development for hyper-production of oxidoreductive enzymes by random mutagenesis, development of bacterial-fungal consortium and reusability of microbial cell cultures. Additionally, this review also compiles the effect of various physico-chemical conditions in decolourisation and degradation of azo dyes.

INTRODUCTION

Dyes are considered as complex organic substances, which give a wide range of colours to substrates when applied to them. They firmly get attached to the substrate by physical adsorption, chemical modification or by the covalent linkage (Kirk-Othmer 2004 & Bafana et al. 2011). Dyes consist of two important compounds, they are chromophore and auxochrome. The colour property of dyes depends on the chemical constituents of dyes and their absorption ability for the visible light. But, according to the Witt theory, the colour of the dye is due to the presence of chromophores, whereas the modern electronic theory states that the colour changes occur due to the excitation of the valance electrons (Murrell 1973).

Historical view about dyes: Natural dyes have been used by the mankind since ancient times or Neolithic period, which took place around 10,200 BCE. These dyes were made by using natural pigments obtained from the plant extracts, insects, sea animals and minerals (Kadolph 2008). The man lived in that age mixed the dyes with solvents and used them for the painting on caves, skin, jewellery and clothes. Nearly, 40,000 years ago during the New Stone Age period,

the yellow and blue colours were considered as the most common one obtained from the plant sources. The types of natural dyes and their sources are presented in Table 1.

Rise of synthetic dyes and the current situation of dying industries in India: The first artificial dye “mauve” was accidentally identified by W. H. Perkin in 1856, which gives a permanent colour when applied to the fabrics. Further, these dyes are highly stable and do not undergo fading even by the exposure to radiation, water, various chemicals and microbial degradation (Rai et al. 2005). In the recent past, original dyes obtained from natural sources have been completely modified by the artificial dyes as the former are highly expensive, less applicability and tend to fade quickly. Over the past five decades, 10,000 artificial dyes have been synthesized worldwide and used for the different applications (Robinson et al. 2001). Currently, the European countries have established many dyeing industries and are able to produce 40% of dyestuff, annually. These dying industries discharge huge amount of effluents into water bodies. Moreover, the water discharged from the textile industries is quite resistant to microbial attack due to unfavourable pH, organic and inorganic matters, and it also contains a

Table 1: Different sources of natural dyes.

S.No	Natural Dyes	Color	Sources
1	Indigo	Deep blue	Obtained from the Dyer's Woad herb (leaves), <i>Isatis tinctoria</i> , <i>Indigofera tinctoria</i>
2	Tyrian Purple	Purple	Glands of snails
3.	Alizarin	Red	Extracted from the madder plant
4.	Carthamin	Yellow	Extract obtained from the flowers of <i>Carthamus tinctorius</i> and weld (leaves) and oak tree (bark)

Table 2: Society of Dyers and Colorists (SDC) classify the azo dyes in colour index (CI) based on the structural complexity.

S.No.	Azo dyes based on chemical structure	Color Index (CI)
1.	Monoazo	11000-19999
2.	Bis-azo	20000-29999
3.	Tri-azo	30000-34999
4.	Polyazo	35000-36999
5.	Azoic	37000-39999

mixture of different types of dyes (Banat et al. 1996). Worldwide, it was reported that 2,80,000 tons of treated or untreated effluents were discharged onto the land or in water every year (Jin et al. 2007). In India, the dye industry grew rapidly for the past 50 years due to the high demand for fabrics. Nevertheless, Gujarat is considered the first leading producer of dyestuff, whereas Mumbai and Tiruppur are the second most producers. Over the past 50 years, the number of bleaching and dyeing units in Tiruppur have considerably increased and currently, the town has established 728 dyeing units out of which 430 units are in operation (Fig. 1). It is estimated that 80,000 tons of dyestuff and pigments are produced every year in India (Marimuthu et al. 2013). The effluents discharged from the dyeing industries contain 2% of dyes, which have been released during the dyeing process. Till 1977, the untreated effluents from the textile industries have been discharged into Noyal River that caused a severe environmental pollution in and around Tiruppur region. To solve this problem, the Tamil Nadu Pollution Control Board (TNPCB) established several Common Effluent Treatment Plants (CETPs), which use physical, chemical and biological methods to eradicate the dye-containing wastewater released from the textile industries. However, these methods failed to achieve satisfactory results to remove completely the structurally different dyes from effluents and also produce the secondary disposal problems.

Classification of synthetic dyes: Generally, the dyes have been classified in two ways based on their structural complexity (nature of chromophores) and their mode of application on fabrics. Based on the nature of chromophores and chemical classification system, the dyes are classified into Acridine dyes, Anthraquinone dyes, Aryl methane dyes,

Triarylmethane dyes, Azo dyes, Cyanine dyes, Diazonium dyes, Nitro dyes, Nitroso dyes, Phthalocyanine dyes, Quinone-imine dyes, Azin dyes, Xanthene dyes, Indophenol dyes, Oxazin dyes, Safranin dyes, Thiazin dyes, Thiazole dyes, Fluorene dyes and Rhodamine dyes. Similarly, based on their mode of applications these dyes have been classified as Reactive dyes, Acid dyes, Basic dyes, Direct dyes, Mordant dyes, Disperse dyes, Vat dyes, Sulphur dyes and Solvent dyes. Azo dyes are predominantly utilized as a dyeing agent in textile industries due to their wide range of applicability. Until 2001, there was no proper nomenclature system to classify the dyes, but presently the Generic Name and Colour Index have been compiled to each dye by the Society of Dyers and Colorists (SDC) and the American Association of Textile Chemists and Colorists (AATCC).

Azo dyes: Azo dyes are synthetic compounds and have been mostly used in different fields, especially in textile industries. As they are very stable, require very less amount for production and generate a wide variety of colours, which accounts for 60-70% of total synthetic dyes (Yingying et al. 2016). Azo dyes have a complex structure with high molecular weight compounds and contain one or more azo bond (-N=N-), which has the ability to absorb light in the visible spectrum of range 400-700 nm (Chang & Kuo 2000). The first azo dye synthesis was started in the year 1861 by Mene (Aniline Yellow) and followed by Martius in 1863 (Bismarck Brown). The modern azo dyes are synthesized by two-step reactions in which during the first step the aniline is used as a derivative for the synthesis of an aromatic diazonium ion, and in the next step, diazonium salt is coupled with an aromatic compound (Fig. 2).

The American Association of Textile Chemists and Colorists (AATCC) classify the azo dyes based on the chemical constituent or by the colour. According to the colour index system, azo dyes are specifically assigned in the range of 11000 to 39999 based on the structural variation and chemical nature of the dyes (Table 2).

Persistent nature of azo dyes: Azo dyes are xenobiotic organic compounds, which cannot be easily degraded by the chemical, light or even by the microbial attack (Zeenat et al. 2014). These dyes are highly recalcitrant in nature due to

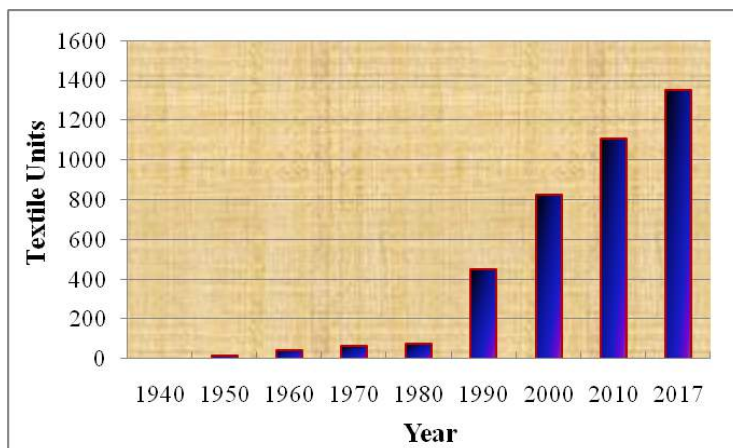
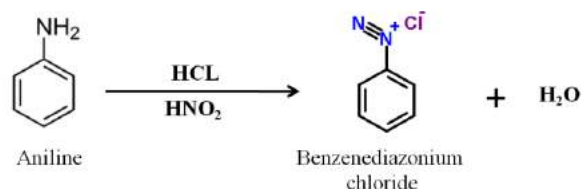


Fig. 1: Number of bleaching and dyeing units in Tirupur (1940-2017).

Step -1: Synthesis of aromatic diazonium ion



Step -2: Diazonium salt coupled with an aromatic compound

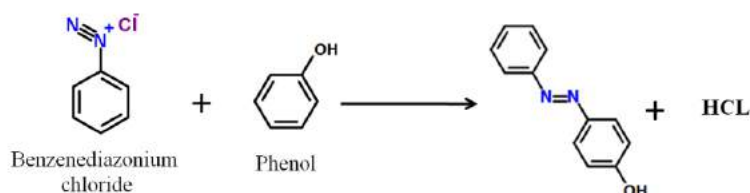


Fig. 2: Synthesis of modern azo dyes.

the presence of one or more azo bond (Anjaneya et al. 2013) and sulphonic ($-\text{SO}_3^-$) electron-withdrawing group (EWG). Sulphonated azo dyes readily obtain electrons from the nearest orbit and generate electron deficiency in the molecules; thereby it provides more stable azo compounds which are found to be more resistant to the oxidative catabolism of microbes (Akpanand & Hameed 2013). Further, the azo dyes containing an EWG in an ortho position are more stable than the azo dyes that have an EWG at the para position. This effect is called a “meta effect” and it could be due to the steric hindrance of the substitute molecules near to the azo bond. Indeed, the azo dyes combined with a different substituent and additionally with one or more sulphonic compounds make them highly persistent to the aerobic environmental conditions.

Impact of azo dyes: Among all the industrial sectors, textile industries are considered as one of the leading polluters of environment due to the release of a large amount of treated and untreated dyes in wastewater. Unfortunately, it is estimated that 2,00,000 tons of dyestuff are released into the environment every year. Azo dyes are dispersed in untreated or improperly treated effluents and their toxic products generated during the partial degradation are discharged into the water bodies that causes unpleasant odour which leads to abnormal changes in the quality of water. Further, it generates mutation of aquatic plants and small animals, and causes acute toxicity to them (Vandevivere et al. 1998). The products obtained after the anaerobic degradation of azo dyes using microorganisms lead to the formation of aromatic amines, which is resulted to have a toxic effect on

Table 3: Physico-chemical treatment methods for azo dye.

Physical/chemical treatment methods	Material used	Advantages	Disadvantages
Coagulation-flocculation	Mg salt, Ferric chloride, and chitosan	Simple and economically feasible	A large amount of Sludge generation
Electrocoagulation	Metal ions (Fe or Al)	-	The high cost of electricity, inefficiency technique
Adsorption	Activated carbon, chitosan, fruit peels, wood chips and alginate	Effectively remove the dyes from the effluent	High cost, requires long retention times
Ion exchange	Calyx arene-based polymer	Routinely used without changing the adsorbent	Dye removal occurs only for specific dyes
Irradiation	Gamma and electron beam radiation	Much effective only for small-scale industry	A huge amount of dissolved O ₂ is required
Membrane filtration	Ultrafiltration and nanofiltration	Removes all type of dyes	Concentrated sludge production
Ozonation	O ₃	High oxidation potential, applied in gaseous state: no alteration of volume	Short half-life (20 min)
Redox-active metals	Fenton reagent (H ₂ O ₂ -Fe(II))	More efficiently remove the color from both soluble and insoluble dyes	The problem in the disposal of sludge
Photochemical treatment	UV rays	Sludge formation was not	Toxic metabolite production, found inefficient in color removal
Electrochemical destruction	Lead dioxide, and boron-doped diamond	Breakdown compounds are non-hazardous and no sludge formation	High cost of electricity and very poor color removal

aquatic ecosystems and even have carcinogenic and mutagenic effects on the organisms (Pinheiro et al. 2004). Besides, an azo dye such as metanil yellow, is found to have hepatotoxicity effect in albino rats (Singh et al. 1988). Nevertheless, in most literature survey it is reported that the continuous exposure of azo dyes on human beings lead to the causes of bladder cancer and also severe damage to the vital organs (Isken et al. 2007). In this review, the primary investigation was carried out to characterize the azo dyes discharged from textile industries and their impact on the environment. In order to achieve high degradation efficiency in bioremediation technology, we focus on three important factors such as strain development through random mutagenesis, development of bacterial-fungal consortium and reusability of microbial cell cultures. Additionally, this review also compiles different strategies to develop optimal parameters for the effective bioremediation of azo dyes.

TREATMENT METHODS OF AZO DYE CONTAINING WASTEWATERS: PAST, PRESENT AND THE FUTURE

Treating azo dye-containing effluents these days has been found to be difficult because azo dyes are xenobiotic compounds having a high complex aromatic molecular structure with different substitutions. It is estimated that 2-50% of dyestuff was released into the environment as wastewater from the textile industries (McMullan et al. 2009). Several

methods have been employed to eradicate the azo dyes from the industrial effluents and they can be broadly classified into three categories such as physical, chemical and biological methods.

Physical and chemical treatments: Over the past three decades, conventional physico-chemical methods have been widely employed to minimize the level of azo dyes present in the effluents. Physical methods such as coagulation-flocculation (Fang et al. 2013), electrocoagulation (Eyvaz et al. 2009), adsorption (Seo et al. 2010), ion exchange (Royer et al. 2010), irradiation (Hosono et al. 1993), ultrasound (Eren & Ince 2010) and membrane filtration (Uzal et al. 2010) were effectively used to remove the dyes from wastewaters. Similarly, the different kinds of chemical treatment methods were also in practice to remove the dyes using the techniques such as ozonation (Santana et al. 2009), sodium hypochlorite (Li et al. 2009), redox-active metals (Gomathi et al. 2009), photochemical treatment (Wang et al. 2010) and electrochemical destruction (Wang 2008 et al. 2008). Recently, among all the chemical methods, advanced oxidation processes (AOPs) are found to be effective methods to remove the dyes with the aid of hydroxyl radicals as strong powerful oxidizing agents. Merits and demerits of the physico-chemical techniques for the removal of dyes from the industrial effluents are presented in Table 3.

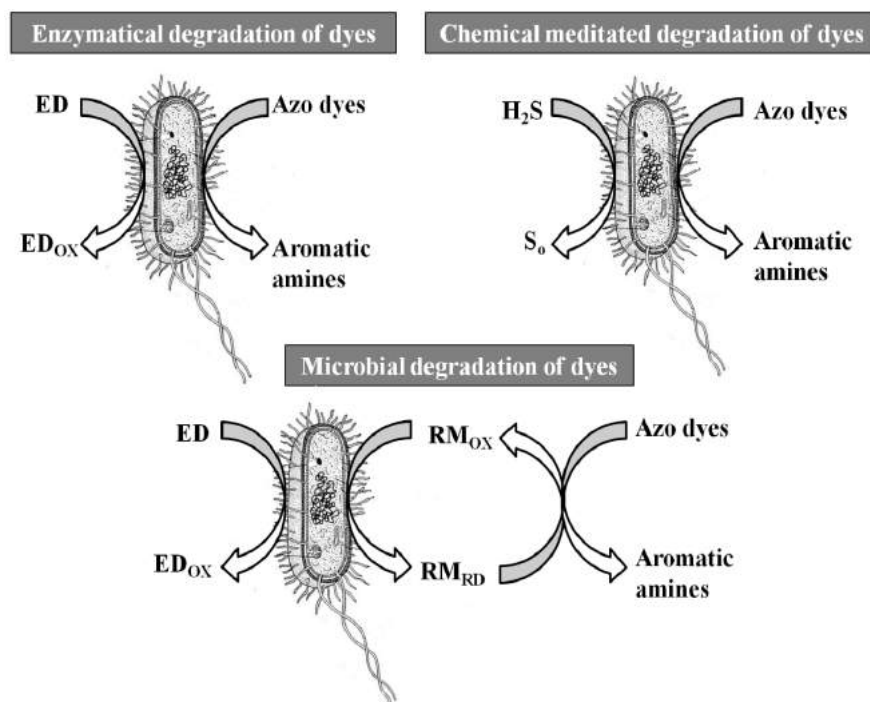


Fig. 3: General mechanism of azo dye degradation.

Biological treatment: “Bioremediation” is a process by which toxic nature of azo dyes is converted to non-toxic by the microbial processes. In the present scenario, using the microbes for treatment of dye polluted water is often considered as an eco-friendly technology when compared with the conventional methods (Liu et al. 2015). Nowadays, extensive research is carried out on biological methods due to their efficiency, low cost, less sludge generation and eco-friendly nature (Liang Tan et al. 2016). Complete detoxification of pollutants can be achieved in the microbial degradation process which results in the reduction of secondary pollution. In order to improve the treatment method feasibly effectively for azo dye polluted water, it is much important to find out new potent azo dye-degrading microbial strains and their mechanisms involved in dye degradation process. Several microorganisms have been intensively used in decolourisation of azo dyes, such as Gram-positive and Gram-negative bacteria (Moosvi et al. 2005), fungi (Miranda et al. 2013), yeast (Song et al. 2017) and algae (Mostafa et al. 2009).

Bacteria and fungi: Bacteria are widely used in bioprocess technology to eradicate the dye-containing pollution due to their variability, adaptability, high activity and cost-effectiveness. Azo dye degradation initially begins with the breakage of the azo bond, aided by azoreductase produced from the bacteria in an anaerobic condition. Nevertheless,

the resulting products formed during anaerobic degradation are aromatic amines, which are highly mutagenic and carcinogenic. These aromatic compounds are further converted into non-toxic molecules by the enzymatical action of hydroxylase and oxygenase produced by certain bacteria (Pandey et al. 2007). Mixed azo dyes present in the effluent could not be easily degraded by the single microbial strain. Further, azo dyes containing a sulphonic compound with strong anionic nature, are found to be more resistant to the bacterial attack and the intermediates formed during decolourisation can also inhibit the activity of bacteria. Considering the aforesaid drawback, the strain development is much required for bioremediation process to improve the activity of enzymes present in the bacteria. In contrast, several fungal biomasses have been reported in the recent literature to effectively degrade the azo dyes by secretion of extracellular oxidoreductive enzymes, including manganese peroxidase (MnP) and laccase (Tan et al. 2013). These days white rot fungi has received much attention in the field of bioremediation technology because it has strong adaptability and has the ability to degrade the phenolic compounds. Generally, the metabolites obtained after the bacterial degradation of azo dyes under anaerobic conditions are found to be toxic and can be converted to nontoxic only by the fungal system (Qu et al. 2012). Fungal cells have the ability to degrade the azo dyes by absorption or by the enzyme

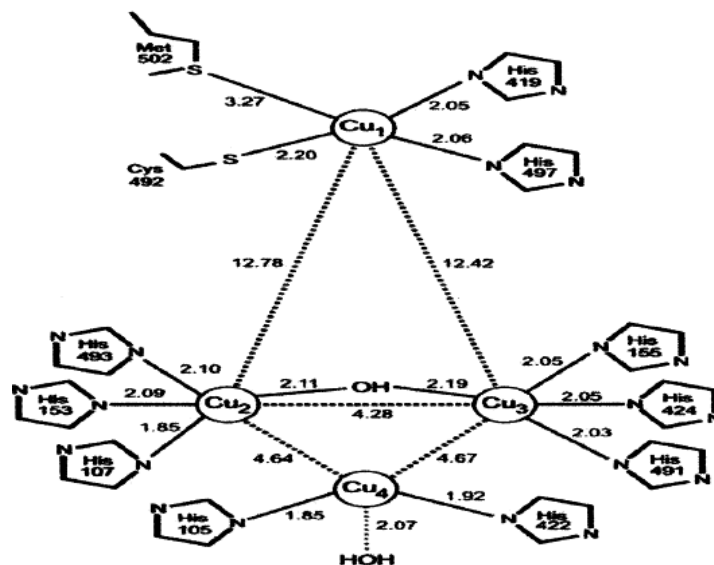


Fig. 4: Structure of laccase.

synthesized by them. Nevertheless, these enzymes could not degrade all types of azo dyes effectively. To establish effective bioprocess technology to remove azo dyes from wastewaters, it is necessary to discover the potent microorganisms which show high enzyme activity with a wide range of substrate specificity.

MICROBIAL OXIDOREDUCTIVE ENZYMES AND THEIR IMPACT ON AZO DYE DECOLOURISATION AND DEGRADATION

In the recent past, the enzymatical decolourisation or degradation of azo dye is found to be more efficient and an alternative method for treating azo dye containing wastewater. The oxidoreductive enzymes generate a high amount of reactive free radicals that help to cleave or remove or transform the phenolic compounds present in the textile effluents. The oxidation of phenolic compounds by oxidoreductive enzymes leads to the formation of oligomeric and polymeric products. These products formed are readily precipitated and settle down due to the increase in molecular weight, which further confirm the detoxification effect of dyes.

However, the initial step of azo dye reduction is breakage of the azo bond by the bacterial action either in aerobic or anaerobic conditions. This kind of reduction may be due to the different mechanisms involved in dye degradation by the oxidoreductive enzymes, redox mediator, sulfide or a combination of these compounds. Generally, this reaction could occur either intracellularly or extracellularly of microbial cells (Fig. 3). Among all the oxidoreductive enzymes, the laccases, manganese peroxidase (MnP) and azoreductase

were seen to have a great potential for azo dye degradation (Ram et al. 2015).

Laccase (benzenediol: oxygen oxidoreductase, EC 1.10.3.2): Laccase is multicopper enzyme containing proteins with four catalytic copper atoms. The copper atoms have been placed in two sites such as T1 site and T2/T3 sites. The T1 site contains one copper atom in which substrate can bind and forms a bluish-green colour during oxidation state Cu^{2+} , whereas T2/T3 site contains a cluster of three copper atoms in which molecular oxygen readily binds to it (Jones et. al. 2015). The structure of laccase is presented in Fig. 4.

Sources: Laccase was first developed by Yoshida in 1883 from the plant extracts obtained from *Rhus vernicifera*. It is found in higher plants, fungi, bacteria, archaea and insects. The laccase from white-rot fungi has great significance in the field of biotechnology due to its higher redox potential (up to +800 mV) when compared to bacterial and plant laccases. Thus, fungal laccases have paved much attention these days in the bioremediation process for the effective degradation of aromatic amines.

Mode of action of laccase: Laccases have been greatly employed as oxidoreductive enzymes for the effective degradation of azo dyes because they have low specificity during the reduction of the substrate (Novotny et al. 2004). Further, these enzymes required NADH or redox mediator to enhance the degradation rate of azo dyes. Generally, the laccase-mediated degradation of azo dyes was performed in a step-wise manner. In the first step, the azo dyes degraded

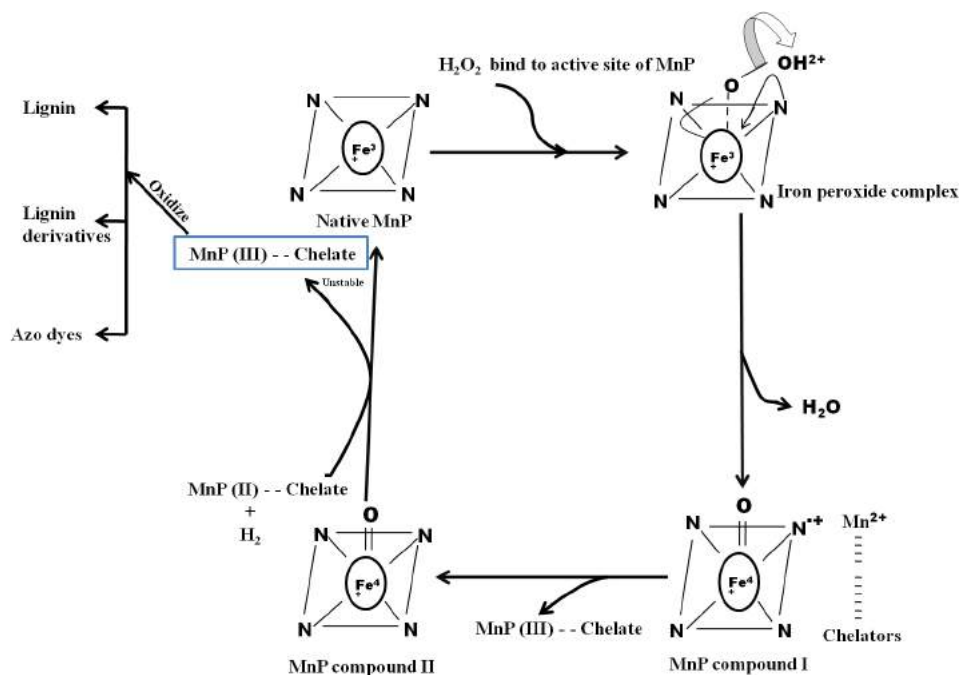


Fig. 5: Catalytic mechanism of MnP in azo dye degradation.

into phenolic compounds by the nonspecific free radical mechanism. In the second step, phenolic compounds are further oxidized to carbonium ion either by the nucleophilic attack or by the phenoxy radicals generated during the reaction. In addition, laccase is able to oxidize various non-phenolic compounds in the presence of redox mediators (Sharma et al. 2007). It is suggested that the laccases have the ability to remove hydrogen atoms from the hydroxyl group of phenolic compounds and aromatic amines (Ram et al. 2015).

Production of laccase enzyme: In the present times, the researchers have focused on the high amount of laccase production by developing the new strains or by regulating the gene expression with the presence or absence of nutrient content (Palmieri et al. 2000). The presence of inducers such as redox mediator, aromatics and phenolic compounds bind to microbial cells, thereby enhancing the laccase production via stress response (De Souza et al. 2004). Many factors influence the level of laccase production such as types of cultivation method (solid-state or submerged), reactor or fermentor, the chemical composition of the nutrient and trace elements present in the cultivation medium. Nearly more than 100 laccases were isolated from the different sources of microorganisms. Nevertheless, the isolated enzymes are found to be similar in structural and functional properties but they are not thermostable and have very fewer

activities towards the substrates. Therefore, most researchers have focused on to obtain novel laccases which have the higher stability to the various temperatures and also to possess high enzyme activity against the wide ranges of the substrate (Li-Qiong et al. 2011).

Azo dye degradation by laccases is a well-studied phenomenon; the reduction of organic dyes in the presence of laccase is considered as an effective method to remove the phenol containing aromatic compounds. Recently, several microorganisms have been employed for the degradation of azo dyes by using laccase as a catalysing agent (Table 4). Although the laccase has a wide range of substrate activity and low specificity, it takes much longer time for the process of dye degradation. To overcome this issue and to improve the bioprocess technology, the redox mediators such as veratryl alcohol (VA), 1-hydroxybenzotriazole (HBT), acetosyringone (AS) and 4-hydroxybenzoic acid (HA) have been extensively used by many researchers to improve the rate of degradation of dyes. The production of laccases in microorganisms is regulated by the nutrient types, amount of nutrients, strain, inducers and substrates (Palmieri et al. 2000). Nevertheless, the proper investigation is still required to improve the strain for effective degradation of azo dyes by using laccase as a catalysing agent.

Manganese Peroxidase (MnP; EC 1.11.1.13): MnP is a special kind of enzyme that belongs to the family of versa-

Table 4: Degradation of azo dyes using laccase as a catalyzing agent.

S.No	Microbial culture	Name of the dyes	% Decolorization	Time (h)	Factors influence laccase production	References
1	<i>Bacillus pumilus</i> W3	Reactive red 11	96	5	Methylsyringate (0.1%)	(Zheng-Bing et al. 2014)
		Reactive blue 171	95	5		
		Reactive blue 4	90	5		
		Reactive brilliant blue	91	5		
2	<i>Trichoderma</i>	Malachite green	100	16	1-hydroxybenzotriazole (HBT) (2 mM)	(Zabin et al. 2017)
		Methylene blue	90	18		
		Congo red	60	20		
3	<i>Marasmiellus palmivorus</i>	Reactive Blue 220	90	24	-	(Camila et al. 2017)
		Acid Green 28	75	24		
4	<i>Spirulina platensis</i> CFTRI	Remazol Brilliant Blue R	90	48	Syngaldehyde (0.1mM)	(Afreen et al. 2017)
5	<i>P. ostreatus</i> MTCC 142	Congo red	37	20	-	(Das et al. 2016)

Table 5: Taxonomic classification of *Pleurotus ostreatus*.

Domain	Eukarya
Super-group	Opisthokonta
Kingdom	Fungi
Phylum	Basidiomycota
Class	Agaricomycetes
Order	Agaricales
Family	Pleurotaceae
Genus	<i>Pleurotus</i>
Species	<i>ostreatus</i>

tile peroxidases (VPs) produced by several white rot fungi and plants (Moreira et al. 2005). This extracellular enzyme was first identified from *Phanerochaete chrysosporium* in 1983. MnP is a haeme-containing glycoprotein (MW 4 20-65 kDa) and initiate the catalytic reaction only in the presence of H₂O₂ and cofactors such as Mn²⁺ (Asgher et al. 2008). MnP catalytic reaction of azo dye degradation occurs in a step-wise manner in which H₂O₂ binds to the active site of the enzyme and then oxidized to form a Mn²⁺. In the second step of the cyclic reaction, the Mn²⁺ is further oxidized to unstable Mn³⁺ which in turn chelated with the organic acid, especially with oxalate molecule. Mn³⁺ or chelated Mn³⁺ was able to oxidize wide range of substrates such as lignin, phenolic compounds and azo dyes due to its less specificity (Fig. 5). The remarkable potential of MnP gained more interest in modern biotechnology due to its wide range of applications in biopulping, biobleaching and bioremediation.

White-rot fungi: White-rot fungi are Basidiomycetes capable of producing unique extracellular peroxidases LME (Lignin Modifying Enzymes) such as laccase, MnP and lignin peroxidases, which have great potential to

decolourize/degrade/mineralize the wide range of toxic organic pollutants due to the broad spectrum of specificity in attacking the substrates (Cerniglia 1997). Recently, a vast number of white-rot fungi such as *Trametes versicolor*, *Phanerochaete chrysosporium*, *Irpex lacteus*, *Ceriporiopsis subvermispora*, *Dichomitus squalens*, *Ganoderma lucidum* and *Pleurotus ostreatus* have been employed to degrade the lignin and toxic azo dyes. In contrast, *Pleurotus ostreatus*, the oyster mushroom, is an easily available mushroom which predominantly releases LME during the degradation process of azo dye. The researchers have paved more attention to this fungus and their enzyme system due to its potential applications in bioremediation technology (Marco-Urrea et al. 2009). The taxonomical classifications of *P. ostreatus* have been summarized in Table 5. However, not much attention was given to the characterization of the extracellular enzymes (MnP) produced by the *P. ostreatus* and their effectiveness in the azo dye degradation.

Azoreductase (also known as Azobenzene reductase EC 1.7.1.6): Azoreductase is a key enzyme produced by azo dye degrading microorganisms, especially bacteria and fungi. It has the ability to decolourize the azo dyes by the reductive cleavage of an azo bond (HN=NH) in anaerobic conditions with the release of toxic aromatic compound (Pandey et al. 2007). This toxic aromatic compound is further oxidized to a non-toxic molecule in an aerobic condition by the other microorganisms (Stolz 2001). Azoreductase increases the catalytic reaction only in the presence of reducing molecules such as NADH, NADPH and FADH₂. The reduction reaction occurs in the cell membrane of bacteria by gaining electrons from the reducing molecules. Over the past few decades, the intensive research has been carried out by most of the researchers to demonstrate theoretically

Table 6: Catalytic activity of bacterial azoreductase on azo dyes decolorization.

S.No	Bacteria	Azo dyes and its concentration (mg/L-1)	% Decolorization	Time (h)	References
1	<i>Pseudomonas</i> species	Remazol black (100) Methyl orange (100) Benzyl orange (100)	75 79 83	24 24 24	(Tuttolomondo et al. 2014)
2	Bacterial consortium - (<i>Microbacterium</i> sp., <i>L. albus</i> , <i>Klebsiella</i> sp. and <i>S. arlettae</i>)	Disperse Red 1 (100)	80	60	(Franciscona et al. 2015)
3	<i>Bacillus</i> sp. strain CH12	Reactive Red 239 (100)	95	96	(Guadie et al. 2017)
4	<i>Comamonas</i> sp. UVS	Direct Red 5B (50)	78	6	(Jadhav et al. 2008)
5	<i>P. aeruginosa</i>	Reactive Blue (500)	48	80	(Bhatt et al. 2005)
6	Mutant <i>Bacillus</i> sp. ACT2	Congo Red (1000)	30	24	(Gopinath et al. 2009)
7	<i>Proteus</i> sp.	Congo Red (200)	67	48	(Perumal et al. 2012)
8	<i>Micrococcus glutamicus</i> NCIM 2168	Reactive Green 19 (50)	100	42	(Saratale et al. 2009)
9	Microbial consortium (white-rot fungus 8-4 and <i>Pseudomonas</i> 1-10)	Direct Fast Scarlet 4BS (50)	99	24	(Fang et al. 2004)
10	Bacterial consortium - (<i>A. faecalis</i> , <i>Sphingomonas</i> sp. EBD, <i>B. subtilis</i> , <i>B. thuringiensis</i> & <i>E. cancerogenus</i>)	Direct Blue-15 (50)	92	24	(Kumar et al. 2009)
11	Bacterial consortium - (<i>Citrobacter freundii</i> (2 strains), <i>Moraxella osloensis</i> , <i>P. aeruginosa</i> and <i>P. aeruginosa</i> BL22)	Mordant Black 17 (100)	95	16	(Karunya et al. 2014)

about the structural diversity of catalytic protein performing azoreductase activity isolated from several microorganisms. Azoreductases obtained from different groups of bacteria and their effects on azo dye decolourisation are summarized in Table 6. Generally, azoreductase has been classified in two groups such as flavin dependant azoreductases (Chen et al. 2005) or flavin independent azoreductases (Blumel & Stolz 2003) based on the structure of amino acids and their functions. Further, flavin dependant azoreductases are subdivided into three groups based on the utilization of coenzymes for reduction of azo dyes such as NADH dependant or NADPH dependent or both. Although, the intracellular azoreductase expressed from the bacterial sources is not able to degrade the most of the azo dyes effectively. This problem is due to the structural complexity of the dyes and also the less specificity of the enzymes. So, there is an urgent need to search for new microorganisms and their enzymes which have broad substrate specificity. Further, the problem can be solved by using low molecular weight redox mediator which can act as an electron shuttle between the dyes and coenzymes. The azoreductase activity will be arrested if the reaction was performed under aerobic condition due to the presence of a

redox mediator. Therefore, it is necessary to identify the oxygen-insensitive azoreductase from the different bacterial sources and make use of it for efficient degradation of azo dyes in wastewater treatment. Additionally, there is only a little information available on the enzyme kinetics and the characterization of these enzymes.

STRAIN DEVELOPMENT FOR IMPROVED DECOLORISATION/DEGRADATION OF AZO DYES

Wastewater discharged from the textile industries containing different groups of azo dyes make them more resistant to microbial attack. Azo dye possesses a complex organic structure with one or more azo bond and hence, they are highly persistent in the environment for many years. A wild microbial strain cannot degrade the mixed azo dyes present in textile effluents. Therefore, it is much important to develop new strains for the effectiveness of the bioprocess technology. Nowadays, genetically modified microorganisms have been employed to eradicate the pollution in an excellent manner. Even though, microbes are considered as tiny organisms they contain a set of genes that is responsible for the production of different sort of catabolic or regulatory enzymes involved in the degradation process. Every

microbe is unique in characteristics with different metabolic regulations and produces various end products. This may be due to the alteration of the gene occurred during spontaneous mutation. Mutation is a permanent change and occurs in the base pair of DNA sequence.

Mutation is broadly classified into two types as spontaneous or induced mutation. The spontaneous mutation occurs naturally in the microbes whereas induced mutation occurs by the physical or chemical mutagens. Exposure of mutagen to the microbial cell will alter the base pair of DNA thereby it may change the pattern of amino acid sequence during protein formation. These variations of the gene may have a good or bad influence on the characteristics of microbes (Schofield & Hsieh 2003). In order to improve the productivity of enzymes from microbes with wide substrate specificity, many researchers have shown more interest in the random mutagenesis approaches. Strain development by exposing the DNA to the physical and chemical mutagenic agents offer a better opportunity to the biotechnologist for the hyperproduction of the enzyme with low cost (Lotfy et al. 2007). In random mutagenesis, mutations are induced to microbial cells by exposing them to one or more mutagenic agents such as UV irradiation, ethyl methyl sulphinate (EMS) and ethidium bromide (EtBr) for a certain period of time. The time of exposure, amount of mutagen and the distance between the microbial cells and radiation are important factors to be considered during the strain development.

In the recent past, a large number of studies have been carried out to improve enzyme production through random mutagenesis (Meleigy et al. 2008). Screened over-production of gibberellic acid mutant strain *Fusarium moniliforme* mutated by gamma rays (Taloria et al. 2012) described the increased alcohol dehydrogenase activity in mutated *S. cerevisiae* during ethanol production with UV mutation. Gopinath et al. (2009) showed the hyper-production of azoreductase by mutant *Bacillus* species which help to improve the degradation rate of Congo red dye. Tannler et al. (2008) developed high yield riboflavin producing bacterial mutant strain *B. subtilis* through the chemical mutagen method. Hyper-production of the oxidoreductive enzymes by mutant species and their potential of biodegradation of azo dyes has not been given much attention.

BACTERIAL-FUNGAL CONSORTIUM FOR DECOLOURISATION/DEGRADATION OF AZO DYES

Taking into account of the most significant environmental problem, the disposal of wastewater from the dyeing industries that are causing serious problems to the living organisms and livelihood, degradation of azo dyes is the topic of

primary concern. As various dyes are wayward to biodegradation, researches are still progressing on developing new biological treatments (Borchert & Judy 2001). Over the past decades, a huge amount of microorganisms including bacteria, fungi, yeasts and algae have been screened out and utilized for the dye decolourisation in an eco-friendly manner. The mixed microbial consortia were suspected to have supremacy over pure isolates in treating azo dye containing the wastewater (Pandey et al. 2007). The azo dyes were supposed to have completely mineralized by co-metabolism of microorganisms (Kapdan & Ozturk 2005). Treating wastewater based on microbial consortium at the contaminated sites is quite efficient as microorganisms habituate to their environment (Thakur 2004). The bacterial-fungal consortium has proved to be effective, eco-friendly, and has the efficiency to degrade the dyes in a short span of time. The strenuous metabolism of the consortium degrades the dye molecule at various positions or carries out intermediate degradation for further mineralization. Further, the synergistic action of bacterial-fungal consortia may lead to faster and complete degradation or detoxification of the azo dyes (Khelifi et al. 2009). Additionally, this consortium releases a huge amount of extracellular oxidoreductive enzymes when compared to monoculture which paves the way for transforming the toxic pollutant into non-toxic metabolites (Kaushika & Malik 2009). The synergistic effect of the microbial consortium on azo dye degradation is given in Table 7. However, only a few reports suggested the bacterial-fungal consortium potential for efficient degradation of azo dyes, but the antagonistic activity among the consortium, positive and negative interaction, optimization and their enzyme system were not clearly elucidated.

OPTIMIZATION PARAMETERS FOR ACCELERATED DEGRADATION OF AZO DYES

The effluents that especially come from the textile industries consist of a different composition of organic pollutants. This effluent when mixed with the environment, undergoes various physico-chemical changes that makes it more resistant to microbial attack. Effective biological treatment methods totally depend upon the optimization parameters such as pH, temperature, the complexity of dye structure, the concentration of dye, treatment methods (aerobic or anaerobic), nutrient sources (carbon, nitrogen), inducers and presence or absence of redox mediators. Thus, to improve the biological treatment methods more effective and rapid in decolourisation, it is essential to find out the appropriate factors which influence the azo dye decolourisation.

Effect of physico-chemical factors on azo dye degradation:

Table 7: Synergistic effect of the microbial consortium on azo dye degradation.

S.No	Consortium	Species	Dye	% Degradation	References
1	Fungal	Trametes sp. SQ01 Chaetomium sp. R01	Acid Violet17	86	(Sharma et al. 2004)
			Acid Blue15	85	
			Crystal Violet	82	
			Malachite Green	82	
			Brilliant Green	85	
2	Fungal	<i>Aspergillus lentulus</i> <i>Aspergillus terreus</i> <i>Rhizopus oryzae</i>	Acid Blue	98	(Mishra et al. 2014)
			Pigment Orange	100	
3	Bacterial	<i>Bacillus flexus</i> NBN2 <i>Bacillus cereus</i> AGP03 <i>Bacillus cytotoxicus</i> NVH <i>Bacillus</i> sp. L10	Direct Blue 151	98	(Lalnunhlumi et al. 2016)
			Direct Red 31	95	
4	Fungal- Bacterial	<i>Aspergillus ochraceus</i> NCIM-1146i <i>Pseudomonas</i> sp. SUK1	Rubine GFL	95	(Lade et al. 2012)
5	Bacterial	<i>Providencia</i> sp. SDS (PS) <i>Pseudomonas aeruginosa</i> strain BCH	Red HE3B	100	(Phugare et al. 2011)
6	Fungal- Bacterial	White-rot fungus 8-4 <i>Pseudomonas aeruginosa</i> 1-10	Direct Fast Scarlet 4BS	99	(Fang et al. 2004)
7	Bacterial	<i>Citrobacter freundii</i> (2 strains), <i>Moraxella osloensis</i> , <i>Pseudomonas aeruginosa</i> and <i>Pseudomonas aeruginosa</i> BL22	Mordant Black 17	95	(Karunya et al. 2014)
8	Bacterial	<i>Proteus vulgaris</i> <i>Micrococcus glutamicus</i>	Green HE4BD	100	(Saratale et al. 2010)
9	Bacterial	<i>Bacillus vallismortis</i> <i>Bacillus megaterium</i>	Congo Red	96	(Tony et al. 2009)
		Brodeaux	89		
		Ranocid fast Blue	81		
		Blue BCC	82		
10	Bacterial	<i>Bacillus cereus</i> (BN-7) <i>Pseudomonas putida</i> (BN-4) <i>Pseudomonas fluorescence</i> (BN-5) <i>Stenotrophomonas acidaminiphila</i> (BN-3)	Acid Red 88	78	(Khehra et al. 2005)
			Acid Red 119	99	
			Acid Red 97	94	
			Acid Blue 113	99	
			Reactive Red 120	82	
11	Fungal- Bacterial	<i>Pseudomonas</i> sp. SUK1 <i>A. ochraceus</i> NCIM-1146	Reactive Navy Blue HE2R	80	(Kadam et al. 2011)

pH and temperature: The variation in pH of the medium has a major effect on azo dye decolourisation/degradation. The degradation efficiency of azo dye mostly depends upon the pH of the medium, tolerance ability of the azo dye degraders and pH stability of the oxidoreductive enzymes. In most of the literature survey, it was reported that the azo dye degradation occurs in the wide range of pH 5.0 to 10 (Kilic et al. 2007). Maximum degradation was achieved only at optimal pH, while the rate of degradation tends to decrease quickly when it reaches strong acid or in alkaline condition. Chang et al. (2001) reported that pH of the medium promotes the transfer of dye molecules across the cell membrane. Hence, pH directly influences or affects the rate of degradation of dyes. During the microbial degradation process, the reduction of azo bond occurs with the formation

of aromatic amines. These aromatic amines increase the pH of the medium and it may be limiting to the growth of microbial biomass. Similarly, the temperature also has a profound impact on azo dye degradation. Microbes always adapt to integrate with the environmental temperature and its variation. But the microbial enzymes are very sensitive to the temperature because they decline from the original activity other than the optimal temperature. Microbes either combine with an endergonic or exergonic reaction during the time of bioremediation process which results in rapid changes in the temperature. This kind of temperature variation can also lead to the loss of cell viability or reduction in activation energy or a decline in growth rate and enzyme activity (Chang & Kuo 2000). However, certain microbes release thermostable oxidoreductive enzymes,

which can adapt to resist up to a temperature of 60°C over a short period of time (Pearce et al. 2003). Therefore, selection of microbial strain or development of that strain, which has the ability to tolerate a wide range of pH and temperature, is considered as prime factors for the effective degradation of azo dyes. Immobilization of cells offers a great protection for microorganisms against the environmental stress such as temperature and pH by the supporting matrix formed during the process.

Dye structure and concentration of dye: Azo dyes are of a diverse group of synthetic dyes with one or more azo bond with different functional groups attached to them. This complexity of structure affects the efficiency of microbial decolourisation. It was reported that the decolourisation efficiency is much faster in monoazo dyes with low molecular weight compared to the diazo or triazo dyes (Hsueh et al. 2009). The dyes with hydroxyl or amino groups are easily degradable compared to those with methyl, methoxy, sulpho or nitro groups. Azo bond containing electron-dense region and a sulphonated group of reactive dye is normally considered to be high recalcitrant in nature which cannot be easily degraded by pure culture (Lorenco et al. 2000). Increasing the concentration of dye gradually decrease the dye degradation rate. This may be due to the toxic effect of the dye or improper biomass and dye ratio or inability of the strain or less amount of oxidoreductive enzymes present in the medium (Tony et al. 2009). Therefore, the development of microbial consortium may be an alternative approach to mineralize the azo dye completely.

Nutrient source and conditions of treatment method (oxy-genic or anoxygenic): Bioreduction of azo dyes can be accomplished only with the supplement of carbon and nitrogen source in degradation medium. Degradation efficiency of azo dyes by the single microbe or consortium can be improved by the addition of one or more organic substances such as glucose, lactose, maltose and sucrose; and also by the addition of nitrogen sources such as sodium nitrate, peptone, beef extract and yeast extract. Pandey et al. (2007) demonstrated that the reductive cleavage of the azo bond by microbes occurs due to the energy obtained from the carbon source. Chang & Kuo (2000) observed that nitrogen source is responsible for the regeneration of NADH which acts as an electron donor for the reduction of dyes. Nitrogen source such as sodium nitrate influences the enzyme system involved in dye degradation (Jadhav et al. 2010). The microbial decolourisation of dyes occurs strictly under anaerobic or facultative anaerobic or aerobic conditions by the various groups of microorganisms. Complete degradation of azo dyes is possible only with the help of aerobic and anaerobic bacteria. Bioremediation of azo dyes occurs in

two-step reactions. In the first step of the reaction, the reduction of azo dyes occurs in an anoxygenic condition by the action of azoreductase produced by the anaerobic bacteria with the release of toxic amines. In the second step, these amines are further converted into the non-toxic compounds with the help of oxidative enzyme produced by aerobic bacteria (Van der Zee & Villaverde 2005). The earlier study suggested that the continuous aeration and agitation in the medium increases the oxygen concentration, thereby affecting the azoreductase activity. This is because the microbial cell utilizes the electron obtained from the oxidation process for the reduction of oxygen rather than the azo dyes. Keeping this in view, the researcher is in search of oxygen sensitive azoreductase from different groups of bacteria to make this process economically feasible by conducting the reaction in one-step mechanism under aerobic condition.

Inducers and redox mediators: Wastewater discharge from the textile industries contains a low amount of substrate, which cannot be readily utilized by the microbes and thus affecting the rate of degradation of azo dyes. This problem can be solved by using the inducer as an external substrate (electron donor) which enhances the degradation efficiency of microbes. Addition of inducer such as glycerol, tween 80 and copper sulphate apparently induces the oxidoreductive enzymes which favour the degradation of azo dyes. Dawkar et al. (2009) observed that the complete degradation of Navy blue 2GL occurs within 18 hrs of incubation by the addition of CaCl_2 due to overexpression of oxidoreductive enzymes. Similarly, Telke et al. (2009) reported that the inducer such as sodium acetate, sodium formate and sodium citrate improve the decolourisation efficiency of C.I. Reactive Orange 16 by the reduced activity of NADH-DCIP reductase produced by the isolated *Bacillus* sp. So far, the concentration of inducers and their effect on azo dye decolourisation were not well understood. Hence, the choice of inducers and their optimizations are more important factors for the colour removal of dyes from the wastewater. Microbes cannot easily uptake azo dyes inside the cell membrane due to their high degree of complexity and also for the wide range of redox potentials (-180 to -430 mV) when they are present in the effluent (Dos Santos et al. 2004). Further, the azo dye, which has a more electron-dense region in the azo bond, is found to be highly resistant to the biological decolourisation process. The redox mediator is the substance which enhances the transfer of reducing equivalents from the co-substrate to the azo dyes. Due to this electron transfer mechanism, steric hindrance of the dye molecule will be reduced, thus facilitating the dye molecule to the bacterial cell membrane (Rau & Stolz 2003). It

has been observed that the redox mediator increases the rate of degradation by improving the substrate specificity of oxidoreductive enzymes (Canas & Camarero 2010). Nowadays, the natural mediators have been extensively used in bioremediation technology when compared to the synthetic mediator because they are less toxic, and eco-friendly. However, the possible concentration of natural mediators and their impact on the oxidoreductive enzymes for effective degradation of azo dye was not well studied.

IMMOBILIZATION OF MICROBIAL CELLS FOR AZO DYE DEGRADATION

Nowadays, immobilization of bacteria/fungi/bacterial-fungal cells has received much attention from biotechnologists due to its wide range of applications in the industrial sector (Ahamad & Kunhi 2011). Further, immobilization has several advantages over freely suspended cells in wastewater treatment because it has higher stability, low-cost, reuse, decrease the cell surface area volume, protect the cells from direct exposure of toxic substances, and eco-friendly (El-Naas et al. 2009). The choice of the supporting materials is an important factor to be considered for the process of cell immobilization (Zacheus et al. 2000). Natural and synthetic gels are the two types of immobilization matrices which have been extensively used in the process of decolourisation of azo dyes. However, the synthetic gel has higher stability, but it does not allow the dye to penetrate the matrix and also will reduce the viability of cells. The natural gels such as alginate offers a wide range of applications in entrapment methods because it has a mild effect on the microbial cells when compared to synthetic gels (Tal et al. 2001). Immobilized biocatalysts act as promising tool to eradicate azo dyes continuously in a controlled manner with low cost and in an eco-friendly way.

CONCLUSIONS

Owing to the high demand for fabrics, the industrial production of azo dyes has drastically increased worldwide. Unfortunately, every year 15% of azo dyes are discharged into the environment from the textile industries and pose a serious problem in aquatic habitats. These effluents contain a mixture of dyes with high complexity of structure and found to have a high alkaline condition, which does not favour the microbial degradation of dyes by monoculture. In the present times, most wastewater treatment plants are obsolete and in need of modern technology to improve the degradation of azo dyes in an eco-friendly manner with low cost. So, there is an urgent need for treating wastewaters using novel methods for complete mineralization of azo dyes. Microbial strain development through random mutations for the production of oxidoreductive enzymes is a

primary initiative for enhanced decolourisation and degradation of azo dyes. Further, bacterial-fungal consortium mediated decolourisation and degradation of azo dyes have significant potential to address this issue in an eco-friendly manner without generating a secondary disposal problem in the form of sludge. The mutated consortium, able to produce different types of oxidoreductive enzymes at an increased level, enhances the degradation rate of mixed dyes. In addition to the above, the immobilization and optimization of parameters for the accelerated decolourisation and degradation of azo dyes are also important. It is well-understood now that the bacterial-fungal consortium developed from the mutated strain increases the production rate of oxidoreductive enzymes. Hence, in near future, the mutated bacterial-fungal consortia may be considered as biological weapons for the effective decolourisation and degradation of azo dyes.

REFERENCES

- Afreen, S., Bano, F., Ahmad, N. and Fatma, T. 2017. Screening and optimization of laccase from cyanobacteria with its potential in decolorization of anthraquinonic dye Remazol Brilliant Blue R. *Biocatalysis and Agricultural Biotechnology*, 10: 403-410.
- Ahamad, P.Y.A. and Kunhi, A.A.M. 2011. Enhanced degradation of phenol by *Pseudomonas* sp. CP4 entrapped in agar and calcium alginate beads in batch and continuous processes. *Biodegradation*, 22: 253-265.
- Akpanand, U.G. and Hameed, B.H. 2013. Development and photocatalytic activities of TiO₂ doped with Ca-Ce-W in the degradation of acid red 1 under visible light irradiation. *Desalination & Water Treatment*, 52(28-30): 5639-5651.
- Anjaneya, O., Shrishailnath, S.S., Guruprasad, K., Nayak, A.S., Mashetty S.B. and Karegoudar, T.B. 2013. Decolourization of Amaranth dye by bacterial biofilm in batch and continuous packed bed bioreactor. *International Biodeterioration & Biodegradation*, 79: 64-72.
- Asgher, M., Bhatti, H.N., Ashraf, M. and Legge, R.L. 2008. Recent developments in biodegradation of industrial pollutants by white rot fungi and their enzyme system. *Biodegradation*, 19: 771-783.
- Bafana, A., Devi, S.S. and Chakrabarti, T. 2011. Azo dyes: past, present and the future. *Environ. Rev.*, 19: 350-370.
- Banat, I.M., Niga, P., Singh, D. and Marchant, R. 1996. Microbial decolorization of textile-dye-containing effluents: a review. *Bioresour. Technol.*, 58: 217-227.
- Bhatt, N., Patel, K., Hareesh, C. and Madmwar, D. 2005. Decolorization of diazo-dye reactive blue 172 by *P. aeruginosa* NBAR12J. *J. Basic Microbiol.*, 45: 407-418.
- Blumel, S. and Stolz, A. 2003. Cloning and characterization of the gene coding for the aerobic azoreductase from *Pigmentiphaga kullae* K24. *Appl. Microbiol. Biotechnol.*, 62: 186-190.
- Borchert, M. and Judy, A.L. 2001. Decolorization of reactive dyes by the white rot fungus *Trametes versicolor* in sequencing batch reactors. *Biotechnol. Bioeng.*, 75: 313-321.
- Camila, C., Fontanaa, R.C., Mezzomoa, A.G., da Rosaa, L.O., Poletob, L., Camassolaa, M. and Dillona, A.J.P. 2017. Production, characterization and dye decolorization ability of a high level laccase from *Marasmiellus palmivorus*. *Biocatalysis and Agricultural Biotechnology*, 12: 15-22.
- Canas, A.I. and Camarero, S. 2010. Laccases and their natural media-

- tors: Biotechnological tools for sustainable eco-friendly processes. *Biotechnology Advances*, 28: 694-705.
- Cerniglia, C.E. 1997. Fungal metabolism of polycyclic aromatic hydrocarbons: Past, present and future applications in bioremediation. *J. Ind. Microbiol. Biotechnol.*, 19: 324-333.
- Chang, J.S. and Kuo, T.S. 2000. Kinetics of bacterial decolorization of azo dye with *Escherichia coli* NO3. *Bioresour. Technol.*, 75: 107.
- Chang, J.S., Chou, C., Lin, Y., Ho, J. and Hu, T.L. 2001. Kinetic characteristics of bacterial azo- dye decolorization by *P. luteola*. *Water Res.*, 35: 2041.
- Chen, H., Hopper, S.L. and Cerniglia, C.E. 2005. Biochemical and molecular characterization of an azoreductase from *Staphylococcus aureus* a tetrameric NADPH dependent flavoproteins. *Microbiology*, 151: 1433-1441.
- Das, A., Bhattacharya, S., Panchanan, G., Navya, B.S. and Nambiar, P. 2016. Production, characterization and Congo red dye decolorizing of a laccase from *Pleurotus ostreatus* MTCC 142 cultivated on co-substrates of paddy straw and corn husk. *Journal of Genetic Engineering and Biotechnology*, 14: 281-288.
- Dawkar, V.V., Jadhav, U.U., Ghodake, G.S. and Govindwar, S.P. 2009. Effect of inducers on the decolorization and biodegradation of textile azo dye Navy blue 2GL by *Bacillus sp.* VUS. *Biodegradation*, 20(6): 777-87.
- De Souza, C.G.M., Tychanowicz, G.K., De Souza, D.F. and Peralta, R.M. 2004. Production of laccase isoforms by *Pleurotus pulmonarius* in response to presence of phenolic and aromatic compounds. *J. Basic Microbiol.*, 3: 129-136.
- Dos Santos, A.B., Cervantes, F.J. and Van Lier, J.B. 2004. Azo dye reduction by thermophilic anaerobic granular sludge, and the impact of the redox mediator anthraquinone- 2,6-disulfonate (AQDS) on the reductive biochemical transformation. *Appl. Microbiol. Biotechnol.*, 64: 62.
- El-Naas, M.H., Al-Muhtaseb, S.A. and Makhlof, S. 2009. Biodegradation of phenol by *P. putida* immobilized in polyvinyl alcohol (PVA) gel. *J. Hazard. Mater.*, 164: 720-725.
- Eren, Z. and Ince, N.H. 2010. Sonolytic and sonocatalytic degradation of azo dyes by low and high frequency ultrasound. *J. Hazard. Mater.*, 177(1-3): 1019-1024.
- Eyvaz, M., Kirilaroglu, M., Aktas, T.S. and Yuksel, E. 2009. The effects of alternating current electrocoagulation on dye removal from aqueous solutions. *Chem. Eng. J.*, 153(1-3): 16-22.
- Fang, H., Wenrong, H. and Yuezhong, L. 2004. Biodegradation mechanisms and kinetics of azo dye 4BS by a microbial consortium. *Chemosphere*, 57: 293.
- Fang, R., Cheng X. and Xu, X. 2013. Synthesis of lignin-base cationic flocculant and its application in removing anionic azo-dyes from simulated wastewater. *Bioresour. Technol.*, 101(19): 7323-7329.
- Franciscona, E., Mendonçaa, D., Sebera, S., Moralesa, D.A., Zocolob, G.J., Zanonib, M.V.B., Grossmanc, M.J., Durrantc, L.R., Freemand, H.S. and Aragão, G. 2015. Potential of a bacterial consortium to degrade azo dye Disperse Red 1 in a pilot scale anaerobic-aerobic reactor. *Process Biochemistry*, 50(5): 816-825.
- Gomathi Devi, L., Girish Kumar, S., Mohan Reddy, K. and Munikrishnappa, C. 2009. Photo degradation of methyl orange an azo dye by advanced fenton process using zero valent metallic iron: Influence of various reaction parameters and its degradation mechanism. *J. Hazard. Mater.*, 164(2-3): 459-467.
- Gopinath, K.P., Murugesan, S., Abraham, J. and Muthukumar, K. 2009. *Bacillus sp.* mutant for improved biodegradation of Congo Red: random mutagenesis approach. *Bioresour. Technol.*, 100: 6295-6300.
- Guadie, A., Tizazu, S., Melese, M., Guo, W., Ngo, H.H. and Xia, S. 2017. Biodecolorization of textile azo dye using *Bacillus sp.* strain CH12 isolated from alkaline lake. *Biotechnology Reports*, 15: 92-100.
- Hosono, M., Arai, H., Aizawa, M., Yamamoto, I., Shimizu, K. and Sugiyama, M. 1993. Decoloration and degradation of azo dye in aqueous solution supersaturated with oxygen by irradiation of high-energy electron beams. *Appl. Radiat. Isot.*, 44(9): 1199-1203.
- Hsueh, C.C., Chen, B.Y. and Yen, C.Y. 2009. Understanding effects of chemical structure on azo dye decolorization characteristics by *Aeromonas hydrophila*. *J. Hazard. Mater.*, 167: 995.
- Iscen, C.F., Kiran I. and Ilhan, S. 2007. Biosorption of reactive black 5 dye by *Penicillium restrictum*: The kinetic study. *J. Hazard. Mater.*, 143(3): 335-340.
- Jadhav, J.P., Kalyani, D.C., Telke, A.A., Phugare, S.S. and Govindwar, S.P. 2010. Evaluation of the efficiency of a bacterial consortium for the removal of color, reduction of heavy metals and toxicity from textile dye effluent. *Bioresour. Technol.*, 101: 165-173.
- Jadhav, U.U., Dawkar, V.V., Ghodake, G.S. and Govindwar, S.P. 2008. Biodegradation of directred 5B, a textile dye by newly isolated *Comamonas sp.*, UVS. *J. Hazard. Mater.*, 158: 507-516.
- Jin, X., Liu, G., Xu, Z. and Yao, W. 2007. Decolorization of a dye industry effluent by *Aspergillus fumigatus* XC6. *Appl. Microbiol. Biotechnol.*, 74: 239-243.
- Jones, S.M. and Solomon, E. I. 2015. Electron transfer and reaction mechanism of laccases. *Cell. Mol. Life Sci.*, 72(5): 869-883.
- Kadam, A.A., Telke, A.A., Jagtap S.S. and Govindwar, S.P. 2011. Decolorization of adsorbed textile dyes by developed consortium of *Pseudomonas sp.* SUK1 and *Aspergillus ochraceus* NCIM-1146 under solid state fermentation. *Journal of Hazardous Materials*, 189(2): 486-494.
- Kadolph, S.J. 2008. Natural dyes: A traditional craft experiencing new attention. *Delta Kappa Gamma Bull.*, 75(1): 14-17.
- Kapdan, I.K. and Ozturk, R. 2005. Effect of operating parameters on color and COD removal of SBR: Sludge age and initial dyestuff concentration. *J. Hazard. Mater.*, 123: 217-222.
- Karunya, A., Valli Nachiyara, C., Ananth, P.B., Sunkar, S. and Jabasingh, S.A. 2014. Development of microbial consortium CN-1 for the degradation of Mordant Black 17. *Journal of Environmental Chemical Engineering*, 2(2): 832-840.
- Kaushika, P. and Malik, A. 2009. Fungal dye decolorization: Recent advances and future potential. *Environment International*, 35: 127-141.
- Khehra, M.S., Saini, H.S., Sharma, D.K., Chadha, B.S. and Chimni, S.S. 2005. Comparative studies on potential of consortium and constituent pure bacterial isolates to decolorize azo dyes. *Water Res.*, 39: 5135.
- Khelifi, E., Bouallagui, H., Touhami, Y., Godon, J. and Hamdi, M. 2009. Enhancement of textile wastewater decolorization and biodegradation by isolated bacterial and fungal strains. *Desalination and Water Treatment*, 2: 310-316.
- Kilic, N.K., Nielsen, J.L., Yuze M. and Donmez, G. 2007. Characterization of a simple bacterial consortium for effective treatment of wastewaters with reactive dyes and Cr(VI). *Chemosphere*, 67: 826.
- Kirk, Othmer 2004. *Encyclopedia of Chemical Technology*. Wiley-Interscience, 7(5).
- Kumar, K., Devi, S.S., Krishnamurthi, K., Dutta, D. and Chakrabarti, T. 2007. Decolorisation and detoxification of Direct Blue-15 by a bacterial consortium, *Bioresour Technol.*, 98(16): 3168-71.
- Lade, H.S., Waghmode, T.R., Kadam, A.A. and Govindwar, S.P. 2012. Enhanced biodegradation and detoxification of disperse azo dye Rubine GFL and textile industry effluent by defined fungal-bacterial consortium. *International Biodeterioration & Biodegradation*, 72: 94-107.

- Lalnunhlmi, S. and Krishnaswamy, V. 2016. Decolorization of azo dyes (Direct Blue 151 and Direct Red 31) by moderately alkaliphilic bacterial consortium. *Brazilian Journal of Microbiology*, 47: 39-46.
- Li, G., Wang, N., Liu, B. and Zhang, X. 2009. Decolorization of azo dye Orange II by ferrate (VI)-hypochlorite liquid mixture, potassium ferrate (VI) and potassium permanganate. *Desalination*, 249(3): 936-941.
- Liang, Tan, He, M., Song, L., Fu, X. and Shi, S. 2016. Aerobic decolorization, degradation and detoxification of azo dyes by a newly isolated salt-tolerant yeast *Scheffersomyces spartinae* TLHS-SF1. *Bioresource Technology*, 203: 287-294.
- Li-Qiong, G., Shuo-Xin, L., Xiao-Bing, Z., Zi-Rou, H. and Jun-Fang, L. 2011. Production, purification and characterization of a thermostable laccase from a tropical white-rot fungus. *World J. Microbiol. Biotechnol.* 27: 731-735.
- Liu, L., Gao, Z.Y., Su, X.P., Chen, X., Jiang, L. and Yao, J.M. 2015. Adsorption removal of dyes from single and binary solutions using a cellulose-based bioadsorbent. *ACS Sustainable Chem. Eng.*, 3(3): 432-442.
- Lorenzo, N.D., Novais, J.M. and Pinheiro, H.M. 2000. Reactive textile dye colour removal in a sequencing batch reactor. *Water Sci. Technol.*, 42(5-6): 321-328.
- Lotfy, W.I., Ghanem, K.M. and El-Helou, E.R. 2007. Citric acid production by a novel *Aspergillus niger* isolate: I. Mutagenesis and cost reduction studies. *Bioresour. Technol.*, 98: 3464-3469.
- Marco-Urrea, E., Perez-Trujillo, M., Vicent, T. and Caminal, G. 2009. Ability of white-rot fungi to remove selected pharmaceuticals and identification of degradation products of ibuprofen by *Trametes versicolor*. *Chemosphere*, 74: 765-772.
- Marimuthu, T., Rajendran, S. and Manivannan, M. 2013. A review on bacterial degradation of textile dyes. *J. Chem. Sci.*, 3: 201-212.
- McMullan, G., Meehan, C., Conneely, A., Kirby, N., Robinson, T., Nigam, P., Banat, I.M., Marchant, R. and Smyth, W.F. 2001. Microbial decolorisation and degradation of textile dyes. *Appl. Microbiol. Biotechnol.*, 56(1-2): 81-87.
- Meleigy, S.A. and Khalaf, M.A. 2008. Biosynthesis of gibberellic acid from milk permeate in repeated batch operation by a mutant *Fusarium moniliforme* cells immobilized on loofa sponge. *Bioresour. Technol.*, 100: 374-379.
- Miranda, R.C., Gomes, E.B., Pereira Marin-Morales, J.N., Machado, M.A. and Gusmão, K.M. 2013. Biotreatment of textile effluent in static bioreactor by *Curvularia lunata* URM 6179 and *Phanerochaete chrysosporium* URM 6181. *Bioresour. Technol.*, 142: 361-367.
- Mishra, A. and Malik, A. 2014. Novel fungal consortium for bioremediation of metals and dyes from mixed waste stream. *Bioresource Technology*, 171: 217-226.
- Moosvi, S., Kehaira, H. and Madamwar, D. 2005. Decolorization of textile dye Reactive Violet 5 by a newly isolated bacterial consortium RVM 11.1. *World J. Microbiol. Biotechnol.*, 21: 667-672.
- Moreira, P.R., Duez, C., Dehareng, D., Antunes, A., Almeida-Vara, E., Frere, J.M., Malcata, F.X. and Duarte, J.C. 2005. Molecular characterization of a versatile peroxidase from a Bjerkandera strain. *J. Biotechnol.*, 118: 339-352.
- Mostafa, M.E.S., Ghariebb M.M. and Abou-El-Souod, G.W. 2009. Biodegradation of dyes by some green algae and cyanobacteria. *International Biodeterioration & Biodegradation*, 63(6): 699-704.
- Murrell, J.N. 1973. *The Theory of the Electronic Spectra of Organic Molecules*. John Wiley & Sons, Inc., New York.
- Novotny, C., Svobodova, K., Kasinath, A. and Erbanova, P. 2004. Biodegradation of synthetic dyes by *Irpex lacteus* under various growth conditions. *International Biodeterioration and Biodegradation*, 54: 215-223.
- Palmieri, G., Giardina, P., Bianco, C., Fontanella, B. and Sanna, G. 2000. Copper induction of laccase isoenzymes in the ligninolytic fungus *Pleurotus ostreatus*. *Appl. Environ. Microbiol.*, 66: 920-924.
- Pandey, A., Singh, P. and Iyengar, L. 2007. Bacterial decolorization and degradation of azo dyes. *Int. Biodeterior. Biodegrad.*, 59: 73-84.
- Pearce, C.I., Lloyd, J.R. and Guthrie, J.T. 2003. The removal of colour from textile wastewater using whole bacterial cells: A review. *Dyes Pigments*, 58: 179.
- Perumal, K., Malleswari, R.B., Catherin, A. and Sambanda-Moorthy, T.A. 2012. Decolorization of Congo Red dye by bacterial consortium isolated from dye contaminated soil, Paramakudi, Tamil Nadu. *J. Microbiol. Biotechnol. Res.*, 2: 475-480.
- Phugare, S.S., Kalyani, D.C., Patil, A.V. and Jadhav, J.P. 2011. Textile dye degradation by bacterial consortium and subsequent toxicological analysis of dye and dye metabolites using cytotoxicity, genotoxicity and oxidative stress studies. *Journal of Hazardous Materials*, 186(1): 713-723.
- Pinheiro, H.M., Touraud E. and Thomas, O. 2004. Aromatic amines from azo dye reduction: status review with emphasis on direct UV spectrophotometric detection in textile industry wastewaters. *Dyes Pigm.*, 61: 121-139.
- Qu, Y., Cao, X., Ma, Q., Shi, S., Tan, L., Li, X., Zhou, H., Zhang X. and Zhou, J. 2012. Aerobic decolorization and degradation of Acid Red B by a newly isolated *Pichia* sp. *TCL. J. Hazard. Mater.*, 223: 31-38.
- Rai, H., Bhattacharya, M., Singh, J., Bansal, T. K., Vats, P. and Banerjee, U. C. 2005. Removal of dyes from the effluent of textile and dyestuff manufacturing industry: A review of emerging techniques with reference to biological treatment. *Crit. Rev. Environ. Sci. Technol.*, 35: 219.
- Ram, L.S., Pradeep Kumar, S. and Singh, R.P. 2015. Enzymatic decolorization and degradation of azo dyes- a review. *International Biodeterioration & Biodegradation*, 104: 21-31.
- Rau, J. and Stolz, A. 2003. Oxygen-insensitive nitroreductases NFSA and NFSB of *Escherichia coli* function under anaerobic conditions as lawsone-dependent azo reductases. *Appl. Environ. Microbiol.*, 69: 3448.
- Robinson, T., McMullan, G., Marchant, R. and Nigam, P. 2001. Remediation of dyes in textile effluent: A critical review on current treatment technologies with a proposed alternative. *Bioresource Technology*, 77(3): 247-255.
- Royer, B., Cardoso, N.F., Lima, E.C., Macedo, T.R. and Airoidi, C. 2010. A useful organo functionalized layered silicate for textile dye removal. *J. Hazard. Mater.*, 181(1-3): 366-374.
- Santana, M.H.P., Da Silva, L.M., Freitas, A.C., Boodts, J.F.C., Fernandes, K.C. and De Faria, L.A. 2009. Application of electrochemically generated ozone to the discoloration and degradation of solutions containing the dye Reactive Orange 122. *J. Hazard. Mater.*, 164(1): 10-17.
- Saratale, R.G., Saratale, G.D., Chang, J.S. and Govindwar, S.P. 2010. Decolorization and biodegradation of reactive dyes and dye wastewater by a developed bacterial consortium. *Biodegradation*, 21(16): 999-1015.
- Saratale, R.G., Saratale, G.D., Chang, J.S. and Govindwar, S.P. 2009. Ecofriendly decolorization and degradation of reactive green 19A using *Micrococcus glutamicus* NCIM- 2168. *Bioresour. Technol.*, 110: 3897.
- Schofield, M.J. and Hsieh, P. 2003. DNA mismatch repair: molecular mechanisms and biological function. *Annu. Rev. Microbiol.*, 57: 579-608.
- Seo, H., Son, M.K., Shin, I., Kim, J.K., Lee, K.J., Prabakar K. and

- Kim, H.J. 2010. Faster dye-adsorption of dye-sensitized solar cells by applying an electric field. *Electrochim. Acta.*, 55(13): 4120-4123.
- Sharma, D.K., Saini, H.S., Singh, M., Chimni, S.S. and Chadha, B.S. 2004. Isolation and characterization of microorganisms capable of decolorizing various triphenylmethane dyes. *J. Basic Microbiol.*, 44: 59-65.
- Sharma, P., Goel, R. and Caplash, N. 2007. Bacterial laccases. *World J. Microbiol. Biotechnol.*, 23: 823-832.
- Singh, R.L., Khanna, S.K. and Singh, G.B. 1988. Acute and short-term toxicity of popular blend of Metanil Yellow and Orange II in albino rats. *Indian J. Exp. Biol.*, 26: 105-111.
- Song, L., Shao, Y., Ning, S. and Tan, L. 2017. Performance of a newly isolated salt-tolerant yeast strain *Pichia occidentalis* G1 for degrading and detoxifying azo dyes. *Bioresource Technology*, 233: 21-29.
- Stolz, A. 2001. Basic and applied aspects in the microbial degradation of azo dyes. *Appl. Microbiol. Biotechnol.*, 56: 69-80.
- Tal, Y., Schwartzburd, B., Nussinovitch, A. and Van Rijn, J. 2001. Enumeration and factors influencing the relative abundance of a denitrifier, *Pseudomonas* sp. JR12, entrapped in alginate beads. *Environ. Pollut.*, 112: 99-106.
- Taloria, D., Samanta, S., Dasa, S. and Pututundaa, C. 2012. Increase in bioethanol production by random UV mutagenesis of *S. cerevisiae* and by addition of zinc ions in the alcohol production Media. *APCBEE Procedia*, 2: 43 - 49.
- Tan, L., Ning, S., Zhang, X. and Shi, S. 2013. Aerobic decolorization and degradation of azo dyes by growing cells of a newly isolated yeast *Candida tropicalis* TL-F1. *Bioresour. Technol.*, 138: 307-313.
- Tannler, S., Zamboni, N., Kiraly, C., Aymerich, S. and Sauer, U. 2008. Screening of *Bacillus subtilis* transposon mutants with altered riboflavin production. *Metab. Eng.*, 10: 216-226.
- Telke, A.A., Kalyani, D.C., Dawkar, V.V. and Govindwar, S.P. 2009. Influence of organic and inorganic compounds on oxidoreductive decolorization of sulfonated azo dye C.I. Reactive Orange 16. *J. Hazard. Mater.*, 172: 298.
- Thakur, I.S. 2004. Screening and identification of microbial strains for removal of colour and adsorbable organic halogens in pulp and paper mill effluent. *Process Biochem.*, 39: 1693-1699.
- Tony, B.D., Goyal, D. and Khanna, S. 2009. Decolorization of textile azo dyes by aerobic bacterial consortium. *Int. Biodeterior. Biodegrad.*, 63: 462-469.
- Tuttolomondo, M.V., Alvarez, G.S., Desimone, M.F. and Diaz, L.E. 2014. Removal of azo dyes from water by sol-gel immobilized *Pseudomonas* sp. *Journal of Environmental Chemical Engineering*, 2: 131-136.
- Uzal, N., Yilmaz, L. and Yetis, U. 2010. Nanofiltration and reverse osmosis for reuse of indigo dye rinsing waters. *Sep. Sci. Technol.*, 45(3): 331-338.
- Van der Zee, F.P. and Villaverde, S. 2005. Combined anaerobic-aerobic treatment of azo dyes-a short review of bioreactor studies. *Water Res.*, 39: 1425.
- Vandevivere, P.C., Bianchi R. and Verstraete, W. 1998. Treatment and reuse of wastewater from the textile wet-processing industry: review of emerging technologies. *J. Chem Technol Biotechnol.*, 72: 289-302.
- Wang, A., Li, Y.Y. and Ru, J. 2010. The mechanism and application of the electro-fenton process for azo dye Acid Red 14 degradation using an activated carbon fibre felt cathode. *J. Chem. Technol. Biotechnol.*, 85: 1463-1470.
- Wang, A., Qu, J., Liu H. and Ru, J. 2008. Mineralization of an azo dye Acid Red 14 by photoelectro-fenton process using an activated carbon fiber cathode. *Appl. Catal. B*, 84(3-4): 393-399.
- Yingying, S., Iswarya, M., Qingzhou, C., Molly, C., Fan, G., Xiaoqi Jacki Z. and Zhiyong, G. 2016. Rapid degradation of azo dye methyl orange using hollow cobalt nanoparticles. *Chemosphere*, 144: 1530-1535.
- Zabin, K.B., Mulla, S.I. and Ninnekar, H.Z. 2017. Purification and immobilization of laccase from *Trichoderma harzianum* strain HZN10 and its application in dye decolorization. *Journal of Genetic Engineering and Biotechnology*, 15: 139-150.
- Zacheus, O.M., Iivanainen, E.K., Nissinen, T.K., Lehtola, M.J. and Martikainen, P.J. 2000. Bacterial biofilm formation on polyvinyl chloride, polyethylene and stainless steel exposed to ozonated water. *Water Res.*, 34: 63-70.
- Zeenat, K., Kunal, J., Ankita, S. and Datta, M. 2014. Microaerophilic degradation of sulphonated azo dye Reactive Red 195 by bacterial consortium AR1 through co-metabolism. *International Biodeterioration & Biodegradation*, 94: 167-175.
- Zheng-Bing, G., Chen-Meng, S., Zhanga, N., Zhoua, W., Cheng-Wen, X., Lin-Xi, Z., Zhaoa, H., Yu-Jie, C. and Xiang-Ru, L. 2014. Overexpression, characterization, and dye-decolorizing ability of a thermostable, pH-stable, and organic solvent-tolerant laccase from *Bacillus pumilus* W3. *Journal of Molecular Catalysis B: Enzymatic*, 101: 1-6.



Erosion Resistance and Aggregate Distribution Characteristics of Vegetation Concrete

Mingtao Zhou^(**), Tianqi Li^{(***)†}, Jiazhen Gao^(**)† and Wennian Xu^(**)

^{*}Hubei Key Laboratory of Disaster Prevention and Mitigation (China Three Gorges University), Hubei Yichang, 443002, China

^{**}Engineering Research Center of Eco-environment in Three Gorges Reservoir Region, Ministry of Education, China Three Gorges University, Hubei Yichang, 443002, China

^{***}College of Hydraulic Engineering & Environmental Engineering, China Three Gorges University, Hubei Yichang, 443002, China

†Corresponding authors: Tianqi Li, Jiazhen Gao

Nat. Env. & Poll. Tech.
Website: www.neptjournal.com

Received: 11-04-2018
Accepted: 02-08-2018

Key Words:

Erosion resistance
Aggregate
Vegetation concrete
Natural soil

ABSTRACT

Soil aggregate property, as a widely accepted soil quality indicator, is closely related to the erosion resistance of soil. In order to quantitatively assess the erosion resistance of vegetation concrete, a typical artificial composite soil, the distribution characteristics of aggregate particle size and eleven evaluation indexes were determined and calculated in laboratory by contrast with natural soil under the same site conditions. The research conclusions could be presented as follows: Compared with the natural soil, mechanical stability macroaggregate, water-stable macroaggregate, mean weight diameter, geometric mean diameter and organic matter content increased by 9.1%, 97.0%, 123.6%, 158.6% and 65.2% respectively. In contrast, erodibility factor, structural failure rate, fractal dimension and dispersion rate decreased by 75.8%, 38.1%, 24.4% and 27.2% respectively. Besides, aggregation status and aggregation degree improved by 63.9% and 38.5%, and the comprehensive principal component value of erosion resistance also increased by 252.6%. Due to the addition of natural organic material and cement, the erosion resistance of vegetation concrete was greatly superior to that of natural soil. Therefore, vegetation concrete was a suitable composite soil to create vegetation habitat on the surface of bare rock slope.

INTRODUCTION

China has been impacted by soil erosion for millennia, which is particularly evident on the slope. Numerous researchers commit to improving soil erosion resistance and reducing soil loss. In addition to climatic conditions, vegetation types and tillage patterns, the soil erosion resistance is closely related to its inherent physical and chemical properties, e.g. organic matter, texture, porosity, infiltration, etc. (Angers & Caron 1998, Barthes & Roose 2002). Soil aggregate can be defined as the basic structural unit formed by the primary fine particles through cementation, coagulation, etc. Aggregate distribution characteristics, which are effective indicators to evaluate the erosion resistance and stability of soil, seriously affected the process of soil erosion (Bronick & Lal 2005). Attention has been drawn to soil aggregates and erosion resistance, thus a series of research achievements have been obtained. An et al. (2008) studied the aggregate characteristics and main influence factors of the typical grassland soil on Loess Plateau during the natural revegetation through field investigations

and laboratory analysis. Soil aggregate stability has been shown to provide a good index of soil erodibility, and the abundance of water-stable aggregates at the soil surface determines the potential for sheet erosion and crust formation (Kay 2000, Li & Fan 2014). Excessive tillage causes changes in soil aggregate size distribution, which leads to the degradation of soil erosion resistance (Parr et al. 1983, Yin et al. 2016). More significantly, soil erosion is substantially controlled by aggregate breakdown process (Selen et al. 2011), and many researchers have demonstrated that surface erosion processes are linked to aggregate stability (Morin & Van 1996, Ramos et al. 2003). Previous studies have provided valuable achievements for the enrichment of soil aggregates theory and the improvement of erosion resistance, while their research subjects were mostly confined to different types of natural soil, limited information has focused on the artificial composite soil aggregate or the quantitative analysis of its erosion resistance.

Vegetation concrete is equably mixed of four solid raw materials, including planting soil, cement, natural organic

material and green additive with a definite ratio, and then a right amount of water is added. As a typical artificial composite soil, vegetation concrete has been widely used throughout the country for it could create suitable vegetation habitat on the surface of bare rock slope, so as to implement ecological restoration and shallow protection for the slope (Xu et al. 2012). Field application indicated that the erosion resistance of vegetation concrete was obviously higher than that of natural soil, but the exact degree and essence of the improvement are yet deficient in specific data and theoretical basis. Therefore, building on the base of comparing with natural soil which is added as the planting soil, this study focused on vegetation concrete and analysed the aggregate distribution characteristics and erosion resistance indexes. Meanwhile, it explored the reason and mechanism of the enhancement of erosion resistance, thereby providing experience reference for the research of artificial composite soil aggregate and offering scientific basis for the soil stabilization in slope ecological restoration

MATERIALS AND METHODS

Study site: Yichang is located in southwest China and has mid-subtropic climate. The average annual rainfall is approximately 1213.6 mm (1998-2010), mainly occurring in June and July with heat and rain in corresponding period. The annual accumulated temperature is high and frost season is short. The average annual temperature is about 16.7°C, varying from 14°C to 19°C.

The slope on the side of Xiazhou Road in Yichang was selected as the study slope. The bedrock of the slope is shallow red mudstone, which has been covered with 15-centimetre-thick vegetation concrete artificially since the late summer of 2005. The vegetation concrete base spraying technique (VCBS) restores the vegetation on slopes by spreading a mix of concrete, greening additives and plant seeds on slope surfaces (Chen et al. 2013). The planting soil was taken from a natural soil slope near the above mudstone slope, and it was classified as a sandy loam with a pH of 6.6. Meanwhile, the natural soil slope for planting soil was taken as the controlled slope, and its site conditions were closer to the study slope, consisting of 58° inclination, 2.6 m height, about 90% vegetation coverage and 30-200 cm plant height.

Sampling: In June 2015, six plots with good vegetative growth were selected for the soil aggregate analysis on the study slope and controlled slope respectively. The size of each plot was set at 1.5 m × 1.5 m and five locations were randomly selected by following S curve at the depth of 0-15 cm to form a composite sample. After being air-dried, all samples were stripped into small blocks along the natural

structure plane, while removing plant roots and small stone tablets. All analyses were repeated thrice for each sample.

Index analysis: There are lots of indexes to characterize the soil aggregate and soil erosion resistance, and many factors should be focused on, e.g. the research object, research conditions, etc. The single index only can reflect the relative sensitivity of soil to the erosion force, while the combination of indexes could be a more comprehensive response to the actual soil erosion resistance. In this paper, the following eleven evaluation indexes were selected from the four aspects.

According to the procedure described by Hofman (1973), the soil was dry-sieved through a set of sieves with openings of 7, 5, 3, 2, 1, 0.5 and 0.25 mm. For aggregates >0.25 mm resistant to external forces, mechanical stability macroaggregate ($MSA_{>0.25}$, %) was chosen and calculated as the cumulative mass percentage of aggregates > 0.25 mm under dry sieving (Choudhury et al. 2014).

According to the procedure described by Elliott (1986), the soil was wet-sieved through a set of sieves with openings of 5, 3, 2, 1, 0.5 and 0.25 mm. For aggregates > 0.25 mm resistant to hydraulic dispersion, six indexes were selected and calculated, including water-stable macroaggregate ($WSA_{>0.25}$, %), mean weight diameter (MWD, mm), geometric mean diameter (GMD, mm), destruction rate (PAD, %), fractal dimension (D) and erodibility factor (K).

WSA_{mac} (%) refers to the cumulative mass percentage of aggregates > 0.25 mm under wet sieving (Young 1984). MWD and GMD are calculated following Nimmo & Perkins (2002):

$$MWD = \sum_{i=1}^n x_i \omega_i \quad \dots(1)$$

$$GMD = \exp \left(\sum_{i=1}^n \omega_i \log_{10} x_i \right) \quad \dots(2)$$

Where, n is the number of aggregate fractions under wet sieving (n=7, with the fractions being < 0.25, 0.25-0.5, 0.5-1.0, 1.0-2.0, 2.0-3.0, 3.0-5.0 and > 5.0 mm); x_i is the mean diameter (mm) of aggregate fraction i under wet sieving, equalling to 0.25, 0.375, 0.75, 1.5, 2.5, 4.0 and 5.0 mm, respectively; and ω_i (%) is the mass proportion of aggregate fraction i under wet sieving.

PAD is calculated as equation (3) (Xu et al. 2013, Su et al. 2004):

$$PAD = \frac{MSA_{>0.25} - WSA_{>0.25}}{MSA_{>0.25}} \times 100\% \quad \dots(3)$$

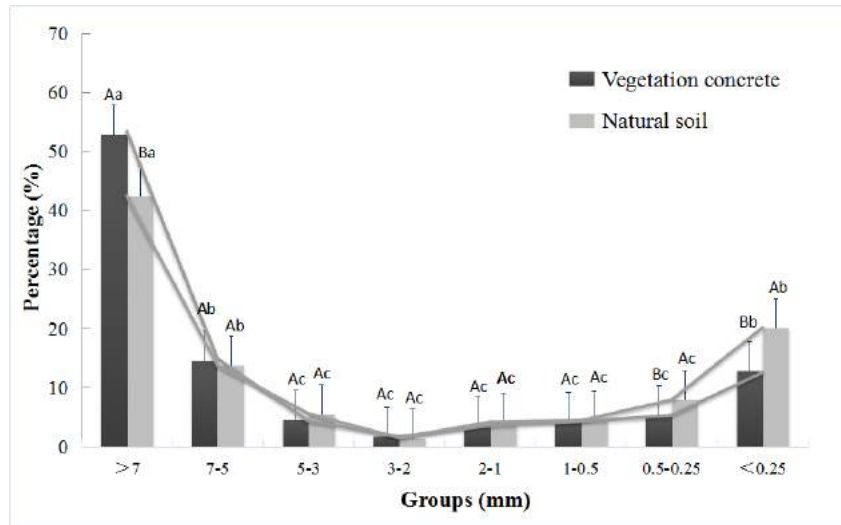


Fig. 1: PSD of mechanical stability aggregates.

*Bars with the same capital letter(s) within each group are not significantly different between vegetation concrete and natural soil at P<0.05, and bars with the same lowercase letter(s) among different groups are not significantly different for the same soil (vegetation concrete or natural soil) at P<0.05.

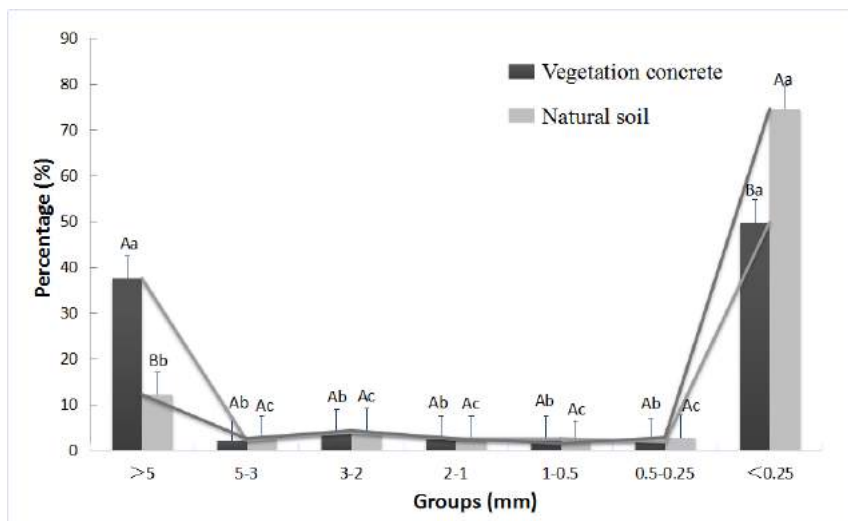


Fig. 2: PSD of water-stable aggregates.

*Bars with the same capital letter(s) within each group are not significantly different between vegetation concrete and natural soil at P<0.05, and bars with the same lowercase letter(s) among different groups are not significantly different for the same soil (vegetation concrete or natural soil) at P<0.05.

D is used to express mass and size information about aggregates and calculated as equation (4) (Chen et al. 2016, Xia et al. 2015):

$$\frac{M(r < R)}{M_T} = \left(\frac{R}{R_L}\right)^{(3-D)} \quad \dots(4)$$

where M(r < R) is the cumulative mass of aggregates with size r smaller than a comparative size R under wet

sieving, i.e., as R is 1.0 mm, M(r < R) refers to the mass of aggregates < 0.25 and 0.25-0.5mm under wet sieving; M_T is the total mass of aggregates under wet sieving; R is the sieve size opening, equalling to 0.25, 0.5, 1.0, 2.0, 3.0 and 5.0 mm, respectively; R_L is the maximum aggregate size defined by the largest sieve size opening, equalling to 5.0 mm.

K is a complex concept and reflects the soil resistance to

erosion (Buttafuoco et al. 2012), which can be calculated in accordance with equation (5) (Wischmeier et al. 1971, Foster et al. 1981, Rosewell 1993):

$$K = 2.77 \times 10^{-7} (12 - \text{OMC}) [(100 - C)(L + \text{Arm}f)]^{1.14} + 4.28 \times 10^{-3} (s - 2) + 3.27 \times 10^{-3} (p - 3) \quad \dots(5)$$

Where OMC is the organic matter content (%), C is the mass proportion (%) of clay (< 0.002 mm), L is the mass proportion (%) of silt (0.002-0.05mm), Armf is the mass proportion (%) of very fine sand (0.05-0.1mm), s is the soil structure code used in soil classification, and p is the profile permeability (SSS, 2006).

For aggregates <0.25mm, which are defined as microaggregates and indicate the structure and dispersion of soil under the condition of immersion, aggregation status (AS, %), aggregation degree (AD, %) and dispersion rate (DR, %) were chosen as follows:

$$\text{AS} = \omega_{(0.05-0.25)} - \omega_{\text{mc}(0.05-0.25)} \quad \dots(6)$$

$$\text{AD} = \frac{\text{AS}}{\omega_{(0.05-0.25)}} \times 100\% \quad \dots(7)$$

$$\text{DR} = \frac{\omega_{<0.05}}{\omega_{\text{mc}(<0.05)}} \times 100\% \quad \dots(8)$$

Where $\omega_{(0.05-0.25)}$ is the mass proportion (%) of microaggregate (0.05-0.25mm), $\omega_{\text{mc}(0.05-0.25)}$ is the mass proportion (%) of soil mechanical composition (0.05-0.25mm), $\omega_{<0.05}$ is the mass proportion (%) of microaggregate (<0.05mm), $\omega_{\text{mc}(<0.05)}$ is the mass proportion (%) of soil mechanical composition (<0.05mm), and all of them were measured through the pipette method described by Xu (2013).

For the organic colloid, organic matter content (OMC, %) was chosen and determined by potassium dichromate-external heating method (Liu et al. 1996).

Statistical analysis: Statistical analysis of all data was conducted by SPSS 16.0, and the results were expressed as mean values. Independent sample T test was used to compare the differences within the same parameter between vegetation concrete and natural soil, one-way ANOVA was performed to test the differences among different parameters of the same soil, correlation analysis was performed to determine the relationships and interactions among different indexes of vegetation concrete, and PC analysis was used to assess the principal components of the two soils.

RESULTS

Distribution characteristics of aggregate particle size: Dry sieving has less damage to the soil particle structure, re-

flecting soil particle size distribution (PSD) in the natural state (Gee & Bauder 1986). The PSD of mechanical stability aggregates for vegetation concrete and natural soil are presented in Fig. 1. For vegetation concrete, it exhibited an inverse J shape. The group >7 mm predominated, constituting about 53% of the total mass, which was significantly higher than any other groups (P<0.05). The groups 7-5 and <0.25 mm were about 15% and 13% respectively, significantly higher than groups 5-3, 3-2, 2-1, 1-0.5 and 0.5-0.25 mm (P<0.05). The least of the group was 3-2 mm in particle size, which was less than 2%. The others, including groups 5-3, 2-1, 1-0.5 and 0.5-0.25 mm, were all about 5% and slightly higher than group 3-2 mm, while there were no significant differences among groups 5-3, 3-2, 2-1, 1-0.5 and 0.5-0.25 mm (P<0.05).

For natural soil, the PSD of mechanical stability aggregates also presented an inverse J shape, which was similar to vegetation concrete. While group >7 mm was 11% less than that in vegetation concrete or so (P<0.05). At the same time, the groups <0.25 and 0.5-0.25 mm were higher than those in vegetation concrete by about 8% and 3% respectively, both of which revealed significant differences, too (P<0.05). However, there were no significant differences between vegetation concrete and natural soil in terms of groups 7-5, 5-3, 3-2, 2-1 and 1-0.5 mm and 0.5-0.25 mm (P<0.05).

The PSD of water-stable aggregates mainly reflects the soil resistance to hydraulic erosion (Kosugi 1996). As shown in Fig. 2, for vegetation concrete, the PSD of water-stable aggregates exhibited a U shape after wet sieving. The groups >5 and <0.25 mm, which accounted for about 37% and 50% of the total mass respectively, were markedly higher than the others (P<0.05). There were no significant differences among groups 5-3, 3-2, 2-1, 1-0.5 and 0.5-0.25 mm with a range of 1-4% (P<0.05).

For natural soil, the PSD of water-stable aggregates presented a J shape and was obviously different from that of vegetation concrete. The group <0.25 mm was the highest, reaching about 74%, which was significantly higher than that in vegetation concrete (P<0.05). However, the group >5 mm was only about 12%, which was significantly lower than that in vegetation concrete (P<0.05). No significant differences were observed in groups 5-3, 3-2, 2-1, 1-0.5 and 0.5-0.25 mm between vegetation concrete and natural soil (P<0.05).

Characteristics of erosion resistance: After determination, eleven evaluation indexes above are presented in Table 1, indicating the significant differences between vegetation concrete and natural soil (P<0.05). On the PSD, $\text{MSD}_{>0.25}$ and $\text{WSA}_{>0.25}$ in vegetation concrete were 87.01% and 50.25% respectively, which were higher than those in natu-

ral soil (79.86% and 25.51%). Under wet sieving, MWD and GMD of vegetation concrete were 2.84 mm and 0.75 mm respectively, significantly higher than those of natural soil (1.27 mm and 0.29 mm), while PAD and K were 42.40% and 0.08 respectively, significantly lower than those of natural soil (68.49% and 0.33). D of vegetation concrete was 2.11, which was significantly lower than those of natural soil (2.79). On the microaggregates, AS and AD of vegetation concrete were 11.18% and 28.23%, remarkably better than those of natural soil (6.82% and 20.39%), while DR of the former was 53.36%, significantly smaller than that in the latter (73.32 %). Additionally, OMC of vegetation concrete was 2.49%, which was also significantly higher than that of natural soil (1.51%).

Correlation analysis of erosion resistance indexes:

Correlation analysis was conducted and among $MSA_{>0.25}$ (X1), $WSA_{>0.25}$ (X2), MWD (X3), GWD (X4), K (X5), D (X6), PAD (X7), AS (X8), AD (X9), DR (X10) and OMC (X11), displaying in Table 2. As a result, the $WSA_{>0.25}$ (X2) of vegetation concrete was closely related to other erosion resistance indexes and had highly significant positive correlations with MWD (X3) ($r = 0.985^{**}$), GWD (X4) ($r = 0.966^{**}$) and OMC (X11) ($r = 0.968^{**}$) at $P < 0.01$. However, it correlated highly negatively with K (X5) ($r = -0.983^{**}$) and D (X6) ($r = -0.950^{**}$) at $P < 0.01$. Furthermore, a significant negative correlation was found between $WSA_{>0.25}$ (X2) and PAD (X7) ($r = -0.923^*$) at $P < 0.05$.

Table 2 shows that OMC (X11) was a key index affecting the erosion resistance of vegetation concrete, too. Specifically, OMC (X11) had highly significant positive correlations with MWD (X3) ($r = 0.982^{**}$) and GWD (X4) ($r = 0.974^{**}$) ($P < 0.01$) and a significant positive correlation with $MSA_{>0.25}$ (X1) ($r = 0.914^*$) ($P < 0.05$). However, it revealed a highly significant negative correlation with K (X5) ($r = -0.950^{**}$) ($P < 0.01$) and significant negative correlations with D (X6) ($r = -0.915^*$) and PAD (X7) ($r = -0.906^*$) ($P < 0.05$). Furthermore, there were different degrees of correlations among other indexes.

PC analysis of erosion resistance indexes: The indexes of soil erosion resistance are various and complex, and there is some mutual information to a certain extent as shown in Table 2. In order to further reveal the contribution of each index to the soil erosion resistance, PC analysis was conducted and results are summarized in Table 3. According to the principle of PC extraction, three principal components (Y1, Y2 and Y3) were extracted from the eleven erosion resistance indexes above, and their characteristic values were 6.305, 2.276 and 1.942 with the contribution rates of 57.32%, 20.69% and 17.66%, respectively. The cumulative contri-

bution rate was 95.67%, meeting the requirement of information loss for PC analysis.

From the load of each index in Table 3, the results of PC analysis suggested that the major contribution indexes to the principal component Y1 were $MSA_{>0.25}$ (X1), $WSA_{>0.25}$ (X2), MWD (X3) and GWD (X4). Accordingly, the major contribution indexes to the principal component Y2 were AS (X8), AD (X9) and DR (X10), and OMC (X11) was the most important index in determining the principal component Y3.

Among them, only DR (X10) was a negative contribution, and others were the positive contribution, including $MSA_{>0.25}$ (X1), $WSA_{>0.25}$ (X2), MWD (X3), GWD (X4), AS (X8), AD (X9) and OMC (X11). PC analysis indicated that stronger erosion resistance of soil was achieved with the higher $MSA_{>0.25}$, $WSA_{>0.25}$, MWD, GWD, AS, AD and OMC as well as the lower DR.

On the basis of index loads and characteristic values in Table 3, the expressions of Y1, Y2 and Y3 could be derived respectively as follows:

$$Y_1 = 0.148X_1 + 0.152X_2 + 0.150X_3 + 0.151X_4 - 0.136X_5 - 0.138X_6 - 0.130X_7 + 0.037X_8 + 0.067X_9 - 0.086X_{10} + 0.022X_{11}$$

$$Y_2 = -0.017X_1 - 0.006X_2 + 0.011X_3 + 0.011X_4 + 0.073X_5 + 0.007X_6 + 0.116X_7 + 0.384X_8 + 0.374X_9 - 0.364X_{10} - 0.007X_{11}$$

$$Y_3 = -0.110X_1 + 0.131X_2 + 0.149X_3 + 0.128X_4 - 0.222X_5 + 0.195X_6 - 0.242X_7 - 0.195X_8 - 0.073X_9 + 0.044X_{10} + 0.506X_{11}$$

According to the expressions, the principal component values of the erosion resistance for vegetation concrete and natural soil were calculated as shown in Table 4.

The comprehensive principal component model $Y = 0.599Y_1 + 0.216Y_2 + 0.185Y_3$ was obtained by taking the proportion of the characteristic value corresponding to each principal component as the total characteristic value, and then comprehensive principal component values of the erosion resistance for vegetation concrete and natural soil were calculated as 0.617 and 0.175, respectively.

DISCUSSION

The research methods of soil erosion resistance could be grossly classified into two main types. One is described in ISSCAS (1981) to study some physical and chemical indexes of soil directly, e.g., the aggregate characteristic and OMC. The other is to study the changes of soil under various external forces, which is controlled by the former (Amezket et al. 1996). This paper used the former to carry out the changes of erosion resistance indexes for vegetation concrete based on natural soil.

It is generally considered that the soil erosion resistance is proportional to $MSA_{>0.25}$, $WSA_{>0.25}$, MWD, GMD, AS, AD

Table 1: Characteristics of erosion resistance indexes of vegetation concrete and natural soil.

Soil type	MSA _{>0.25} (%)	WSA _{>0.25} (%)	MWD (mm)	GMD (mm)	K	D	PAD (%)	AS (%)	AD (%)	DR (%)	OMC (%)
Vegetation concrete	87.01A	50.25A	2.84A	0.75A	0.08 B	2.11B	42.40B	11.18A	28.23A	53.36B	2.49A
Natural soil	79.86B	25.51B	1.27B	0.29B	0.14A	2.79A	68.49A	6.82B	20.39B	73.32A	1.51B

*The same capital letter(s) within each index are not significantly different between vegetation concrete and natural soil at P<0.05.

Table 2: Correlation analysis of erosion resistance indexes for vegetation concrete.

	X ₁	X ₂	X ₃	X ₄	X ₅	X ₆	X ₇	X ₈	X ₉	X ₁₀	X ₁₁
X ₁	1.000										
X ₂	0.954**	1.000									
X ₃	0.961**	0.985**	1.000								
X ₄	0.957**	0.966**	0.974**	1.000							
X ₅	-0.853	-0.983**	-0.864	-0.868	1.000						
X ₆	-0.912*	-0.950**	-0.915*	-0.907*	0.879	1.000					
X ₇	-0.907*	-0.923*	-0.921*	-0.913*	0.910*	0.864	1.000				
X ₈	0.773	0.875	0.768	0.774	-0.562	-0.798	-0.865	1.000			
X ₉	0.832	0.845	0.821	0.830	-0.764	-0.690	-0.675	0.903*	1.000		
X ₁₀	-0.814	-0.891	-0.879	-0.871	0.745	0.619	0.902*	-0.921*	-0.911*	1.000	
X ₁₁	0.914*	0.968**	0.982**	0.974**	-0.950**	-0.915*	-0.906*	0.865	0.871	-0.821	1.000

** indicated that it is significant at P<0.01, * indicated that it is significant at P<0.05.

Table 3: PC analysis of erosion resistance indexes.

Principal component	Index load											Characteristic	Cumulative contribution rate %
	X ₁	X ₂	X ₃	X ₄	X ₅	X ₆	X ₇	X ₈	X ₉	X ₁₀	X ₁₁ value		
Y ₁	0.932	0.961	0.943	0.952	-0.858	-0.870	-0.822	0.231	0.425	-0.543	0.141	6.305	57.32
Y ₂	-0.038	-0.013	0.024	0.026	0.167	0.015	0.264	0.874	0.852	-0.828	-0.015	2.276	78.01
Y ₃	-0.213	0.254	0.289	0.249	-0.431	0.379	-0.469	-0.379	-0.142	0.086	0.983	1.942	95.67

Table 4: Principal component values of erosion resistance for vegetation concrete and natural soil.

Soil type	Y ₁	Y ₂	Y ₃	Y
Vegetation concrete	0.249	0.006	0.361	0.617
Natural soil	-0.072	0.040	0.207	0.175

and OMC, while it is inversely proportional to PAD, K, D and DR (Staricka & Beniot 1995, Cotler & Ortega-Larrocea 2006, Liu et al. 2012), which was consistent with the PC analysis in this paper. Compared with natural soil, all the erosion resistance indexes of vegetation concrete had improved. On the distribution characteristic of aggregate particle size, MSA_{>0.25} and WSA_{>0.25} of vegetation concrete increased by 9.1% and 97.0% respectively, and the variation was particularly noticeable in WSA_{>0.25}. On the indexes resistant to hydraulic dispersion, MWD and GWD of vegeta-

tion concrete increased by 123.6% and 158.6%, while K, PAD and D decreased by 75.8%, 38.1% and 24.4%. On the indexes of microaggregate, AS and AD of vegetation concrete improved by 63.9% and 38.5%, while DR decreased by 27.2%. On the organic colloid indexes, OMC of vegetation concrete increased by 65.2%. Especially, the comprehensive principal component value (Y) of erosion resistance for vegetation concrete also increased by 252.6%. Therefore, the connection capability between particles had been improved and the anti-dispersion ability had been

strengthened for vegetation concrete, and its erosion resistance was obviously better than that of natural soil.

The erosion resistance of vegetation concrete was obviously better than that of natural soil because of the addition of a large amount of natural organic material and cement in the latter when mixing vegetation concrete. On the one hand, as a kind of natural organic material, the fir sawdust added into natural soil would be decomposed into organic matter after a long time of decay, which made the OMC in vegetation concrete much higher than that of natural soil. Data in this article displayed that OMC had highly significant positive correlations with $WSA_{>0.25}$, MWD and GWD and the very significant negative correlation with K. At the same time, PC analysis above also presented that OMC made a greater contribution to the erosion resistance of vegetation concrete. To a great extent, the erosion resistance of soil depended on the ability of organic and inorganic cementing materials to connect soil particles (Tisdall et al. 1982, Bandyopadhyay et al. 2010, Yin et al. 2016). Blazejewski et al. (2005) have pointed out that macroaggregates and organic matter were the basis of stable soil structure. Studies by Yao (2009) also showed that higher OMC would facilitate the formation of soil aggregates and the increase of erosion resistance. Further, organic colloids in organic matter have cementation and flocculation, which could promote the formation of macroaggregates in soil, enhance the cohesive force between soil particles and improve the soil erosion resistance (Barral et al. 1998). In addition, organic matter would decompose under the action of microorganisms and organic acids would be produced to prevent agglomerates from dissipating, which also enhance the stability and erosion resistance of soil (Wu et al. 1997).

On the other hand, the cement added into natural soil would react with water and directly convert into hydrated calcium silicate, hydrated calcium aluminate, $Ca(OH)_2$ crystal and other compounds. These crystalline compounds would make microaggregates agglomerate together to form crystalline networks and solid compact structures under the action of strong chemical bonds, so as to improve the content of macroaggregates ($MSA_{>0.25}$, $WSA_{>0.25}$) in vegetation concrete and enhance its erosion resistance. This view was similar to the result of Su (2011) that the addition of EN-1 curing agent could improve the erosion resistance of slope soil. After adding cement into natural soil, complex substance has essentially become a kind of cement soil. The effect of cement and curing agent were the similar, which could improve the erosion resistance of vegetation concrete.

It is a prerequisite to create the vegetation habitat with the strong erosion resistance as carrying out ecological res-

toration work on the surface of bare rock slope. The erosion resistance of vegetation concrete is much higher than that of natural soil, and its damage degree is lower under the hydraulic force as well as the better stability. Thus, vegetation concrete has a broad prospect in the future of engineering applications.

In the distribution characteristics of aggregates particle size, mechanical stability aggregates of vegetation concrete and natural soil, both presented an inverse J shape, while water-stable aggregates of vegetation concrete and natural soil exhibited a U shape and a J shape respectively. As a whole, the group <0.25 mm in natural soil was significantly higher than that in vegetation concrete ($P<0.05$).

Compared with natural soil, all the erosion resistance indexes of vegetation concrete were significantly improved ($P<0.05$). $MSA_{>0.25}$, $WSA_{>0.25}$, MWD, GWD, AS, AD and OMC increased by 9.1%, 97.0%, 123.6%, 158.6%, 63.9%, 38.5% and 65.2% respectively, while K, PAD, D and DR decreased by 75.8%, 38.1%, 24.4% and 27.2% respectively. Meanwhile, the comprehensive principal component value (Y) of erosion resistance for vegetation concrete also enhanced by 252.6%.

Correlation analysis showed that there were highly significant correlations among erosion resistance indexes of vegetation concrete ($P<0.01$), e.g. $WSA_{>0.25}$, OMC, MWD, GWD, K, etc.

The natural organic material and cement added in the preparation of vegetation concrete were the main reasons for its erosion resistance obviously better than that of natural soil. Therefore, vegetation concrete was a suitable compound to create vegetation habitat with the strong erosion resistance on the surface of bare rock slope.

ACKNOWLEDGEMENTS

This study was supported by the Hubei Key Laboratory of Disaster Prevention and Mitigation, China Three Gorges University (No. 2016KJZ11) and CRSRI Open Research Program (No. CKWV2017514/KY)

REFERENCES

- Amezketta, E., Singer, M.J. and Le Bissonnais, Y. 1996. Testing a new procedure for measuring water-stable aggregation. *Soil Sci. Soc. Am. J.*, 60: 888-894.
- An, S.S., Huang, Y.M. and Zheng, F.L. 2008. Aggregate characteristics during natural revegetation on the Loess Plateau. *J. Pedosphere*, 06: 809-816.
- Angers, D.E. and Caron, J. 1998. Plant-induced changes in soil structure: processes and feedbacks. *Biogeochemistry*, 42: 55-72.
- Bandyopadhyay, P.K., Saha, S., Mani, P.K. and Mandal, B. 2010. Effect of organic inputs on aggregate associated organic carbon concentration under long-term rice-wheat cropping system. *Geoderma*, 154: 379-386.

- Barral, M.T., Arias, M. and Guerif, J. 1998. Effects of iron and organic matter on the porosity and structural stability of soil aggregates. *Soil Till. Res.*, 46: 261-272.
- Barthes, B. and Roose, E. 2002. Aggregate stability as an indicator of soil susceptibility to runoff and erosion; validation at several levels. *Catena*, 47: 133-149.
- Blazejewski, G. A., Stolt, M. H., Gold, A. J. and Groffman, P. M. 2005. Macro- and micromorphology of subsurface carbon in riparian zone soils. *Soil Sci. Soc. Am. J.*, 69: 1320-1329.
- Bronick, C. J. and Lal, R. 2005. Soil structure and management: a review. *Geoderma*, 124: 3-22.
- Buttafuoco, G., Conforti, M., Auccelli, P.P.C., Robustelli, G. and Scarciglia, F. 2012. Assessing spatial uncertainty in mapping soil erodibility factor using geostatistical stochastic simulation. *Environmental Earth Sciences*, 66(4): 1111-1125.
- Chen, F., Xu, Y., Wang, C. and Mao J. 2013. Effects of concrete content on seed germination and seedling establishment in vegetation concrete matrix in slope restoration. *Ecological Engineering*, 58: 99-104.
- Chen, S.N., Ai, X.Y. and Dong, T.Y. 2016. The physico-chemical properties and structural characteristics of artificial soil for cut slope restoration in Southwestern China. *Scientific Reports*. DOI, 10.1038 (in Chinese).
- Choudhury, S.G., Srivastava, S. and Singh, R. 2014. Tillage and residue management effects on soil aggregation, organic carbon dynamics and yield attribute in rice-wheat cropping system under reclaimed sodic soil. *Soil Till. Res.*, 136: 76-83.
- Cotler, H. and Ortega-Larrocea, M.P. 2006. Effects of land use on soil erosion in a tropical dry forest ecosystem, Chamela watershed, Mexico. *J. Catena*, 65(02): 107-117.
- Elliott, E.T. 1986. Aggregate structure and carbon, nitrogen and phosphorus in native and cultivated soils. *Soil Sci. Soc. Am.*, 50: 627-633.
- Foster, G.R., McCool, D.K., Renard, K.G. and Moldenhauer, W.C. 1981. Conversion of the universal soil loss equation to SI metric units. *Journal of Soilless and Water Conservation*, 36(6): 355-359.
- Gee, G. W. and Bauder, J. W. 1986. Particle-size analysis. In: Klute, A. (ed.) *Methods of Soil Analysis. Part I. Physical and Mineralogical Methods*. 2nd ed., Agron. Monogr. ASA and SSSA, Madison, WI., pp. 383-409.
- Hofman, G. 1973. Kritische studie van de instabiliteit van bodemaggregaten en de invloed op fysische bodemparameters (Doctoral dissertation, Dissertation. Faculty of Agricultural Sciences, University of Ghent, Belgium).
- ISSCAS (Institute of Soil Science of Chinese Academy of Science) 1981. *Soil Chemical and Physical Analysis*. Shanghai Science and Technology Publishing House, Shanghai (in Chinese).
- Kay, B.D. 2000. Soil structure. In: Summer, E.M. (ed.) *Hand-book of Soil Science*. Boca Raton, London, New York., pp. A229-A264.
- Kosugi, K. 1996. Lognormal distribution model for unsaturated soil hydraulic properties. *Water Resour. Res.*, 32: 2697-2703.
- Li, G.Y. and Fan H.M. 2014. Effect of freeze-thaw on water stability of aggregates in a black soil of northeast China. *Pedosphere*, 24(2): 285-290.
- Liu, G.S., Jiang, N.H., Zhang, L.D. and Liu, Z.L. 1996. *Soil Physical and Chemical Analysis & Description of Soil Profiles*. Beijing: Standards Press of China, pp. 166-167.
- Liu, X.H., Han, F.P. and Zhang, X.C. 2012. Effect of biochar on soil aggregates in the Loess Plateau: results from incubation experiments. *International Journal of Agriculture and Biology*, 6(14): 975-979.
- Morin, J. and Van Winkel, J. 1996. The effect of raindrop impact and sheet erosion on infiltration rate and crust formation. *Soil Sci. Soc. Am. J.*, 60: 1223-1227.
- Nimmo, J.R. and Perkins, K.S. 2002. Aggregate stability and size distribution. In: Dane, J.H., Topp, G.C. (Eds.), *Methods of Soil Analysis, Part 4. Physical Methods*, SSSA Book, Ser., Vol. 5. SSSA, Madison, WI, pp. 317-328.
- Ramos, M.C., Nacci, S. and Pla, I. 2003. Effect of raindrop impact and its relationship with aggregate stability to different disaggregation forces. *Catena*, 53: 365-376.
- Parr, J.F., Papendick, R.I. and Youngberg, I.G. 1983. Organic farming in the United States: Principles and perspectives. *Agro-Ecosystems*, 8: 183-201.
- Rosewell, C.J. 1993. SOLOSS: a program to assist in the selection of management practices to reduce erosion. Tech handbook No. 11 (2nd ed.). Conservation Service of New South Wales, Department of Conservation and Land Management, Sydney.
- Selen, D.S., Wim, M.C., Gunay, E. and Donald, G. 2011. Comparison of different aggregate stability approaches for loamy sand soils. *Applied Soil Ecology*, 54: 1-6.
- Soil Survey Staff (SSS) 2006. *Keys to Soil Taxonomy*. 10th Edition. Soil Conservation Service. Agricultural US Government Printing Office, Washington, D.C., USA.
- Staricka, J.A. and Benoit, G.R. 1995. Freeze-drying effects on wet and dry soil aggregate stability. *Soil Sci. Soc. Am. J.*, 59: 218-223.
- Su, T. 2011. Mechanism on scour resistance stability of EN-1 solidified slope in Pisha sandstone region. D. Northwest A&F University.
- Su, Y.Z., Zhao, H.L., Zhao, W.Z. and Zhang, T.H. 2004. Fractal features of soil particle size distribution and the implication for indicating desertification. *Geoderma*, 122: 43-49.
- Tisdall, J. M. and Oades, J. M. 1982. Organic matter and water-stable aggregates in soils. *J. Soil Sci.*, 33: 141-163.
- Wischmeier, W.H., Johnson, C.B. and Cross, B.V. 1971. Soil erodibility nomograph for farmland and construction sites. *Journal of Soil and Water Conservation*, 26(5): 189-193.
- Wu, Y., Liu, S.Q. and Wu, X.Q. 1997. Study on improving soil's waterstable aggregates amounts by botanic roots. *Journal of Soil Erosion and Soil and Water Conservation*, 1(3) (in Chinese).
- Xia, D., Deng, X. S. and Wang S. L. 2015. Fractal features of soil particle-size distribution of different weathering profiles of the collapsing gullies in the hilly granitic region, south China. *Nat Hazards*, 79: 455-478
- Xu, G., Li, Z. and Li, P. 2013. Fractal features of soil particle-size distribution and total soil nitrogen distribution in a typical watershed in the source area of the middle Dan River, China. *Catena* 101: 17- 23.
- Xu, W.N., Xia Z.Y. and Zhou, M.T. 2012. Theory and practice of ecological protection technology of vegetation concrete. *Water Resources and Hydropower Engineering*. China Water & Power Press, Beijing (in Chinese).
- Yao, S. H., Qin, J. T., Peng, X. H. and Zhang, B. 2009. The effects of vegetation on restoration of physical stability of a severely degraded soil in China. *J. Ecological Engineering*, 35(05): 723-734.
- Yin, Y., Wang, L. and Liang, C.H. 2016. Soil aggregate stability and iron and aluminium oxide contents under different fertiliser treatments in a long-term solar greenhouse experiment. *J. Pedosphere*, 26(5): 760-767.
- Young, R.A. 1984. A method of measuring aggregate stability under waterdrop impact. *Trans. Am. Soc. Agric. Eng.*, 27: 1351-1353.



Statistical Modelling of 4-hourly Wind Patterns in Calcutta, India

Prashanth Gururaja*, Nittaya McNeil**(*)† and Bright Emmanuel Owusu*(***)

*Department of Mathematics and Computer Science, Faculty of Science and Technology, Prince of Songkla University, Mueang Pattani, 94000, Thailand

**Centre of Excellence in Mathematics, Commission on Higher Education (CHE), Ministry of Education, Ratchathewi, Bangkok, 10400, Thailand

***Department of Information and Communication Technology/Mathematics, Faculty of Science and Technology, Presbyterian University College, Ghana

†Corresponding author: Nittaya McNeil

Nat. Env. & Poll. Tech.

Website: www.neptjournal.com

Received: 05-05-2018

Accepted: 02-08-2018

Key Words:

Wind prevalence

Wind patterns

Logistic and linear regression

Speed and gust

ABSTRACT

The rising energy demands of the world and minimal availability of conservative energy sources have considerably increased the role of non-conventional sources of energy like solar and wind. The modelling of the prevalence of wind speed and trends helps in estimating the energy produced from wind farms. This study uses statistical models to analyse the wind patterns in India. Hourly wind data during 2004-2008 were obtained from the National Renewable Energy Laboratory for the study. A logistic regression model was initially used to investigate 4-hourly wind prevalence and the pattern of wind gust. A linear regression model was then applied to investigate wind speed trends. The 4-hour periods of the day, months, and year factors of wind were used as the independent variables in the statistical analysis. The results showed that wind prevalence was mostly higher between 4 AM to 4 PM within the day (90%). Analysis of the monthly wind prevalence revealed higher percentage between April to June (90%), while higher annual prevalence was revealed in 2007 and 2008 (85%). Wind speed trends (4-hourly periods) was observed to increasing from 4 AM to 4 PM within which the maximum occurred. Monthly wind speed was seen to be increasing from January to April where it attains the maximum (13 ms^{-1}) and reduces it to minimum in November (3 ms^{-1}). Annual mean wind speed has reduced by 4 ms^{-1} between 2004 and 2008.

INTRODUCTION

Wind plays a pivotal role in climate and weather on Earth's surface. The movement of wind on Earth's surface has diverse ranges of magnitudes, different directions and various time intervals from minute to few hours. Wind circulation on the Earth's surface commonly known as wind prevalence describes the motion of wind with intermittent momentarily rates (Greene et al. 2010). The wind speed intriguing behaviour has a vast impact on global climate and weather conditions (Csavina et al. 2014) nurturing of ecosystems, and human life imbalance (Mitchell 2012). Wind gusts rapid and intermittent speeds have an enormous influence on climate and weather events (Cheng et al. 2014). In addition, its extreme can cause enormous damages or destruction to human-made structures, devastation to humans and ecosystems, and dangerous situations in aircrafts (Jain et al. 2001, Schindler et al. 2012, Jamaludin et al. 2016). It plays a significant factor in wind characteristics often combined and denoted as wind velocity. Further, six major wind belts, three each in the northern and southern hemisphere, encircle the surface of the Earth. These belts lie from pole to equator

namely polar easterlies, westerlies, and trade winds describe the wind pattern on the Earth's surface (Myrl 2012).

The variant behaviours of wind cause a difference in absorption of solar energy among the climate zones of earth and atmospheric circulation by differential heating between equator and poles (Chapin et al. 2002). Therefore, wind with its volatile behaviour can be used productively to harness energy, operate transport and warfare equipment. Thus, statistical analysis of wind characteristics will be beneficial.

In recent decades, many studies have investigated wind patterns over the Earth's surface. A study by Klink (2002) investigated trends and interannual variability of wind speed distributions in Minnesota. The research results showed reducing wind speed trend below the overall mean for most of the stations. However, only few stations showed increasing trends above the overall mean. Nchaba et al. (2016) studied long-term austral summer wind speed trends over southern Africa. The results revealed evidence of a decline in wind speeds, results in deceleration of mid latitude westerly, and Atlantic southeasterly winds with a poleward shift in the subtropical anticyclone. Increasing trends in the annual

frequency of summer circulation weather types, and the weakening of the subtropical continental heat. Another study by Klink (1999) studied on trends in mean monthly maximum and minimum surface wind speeds in the coterminous United States, 1961 to 1990. The results showed reducing trends in the maximum and minimum winds observed in spring and summer reduced. The decreasing wind speed occurred in western and southeastern United States may be due to variable topography and high pressure mostly all through the year. However, central and the northeastern United States having gentle topography and are near common storm tracks had the highest maximum and minimum winds. Also, a study by Bett et al. (2013) investigated European wind variability over 140 years. The results revealed strong highly-variable wind in the northeast Atlantic. Also, findings do not show any clear long-term trends in the wind speeds across Europe and the variability between decades is large. However, the year 2010 had the lowest mean wind speed on record for this region. Mohanan et al. (2011) investigated the probability distribution of land surface wind speeds. The results illustrated daytime surface wind speeds to be broadly consistent, whereas night time surface wind speeds are more positively skewed. However, in the mid latitudes, these strongly positive skewnesses are shown to be associated with conditions of strong surface stability and weak lower-tropospheric wind shear. Moreover, research by Troccoli et al. (2012) studied long-term wind speed trends over Australia. The results showed that light winds tend to increase more rapidly than the mean winds, whereas strong winds increase less rapidly than the mean winds. The trends in both light and strong winds vary in line with the mean winds. Chen et al. (2013) investigated wind speed trends over China, quantifying the magnitude and assessing causality. The results exhibited pronounced downward trends especially in the upper percentiles and during spring. The warm and cold Arctic Oscillation and El Niño-Southern Oscillation phases have significant influence on the probability distribution of wind speeds. Thus, internal climate variability is a major source of both interannual and long-term variability.

Reddy et al. (2015) used statistical analysis to estimate wind energy over Gadanki, India from 2007 to 2012 using Weibull, Rayleigh and Gamma parametric methods. They showed that Weibull distribution fitted well. A study by Gupta & Biswas (2010) analysed wind velocity of Silchar (Assam, India) from 2003-2007 by applying Rayleigh's and Weibull methods. The results revealed that average wind velocity in Silchar is about 3.11 kmh^{-1} , which is considerably low. Lakshmanan et al. (2009) studied on the basic wind speed map of India with long-term hourly wind data

from 1983-2005 using Gumbel method. The study results showed that certain regions require improvement to higher wind zones from the current benchmark wind zones. They also suggested the need to revised basic wind speed map with upgraded wind speed zones for India. Even though many aspects of wind in India have been analysed, not much has been on the description of wind prevalence rates, wind speed trends and wind gust patterns. The objectives of this study are to describe the wind and wind gust prevalences and analyse the wind speed patterns using statistical models.

MATERIALS AND METHODS

India has nine meteorological stations specified by National Renewable Energy Laboratory (NREL). Hourly wind observations from Calcutta during 2004-2008 were obtained from NREL (https://www.nrel.gov/international/ra_india.html) for the study. This station was selected due to its subtropical climate with moist (rain-bearing) winds and frequent thunderstorms (Mukhopadhyay et al. 2009). The winds can vary from frigid winds, may be related to large storm systems such as Nor'westers and Western disturbances (Reddy 2008). It is also in wind and cyclone zone of very 'high damage risk' (UNDP 2006).

Data were arranged based on the Earth's surface wind direction patterns for Indian subcontinent (Wiegand 2004, Kious & Tilling 1996, IMD 2015). The data, which did not fall under the wind direction for the particular month, were discarded from the study resulting in 38,157 observations during the period of study. The hourly wind occurrence had fluctuations that were smoothed by accumulating data to 4 hour periods, and these were used for the analysis. The measurements recorded for consecutive 4-hourly periods were associated as per the well-known ancient time metrics of Babylon and Egyptian system which can be represented in 4-hourly periods of 6 intervals of a day (Gillings 1972). Moreover, 6 periods of 4 hours each of the day classified into clear time intervals like mid-night, dawn, morning, noon, mid-noon, night (Glickman & Zenk 2000) which is indicated as a period of the day, and other predictors are months and year. Observations on February 29 were discarded to have uniform number of observations for each year and also associated with heuristic 365 day climate data observations, therefore totalling to 9,540 observations for the study.

STATISTICAL METHODS

Logistic regression was initially fitted to model the prevalence of 4-hourly wind. The 4-hourly wind speed less than 0.775 ms^{-1} was kept as the non-occurrence of wind, and at least 0.775 ms^{-1} was considered as the occurrence of wind.

In modelling the prevalence of 4-hourly wind, if p_i is the probability of wind for the i th period in the data set, restricted on the variables x_i , then the model takes the form:

$$\ln\left(\frac{p_i}{1-p_i}\right) = \alpha + \beta_1 x_1 + \beta_2 x_2 + \dots + \beta_m x_m, \quad \dots(1)$$

Where, α is a constant, β_i ($i = 1, 2, 3, \dots, m$) are the slope coefficients of the model and x_i ($i = 1, 2, 3, \dots, m$) are the predictors and m is the number of predictors. The predictors are the 4-hourly periods, month and year factors.

Model (1) was also used to estimate the prevalence of wind gust. Wind speed of at least 5 ms^{-1} (Geer 1996) was classified as gust occurrence and classified as the non-occurrence of a gust if otherwise. The modelling process of estimating the wind gust occurrence is similar to that of the wind prevalence. The predictors are also the 4-hourly periods, month and year factors. These models were assessed using the receiver operating characteristic (ROC) curve.

The ROC curve is popularly known for determining the capability of prediction a binary outcome (Westin 2001). The ROC curve plots sensitivity against the false positive rate of the 4-hourly wind prevalence.

Multiple regression was then used to describe the trends of wind speed of at least 0.775 ms^{-1} . The model takes the form

$$y_{ijk} = \alpha + \beta_1 x_i + \beta_2 x_j + \beta_3 x_k + \gamma_{t-1}, \quad \dots(2)$$

Where, y_{ijk} represents wind speed trends, α is a constant, β 's are the regression coefficients, x_i, x_j, x_k is time indicating the predictors 4-hour periods, month and year, γ denotes the regression coefficients of the trimmed lag 1 term and $t-1$ indicates lag 1 period. The goodness of fit of the model was assessed using the coefficient of determination (R-square) and the Q-Q plots.

Further, since the normality assumption was not satisfied as the data were not normally distributed, due to heavy tails; the wind speed values were transformed by square roots, to satisfy the statistical assumption of normality. Subsequently, the wind speed observation anomalies were filtered by removing the auto correlations at lag 1 term (Chatfield 1996). The filtered autocorrelations at lag 1 term were then added to fit linear regression model (Venables & Ripley 2002) that investigated the wind speed trends.

The sum contrasts (Tongkumchum & McNeil 2009) were applied to obtain 95% confidence intervals (CI) to compare the fitted model means with the overall wind means. This contrast gives criteria to classify levels of the factor into three groups, according to whether each relating CI is greater than or equal to, or is less than the overall mean. All analy-

sis was done in R (R Development Core Team 2008)

RESULTS

A logistic regression model was fitted to 4-hourly wind periods for 2004-2008.

The model for the 4-hourly mean of wind prevalence was made of 3 predictors. The first predictor was the 4-hourly period of the day and had 6 factors, the second predictor was the months with 12 factors, and the third factor was the year having 5 factors. There were 24 parameters including the constant term in the model. The parameters were highly significant and influential in the model.

Assessing the goodness of fit of the model by the ROC curve (Fig. 1) revealed an area under ROC curve (AUC) value of 0.75 which show a sound classification of the prevalence and non-occurrence of wind.

The overall accuracy of the classification on the occurrence and non-occurrence of wind was 85% having a true positive rate of 99.7% with a false positive rate of 61.5%.

The plot of confidence intervals illustrates the pattern of wind prevalence percentage for period of the day, month and year and the crude percentage (Fig. 2). The horizontal red line denotes the overall mean of the wind prevalence, which is approximately 70%.

Analysis of the 95% confidence interval plots revealed that the wind prevalence patterns for period of the day were significantly different from the overall mean.

The period from dawn (period 2) to afternoon (period 4) observed high wind prevalence rates with the maximum

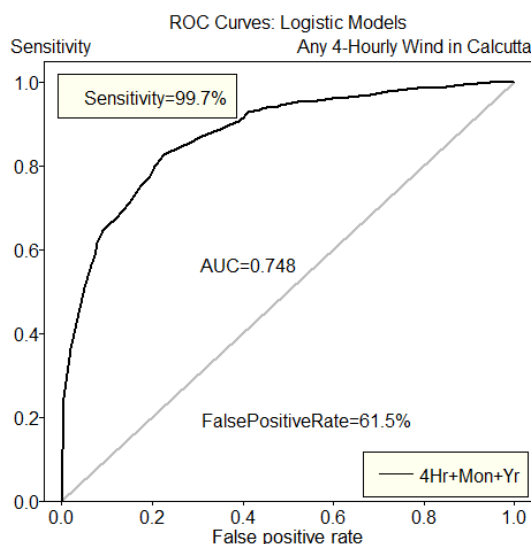


Fig. 1: ROC curve of the logistic model for 4-hour period of wind to investigate the prevalence of wind.

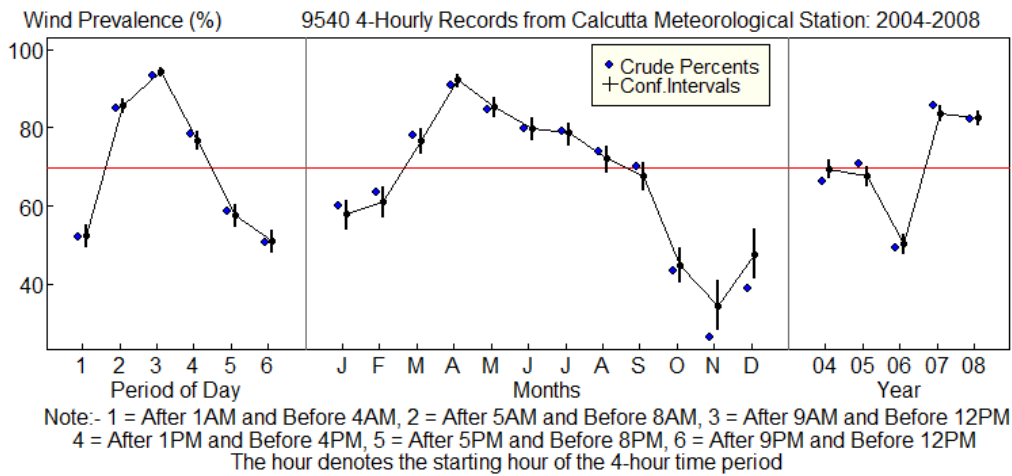


Fig. 2: Logistic model confidence interval plot for percentages of wind prevalence.

prevalence of around 90% observed in noon (period 3). The low wind prevalence rates were observed from midnight to dawn (period 1), evening (period 5) tonight (period 6) with the minimum prevalence of around 50 % in the night (period 6) respectively.

The monthly wind prevalence patterns were observed to have high wind prevalence rates from March to July with maximum wind prevalence of 90% observed in April. Moderate wind prevalence rate was observed during August and September with modest wind prevalence of 70% aligned with the overall mean. Wind prevalence rates were observed to be less than the overall mean during January and February. It increases gradually to attain its maximum (90%) in April,

decreases steadily, attain its minimum (30%) in November.

The yearly wind prevalence patterns were not significantly different from the overall mean between 2004 and 2005. It reduced considerably to its minimum in 2006 and rose steadily to its maximum in 2007, where it began to reduce slightly. The yearly wind prevalence ranged from 50 to 85% and observed to be higher than the overall mean between 2007 and 2008.

Model (1) was also used to examine the 4-hourly period wind gust prevalence from 2004-2008. The 4-hourly mean wind gust prevalence model was also made of 3 predictors.

Assessing the goodness of fit of the model by the ROC curve (Fig. 3) revealed an area under ROC curve (AUC) value of 0.61 which show classification of the occurrence and non-occurrence of wind. The overall accuracy of the classification on the occurrence and non-occurrence of wind gust was 81.67% having a true positive rate of 89.7% with a false positive rate of 23.7%.

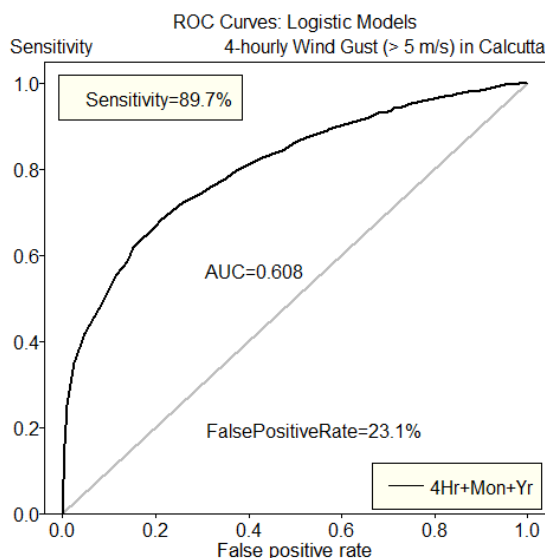


Fig. 3: ROC curve of the logistic regression model for the 4-hourly wind gust prevalence.

In Fig. 4, the horizontal line denotes the overall mean of the prevalence of wind gusts, which is around 10 % during the study period. The wind gust patterns for period of the day were significantly different from the overall mean. The period from midnight (period 1) to noon (period 3) observed increasing wind gust prevalence rates with the maximum prevalence of around 18% observed in noon (period 3). It then decreases steadily from this period to the night. The minimum wind gust prevalence of 4% occurred in midnight (period 1).

The monthly wind gust patterns revealed increasing pattern from January to April, where the maximum was attained. It was constant between April and decreases steadily until August, where it increased again until September. It then decreases sharply to minimum in November. The wind

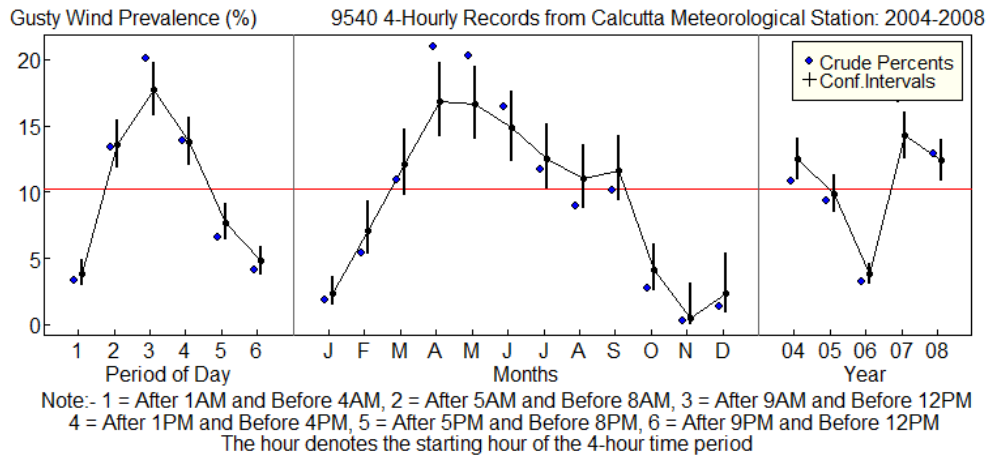


Fig. 4: The 95% confidence interval plot for the percentage of wind gusts using logistic regression.

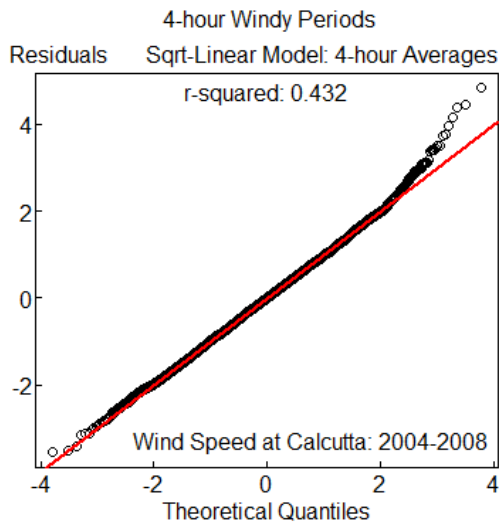


Fig. 5: Q-Q plots for the linear model of the wind speed.

gust prevalence was observed to be mostly above the overall mean between March and September.

The yearly wind gust prevalence revealed decreasing pattern from 2004 to 2006, where it attained the minimum of 4% and increased sharply to its maximum of 14% in 2007. There was a decreasing pattern between 2007 and 2008.

The linear regression model (model 2) was fitted to the 4-hourly wind speed to examine the trends. The model for 4-hourly period wind speed from 2004 -2008 was also made of 3 predictors. There were 25 parameters including the constant and AR(1) terms in the model. Most of the parameters were highly significant and influential in the model. The coefficient of determination (r-squared) and the quantile-quantile plots was used to evaluate the goodness of fit of the model. The r-squared value of 0.432 shows that 43% of the wind speed patterns are explained by the model (2).

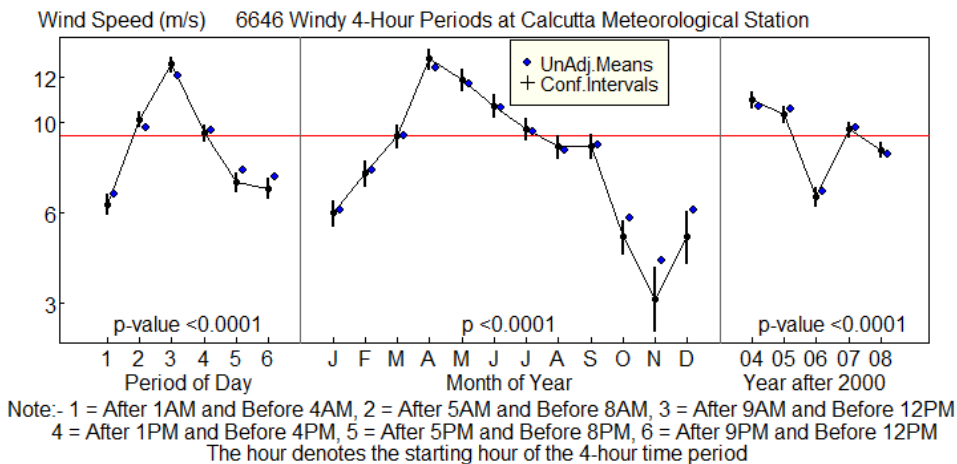


Fig. 6: Linear model confidence interval plot of wind speed trends.

The quantile-quantile (Q-Q) plot illustrates that the residuals from the model are approximately normally distributed (Fig. 5) which shows that the model fitted the data reasonably well. However, there were some deviations from the upper tail of the model. This deviation may be due to extreme values in the data and some variations that could not be explained by the predictors.

Fig. 6, the horizontal line denotes the overall mean of the wind speed is approximately 9 ms^{-1} . The wind speed trends for the period of the day were significantly different from the overall mean. The period during dawn (period 2) to noon (period 3) had the maximum wind speed of around 13 ms^{-1} observed during noon (period 3). Moderate wind speed trend was observed during the afternoon (period 4) with a modest wind speed of approximately 9 ms^{-1} aligning with overall mean. The low wind speed trends were observed during midnight (period 1) to dawn (period 2), evening (period 5) to night (period 6) with a minimum wind speed of around 6 ms^{-1} in midnight (period 1) respectively.

The monthly wind speed trends revealed rising trends during April to June with a maximum wind speed of around 13 ms^{-1} observed during April. Moderate wind speed trend was observed during March and July to September with a modest wind speed of approximately 9 ms^{-1} aligning with overall mean. The low wind speed trends were observed during January to February, and October to December with a minimum wind speed of around 3 ms^{-1} in November. The monthly and yearly wind speed trends revealed values either greater, equal to or lower than the overall mean. The yearly wind speed revealed increasing trends during 2004 and 2005 with a maximum wind speed of around 11 ms^{-1} observed during 2004. Moderate wind speed was observed during 2007 with a modest wind speed of approximately 9 ms^{-1} aligning with overall mean. The reducing trends were observed during 2006 and 2008 with a minimum wind speed of around 7 ms^{-1} in 2006.

CONCLUSION AND DISCUSSION

Statistical models were used to investigate the 4-hourly wind observations of Calcutta, India during 2004-2008. The wind and wind gust prevalence patterns together with the wind speed trends were investigated. The wind prevalence pattern, wind speed trend and wind gust prevalence for the period of the day, month and year illustrated distinct divergent patterns. Logistic regression model fitted wind prevalence and wind gust pattern reasonably well. The overall wind prevalence was observed to be 70% all through the year. The period of the day factors revealed the wind prevalence above the overall mean between period 2 and period 4. This pattern may be due to stronger breeze during

early morning to afternoon (Zhong 1992). The observed wind prevalence below the overall mean during the other periods of the day may be due to lighter land breeze during the night (Mandal et al. 2013). The observed monthly maximum wind prevalence of 90% during March and June may be due to the high rates of wind such as breeze, storm during the first and second quarter of the year (Gadgil 2003, Rajeevan et al. 2012). However, the minimum wind prevalence occurred between October and December which may be as a result of the lighter rates of wind blown such as squall on the surface of the Earth (Gadgil 2003, Rajeevan et al. 2012). The yearly wind prevalence was mostly below the overall mean during 2004 to 2006, but above the overall mean between 2007 and 2008 where the maximum occurred (85%). This pattern was partly because of stronger breeze and monsoon winds during the initial period of the decadal period from the year 2000, and lighter and weak monsoon winds from the final period of decade 2000 (Kumar et al. 2006). The results of the 95% confidence interval plot for the wind gust was similar to that of wind prevalence.

Linear regression model revealed an increasing trend for the period of the day factors period 1 to period 3 and decreasing trend between period 3 and period 6. The observed trend may be due to the stronger intensity of sea breeze and prevailing wind during early morning to afternoon and low intensity of land breeze and prevailing wind during the night (Chaudhuri et al. 2013). The monthly wind speed trend showed increasing trend between January and April and reducing trend from April to November. These trends observed partly due to vigorous variation of wind speed near to the surface of the land (Torralba et al. 2017), global warming (McInnes et al. 2011) strong monsoon (Loo et al. 2015), and weaker monsoon (Vishnu et al. 2016). The yearly wind speed trend displayed reducing trend between 2004 and 2006 and increasing trend between 2007 and 2008. This observed trends may be due to the effect of global warming and ocean warming on monsoon patterns (Mojgan et al. 2017).

This study has provided a description of wind trends and patterns, which helps in obtaining descriptive and knowledgeable information of wind circulation over Calcutta, India. These trends are vital in the development of wind resources distribution in several areas of India. Future studies on wind could include data on dewpoint, wind chill and heat index along with different statistical methods.

ACKNOWLEDGMENT

The work has been supported by the Higher Education Research Promotion and Thailand's Education Hub for Southern Region of ASEAN Countries Project Office of the Higher

Education Commission under grant no. THE/033. We thank Emeritus Prof. Dr. Don McNeil for supervising this work. Thanks to Centre of Excellence in Mathematics, Commission on Higher Education, Thailand.

REFERENCES

- Bett, P.E., Thornton, H.E. and Clark, R.T. 2013. European wind variability over 140 yr. *Advances in Science and Research*, 10(1): 51-58.
- Chapin, F.S., Matson III, P.A. and Mooney, H. 2002. *Principles of Terrestrial Ecosystem Ecology*. Springer-Verlag, New York, New York, USA.
- Chatfield, C. 1996. *The Analysis of Time Series*. Chapman and Hall: Melbourne.
- Chaudhuri, S. and Middey, A. 2013. Nowcasting lightning flash rate and peak wind gusts associated with severe thunderstorms using remotely sensed TRMM-LIS data. *International Journal of Remote Sensing*, 34(5): 1576-1590.
- Chen, L., Li, D. and Pryor, S.C. 2013. Wind speed trends over China: quantifying the magnitude and assessing causality. *International Journal of Climatology*, 33(11): 2579-2590.
- Cheng, C.S., Lopes, E., Fu, C. and Huang, Z. 2014. Possible impacts of climate change on wind gusts under downscaled future climate conditions: Updated for Canada. *Journal of Climate*, 27(3): 1255-1270.
- Csavina, J., Field, J., Félix, O., Corral-Avitia, A.Y., Sáez, A.E. and Betterton, E.A. 2014. Effect of wind speed and relative humidity on atmospheric dust concentrations in semi-arid climates. *Science of the Total Environment*, 487(1): 82-90.
- Gadgil, S. 2003. The Indian monsoon and its variability. *Annual Review of Earth and Planetary Sciences*, 31: 429-467.
- Geer, I.W. 1996. *Glossary of Weather and Climate: With Related Oceanic and Hydrologic Terms*. Boston, Mass: American Meteorological Society, pp. 272.
- Greene, S., Morrissey, M. and Johnson, S.E. 2010. Wind climatology, climate change, and wind energy. *Geography Compass*, 4(11): 1592-1605.
- Gillings, R.J. 1972. *Mathematics in the Time of the Pharaohs*. Dover Publications Inc, New York, USA.
- Glickman, T.S. and Zenk, W. 2000. *Glossary of Meteorology*. American Meteorological Society, Boston, USA.
- Gupta, R. and Biswas, A. 2010. Wind data analysis of Silchar (Assam, India) by Rayleigh's and Weibull methods. *Journal of Mechanical Engineering Research*, 2(1): 010-024.
- IMD 2015. Indian Meteorological Department, Monsoon. Available at http://www.imd.gov.in/pages/monsoon_main.php [February 5, 2017].
- Jain, A., Srinivasan, M. and Hart, G.C. 2001. Performance based design extreme wind loads on a tall building. *Structural Design of Tall Buildings*, 10(1): 9-26.
- Jamaludin, A.R., Yusof, F., Kane, I.L. and Norulasikin, S.M. 2016. A comparative study between conventional ARMA and Fourier ARMA in modeling and forecasting wind speed data. In: *Advances in Industrial and Applied Mathematics, Proceedings of 23rd Malaysian National Symposium of Mathematical Sciences (SKSM23)*, 1750: 60022.
- Kious, W.J. and Tilling, R.I. 1996. *This Dynamic Earth: The Story of Plate Tectonics*. DIANE Publishing, Darby, USA.
- Klink, K. 2002. Trends and interannual variability of wind speed distributions in Minnesota. *Journal of Climate*, 15(22): 3311-3317.
- Klink, K. 1999. Trends in mean monthly maximum and minimum surface wind speeds in the coterminous United States, 1961 to 1990. *Climate Research*, 13(3): 193-205.
- Kumar, K.K., Rajagopalan, B., Hoerling, M., Bates, G. and Cane, M. 2006. Unraveling the mystery of Indian monsoon failure during El Niño. *Science*, 314(5796): 115-119.
- Lakshmanan, N., Gomathinayagam, S., Harikrishna, P., Abraham, A. and Ganapathi, S.C. 2009. Basic wind speed map of India with long-term hourly wind data. *Current Science*, 96(7): 911-922.
- Loo, Y.Y., Billa, L. and Singh, A. 2015. Effect of climate change on seasonal monsoon in Asia and its impact on the variability of monsoon rainfall in Southeast Asia. *Geoscience Frontiers*, 6(6): 817-823.
- Mandal, S., Choudhury, B.U., Mondal, M. and Bej, S. 2013. Trend analysis of weather variables in Sagar Island, West Bengal, India: a long-term perspective (1982-2010). *Current Science*, pp. 947-953.
- McInnes, K.L., Erwin, T.A. and Bathols, J.M. 2011. Global climate model projected changes in 10 m wind speed and direction due to anthropogenic climate change. *Atmospheric Science Letters*, 12(4): 325-333.
- Mitchell, S.J. 2012. Wind as a natural disturbance agent in forests: a synthesis. *Forestry*, 86(2): 147-157.
- Mojgan, G.M., Mehdi, M.M. and Reza, B.M. 2017. The trend of changes in surface wind in the Indian Ocean, in the period from 1981 to 2015, using reanalysis data, NCEP/NCAR. *Open Journal of Marine Science*, 7(4): 445-457.
- Mohan, A.H., He, Y., McFarlane, N. and Dai, A. 2011. The probability distribution of land surface wind speeds. *Journal of Climate*, 24(15): 3892-3909.
- Mukhopadhyay, P., Mahakur, M. and Singh, H.A. 2009. The interaction of large scale and mesoscale environment leading to formation of intense thunderstorms over Kolkata Part I: Doppler radar and satellite observations. *Journal of Earth System Science*, 118(5): 441-466.
- Myrl, S. 2012. *The Earth's Prevailing Wind Belts*. Greensboro: Mark Twain Media.
- Nchaba, T., Mpholo, M. and Lennard, C. 2016. Long-term austral summer wind speed trends over southern Africa: Austral summer wind speed trends over Southern Africa. *International Journal of Climatology*, 37(6): 2850-2862.
- R Development Core Team 2008. *A Language and Environment for Statistical Computing*, R Foundation for Statistical Computing, Vienna, Austria.
- Rajeevan, M., Unnikrishnan, C.K., Bhate, J., Kumar, K.N. and Sreekala, P.P. 2012. Northeast monsoon over India: variability and prediction. *Meteorological Applications*, 19(2): 226-236.
- Reddy, G.K.K., Reddy, S.V., Sarojamma, B. and Ramkumar, T.K. 2015. Statistical analysis for wind energy estimation over Gadanki, India. *Research Journal of Engineering and Technology*, 1(2): 30-40.
- Reddy, S.J. 2008. *Climate Change: Myths and Realities*. JCT, Hyderabad, India.
- Venables, W.N. and Ripley, B.D. 2002. *Modern Applied Statistics with S* Fourth edition. Springer.
- Tongkumchum, P. and McNeil, D. 2009. Confidence intervals using contrasts for regression model. *Songklanakarin Journal of Science and Technology*, 31(2): 151-156.
- Torralba, V., Doblas-Reyes, F.J. and Gonzalez-Reviriego, N. 2017. Uncertainty in recent near-surface wind speed trends: a global reanalysis intercomparison. *Environmental Research Letters*, 12(11): 114019.
- Troccoli, A., Muller, K., Coppin, P., Davy, R., Russell, C. and Hirsch, A.L. 2012. Long term wind speed trends over Australia. *Journal of Climate*, 25(1): 170-183.

- UNDP 2006. Hazard profile of Indian districts, Available at <https://web.archive.org/web/20060519100611/http://www.undp.org.in/dmweb/hazardprofile.pdf> [August 23, 2006].
- Schindler, D., Bauhus, J. and Mayer, H. 2012. Wind effects on trees. *European Journal of Forest Research*, 131(1): 159-163.
- Vishnu, S., Francis, P.A., Sheno, S.S.C. and Ramakrishna, S.S.V.S. 2016. On the decreasing trend of the number of monsoon depressions in the Bay of Bengal. *Environmental Research Letters*, 11(1): 14011.
- Westin, L.K. 2001. Receiver operating characteristic (ROC) analysis: evaluating discriminant effects among decision support systems. UMINF report, Department of Computer Science, Umea University, Sweden: Available from: <https://www8.cs.umu.se/research/reports/2001/018/part1.pdf> [December, 08 2017]
- Wiegand, P. 2004. *Oxford International Student Atlas*. Oxford University Press, Chennai, India.
- Zhong, S. and Takle, E.S. 1992. An observational study of sea- and land-breeze circulation in an area of complex coastal heating. *Journal of Applied Meteorology*, 31(12): 1426-1438.



Distribution of Zooplankton Population in Different Culture Ponds from South China

Yuan Gao, Zi-Ni Lai[†], Guang-Jun Wang, Qian-Fu Liu and Er-Meng Yu[†]

Pearl River Fisheries Research Institute, Chinese Academy of Fishery Science, Guangzhou 510380, China

[†]Corresponding author: Zi-Ni Lai and Er-Meng Yu

Nat. Env. & Poll. Tech.
Website: www.neptjournal.com

Received: 07-05-2018
Accepted: 02-08-2018

Key Words:

Fish ponds
Zooplankton
Population distribution
Biodiversity

ABSTRACT

To understand the population distribution characteristics of zooplankton in typical densely populated freshwater fish ponds, we intensively studied the species composition, abundance, and biodiversity of zooplankton in the *Oxyeotris marmoratus*, *Ctenopharyngodon idellus*, *Micropterus salmoides*, and *Channa argus* culture ponds in the Pearl River Delta region in China during May to December in 2012. The number of zooplankton species in the four ponds were 66, 54, 55, and 68, respectively. The average abundance was 16466.78 ind./L, 8408.17 ind./L, 7397.77 ind./L, and 33632.53 ind./L, respectively. The average biodiversity index and species evenness were 1.360 and 0.628 in the *Oxyeotris marmoratus* culture pond, 1.150 and 0.587 in the *Ctenopharyngodon idellus* culture pond, 1.438 and 0.755 in the *Micropterus salmoides* culture pond, and 1.234 and 0.580 in the *Channa argus* culture pond. The canonical correspondence analysis (CCA) results indicated that the most significant environmental factors that significantly affected the distribution of zooplankton species were: dissolved oxygen was for *Oxyeotris marmoratus* culture pond, total phosphorus content for *Ctenopharyngodon idellus* culture pond, chlorophyll *a* for *Micropterus salmoides* culture pond and pH value for *Channa argus* culture pond. These study results demonstrated that different culture fish species might change the contents of environmental factors in the pond, and significant environmental factors would further impact the species composition, abundance, and biodiversity of zooplankton. The research results could provide a scientific basis for the management of pond water quality.

INTRODUCTION

Zooplankton are important biological components of aquatic ecosystems. They play important roles in the fisheries production as the bait for commercial fishes, and regulate the genesis and development of phytoplankton and microorganisms in water (Sun 2001). In addition, zooplankton are important components of the matter cycle and energy flow in the aquatic ecosystems. The composition and biodiversity of zooplankton species directly reflect the structure and function of an aquatic ecosystem (Luo 2004, Pinel-Alloul et al. 1991, Wei et al. 2013).

The biodiversity and community structure of zooplankton varied in different culture ponds due to different cultivation modes (Zhang et al. 2015). Several indicators, including species composition, abundance, and biomass of zooplankton can be used to show the productivity of the culture ponds (Gozdziejewska & Tucholski 2011). Zhang et al. (2014) studied the characters of the zooplankton community structure in *Ctenopharyngodon idellus* culture ponds, and found that the dominant species of zooplankton were *Coleps irtus*, *Askenasia faurei*, *Askenasia volvox*, *Tetrahymena pyriformis* and *Halteria grandinella*. Zhao et al. (2014) investigated the effects of *Channa argus* culturing

on the community structure of zooplankton and found the dominant species *Daphnia magna* and *Brachionus calyciflorus*. So far, few studies have focused on the impact of aquaculture species on zooplankton species, and this study will explore the relationships between aquaculture species and zooplankton species.

Oxyeotris marmoratus, *Micropterus salmoides*, *Ctenopharyngodon idellus*, and *Channa argus* are important commercial freshwater products in Pearl River Delta region of south China. In the present study, the zooplankton species composition, abundance, and biodiversity in these aquaculture ponds were analysed, so as to demonstrate the ecological and environmental conditions of the aquaculture ponds, and to provide a scientific basis for the maintenance of the quality of aquaculture pond water and the improvement of aquatic breeding.

MATERIALS AND METHODS

Sampling timing and location: The investigation was carried out by continuous sampling for 13 times from May to December in 2012. In May, June, July, September, and October, the samples were collected semi-monthly. In August, November, and December, the samples were collected monthly.

Table 1: The locations of the four aquaculture ponds.

Sampling pond	Longitude	Latitude
OM	113°05'46.6"	22°48'26.5"
CI	113°11'54.6"	22°50'20.7"
MS	113°09'32.0"	22°49'33.0"
CA	113°07'43.0"	22°52'12.1"

OM, *Oxyeleotris marmoratus*; CI, *Ctenopharyngodon idellus*; MS, *Micropterus salmoides*; CA, *Channa argus*

The samples were collected from four aquaculture ponds that were culturing *Oxyeleotris marmoratus*, *Ctenopharyngodon idellus*, *Micropterus salmoides*, and *Channa argus* in Shunde District, Foshan, Guangdong Province, PR China. The location of the four aquaculture ponds is given in Table 1.

Methods: The methods for the collection, identification, and quantification of zooplankton were carried out according to the Research Methods of Freshwater Plankton (Zhang & Huang 1995).

Protozoans and rotifers: The samples for the species identification were collected by No. 25 plankton net (mesh size of 64 μm , produced by the Institute of Hydrobiology, Chinese Academy of Sciences in Wuhan, PR China) in a “ ∞ ” shape movement across the water for 3 to 5 minutes. The collected samples were then taken to the lab for species identification. The samples for quantification were collected by taking 1 L of surface water using a water sampler, and immediately fixed with formalin solution (formalin was added to a final concentration of 4%). The samples were taken to the lab and concentrated into 10–20 mL. For protozoan counting, 0.1 mL of well mixed concentrated water sample was taken and examined under microscope at 10 \times 20 fold magnification. For rotifer counting, 0.1 mL of well mixed concentrated water sample was taken and examined under microscope at 10 \times 10 fold magnification. Two slides were counted for each sample.

Cladocerans and copepods: The samples for species identification were collected by No. 13 plankton net (mesh size of 113 μm , produced by the Institute of Hydrobiology, Chinese Academy of Sciences in Wuhan, PR China) in a

“ ∞ ” shape movement across the water for 3 to 5 minutes. The samples for quantification were collected by taking 30 L of surface water using a 5 L water sampler, then filtered with No. 25 plankton net, and immediately fixed with formalin solution (formalin was added to a final concentration of 4%). The samples were then taken to the lab and concentrated into 20 mL. The numbers of cladocerans and copepods were counted under microscope at 10 \times 10 fold magnification using 1 mL plankton counting chamber.

The water temperature, pH value, dissolved oxygen, and transparency were detected during the sampling. Additional water samples were collected to determine chlorophyll *a* content and nutrients in the lab.

Data processing: Dominance index (Y) = $f_i \cdot n_i / N$. In the formula, f_i indicates the frequency of the species i in each sampling site, n_i indicates the abundance of species i , N indicates the total abundance (Xu et al. 1995).

Shannon-Wiener diversity index (H) =

$$-\sum_{i=1}^S (n_i / N) \log_2 (n_i / N)$$

In the formula, S indicates the number of species, n_i indicates the number of species i , N indicates the total number (Shannon & Weaver 1963).

Evenness index (J) = $H / \log_2 S$. In the formula, H indicates Shannon-Wiener diversity index, S indicates the number of species (Pielou 1966).

SPSS 18.0 software was used for data analysis, Origin 8.6 software was used for chart plotting, and Canoco 4.5 software was used to analyse the correlation between zooplankton community and environmental factors. $P < 0.05$ was considered statistically significant.

RESULTS

Environmental factors: The mean values of the main environmental factors in the four culture ponds are shown in Table 2. In all of the four ponds, the total nitrogen, total phosphorus, ammonia nitrogen, and chlorophyll *a* were at high levels (Table 2).

Table 2: Levels of main environmental factors in the four ponds.

Sampling ponds	Total nitrogen (mg/L)	Total phosphorus (mg/L)	Ammonia nitrogen (mg/L)	Chlorophyll <i>a</i> ($\mu\text{g/L}$)
OM	5.39 \pm 3.31	0.36 \pm 0.12	1.56 \pm 1.01	45.18 \pm 22.27
CI	5.09 \pm 1.91	0.42 \pm 0.11	1.47 \pm 0.73	271.45 \pm 69.57
MS	9.06 \pm 5.33	0.47 \pm 0.26	1.17 \pm 1.14	92.64 \pm 36.41
CA	16.34 \pm 7.62	1.57 \pm 1.42	3.39 \pm 3.58	154.77 \pm 63.46

OM, *Oxyeleotris marmoratus*; CI, *Ctenopharyngodon idellus*; MS, *Micropterus salmoides*; CA, *Channa argus*

Table 3: Richness of zooplankton species in the four ponds.

Species numbers	Sampling ponds			
	OM	CI	MS	CA
Protozoa	18	15	12	20
Rotatoria	22	29	21	29
Cladocera	14	6	11	10
Copepoda	12	4	11	9
Zooplankton	66	54	55	68

OM, *Oxyeleotris marmoratus*; CI, *Ctenopharyngodon idellus*; MS, *Micropterus salmoides*; CA, *Channa argus*

Species composition: We identified 66 and 68 zooplankton species in the *Oxyeleotris marmoratus* and *Channa argus* culture ponds. In comparison, we found fewer zooplankton species in *Ctenopharyngodon idellus* and *Micropterus salmoides* culture ponds (54 and 55 species, respectively). Microzooplankton were dominant in all the four ponds, and the number of rotifer species was the highest, followed by protozoans, cladocerans and copepods (Table 3).

Dominant species and dominance index: The dominant zooplankton species varied in different types of culture ponds ($Y > 0.02$) (Table 4). The numbers of dominant species in *Oxyeleotris marmoratus*, *Ctenopharyngodon idellus*, *Micropterus salmoides* and *Channa argus* ponds were 8, 5, 5 and 5, respectively, and all the dominant species belonged to microzooplankton including protozoans and rotifers. *Paramecium caudatum* was the most dominant species in *Oxyeleotris marmoratus* and *Channa argus* ponds.

Species abundance and distribution: The distribution of zooplankton in the four types of ponds is shown in Fig. 1. At all the sampling times, abundances of zooplankton in

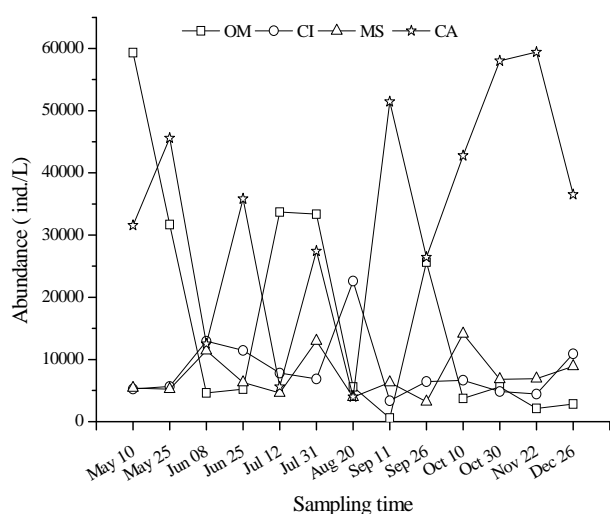


Fig.1: The distribution of zooplankton in four types of ponds.

Oxyeleotris marmoratus pond ranged from 570.00 ind./L to 59339.00 ind./L, with an average value of 16466.78 ind./L. The lowest value appeared on September 11 and the highest value on May 10. The *Ctenopharyngodon idellus* pond had the lowest zooplankton abundance on September 11 (3352.33 ind./L) and the highest abundance on August 20 (22600.00 ind./L), with an average abundance of 8408.17 ind./L. The abundances of zooplankton in *Micropterus salmoides* culture pond ranged from 3209.00 ind./L to 14124.44 ind./L, with an average value of 7397.77 ind./L. The lowest value existed on September 26 and the highest value on October 10. The abundances of zooplankton in *Channa argus* culture pond ranged from 3984.00 ind./L to 59415.00 ind./L, with an average value of 33632.53 ind./L. The lowest value appeared on August 20 and the highest value on November 22.

Time distribution of zooplankton diversity: In *Oxyeleotris marmoratus* pond, the zooplankton diversity index ranged from 0.530-2.002, with an average value of 1.360; and the evenness index ranged from 0.228-0.881, with an average value of 0.628 (Fig. 2). In *Ctenopharyngodon idellus* pond, the lowest zooplankton diversity index and evenness index values were 0.727 and 0.293, respectively, both appearing on August 20, while the highest values were 1.742 and 0.905, respectively, both appearing on June 8 (Fig. 2). In *Micropterus salmoides* pond, the average zooplankton diversity index value was 1.438, with the lowest value (1.020) appearing on October 30 and the highest value (1.759) appearing on October 10 (Fig. 2). The average zooplankton evenness index for the *Micropterus salmoides* pond was 0.755, with the lowest value (0.440) appearing on October 30 and the highest value (0.925) on June 8 (Fig. 2). In the *Channa argus* pond, the lowest zooplankton diversity value was 0.813, appearing on June 8, and the highest value was 1.932, appearing on July 31 (Fig. 2). The zooplankton evenness indexes of the *Channa argus* pond ranged from 0.369-0.891, with an average value of 0.580 (Fig. 2).

Relationship between zooplankton community and environmental factors: The dominant zooplankton species in the four aquaculture ponds were listed in Table 4 based on their frequencies. The canonical correspondence analysis (CCA) was carried out using Canoco software to investigate the correlation between the abundance of dominant zooplankton and the environmental factors such as water temperature, pH value, dissolved oxygen, total nitrogen, total phosphorus, and chlorophyll *a* content (Fig. 3).

CCA analysis results showed that the first two ordination axes accounted for 78.6%, 80.3%, 65.7%, and 62.4% of the species variables in ponds culturing *Oxyeleotris marmoratus*, *Ctenopharyngodon idellus*, *Micropterus*

Table 4: Dominance of dominant zooplankton species in the four ponds.

Sampling pond	Dominant species	Dominance
OM	<i>Paramecium caudatum</i>	0.631
	<i>Polyarthra trigla</i>	0.089
	<i>Brachionus angularis</i>	0.046
	<i>Trichocerca gracilis</i>	0.043
	<i>Tintinnopsis wangi</i>	0.039
	<i>Askenasia volvox</i>	0.026
CI	<i>Pompholyx complanata</i>	0.021
	<i>Trichocerca cylindrica</i>	0.085
	<i>Brachionus angularis</i>	0.030
	<i>Polyarthra trigla</i>	0.028
	<i>Acanthocystis chaetophora</i>	0.026
MS	<i>Dileptus binucleatatus</i>	0.025
	<i>Askenasia volvox</i>	0.060
	<i>Polyarthra trigla</i>	0.050
	<i>Tintinnopsis conus</i>	0.050
	<i>Tintinnidium fluviatile</i>	0.041
CA	<i>Paramecium caudatum</i>	0.038
	<i>Paramecium caudatum</i>	0.426
	<i>Filinia maior</i>	0.103
	<i>Polyarthra trigla</i>	0.047
	<i>Brachionus calyciflorus</i>	0.034
	<i>Brachionus forficula</i>	0.025

OM, *Oxyeleotris marmoratus*; CI, *Ctenopharyngodon idellus*; MS, *Micropterus salmoides*; CA, *Channa argus*

salmoides and *Channa argus*, respectively. Thus, the first two ordination axes can be considered as the significant canonical axes. The coefficients of the correlation between environmental variables and species variables and the two significant canonical axes were shown in Table 5.

In the *Ctenopharyngodon idellus* pond, the abundance of dominant zooplankton species including *Tintinnopsis wangi*, *Askenasia volvox*, *Trichocerca gracilis*, *Pompholyx complanata* and *Polyarthra trigla* was significantly nega-

tively correlated with the dissolved oxygen content; the abundance of dominant zooplankton species including *Tintinnopsis wangi*, *Askenasia volvox*, *Trichocerca gracilis* and *Brachionus angularis* was significantly negatively correlated with the total dissolved solid content and significantly positively correlated with the total nitrogen content; and the abundance of *Pompholyx complanata*, *Paramecium caudatum* and *Polyarthra trigla* showed significant positive correlation with the nitrite content (Table 5, Fig. 3a).

In the *Ctenopharyngodon idellus* pond, the abundance of dominant zooplankton species *Acanthocystis chaetophora* and *Trichocerca cylindrical* showed a significant positive correlation with the total dissolved solids content, and significant negative correlation with water temperature and the nitrite nitrogen content; and the abundance of *Brachionus angularis* and *Polyarthra trigla* showed a significant positive correlation with total phosphorus content (Table 5, Fig. 3b).

In the *Micropterus salmoides* pond, the abundance of *Tintinnopsis conus* was significantly positively correlated with the total dissolved solids content and chlorophyll *a*; and the abundance of *Polyarthra trigla* and *Paramecium caudatum* showed significant negative correlations with the total phosphorus content and water temperature (Table 5, Fig. 3c).

In the *Channa argus* pond, the abundance of *Polyarthra trigla* and *Filinia maior* was significantly negatively correlated with water temperature, but significantly positively correlated with pH value (Table 5, Fig. 3d).

DISCUSSION

Many studies have shown that fish predation strongly in-

Table 5: The coefficients of the correlation between environment variables, species variables, and the two significant canonical axes.

Environmental factors	OM		CI		MS		CA	
	SPAX1	SPAX2	SPAX1	SPAX2	SPAX1	SPAX2	SPAX1	SPAX2
Water temperature	0.233	0.339	-0.494*	0.194	-0.420*	-0.194	0.324	-0.549*
Transparency	-0.323	-0.344	0.386	-0.013	-0.007	0.267	-0.317	-0.135
pH value	-0.105	-0.015	-0.112	0.257	-0.165	-0.070	0.053	0.460*
Dissolved oxygen	-0.700*	-0.103	-0.318	0.076	0.310	-0.299	-0.032	-0.370
Total dissolved solids	0.009	-0.530*	0.543*	-0.219	0.422*	0.238	-0.253	-0.367
Total phosphorus	-0.003	-0.125	-0.080	0.566*	-0.444*	-0.070	0.326	0.362
Total nitrogen	0.481*	0.007	0.187	0.484*	0.246	0.268	-0.248	0.049
Nitrite	0.554*	-0.076	-0.453*	0.123	0.291	-0.059	-0.080	0.100
Ammonia nitrogen	0.301	0.083	-0.186	-0.228	-0.217	-0.222	-0.338	-0.221
Chlorophyll <i>a</i>	-0.178	-0.339	0.013	0.072	0.450*	0.254	0.073	-0.060

* $P \leq 0.05$

SPAX1 indicates the first ordination axis and SPAX2 represents the second ordination axis.

OM, *Oxyeleotris marmoratus*; CI, *Ctenopharyngodon idellus*; MS, *Micropterus salmoides*; CA, *Channa argus*

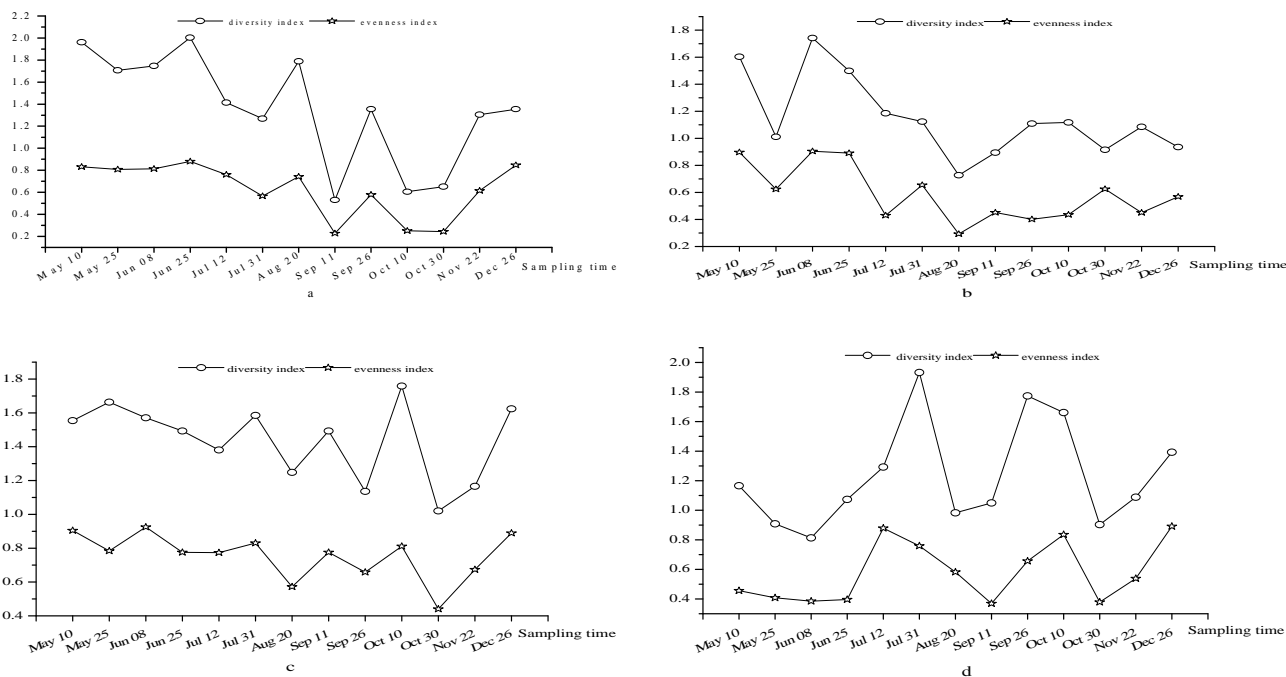


Fig.2: Time distribution of zooplankton diversity index and evenness index.

influenced the community structure of zooplankton (Anton-Pardo & Adámek 2015). According to the studies of Zheng et al. (2009) and Wu et al. (2011), in the culture ponds of filter-feeding fishes *Aristichthys nobilis* and *Hypophthalmichthys molitrix*, macrozooplankton such as copepods were favoured by these two types of fishes, which helped the growth of protozoans and rotifers, and thus they became the major zooplankton components in these ponds. Macrozooplankton larvae were the main food for the cultured juvenile fish. When no macrozooplankton larvae was put into the ponds as supplement, and the adult fish continued to feed on macrozooplankton, the proportion of macrozooplankton in aquaculture ponds would become low.

Zhang (2014) found that the dominant species of zooplankton in the *Ctenopharyngodon idellus* ponds in May to October 2012 were protozoa and rotifer, and the number of protozoa and rotifer accounted for 92.5% of the total number of species of zooplankton. Li (2012) found that protozoans and rotifers were the major zooplankton species in partitioned pond culturing ground fish, followed by cladocera, and copepod was the least. Chen et al. (2012) reported that the mini type protozoa increased and remained superiority from April to December in 2009 in the ponds with paddlefish as the assistant cultured species. Consistent with the above findings, in the ponds we studied, as far as the number of species and abundance were concerned, the proportion of microzooplankton (protozoans and rotifers)

was highest among all zooplankton species, while the proportion of cladocerans and copepods was much less.

In aquaculture ponds, artificial influences are significant. For example, sludge clearing and disinfection in the ponds before adding the fries and regular disinfection with quicklime or copper sulphate greatly affected the growth of zooplankton (Hu et al. 2007). In these processes, since the protozoans and rotifers were of small size, and fast growing with short life cycle, they would quickly become dominant zooplankton groups in the aquaculture ponds. Eutrophication will lead to the decrease of the number of intolerant species and the increase of tolerant species (Dumont 1983, Dussart et al. 1984). Our results showed that the four ponds were in a eutrophic state. In all the four ponds, tolerant species, such as *Paramecium caudatum*, *Polyarthra trigla*, *Brachionus angularis* and *Brachionus calyciflorus*, became dominant species in these ponds, which were of certain indication function for the eutrophic state of the ponds (Shen et al. 1990, Wang et al. 2006). Our results can be confirmed by the comprehensive evaluation based on Shannon-Wiener diversity index and Pielou evenness index of zooplankton. The high eutrophic state might be due to the high content of nitrogen and phosphorus from bait residues and fish faeces in the ponds.

Studies have shown that the species composition and abundance of zooplankton are closely correlated with the nutritional state of water (Chen et al. 2008, Dumont 1983). The nitrogen and phosphorus contents are important fac-

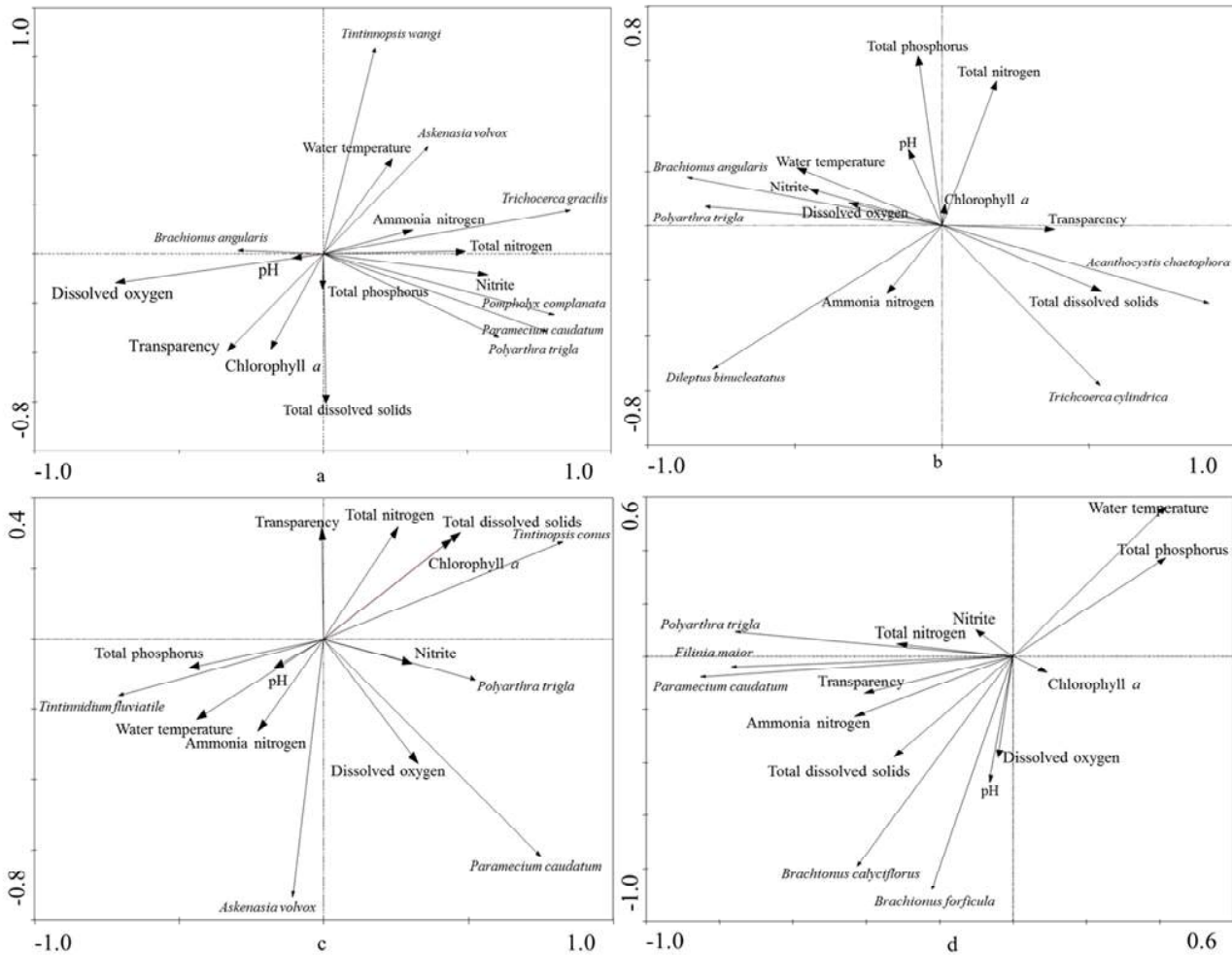


Fig. 3: Ordination diagram of the first two axes of canonical correspondence analysis of zooplankton community index and environmental factors. a, *Oxyeleotris marmoratus*; b, *Ctenopharyngodon idellus*; c, *Micropterus salmoides*; d, *Channa argus*

tors that affect the abundance of zooplankton. Zooplankton species vary in different water systems depending on their demands of nutrients. In the freshwater ecosystems, nitrate, nitrite and ammonia nitrogen at certain concentration showed suppressing effects on the growth of zooplankton. Chen et al. (2008) found that, in the West Lake of Huizhou, the nitrogen and phosphorus contents affected the abundance and biomass of zooplankton to a certain degree, and the phosphate content was positively correlated with zooplankton biomass. The study of Qiu & Zhao (2012) in Sand Lake found that the total phosphorus content was negatively correlated with zooplankton abundance.

In the present study, the zooplankton community structures in all the four ponds were highly correlated with total nitrogen, total phosphorus and nitrite contents. These re-

sults were consistent with published studies (Li 2013, Zhang 2014, Zhou et al. 2010). Excessively high levels of total dissolved solids in water will deteriorate the conditions of macrozooplankton (cladocerans and copepods), especially cladocerans as they will die due to the clogging of the filter. In this study, the total dissolved solids were negatively correlated with zooplankton abundance, and the increase in suspended solids will cause rapid growth of algae, and microzooplankton (protozoans and rotifers) with short life cycle will also multiply. Water temperature is a distinctively important environmental factor that affects the growth, development, community composition, quantity and distribution of zooplankton (Dussart et al. 1984). Jin et al. (1991) found that the abundance of zooplankton increased with the temperature when it is between 20°C and 30°C. However, the abundance of zooplankton decreased in July and

August, when the temperature was highest. This might be due to the diapause of zooplankton under excessively high temperature (Marcus 1982). Our study also demonstrated that the dominant zooplankton abundance was negatively correlated with the water temperature in July and August. The dissolved oxygen level in water, which varies in different culture ponds and shows remarkable seasonal variation, directly determines the living condition of most aquatic organisms. As the biological metabolism level and oxygen utilization rate of organisms increase with water temperature, the dissolved oxygen level in water directly determines the biological abundance under high temperature (Wang 2007). In spring and winter, the level of dissolved oxygen is high, the activity and standing stock of the zooplankton are low, hence the dissolved oxygen level is not the limiting factor for zooplankton abundance. However, in summer and autumn, when the dissolved oxygen level decreases, while zooplankton activity become frequent and the standing stock of zooplankton is high, their oxygen demand increases, and thus the dissolved oxygen will be a factor affecting the living of zooplankton. The acidity or alkalinity of water is indicated by the pH value, which is closely related to the number of rotifer species in freshwater. Rotifers, according to their pH value preference, can be divided into alkaliphile species, acidophile species, and facultative species. The abundance of rotifers is high in water with high pH value, and low in water with low pH value (Zhou 2007). In the present study, the abundance of dominant rotifers in *Channa argus* ponds, such as *Polyarthra trigla* and *Filinia maior*, showed a significant positive correlation with pH value of the water.

In addition to the direct effects, environmental factors may also indirectly influence the standing stock of zooplankton through affecting the growth of phytoplankton (Lu & Zhu 2008), which sometimes even counteracts the direct effects. In the present study, the zooplankton community structure showed a remarkable positive correlation with the chlorophyll *a* content in the *Micropterus salmoides* pond, which is an indicator for phytoplankton abundance, and is also an indirect indicator for the regulation effects of phytoplankton on zooplankton populations.

CONCLUSIONS

The species composition, abundance and biodiversity of zooplankton varied in different types of culture ponds. Changes of the structure and dynamics of zooplankton in the investigated ponds were determined mostly by trophic relationships and interspecies interactions, while fish predation pressure supported greater species diversity and its reinstatement.

ACKNOWLEDGEMENTS

We thank Shi-Xun Pang, Wan-Ling Yang, Chao Wang and Wei-Zhen Zhang for their sampling assistance and logistic support.

REFERENCES

- Anton-Pardo, M. and Adámek, Z. 2015. The role of zooplankton as food in carp pond farming: A review. *J. Appl. Ichthyol.*, 31: 7-14.
- Chen, G.R., Zhong, P., Zhang, X.F., Xie, Y.F. and Li, C.H. 2008. Zooplankton and its relationship with water quality in Huizhou West Lake. *J. Lake Sci.*, 20: 351-356 (In Chinese).
- Chen, J.W., Zhu, Y.J., Zhao, J.H., Feng, X.B., Li, Q. and Yang, D.G. 2012. The varieties of plankton in ponds with paddlefish as the assistant cultured species. *Journal of Fujian Agriculture and Forestry University (Natural Science Edition)*, 41: 503-508 (In Chinese).
- Dumont, H.J. 1983. Biogeography of rotifers. *Hydrobiologia*, 104: 19-30.
- Dussart, B.H., Fernando, C.H., Matsumura-Tundisi, T. and Shiel, R.J. 1984. A review of systematic, distribution and ecology of tropical freshwater zooplankton. *Hydrobiologia*, 113: 77-91.
- Gozdziejewska, A. and Tucholski, S. 2011. Zooplankton of fish culture ponds periodically fed with treated wastewater. *Pol. J. Environ. Stud.*, 20: 67-79.
- Hu, X.Y., Wu, S.G. and Mao, D.S. 2007. High efficiency and healthy culture technology in snakehead culture pond. *China Fisheries*, 3: 23-25 (In Chinese).
- Jin, Q.B., Sheng, L.X. and Zhang, R. 1991. Effects of temperature on zooplankton community. *J. Northeast Normal University*, 4: 103-115 (In Chinese).
- Li, L.C. 2012. Analysis and research on plankton in partitioned pond. *Chin. Agricultural Sci. Bull.*, 28: 104-108 (In Chinese).
- Li, X.Y. 2013. Study on the community structure and diversity of metazoan zooplankton in Xiaoheli River reservoir. Dissertation, Northeast forestry University, Harbin, China (In Chinese).
- Lu, K.H., Zhu, J.Y., Wang, Y.C., Jin, C.H., Zheng, Z.M., Hu, Z.Y. and Pan, J.H. 2008. Structure and dynamics of plankton community and their impact factors based on CCA analysis in Hunanzhen Reservoir. *J. Fishery Sci. China*, 15: 950-960 (In Chinese).
- Luo, D.L. 2004. Quantitative distribution characteristic of zooplankton from three important mariculture areas of Xiamen. *Journal of Oceanography in Taiwan Strait*, 23: 458-468 (In Chinese).
- Marcus, N.H. 1982. The reversibility of subitaneous and diapause egg production by individual females of *Labidocera aestiva* (Copepoda: Calanoida). *Biological Bulletin*, 162: 39-44.
- Pielou, E.C. 1966. Species-diversity and pattern-diversity in the study of ecological succession. *J. Theoret. Biol.*, 10: 370-383.
- Pinel-Alloul, B. and Pont, D. 1991. Spatial distribution patterns in freshwater macrozooplankton: Variation with scale. *Can. J. Zool.*, 69: 1557-1570.
- Qiu, X.C., Zhao, H.X. and Sun, X.X. 2012. Relationships between zooplankton and water environmental factors in Shahu Lake, Ningxia of Northwest China: A multivariate analysis. *Chin. J. Ecology*, 31: 896-901 (In Chinese).
- Shannon, C.E. and Weaver, W. 1963. *The Mathematical Theory of Communication*. University of Illinois Press, Urbana.
- Shen, Y.F., Zhang, Z.S. and Gong, X.J. 1990. *New Technology of Microbiological Monitoring*. China Building Industry Press, Beijing, pp. 1-524 (In Chinese).

- Sun, R.Y. 2001. Principles of Animal Ecology. Beijing Normal University Press, Beijing (In Chinese).
- Wang, F.J., Hu, Z.Q., Tang, J., Liu, L.S. and Zhao, H.Q. 2006. Evaluation of water quality and the type of nourishment in the eastern zone of Lake Chaohu by means of zooplankton. *Ecol. Sci.*, 25: 550-553 (In Chinese).
- Wang, X.M. and Song, X.M. 2007. Investigation on relevance between zooplankton in GaoTangLake and water environmental factors in Huainan City. *J. Beijing Institute of Education (Natural Science)*, 2: 19-23 (In Chinese).
- Wei, X.L., Li, C.H., Xie, X.Y., Dai, M., Liao, X.L., Hu, W.A., Xiao, Y.Y. and Li, P. 2013. Ecological characteristics of zooplankton in the higher place pond of shrimp recirculating aquaculture system. *J. Agro-Environ. Sci.*, 32: 141-152 (In Chinese).
- Wu, L., Feng, W.S., Zhang, T.L. and Yu, Y.H. 2011. Characteristics of zooplankton community and its relation to environmental factors in Lake Wuhu in spring and autumn. *J. Hydroecol.*, 32: 31-37 (In Chinese).
- Xu, Z.L., Wang, Y.L. and Chen, Y.Q. 1995. An ecological study on zooplankton in maximum turbid of estuarine area of Changjiang (Yangtze) River. *J. Fishery Sci. China*, 2: 39-48 (In Chinese).
- Zhang, N. 2014. Community structure characteristics of zooplankton in the *Ctenopharyngodon idellus* aquaculture ponds and correlations between zooplankton and environmental factors. Dissertation, Huazhong Agriculture University, Wuhan, China (In Chinese).
- Zhang, N., Xie, C.X., Zhao, F., Lv, Y.J. and Li, R.J. 2014. Community structure characteristics of zooplankton in the *Ctenopharyngodon idellus* aquaculture ponds and correlations between zooplankton and environmental factors. *Freshwater Fisheries*, 44: 89-100 (In Chinese).
- Zhang, Z.S. and Huang, X.F. 1995. Studying Methods on Freshwater Plankton. Science Press, Beijing (In Chinese).
- Zhao, C., Zhang, H.M., Chen, L., Sha, W.L., Shu, F.Y. and Zhang, J. 2014. Effects of snakehead culture on zooplankton community structure. *Chin. J. Zool.*, 49: 63-70 (In Chinese).
- Zheng, X.Y., Wang, L.Q., Gai, J.J., Ji, G.H., Fan, Z.F. and Zhang, R.L. 2009. Dynamic and community structure of zooplankton in Dianshan Lake. *Chin. J. Zoology*, 44: 78-85 (In Chinese).
- Zhou, S.C. 2007. The ecological studies of zooplankton in Xiangxi River system. Dissertation, Institute of Aquatic Biology, Chinese Academy of Sciences (In Chinese).
- Zhou, X.M. 2010. Comparative study on community structures of zooplankton in Dishui Lake and its surrounding waters. Dissertation, Shanghai Normal University, Shanghai, China (In Chinese).



Environmental Pollution Status Quo and Legal System of Third-Party Governance in Hebei Province, China

Kehui Cheng[†] and Fang Lv

Hebei College of Industry and Technology, Shijiazhuang, Hebei, 050091, China

[†]Corresponding author: Cheng Kehui

Nat. Env. & Poll. Tech.
Website: www.neptjournal.com

Received: 12-01-2019
Accepted: 14-02-2019

Key Words:

Environmental pollution
Pollution status
Third-Party governance
Legal system

ABSTRACT

Environmental pollution has consistently been a serious obstacle to the sustainable development of China's national economy. The proposed third-party governance mode for environmental pollution is suitable for China's development and could fundamentally solve pollution problems. The construction of the legal system of third-party governance is the primary prerequisite for determining the relationship between relevant government departments and enterprises discharging and managing pollution and for upgrading market and competitive mechanisms. Taking Hebei Province as an example, this study analyses the design and implementation of legal systems adopted by developed countries to prevent environmental pollution, and concludes pollution regularity in recent years. The study also summarizes the main modes of the third-party legal system for environmental pollution governance and proposes relevant suggestions. Results show that third-party governance can improve the effect of environmental pollution control under the market mechanism. The unreasonable industrial structure and extensive economic growth in Hebei Province lead to increased fluctuations in wastewater emissions and industrial solid waste, and the main pollutants in industrial exhaust emissions are relatively large in number. Moreover, entrusted governance, trust operation, and public-private partnership are the major modes of the third-party governance's legal system. The study's results are of considerable importance in clarifying different subject responsibilities of third-party environmental pollution governance and in upgrading its market and competitive mechanisms. The results also provide a valuable reference to the perfection of an assessment system to the governance effect and the establishment of public participation and legal systems of third-party governance.

INTRODUCTION

As a developing country, China's economic development lags behind that of developed countries. Numerous environmental pollution issues have emerged due to economic development. Haze and sand-dust events often occur in provinces with highly developed industries. Air has been severely polluted, and this endangers people's health and safety outdoors. Water, soil, and atmosphere improvement should be emphasized to strengthen the protection of the ecological environment, and the prevention and management of pollution should be reinforced. In the traditional polluter governance mode, promoting third-party governance is an inevitable choice for professional and social pollution management. Manufacturers only focus on their business operation and "transfer" the pollution governance responsibility to professional enterprises by signing contracts to maximize economic benefits and solve environmental pollution simultaneously.

Hebei Province is one of China's major provinces with large energy consumption and high pollution discharge. The resources and environment of Hebei Province are under

considerable pressure, and the pollution improvement task is heavy. As shown in Fig. 1, per capita GDP increased from 2006-2017. Although the proportion of the secondary industry has declined, this industry still accounts for the largest part in the industrial structure, with heavy industry as the leading industry. Environmental pollution has become increasingly serious along with the rapid development of the economy. The ecology is relatively fragile, and haze and sand-dust events occur frequently. Therefore, the third-party governance mode is urgently needed to prevent environmental pollution and improve environmental quality, thereby realizing coordinated economic and environmental development in Hebei Province. A third-party governance system has several advantages in improving enterprise pollution management efficiency and reducing the pollution control cost. This system provides convenience to the supervision of environmental protection administration and alleviates the government's financial pressure. However, in practice, the limitations of the legal system, inadequate market access and exit mechanisms, existing financing obstacles of third-party governance enterprises, and business risks caused by the discontinuous policy restrict the devel-

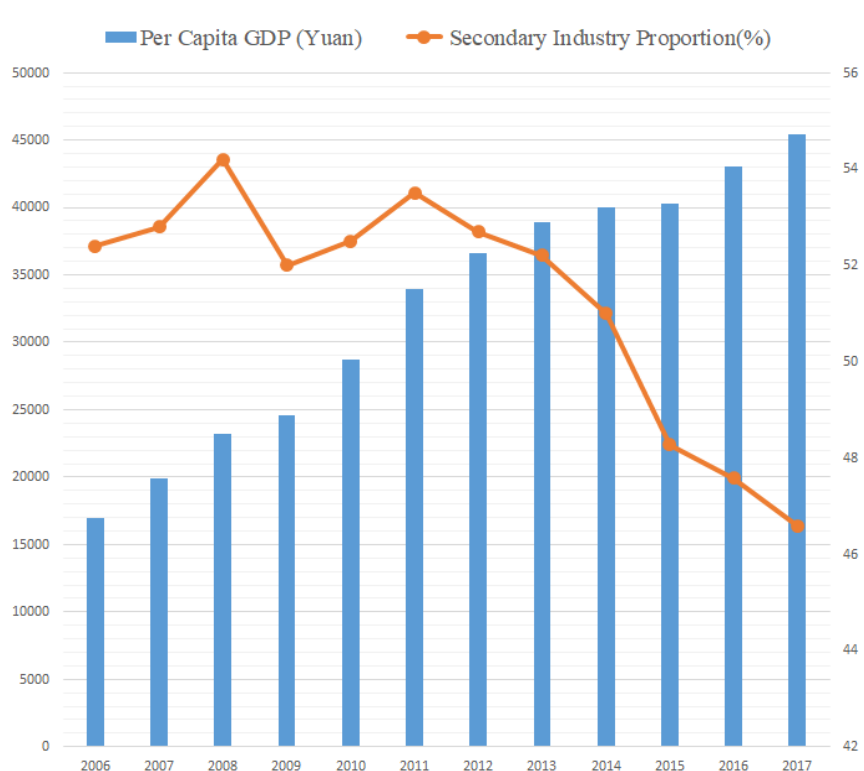


Fig. 1: Per capita GDP and the secondary industry proportion in Hebei Province from 2006 to 2017. (Data from <http://olap.epsnet.com.cn/>).

opment of the third-party governance system.

EARLIER STUDIES

Some developed countries have undertaken studies on third-party governance (or market operations) of environmental pollution. In view of the early start of the industrial revolution in these countries, environmental issues were immediately recognized and received considerable attention. These countries, with their pollution discharge rights in the international community, have gained rich experiences and advanced technologies in dealing with environmental pollution. A considerable amount of literature shows that third-party governance can not only improve the pollution control effect, but also promote ecological civilization construction under the market mechanism. Jackson (1992) analysed the quantitative relationship among pollution pricing, government regulation, and environmental pollution. Yhdego (1995) provided a general introduction of water, air, and noise pollution in Tanzania and believed that the country lacks a conceptual framework, public support, government motivation, and legislative and regulatory infrastructure, all of which were necessary for efficient environmental pollution management. In the end of the study, the

author proposed a simplified pollution prevention strategy. Blakemore et al. (1998) showed that Britain's demand for primary energy resources increased slightly from 1970 to 1994, and its carbon dioxide emissions considerably decreased during this period due to the enacted UK/EU environmental policy. Blakemore et al. (2001) believed that laws have been enacted to increase the use of new energy sources and therefore restrict large pollutant emissions from power plants and gasoline-powered vehicles; evidently, nitric oxide emissions from power plants decreased. Mugabi et al. (2007) analysed relevant recycling policies for water resources in developing countries and proposed suggestions from the perspective of legal governance. Wang et al. (2010) argued that the number of discarded electrical and electronic equipment in China had rapidly increased, but a corresponding administrative supervision and recycling system had not been established to date. The government should regulate the manufacturing, recycling, and disposal of household appliances through legislation. Hua et al. (2011) stated that clean production is one of the voluntary environmental management tools that could effectively solve resource shortages and environmental pollution issues. Clean production technology is a quasi-public prod-

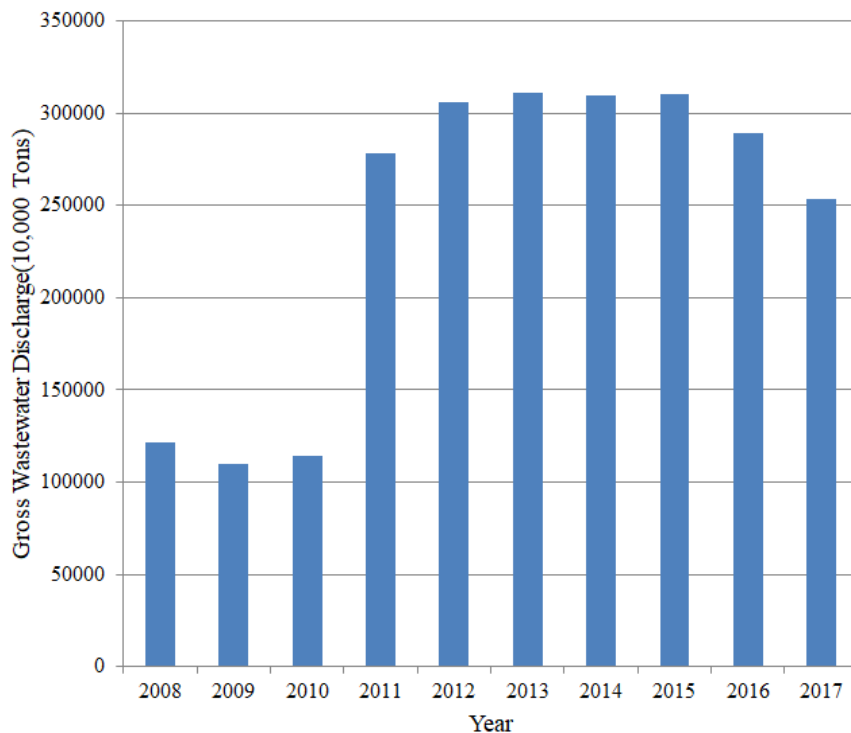


Fig. 2: Gross wastewater discharge in Hebei Province from 2008 to 2017. (Data from the China Environmental Statistics Yearbook).

uct with positive externality. Guosheng et al. (2011) proposed the upgrading of the systems of environmental protection infrastructure, ecological compensation, technical support, performance evaluation, and industry and introduced several countermeasures related to environmental protection. Wang et al. (2011) believed that environmental pollution coexists with environmental improvement. However, an evident increase in environmental pollution pressure was observed; therefore, environmental governance should be considerably enhanced. Swartjes et al. (2012) summarized the management status quo of contaminated sites in the Netherlands and argued that the legislative work on these contaminated sites should be reinforced. Feng et al. (2014) analysed the development of environmental pollution liability insurance in China and found that the imperfect law weakened the legal basis of pollution insurance, and the inadequate technical support hindered the further improvement of insurance. Basijrasikh (2015) showed that Afghanistan established its National Environmental Protection Agency with the help of the United Nations Environment Program and analysed the measures implemented by the government to cope with environmental issues. Horne et al. (2016) focused on the direct relation between environmental regulators from the government and business own-

ers of third-party governance enterprises. The author also provided new perspectives on measures, such as pollution prevention, site remediation, and waste management, for individuals engaged in environmental protection. Zhang et al. (2016) studied the information transparency and disclosure issues in environmental governance in China and proposed suggestions for improving the information release of third-party environmental governance. Through a service evaluation of third-party governance, Xu et al. (2017) proposed an evaluation system comprising five main indicators, including enterprise capacity, equipment operation, and economic and environmental benefits of techniques. Feng et al. (2017) introduced China's environmental protection legislation from the perspective of national, local, and international communities. The author also clarified the definitions of legislation, plan, and policy and established a preliminary analysis framework to evaluate their integration. Yousefi et al. (2017) argued that in consideration of the importance and challenges posed by air pollution in Teheran, the Iranian government should require enterprises to use renewable energy and reduce environmental pollution by enacting relevant laws.

These studies have shown that third-party governance is necessary for managing environment pollution. Under

the premise of a sound legal system, the binding force of national administration should be enhanced, and third parties should be supervised and governed by multiple parts. The supervision of the government environmental department should be strengthened, and multiple parties must be allowed to participate. Relevant regulations and laws should emphasize the responsibility of polluters and require polluters and third parties to control pollution at the source and pay the penalty after pollution is generated. Taking Hebei Province as an example, this study examines environmental pollution regularity in recent years, summarizes the main modes of the third-party legal system for environmental pollution governance, and proposes relevant suggestions. Third-party governance is a new mode of pollution management. This study is of heuristic value to the legal mechanism construction, legal responsibility determination, and top-level design of third-party governance.

STATUS QUO OF ENVIRONMENTAL POLLUTION IN HEBEI PROVINCE

Water pollution: Water pollution is caused by many factors, among which industrial wastewater generated by industrial activities is regarded as the main one. Many complex chemicals exist in wastewater, and these chemicals pollute water and pose a threat to people's health. Fig. 2 shows that in 2008, the wastewater discharge of Hebei Province was 1211.72 million tons. The amount reached 2536.85 million tons in 2014, with an average annual growth rate of 12.15%. However, the amount of industrial wastewater discharge declined from 2009 to 2010. After 2011, the wastewater discharge continued to increase, but the overall amount of increase was small. In 2015, wastewater discharge began to increase again. This situation shows that controlling industrial wastewater discharge is necessary, and the management of pollution and polluted waters should be considerably strengthened.

Air pollution: Air pollution is primarily caused by natural sources and human activities. The natural sources mainly originate from natural disasters, such as earthquakes, tsunamis, mudslides, and fire. Air pollution caused by human activities refers to the exhaust gas generated by humans' daily life and industrial activities. The pollutants emitted by enterprises that produce steel, petroleum chemicals, and ferrous metal contain large amounts of toxic gases, such as sulphur dioxide and nitrogen dioxide, which damage the air and people's health. Industrial waste gas is the primary cause of waste gas. As shown in Fig. 3, the amount of sulphur dioxide emissions in Hebei Province was 789,443 tons, showing a 44% decrease compared with that in 2011. The amount of nitrogen oxide was 1,126,640 tons, showing a 37% decrease. Smoke (power) dust emission was 1,322,477

tons in 2011 and reached a peak of 1,797,683 tons in 2014. This emission was 1,256,835 tons in 2016, showing a decrease of 4.9% compared with that in 2011.

Solid waste pollution: Solid waste primarily originates from urban household waste, agricultural waste, and waste generated by industrial activities. Urban household waste refers to food and plastic waste generated by residents' daily life. Agricultural waste refers to animal waste, crop straw, agricultural fertilizer, and plastics produced by agricultural activities, and waste generated by industrial activities refers to various waste fuels, residues, foam, and dust emitted by enterprises during production. The primary source of solid waste is industrial activities. Fig. 4 shows that the amount of industrial solid waste generated in Hebei Province in 2005 was 162.79 million tons. This amount continued to increase until 2015, reached a peak of 455.75 million tons in 2012, and declined to 327.21 million tons in 2017, with an annual average increase of 8.42% compared with the amount in 2005. The overall consumption of industrial solid waste in Hebei Province was 83.74 million tons in 2005. The figure was 187.4 million tons in 2017, with an annual average increase of 10.32% compared with that in 2005. The higher the utilization rate of industrial solid waste is, the better the waste is re-utilized. Improved waste utilization saves energy and natural resources; protects the environment; improves environmental quality, and enhances energy efficiency.

MAIN MODES OF THE THIRD-PARTY GOVERNANCE'S LEGAL SYSTEM FOR ENVIRONMENTAL POLLUTION

Entrusted governance: Entrusted governance service refers to the manner in which an enterprise that discharges pollutants entrusts a third-party enterprise to provide particular services by signing an entrusted operation contract and pays for pollution management according to the contract. The services include financing, operation maintenance, upgrade, and transformation towards newly built or expanded pollution control equipment. The contract stipulates that the third-party shall ensure satisfaction of the emission reduction target through operation and bear the corresponding legal responsibilities. Two main types of entrusted governance service modes are available. Firstly, the enterprise that discharges pollutants entrusts a third-party enterprise to provide a service package from project design, engineering construction, and tests to operation management after the project is completed. The pollution control assets are owned by the enterprise that discharges pollutants, and the third-party enterprise only provides operation and maintenance for the equipment while ensuring that the pollution control effect stipulated in the contract is achieved. Sec-

only, the enterprise that discharges pollutants does not own the pollution control equipment. The pollution control assets are owned by the third-party enterprise. The third party takes charge of equipment construction and operation and brings the equipment to enterprise management to be accounted for independently.

Trust operation: Trust operation refers to the manner in which an enterprise that discharges pollutants entrusts a third-party enterprise to provide particular services by signing a trust contract and pays for trust operation according to the contract. The services include operation, maintenance, upgrade, and transformation toward existing pollution control equipment. The contract stipulates that the third party shall ensure satisfaction of the emission reduction target through operation and bear the corresponding legal responsibilities. Two types of trust service are available. Firstly, the third-party enterprise is responsible for the operation of pollution control facilities owned by the enterprise that discharges pollutants. Secondly, the third party is also fully involved in the environmental pollution management of the enterprise discharging pollutants. The difference between the two modes is the ownership of pollution control equipment by the third-party enterprise. In the entrusted governance mode, the third-party enterprise owns or partially owns the pollution control equipment, whereas the third party does not own the equipment in the trust operation mode. The third-party enterprise is only responsible for the operation, management, maintenance, upgrade, and transformation of the equipment based on the trust request proposed by the enterprise discharging pollutants.

Public-private partnerships: Public-private partnerships (PPP) refer to governmental agencies and other enterprises or investors that construct or operate public utilities together with the use of joint stock. PPP is an important tool for public management in developed countries. The scale and management level of PPP projects in developed countries, such as Australia, the United States, Spain, and Germany, is at the leading level worldwide. The application of the PPP mode and third-party governance system to environmental pollution is effective in attracting social capital and professional environmental protection forces. These approaches can remarkably alleviate or even eliminate financial dilemmas and guarantee the benefits and development space of investors who pursue stable medium and long-term investment return. In this way, a win-win situation can be achieved to compensate for government regulation, and reduce the cost of polluters, and promote the healthy and orderly development of the environmental protection industry.

POLICY RECOMMENDATIONS

Clarify the legal responsibility in the third-party

governance mode: In the third-party governance mode, the enterprise that discharges pollutants entrusts environmental pollution control work to a third-party enterprise by signing an entrustment contract. The purchase of pollution control services from the third party is the main indicator of the third-party governance mode. According to the principle of “polluter pays”, the purchase is a contractual relationship that obeys private laws. The pollution control responsibility of the enterprise that discharges pollutants is also the obligation requested by the public law. The contractual relationship between the two enterprises is subject to laws. Enterprises discharging pollutants have the responsibility to control pollution, and their pollutant discharge should meet national emission standards. Pollution control enterprises that discharge pollution should inform other enterprises of their operation state, emission types, and concentrations. Rights and obligations supplement each other, and one cannot exist without the other. Improved cooperation between the two parties of pollution control management can only be achieved through mutual understanding and trust. Therefore, clarification of the relationship and responsibility of each entity in pollution control benefits the determination of their rights and obligations and allows law enforcement agencies to easily distinguish and investigate their specific responsibilities.

Strengthen the legal standing of government supervision in third-party governance: Strengthening the supervision of the government’s environmental protection department is crucial in solving the current environmental issue. At present, in the environmental protection market, many enterprises that discharge pollutants build pollution control equipment but do not utilize the equipment; meanwhile, pollution control enterprises cannot provide accurate monitoring data. The lack of effective and necessary supervision is the main problem. Given that the market entity considers the nature of the “economic man,” the market aims to achieve maximal benefits. The market entity would rather accept punishment from the environmental protection department than equip itself with expensive pollution control facilities, let alone third-party governance. In addition, the third-party governance mode changes only the entity that is responsible for pollution control based on the contract. Although a pollution control enterprise has a certain obligation to supervise the pollution management work of the enterprise that discharges pollutants, it cannot replace the environmental law enforcement department because enterprises that discharge pollutants ignore their damage to the environment. The success of third-party governance requires strict supervision from the government’s environmental protection department. In this way, enterprises discharging pollutants are “forced” to take actions to pre-

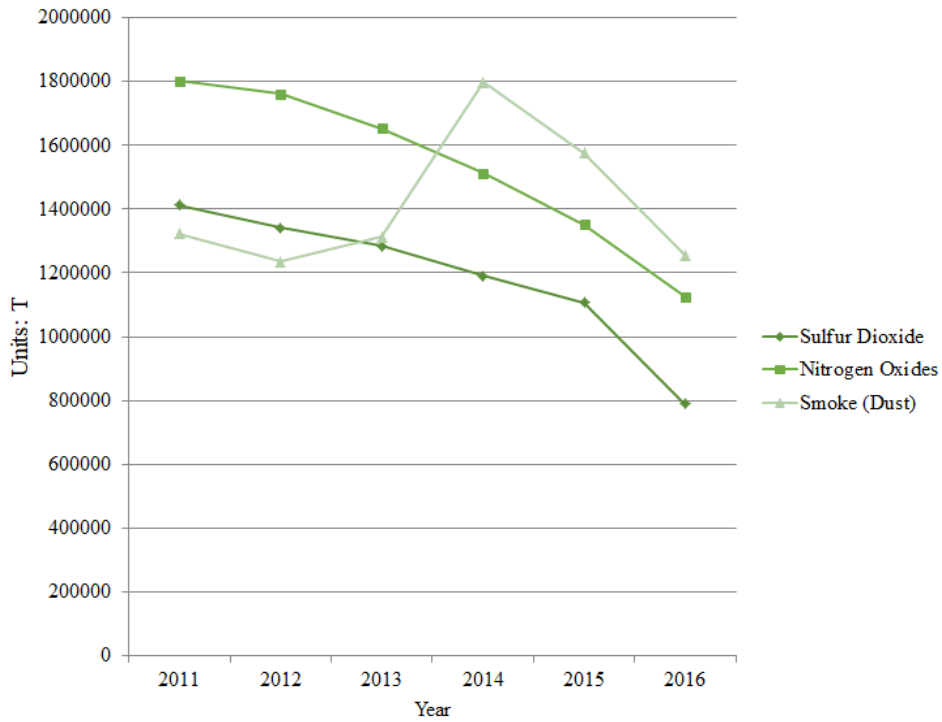


Fig. 3: Amount of main pollutants in industrial waste gas in Hebei Province from 2011 to 2016. (Data from the China Environmental Statistics Yearbook).

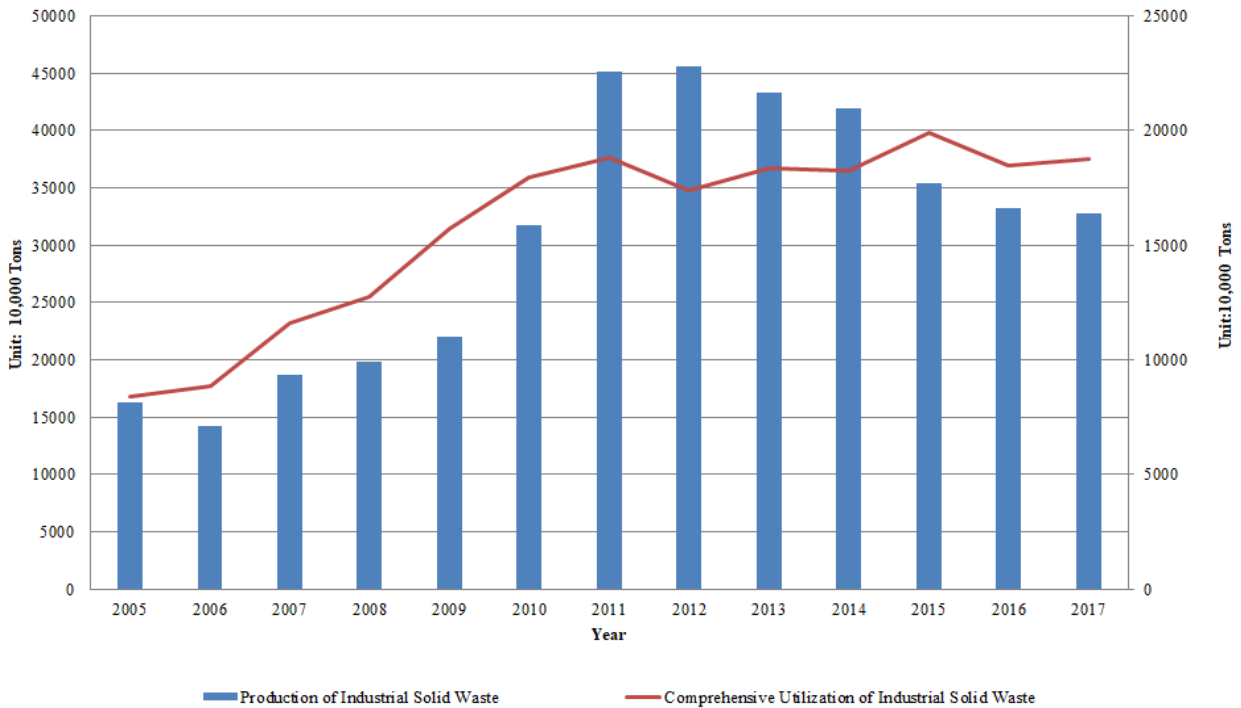


Fig. 4: Amount of produced and consumed industrial solid waste in Hebei Province from 2005 to 2017. (Data from the China Environmental Statistics Yearbook).

vent pollution, and enterprises managing pollution are “forced” to take actions to control pollution.

Establish an environmental credit evaluation system for third-party governance enterprises: The premise of healthy and effective market development is that each market entity should strictly follow the market order, undertake relevant marketing obligations, and be responsible for its actions while enjoying its rights. In practice, many professional governance companies refuse to bear their legal responsibilities by seeking pretext that they have not obtained permission nor a contract or they are treated unjustly. The existing law does not determine the legal relationship between relevant market entities under the third-party governance mode, leaving enterprises that discharge pollutants at a disadvantage in terms of taking responsibilities. Relevant service companies should be supervised from the very beginning (from their entry into the market) to punish the appropriate responsible party. Enterprises with an incomplete certificate and poor credit should be eliminated from the market, and well-qualified ones with high credit should be given priority to enter the market.

Standardize the entry mechanism of third-party governance in environmental pollution management: Relevant documents can be refined according to pollution types. An enterprise entry standard could be set from the aspects of company’s registered capital, technology, and market threshold price so that the scale of the third-party governance enterprise can be legalized and the management entity can be regulated. The market entry standard of the third-party governance enterprise should be strictly controlled to provide an institutional guarantee for regulatory market operation of the third-party governance from the source. Given that the market entry and exit mechanism is still incomplete, the environmental supervision department should formulate and adjust the environmental service threshold price provided by the third-party governance market based on material and technical limits for different pollution types and fields and the average level of third-party governance market profits in each field. This department should also establish and upgrade the pricing system in the third-party governance market and strictly control the market entry price. Adhering to a marketable operation mode in third-party governance and allowing the market discipline to play its role are necessary in establishing systems for pricing, credit, and qualification evaluation standards of third-party governance in a fair market. Outside the market, the government should pay attention to market supervision and risk control, thus mitigating the gap in the market mechanism.

CONCLUSIONS

As an important legal system promoted by China for envi-

ronmental governance, third-party governance establishes a pollution control mechanism and provides a new means of environment management and ecological restoration. The legal system of third-party governance is a crucial driving force in promoting professional and industrial environment management. It is also an effective incentive for the development of the environmental protection industry. The third-party governance mode is a new choice for resolving environmental pollution issues. Taking Hebei Province as an example, this study analyses the design and implementation of the legal system adopted by developed countries to prevent environmental pollution and concludes pollution regularity in recent years. It also summarizes the main modes of the third-party legal system for environmental pollution governance. The research results show that the implementation of third-party governance under the market mechanism can completely improve the effect of environmental pollution control. Increased fluctuations in wastewater emissions and industrial solid waste are observed in Hebei Province, and the main pollutants in industrial exhaust emissions are relatively large in number. Moreover, the major modes of the third-party governance’s legal system, which include entrusted governance, trust operation, and PPP, are used to prevent environmental pollution. Several suggestions, such as clarifying the legal responsibility in the third-party governance mode, strengthening the legal standing of government supervision in third-party governance, and establishing an environmental credit evaluation system for third-party governance enterprises, are also proposed in this study. The author suggests that several aspects, such as clarifying the entity responsibility of third-party’s environmental pollution governance, upgrading market entry and exit mechanisms, removing financing barriers for the third-party governance, and improving the insurance system of third-party governance, should be further studied.

REFERENCES

- Basijrasikh, M. 2015. Assessing environmental policy in Afghanistan through water pollution: What Afghan citizens and the government can do to improve the environmental state in Afghanistan. *Soil Biology and Biochemistry*, 78(11): 1-9.
- Blakemore, F.B., Davies, C. and Isaac, J.G. 1998. The effects of changes in the UK energy demand and environmental legislation on atmospheric pollution by carbon dioxide. *Applied Energy*, 59(4): 273-303.
- Blakemore, F.B., Davies, C. and Isaac, J.G. 2001. Effects of changes in the UK energy-demand and environmental legislation on atmospheric pollution by oxides of nitrogen and black smoke. *Applied Energy*, 68(1): 83-117.
- Feng, L. and Liao, W. 2017. Legislation, plans, and policies for prevention and control of air pollution in China: Achievements, challenges, and improvements. *Journal of Cleaner Production*, 112: 1549-1558.
- Feng, Y., Mol, A.P. and Lu, Y. 2014. Environmental pollution liability insurance in China: in need of strong government backing.

- Ambio, 43(5): 687-702.
- Guosheng, C., Jianhui, Z. and Chan, C. 2011. The research on restrictive factors and countermeasures of environment governance in reservoir: An experimental study on Shanxi hydraulic project in Wenzhou. *Energy Procedia*, 5(4): 725-733.
- Horne, R., Strengers, Y. and Stempel, A. 2016. Policing and polluting: The role of practices in contemporary urban environmental pollution governance. *Environmental Science and Policy*, 66: 112-118.
- Hua, Z.J. and Hua, J. 2011. Clean production and third-party governance. *IEEE*, 2: 730-733.
- Jackson, T. 1992. Pricing for pollution: Market pricing, government regulation, environmental policy: Hobart paper 66, 2nd edition, Institute of Economic Affairs, London, UK, 1990. *Energy Policy*, 20(1): 84-86.
- Mugabi, J., Kayaga, S. and Njiru, C. 2007. Strategic planning for water utilities in developing countries. *Utilities Policy*, 15(1): 1-8.
- Swartjes, F.A., Rutgers, M. and Lijzen, J.P.A. 2012. State of the art of contaminated site management in the Netherlands: Policy framework and risk assessment tools. *Science of the Total Environment*, 427-428.
- Wang, H., Chen, F. and Yao, C. 2011. Analysis on the environmental conditions for economic development in central China. *Energy Procedia*, 5(5): 1243-1250.
- Wang, Y., Ru, Y. and Veenstra, A. 2010. Recent developments in waste electrical and electronics equipment legislation in China. *International Journal of Advanced Manufacturing Technology*, 47(5-8): 437-448.
- Xu, Bingsheng, Lin, L. and Huang, J. 2017. Research on standardization system of third-party governance on environmental pollution. *IOP Conf. Ser. Earth Environ. Sci.*, 94 012079.
- Yhdego, M. 1995. Environmental pollution management for Tanzania: towards pollution prevention. *Journal of Cleaner Production*, 3(3): 143-151.
- Yousefi, H., Roumi, S. and Tabasi, S. 2017. Economic and air pollution effects of city council legislations on renewable energy utilisation in Tehran. *International Journal of Ambient Energy*, 39(3): 1-16.
- Zhang, L., Mol, A.P. and He, G. 2016. Transparency and information disclosure in China's environmental governance. *Current Opinion in Environmental Sustainability*, 18: 17-24.



Biodegradation of Reactive Red 195 By A Novel Strain *Enterococcus casseliflavus* RDB_4 Isolated from Textile Effluent

Radhika Birmole, Azza Parkar and K. Aruna†

Department of Microbiology, Wilson College, Mumbai-400 007, Maharashtra, India

†Corresponding author: K. Aruna

Nat. Env. & Poll. Tech.

Website: www.neptjournal.com

Received: 07-08-2018

Accepted: 21-10-2018

Key Words:

Decolourisation

Degradation

Enterococcus casseliflavus

RDB_4

Reactive Red 195

ABSTRACT

Reactive Red 195 (RR-195) is a sulphonated azo-dye used extensively in textile industries. The current study was carried out to investigate the decolourisation of RR-195 dye using a novel bacterial strain, in an attempt to overcome the environmental hazards caused due to the unopposed industrial laws and standard waste management systems. The most promising bacterial strain isolated from textile effluent was identified as *Enterococcus casseliflavus* RDB_4 by 16s rRNA analysis. It showed complete decolourisation of 50 ppm dye in optimized M9 medium (pH 7) supplemented with 3% yeast extract, within 4 h at 35°C using inoculum size of 0.2 O.D._{530nm} under static conditions. Moreover, it showed tolerance to high NaCl (1 to 6%) and dye (1000 ppm) concentrations in batch as well as continuous culture systems; thus making it ideal for industrial dye waste management. Furthermore, the biodegradation of RR-195 dye was confirmed by high-performance liquid chromatography and Fourier transform infrared spectroscopy analysis into nontoxic metabolites ensured by ecotoxicity studies.

INTRODUCTION

An immense obsession with exquisite lifestyle has pressurized the textile industry to use coloured dyes in order to chaperone the appearance of finished goods. A similar situation is prevalent in other industries producing paper, leather, food, drug, cosmetics, fashion products and plastic merchandise (Thakur 2006). These profit-driven industries have collectively managed to crown the dye-related trades as the most important sector of the chemical industry and contaminate the environment in the process.

Dyes are basically derived from petroleum products containing unsaturated chromophore group of molecules which are capable of absorbing light in the visible region of the electromagnetic spectrum (400 to 750 nm). Most dyes are recalcitrant molecules that chemically lock the colour onto fibres or other materials and resist decolourisation on exposure to soap, water, light or other mild chemical agents (Robinson et al. 2001, Banat et al. 1996, Plumb et al. 2001). It is estimated that approximately 7×10^5 metric tons of 10,000 different dyes are produced annually, worldwide (Thakur 2006). This roughly quantifies to more than 1 million tons of dye production; of which about 40% ends up in wastewaters. Among these, azo-dyes constitute nearly over 70% of the synthetically produced dyes (Suteu et al. 2010).

The extensive utilization of azo-dyes by industries can be attributed to the complex structure of the dye that allows

the possibility of diverse shades without compromising its stability (Neil et al. 2000). Azo dyes generally contain at least one N=N double bond and are connected to benzene and naphthalene rings. In certain cases, a sulphonate substituent group may be present, in which case it is termed as a "sulphonated azo-dye". These complex structures may be favourable for industrial requirement; however, it poses a serious challenge for waste disposal systems.

The presence of dyes in textile effluents significantly affects the photosynthesis activity in aquatic life because of reduced light penetration. The luminosity can be affected even by the presence of less than 1 ppm dye concentration in water bodies. Along with other contaminants, these dyes also aid in subsequent depletion of dissolved oxygen concentration and hence alter the aquatic ecosystem (Moreira et al. 2004). The resilience to disintegration observed in the complex chemical structure of these dyes further compromises the environmental safety. Hence, regulatory acts affirm the prerequisite treatment of industrial effluent containing synthetic dyes to its discharge in the environment.

The routinely operated physical and chemical techniques of effluent treatment including sedimentation, filtration, segregation, coagulation/flocculation, etc., have been in practice for over decades. However, they suffer several drawbacks associated with the excess use of chemicals and high expenditure. Besides, these techniques are labour intensive and trigger problems with sludge disposal. Also, many times,

the disappearance of colour is believed to be an indication of dye degradation. This can further aggravate the intensity of the situation, since the incomplete degradation of several dyes may produce end products that are more toxic than the native dyes. The intermediate compounds produced during the breakdown of complex dyes are aromatic amines with constituent side groups. Contamination in such cases may not be perceptible, but it creates a larger and more deleterious problem (Brown & Stephen 1993). Thus, the complete degradation of dyes from aromatic amines to simple compounds is a priority research venture that satisfies the current need of the environment. Most evidently, the biological processes of effluent treatment may be able to surpass these drawbacks and provide a more economical and environment-friendly alternative to the existing technologies (Jacob & Azariah 2000, Ngwasiri et al. 2011). There have been reports of bacterial, fungal, yeast and algal (Kurade et al. 2017, Pillai 2017, Chen & Ting 2017, Dellamatrice et al. 2017) degradation of dyes into simple compounds. Although the biological approach of effluent treatment may face challenges like alkaline pH and the presence of high amounts of inorganic salts, it can be prevented by exploiting the salt-tolerant and alkaliphilic microorganisms.

The present study focuses on the use of a novel salt-tolerant and alkaliphilic bacterium *Enterococcus casseliflavus* RDB_4 isolated from textile effluent, to degrade one of the frequently used textile dyes i.e., Reactive Red 195 (RR-195). It is a sulphated azo-dye containing reactive groups which are often a heterocyclic aromatic ring substituted with chloride. It is mainly used for dyeing of cellulose fabrics, but other uses also include viscose fibre printing. Considering the possibility of toxic nature of biodegraded components of RR-195, our study also emphasizes the toxicological investigation of pure and decolourised dye using germinating seeds of *Phaseolus mungo* and *Triticum aestivum*.

MATERIALS AND METHODS

Chemicals and media used in the study: The dyes used in our study viz., RR-195, Disperse blue B3, Reactive brilliant blue 198, Reactive brilliant blue 19, Reactive Red 120, Direct red 5B, Reactive Orange 16, Reactive black 5, Coracion green HE4B, Blue MEBRF 150%, Navy blue ME2G, Navy blue MEBL, Reactive yellow, Coracion red HE3B-N, Coracion orange HE2R, Orange ME2R and Corafix red ME4B were procured from Atul dyes, Mumbai, India. Other common dyes used in the laboratory such as methylene blue and congo red were procured from Merck chemicals. All other growth media like Nutrient Broth (NB) and media components were obtained from Hi-media Pvt. Ltd., Mumbai, India. Dye stock solution of 10 mg/mL was

prepared in sterile distilled water and used for further experiments.

Sample collection: The screening of dye decolourising and degrading bacteria was carried out from the textile effluent collected from Dhanlakshmi Textile Mill, Mumbai.

Enrichment of dye degraders: A 10 mL volume of the textile effluent was diluted 1:10 using sterile phosphate buffered saline (pH 7.2). The solid particles in the above mixture were allowed to settle for a period of 1 h and 10 mL of the supernatant was inoculated into two flasks, each containing 90 mL of NB incorporated with 50 ppm of RR-195 dye. For enrichment of dye degraders, one of the inoculated media was kept on a rotary shaker (150 rpm) while the other was kept under static conditions and incubated at 30°C for 7 days.

Isolation of dye degrading bacteria: Isolation of bacterial species was carried out from the flask showing decolourisation on Luria Bertani (LBM) agar medium containing 50 ppm RR-195 dye. The promising isolate showing most efficient decolourisation in the shortest time period was selected for the present study and maintained on LBM agar slants containing 50 ppm RR-195 dye.

Identification of dye degrading bacteria: Primary identification of the isolate was done on the basis of morphological, cultural and biochemical tests. The strain was confirmed by 16s rRNA gene sequence analysis. PCR based 16S rRNA gene amplification and sequencing of the isolated bacterium was carried out using universal primers at SciGenom Labs Pvt. Ltd., Kerala, India.

Dye decolourisation assay: For decolourisation studies, 20 mL sterile LBM broth containing 50 ppm RR-195 dye was inoculated with 1 mL of 18-24 h old test isolates (0.2 O.D._{530nm}) and incubated at 30°C under static and shaker conditions until decolourisation was observed. Following incubation, the cell-free supernatant was collected by centrifuging small aliquots (3 mL) of the inoculated media at 10,000 rpm for 10 min. The decolourisation activity was expressed in terms of percentage (%) decolourisation using a UV-Vis spectrophotometer and determined by monitoring the decrease in absorbance at the maximum wavelength of dye (540 nm). The uninoculated culture medium containing 50 ppm RR-195 dye was used as the experimental control to check abiotic loss of the dye, and sterile LBM broth without test culture or dye was set up as blank.

All experiments were carried out in triplicate and the mean values were represented. The data obtained were checked statistically for the standard error and standard deviation. The % decolourisation was calculated using the following equation:

$$\% \text{ Decolourisation} = \frac{A - B}{A} \times 100$$

Where, A is the initial absorbance of control dye and B is the observed absorbance of the decolourised dye (Dhanve et al. 2008).

Optimization of various physico-chemical parameters:

The biological decolourisation and degradation of any pollutant are affected by several environmental factors like pH, temperature, oxygen, incubation time, substrate concentration, etc. In our study, the optimization experiments were initiated by determining the optimum nutrient medium for dye decolourisation assay. The different nutrient media used in our study were LBM, mineral salt medium, NM9 medium, M9 medium, synthetic medium and NB. The decolourisation was monitored by using 20 mL of various culture media containing 50 ppm of RR-195 dye, inoculated with 1 mL of 18-24 h old test culture (0.2 O.D._{530nm}) and incubated at 30°C under static and shaker conditions until decolourisation was observed.

The optimization of physico-chemical parameters for biodegradation of RR-195 was investigated by varying one parameter at a time while keeping the others constant. These varying parameters included the initial optical density of test isolate (O.D._{530nm} 0.2, 0.4, 0.6, 0.8, 1.0, 1.5 and 2.0), temperature (5°C, 30°C, 35°C, 45°C and 55°C), pH (1 to 10), concentration of NaCl (1 to 10%), aeration i.e., static or shaking (150 rpm) and initial dye concentration (50 ppm to 1000 ppm). We also carried out an addition, substitution and deletion assay of organic nitrogen sources to check the effect of an individual component of LBM broth showing most effective dye decolourisation. For this purpose, in one set of experiments, the yeast extract and tryptone in the LBM broth was substituted with meat extract (0.5%) and peptone (0.5%) respectively and in the other set, the same was supplemented to LBM broth. To check the effect of an individual component of LBM broth on the dye degradation, the individual component of the medium was deleted one at a time and the decolourisation assay was carried out.

In addition, the M9 medium was also used to study the effect of varying concentrations of yeast extract (1-5%), electron donors (sodium lactate, sodium pyruvate, sodium formate, sodium acetate and various carbohydrates viz., glucose, lactose, maltose, mannitol, and sucrose), and electron acceptors (ammonium nitrate, sodium nitrate, sodium nitrite and potassium nitrate) to examine their effect on dye decolourisation.

Moreover, the effect of pre-grown cell mass was also studied on decolourisation of RR-195 dye under optimized conditions. The results for optimization assays were recorded

in the shortest time during which maximum decolourisation of RR-195 was observed. At the end of incubation period, cell-free supernatant was collected and % decolourisation was determined to optimize the culture conditions.

Mode of decolourisation: In order to determine the possibility of decolourisation due to extracellular adsorption by microbial cells over biodegradation, the % decolourisation of RR-195 dye by heat-killed and live test culture were assessed in our study. For this purpose, the test culture was inoculated into sterile M9 medium containing 3% yeast extract and allowed to grow at 30°C for 24h. Following incubation, the M9 medium was divided into two equal portions; one of which was autoclaved to kill the grown test culture. Later, 50 ppm of RR-195 dye was added to both the portions and incubated at 30°C until decolourisation was observed (Shah & Patel 2014).

Repeated dye decolourisation in the fed-batch process with pregrown cell mass:

In order to study the continuous decolourisation potential of the test culture, a repetitive fed-batch system was set up. In this system, a pregrown cell mass of the test culture was inoculated in optimized culture media and incubated at 35°C. A 50 ppm RR-195 dye concentration was added repeatedly to this system after an appropriate time interval when complete decolourisation was observed (Sahasrabudhe & Pathade 2012). This cycle was repeated until significant decolourisation activity was observed.

Immobilization of test culture in calcium alginate beads:

In order to carry out immobilization, 1 mL of the test isolate (5% w/v) was added to 100 mL of sterilized and chilled sodium alginate solution (4% w/v). This alginate-cell mixture was extruded drop by drop, using a 10 mL pipette, into a chilled and sterile 0.2 M CaCl₂ solution. Gel beads of approximately 2 mm diameter were obtained which were hardened by re-suspending it into a fresh CaCl₂ solution for 2 h with gentle agitation. Finally, these beads were washed with sterile distilled water and used for decolourisation experiment under optimized conditions (Cheetham & Bucket 1984, Usha et al. 2010).

Ecotoxicity studies: In order to assess the toxicity of the RR-195 dye and its degradation products, their effect was studied on germination of *Phaseolus mungo* and *Triticum aestivum* seeds. The investigation was carried out by exposing 10 seeds each to the 5 mL solution of pure dye (600 ppm) and its degradation products respectively.

The degradation products of RR-195 dye were extracted with equal volume of dichloromethane, dried and dissolved in distilled water. The length of plumule (shoot) and radicle (root) was recorded after seven days and compared with a control set which was soaked in distilled water (Dhanve et

al. 2008, Usha et al. 2010. Patil et al. 2010).

Analytical methods: Metabolites produced during biodegradation of the RR-195 dye were extracted with equal volumes of dichloromethane and concentrated using rotary vacuum evaporator (Celik et al. 2011). The concentrated dry residue of the extracted metabolites and dye (control) were analysed by a high-performance liquid chromatography (HPLC) and Fourier transform infrared spectroscopy (FTIR). The HPLC analysis was performed at IIT (Mumbai), and FTIR analysis was carried out in our laboratory using Agilent Technologies Cary 630 instrument. The Agilent Resolution Pro software was used for the spectral scan.

Decolourisation spectrum of various textile dyes and dye mixture by the test isolate: Textile effluent is a mixture of various dyes; hence it is necessary to exploit the ability of test isolates to decolourise diverse dyes and even mixtures of dyes. For this purpose, the % decolourisation of the different dyes (50 ppm) such as Dispersive blue B3, Reactive brilliant blue 198, Reactive brilliant blue 19, Reactive Red 120, Direct Red 5B, Reactive Orange 16, Reactive black 5, Coracion green HE4B, Blue MEBRF 150%, Navy blue ME2G, Navy blue MEBL, Reactive yellow, Coracion red HE3B-N, Coracion orange HE2R, Orange ME2R, Corafix red ME4B was determined in optimized culture medium over 5 h. Various combinations of different dyes (50 ppm of each dye) were also used in our study.

RESULTS AND DISCUSSION

RR-195 decolourisation studies: Seven distinct isolates were obtained from the dye effluent sample and all these were subjected to decolourisation assay. Fig. 1 represents the decolourisation activities of test isolates. Isolate 3 showed the most promising decolourisation activity under static conditions, and hence was selected for the present study.

Identification of the isolate: The cultural, morphological and biochemical tests identified the promising isolate (isolate 3) as *Enterococcus casseliflavus* and 16s rRNA analysis also confirmed the same. The nucleotide sequence analysis of the isolate was done at BlastN site on NCBI server (<http://www.ncbi.nlm.nih.gov/BLAST>) and corresponding sequences were downloaded. The identified isolate was deposited as *Enterococcus casseliflavus* RDB_4 at National Centre for Biotechnology Information (NCBI) with an accession number KP268598.

Optimization of physico-chemical parameters for dye decolourisation: The results for optimization of physico-chemical parameters for dye degradation are represented in Figs. 2-14. The optimized culture condition for the growth of *E. casseliflavus* RDB_4 (2.0 O.D_{530nm}) to effectively

decolourise 50 ppm of RR-195 dye was achieved when it was incubated at 35°C for 10 h under static conditions using LBM (pH 7). However, the most effective decolourisation was observed in M9 medium containing 3% yeast extract that resulted in complete decolourisation of 50 ppm RR-195 dye within 4 h.

Prior to optimization of physico-chemical parameters, it is essential to optimize the nutrient media in order to ensure maximum growth, and hence degradation of the dye. In our study, the decolourisation potential of *E. casseliflavus* RDB_4 was studied in various liquid media indicated in Fig. 2. Among the tested media, LBM supported maximum (88.24%) decolourisation of RR-195 dye in 10 h. The synthetic and mineral media, on the other hand, supported negligible decolourisation of RR-195 dye. Our previous study also showed effective biodegradation of Reactive blue 172 by *Shewanella haliotis* DW01 in LBM (Birmole et al. 2014). Other authors have also indicated the positive effect of tryptone and yeast extract in LBM that acts as readily available carbon as well as nitrogen sources for bacterial growth and hence promote effective decolourisation of the dye (Dhanve et al. 2008).

One of the important parameters for any microbiological process is the initial density of microbes used for the experiment. In cases where a lower density of starter culture is used, their potential activity may not be exploited and in cases where more than optimum concentrations are used, the nutrients may become exhausted before effective activity initiates. In our study, a maximum decolourisation of 83% was obtained with 2.0 O.D_{530nm} (Fig. 3) in 10 h. However, a culture density of 0.2 was used in further experiments, since there was no significant change observed in the decolourisation process with very dense cultures. Also, using a lower cell number is economical and feasible for the degradation process.

The optimum growth temperatures enable proper microbial metabolism and hence release an optimum concentration of enzymes required for the degradation process. In our study, dye decolourisation process was inhibited at low (5°C) and high (55°C) temperatures probably due to inactivation of enzymes or loss of cell viability. Our study showed significant decolourisation of RR-195 dye by *E. casseliflavus* RDB_4 at temperatures in the range of 30 to 45°C (Fig. 4) in 10 h with maximum decolourisation (97.99%) observed at 35°C. This also confirms that the degradation of dye is due to microbial metabolism that is dependent on temperature, and not due to adsorption (Bhatt et al. 2005). These results are in accordance with those of Sahasrabudhe & Pathade (2012), who reported maximum decolourisation of azo dye at 40°C by *Enterococcus faecalis* YZ66. Other studies have

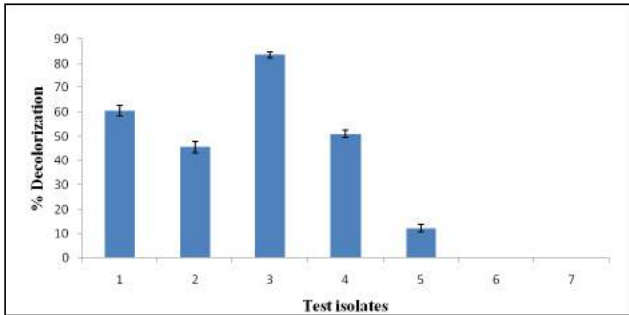


Fig. 1: Decolorisation of RR-195 dye by test isolates.

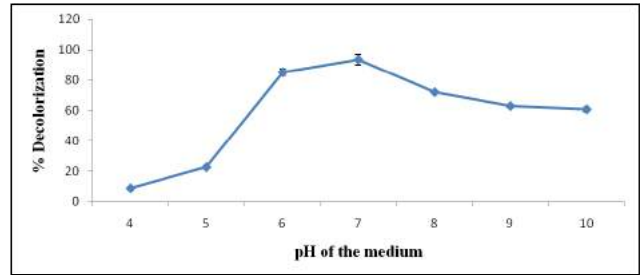


Fig. 5: Optimization of pH for decolourisation of RR-195 by *E. casseliflavus* RDB_4.

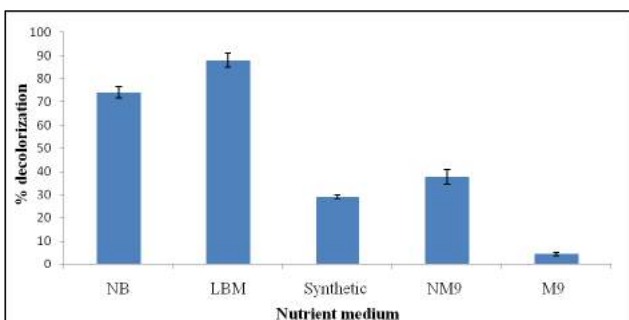


Fig. 2: Optimization of nutrient media for decolourisation of RR-195 by *E. casseliflavus* RDB_4.

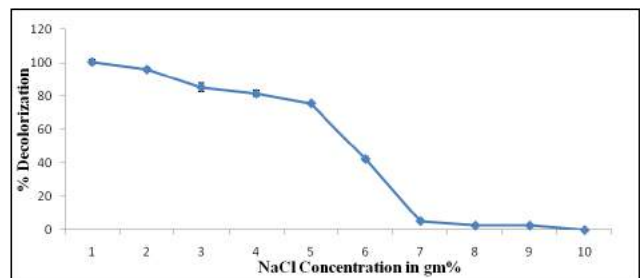


Fig. 6: Optimization of NaCl concentration for decolourisation of RR-195 by *E. casseliflavus* RDB_4.

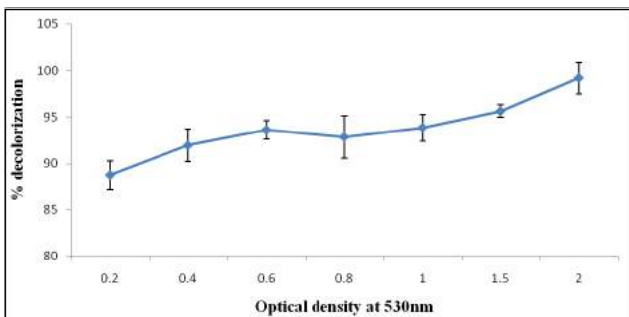


Fig. 3: Optimization of optical density for decolourisation of RR-195 by *E. casseliflavus* RDB_4.

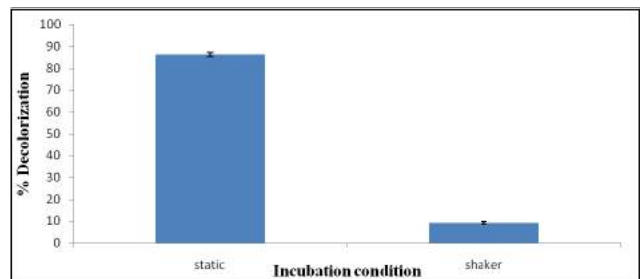


Fig. 7: Optimization of incubation conditions (aeration) for decolourisation of RR-195 by *E. casseliflavus* RDB_4.

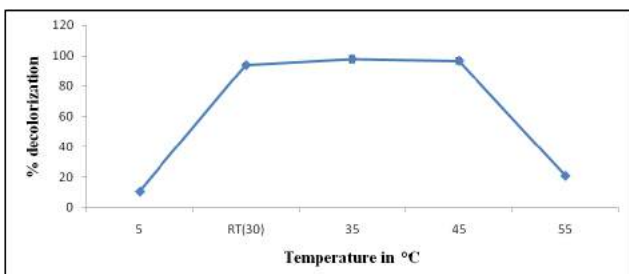


Fig. 4: Optimization of temperature for decolourisation of RR-195 by *E. casseliflavus* RDB_4.

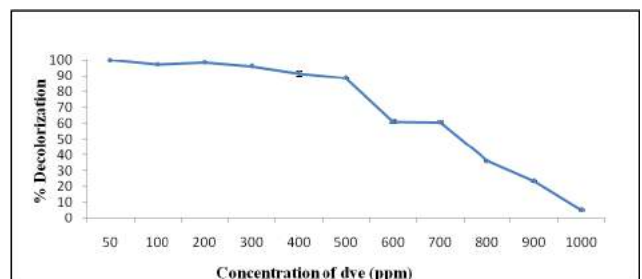


Fig. 8: Optimization of dye concentration for decolourisation of RR-195 by *E. casseliflavus* RDB_4.

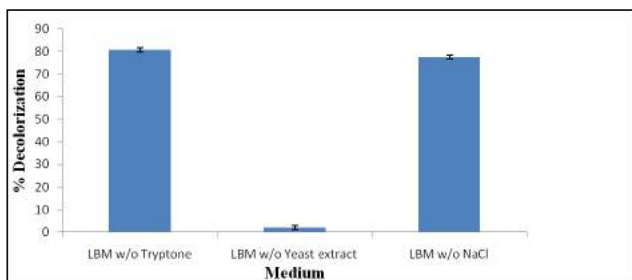


Fig. 9: Deletion assay of LBM for decolourisation of RR-195 by *E. casseliflavus* RDB_4.

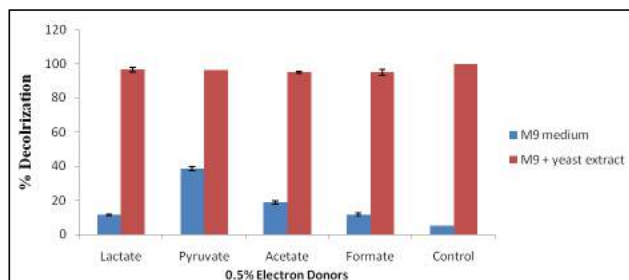


Fig. 13: Effect of electron donors (organic acids) on decolourisation of RR-195 by *E. casseliflavus* RDB_4.

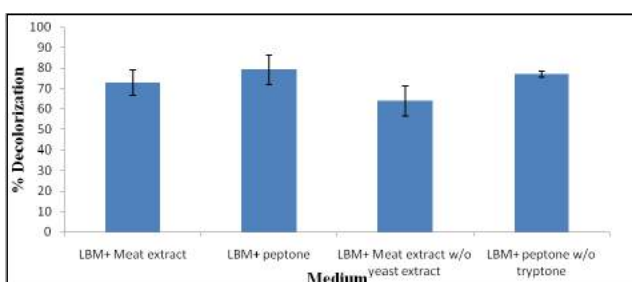


Fig. 10: Addition and substitution assay of LBM for decolourisation of RR-195 by *E. casseliflavus* RDB_4.

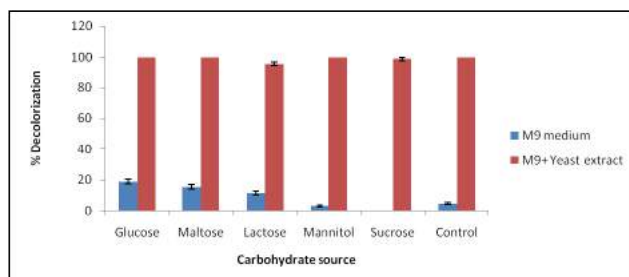


Fig. 14: Effect of electron donors (sugars) on decolourisation of RR-195 by *E. casseliflavus* RDB_4.

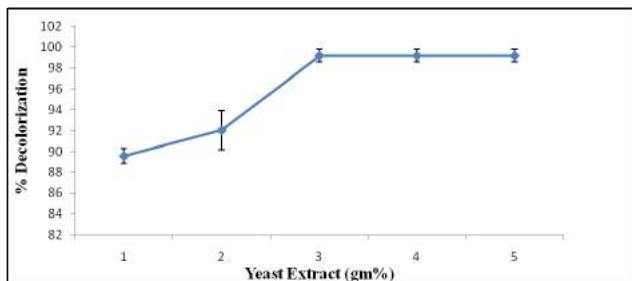


Fig. 11: Optimization of yeast extracts concentration for decolourisation of RR-195 by *E. casseliflavus* RDB_4.

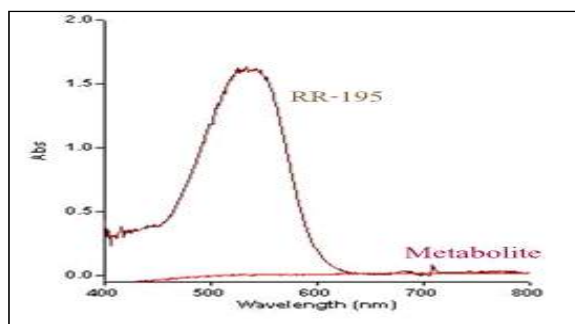


Fig. 15: Variation in UV-Vis spectra of RR-195 before and after decolourisation by *E. casseliflavus*.

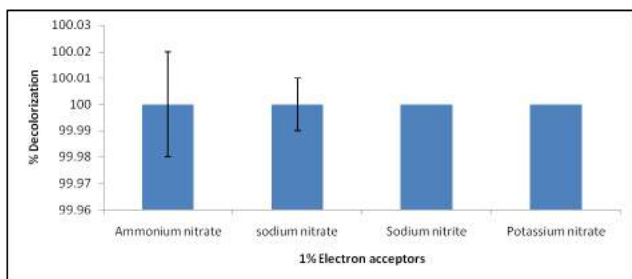


Fig. 12: Effect of inorganic nitrogenous compounds as electron acceptors for decolourisation of RR-195 by *E. casseliflavus* RDB_4.

reported 37°C as an optimal temperature for dye decolourisation by bacterial isolates (Kolekar et al. 2008) as well as by bacterial consortium (Saratale et al. 2010).

The optimum pH of the medium is critical for the growth, metabolic activity and enzyme production required for the decolourisation process. Our study showed significant decolourisation activity in the pH range of 6.0 to 10 (Fig. 5) with maximum decolourisation (93.66%) observed at pH 7 in 10 h. Tolerance to high pH is an added advantage in dye decolourisation studies since the processing of textile dyes includes steps involving the use of alkaline conditions and high temperatures (Aksu 2003). Our observation is also in accordance with Bhatt et al. (2005), where *E. coli* and *Pseu-*

domonas luteola were reported to exhibit maximum decolourisation at pH 7. In another study, *E. faecalis* showed maximum decolourisation of RO-16 in the pH range of 5 to 8 (Sahasrabudhe & Pathade 2012). Similar studies showing optimum activity in the pH range of 6.0-10.0 have been reported by several authors (Chen et al. 2003, Guo et al. 2007, Kilic et al. 2007).

The dyeing industries use a high amount of salts in industrial dye baths to ensure fixation of dye to the cellulose fibres (Gupta et al. 1990, Zollinger 1991). Salt concentrations up to 15 to 20% have been measured in wastewaters from dyestuff industries. Sodium levels are also elevated when sodium hydroxide is used in the dye bath to increase the pH. These high concentrations of sodium generally suppress microbial growth at levels above 3g% (Panswad & Anan 1999, Khalid et al. 2008). Hence, tolerance to high salt concentration for decolourisation studies is an essential requirement. In our study, *E. casseliflavus* RDB_4 showed significant decolourisation in LBM containing NaCl concentrations ranging from 1% to 5% with maximum decolourisation (100%) observed at 1% NaCl concentration (Fig. 6). In a recent study carried out on the detoxification of Direct black G, an azo dye, a thermophilic bacteria was also reported to tolerate salinity levels up to 5g% (Chen 2018).

The current study also reported that the decolourisation of RR-195 by *E. casseliflavus* RDB_4 was sensitive to oxygen since the optimum activity was observed under static conditions (Fig. 7). It may be due to the anoxic nature of *E. casseliflavus* RDB_4 which is a facultative anaerobic bacterium. Similar findings were also reported by other authors (Pearce et al. 2003, Sahasrabudhe & Pathade 2012). Bacterial degradation of azo dyes under oxygen-limiting conditions can be attributed to its strong reductive nature (Wuhrmann et al. 1980, Zimmermann et al. 1982, Banat et al. 1996, Chen et al. 2003). Since oxygen is a preferred electron acceptor in a bacterial system, it can be suggested that the dominance of aerobic respiration under agitation conditions may deprive the azoreductase enzymes of getting reduced by NADH, and hence minimize the decolourisation process (Stolz 2001, Kaushik & Malik 2009, Hu 1998).

The decolourisation potential of *E. casseliflavus* RDB_4 for RR-195 dye showed variations at different initial dye concentrations as indicated in Fig. 8. Complete decolourisation was observed in the concentrations ranging from 50 to 200 ppm and over 90% decolourisation was observed up to a 500 ppm concentration of RR-195 dye within 10 h. The natural environment contaminated with dyes and other toxic agents may possess higher concentrations of diverse dyes making it difficult for the bacteria to survive in such a strenu-

ous environment. Inhibition of microbial cell growth due to interference with the synthesis of nucleic acids has been reported at higher dye concentrations (Shah & Patel 2014). Our study thus offers challenging application of *E. casseliflavus* RDB_4 for bioremediation of polluted dye effluents. Similar to our findings, *Georgenia* sp. CC-NMPT-T3 and an unidentified microflora have also shown decolourising ability up to 200 ppm of RR-195 dye and 600 ppm of Direct black G azo dye respectively (Sahasrabudhe & Pathade 2012, Chen et al. 2018).

Figs. 9 and 10 indicate the effect of deletion, addition and substitution assay to determine the effect of media components on the decolourisation potential of RR-195 by *E. casseliflavus* RDB_4. The deletion assay carried out, indicated the absolute necessity of yeast extract in the dye degradation process. In contrast, there was no significant difference observed in the dye degradation process in absence of NaCl and tryptone. The substitution of nutrient sources like yeast extract and tryptone from LBM with meat extract and peptone respectively, showed a decrease in decolourisation activity. Also, the addition of extra nutrient sources (meat extract and peptone) to LBM did not show any increased activity. All the above observations clearly indicate the positive role of yeast extracts for dye decolourisation processes. Hence, in further studies, the optimization of yeast extract concentration in the M9 medium was carried out. It was observed that 3% yeast extract was capable of decolourising 50 ppm RR-195 dye in 4 h as indicated in Fig. 11. Thus, yeast extract was supplemented in the minimal medium for all the further investigations. In contrast to the current study, our previous study reported a significant role of tryptone in addition to yeast extract for the decolourisation process (Birmole et al. 2014). Increased decolourisation in presence of yeast extract has also been reported for decolourisation of RR-195 by *Georgenia* sp. CC-NMPT-T3 (Sahasrabudhe & Pathade 2012) and other azo dyes by *P. Chrysogenum* (Praveen & Bhat 2012). Many investigators have reported yeast extract (50 g.L⁻¹) to be the most effective carbon and nitrogen source for the decolourisation of azo dye (Hosono et al. 1993, Lie et al. 1996). Dyes are deficient in carbon content and biodegradation without any extra carbon source is difficult (Coughlin et al. 1999).

In addition to various physical parameters, we also checked the effect of several electron acceptors for decolourisation of RR-195 by *E. casseliflavus* RDB_4. Complete decolourisation of RR-195 dye was observed in presence of various nitrates and nitrites added to M9 medium supplemented with 3% yeast extract (Fig. 12). Our results are not in agreement with those published by other researchers who have evaluated the interference of nitrate with azo

dye biodegradation. Thus, the bioremediation using *E. casseliflavus* RDB_4 has an advantage over other biological systems as this organism can decolourise RR-195 in the presence of nitrate and nitrite salts. Nitrate is used as an electron acceptor for anaerobic growth and is a potent regulator of the enzymes required for respiration using other electron acceptors (Pearce et al. 2006). Decolourisation is an oxidation-reduction process in which azo dyes serve as electron acceptors. Sodium nitrate is one of the typical salts included in the dye baths for improvement of dye fixation to the textile fibres and concentrations can reach 40-100 g dm⁻³. Thus, nitrates can be present in dye wastewater and may, therefore, play a role in reducing the effectiveness of dye reduction; potentially down regulating azo reduction activity or acting as an electron sink in preference to azo bonds. Thus, in many other biological treatment systems colour removal is much slower when nitrate and nitrites are present in the system, with rapid denitrification preceding dye reduction, which suggests that the nitrate can compete with the dye for reducing equivalents by the biocatalysts (Dubin & Wright 1975, Pearce et al. 2006, Radhika et al. 2014).

Various organic acids (Fig. 13) and carbohydrates (Fig. 14) incorporated in the M9 medium were also checked for their potential to act as an electron donor for RR-195 decolourisation by *E. casseliflavus* RDB_4. The results indicated that none of the provided organic acids and carbohydrates could act as an electron donor. *E. casseliflavus* RDB_4 required yeast extract as the carbon and nitrogen source, and also as the electron donor for decolourising RR-195. Addition of carbon sources seemed to be less effective in promoting the decolourisation process, probably due to the preferences of the cells in assimilating the added carbon sources over the dye compound as the carbon source (Sahasrabudhe & Pathade 2012).

Mode of decolourisation: Investigations show that remediation of dyes by bacteria could be due to adsorption or biodegradation (Shah & Patel 2014). In our study, the non-autoclaved media containing live cells showed decolourisation and the autoclaved media containing dead cells did show decolourisation. The optimization experiments also suggested that the decolourisation process is

dependent on various physical and biochemical factors which would not be the case if it was due to adsorption. Hence, it can be confirmed that the decolourisation of RR-195 dye is due to the metabolic process of *E. casseliflavus* RDB_4.

Effect of repeated dye decolourisation in a fed-batch process: The use of microbial isolates for commercial applications is relevant only if it can be used repeatedly in the continuous culture system. In our study, *E. casseliflavus* RDB_4 showed the ability to decolourise repeated addition of RR-195 dye aliquot (50 ppm) in M9 medium containing 3% yeast extract under a static condition. It exhibited the potential to completely decolourise the dye up to the third cycle. The first two cycles were complete within 2 and 3 h respectively, whereas the third cycle took 15 h for complete decolourisation. The eventual cessation of decolourisation was likely due to nutrient depletion (Kalyani et al. 2008, Sartale et al. 2009).

Immobilization: The process of immobilization of bacterial cells in calcium alginate also offers advantages of continuous processing of dyes in industrial wastes. This is because the process prevents washout of cells and allows high cell density to be maintained in the beads. Immobilization of cells in calcium alginate provides both aerobic and anaerobic conditions for cells to act on dyes which efficiently degrade textile dyes. Unfortunately, the immobilization of cells in our study did not support efficient decolourisation of RR-195 dye. It took 24 h for immobilized cells to decolourise 50 ppm of RR-195, whereas free cells of *E. casseliflavus* strain RDB_4 decolourised RR-195 within 4 h in the M9 medium. Immobilized cultures tend to have a higher level of activity and are more resilient to environmental perturbations with respect to pH or exposure to toxic chemicals. In our study, the inefficiency of the immobilized cells might be due to the anoxic condition produced in the beads which could not support the metabolism of the organism and therefore decolourisation of the dye.

Ecotoxicity studies: Table 1 represents the observed effects of RR-195 dye and its degraded metabolites on germination of *P. mungo* and *T. aestivum* seeds. It clearly reflects the toxic effect of untreated RR-195 dye as indicated by the stunted radicle and plumule length as compared to control.

Table 1: Ecotoxicity study of RR-195 and its degraded metabolites by *E. casseliflavus* RDB_4.

Plant name	Average length in cm					
	Control		RR-195		Metabolites	
	Radicle	Plumule	Radicle	Plumule	Radicle	Plumule
<i>P. mungo</i>	3.3	1.8	0.4	0.2	3	1.6
<i>T. aestivum</i>	2.7	1.2	0.3	0.2	2.5	1.2

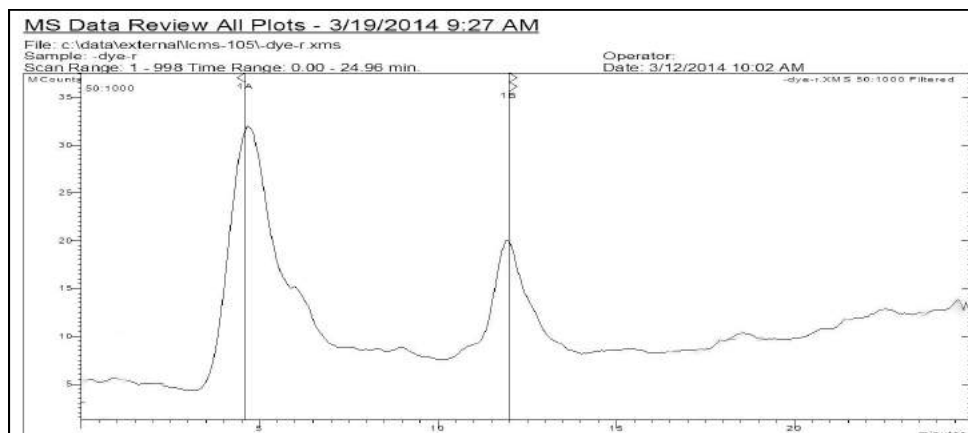


Fig. 16: HPLC chromatogram of RR-195 dye.

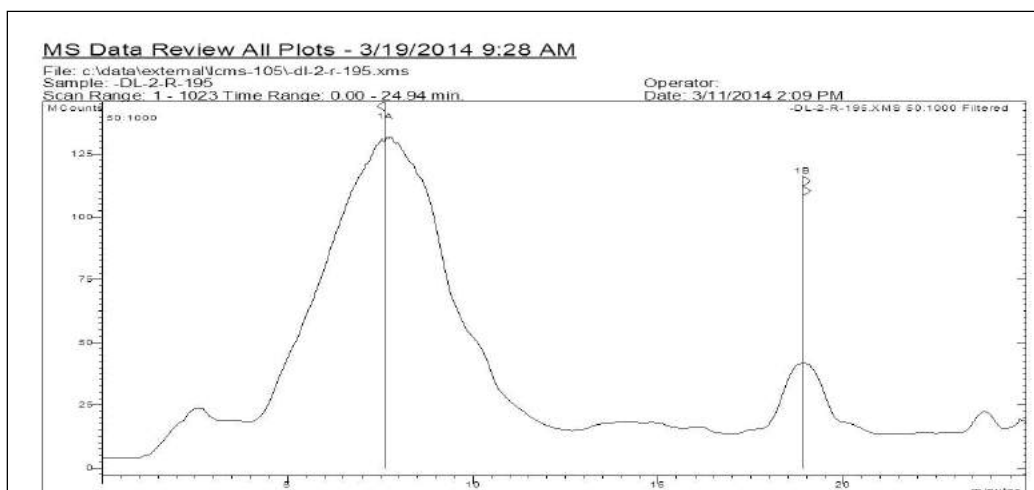


Fig. 17: HPLC chromatogram of degraded RR-195 dye metabolites.

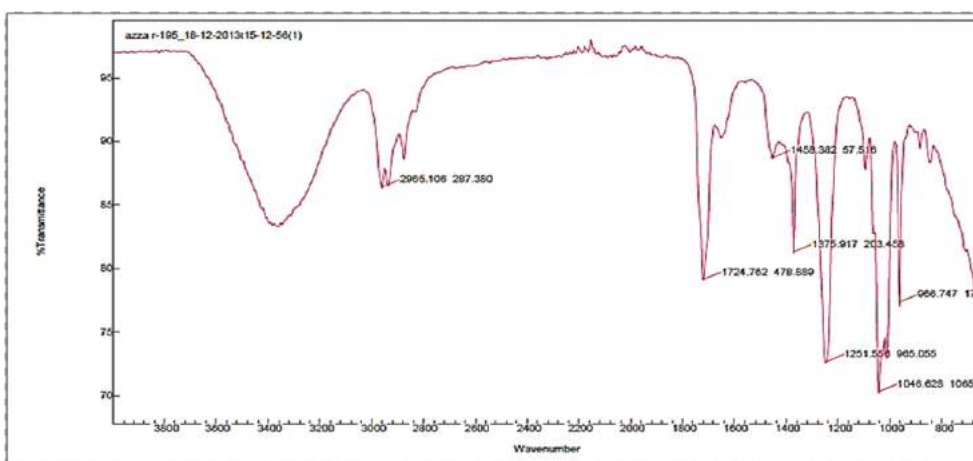


Fig. 18: FTIR spectrum of RR- 195 dye.

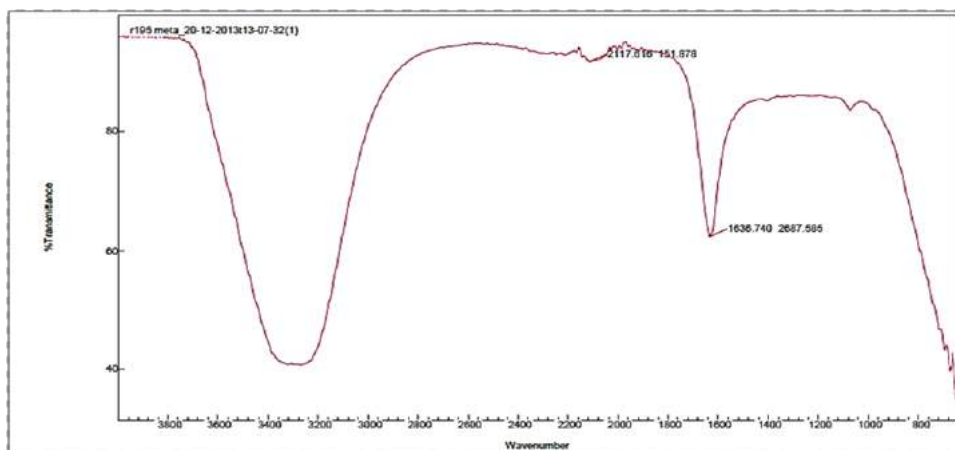


Fig. 19: FTIR spectrum of degraded RR-195 dye metabolites.

The degraded metabolites, on the other hand, showed no growth inhibition indicating that the biodegraded metabolites of RR-195 are non-toxic.

Dye effluents contain diverse contaminants, which when discarded into water-bodies, may cause serious environmental and health hazards. Unfortunately, in spite of the known hazards, untreated dye effluents commonly find their way into neighbouring water resources including rivers and lakes and ultimately into agricultural fields. Our study indicated that the metabolites obtained after degradation of RR-195 dye are nontoxic to the germination of the seeds. This opens a new dimension for application of our test isolate i.e. *E. casseliflavus* RDB_4 for treatment of industrial dye RR-195. Similar studies have shown effective degradation of azo-dyes by *Pseudomonas aeruginosa* (Elfarash et al. 2017) and *Staphylococcus hominis* subsp. *hominis* DSM 20328 (Parmar & Shukla 2017). A phytotoxicity assay carried out using *Vigna radiata* also indicated effective detoxification of AB dye. In the same study, the genotoxicity assay with *Allium cepa* showed that pure AB dye solutions significantly reduced mitotic index (MI) and induced various chromosomal abnormalities, whereas, bio-remediated dyes induced relatively less genotoxicity in nature (Haq et al. 2017).

Bio-decolourisation and biodegradation analysis: The UV-Vis spectral analysis of RR-195 dye showed a decrease in absorbance from 1.161 to -0.1210 at 540 nm after the biodegradation process (Fig. 15). The decrease in absorbance or disappearance of the absorbance peak at the maximum wavelength of the dye is indicative of biodegradation due to microbial metabolism (Novotny 2004). In order to confirm complete degradation of dye, the cell pellet was recovered to further extract the adsorbed dye if any, using methanol and subjected to UV- Vis Spectrophotometric

analysis. It showed no absorbance at 540 nm, hence confirming complete degradation.

Figs. 16 and 17 indicate the HPLC elution profile of RR-195 and its degraded metabolites respectively. Both chromatograms showed different retention times. RR-195 dye showed major peaks at retention time 4.598 min and 11.988 min, whereas degradation products showed major peaks at retention time 7.629 min and 18.892 min. The disappearance of peaks in the dye chromatogram and occurrence of new peaks in the metabolite chromatogram clearly indicates successful biodegradation of RR-195 dye.

A noticeable difference was also observed between FTIR spectra of RR-195 and its metabolites (Figs. 18 and 19) further implying the biodegradation of RR-195 by *E. casseliflavus* RDB_4. Table 2 represents the probable functional groups of the peaks observed in the FTIR spectrum of the RR-195 dye and its degraded metabolites. The peak of sulfide and sulphone (S=O bond) stretching at 1375.917,

Table 2: Probable functional groups of the peaks observed in FTIR spectrum of RR-195 dye and its degraded metabolites.

Wave number	Probable functional group
RR-195 dye	
2965.108	Asymmetric aliphatic C-H
1724.762	C=O ketone group
1458.382	N=N stretching of the azo group
1375.917	S=O stretching of SO ₃
1251.556	The C-N stretching vibration of aromatic primary amine
1046.628	C-O or C-N
Degraded metabolites	
2117.616	Amines
1636.740	C=C stretching indicating aromatic nature

Table 3: Decolourisation of different textile dyes by *E. casseliflavus* RDB_4.

Name of the dye	λ max(nm)	% Decolourisation
Dispersive blue B3	634	25.7
Reactive brilliant blue-198	628	35.08
Reactive brilliant blue-19	600	54.69
Reactive red-120	51	89.08
Direct red 5B	507	100
Reactive orange-16	495	95.63
Reactive black-5	600	100
Coracion green HE4B	652	98.27
Blue MEBRF 150%	624	100
Navy blue ME2G	611	100
Navy blue MEBL	617	100
Reactive yellow	425	100
Coracion red HE3B-N	415	100
Coracion orange HE2R	491	100
Orange ME2R	491	45.38
Corafix red ME4B	541	91.50

Table 4: Decolourisation of different dye mixtures by *E. casseliflavus* RDB_4.

Dye mixture	λ max(nm)	% Decolorization
Navy blue MEBL + RR-195	552	100
Direct red 5B + RR-195	541	98.64
Reactive red-120 + RR-195	527	97.91
Reactive black -5 + RR-195	551	80.69
Coracion green HE4B + RR-195	551	91.10
Blue MEBRF 150% + RR-195	552	100
Navy blue ME2G + RR-195	551	98.06
Reactive orange - 16 + RR-195	521	98.45
Reactive brilliant blue -19 + RR-195	540	74.65
Reactive yellow + RR-195	545	100
RR-195+ Navy blue MEBL +		
Reactive Red-120 + Reactive yellow	552	100

1251.558 and 1045.628 was observed in control dye spectrum. These stretching peaks were completely absent in the metabolite spectra indicating a breakdown of S=O bond in biodegradation of the RR-195 dye. The peak of the azo bond (N=N) at 1458.382 was observed in the control dye spectrum but was completely absent in the metabolite spectra indicating a breakdown of N=N bond in the RR-195 dye. The breakdown of asymmetric aliphatic -CH, C-O, C-N and C-H groups was also observed in the metabolite spectra. The metabolite spectra also showed the presence of amines which must have been produced during the biodegradation process of the dye.

The different chemical structures in azo dyes have a prominent effect on the decolourisation and biodegradation rate (Wuhrmann et al. 1980, Mendez et al. 2005). Depending on the number and placement of the azo linkages, some dyes are biodegraded more rapidly than others. In gen-

eral, more the number of azo linkages, the slower is the rate of degradation. In this effect, Brown & Laboureur (1983) have reported that two poly-azo dyes showed very low decomposition rate when compared to dyes having four mono azo and six diazo linkages. Fibre-reactive azo dyes often have side groups responsible for solubilization, along with reactive groups being nucleophilic in nature. Depending on the type of these substituents, biodegradation rate might be changed.

Decolourisation of various textile dyes and mixture of dyes: Synthetic dyes of different structure are often manufactured by industries, and therefore, the effluents are markedly variable in composition. Due to this reason, there is a need for screening of cultures which possess the ability to decolourise a range of dyes and even mixtures of several dyes. Our study showed that *E. casseliflavus* RDB_4 could decolourise twelve azo-dyes in addition to RR-195 and also methylene blue and Congo red in M9 medium containing 3% yeast extract within 5 h. Amongst azo-dyes, *E. casseliflavus* RDB_4 showed complete decolourisation (100%) of 8 dyes under static condition, and above 90% decolourisation was observed for 5 other dyes (Table 3). In addition, it also showed considerable decolourisation ability towards the mixture of two to four dyes within 5 h (Table 4). Chen et al. (2003) have reported significant decolourisation for mixtures of dyes within two days by *Aeromonas hydrophila*. *E. faecalis* YZ66 had the ability to decolourise mixtures of various dyes such as RR-195, Direct Red 81, Acid blue 113, Reactive orange 16 and Reactive yellow 145. The rate of decolourisation was very fast and colour removal was 80.58% within 2 h (Sahasrabudhe & Pathade 2012).

CONCLUSIONS

The RR-195 dye is a sulphonated azo-dye used extensively in the textile industries and discharged in the environment, thus compromising the well-being of its inhabitants. Our study offers a solution to this problem by exploiting the capability of *E. casseliflavus* RDB_4 to degrade RR-195 into nontoxic compounds. The tolerance of *E. casseliflavus* RDB_4 to high salt and dye concentrations in alkaline conditions makes it a perfect candidate for bioremediation of industrial dye wastes.

REFERENCES

- Aksu, Z. 2003. Reactive dye bioaccumulation by *Saccharomyces cerevisiae*. *Process Biochem.*, 38: 1437-44.
- Banat, I.M., Nigam, P., Singh, D. and Marchant, R. 1996. Microbial decolourisation of textile dye containing effluents: A review. *Biores. Technol.*, 58: 217-27.
- Bhatt, N., Patel, K.C., Keharia, H. and Madamwar, D. 2005. Decolorization of diazo-dye Reactive Blue 172 by *Pseudomonas*

- aeruginosa* NBAR12. *J. Basic Microbiol.*, 45: 407-18.
- Birmole, R., Patade, S., Sirwaiya, V., Bargir, F. and Aruna, K. 2014. Biodegradation study of Reactive blue 172 by *Shewanella haliotis* DW01 isolated from lake sediment. *Indian J. Sci. Res.*, 5: 139-52.
- Brown, D. and Laboureur, P. 1983. The degradation of dyestuffs: Part I. Primary biodegradation under anaerobic conditions. *Chemosphere*, 12: 397-404.
- Brown, M.A. and Stephen, C.D. 1993. Predicting azo dye toxicity. *Critical Rev. Env. Sc. Tech.*, 23: 249-324.
- Celik, L., Ozturk, A. and Abdullah, M.I. 2011. Biodegradation of reactive red 195 azo dye by the bacterium *Rhodopseudomonas palustris* 51ATA. *African J. Microbiol. Res.*, 6: 120-6.
- Cheatham, P.S.J. and Bucket, C. 1984. Immobilisation of microbial cells and their use in waste water treatment. In: Grainger J.M., Lynch J.M. (eds.) *Microbial Methods for Environmental Biotechnology*. Academic Press Inc, London, UK, pp. 219.
- Chen, K.C., Wu, J.Y., Liou, D.J. and Hwang, S.C.J. 2003. Decolorization of the textile azo dyes by newly isolated bacterial strains. *J. Biotechnol.*, 101: 57-68.
- Chen, S.H. and Ting, A.S.Y. 2017. Microfungi for the removal of toxic triphenylmethane dyes. In: Kalia V., Shouche Y., Purohit H., Rahi P. (eds.) *Mining of Microbial Wealth and MetaGenomics*. Springer, Singapore.
- Chen, Y., Feng, L., Li, H., Wang, Y., Chen, G. and Zhang, Q. 2018. Biodegradation and detoxification of Direct Black G textile dye by a newly isolated thermophilic microflora. *Bioresour. Technol.*, 250: 650-7.
- Coughlin, M.F., Kinkle, B.K. and Bishop, P.L. 1999. Degradation of azo dyes containing amino naphthol by *spingomonas* sp. strain ICX. *J. Industrial Microbiol. Biotechnol.*, 23: 341-6.
- Dellamatrice, P.M., Stenico, E.M., Beraldo, L.A., Moraesc, M., Regina, F.F. and Monteiro, T.R. 2017. Degradation of textile dyes by cyanobacteria. *Brazilian J. Microbiol.*, 48: 25-31.
- Dhanve, R.S., Shedbalkar, U.U. and Jadhav, J.P. 2008. Biodegradation of diazo reactive dye Navy blue HE2R (Reactive blue 172) by an isolated Exiguobacterium sp. RD3. *Biotechnol. Bioprocess Eng.*, 13: 53-60.
- Dubin, P. and Wright, K.L. 1975. Reduction of azo food dyes in cultures of *Proteus vulgaris*. *Xenobiotica*, 5: 563-71.
- Elfarash, A., Mawad, M.M., Yousef, M.M. and Shoreit, A.M. 2017. Azoreductase kinetics and gene expression in the synthetic dyes-degrading *Pseudomonas*. *Egyptian J. Basic Appl. Sc.*, 4: 315-22.
- Guo, J.B., Zhou, J.T., Wang, D., Tian, C.P., Wang, P., Uddin, M.S. and Yu, H. 2007. Biocatalyst effects of immobilized anthraquinone on the anaerobic reduction of azo dyes by the salt-tolerant bacteria. *Water Res.*, 41: 449-505.
- Gupta, G.S., Prasad, G. and Singh, V.H. 1990. Removal of chrome dye from aqueous solutions by mixed adsorbents: Fly ash and coal. *Water Res.*, 24: 45-50.
- Haq, I. and Raj, A.M. 2017. Biodegradation of Azure-B dye by *Serratia liquefaciens* and its validation by phytotoxicity, genotoxicity and cytotoxicity studies. *Chemosphere*, 196: 58-68.
- Hosono, M., Aral, H., Aizawa, M., Yamamoto, I., Shimizo, K. and Sugiyama, M. 1993. Decoloration and degradation of azo dye in aqueous solution of supersaturated with oxygen by irradiation of high energy electron beams. *Appl. Rad. Iso.*, 44: 1199-203.
- Hu, T.L. 1998. Degradation of Azo Dye RP2B by *Pseudomonas luteola*. *Water Sc. Tech.*, 38: 299-306.
- Jacob, C.T. and Azariah, J. 2000. Environmental ethical cost of t-shirts, Tiruppur, Tamil Nadu, India. In: Fujiki N., Macer D.R.J., (eds) *Bioethics in Asia*, pp. 191-195.
- Kalyani, D.C., Patil, P.S., Jadhav, J.P. and Govindwar, S.P. 2008. Biodegradation of reactive textile dye Red BLI by an isolated bacterium *Pseudomonas* sp. SUK1. *Biores. Technol.*, 99: 4635-41.
- Kaushik, P. and Malik, A. 2009. Fungal dye decolorization: Recent advances and future potential. *Environ Int.*, 35: 127-41.
- Khalid, A., Arshad, M. and Crowley, D.E. 2008. Decolorization of azo dyes by *Shewanella* sp. under saline conditions. *Appl. Microbiol. Biotechnol.*, 79: 1053-9.
- Kilic, N.K., Nielsen, J.L., Yuce, M. and Donnez, G. 2007. Characterization of a simple bacterial consortium for effective treatment of waste waters with reactive dyes and Cr(VI). *Chemosphere*, 67: 826-31.
- Kolekar, Y.M., Powar, S.P., Gawai, K.R., Lokhande, P.D., Shouche, Y.S. and Kodam, K.M. 2008. Decolorization and degradation of Disperse Blue 79 and Acid Orange 10 by *Bacillus fusiformis* KMK5 isolated from the textile dye contaminated soil. *Biores. Technol.*, 99: 8999-9003.
- Kurade, M.B., Waghmode, T.R., Patil, S.M., Jeona, B.H. and Govindwar, S.P. 2017. Monitoring the gradual biodegradation of dyes in a simulated textile effluent and development of a novel triple layered fixed bed reactor using a bacterium-yeast consortium. *Chem. Eng. J.*, 307: 1026-36.
- Lie, T.J., Pitt, T., Leadbetter, E.R., Godchaux, W. and Leadbetter J.R. 1996. Sulphonates: Novel electron receptor in anaerobic respiration. *Archives Microbiol.*, 166: 204-10.
- Mendez, P.D., Ormill, F. and Lema, J.M. 2005. Anaerobic treatment of azo dye acid orange 7 under fed-batch and continuous conditions. *Water Res.*, 39: 771-8.
- Moreira, M.T., Viacava, C. and Vidal G. 2004. Fed-batch decolorization of poly R-478 by *Trametes versicolor*. *Brazilian Arch. Biol. Technol.*, 47: 179-83.
- Neil, C., Lopez, A., Esteves, S., Hawkes, F.R., Hawkes, D.L. and Wilcox, S. 2000. Azo dye degradation in an anaerobic-aerobic treatment system operating on simulated textile effluent. *Appl. Micro. Biol. Biotechnol.*, 53: 249-54.
- Ngwasiri, P., Nda;si, M., Augustin, T. and Jean, B. 2011. Biodecolourisation of textile dyes by local microbial consortia isolated from dye polluted soils in ngaoundere (Cameroon). *Int. J. Env. Sc.*, 1: 1403-19.
- Novotny, C., Svobodova, K., Kasinath, A. and Erbanova, P. 2004. Biodegradation of synthetic dyes by *Irpex lacteus* under various growth conditions. *Int. Biodeterioration Biodegrad.*, 54: 215-23.
- Panswad, T. and Anan, C. 1999. Impact of high chloride wastewater on an anaerobic/anoxic/aerobic process with and without inoculation of chloride acclimated seeds. *Water Res.*, 33: 1165-72.
- Parmar, N.D. and Shukla S.R. 2017. Biodegradative decolorization of Reactive Red 195-A by an isolated bacteria *Staphylococcus* sp: Studies on metabolites and toxicity. *Desalin. Water Treat.*, 63: 241-53.
- Patil, P.S., Phugare, S.S., Jadhav, S.B. and Jadhav, J.P. 2010. Communal action of microbial cultures for Red HE3B degradation. *J. Hazard. Mater.*, 181: 263-70.
- Pearce, C.I., Christie, R., Boothman, C., Canstein, H., Guthrie, J.T. and Lloyd, J.R. 2006. Reactive azo dye reduction by *Shewanella* strain J18 143. *Biotechnol. Bioeng.*, 95: 692-703.
- Pearce, C.I., Lloyd, J.T. and Guthrie, J.T. 2003. The removal of colour from textile waste water using whole bacteria cells: A review. *Dyes and Pigments*, 58: 179-96.
- Pillai, J.S. 2017. Optimization of process conditions for effective degradation of azo blue dye by *Streptomyces* DJP15 H.P. *J. Pure Appl. Microbiol.*, 11: 1757-65.
- Plumb, J.J., Bell, J. and Stuckey, D.C. 2001. Microbial populations associated with treatment of an industrial dye effluent in an anaerobic baffled reactor. *Appl. Environ. Microbiol.*, 67: 3226-35.
- Praveen, K.G.N. and Bhat, S.K. 2012. Decolorization of azo dye Red 3BN by bacteria. *Int. Res. J. Biol. Sc.*, 1: 46-52.
- Robinson, T., McMullan, G., Marchant, R. and Nigam, P. 2001.

- Remediation of dye in textile effluent: A critical review on current treatment technologies with proposed alternative. *Biores. Technol.*, 77: 247-55.
- Sahasrabudhe, M.M. and Pathade G.R. 2012. Decolourization of C.I. reactive yellow 145 by *Enterococcus faecalis* strain YZ66. *Archives of Appl. Sc. Res.*, 3: 403-14.
- Saratale, R.G., Saratale, G.D., Changand, J.S. and Govindwar, S.P. 2010. Decolorization and degradation of reactive dyes and dye wastewater by a developed bacterial consortium. *Biodegradation*, 21: 999-1015.
- Sartale, R.G., Sartale, G.D., Kalyani, D.C., Chang, J.S. and Govindwar, S.P., 2009. Ecofriendly degradation of sulphonated diazo dye C.I. Reactive Green 19A using *Micrococcus glutamicus* NCIM-2168. *Biores. Technol.*, 100: 3897-905.
- Shah, M.P. and Patil, K.A. 2014. Microbial degradation of Reactive Red 195 by three bacterial isolates in anaerobic-aerobic bioprocess. *Int. J. Env. Bioremediation & Biodegradation*, 2: 5-11.
- Stolz, A. 2001. Basic and applied aspects in the microbial degradation of azo dyes. *Appl. Microbiol. Biotechnol.*, 56: 69-80.
- Suteu, D., Malutan, T. and Bilba, D. 2010. Removal of reactive dye Brilliant Red HE-3B from aqueous solutions by industrial lignin: Equilibrium and kinetics modeling. *Desalination*, 255: 84-90.
- Thakur, 2006. *Industrial Biotechnology-Problems and Remedies*. I.K International. Chapter-7, pp. 213-237.
- Usha, M.S., Sanjay, M.K., Gaddad, S.M. and Shivannavar, C.T. 2010. Degradation of h-acid by free and immobilized cells of *Alcaligenes latus*. *Braz. J. Microbiol.*, 41: 931-45.
- Wuhrmann, K., Menscher, K. and Kappeler, T. 1980. Investigation on rate determining factors in microbial reduction of azo dyes. *Eur. J. Appl. Microbiol. Biotechnol.*, 9: 325-38.
- Zimmermann, T., Kulla, H.G. and Leisinger, T. 1982. Properties of purified orange II azo reductase, the enzyme initiating azo dye degradation by *Pseudomonas* KF46. *J. Biochem.*, 129: 197-203.
- Zollinger, H. 1991. *Colour Chemistry, Synthesis, Properties and Applications of Organic Dyes and Pigments*. 2nd ed. VCH, Weinheim, Germany.



Inter-regional Differences in Environmental Regulation Intensity Among Chinese Provincial Governments and the Overall Planning Countermeasures

Gang Ding[†], Xiajing He and Ling Ye

School of Economics and Management, Fuzhou University, Fuzhou 350100, China

[†]Corresponding author: Gang Ding

Nat. Env. & Poll. Tech.
Website: www.neptjournal.com

Received: 15-05-2018
Accepted: 02-08-2018

Key Words:

Environmental regulation intensity
Global entropy method
Quartile analysis method

ABSTRACT

This research establishes a set of multi-layer comprehensive evaluation index system through global entropy method and conducts comprehensive evaluation of the environmental planning intensity among Chinese provincial governments. Based on the above, the inter-regional differences in environmental regulation intensity among 30 Chinese provincial governments are further analysed with methods of quartile analysis and coefficient of variance, revealing the status of spatial differences in environmental regulation level among provincial governments. In addition, corresponding overall planning countermeasures are proposed. Research results show that during 2006-2014, the environmental regulation intensity of various Chinese provincial governments had all seen certain improvement, but the inter-regional differences tended to be widening after experiencing certain amplitude of narrowing; and there was obvious difference in cognition of the importance of environmental governance investment among different provincial regions. To promote synergistic advancement of environmental regulation in Chinese provincial governments, the environmental regulation cooperation mechanism for cross-administrative regions has to be perfected, scientific and reasonable regional government performance examination mechanism has to be established, and multi-subject synergistic governance mechanism has to be set up as well.

INTRODUCTION

Government environmental regulation is a general term of various environmental laws, regulations, policies and measures formulated and implemented for environmental protection, and its intensity determines the effect of regional eco-environmental governance. At present, research on regional environmental regulation intensity is focused on the aspects of measurement method and inter-regional competition behaviours. Besides, the research on measurement methods of environmental regulation also displays the feature of diversity. Gray (1997) used the financial budget outlays for environmental and natural resources protection against America as the substitute index for environmental regulation. Levinson (1996) and Cole et al. (2008) respectively used the average number of staff in environmental organs and the number of environmental protection related cases of administrative penalty per enterprise as the substitute index for regional environmental regulation intensity. Pearce & Palmer (2001) advocated to combine government pollution treatment investment and corporate pollutants discharge reduction expenditures to measure the regional environmental regulation intensity. Zhang et al. (2011) used the regional pollutants discharge reduction expenditures per unit output valued to measure the regional environmen-

tal regulation intensity. Smarzynska & Wei (2004) used CO₂, lead and wastewaters to discharge reduction per output value as the measurement for environmental regulation intensity. Zhang et al. (2012) used industrial wastewater discharge standard-reaching rate and industrial sulphur dioxide removal rate to express environmental regulation intensity. Levinson (1996) believed that the evaluation of environmental regulation intensity should be handled from the three aspects of effort level, affordable cost and direct measurement. Sauter (2014) held that environmental regulation was a process of output-input, and the measurement should include three dimensions, namely input, process and result. The environmental regulation indexes built by Chen et al. (2012) include the four systems of environmental regulation law, environmental regulation supervision, environmental regulation methods and environmental regulation support. Li et al. (2011) studied the issue of undesirable output with directional environmental function model, and studied the environmental efficiency under four types of environmental regulation policies by selecting relevant indexes. Besides, there were also many scholars shaving explored the competition behaviours of environmental regulation in local governments. Yang et al. (2008) held that influenced by GDP-oriented government performance evaluation system and fiscal decentralization over the long run,

Table 1: Basic framework of evaluation index system for status quo of environmental regulation intensity in Chinese provincial governments.

Layer of Goal	Layer of Norm	Basic Indexes
Environmental regulation intensity level	Environmental Regulation Input	Ratio of environmental pollution treatment investment in GDP (%) Ratio of industrial pollution treatment completion investment in industrial added value (%)
	Environmental Regulation Effect	Multipurpose utilization rate of industrial solid waste (%) Concentrated treatment rate of wastewater (%) Industrial soot discharge standard-reaching rate (%) Harmless treatment rate of domestic waste (%)

Table 2: Weight of evaluation indexes for status quo of environmental regulation intensity in provincial governments.

Layer of Goal	Layer of Norm	Basic Indexes	Weight of Index Layer
Spatial Differences in Environmental Regulation among Provincial Governments	Environmental Regulation Input	Ratio of environmental pollution treatment investment in GDP (%)	0.2655
		Ratio of industrial pollution treatment completion investment in industrial added value (%)	0.3616
	Environmental Regulation Effect	Multipurpose utilization rate of industrial solid waste (%)	0.1494
		Concentrated treatment rate of wastewater (%)	0.0839
		Industrial soot discharge standard-reaching rate (%)	0.0648
	Harmless treatment rate of domestic waste (%)	0.0747	

provinces were more likely to keep up with regions with a relatively weak regulation intensity, leading to comparing competition. Cui et al. (2009) found out that local governments would lead their environmental regulation to deviate from the goal of overall social welfare, so as to obtain a competitive edge of economic growth. Zhang et al. (2010) utilized two-zone Durbin fixed effects model to discuss the relations among features of environmental regulation strategy interaction.

Through retrieval of literature, it can be known that although there is a plenty of literature involving the area of environmental regulation intensity, little focuses on comparing the spatial differences in environmental regulation among Chinese provincial governments. To this end, this paper proposes to establish a set of multi-layer comprehensive index system using global entropy method and analyse the inter-regional differences in environmental regulation among 30 Chinese provincial governments using methods of quartile analysis and coefficient of variance. Furthermore, based on the above, corresponding overall planning countermeasures are put forward, which are of great referable value of planning the environmental regulation in Chinese provincial governments.

MATERIALS AND METHODS

Construction principles of evaluation index system: To evaluate the status quo of environmental regulation in Chinese provincial governments, an evaluation index system for environmental regulation level of Chinese provincial governments has to be firstly established. This paper follows three major principles. The first one is the principle of being scientific. Whether the design of the evaluation index system is reasonable and scientific, it will directly affect the quality of results, so the index system has to be able to objectively and comprehensively evaluate the status quo of environmental regulation level in Chinese provincial governments. The second one is the principle of being economical. It mainly refers to that the evaluation index system needs to be coordinated, complete, concise and clear, so the indexes to be selected should be advisable, large information-containing, representative and summarizing. The third one is the principle of being comparable. The content and meaning of evaluation indexes can be clearly defined, the indexes are comparable both horizontally and vertically, and the index system can objectively reflect the status quo of environmental regulation intensity level in Chinese provincial governments.

Selection of measurement indexes for environmental regulation intensity:

After dissecting the existing research results, the contents involving environmental regulation mainly include public environment policy, environmental governance input and law enforcement effort, so environmental regulation intensity level can be measured from the two aspects of input and output. On the basis of existing research results, this paper selects indexes like ratio of environmental pollution treatment investment in GDP, ratio of industrial pollution treatment completion investment in industrial added value, concentrated treatment rates of wastewater, harmless treatment rate of domestic waste, industrial soot discharge standard-reaching rate, and multi-purpose utilization rate of industrial solid wastes. Besides, it also establishes comprehensive evaluation index system containing the two dimensions of environmental regulation input and environmental regulation effect. The specific index system is as shown in Table 1.

Global entropy method: On the basis of building a comprehensive evaluation index system, this paper adopts the global entropy method that features objective weighting and dynamic comparability to obtain data on the level of environmental regulation intensity in provincial governments (Sun et al. 2009). The steps are as follows:

Build a global evaluation matrix and standardize it. n indexes are used to evaluate the science popularization resource development of m provincial regions over a duration of T years and ultimately build an initial global evaluation matrix for the evaluation system, which is recorded as X :

$$X = (x_{ij}^t)_{mT \times n} = \begin{bmatrix} x_{11}^1 & x_{12}^1 & \cdots & x_{1n}^1 \\ x_{21}^1 & x_{22}^1 & \cdots & x_{2n}^1 \\ \cdots & \cdots & & \cdots \\ x_{m1}^1 & x_{m2}^1 & \cdots & x_{mn}^1 \\ \cdots & \cdots & & \cdots \\ x_{11}^T & x_{12}^T & \cdots & x_{1n}^T \\ x_{21}^T & x_{22}^T & \cdots & x_{2n}^T \\ \cdots & \cdots & & \cdots \\ x_{m1}^T & x_{m2}^T & \cdots & x_{mn}^T \end{bmatrix} \quad \dots(1)$$

Where, x_{ij}^t is the assigned value of the j^{th} evaluation index of the i^{th} provincial region at the t^{th} year, and $n = 24$, $m = 30$, $T = 5$. Given that the dimension, magnitude and positive and negative assignment of each index vary, X has

to be standardized to make $x_{ij}^t \in [0, 100]$, as shown in formula (2) and formula (3), $(x_{ij}^t)'$ is the equally standardized index value, $x_{j\min}$ is the minimal value of the j^{th} index, $x_{j\max}$ is the maximal value of the j^{th} index. Formula (2) and formula (3) are respectively for the standardization of the positive index and negative index.

$$(x_{ij}^t)' = \frac{x_{ij}^t - x_{j\min}}{x_{j\max} - x_{j\min}} \times 99 + 1 \quad (i = 1, 2, \dots, m; j = 1, 2, \dots, n; t = 1, 2, \dots, T) \quad \dots(2)$$

$$(x_{ij}^t)' = \frac{x_{j\max} - x_{ij}^t}{x_{j\max} - x_{j\min}} \times 99 + 1 \quad (i = 1, 2, \dots, m; j = 1, 2, \dots, n; t = 1, 2, \dots, T) \quad \dots(3)$$

The formula for measuring the information entropy of the j^{th} index is as follows:

$$e_j = -K \sum_{t=1}^T \sum_{i=1}^n y_{ij}^t \ln y_{ij}^t \quad \dots(4)$$

Where $y_{ij}^t = \frac{(x_{ij}^t)'}{\sum_{t=1}^T \sum_{i=1}^n (x_{ij}^t)'}$, constant $K = \frac{1}{\ln mT}$, which is

related to the number m of samples in the system. When the information in the system is distributed disorderly, then the degree of order is 0 and information entropy $e_j=1$. When samples are all in a disorderly state, $y_{ij}^t=1$.

According to information entropy index, the weight w_j of the j^{th} index can be calculated. When $0 \leq w_j \leq 1$,

$\sum_{j=1}^n w_j = 1$ as follows:

$$w_j = \frac{1 - e_j}{n - \sum_{j=1}^n e_j} \quad \dots(5)$$

After obtaining the results of the index weight, formula (6) can be used to calculate the comprehensive evaluation score:

$$s_i = \sum_{j=1}^n w_j (x_{ij}^t)' \quad \dots(6)$$

Data source: According to related materials like China Statistical Yearbook (2006-2014), this paper builds the index datasheet for status quo of environmental regulation intensity in Chinese provincial governments. Following the implementation steps of comprehensive evaluation in global entropy method, the original data involved in evaluation go through forward and standardization processing. Then the non-dimensional data obtained are used to calculate the

Table 3: Comprehensive evaluation scores for the overall environmental regulation intensity level in provincial governments.

Region		Comprehensive evaluation score for the overall environmental regulation intensity level								
	Province	2006	2007	2008	2009	2010	2011	2012	2013	2014
Eastern region	Beijing	49.17	45.75	40.79	40.61	37.7	34.97	43.13	44.07	50.18
	Shanghai	35.14	40.14	39.76	40.01	37.82	36.89	38.31	38.63	43.18
	Tianjin	43.99	45.08	44.51	47.4	45.28	46.59	44.48	45.2	49.52
	Zhejiang	37.76	37.02	47.29	38.24	40.41	37.57	41.23	43.38	45.13
	Jiangsu	42.97	43.34	42.01	39.44	39.21	40.04	41.98	44.32	42.93
	Guangdong	30.05	29.46	28.62	31	50.11	32.05	32.83	34.94	34.32
	Shandong	42.55	44.58	45.92	45.13	43.47	44.9	46.35	48.07	49.82
	Fujian	34.35	32.01	33.11	35.33	36.85	37.89	41.59	43.08	39.77
	Liaoning	39.94	26.5	27.47	28.23	27.42	30.6	39.67	31.84	31
	Hebei	30.5	31.73	33.41	35.76	36.39	42.59	34.84	40.39	42.96
Central region	Hainan	37.96	34.69	32.28	32.36	31.85	37.67	45.68	41.96	44.25
	Heilongjiang	23.81	22.95	26.48	27.66	28.84	29.48	32.34	40.79	34.86
	Jilin	21.83	25.5	25.35	26.69	32.13	28.5	28.72	29.55	30.92
	Hubei	30.41	30.25	30.31	36.97	36.01	34.86	36.39	37.38	38.82
	Henan	29.09	31.06	31.32	31.55	32.37	33.27	33.33	30.87	38.27
	Hunan	30.83	26.39	28.86	31.93	31.87	30.52	33.02	35.91	34.33
	Anhui	29.72	34.01	38.14	37.35	37.09	39.39	45.32	54.36	46.86
	Jiangxi	20.33	21.56	20.77	25.51	33.08	35.52	40.09	35.29	33.35
	Shanxi	40.16	44.4	49.16	48.6	46.57	44.59	50.99	55.08	48.23
	Western region	Shanxi	23.56	24.3	25.87	35.73	42.01	33.95	38.19	40.02
Sichuan		29.42	26.89	31.23	27.19	24.77	26.83	26.14	29.24	30.99
Inner Mongolia		37.77	32.37	34.53	34.41	37.65	45.17	41.87	52.06	55.95
Guangxi		29.59	35.53	34.2	37.11	36.55	33.45	38.39	37.79	35.82
Yunnan		25.83	26.81	29.8	33.98	36.85	36.6	37.44	40.89	37.73
Xinjiang		21.67	22.79	26.6	37.45	27.97	33.02	43.81	52.19	58.77
Ningxia		53.9	58.2	60.76	41.58	42.66	45.35	51.38	66.18	79.83
Gansu		33.98	35.46	26.7	30.27	34.65	27.42	43.46	43.26	39.93
Guizhou		28.36	20.17	25.86	26.58	29.58	36.5	36.37	38.18	40.39
Qinghai		15.64	19.09	22.09	23.23	19.11	23.65	26.44	27.38	30.71
Chongqing	34.03	41.84	40.33	42.15	45.67	46.89	40.37	39.72	37.36	

weight of corresponding evaluation indexes (as given in Table 2).

Analyses result based on global entropy method: According to the Formula (6) for integrated score calculation, we can work out the comprehensive evaluation scores for the overall environmental regulation intensity status in provincial governments across the country as shown in Table 3.

According to the evaluation scores of environmental regulation intensity level for provincial governments 2006-2014, the average for national environmental regulation intensity during this period can be calculated for histogram as shown in Fig. 1.

From Table 3, it can be seen that for the progress of environmental regulation in provincial regulation, there is certain imbalance in overall current status evaluation scoring. Take the overall current status score as an example. From 2006 to 2014, the evaluation score for status quo of environmental regulation intensity in provincial governments displayed the development trend of stable growth;

the average score increased from 32.81 in 2006 to 42.24 in 2014, with an increase of 9.43 in integrated score, indicating that the overall environmental regulation level in provincial governments during that period showed a sound development trend. From 2006 to 2014, the current status evaluation scores of environmental regulation in east, middle and west provincial governments increased with the same trend of national average score. Within the evaluation range, the average scores in east region over the years were obviously higher than national average and those of middle and east regions; while the average scores of middle and west regions were always slightly lower than national average.

Based on the above, it can be known that there were relatively obvious differences in environmental regulation level in provincial governments across the country. The score in east region was far higher than those of middle and west regions; the scores of middle and west regions were close; and the score in middle region was slightly higher than west region. However, seen from the growth amplitude

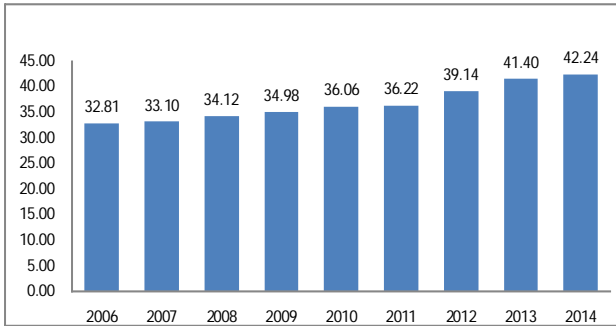


Fig. 1: The average evaluation scores of environmental regulation intensity level for provincial governments 2006-2014.

of regions, the growth amplitude of west region took the lead of middle and east regions, and that of east region with the highest score was the least. It can be deduced that the differences in environmental regulation level among provincial governments are narrowing, but the overall imbalance remains obvious.

ANALYSIS OF INTER-REGIONAL DIFFERENCES IN ENVIRONMENTAL REGULATION INTENSITY AMONG CHINESE PROVINCIAL GOVERNMENTS

Overview of quartile method: Quartile method, as an important method in analysing data set distribution features in statistics, takes the median as the mean value for estimation and interquartile range (IQR) as the standard deviation for estimation. The median and IQR can be used to describe the features of any distribution data like skewed distribution, unknown distribution, no determined value of the terminal of distribution. Besides, they can exempt from the influence of large number, and show more stability than mean value and standard deviation, with the formula shown below.

Assume that one set of observation data is X, $X = X(x_1, x_2, \dots, x_N)$, and X is arranged in a small-to-large order. When N is odd, the data in the center is called median (M) as shown in Formula (7); when N is even, the average of the two numbers in the center is taken as median (M) as shown in Formula (8).

$$\text{When } N \text{ is odd, } M = x_{(\frac{N+1}{2})} \quad \dots(7)$$

$$\text{When } N \text{ is even, } M = \frac{1}{2} \left(x_{(\frac{N}{2})} + x_{(\frac{N}{2}+1)} \right) \quad \dots(8)$$

Quartile method arranges all values in order and divides them into 4 equal parts, and the data at the third break point will be the quartile. The minimal quartile is called lower quartile or the 1st quartile (Q1). In all values, 25% are smaller than lower quartile, and 75% larger than quartile. The quar-

tile at the midpoint is the median or the 2nd quartile (Q2). The largest quartile is called upper quartile or the 3rd quartile (Q3). In all values, 75% are smaller than upper quartile, and 25% are larger than upper quartile. The IQR is obtained through Q3 minus Q1 as shown in Formula (9).

$$IQR = Q_3 - Q_1 \quad \dots(9)$$

IQR is normally taken with the median to describe the distribution features of data.

This paper takes the comprehensive evaluation scores (average for 2006-2014) of environmental regulation level in Chinese provincial governments as the set of observation data, which can be obtained from Table 3. N=30, i.e., it is even.

Analyses result based on quartile method: In order to further dissect the overall level of environmental regulation intensity in 30 provincial governments of China, we divide Chinese provinces into four classes according to their scores adopting quartile analysis method based on the comprehensive evaluation scores (average for 2006-2014) of environmental regulation intensity level in Chinese provincial governments (Table 4). Among them, there are 8 provinces and municipalities directly under the Central Government at the fourth class, namely Inner Mongolia, Ningxia, Shanxi, Beijing, Tianjin, Shandong, Jiangsu and Chongqing, which are the regions with the highest comprehensive score in government environmental regulation within the country and mostly located at the east region; there are 7 provinces and municipalities directly under the Central Governmental the first class, namely Heilongjiang, Jilin, Liaoning, Jiangxi, Sichuan, Chongqing and Qinghai, which are the regions with the lowest comprehensive score in government environmental regulation within the country and mostly located at the middle and west regions. It can be seen that there have been relatively obvious spatial differences in environmental regulation level among inter-regional governments of China.

From 2006 to 2014, when the end of term (2014) is compared with the start of term (2006), there is no obvious change in the number of provinces in the first to the fourth class, but there are slight changes in the structure. When the end of term is compared with the start of term, Beijing, Tianjin, Shanxi, Shandong and Ningxia are still in the fourth class, which are the regions with the highest scores for status quo in environmental regulation of Chinese provincial governments. Jiangsu and Hainan recedes into the third class, and Liaoning into the first class, which means that the score for environmental regulation status quo drops when compared with the start of term. And the provinces that newly move into the fourth class are Xinjiang, Inner Mongolia

Table 4: quartile analysis results of environmental regulation status quo evaluation score in chinese provincial governments 2006-2014 coefficient of variance based inter-regional differences measurement.

Classes	Provinces	
	2006	2014
The first class	Xinjiang, Qinghai, Yunnan, Shanxi, Jiangxi, Heilongjiang, Jilin	Qinghai, Sichuan, Hunan, Jiangxi, Jilin, Liaoning, Guangdong
The second class	Hebei, Henan, Hebei, Anhui, Sichuan, Guizhou, Guangxi, Guangdong	Ansu, Yunnan, Guangxi, Chongqing, Hunan, Fujian, Henan, Haerbing
The third class	Inner Mongolia, Ansu, Chongqing, Hunan, Zhengjiang, Fujian, Shanghai	Hebei, Shanxi, Jiangxi, Zhengjiang, Shanghai, Guizhou, Hainan
The fourth class	Liaoning, Beijing, Tianjin, Shanxi, Ningxia, Shandong, Jiangsu, Hainan	Xinjiang, Inner Mongolia, Ningxia, Shanxi, Beijing, Tianjin, Shandong, Anhui

Table 5: Coefficient of variance for evaluation score of environmental regulation intensity in chinese provincial governments

Year	Coefficient of variance for evaluation score of environmental regulation intensity		
	The mean value	The standard deviation	CV
2006	32.81	8.76	0.27
2007	33.10	9.22	0.28
2008	34.12	9.12	0.27
2009	34.98	6.54	0.19
2010	36.06	6.91	0.19
2011	36.22	6.29	0.17
2012	39.14	6.36	0.16
2013	41.40	8.58	0.21
2014	42.24	10.21	0.24

and Anhui. And the provinces in the first class are still 7, but there are changes in specific provinces: apart from Jiangxi, Qinghai and Jilin that remain in the first class, other provinces that used to be in the first class drop into other classes. And the provinces that newly rise into the first class are Sichuan, Hunan, Liaoning and Guangdong. The provinces in the second and third class also see changes in evaluation range. Gansu, Fujian, Hunan and Chongqing recede from the third class into the second class, and Hebei and Guizhou rise from the second class into the third class. Results show that the provinces contained in the fourth class with the highest score for environmental regulation status quo by Chinese provincial governments shift from major distribution in the east region (6/8) in 2006 to even distribution across the country in 2014, and the provinces in the first class with the lowest score for environmental regulation status quo by Chinese provincial governments are all located in middle and west regions, showing that the environmental regulation level of provincial governments at the east region is commonly higher while that at the middle and west regions is low, so there has been relatively obvious development gap in environmental regulation level of provincial governments between east region and middle and west regions.

Coefficient of variance, also called coefficient of variation, is a common statistical magnitude in measuring the variation degree of observation values in data, marked as coefficient of variance (CV) as shown in Formula (10). CV can eradicate the influence of different units and/or average upon comparison of variation on two or more data.

$$CV = \delta / \mu \quad \dots(10)$$

Where, δ is the standard deviation, and μ is the mean value.

From Table 5, it can be seen that there were certain spatial differences in environmental regulation level among different provincial governments in China; from 2006 to 2014, it displayed the development trend of narrowing followed by widening, with imbalance in spatial distribution. The specific changing trends were basically stable for the three years of 2006, 2007 and 2008; to 2009, the CV dropped to below 20%, and kept this way to 16% in the following three years; to 2013, the CV of evaluation score for environmental regulation intensity in provinces some how rose to above 20%. Further measurement results show that among the six indexes, the one with the largest spatial differences in provinces is the ratio of industrial pollution treatment completion investment in industrial added value, with the

CV exceeding 60% over the years; the CV for ratio of environmental pollution treatment investment in GDP also exceeds 50%. This means that there are obvious differences in the cognition of the importance of environmental governance investment of provinces.

OVERALL PLANNING COUNTERMEASURES

Improving environmental regulation cooperation mechanism for cross-administrative regions: The holistic nature of eco-civilization construction determines that the boundary of environmental regions cannot be divided by administration regions, which then requires the cooperation of local governments for environmental governance, especially cross-regional environmental regulation. Firstly, the law system for regional environmental pollution treatment has to be improved. The Environmental Protection of Law has to be based on to establish the law system for cross-regional environmental pollution governance, remove or abolish laws and regulations conflicting with regional eco-environmental governance cooperation, and specify the limits of authority on local governments in eco-environmental governance cooperation with law, so as to form a binding cooperation mechanism and realize legalization and standardization of regional environmental governance. Secondly, the mechanism of joint negotiation for decision-making has to be set up to solve the contradictions and conflicts among regions in environmental governance schemes and goals, and timely deal with prominent cross-regional environmental events. Thirdly, information coordination mechanism has to be put in place. Within the regions, environmental management information application system and environment basic information database have to be established to realize information sharing about environmental governance, make effective communication, exchange and coordination, and ultimately properly handle eco-environmental issues amid cooperation.

Establishing scientific and reasonable regional government performance examination mechanism: A scientific and reasonable performance examination mechanism has to be established to overcome the problem of excessive stress on economic growth by local government officials to the neglect of eco-environmental protection. Firstly, the multidimensionality of examination indexes has to be held on to. The performance examination of local governments by central government has to shift from being singular to multidimensional, that is, shift from economic growth of multidimensional index system covering economic development index, social development index, eco-environmental protection index, etc. Secondly, differentiated examination methods have to be adopted according to the division of

main functions. The resources and environment of different main functional areas is varying, so different function orientation determines that the weight of indexes like economic growth and eco-environmental protection has to be differentiated. Thirdly, the mechanism of reward and punishment has to be put in place. Examination results will be taken as the foundation for reward or punishment for related government officials. For cadres with sound performance, promotion will be granted; for cadres who make blind decisions and thus cause waste of resources and eco-environmental destruction, they will be held accountable. Moreover, the reward and punishment procedures and results will be made public.

Establishing multi-subject synergistic governance mechanism: Firstly, marketized eco-compensation mechanism has to be improved by considering protection against eco-environment and holding on to the principle of sharing benefit and spreading risk. This requires putting in place horizontal eco-compensation mechanism across regions, adhering to the principle of “whoever pollutes the environment must pay, and whoever profits from it must compensate”, and perfecting the relationship between ownership and management to give full play to the role of market in allocating eco-resources. Meanwhile, it also requires offsetting the problem of less vertical compensation and enhancing compensation efforts in regions with fragile ecology and restricted development. Secondly, the public engagement system has to be better. Public engagement on environmental protection mainly includes three means, namely engagement on environmental decision-making, environmental management and environmental relief. Public engagement on environmental decision-making is the legal right of citizens. Through engaging in collecting, collating and releasing environmental governance related information, the public can provide references to the government in formulating environmental protection laws and regulations as well as policies, thereby guaranteeing individual interests through the means of environmental relief. This requires the government to enhance the promotion of environmental protection against one hand, and devise one set of open and transparent engagement mechanism on the other hand for environmental protection that can more gather the wisdom of the people, express the will of the people.

CONCLUSIONS

The research used global entropy method to conduct comprehensive evaluation of the environmental planning intensity among Chinese provincial governments, then combining methods of quartile analysis and coefficient of variance to further analyse the China 30 provincial government

environmental regulation level of inter-regional differences. The results show that during 2006-2014, the differences in environmental regulation level among provincial governments are narrowing, but the overall imbalance remains obvious. This is also verified by the analysis of the quartile method. Meanwhile, further measurement results show that there are obvious differences in the cognition of the importance of environmental governance investment of provinces. Therefore, the environmental regulation cooperation mechanism for cross-administrative regions has to be perfected, scientific and reasonable regional government performance examination mechanism has to be established, and multi-subject synergistic governance mechanism has to be set up as well. All above measures are conducive to the promotion of the cooperation of provincial government environmental supervision.

ACKNOWLEDGEMENT

This work was supported by these projects: Fuji-An Science and Technology Association Science and Technology Think Tank Major Project (Project No. FJKX-ZD1401); Chinese Academy of Sciences Strategic Research and Decision Support System Construction Project (Project No. GHJ-ZLZX-2016-11); the National Social Science Fund of China (Project No. 13CJL071); Philosophy and Social Science Innovation Team Project of Fuzhou University (Project No. 17TD06).

REFERENCES

- Cole, M.A., Elliott, R.J. and Fredriksson, P.G. 2006. Endogenous pollution havens: Does FDI influence environmental regulations? *Scandinavian Journal of Economics*, 108(1): 157-178.
- Chen, Demin and Zhang, Rui 2012. Influence of environmental regulation upon Chinese total-factor energy efficiency: An empirical verification based on inter-provincial panel data. *Economic Science*, 4: 49-65.
- Cui, Yafei and Liu, Xiaochuan 2009. Game theory analysis of environmental pollution governance strategies among Chinese local governments: From the perspective of government social welfare goal. *Theory and Reform*, 6: 62-65.
- Gray, W.B. 1997. Manufacturing plant location: Does state pollution regulation matter? (No. w5880). National Bureau of Economic Research.
- Levinson, A. 1996. Environmental regulations and manufacturers' location choices: Evidence from the census of manufactures. *Journal of Public Economics*, 62(2): 5-29.
- Li, Jing and Rao, Meixian 2011. China in industry's environmental efficiency and rule research. *Ecological Economy*, 02: 23-32.
- Pearce, D. and Palmer, C. 2001. Public and private spending for environmental protection: a cross-country policy analysis. *Fiscal Studies*, 22(4): 403-456.
- Sauter, C. 2014. How should we measure environmental policy stringency? A new approach. IRENE Working Paper No. 14-01.
- Smarzynska, B.J. and Wei, S.J. 2004. Pollution havens and foreign direct investment: Dirty secret or popular myth. *The B.E. Journal of Economic Analysis and Policy*, Berkeley Electronic Press, 1-34.
- Sun, Y.T., Liu, F.C. and Li, B. 2009. A comparison of national innovation capacity and development mode between central European countries. *Studies in Science of Science*, 27(3): 440-444.
- Yang, Haisheng 2008. Local government competition and environmental policy: Empirical evidence from province's governments in China. *South China Journal of Economics*, 06: 15-30.
- Zhang, Cheng, Lu, Yang, Guo, Lu and Yu, Tongshen 2011. The intensity of environmental regulation and technological progress of production. *Economic Research Journal*, 2: 113-124.
- Zhang, Zhongyuan and Zhao, Guoqing 2012. FDI, environmental regulation and technical progress. *The Journal of Quantitative & Technical Economics*, 4: 19-32.
- Zhang, Wenbin 2010. Inter-provincial competition forms and their evolution of Chinese environmental regulation intensity: An analysis based on two-zone Durbin fixed effects model. *Management World*, 12: 34-44.



Iron-Manganese Silicate Polymerization (IMSP) Catalytic Ozonation for Removal of *p*-Chloronitrobenzene in Aqueous Solution

Yue Liu[†], Laiqun Zhao, Yanyan Dou, Weijin Gong, Haifang Liu, Jingjing Lv, Zizhen Zhou and Fuwang Zhao

School of Energy & Environment Engineering, Zhongyuan University of Technology, Zhengzhou, 451191, China

[†]Corresponding author: Yue liu

Nat. Env. & Poll. Tech.
Website: www.neptjournal.com

Received: 15-05-2018
Accepted: 02-08-2018

Key Words:

Catalytic ozonation
p-chloronitrobenzene
Hydroxyl radicals
Iron-Manganese silicate

ABSTRACT

Iron-manganese silicate polymer (IMSP) was synthesized in the laboratory and characterized by using X-ray diffraction (XRD), scanning electron microscope (SEM), energy dispersive X-ray spectroscopy (EDX), Fourier transformation infrared (FT-IR) and Brunauer-Emmett-Teller (BET). The mesopores and amorphous sample had nanorods structure, and on the surface was contained with abundant of surface hydroxyl groups. The catalytic activity of IMSP was investigated in terms of *p*-chloronitrobenzene (*p*CNB) and TOC removal. Ozonation catalysed by IMSP exhibited extraordinarily high catalytic performance over other studied processes. In the IMSP-catalytic ozonation process, 99.5 % conversion of *p*CNB and 50.7 % TOC was achieved in 15 min. Ozone dosage and catalyst dosage exert a positive influence on the removal rate of the *p*CNB. And the initial water pH of 7.0 ± 0.1 (the solution pH was close to the point of zero charge of IMSP) achieved the highest *p*CNB removal among all the tested conditions.

INTRODUCTION

In recent years, the increasing organic pollution in water sources promoted the development of water treatment technologies. Heterogeneous catalytic ozonation using metal materials as ozonation catalyst at mild experimental conditions and without any additional thermal and light energy was considered to be one of the most effective techniques for water remediation (Ikhlaq et al. 2015). Recent studies have found that many transition metals and oxides were an effective catalyst for ozone oxidation. For example, MnO_2 was used in the ozonation of 4-nitrophenol (Nawaz et al. 2017). Ferrocene was used in the ozonation of toxic contaminants in aqueous solution (Lin et al. 2017). Manganese silicate and iron silicate were used as catalysts, which were highly effective in catalysing ozone of *p*CNB in aqueous solution (Liu et al. 2011a, Liu et al. 2012). Many researchers have reported that heterogeneous catalysts with ozonation could significantly enhance the degradation efficiency of organic pollution and improvement of TOC removal by ozone decomposition and hydroxyl radicals ($\cdot\text{OH}$) generation compared with ozonation alone (Gao et al. 2017). $\cdot\text{OH}$ is a high-oxidation-potential and non-selective radical, which could effectively remove the organic pollutants in aqueous solutions (Ikhlaq et al. 2013). Moreover, heterogeneous catalysts in water treatment are limited by their easy to lead secondary pollution, hard to recycle, high cost and so on. So, it is very important for heterogeneous catalytic ozonation process to choose as a catalyst.

According to our previous work (Liu et al. 2011a, Liu et al. 2012), iron silicate and manganese silicate are effective heterogeneous catalysts. Moreover, compared with manganese silicate, iron silicate has a high catalytic activity and relatively weak recovery and utilization. So, we intend to use the advantages of iron silicate and manganese silicate to synthesize a compound silicate. With this in mind, the scope of the present paper was to fabricate a novel sample iron-manganese silicate polymerization (IMSP) and to study its catalytic performance in ozonation of organic pollution in aqueous solution.

As a typical halogenated nitro aromatic compound, *p*-chloronitrobenzene (*p*CNB) was selected as a model pollutant to test the catalytic activity of the IMSP. To the best of our knowledge, there was no reported research on the IMSP used in the ozonation process.

The primary objectives of this study were to synthesize and identify the characteristics of IMSP as an ozonation catalyst, to investigate the degradation efficiency of *p*CNB in the presence of a catalyst in an aqueous solution.

MATERIALS AND METHODS

Materials: All the solutions were prepared by using Milli-Q ultra-pure water. Catalysts were synthesized in the laboratory as follows: The catalyst crystalline phases were confirmed by X-ray diffraction (XRD). A stock solution of *p*CNB (Chem Service, USA) was prepared at 100 mg/L by dissolving 100 mg *p*CNB in 1000 mL ultra-pure water.

Methanol of HPLC grade was purchased from Sigma Aldrich (USA). Other reagents were all of analytic grade without further purification.

Catalyst synthesis: The IMSP catalyst was synthesized as follows: 150 mL 0.2 M $\text{Fe}(\text{NO}_3)_3$ and 150 mL 0.2 M $\text{Mn}(\text{NO}_3)_2$ were mixed intensively. Then 300 mL of 0.1 M Na_2SiO_3 was slowly added into the mixed liquor at room temperature under magnetic stirring. When the pH of the suspension was 7.0, the dropping of Na_2SiO_3 solution was stopped. The pH of the suspension was adjusted higher than 12 by NaOH solution, and it was incubated at 40°C for 24 h. The precipitate was then collected and washed with ultra-pure water for several times until the conductivity of the rinse water remained constant over three consecutive rinses. Finally, the precipitate was dried at 60°C for 10 h and then ground. Particles with diameters between 0.075 mm and 0.3 mm were used in the experiment.

Analysis methods: According to our previous work (Liu et al. 2011b), the concentration of pCNB was determined by a 1200 high performance liquid chromatography (HPLC, Agilent, USA) with UV detection at 265 nm. The pCNB mineralization was determined using a TOC analyser (TOC-VCPH, Shimadzu, Japan). Scanning electron microscope (SEM, Quanta 200FEG, FEI Corporation, USA) and energy dispersive X-ray spectroscopy (EDX) was used to measure the morphology and composition of the catalyst. The FTIR spectrum of the synthesized catalyst was determined using the KBr disc method and measured on a SHIMADZU (1730, Japan) spectrometer. The Brunauer-Emmet-Teller (BET) method on a surface area and porosity analyser (Micromeritics ASAP 2020, USA) with krypton adsorption at liquid nitrogen temperature was used to measure the surface area and pore volume of the catalyst. The metals leaching from the catalyst into the solution were determined by inductively coupled plasma atomic emission spectrometer (ICP-AES, Optima 5300DV, Perkin Elmer, USA). A saturated deprotonation method was used to determine the density of surface hydroxyl groups of the catalyst (Laiti et al. 1995).

Catalytic ozonation experiments: Batch experiments were carried out with a 1.2-L flat-bottom flask reactor. 1-L ultra-pure water was first transferred into the flask reactor. The desired concentration of gaseous ozone, which was produced by CF-G-3-010g ozone generator (Qingdao Guolin, China) was bubbled into the reactor and dispersed into the solution by means of a porous fritted diffuser. Then, the ozone generator was turned off and immediately dosed with the desired amounts of catalyst and pCNB stock solution into the reactor. The solution was continuously stirred with a magnetic stirrer at 300 rpm. All the experiments were operated

at 20°C by a thermostatic water bath. The experiment of ozonation alone (without catalyst) was carried out under the same conditions. The adsorption experiments were conducted under the same experimental conditions as used in the previous tests, but with the pure oxygen been replaced with ozone gas. After the designated time intervals in the course of the experiments, 15 mL of the solution in the reactor was sampled. The residual dissolved ozone in the samples was immediately quenched by 0.1 mL $\text{Na}_2\text{S}_2\text{O}_3$ (0.1 mol/L). The quenched samples were then analysed for pCNB quantification.

RESULTS AND DISCUSSION

Characterization of IMSP: The structure of the synthesized IMSP sample was examined by XRD, and the result is shown in Fig. 1. According to the literature, the broad peak in the range of 20° to 40° was typical of amorphous silica peak (Liu et al. 2011b, Aderson et al. 2000). However, due to the significant content of the amorphous phase in the sample, most of the crystals were covered. No obvious peaks belonging to IMSP or manganese oxide or iron oxide were seen.

The SEM micrographs of the synthesized IMSP are displayed in Fig. 2(a) and (b). Aggregates of nanorods were obtained for the ternary crystals. EDX was used to analyse the composition of the prepared IMSP (Fig. 2 c). The EDX analysis area was marked with a black cross in the SEM images (Fig. 2 a). The EDX result showed that this area was mainly composed of the four elements Fe, Mn, Si and O, and the weight percentages of the four elements were: Fe 20.56%, Mn 11.35%, Si 16.15% and O 51.94%, respectively. Combined with the results of Fig. 1, we could infer that

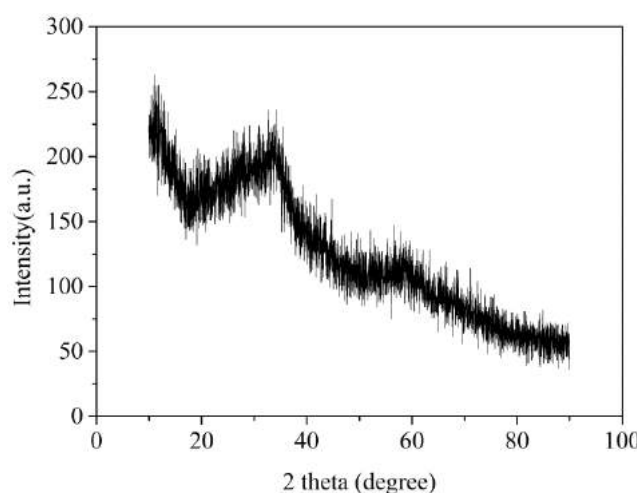


Fig. 1: XRD pattern of the catalyst.

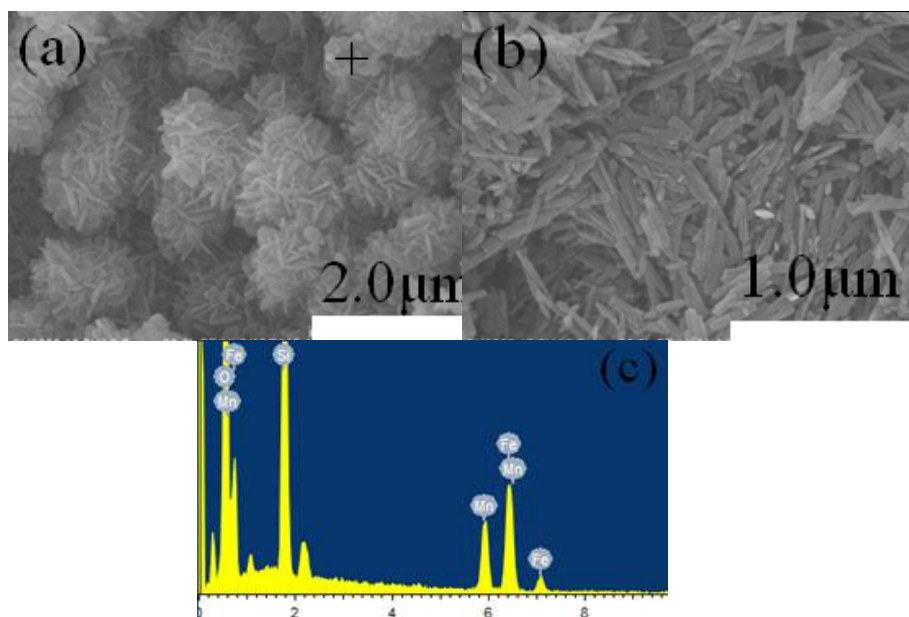


Fig. 2: SEM photographs of the IMSP catalyst (a) $\times 5000$, (b) $\times 10000$, (c) EDX analysis results of the catalyst, using a black cross to mark the structure in (a).

most of the iron oxide or manganese oxide crystals were wrapped by the amorphous silicon. The average surface area of the IMSP was found to be $312 \text{ m}^2\text{g}^{-1}$, and the pore volume of $0.37 \text{ cm}^3\text{g}^{-1}$.

The FTIR spectrum of the IMSP is depicted in Fig. 3. The band at 790 cm^{-1} is attributed the Si-O bond and the band at 1297 cm^{-1} is attributed to OH deformation vibrations of hydration of iron-manganese oxide (Abebe et al. 2017). The bands at 3452 cm^{-1} are corresponding to the O-H stretching vibrations and the peaks at 1690 cm^{-1} may be attributed to bending vibrations of adsorbed H_2O (Lu et al. 2013, Yu et al. 2015). These surface hydroxylation groups on the iron-manganese oxide surface might result in the formation of surface functional groups. Valdés et al. (2012) reported that in the heterogeneous catalytic ozonation process, the surface hydroxyl groups could accelerate the decomposition of the ozone to generate $\cdot\text{OH}$ radicals.

Catalytic activity of IMSP: Ozonation alone, IMSP-catalytic ozonation and adsorption of IMSP were conducted to investigate the catalytic activity of IMSP on the degradation of *p*CNB, and the results are shown in Fig. 4. The residual ion concentrations in aqueous solution and the TOC removal efficiency of different processes were also studied. As shown in Fig. 4, the concentration of *p*CNB decreased with the increased reaction time in all the three processes mentioned above. After 15 min reaction time, the degradation efficiency of *p*CNB in the process of ozonation alone

was 54.2%. Under the same experimental conditions, IMSP-catalytic ozonation process led to about 99.5% *p*CNB removal. And the adsorption of *p*CNB was only 7.5% in 15 min. Comparing the IMSP-catalytic ozonation process with the cumulative effect of ozonation alone and adsorption of IMSP, an increment of approximately 37.8% of *p*CNB degradation was observed.

As shown in Fig. 5, after 15 min reaction, the IMSP-catalytic ozonation and ozonation alone led to nearly 50.7% and 21.9% mineralization of TOC, respectively. And after 15 min reaction, the metal ion concentrations in the solution were far below the relevant level of international standards for drinking water.

Influence of initial pH: The initial pH of the solution exhibited a complicated effect on both ozone stability and catalyst surface properties. So it is important to examine the influence of the initial pH on IMSP-catalytic ozonation process. As shown in Fig. 6, in neutral water ($\text{pH} = 7.0 \pm 0.1$), the removal efficiency by the ozonation alone was less than 60% and with IMSP-catalysed ozonation process was 99.5%. However, under acidic conditions ($\text{pH} = 3.8$), the removal efficiency of ozonation alone and the IMSP-catalysed ozonation process were reduced to 16% and 30%, respectively. In contrast, when the pH of the solution was raised to 9.5, the degradation rate of ozonation alone increased to 89.7%, under the same experimental conditions, the degradation rate of the IMSP-catalysed ozonation process was

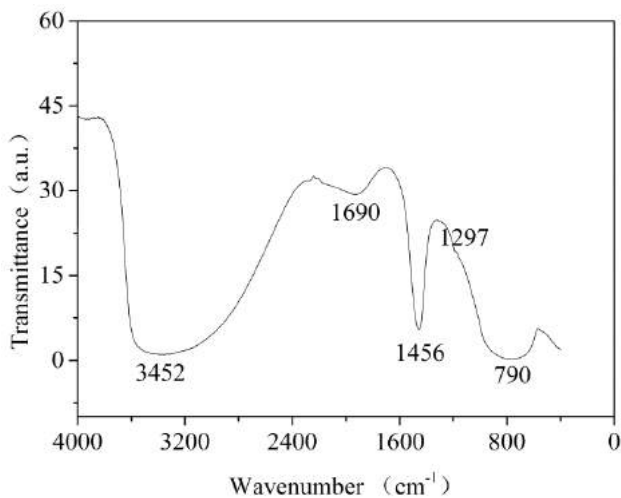


Fig. 3: FTIR spectrum of IMSP catalyst.

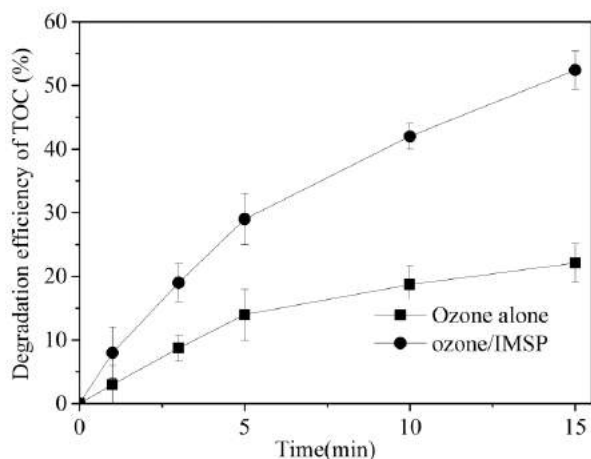


Fig. 5: TOC removal efficiency in the different process. Experiment conditions were: $[p\text{CNB}]_0 = 100 \mu\text{g/L}$, $[\text{O}_3]_0 = 1.0 \text{ mg/L}$, $[\text{IMSP}]_0 = 500 \text{ mg/L}$, $\text{pH} = 7.0 \pm 0.1$.

91.9%. For IMSP, its surface charge was affected by both, pH value of the solution and its pH_{pzc} . The pH_{pzc} of IMSP was determined to be 7.1. The results in Fig. 6 indicated that at a $\text{pH} 7.0 \pm 0.1$, IMSP had a greater influence on the catalytic ozonation of *p*CNB than at acidic and alkaline conditions. According to the characteristics of ozone, this phenomenon could be explained as follows: Under different solution pH conditions, surface hydroxyl groups of catalyst exhibited different charge properties. Under acidic ($\text{pH} < \text{pH}_{\text{pzc}}$) or alkaline conditions ($\text{pH} > \text{pH}_{\text{pzc}}$), the hydroxyl groups on the surface of the catalyst undergoes protonation or deprotonation. Moreover, when the solution is equal to the catalyst pH_{pzc} , the charge of metal oxide surface and surface hydroxyl groups was zero, which could accelerate

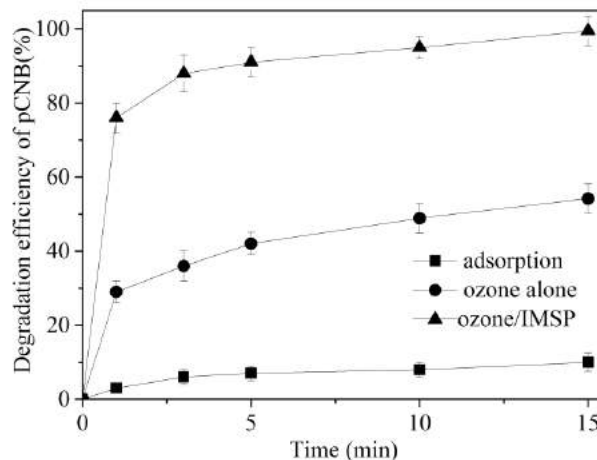


Fig. 4: Promotion of the *p*CNB degradation in different processes. Experiment conditions were: $[p\text{CNB}]_0 = 100 \mu\text{g/L}$, $[\text{O}_3]_0 = 1.0 \text{ mg/L}$, $[\text{IMSP}]_0 = 500 \text{ mg/L}$, $\text{pH} = 7.0 \pm 0.1$.

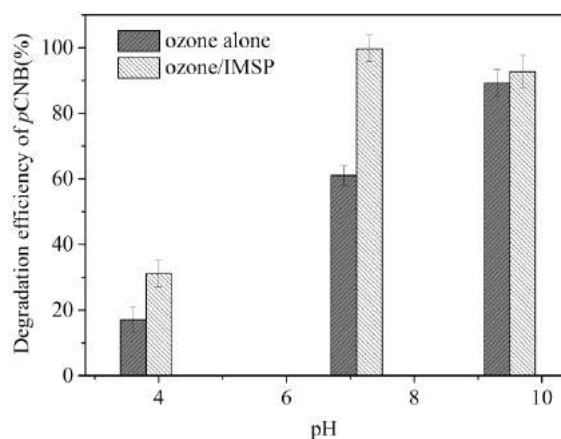


Fig. 6: Effect of initial pH on catalyzed ozonation of *p*CNB. Experiment conditions were: $[p\text{CNB}]_0 = 100 \mu\text{g/L}$, $[\text{O}_3]_0 = 1.0 \text{ mg/L}$, $[\text{IMSP}]_0 = 500 \text{ mg/L}$.

the ozone decomposition to generate high activity $\cdot\text{OH}$ radical (Qi et al. 2009). Our previous research also showed that the uncharged surface was more active than protonated or deprotonated form (Liu et al. 2012).

Influence of catalyst dosage: In the heterogeneous catalytic ozonation process, more dosage of catalyst could give more active sites for the catalytic ozonation, and the increasing of the more active sites could promote more ozone decomposition to generate more $\cdot\text{OH}$ radicals (Xu et al. 2009, Huang et al. 2015, Wang et al. 2015). The influence of catalyst dosage on the degradation of *p*CNB as a function of reaction time by IMSP-catalytic ozonation process can be observed in Fig. 6. It can be seen that the catalyst dosage exerts a positive influence on the removal rate of *p*CNB

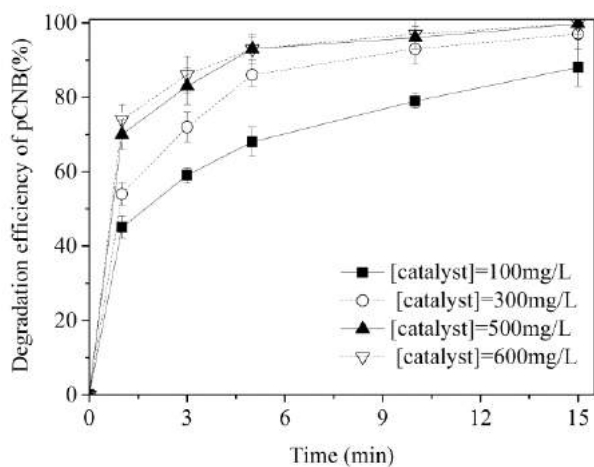


Fig. 7: Effect of catalyst dosage on catalyzed ozonation of *p*CNB. Experiment conditions were: $[pCNB]_0 = 100 \mu\text{g/L}$, $[O_3]_0 = 1.0 \text{ mg/L}$, $\text{pH} = 7.0 \pm 0.1$

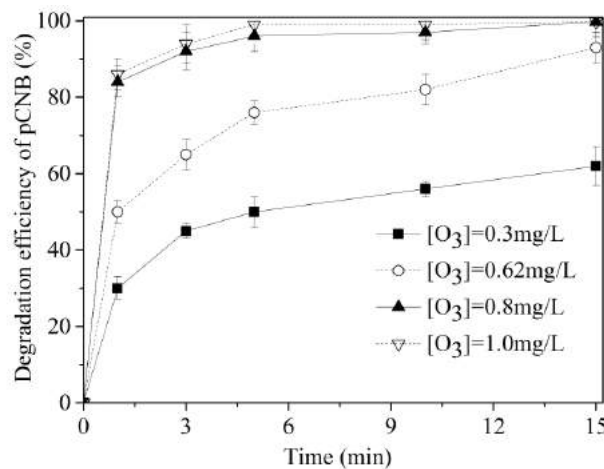


Fig. 8: Effect of ozone dosage on catalyzed ozonation of *p*CNB. Experiment conditions were: $[pCNB]_0 = 100 \mu\text{g/L}$, $[IMSP]_0 = 500 \text{ mg/L}$, $\text{pH} = 7.00.1$.

appreciably. Increasing the IMSP dosage, the removal efficiency of *p*CNB was enhanced. So the dosage of catalyst was positive in the IMSP-catalytic ozonation process for the degradation of *p*CNB. Previous research also reported that the surface hydroxyl groups of iron silicate and manganese silicate were the active sites for catalysed ozonation (Liu et al. 2011a, Liu et al. 2012). IMSP was a mixture of iron oxide, manganese oxide and so on. FTIR results showed that surface hydroxyl groups covered the surface of the IMSP. According to results of the saturated deprotonation experiment, the density of surface hydroxyl groups on iron silicate was $2.573 \times 10^{-2} \text{ mol/g}$ and IMSP was $3.169 \times 10^{-2} \text{ mol/g}$, respectively, which was much more than the efficient catalyst FeOOH (Sui et al. 2010). That was to say, more dosage of the IMSP could give more surface hydroxyl groups as active sites of catalysed ozonation reaction.

By combing the results shown in Figs. 4-7, the mechanism of IMSP catalysed ozonation of *p*CNB could be deduced as follows: In aqueous solution, surface hydroxyl groups as active sites of IMSP-catalysed ozonation reaction can accelerate the ozone decomposition to generate $\cdot\text{OH}$ radicals, which could oxidize *p*CNB efficiently.

Influence of ozone dosage: Ozone as the oxidant and treatment agent was a very important parameter in the process of heterogeneous catalytic ozonation. To determine the effect of the ozone dosage on the *p*CNB removal efficiency, a series of experiments were conducted by varying the ozone dosage from 0.3 mg/L to 1.0 mg/L, and the results are shown in Fig. 8. With an ozone concentration of 0.3 mg/L, the removal of *p*CNB in 15 min was 46%. When the ozone concentration was increased to 1.0 mg/L, its removal effi-

ciency was 99.8%. An approximately 3 times increase in ozone dosage led to about 2.5 times increase in *p*CNB removal in 15 min.

CONCLUSIONS

Based on the experimental data, the following conclusions can be drawn:

1. IMSP was synthesized in the laboratory and XRD, SEM, EDX, FTIR and BET analysis results confirmed that the amorphous IMSP contained an abundance of hydroxyl groups on the surface.
2. IMSP exhibited significant catalytic activities on the degradation of *p*CNB.
3. The degradation of *p*CNB in the IMSP-catalysed ozonation processes followed the $\cdot\text{OH}$ radicals oxidation mechanism.
4. $\text{pH} 7.0 \pm 0.1$, which nearly zero charged the surfaces of the IMSP, was found as the optimum value for the catalytic ozonation of *p*CNB. And the *p*CNB removal efficiency increased with the increased catalyst and ozone dosages.

ACKNOWLEDGEMENTS

This work was financially supported by the National Natural Science Foundation of China (51308561), Key Scientific Program of Higher Education Institutions (19B560012), and Supported by the Research Funds of Key Laboratory of Heating and Air Conditioning, the Education Department of Henan Province (2016HAC205 & 2016HAC202), and the Henan Province Colleges and Universities Youth Backbone Teachers Training Plan (2015GGJs-189).

REFERENCES

- Abebe, B., Tadesse, A.M., Kebede, Teju, T. and Diaz, E.I. 2017. Fe-Al-Mn ternary oxide nanosorbent: Synthesis, characterization and phosphate sorption property. *J. Environ. Chem. Eng.*, 5: 1330-1340.
- Anderson, D., Roy, A., Seals, R.K., Cartledge, F.K. and Jones, S.C. 2000. A preliminary assessment of the use of an amorphous silica residual as a supplementary cementing material. *Cement Concrete Res.*, 30: 437-445.
- Gao, G., Shen, J., Chu, W., Chen, Z. and Yuan, L. 2017. Mechanism of enhanced diclofenac mineralization by catalytic ozonation over iron silicate-loaded pumice. *Sep. Purif. Technol.*, 2: 55-62.
- Huang, Y., Cui, C., Zhang, D., Li, L. and Pan, D. 2015. Heterogeneous catalytic ozonation of dibutyl phthalate in aqueous solution in the presence of iron-loaded activated carbon. *Chemosphere*, 119: 295-301.
- Ikhlaq, A., Brown, D.R. and Kasprzyk-Hordern, B. 2015. Catalytic ozonation for the removal of organic contaminants in water on alumina. *Applied Catalysis B: Environmental*, 165: 408-418.
- Ikhlaq, A., Brown, D.R. and Kasprzyk-Hordern, B. 2013. Mechanisms of catalytic ozonation: An investigation into superoxide ion radical and hydrogen peroxide formation during catalytic ozonation on alumina and zeolites in water. *Appl. Catal. B: Environ.*, 129: 437-449.
- Laiti, E., Ohman, L.O., Nordin, J. and Sjöber, G.S. 1995. Acid/base properties and phenylphosphonic acid complexation at the aged $\text{I-Al}_2\text{O}_3/\text{water}$ interface. *J. Colloid Interface Sci.*, 175: 230-238.
- Lin, K.A., Lin, T., Chen, Y. and Lin, Y. 2017. Ferrocene as an efficient and recyclable heterogeneous catalyst for catalytic ozonation in water. *Catal. Commun.*, 95: 40-45.
- Liu, Y., Chen, Z., Yang, L., Han, Y., Shen, J. and Wang, H. 2012. Ozonation catalyzed by iron silicate for the degradation of *o*-chloronitrobenzene in drinking water. *Water Sc. Tech-W. Sup.*, 12: 31-37.
- Liu, Y., Shen, J., Chen, Z. and Liu, Y. 2011a. Degradation of chloronitro-benzene in drinking water by manganese silicate catalyzed ozonation. *Desalination*, 278: 219-224.
- Liu, Y., Shen, J., Chen, Z., Yang, L., Liu, Y. and Han, Y. 2011b. Effects of amorphous-zinc-silicate-catalyzed ozonation on the degradation of *p*-chloronitrobenzene in drinking water. *Appl. Catal. A: Gen.*, 403: 112-118.
- Lu, J., Liu, H., Liu, R., Zhao, X., Sun, L. and Qu, J. 2013. Adsorptive removal of phosphate by a nanostructured Fe-Al-Mn trimetal oxide adsorbent. *Powder Technol.*, 233: 146-154.
- Nawaz, F., Cao, H., Xie, Y., Xiao and Ghazi, J.Z.A. 2017. Selection of active phase of MnO_2 for catalytic ozonation of 4-nitrophenol. *Chemosphere*, 168: 1457-1466.
- Qi, F., Xu, B., Chen, Z., Ma, J., Sun, D. and Zhang, L. 2009. Influence of aluminum oxides surface properties on catalyzed ozonation of 2,4,6-trichloroanisole. *Sep. Purif. Methods*, 429: 405-410.
- Sui, M., Sheng, L., Lu, K. and Tian, F. 2010. FeOOH catalytic ozonation of oxalic acid and the effect of phosphate binding on its catalytic activity. *Appl. Catal. B: Environ.*, 96: 94-100.
- Valdés, H., Tardón, R.F. and Zaror, C.A. 2012. Role of surface hydroxyl groups of acid-treated natural zeolite on the heterogeneous catalytic ozonation of methylene blue contaminated waters. *Chem. Eng. J.*, 211-212: 388-395.
- Wang, Z., Chen, Z., Chang, J., Shen, J., Kang, J. and Chen, Q. 2015. Fabrication of a low-cost cementitious catalytic membrane for *p*-chloronitrobenzene degradation using a hybrid ozonation-membrane filtration system. *Chem. Chem. Eng. J.*, 262: 904-912.
- Xu, Z.Z., Chen, Z., Joll, C., Ben, Y., Shen, J. and Tao, H. 2009. Catalytic efficiency and stability of cobalt hydroxide for decomposition of ozone and *p*-chloronitrobenzene in water. *Catal. Commun.*, 10: 1221-1225.
- Yu, Y. and Chen, J.P. 2015. Key factors for optimum performance in phosphate removal from contaminated water by a Fe-Mg-La trimetal composite sorbent. *J. Colloid Interface Sci.*, 445: 303-311.



The Role of Advanced Technologies in the Remediation of Oil-Spilled Environment: A Decision-Matrix Approach

C.I.C. Anyadiegwu*, A.C. Igbojionu**, N.P. Ohia* and R.C. Eluagu*

*Department of Petroleum Engineering, Federal University of Technology, Owerri, Nigeria

**Mobil Producing Nigeria Unlimited, Port Harcourt Shore Base, Onne, Nigeria

Nat. Env. & Poll. Tech.
Website: www.neptjournal.com

Received: 19-05-2018
Accepted: 02-08-2018

Key Words:

Oil spill
Remediation
Decision matrix
Effective score
Advanced technologies

ABSTRACT

The role of advanced technologies in the remediation of oil spilled environment was investigated. Oil spill remediation technologies for the clean-up of soil and groundwater contamination from petroleum industry activities have advanced considerably over the past decade. This has been the result of increasing regulatory pressures in many parts of the world, mounting liability exposure, changing public perceptions, and the drive towards enhanced remediation in terms of cost effectiveness, health and environmental concerns, operation and maintenance requirement, applicability and efficiency. This paper examined the state of remedial technologies for petroleum industry applications in ex-situ and in-situ conditions, and used an effective score drawn from research to develop a decision matrix for selection evaluation. Ex-situ technologies involve excavation and treatment of contaminated soil. These include methods such as pyrolysis, solvent extraction, oxidation/reduction, and bioremediation, designed to remediate the soil to acceptable standards. In-situ technologies involve alteration of sub-surface flow, pressure, chemical or biological regimes to achieve containment, redirection, removal or destruction of contaminants. They include soil vapour extraction, bioventing, bio-sparging, and the use of horizontal wells and semi-passive barrier systems. A decision matrix was then developed using Microsoft Excel to aid decision making. This was developed using an effective research score allocated to each evaluation criterion and weighted using the ratio of this effective score to the total score by hundred percent. The optimal remedial approach depends on the highest ranked score as computed and documented in the MS-excel spreadsheet. From the analyses shown in the ex-situ decision matrix, advanced bioremediation was found to be the best placed technique with a weighted score of 7.048 and the highest rank of 1, while wet oxidation was found to be the least impressive technique with a weighted score of 2.022.

INTRODUCTION

Due to environmental, economic and social costs of hydrocarbon leaks, the oil and gas industry places great importance to the need to minimize ugly events of oil spill or pollution from occurring. Hydrocarbon contaminations of soil and groundwater are amongst the most evident negative effects of industrial life. There are multiple causes from oil well drilling, production, transportation and storage in the upstream industry, refining, transportation and marketing in the downstream industry (Seitinger et al. 1994).

Also, the recent oil spill incidents have shown that the cost is much more than the associated downtime and clean-up expenses as it goes a long way to affect the social welfare, aggravates poverty, population displacement, social conflict, production reduction and also affects the profit margin of the companies involved (McAllister 2005). Clean-up operations in response to an oil spill can generate large volume of oily liquid and solid wastes, (melanges of oil, seawater, sand and debris such as seaweed, sediments, peb-

ble, flotsam, jetsam and probably dead fauna). The volume of the waste material generated from the clean-up depends on: type and volume of oil; oil characteristics (viscosity, pour point, etc.); oil weathering processes, environmental conditions (climate, weather); shoreline, salt marsh, mangroves, etc.) and the clean-up strategies employed (Massoura et al. 2009). The integrity of a leak detection system is not limited, but may be compromised by a poor oil spill response/remediation technique.

Marine oil pollution receives much attention all over the world due to the perception of the magnitude, longevity and extent of damage it inflicts on the environment. In reality the impacts on the marine environment and coastline when the incident is well managed are often short-lived. The waste generated, however, may present a longer-term problem if not correctly managed and treated (Massoura et al. 2009). Massoura et al. (2009), in their paper examined some of the remediation techniques now being used for treatment of oily wastes and the criteria for determining and selecting the most appropriate techniques. They examined

various techniques and oil spill incidents in which they were used to illustrate the issues.

The management of waste streams is dependent on the type of pollutant, the composition of the impacted area, cleanup methods employed, nature of removed material and finally the volume of waste generated. The remediation techniques available can be broadly grouped into physicochemical, biological and thermal techniques. While all have limitations such as increasing the area of contaminated material, potential groundwater contamination, air emissions or need for long-term management, these are more acceptable than the historic landfill disposal strategies. It has been determined that these techniques have potential separately, or in combination, to increase the rate of degradation of contaminants. The residual contamination concentrations, which will be acceptable are not universally agreed, but defined by an assessment of the health, ecological risks of the contaminants. Remedial technologies must be chosen based on their ability to achieve those goals in a cost-effective and timely manner (Massoura et al. 2009). Their paper looked to the future of each technique based on parameters such as effectiveness, reasonableness, cost, practicability, durability, technological and scientific advances, and discussed future implementation in accordance with good practice and quality assurance procedures.

According to Engler et al. (2017), an ongoing issue for many operators is the need to be able to safely and quickly remediate environmental issues. Of particular interest are the cleanup of petroleum products, and the cleanup of produced water, which often has extremely high levels of chlorides (Cl⁻), and may include hydrocarbon components. Methods used in the past have been difficult and expensive, often causing issues with the disposal of contaminated soil. Attempts have been made for many years to perform in-situ remediation. In the 1950's, processes were developed that enhance the growth of naturally occurring microbes by applying a culture of microbes and enzymes to the affected area. The process studied has been used in over 1400 individual locations, providing a rich data set for analysis. Differences in how the processes were executed have resulted in variances in the results and the scope of the treatment required to meet environmental standards. In their paper, they discussed a methodology that has been applied in over 1400 locations. Their paper documented the work, and identified features and techniques that enhanced or diminished success rates. Processes were optimized to maximize the consistency of results at minimum cost. Six treatments were illustrated as representative examples of the effectiveness of the process. The first treatment reviewed involved remediation of a well site in West Texas near Garden City, TX. The treatment resulted in reductions of Cl⁻ contamination by 83% to

99%. The second treatment reviewed was completed on another site near Garden City, TX where a produced water spill had contaminated cotton fields. Reduction of contaminants at this site was over 99%. The third treatment reviewed was a site in Fisher County, TX, where a spill contaminated a pond on the site. Reductions of Cl⁻ up to 84% were observed, and hydrocarbon contaminants were reduced over 99%. The fourth description involved a site in Gaines County, Texas that experienced a produced water spill in April 2016. As a result of the spill, the initial contamination of the soil was tested to be 30,000 ppm. The area was treated using the process and the biological agent. Within twenty-one days, the salt level in the soil had been reduced to 900 ppm. Local plant life was observed to be growing in the formerly contaminated soil within twenty-eight days. The fifth description involved a site in Fisher County, Texas, where a pipeline leak contaminated soil. Samples were taken at several locations at the surface, and at depths of 48" and 60" to evaluate ground penetration. Post treatment, samples indicated reductions of 57% to 99.99%. The sixth description involved a site in Jal, New Mexico where crude oil was spilled into a storm sewer, and the oil flowed into a sewage treatment plant. The site and the sewage plant were treated, and reductions of hydrocarbons were observed to be 98%-99% of the original sample values. The processes described in their paper offered a significant benefit not only to the oil and gas producing community, but also to the general public in that the ability to restore previously damaged soil enhances the environment we live and work in.

Imtiaz et al. (2016) did a very great work on the use of advanced technology for the remediation of aquatic oil spills. According to Imtiaz et al. (2016), the utilization of automated unmanned boats for the skimming of oil has not been introduced. Their paper underscored on the feasibility and the advantages of deploying an autonomous vehicle for the same. The paper briefly discussed the trend in removal of slick, and put forward a revolutionary methodology for the same in the form of CSASSB, Cok Sorbent carrying Automated Sub-Surface Boats. It discussed the effectiveness of the use of CSASSB's and compared it with the currently used counterparts. It also discussed the suitability of cork as the appropriate absorbing material. The cork absorbent material was subjected to a heat treatment to increase its hydrophobicity, its lightness and absorption capacity. The working of CSASSB's involved a five step process and the paper discussed all the above-mentioned steps in detail. The CSASSB was found to be considerably more fuel effective and eco-friendly than the current ships that are used for the remediation of aquatic oil spills. The system is simple, yet effective. Moreover, the heat treated cork as a sorbent for oil removal in aquatic environment with

advantage of being a natural and ecological product. Hence, the CSASSB system with the aid of cork sorbent keeps the ecosystem healthy by removing toxic slick.

Oil spills are one of the major concerns of the up and downstream oil industry. Although land operations do not cause spill accidents and volumes like offshore, the damage and the loss in public credibility is severe and long term (Seitinger et al. 1994). Solubility of hydrocarbons (HC) in water is generally small. The movement of oil in porous media must be described using a two phase flow concept. The spread is a four stage process: migration in the subsoil; invasion into the capillary fringe; spreading on the water table; stabilization of the spill, HC solubility (plume). Seitinger et al. (1994) analysed these four steps in detail in their paper. According to Seitinger et al. (1994), the main concern of the environmental groups, authorities, etc. is the presence of a floating oil layer on the groundwater table. Further in-situ remediation methods are based upon the removal of the liquid hydrocarbons (bioremediation, soil-vapour extraction, etc.). Their paper presented various directional drilling techniques including their pros and cons for oil spill remediation. Also, a brand-new technology to drill directional wells in heterogeneous, unconsolidated sands was presented. The method was used to drill directional wells in unconsolidated, coarse gravel formations (river sedimentation). Directional changes of 25-30/30 m were reached. A case study and experience from oil spill production was also presented, including a comparison in cost and success to vertical extraction wells. In their study, they found out that horizontal or strongly deviated wells offer significant advantages in the cleanup of thin, floating oil spills. The advantages are similar to horizontal wells in oil production (linear drainage along wellbore instead of radial drainage, low drawdown during production, increased net pay, etc.). A moving groundwater table is one of the most obvious differences to traditional oil production. High angle wells combine inflow advantages of horizontal wells with moving water table.

According to Olayinka et al. (2013), the impacts of oil spills are not limited to the direct effect on the ecosystem; it goes a long way to affect the social welfare, aggravates poverty, population displacement, social conflict, production reduction and also affects the profit margin of the companies involved. Their study was aimed at providing a review and comparison of the remediation techniques currently in use and suggest the most suitable methods of oil spill cleanup and remediation in Nigeria Niger Delta region based on certain criteria and to also suggest ways of mitigating oil spill occurrences in this region. In the course of their research, data collection was on primary and secondary data. For the primary data, a structured questionnaire was drafted and used for survey relating to the research to rank and

evaluate different perspectives of stakeholders on various remediation techniques that are in consideration. For the secondary data, the study was carried out with a literature study to gain an overview of the different remediation methods for PHCs contaminated soils. Finally, using specific criteria, including cost efficiency, operation and maintenance of the technique, environmental friendliness, time frame of achieving remedial objectives, health concerns, and applicability of the techniques were used to make an evaluation design for the different remediation techniques for hydrocarbons contaminated soils. The results from these studies showed that single remedial action cannot be used for cleanup, but the thermal desorption and remediation by enhanced natural attenuation (RENA) was the best placed technique ranking highest under the different criteria of the evaluation design and the sample survey of the remediation techniques considered.

Olayinka et al. (2013) was able to establish that in-situ vitrification is the most cost effective technique with little or no disturbance of site.

Also regarding costs, Esak et al. (2000) gave a good illustration of successful co-compost remediation practical project which was able to achieve about 45% reduction in oil spill contaminated soil remediation costs. The said project was a co-compost remediation program involving oil contaminated soil at a pipeline break located near Gilby, Alberta. This was undertaken from the fall of 1998, by Millennium EMS Solutions Ltd. on behalf of Gulf Canada Resources Limited. Approximately 1100 m³ of heavy clay textured, hydrocarbon contaminated soil (5,000 to 6,000 µg/g TPH) was windrowed, treated with soil amendments (manure, fertilizer and wood waste), windrow turned two times and left to digest over the cold winter months. In early spring, the windrows were turned two more times. The results of the soil sampling and analysis completed 210 days after initiation show the soil to have been remediated to below Alberta Tier 1 cleanup criteria (1000 µg/g). Toxicological tests for aquatic and terrestrial systems were also successfully conducted to confirm the clean levels of the remediated soil.

According to Lessard et al. (1998), the focus of industry and government activities with respect to oil spills is on prevention. Despite best prevention efforts, however, some spills will occur and industry and government must be fully prepared to respond. After 30 years of studies and practical experience, there is now a definitive body of evidence that the use of dispersants to counter the effects of an oil spill can result in lower overall environmental impact than relying on other countermeasures, and for many large spills, it is often the only practical at-sea response technique. This conclusion is supported by numerous international organiza-

tions. A number of countries, including the U.S. have recently become more pro-active in supporting and advocating dispersant use. One major reason for this support has been the development of new dispersants with increased capability and improved toxicity characteristics. Their paper focused on new capability to disperse heavy and/or weathered oils such as bunkers. It summarized the mechanism by which dispersants work, listed their advantages and reviewed the results of recent large-scale field tests in the North Sea which conclusively demonstrated the capability of new products to disperse heavy and weathered oils.

In recent years, advances in computer technology allowed the development of sophisticated software applications able to simulate the effects of oil spills on the marine environment. The need for such modelling arises from the perception of oil spills as long lasting and highly damaging events because of their wide range of potential impacts on the environment, human health and economic activities. Modelling tools can predict the consequences of these events and allow a targeted response planning to be made. Iazeolla et al. (2016), in their paper presented an innovative application of oil spill modelling tools aimed at supporting the emergency response system along the different stages of the project life-cycle. Three case studies were presented, from exploration, to response planning during production, to contingency response during an emergency. The oil spill modelling approach for each case study was detailed, as well as the specific support provided to the decision making process. Two different methods for oil spill modelling and environmental consequences assessment in Eni exploration and production activities were shown. Preventive modelling, based on a statistical approach, identifies the range of possible outcomes of an event. Through this simulation, the consequence assessment of a spill provides useful information for a targeted emergency response planning. Emergency modelling, on the other hand, is based on a deterministic approach and simulates the evolution of a single event, whose characteristics are known. In this case, oil spill models can predict the fate of an oil spill in an emergency, providing an insight on its future evolution and driving the decision on the most appropriate response actions. Their results highlighted the contribution of oil spill modelling in making the emergency response system an active player during all the project life-cycle, enabling its complete integration within the project management structure. Oil & gas operators may benefit of this advanced approach that contributes to the improvement of their emergency response management system. Through a prompt and proper response, the effect of oil spills can be excluded or mitigated, saving human lives as well as protecting the environment, the facilities and Company's reputation.

Still on oil spill modelling, Michel et al. (2012) explained the global methodology developed by Total Exploration and Production Limited to improve the reliability of oil spill drift modelling by developing metocean skills in-house. According to Michel et al. (2012), actually, model predictions should make it possible to forecast the drift of an oil slick, identify the areas where the intervention teams should take action, predict the period and areas that could be impacted, and inform neighbouring installations, authorities and NGOs. Total Exploration and Production Limited created a metocean oil spill modelling system to improve the quality and in turn bring an improvement to oil-spill drift modelling results. Thanks to the improvements, oil spill models can be considered as reliable tools for use in oil spill response.

Aiello et al. (2014) also developed a web application, SmartGIS based on a continuous improvement project focused on oil spill management processes to perform a large-scale harmonization of procedure and strategies. The main scope was the development of an Oil Spill Best Practice which provides a guideline addressed to Eni subsidiaries for oil spill preparedness and for the selection of the most suitable tactics and technologies for response and remediation. This is based on the habitat types present in each country where Eni operates. To reach this goal, the habitat mapping and benchmarking activities were performed as intermediate deliverables. Habitat mapping is based on the mapping and classification of all the habitat types using certified reference datasets. Three marine and seven terrestrial habitats were identified. Benchmarking analysis provides a detailed overview over the current status and development trends of oil spill response and remediation tactics and technologies applied worldwide. They have then been categorized into habitat types. A webGIS application was identified as the best solution to manage all the data and information acquired through the project. It works wherever an internet connection is available and allows an effective remote support of the accidental oil spill scenario. For this reason the SmartGIS was launched with the development of an environmental analysis tool within the 3Ter Advanced Emergency System, already applied in Eni in case of emergency. The environmental analysis tool is characterised by different layers on habitats, countries, marine regions, active concessions and protected areas. In addition it can be supplemented by other information such as meteomarine data, nautical charts, bathymetry and vessel tracking as well as thickness and concentration of oil. Aiello et al. (2014) illustrated how the data and information presented in the SmartGIS can be applied worldwide in case of an accidental oil spill, providing a fruitful contribution to handle the emergency.

For years, even decades, microbial biologists have been

aware of the ability of some naturally-occurring microorganisms to degrade certain fractions of petroleum into simpler substances. This process is known as biodegradation and refers specifically to the natural process whereby, bacteria or other microorganisms alter and break down organic molecules into other substances, such as fatty acids and carbon dioxide. The possibility that this natural process could be harnessed as a practical oil spill response technology motivated some of the early investigations into the factors that affect biodegradation, the kinds of hydrocarbons capable of being degraded by microorganisms, rates of biodegradation, and the species and distributions of microorganisms involved in biodegradation. Research into these topics has led to the development of several types of methods for using microorganisms to restore sites polluted by oil. Collectively, they are known as bioremediation techniques, and they involve the addition of materials to contaminated environments to cause an acceleration of the natural biodegradation process. Fertilization is the bioremediation method of adding nutrients, such as nitrogen and phosphorus, to a contaminated environment to stimulate the growth of indigenous microorganisms. This approach is also known as nutrient enrichment. Seeding refers to the addition (usually of non-native) of microorganisms to a spill site. Such microorganisms may or may not be accompanied by nutrients. Current seeding efforts use naturally occurring microorganisms, but seeding with genetically engineered microorganisms may also be possible. This approach, bio-remediation is now widely considered for the remediation of oil spills (Westermeyer 1992).

So many oil spill remediation techniques abound, which have been described briefly in this section. However, most of the conventional oil spill response/remediation technologies to date, have in general failed to perform optimally within the criteria of cost and efficiency.

MATERIALS AND METHODS

Ex-situ Technologies

Ex situ treatment involves excavation of contaminated soils, followed by treatment or disposal. Ex-situ technologies have evolved from simple removal and landfill disposal (dig and dump), to technologies designed to treat contaminated soil and water onsite. Recently, many owners of contaminated sites have required that all treated soil and water remain on the site, to minimize future liability associated with transportation and off-site disposal. The move to on-site treatment has been accelerated in many countries by the increasing difficulty in siting fixed waste treatment facilities. Public concerns over the safety of such facilities, and the dangers of long-term exposure to nearby residents have led

to the increased popularity of mobile treatment technologies. These systems can be moved quickly on-site, the waste treated over a relatively short period, and then moved away. This tends to improve public acceptance, reduce costs, and provide for a site-specific solution.

Pyrolysis or thermal phase separation or indirect fired thermal desorption: Thermal desorption is a process that uses high temperatures (usually below 400°C) to drive organics out of soil by volatilization. The method is done in the absence of oxygen and it uses temperature much less than that required for combustion. Unlike the incineration process that heats the soil to higher temperatures in an oxygenated atmosphere which both volatilizes and combusts the organics simultaneously, thermal desorption offers several advantages over incineration including reduced amount of gases produced, thereby reducing the size of the off-gas handling system.

Bioremediation: This refers to the degradation of organics in soil using indigenous or inoculated microbes in bio-piles or land spreading process. The process is natural and it usually takes longer time to achieve the intended aim. It requires large areas and control of fugitive emissions.

Leaching/soil washing: This involves an on-site set-up to scrub soil and remove hydrocarbons which are then treated separately. Soil flushing is flooding a zone of contamination with an appropriate solution to remove the contaminant from the soil. The two technologies are not well developed, but looks promising for some applications (Wilson 1994). The contaminants are mobilized by solubilisation, formation of emulsion, or a chemical reaction with the flushing solutions. After passing through the contamination zone, the contaminant-bearing fluid is collected and brought to the surface for disposal, recirculation, or on-site treatment and reinjection (US EPA 2008).

Vitrification: This process involves melting of contaminated soil, buried wastes, or sludges in place to render the material non-hazardous. It uses electricity to heat soil to remove organics and encapsulate heavy metals into glass. Heating is as high as 1,600 to 2,000°C. The high temperature destroys organic pollutants by pyrolysis.

Acid extraction: This involves leaching of heavy metals using an acid based reagent. Its application is limited to use in inorganic environments since it may affect the treatments of organics.

Dechlorination: This involves the treatment of chlorinated contaminated soils using proprietary chemical systems. It's limited in application to chlorine contaminated environ-

ments and has no effect on non-halogenated organics.

Oxidation/reduction: This can be traced back to the concept of REDOX reaction where organics are treated using hydrogen and temperature. Oxidation involves the loss of hydrogen while reduction is the gain of hydrogen. It's limited in application to chlorinated organic compounds and it's not suitable for inorganics.

Solvent extraction: This requires the use of solvent to extract organics of high concentration from the soil. Organics of high concentration here are those ones that emanate from hydrocarbon operations/spills. Also, various applications identify weakness in its effectiveness with heavy metal contaminated soils.

Wet oxidation: In wet oxidation, slurry flows through reaction tube, oxygen is injected and oxidation of organics is achieved. No air is emitted during the process. It is successful in applications in organics and hydrocarbon contaminated environments.

In-Situ Technologies

Soil vapour extraction (SVE): SVE, also known as soil venting or vacuum extraction, is an in-situ remedial technology that reduces concentrations of volatile constituents in petroleum products adsorbed to soils in the unsaturated (vadose) zone.

Bio-venting: This is the stimulation of aerobic bioactivity through inducement of air flow in the unsaturated zone as part of conventional SVE, thereby reducing the concentration of contaminants in the unsaturated zone only.

Bio-sparging: This refers to the removal of volatile compounds from saturated zone by injection of air/oxygen below groundwater surface. It is also used in conjunction with SVE thereby stimulating aerobic bioactivity in the saturated zone.

In-situ bioremediation: This involves degradation by active microbes in soil. Microbes used are mainly indigenous or inoculated microbes. Delivery systems and stimulants used involve both aerobic and anaerobic processes.

Wetland treatment: This approach focuses on the treatment of pumped groundwater or contaminated discharge through natural or engineered systems.

Horizontal wells: This is an emerging technology where wells are screened horizontally or at an angle to intercept thin of oriented geologic zones or contaminant plumes.

In-situ passive barriers (funnel and gate) method: This is also an emerging technology yet to be adopted where an in-

situ barrier is used to directly flow to a central point. Treatment occurs by natural gradient through-flow. Variation in treatment arises from the difference in the concentrations and compositions of contaminants.

Decision Matrix Development

Based on the findings in the literature study above, some criteria were set as guiding factors in order to determine the differences in each remediation technique with respect to the criteria. A decision matrix was developed using these criteria. This served as our basis of selection to the efficient deployment of a sole or hybrid technique. The decision matrix covers some of the main criteria influencing the selection of remedial methods for contaminated soils. It also determines the degree of overall importance of a remediation technique. Criteria used to design this decision matrix include:

1. Cost efficiency
2. Applicability of the technique
3. Operation and maintenance of the technique
4. Environmental Impact
5. Time frame of achieving remedial objectives/Ease of deployment
6. Health concerns
7. Efficiency/foot print after clean-up

Data Collection

Primary data: Primary data collection was carried out with a wide number of literature studies to gain an overview of the different remediation methods for Niger Delta contaminated soils. Through this study, different factors responsible for the design of the decision matrix table were identified and analysed. Specific literature studies include USEPA, UNEP report on Ogoni land, NOSDRA report and various SPE papers and thesis of different scholars collected from web searches.

Assessment/ranking scales: The study used the following assessment scales by allocating an effective score to each technique which is based on the assessment criteria discussed in the section above.

1-Very low, 3-Low, 5-Medium, 7-High, 10-Very High

RESULTS

Matrix Weight Computation

Preference Scale - 1 = about the same, 2 = preferred, 3 = strongly preferred.

The matrix weight percent was computed in MS-Excel using an effective computational score allocated to each criterion stipulated. Stated clearly below is the equation used for this computation:

Table 1: Selection criteria ranking for oil spill remediation techniques (paired comparison).

	B	C	D	E	F	G	SELECTION CRITERIA	SCORE	WEIGHT(%)	RANKING
A	A1B1	A1C1	A1D1	E2	F2	A1G1	A: Applicability	4	9.30	1
B		B1C1	B1D1	E2	F2	B1G1	B: Ease of Deployment	4	9.30	1
C			C3	C1E1	C1F1	C1G1	C: Operation and maintenance Requirement	8	18.60	2
D				E2	F2	G2	D: Health Concerns	2	4.65	2
E					E1F1	E1G1	E: Environmental Impact	9	20.93	3
F						F1G1	F: Cost Effectiveness	9	20.93	3
G							G: Efficiency	7	16.28	2
							TOTAL	43		

Table 2: Ex-situ technologies decision matrix.

		Ex-Situ Technologies Decision Matrix								
		Applicability +	Time Frame/Ease of Deployment +	Operation & Maintenance Requirement -	Health effectiveness +	Environmental Friendliness +	Cost-effectiveness +	Efficiency +	Weighted Score	Ranking
Criteria Weight		0.093	0.093	0.186	0.047	0.209	0.209	0.163		
TYPE OF REMEDIATION TECHNIQUE	Pyrolysis	10	5	5	3	1	5	5	2.675	5 th
	Bioremediation	10	7	1	10	10	7	10	7.048	1 st
	Soil Washing	10	3	5	3	5	5	7	3.325	2 nd
	Vitrification	7	5	5	3	5	3	1	2.162	7 th
	Acid Extraction	3	5	5	1	5	5	7	3.092	3 rd
	De-chlorination	3	5	5	1	5	5	7	3.092	3 rd
	Solvent Extraction	10	5	7	1	5	5	3	2.719	4 th
	Wet Oxidation	3	5	5	1	5	3-5	3	2.022	8 th
	REDOX	5	7	5	3	5	3	3	2.488	6 th

$$\text{Weight Percent} = \text{Score/Total} \times 100 \quad \dots(1)$$

Results from this computation can be seen in Table 1.

Application of Weight Percent

Based on the weight matrix developed in Table 1, the different remediation techniques were ranked and displayed in Table 2 to explain the results. The results show, in general, that how different techniques compare with each other and how each technique outweighs the other.

DISCUSSION AND CONCLUSION

From the ex-situ decision matrix in Table 2, advanced bioremediation is the best placed technique with a highest

rank of 1 as seen in the second row.

Bioremediation is the most efficient and cost effective technique with little or no disturbance on site. It has very low health risks as it is a natural process despite the fact that it takes quite considerable amount of time to complete. Its applicability is high as regulatory bodies are seriously buying the idea. In terms of management, it requires virtually no or low cost to operate and maintain processes/equipment used.

Pyrolysis requires professionalism and technicality to operate and maintain. Its wide applicability can be attributed to successful applications in various spill sites (Someus 1994) with high moderation in terms of cost, time frame of

deployment and efficiency. Professionalism and technicality as stated before is highly needed to manage its health and environmental implications.

Conclusively, an extensive review has been done based on the role played by technology in remediating oil spilled sites. The review was grouped under two broad categories - the Ex-situ and In-situ remediation technologies.

Ex-situ technologies involve excavation and treatment of contaminated soil. These techniques tend to be more intensive and expensive than in-situ methods, but a higher degree of clean-up certainty is provided more quickly.

In-situ technologies deal with soil and groundwater contaminants in place. Because of the heterogeneity of the subsurface, remediation is rarely complete, and processes are slower. However, on the whole, costs tend to be lower.

A decision matrix was developed during the course of this work to serve as a guide for selection of remediation technique based on different criteria clearly stated in the paper.

The criteria are peculiar to different arms of the business. For example, applicability and operation are peculiar to the cleanup contractors; cost, time and health concerns are peculiar to government regulators; environmental friendliness, time frame and also health concerns are peculiar to the public.

Finally, bioremediation has been identified as the most favourable of all the Ex-situ techniques that were in consideration.

RECOMMENDATION/FURTHER WORK

There is no universally acceptable remediation technique for a particular area or type of spill. This study only serves as a guide to select remediation measures based on our preferences.

Further research should be carried out in the area of hybrid remediation technique application to ascertain its feasibility in terms of cost, applicability, health and efficiency.

Proactive measures like oil spill prevention techniques should be strengthened and regulatory agencies empowered to carry out their work without prejudice.

A secondary data collection approach in form of questionnaire should further be conducted amongst stakeholders/professionals involved in the decision making process of the various remediation techniques applied in events of oil spill.

REFERENCES

Aiello, G., Buffagni, M., Pavanel, E., Bracco, L., Thorbjornsen, S.

- and Meregaglia, M. 2014. SmartGIS project: a web application for global oil spill management. In: SPE International Conference on Health, Safety, and Environment. Society of Petroleum Engineers, 17-19 March, Long Beach, California, USA.
- Engler, R.A., Rome, G., Rainey, R., DeLeon, V. and Good, M. 2017. Environmental remediation using advanced microbial techniques. In: SPE Health, Safety, Security, Environment, & Social Responsibility Conference-North America. Society of Petroleum Engineers, 18-20 April, New Orleans, Louisiana, USA.
- Esak, L.K. and Osborne, A.E. 2000. Successful co-compost remediation project points the way to 45% reduction in oil spill contaminated soil remediation costs. In: 16th World Petroleum Congress, 11-15 June, Calgary, Canada.
- Iazeolla, G., Mariani, M., Cassina, L., Marconi, M., Deffis, J.M. and Buffagni, M. 2016. Advanced oil spill modelling in the offshore oil & gas industry: Improving the emergency response management along the project life-cycle. In: SPE International Conference and Exhibition on Health, Safety, Security, Environment, and Social Responsibility. Society of Petroleum Engineers, 11-13 April, Stavanger, Norway.
- Intiaz, M., Rajak, V.K., Dei, S., Chhateja, J. and Biswas, A., 2016. Aquatic oil spill remediation by using automated unmanned boat AUB. In: Offshore Technology Conference Asia, 22-25 March, Kuala Lumpur, Malaysia.
- Lessard, R.R., DeMarco, G., Fiocco, R.J., Lunel, T. and Lewis, A. 1998. Recent advances in oil spill dispersant technology with emphasis on new capability. In: SPE International Conference on Health, Safety, and Environment in Oil and Gas Exploration and Production. Society of Petroleum Engineers, 7-10 June, Caracas, Venezuela.
- Massoura, S.T. and Sommerville, M. 2009. Realities of spill: Waste remediation strategies. In: Asia Pacific Health, Safety, Security and Environment Conference & Exhibition, Jakarta, Indonesia, 4-6 August.
- McAllister, E. W. 2005. Pipeline Rules of Thumb Handbook: Quick and Accurate Solutions to Your Everyday Pipeline Problems. 6th Edition, pp. 547-556.
- Michel, C., Quiniou, V. and Vigan, X. 2012. Metocean and oil spill modelling. International Conference on Health, Safety and Environment in Oil and Gas Exploration and Production, 11-13 September, Perth, Australia.
- Olayinka, E. D. and Ogbonna, F. J. 2013. Environmental remediation of oil spillage in Niger delta region. In: SPE Nigeria Annual International Conference and Exhibition, 5-7 August, Lagos, Nigeria.
- Seitinger, P. and Baumgartner, A. J. 1994. Oil spill remediation: An integrated approach for in-situ site clean-up. SPE Health, Safety and Environment in Oil and Gas Exploration and Production Conference, 25-27 January, Jakarta, Indonesia.
- Someus, G. E. 1994. Advanced waste management: Indirect fired thermal treatment technologies. USEPA 5th Forum on Innovative Hazardous Waste Treatment.
- U.S. EPA 2008. Green Remediation: Incorporating Suitable Environmental Practices into Remediation of Contaminated Sites. EPA 542-R-08-002.
- Westermeyer, W. E. 1992. Bioremediation: A new tool for marine oil spill response? The Second International Offshore and Polar Engineering Conference, 14-19 June, San Francisco, California, USA.
- Wilson, D. J. and Clarke, A. N. 1994. Hazardous Waste Site Remediation. Marcel Dekker, New York.



Interaction Between Foreign Trade and Environmental Pollution: A Case Study of Guizhou Province, China

Mengxi Gao

Guizhou Normal University, School of International Education, Guiyang, Guizhou, 550000, China

Nat. Env. & Poll. Tech.
Website: www.neptjournal.com

Received: 12-01-2019
Accepted: 14-02-2019

Key Words:

Foreign trade
Environmental pollution
Guizhou province

ABSTRACT

Economic globalization is deepening China's opening up to the world. China has promoted the development of foreign trade by extensively improving the level of its open economy. However, to determine whether the development of foreign trade has aggravated environmental pollution, attention needs to be paid. Taking Guizhou Province as an example, this study examines the relevant studies on the interaction between foreign trade and environmental pollution, and summarizes the current environmental pollution in Guizhou Province, and uses panel data at the municipal level of Guizhou Province from 2007 to 2016 to analyse the dynamic relationship between foreign trade and environmental pollution and further explore the environmental effect law of foreign trade. Results are found to be inconsistent with those of existing studies on the relationship between foreign trade and environmental pollution possibly due to the incorrect source of sample data and different estimation methods. The current situation of environmental pollution in Guizhou Province shows that the total discharge of industrial wastewater and industrial waste gas is on the rise and that the discharge of industrial solid waste increases in a small fluctuation. Emissions of environmental pollutants, gross domestic product, and foreign investment show a U-shaped relationship. Foreign trade layout affects the adjustment of the industrial structure, and its growth has resulted in negative effects. This study can provide a reference for understanding the internal relationship between trade and the environment, and diminishing the negative effects of foreign trade on the environment, and providing advice on environmental regulation, and promoting the coordinated development of trade and the environment in Guizhou Province.

INTRODUCTION

China's economy continues to develop rapidly, with its total economic output ranking second in the world and its development achievements attracting worldwide attention. However, the extensive growth mode of China's economy has not been fundamentally changed. China's high economic growth comes at the cost of over-exploitation and inefficient utilization of natural resources and destruction of the environment. Notably, the reserve of natural resources and the environmental carrying capacity are limited. Environmental problems have become a major issue that hinders the sustainable development of China's economy. The total volume of import and export trade also continues to grow at a fast pace with the rapid development of the economy. These developments cause a series of problems, such as environmental pollution and ecological deterioration, which cannot be ignored. As a party engaging in trade openness, China's expansion of economic activities has increased resource consumption and damaged the ecological environment. Moreover, because of the large proportion of pollution-intensive products, the increase in export trade leads to a rise in pollution emissions.

Guizhou Province is one of the China's important provinces in the western region. With the advancement of China's opening up to the west and relying on its own energy advantages and industrial and agricultural bases, Guizhou has ushered its economy into a period of rapid development and has become an important energy and heavy industry base in the southwestern region of China. The foreign trade of Guizhou has developed rapidly, but its fragile environment exerts strong binding forces on economic development and opening up. The benefits attributed to the rapid growth of foreign trade have not kept pace with the growth, and the situation of resource waste and environmental pollution is becoming increasingly serious with the expansion of the trade scale. The negative effects of foreign trade have also become increasingly prominent. As shown in Fig. 1, the economic structure of Guizhou is unbalanced. Its economic development mode is defective, and its economic growth depends on the prolonged exploitation and utilization of natural resources, especially coal. Moreover, the environmental pollution accumulated through extensive economic growth is serious. Therefore, we must pay attention to the study of the relationship between foreign trade and environment. Taking Guizhou Province as an example,

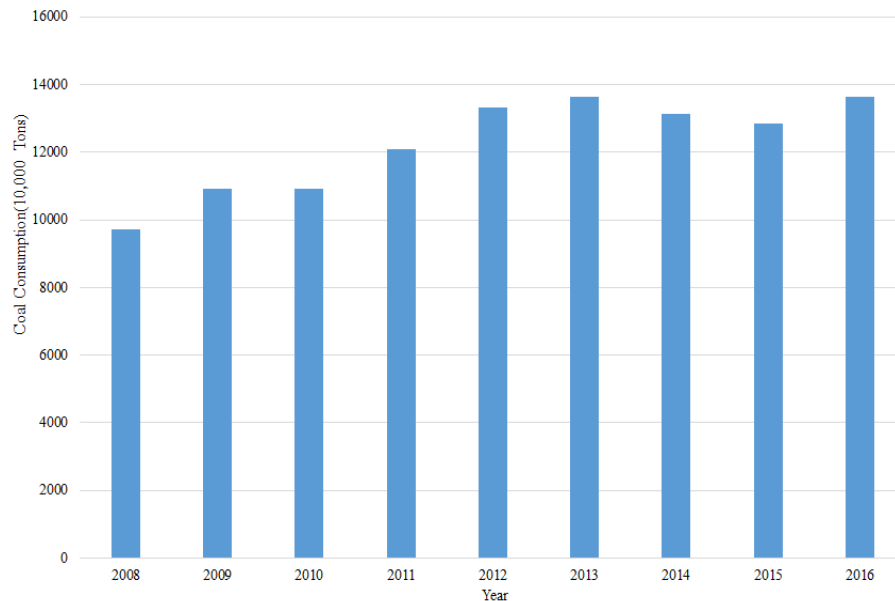


Fig. 1: Coal consumption in Guizhou Province from 2008-2016.
(Data from the China Statistics Database, <http://data.stats.gov.cn/index.htm>)

this study identifies the relationship between foreign trade and the environment, and determines the means to achieve coordinated development, and establishes Guizhou into an economic development-oriented and environment-friendly society to promote the coordinated development of the opening up policy and the environment.

EARLIER STUDIES

Foreign research on foreign trade and the environment began early, and the research results are abundant. However, the research conclusions still lack consistency. The numerous complex issues involved in the relationship between foreign trade and environmental quality have been heatedly debated in the international academia. Discussing the environmental effects of trade at the theoretical level and studying the relationship among economic growth, trade openness, and environmental pollution can enrich theoretical contents. Grossman et al. (1991) believed that the positive and negative impacts of scale, structural, and technological effects determine whether the impact of foreign trade on environmental pollution was positive or negative. Birdsall et al. (1993) believed that development of foreign trade expanded the economic scale, thus directly increasing environmental pollution. Considering the principle of comparative advantage, Copeland et al. (1995) argued that the impact of foreign trade on the environment was that pollution-intensive industries were transferred from developed to developing countries or from countries with strong environmental control to those with weak

environmental control. By comparing Mexico and Chile, two countries with different degrees of development, Beghin et al. (1995) found that the trade openness led to increased pollution to the ecological environment regardless of the degree of development. Copel et al. (1995) studied the trading system of emission permits and concluded that the development of free trade led to increased emissions of global pollutants. Azhar et al. (2007) investigated the relationship between changes in the industrialization patterns of foreign trade and specialization and environmental pollution. McAusland et al. (2013) compared the different impacts of Chinese and international trade on the environment and reported that the former and the latter increase and decrease pollution emissions, respectively. Erdogan (2014) analysed the impacts of international productivity differences on environmental quality and found that complete free trade could help reduce pollution levels in member countries of the Organisation for Economic Cooperation and Development and that approximately half of the reduction was from international productivity differences. Cherniwchan et al. (2016) summarized the literature on linkages between international trade and the environment and provided the structure of this review by linking changes in emissions with those in production activities at all levels in factories, companies, and industries. Copeland (2016) reviewed recent studies on the implications of endogenous policies on the impact of trade on environmental sustainability and the stock of renewable resources. He reported that pollution policies were recognized as endog-

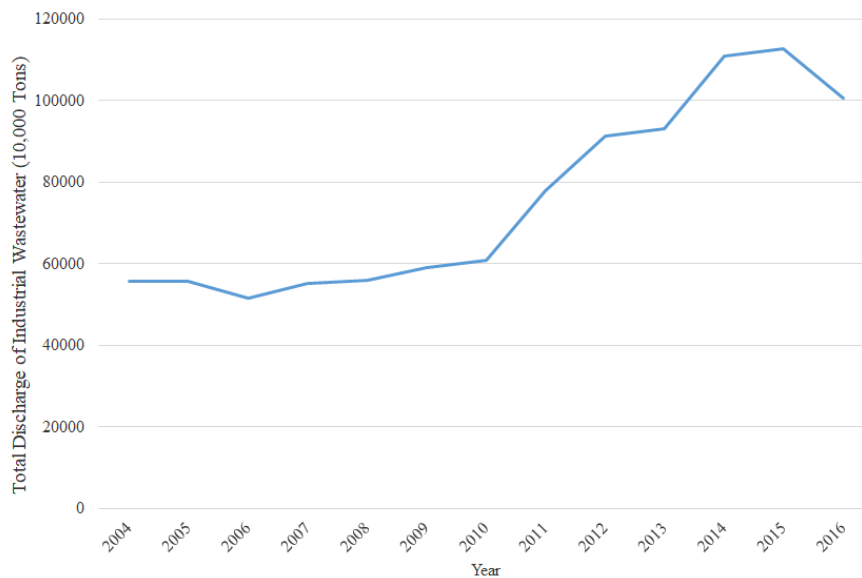


Fig. 2: Total discharge of industrial wastewater in Guizhou Province from 2004-2016. (Data from the China Statistics Database, <http://data.stats.gov.cn/index.htm>)

enous. The study of Cherniwchan (2017) showed that trade liberalization decreased the number of plants affected by pollutants. The 2/3 reduction in PM10 and SO2 emissions from manufacturing in the United States between 1994 and 1998 could be attributed to trade liberalization. Bildirici et al. (2017) explored the relationship among environmental pollution, economic growth, and energy consumption of hydropower under the different economic cycle systems of the G7 countries during 1961-2013. The studies of Duan et al. (2017) were based on the World Input-Output Database and used the revised terms of trade (PTT) index. The results showed that the change in global trade pattern is an important driving force behind the different changes in PTT. Sakamoto et al. (2017) studied the relationship between environment-related efficiency and export performance, and the empirical results showed that efficiency has a minimal impact on export performance in industries with relatively low freedom, and the impact of efficiency depends on industry characteristics. Wang et al. (2017) discovered that international exports and inter-provincial trade increased the health burden of air pollution in China's inland underdeveloped provinces. In China's effective regional air quality planning, trade plays an important role but is often easily ignored. The conclusions of existing research on the relationship between foreign trade and environmental pollution level are inconsistent, possibly because of the different sources of sample data and various estimation methods. Therefore, taking Guizhou Province as an example, this study establishes dynamic panel data at the municipal level in Guizhou Province, and analyses the relationship between

foreign trade and environmental pollution, and draw conclusions of their relationship from the perspective of empirical research. In addition, this work proposes suggestions for environmental regulations and policies and for the trade and economic development of Guizhou. This study has practical importance for the coordinated development of the economy and the environment in Guizhou Province.

CURRENT SITUATION OF ENVIRONMENTAL POLLUTION IN GUIZHOU PROVINCE

Water Pollution

Guizhou Province is experiencing a serious shortage of water resources. The per capita water resource possession is lower than the national average level, and the distribution of water resources is seriously uneven. Guizhou Province is located in China's inland, and the lack of ocean vapour leads to the shortage of water resources. Aside from water shortage, Guizhou also suffers from widespread water pollution. The discharge of industrial wastewater is an important reason behind the aggravated water pollution. As shown in Fig. 2, the total discharge of industrial wastewater in Guizhou Province increased from 2004 to 2016 and reached 128.0312 million tons in 2015, with an average annual growth rate of 6.74%. As shown in Table 1, the content of main pollutants in industrial wastewater decreases yearly, which indicates that Guizhou Province has effectively reduced the content of major pollutants in industrial wastewater by strengthening the treatment of industrial pollutants and upgrading the technology of industrial emission reduction.

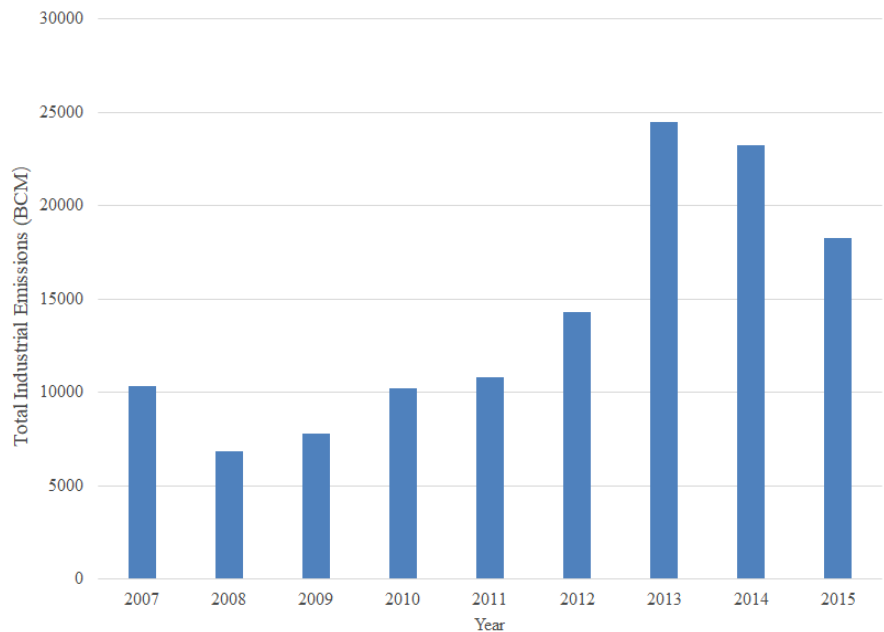


Fig. 3: Total emissions of industrial waste gas in Guizhou Province from 2007-2015.
(Data from the EPS Data Platform, <http://olap.epsnet.com.cn>)

Air Pollution

Energy mining and coal-heavy chemical enterprises in Guizhou Province cause serious air pollution. In several small- and medium-sized enterprises, pollutant smuggling occasionally occurs, resulting in frequent air pollution problems, such as smog, in winter and spring. As shown in Fig. 3, the main pollutant emissions from industrial exhaust in Guizhou Province increased from 10.356 billion standard cubic meters in 2007 to 2446.6 billion standard cubic meters in 2013 then decreased in 2014 and 2015. Overall, the industrial exhaust emissions in Guizhou Province have been increasing.

Solid Waste Pollution

The discharge of industrial solid waste in Guizhou Province increased steadily in a small fluctuation from 598.588 million tons in 2007 to 935.599 million tons in 2017. The average annual growth rate of industrial solid waste production is 5.62%. Overall, industrial solid waste production slightly increased annually before 2013 and sharply increased in 2015, then remained at a high level. The overall upward trend is evident (Fig. 4).

EMPIRICAL RESEARCH

Econometric Model

Considering the factors related to data availability in Guizhou Province, an econometric model of panel data is established as shown in Formula (1).

$$\ln Z_{it} = \alpha_1 \ln Y_{it} + \alpha_2 (\ln Y_{it})^2 + \alpha_3 \ln FDI_{it} + \alpha_4 (\ln FDI_{it})^2 + \alpha_5 \ln TR_{it} + \alpha_6 \ln ST_{it} + c + \varepsilon_{it} \quad \dots(1)$$

Where it represents the corresponding data of city i in t year and Z_{it} represents the pollutant discharge situation of city i in t year. In this study, “solid” is used to represent the production of industrial solid wastes, and “water” is used to represent the discharge of industrial wastewater. Y_{it} is the GDP output of city i in t year. FDI_{it} indicates the foreign direct investment of city i in t year. TR_{it} expresses the foreign trade situation of city i in t year, reflecting the scale effect. ST_{it} expresses the industrial structure of city i in t year, reflecting the structural and product effects. c represents the intercept term, and ε_{it} denotes the error term.

Data Sources and Explanations

According to the specific situation of Guizhou Province, this study uses the dynamic panel data of cities at all levels to conduct an empirical analysis of the impact of environmental pollution on trade. On the basis of the statistical data of six prefecture-level cities and three autonomous prefectures in Guizhou Province from 2007 to 2016, this study analyses the relationship between foreign trade and the environment of cities' panel data in Guizhou Province. The statistical data on GDP, industrial wastewater discharge, industrial solid waste production, foreign investment, foreign trade, and related influencing factors are mainly from the State Statistical Yearbook of Guizhou (<http://www.gz.stats.gov.cn/>).

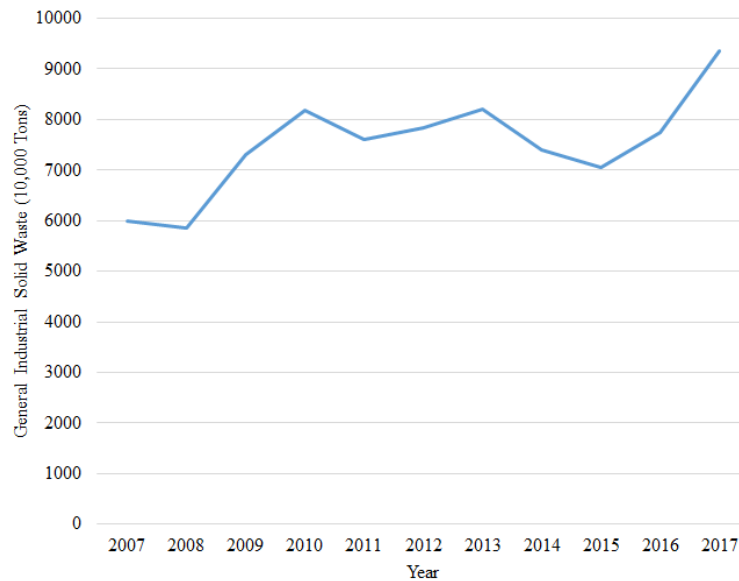


Fig. 4: General industrial solid waste in Guizhou Province from 2007-2017. (Data from the Zhongjing Statistical Database, <http://db.cei.cn>)

Result Analysis

A fixed-effect regression model is established by using the research methods adopted by most studies. Three models, namely, hybrid, individual fixed-effect, and time fixed-effect models, are used for the analysis. The specific regression results are shown in Table 2.

The following conclusions are obtained from Table 2:

1. A U-shaped relationship exists between environmental pollutant emissions and GDP in Guizhou Province, that is, the income and scale effects of economic growth are initially reduced, and then increased pollutant emissions. Given that the environment has a certain self-purification capacity, the discharge of pollutants within this capacity range does not cause environmental pollution, which belongs to the free use of the environment (the marginal environmental cost is zero). Therefore, "zero pollution" does not conform to the principles of environmental economics.
2. The growth of foreign investment and the discharge of industrial solid wastes and wastewater in Guizhou Province show an inverted U-shaped change. This conclusion verifies the environmental Kuznets curve hypothesis that short-term foreign investment results in negative technological effects, and the growth of foreign investment increases the discharge of industrial wastewater and the production of solid wastes. However, in the long run, given that foreign direct investment leads to advanced technology and production management standards, and pollu-

tion emissions gradually decrease when the emission peaks.

3. The layout of Guizhou's foreign trade and economy affects the adjustment of the industrial structure. The product and structure effects show significant negative effects. The increase in industrial proportion caused by foreign trade promotes the growth of industrial solid waste and industrial wastewater. Statistically significant estimates show that for Guizhou Province, when the proportion of the industrial output value to GDP is large, the emissions of industrial pollutants measured by different indicators are low.
4. The negative scale effect of Guizhou's foreign trade growth is consistent with the current theory of "polluter's paradise," which supports the establishment of the hypothesis in Guizhou Province. Guizhou's foreign trade belongs to the "high energy consumption, high pollution, and resource-based" export mode. For a long time, processing trade has been the main mode, with low added value of export manufactured goods and poor terms of trade. The vast majority of Guizhou's foreign trade is composed of resource, pollution, and emission intensive industries. The growth of Guizhou's foreign trade and the extensive foreign trade model have placed tremendous pressure on Guizhou's ecological, environmental and resource systems and increased other pollutant emissions.

POLICY RECOMMENDATIONS

Expanding the Participation in Foreign Trade and Ac-

Table 1: Emissions of major pollutants from industrial wastewater in Guizhou Province from 2011-2016. (Data from the China Statistics Database, <http://data.stats.gov.cn/index.htm>)

Index	2016	2015	2014	2013	2012	2011
Chemical oxygen demand emissions (10,000 tons)	25.59	31.83	32.67	32.82	33.3	34.22
Ammonia nitrogen emissions (10,000 tons)	3.08	3.64	3.8	3.83	3.87	3.98
Total nitrogen emissions (10,000 tons)	4.25	4.76	4.7	4.38	4.68	4.44
Total phosphorus emissions (10,000 tons)	0.39	0.48	0.49	0.44	0.45	0.45
Petroleum emissions (tons)	136.61	412.76	330.79	437.39	461.81	483.83

Table 2: Regression results.

Explanatory variable	Solid			Water		
	Hybrid model	Individual fixed-effect model	Time fixed-effect model	Hybrid model	Individual fixed-effect model	Time fixed-effect model
C	-1.621	2.012*	-1.201	1.641***	8.241*	0.412
$\ln Y_{it}$	1.012*	0.614*	1.654*	1.325*	-0.254*	1.245*
$(\ln Y_{it})^2$	0.001	0.004*	-0.142*	-0.064	0.017	0.006*
$\ln FDI_{it}$	0.214	0.541***	-0.541	0.674	0.034	0.011***
$(\ln FDI_{it})^2$	-0.026*	-0.012*	-0.154*	0.004*	-0.741*	0.019*
$\ln TR_{it}$	-0.214*	0.141**	-0.364*	-0.087**	0.011**	-0.697*
$\ln ST_{it}$	0.245*	0.110*	0.003*	0.451	0.234*	0.221*
R-squared Adjusted	0.741	0.904	0.845	0.421	0.931	0.845
AIC	1.801	0.354	1.647	2.221	0.108	1.414
SC	1.845	0.641	1.845	2.303	0.478	1.254
DW	0.147	0.365	0.098	0.654	0.574	0.109

(In the table, *, ** and *** indicate significance at 1%, 5% and 10% levels, respectively)

celerating the Opening Up

The scale of import and export trade in Guizhou Province is gradually expanding. Heavy industries, such as petroleum and minerals, account for a large proportion of the industry and provide a small contribution to foreign trade. By contrast, light industries, such as textile and garment, account for a small proportion of the industry and a large proportion of foreign trade commodities. We should further study and develop the strategy of opening up to the west, change geographic and resource advantages into the actual driving force of economic development, and establish trade cooperation with other countries. In addition, investment attraction should be increased, and the scope of foreign capital utilization should be broadened. Innovating technology, building a brand, and realizing the sound and rapid development of foreign trade are crucial. Furthermore, the export of products from high-polluting industries should be reduced, and the comparative advantages of production factors in Guizhou Province should be fully utilized, and a sustainable development route of trade development and ecological environment coordination in Guizhou Province should be realized.

Adjusting the Structure of Import and Export Products to Reduce Environmental Damage

Guizhou Province should pay attention to the marketing of green products in the international market during the development and production of its own green products and take this as a guide to promote the optimization and upgrading of the export structure. To further improve the construction of a green food standard system and strengthen the management of green food labels, international registration of green food trademarks must be conducted in an organized manner; the selection and certification of the origin of raw materials must be carefully examined, and follow-up supervision and management should be performed. In the development of green food, attention should be provided to the development, introduction, and screening of production methods to tackle key technical problems and form a means of green food production and its supporting technical service system. Attention should also be provided to expanding the scale of green products, continuously optimizing products, enriching varieties, and steadily promoting the pace of market construction to gradually occupy and expand the international market scale.

Formulating Proper Import and Export Strategies and Setting Proper Environmental Standards

The growth mode of foreign trade, especially the structure of import and export products, should be changed. The export of self-owned brand products must be expanded with environmental protection technologies, and the export of highly polluting products must be controlled, and imports of advanced production technologies, environmental protection technology, and equipment from abroad should be encouraged. In foreign trade, the research, development, and introduction of clean production technology should be emphasized, and the green industry should be supported, and the production and export of green products should be developed. In addition, we should give appropriate tax credit preferences and prohibit the import of technologies and equipment that seriously pollute the environment. Proper environmental standards can put pressure on the export of polluting products, thus reducing the pollution intensity of export products. Exports can also efficiently pass the strict environmental standards of developed countries, thereby reducing the number of local enterprises that fail to reach foreign countries. The economic loss caused by the return of environmental standards can be reduced, and a good reputation can be established for products in the international market.

Optimizing the Self-Investment Environment and Developing the Environmental Protection Industry

Guizhou Province should strive to improve its own environment, including its natural and investment economic environments. The quality of the environment should be improved by making the environment an important means of attracting foreign investment, and sustainable development of environmental protection should be realized by expanding the use of foreign capital. Efforts to protect the natural environment must be intensified, and improvement of the fragile ecology of Guizhou should be attempted to prevent difficulties in introducing foreign capital due to the harsh natural environment. Efforts should be exerted to improve the management system related to the introduction of foreign capital, enhance the quality and efficiency of government services, and create a fair market environment, an open and transparent legal environment, and an efficient and nondiscriminatory administrative environment for the maximal use of foreign capital. At present, the main environmental protection scheme is the development of new clean energy. The market potential of clean energy is large. The excessive consumption of resources can be inferred as a broad market prospect of emerging energy. Many countries currently regard environmental protection as a key industry, in which the policy support is strong and the emphasis

is strengthened. Attention should also be provided to pollution control equipment, technology, services, energy saving, and bio-energy development.

CONCLUSIONS

In the early and middle stages of the sustainable development of foreign trade, China provided too much attention to economic interests and neglected the cost of the environment and resources. Therefore, China welcomed a large number of industries with high pollution, emissions, and energy consumption, which has resulted in a long-term surplus in foreign trade and a deficit in natural resources and has affected the sustainable development of the economy and environment. Taking Guizhou Province as an example, this study explores relevant studies on the interaction between foreign trade and environmental pollution, and summarizes the current situation of environmental pollution in Guizhou Province, and analyses the dynamic relationship between foreign trade and environmental pollution by using panel data at the municipal level of Guizhou Province from 2007 to 2016. Specific measures are introduced to control environmental pollution. The results show that the different sources of sample data and various estimation methods used in Chinese and foreign studies led to the inconsistency of existing conclusions on the relationship between foreign trade and environmental pollution. The main manifestations of environmental pollution in Guizhou Province are evident in the rising trends of industrial wastewater discharge, waste gas discharge, and solid waste discharge with a small fluctuation. The panel data regression model confirms that the relationship among environmental pollutant emissions, GDP, and foreign investment in Guizhou Province is U-shaped. The layout of the foreign trade economy affects the adjustment of the industrial structure. The growth of foreign trade has also exerted a negative scale effect. Therefore, further studies should be conducted in the following aspects: increasing the emission targets of environmental pollutants, prolonging the length of the study objects, and investigating the short-term impact principle of environmental pollution and foreign trade at different economic levels. Moreover, the construction of the coordination mechanism of international environmental and economic policies is worth studying.

REFERENCES

- Azhar, A. K. and Elliott, R. J. 2007. Trade and specialisation in pollution intensive industries: North-South evidence. *International Economic Journal*, 21(3): 361-380.
- Beghin, J., Roland-Holst, D. and Mensbrugge, D.V.D. 1995. Trade liberalization and the environment in the Pacific basin: Coordinated approaches to Mexican trade and environment policy. *Staff General Research Papers Archive*, 77(3): 778-785.

- Bildirici, M. E. and Gökmenođlu, S. M. 2017. Environmental pollution, hydropower energy consumption and economic growth: Evidence from G7 countries. *Renewable & Sustainable Energy Reviews*, 75: 68-85.
- Birdsall, N. and Wheeler, D. 1993. Trade policy and industrial pollution in Latin America: Where are the pollution havens? *The Journal of Environment and Development*, 2(1): 137-149.
- Cherniwchan, J., Copeland, B. and Taylor, M. S. 2016. Trade and the environment: New methods, measurements, and results. *Cesifo Working Paper*, 9(1).
- Cherniwchan, J. 2017. Trade liberalization and the environment: Evidence from NAFTA and U. S. manufacturing. *Journal of International Economics*, 105: 130-149.
- Copel, B. R. and Taylor, M. S. 1995. Trade and transboundary pollution. *American Economic Review*, 85(4): 716-737.
- Copeland, B. R. and Taylor, M. S. 1995. Trade and transboundary pollution. *The American Economic Review*, 85(4): 716-737.
- Copeland, B. R. 2016. Policy endogeneity and the effects of trade on the environment. *Agricultural and Resource Economics Review*, 34(1): 1-15.
- Duan, Y. and Jiang, X. 2017. Temporal change of China's pollution terms of trade and its determinants. *Ecological Economics*, 132: 31-44.
- Erdogan, A. M. 2014. Bilateral trade and the environment: A general equilibrium model based on new trade theory. *International Review of Economics and Finance*, pp. 52-71.
- Grossman, G. M. and Krueger, A. B. 1991. Environmental impacts of a North American free trade agreement. *Social Science Electronic Publishing*, 8(2): 223-250.
- Mcausland, C. and Millimet, D. L. 2013. Do national borders matter? Intranational trade, international trade, and the environment. *Journal of Environmental Economics and Management*, 65(3): 411-437.
- Sakamoto, T. and Managi, S. 2017. New evidence of environmental efficiency on the export performance. *Applied Energy*, 185: 615-626.
- Wang, H., Zhang, Y. and Zhao, H. 2017. Trade-driven relocation of air pollution and health impacts in China. *Nature Communications*, 8(1): 738.



Effect of Process Parameters on Adsorption of Cadmium from Aqueous Solutions by Activated Carbon Prepared from *Bauhinia purpurea* Leaves

H. Joga Rao*†, P. King** and Y. Prasanna Kumar***

*Department of Chemical Engineering, GMR Institute of Technology, Rajam, Andhra Pradesh, 532 127, India

**Department of Chemical Engineering, Andhra University College of Engineering, Visakhapatnam, Andhra Pradesh, 530027, India

***Visakha Institute of Engineering and Technology, Visakhapatnam, Andhra Pradesh, 530 008, India

†Corresponding author: H. Joga Rao

Nat. Env. & Poll. Tech.
Website: www.neptjournal.com

Received: 01-06-2018
Accepted: 02-08-2018

Key Words:

Bauhinia purpurea leaves
Activated carbon
Adsorption efficiency
Process parameters
Thermodynamic studies

ABSTRACT

Adsorption is one of the most versatile and widely used techniques for the removal of toxic metals from the aqueous solutions. Cadmium is the toxic metal selected for adsorption in this study and adsorbent of interest was activated carbon prepared from *Bauhinia purpurea* leaves as a plant biomass. The following process parameters were investigated during the batch adsorption process: The adsorption efficiency and cadmium deposition on the adsorbent surface were increased from 15.95 to 89.98%, 0.074 to 0.418 mg/g, and 7.27 to 89.97%, 0.034 to 0.418 mg/g with increasing contact time from 2 to 50 min and pH from 2 to 6.5, respectively. The adsorption efficiency was decreased from 89.98 to 45.96% and the amount of cadmium deposited on the surface of the ACBPL adsorbent was increased from 0.418 to 1.032 mg/g with an increase in solute concentration. The adsorption efficiency of cadmium decreased from 98.41 to 84.51% and 0.457 to 0.392 mg/L with an increase in particle size from 74 to 177 μm . The rate of adsorption of cadmium was increased from 61.31 to 96.34% with an increase in dosage of the ACBPL adsorbent from 0.05 to 0.15 g. The adsorption efficiency and cadmium deposition was decreased from 89.98 to 97.90%, 0.418 to 0.454 mg/g as the temperature increased from 303K to 323K. The variation of thermodynamic energy parameters (ΔG° , ΔH° and ΔS°) with the solution temperature described that the adsorption process is endothermic, spontaneous at high temperatures and non-spontaneous at low temperatures. The positive value of ΔS , reflecting the high degree of disorder in the adsorbent/adsorbate interface that is formed during the transition.

INTRODUCTION

Freshwater is a limited resource in many parts of the world. The major fact for this paucity of freshwater is not only due to demand for water, but also due to pollution of freshwater ecosystems. Due to the pollution created by human beings, the usable water has decreased drastically and the cost of purifying the water has increased dramatically. The rapid pace of population growth, industrialization and improper planning of urban development activities have been severely contributing to the contamination of water and soil systems. The persistence of heavy metals (zinc, copper, nickel, lead, chromium, cadmium, mercury, etc.) in the aquatic ecosystems results in a serious threat because of their toxicity, bioaccumulation, and bio-magnification in the food chains (Momodu et al. 2010, Rao et al. 2010). Among all the heavy metals, Cd(II) is the predominant one as it is generated from a majority of industrial operations such as metal plating industries, electroplating industries, petrochemical industries, refining of ores, and battery production (Fu et al.

2011, Akunwa et al. 2014). Cadmium is discharged into the environment due to the industrial processing of metals like zinc, aluminium, etc. The cadmium enters the food chain through the uptake of contaminated water and soil by the plants. A 0.005 mg/L is set as the maximum cadmium concentration in the domestic water supplies by the World Health Organization and the EUD directive. Excessive cadmium concentration in drinking water can lead to a number of health effects, mainly cancer, malfunctions of human kidneys, damage of bones, and many other ailments (Akunwa et al. 2014, Debasree et al. 2014). Formation of stones in the kidney and calcium metabolism is caused due to the excessive intake of cadmium. Adsorption is one of the most versatile and widely used techniques for the removal of metal ions. Activated carbon is the most effective and widely used adsorbent, because it has large specific surface area, micro-porous structure and excellent adsorption ability (Kannan et al. 2005). Activated carbon has been the water industry's standard adsorbent for the reclamation of municipal and industrial wastewater for potable use for decades. Despite its pro-

lific use in the water and wastewater treatment plants, activated carbon remains an expensive material. In recent years, research interest in the production of low cost (Akunwa et al. 2014, Kannan et al. 2005) activated carbon produced from diverse materials has grown. Low cost activated carbons are prepared by thermo-chemical methods from various materials and plant biomass to remove heavy metals from effluents (Venkatesan et al. 2013). The aim of the present study is to investigate the feasibility of alternative, low cost and novel adsorbents for efficient removal of cadmium from an aqueous solution. From the survey of the literature, no information is available for the adsorptive removal of cadmium by activated carbons prepared from *Bauhinia purpurea* leaves as adsorbent. The present work focuses on the adsorption process parameters. Initial metal ion concentration, pH, temperature and adsorbent dosage are the input variables considered for the optimization of heavy metal removal. Thermodynamic studies have been used to evaluate the thermodynamic energy parameters and compare the adsorption capacities of metals used with activated carbon prepared from *Bauhinia purpurea* leaves.

MATERIALS AND METHODS

***Bauhinia purpurea* leaves:** The adsorbent, *Bauhinia purpurea* leaves used in the present study were collected from Rajam and Srikakulam, Andhra Pradesh, India. *Bauhinia purpurea* is used in several traditional medicine systems to treat various diseases. Water extracts of *Bauhinia purpurea* leaves have been shown to have anti-ulcer activity in animals in the 'ethanol-induced gastric ulcer model'. *Bauhinia purpurea* may possess antibacterial, antidiabetic, analgesic, anti-inflammatory, anti-diarrheal, anticancerous, nephroprotective, and thyroid hormone-regulating activity (Zakaria et al. 2011, Kumar et al. 2011).

Chemicals and reagents: The chemicals of AR/LR grades supplied by different standard manufacturing industries are given in Table 1.

Preparation of adsorbent: The *Bauhinia purpurea* leaves were washed several times with deionized water until the wash water contains no dirt. The washed leaves were completely dried under sunlight for 30 days and cut into small pieces and powdered using domestic mixer. The powder was dried in an oven at 100°C for 120 min. The dried material was now placed in the cooker for carbonization and it was heated continuously for 10 min. The dried material was activated to 650°C for 120 min in a covered silica crucible by heating in a muffle furnace. After that, 100 g of carbon powder was taken and mixed with 100 g ZnCl₂ dissolved in 500 mL of distilled water containing 22 g of HCl. The chemically treated material was left overnight and carbonized.

Table 1: Chemicals and reagents.

Reagent	Company	Purity
Cadmium Nitrate Cd (NO ₃) ₂	S. D. Fine Chem. Pvt. Ltd.	99.5%
Hydrochloric Acid (HCl)	Sarabai Company, India	35%
Zinc Chloride (ZnCl ₂)	Fischer Inorganics Ltd.	70%

Table 2: Range of adsorption process parameters covered in the present study.

Process parameter	Cadmium	
	Min	Max
Contact time, <i>t</i> (min)	2	80
Initial metal ion concentration of the solution, <i>C_i</i> (mg/L)	2	10
Solution pH	2	10
Average particle size of the adsorbent, <i>d</i> (μm)	74	177
Dosage of the adsorbent, <i>w</i> (g)	0.025	0.15
Temperature, <i>T</i> (K)	303	323

Carbonized material was refluxed with 10% HCl solution for 180 min and filtered. This was followed by drying of the material at 100°C for 24 hrs. The dried product was sieved to desired particle size range of 74-177 μm (Fig. 1).

Preparation of metal solutions: Adsorbate solutions of cadmium with a concentration of 1000 mg/L were prepared separately by dissolving 2.7442 g of 100% Cd(NO₃)₂ in 1000 mL of double distilled water. From the standard stock solution, working solutions of lower concentrations were prepared with cadmium (2, 4, 6, 8 and 10 mg/L), used for batch experiment. After adsorption, the final effluent solution was analysed by atomic absorption spectrophotometer of Perkin Elmer model-3100, a flame type AAS.

Batch adsorption experimental studies: The adsorption study of cadmium was conducted in the exploratory conditions of various effective parameters like pH 2-10, contact time of 2-120 min, metal ion concentration of 2-10 mg/L, the dosage of the adsorbent 0.025-0.15 g and the particle size of the adsorbent from 74 (200 mesh)-177 (80 mesh) μm. Agitation speed of 250 rpm was kept constant in the orbital shaker with the suitable time interims from 2 -120 min. The mixed adsorbent solutions were taken out and filtered through Whatman filter paper and analysed for metal ion concentration in an Atomic Absorption Spectrophotometer (Perkin Elmer model-3100). Batch experiments were conducted at various temperatures (303 K-323 K) of the metal solution using orbital shaker with optimum contact time of 50 min at pH of 6.5. Samples were analysed by AAS for metals to assess the thermodynamic parameters and study the feasibility of the process with temperature.

Metal adsorption capacity: The amount of metal deposited on the adsorbent surface was determined by performing at different contact times (2-90 min), temperatures (303-323K) and pH (2-8) etc., for both the adsorbents. After experimentation, the amount of metal deposited on the adsorbent surface was calculated by using the following equation:

$$q_t = \frac{V(C_i - C_f)}{1000w} \quad \dots(1)$$

Where, q_t is the amount of metal deposited on the adsorbent surface (mg/g), C_i is the initial solute concentration in the solution before adsorption (mg/L), C_f is the final concentration of solute in the solution after adsorption (mg/L), V is the volume of metal solution (L) and w is the dosage of the adsorbent (g).

Thermodynamic studies: Thermodynamic studies provide information about the feasibility of the adsorption process. It also plays an important role in the study of the nature of adsorption process. The thermodynamic energy parameters like enthalpy change (ΔH°), entropy change (ΔS°), and Gibb's free energy (ΔG°) are used to determine the spontaneity, heat change and affinity of the adsorption process. The Van't Hoff equation describes the thermodynamic parameters by using the following linear and nonlinear equations,

$$\frac{d \ln K_e}{dT} = \frac{\Delta H}{RT^2} \quad \dots(2)$$

$$\ln K_e = \frac{\Delta S^\circ}{R} - \frac{\Delta H^\circ}{RT} \quad \dots(3)$$

Where, R is gas constant (8.314 J/mol K) and K_e is the adsorption equilibrium constant equivalent to q_e/C_e . Van't-Hoff plot with $\ln K_e$ as a function of $1/T$ yields a straight line and ΔH° and ΔS° can be evaluated from the slope and intercept, respectively. The relationship between ΔG° and K_e is given by the following equation,

$$\Delta G^\circ = -RT \ln K_e \quad \Delta G^\circ = -RT \ln K_e \quad \dots(4)$$

For significant adsorption to occur, the Gibb's free energy change of adsorption, ΔG° , must be negative. As a thumb rule, a decrease in the negative value of ΔG° with an increase in temperature indicates that the adsorption process is more favourable at higher temperatures. This could be possible because the mobility of adsorbate ions/molecules in the solution increase with an increase in temperature and that the affinity of adsorbate on the adsorbent is higher at high temperatures. On the contrary, an increase in the negative value of ΔG° with an increase in temperature implies that lower temperatures make the adsorption easier. A negative value of ΔH° implies that the adsorption phenomenon



Fig.1: Activated carbons prepared from *Bauhinia Purpurea* leaves with average particlesize of 149 μm .

is exothermic while a positive value implies that the adsorption process is endothermic. In an endothermic process, the adsorbate species has to displace more than one water molecule for their adsorption and this results in the endothermicity of the adsorption process (Awwad et al. 2014, Venkatesan et al. 2013). A positive value of ΔS° reflects the affinity of the adsorbent towards the adsorbate species.

RESULTS AND DISCUSSION

Batch experiments were carried out to study the effect of process parameters such as contact time (t), solution pH, initial metal concentration (C_i), the dosage of the adsorbent (w), average particle size of the adsorbent (d) and temperature of the solution (Fig. 2). This section also deals with thermodynamic studies of the adsorption of cadmium using activated carbon prepared from *Bauhinia purpurea* leaves as an adsorbent.

Effect of contact time: The adsorption efficiency and metal accumulated on the adsorbent surface determined at different contact times are shown in Figs. 2 & 3. The percentage removal and cadmium accumulated on the adsorbent surface were increased with an increase in contact time from 2 to 50 min and thereafter reached plateau after attaining equilibrium at 50 min. The rapid adsorption at the early stages of contact period indicates the availability of more number of active sites on the surface of the adsorbent and also due to the thermal-chemical treatment process during the preparation of activated carbon from *Bauhinia purpurea* leaves. At later stages of adsorption, the external adsorbent surface was saturated with cadmium molecules, thus the adsorption proceeds on interior walls of the adsorbent surface. The slower adsorption rate towards equilibrium was due to the availability of less number of vacant sites on the adsorbent surface (Fu et al. 2011). After equilibrium, the adsorption rate was very slow with longer contact time, concluded the possible involvement of chemical bonding between cadmium

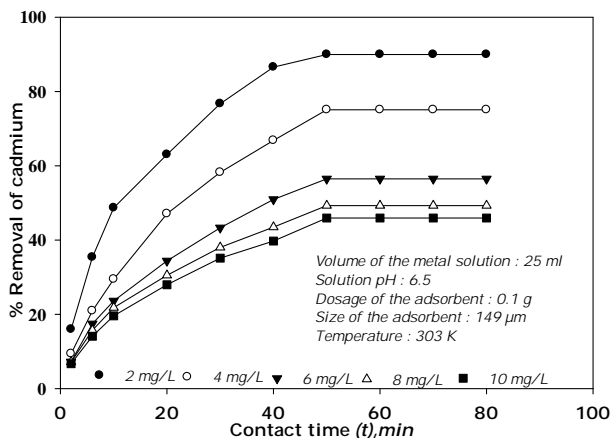


Fig. 2: Effect of contact time on % removal of cadmium.

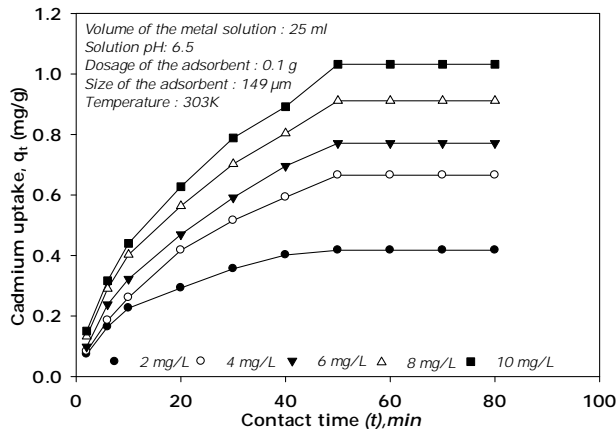


Fig. 3: Effect of contact time on cadmium uptake.

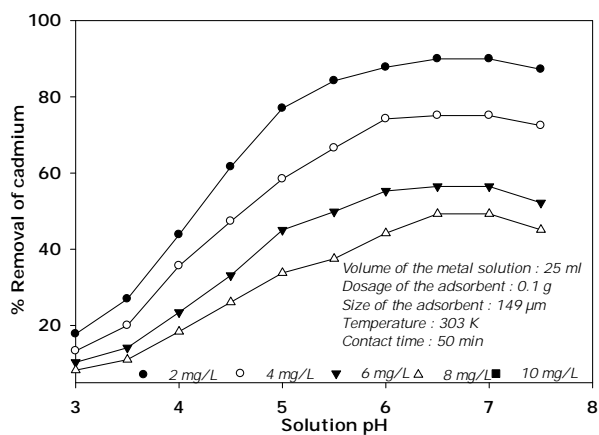


Fig. 4: Effect of solution pH on % removal of cadmium.

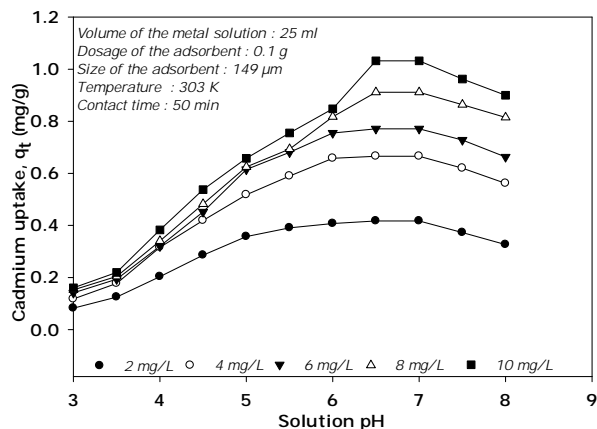


Fig. 5: Effect of solution pH on cadmium uptake.

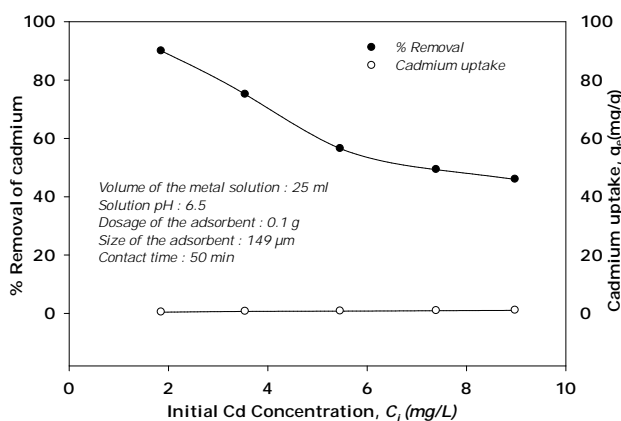


Fig. 6: Effect of initial concentration on % removal and cadmium uptake using ACBPL as an adsorbent.

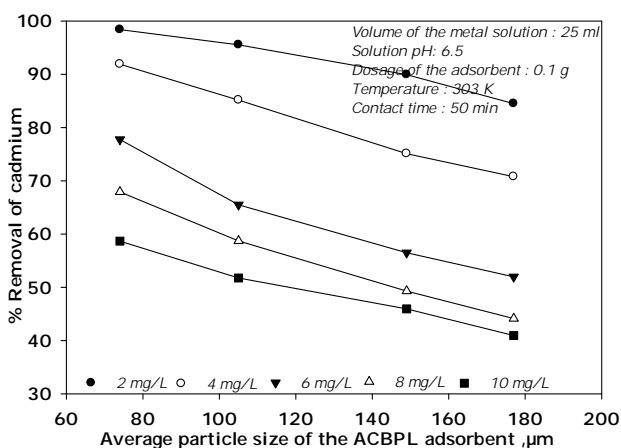


Fig. 7: Variation of % removal of cadmium with average particle size of the adsorbent.

molecule and adsorbent surface. The adsorption efficiency and cadmium accumulated on adsorbent surface were increased from 15.95 to 89.98% and 0.074 to 0.418 mg/g, respectively with increasing contact time from 2 to 50 min for 2 mg/L initial concentration. A similar procedure was repeated for 4, 6, 8 and 10 mg/L metal concentrations of cadmium and the results showed the same contact time of 50 min.

Effect of solution pH: The adsorption process, mostly affected by changing the pH of metal solution. The pH of the solution will affect the surface charges of the adsorbent as well as the degree of ionization of different metal ions in the aqueous solution. The effect of pH on adsorption of Cd at constant temperature (303 K) for varying concentrations and contact time of 50 min is shown in Figs. 4 and 5. It was observed that as the pH of the solution varied from 3 to 5, the adsorption efficiency was very low because repulsion was taking place between the solution and *ACBPL* adsorbent. The adsorption efficiency and cadmium deposition were highly increased with an increase in pH from 5 to 6.5, because the effluent solution was exposed to the negative charges and strongly attracted the Cd^{+2} ions with the adsorbent surface (Leandro et al. 2014). The increase in solution pH from 6.5 to 8 leads to undergo hydrolysis process forming a precipitation of cadmium hydroxide ($\text{Cd}(\text{OH})_2$) and carbonate ($\text{Cd}(\text{CO}_3)_2$) in the metal solution (Bohli et al. 2013). Therefore the adsorption efficiency and cadmium deposition increased from 7.27 to 89.97% and 0.034 to 0.418 mg/g respectively, with an increase in solution pH from 2 to 6.5 for 2 mg/L of the initial concentration.

Effect of initial concentration of metal in solution: At low initial metal concentration, numbers of unoccupied active sites are available on the adsorbent surface for the adsorption of metal from the solution. Under these conditions, the ratio of available adsorption active sites to the solute concentration was higher and hence leads to higher adsorption efficiencies. When the initial solute concentration increases, the active sites required for the adsorption of the solute will not be sufficient to accommodate the increased solute concentration in the solution. This led to the available active sites on the adsorbent surface completely filled with the solute and decreased the adsorption efficiency. The Fig. 6 shows that the adsorption efficiency of cadmium was decreased from 89.98 to 45.96% and the amount of cadmium deposited on the surface of the *ACBPL* adsorbent was increased from 0.418 to 1.032 mg/g with an increase in solute concentration. At lower concentrations, all cadmium ions present in the solution could interact with the binding sites and accordingly the rate of adsorption was higher than those at higher initial cadmium ion concentrations (Umar et al. 2015). At higher concentrations, the lower adsorption yield

is due to the saturation of adsorption sites.

Effect of average particle size of adsorbent: The number of active sites per unit volume of adsorbent for solid-liquid interface highly influences the adsorption efficiency and metal deposited on *ACBPL* surface. The contact of the solid-liquid is higher for smaller particles when compared with larger particles, which shows that there was more rapid adsorption and high mass transfer to enhance the adsorption process (Venkatesan et al. 2013). Figs.7 & 8 show that the removal efficiency of the cadmium adsorption process was increased with the decrease of the particle size of activated carbon of *Bauhinia Purpurea* leaves indicating that the cadmium ion adsorption occurs by a surface phenomenon. It reveals that the percent removal and cadmium accumulated on the activated carbon of *Bauhinia Purpurea* leaves was decreased from 98.41 to 84.51% (at t : 50 min, pH: 6.5 and T : 303 K) and 0.457 to 0.392 mg/L respectively, with an increase in particle size from 74 to 177 μm for 2 mg/L of cadmium concentration in solution.

Effect of dosage of adsorbent: The dosage of the adsorbent is an important parameter to determine the capacity of an adsorbent for a given initial concentration of the effluent. The rate of adsorption of cadmium was increased from 61.31 to 96.34% with an increase in dosage of the *ACBPL* adsorbent from 0.05 to 0.15 g at an initial concentration of 2 mg/L, pH 6.5 and contact time of 50 min as shown in Fig. 9. Similar trends were obtained for the initial metal concentration of 4, 6, 8 and 10 mg/L of cadmium by varying dosage of the *ACBPL* adsorbent from 0.05 to 0.15 g. Fig.10 shows that the amount of cadmium deposited on the *ACBPL* adsorbent surface was decreased from 1.14 to 0.30 mg/g with an increase in dosage of the adsorbent from 0.05 to 0.15 g/25 mL of solution. These results illustrate that the percent removal was increased with an increase in dosage of the *ACBPL* adsorbent, because of an increase in the number of available active sites on the adsorbent surface. The decrease in metal deposition on the adsorbent surface with an increase in dosage of the adsorbent could be due to the reduction in the available surface area of the adsorbent for the adsorption of metals due to overlapping of adsorbent particles (Mona et al. 2014).

Effect of temperature: Temperature plays an important role in the adsorption, since it is an energy dependent mechanism which involves the binding of metal onto cell wall. It alters the cell wall stability, configuration and ionization of the functional groups on the cell wall surface. The above factors parallelly affect the binding sites on the adsorbent cell wall which results in the reduction of metals. These changes may play positive or negative roles in the adsorption of metals. The temperature has two major effects on the

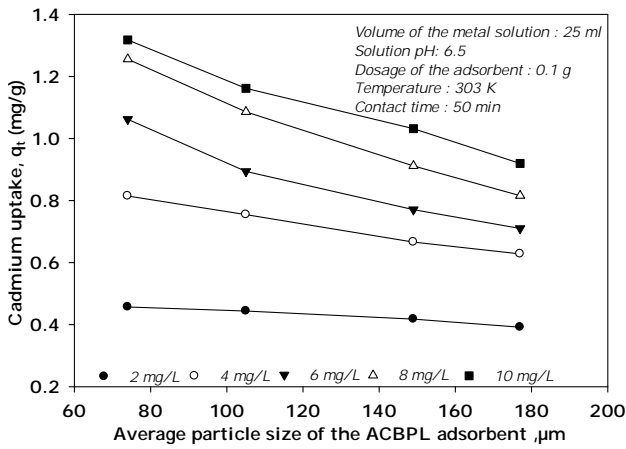


Fig. 8: Variation of cadmium uptake with average particle size of the adsorbent.

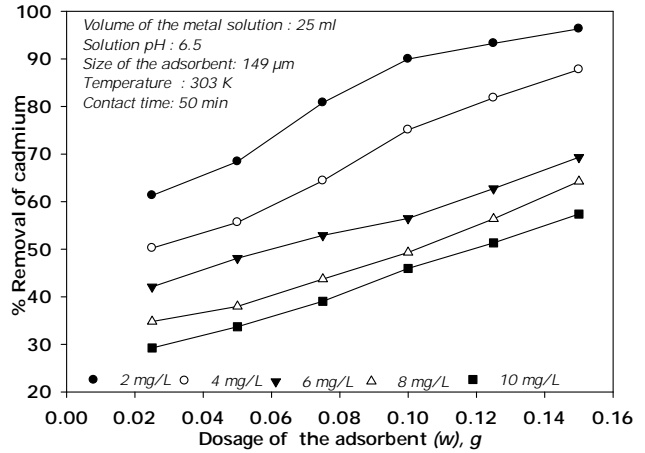


Fig. 9: Effect of dosage of the adsorbent on % removal of cadmium.

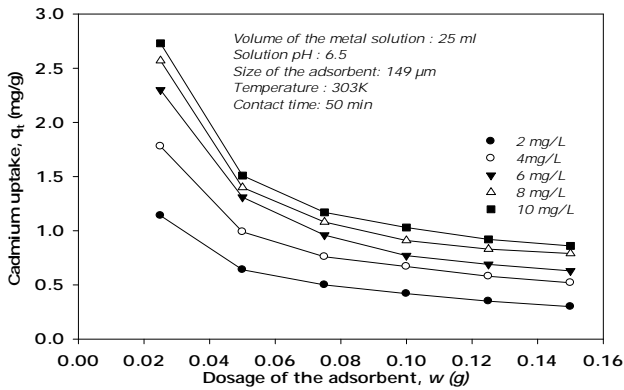


Fig. 10: Variation of cadmium uptake on the adsorbent surface with dosage of the adsorbent.

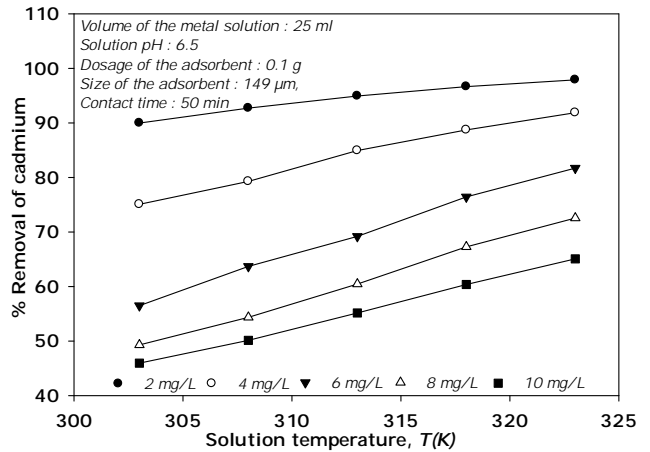


Fig. 11: Effect of temperature on % removal of cadmium.

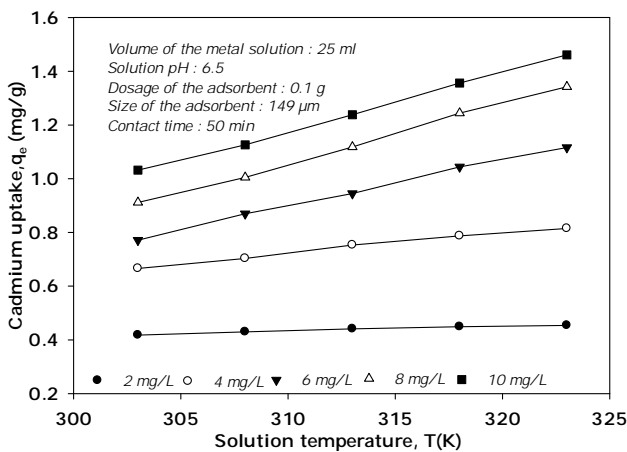


Fig. 12: Effect of temperature on cadmium uptake.

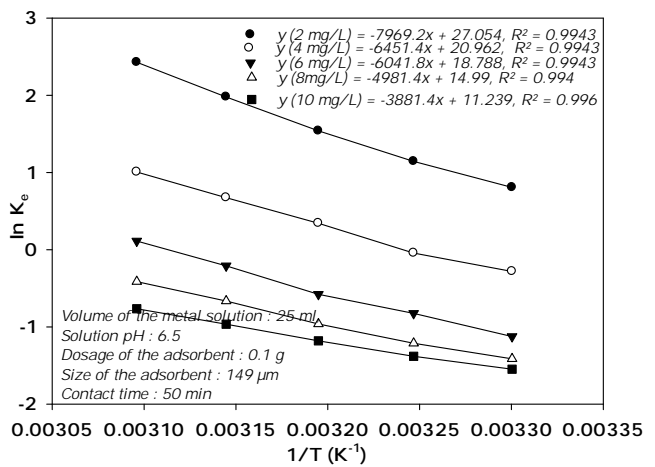


Fig. 13: Estimation of thermodynamic energy parameters for cadmium adsorption process.

Table 3: Thermodynamic energy parameters for the adsorption of cadmium using *ACBPL* as an adsorbent.

C_i (mg/L)	ΔH° (kJ/mol)	ΔS° (kJ/mol.K)	$-\Delta G^\circ$ (kJ/mol)				
			303K	308K	313K	318K	323K
2	66.255	0.224	7.08	5.87	4.68	3.44	2.22
4	53.636	0.174					
6	50.231	0.156					
8	41.410	0.124					
10	32.260	0.093					

Table 4: The optimal experimental values of the process variables and responses (% removal).

Process variable	Optimum value
Contact time (t), min	50
Solution pH	6.5
Initial metal concentration (mg/L)	4
Dosage of the adsorbent (g)	0.15
Solution temperature (K)	313
Maximum % removal	88.76

adsorption process. As the temperature increases, the rate of diffusion of adsorbate molecules across the external boundary layer and internal pores of the adsorbent particle increases (Safa et al. 2009). In addition, changing temperature will change the equilibrium capacity of the adsorbent for particular adsorbate. The rate of adsorption of cadmium and deposition of cadmium onto *ACBPL* adsorbent surface with changing temperature (303K to 323K) were increased from 89.98 to 97.90 % and 0.418 to 0.454 mg/g with an initial concentration of 2 mg/L (pH: 6.5 and t : 50 min) of cadmium solution. When the temperature increases, the pores enlarge, thereby more surface will be available for adsorption, diffusion and penetration of Cd^{+2} ions favouring adsorption and hence there is an increase in the % removal and metal accumulation on the adsorbent surface of cadmium ions. The results are shown in Figs. 11 & 12.

Thermodynamic studies: Thermodynamic energy parameters (ΔH° , ΔS° , and ΔG°) give the evidence of the direction of the adsorption process. The equilibrium constant (K_e) obtained from Eq. 3 was used to evaluate the thermodynamic energy parameters. The values of ΔH° , ΔS° and ΔG° were calculated from the slope and intercept of the linear Vant-Hoff's plot i.e., $\ln K_e$ vs $\left(\frac{1}{T}\right)$ as shown in Fig. 13. The estimated thermodynamic energy parameter values of ΔH° , ΔS° and ΔG° are presented in Table 3. The thermodynamic feasibility of cadmium adsorption process described that the % removal of cadmium increased with increasing temperature. According to Eq. (3), the values of ΔH° , ΔS° and ΔG° at various initial concentrations of cadmium with different temperatures are given in Table 3. The adsorption

process is endothermic, spontaneous at high temperatures and non-spontaneous at low temperatures. Based on the experimental results, the *ACBPL* adsorbent is efficient for the removal of cadmium at higher temperatures (Awwad et al. 2014). The positive value of ΔS° reflects the high degree of disorder in the adsorbent/adsorbate interface that is formed during the transition.

CONCLUSIONS

The activated carbon prepared from *Bauhinia purpurea* leaves demonstrate a good capacity of adsorption of cadmium, highlighting its potential as an effective adsorbent for the treatment of industrial effluent. The following conclusions could be drawn from the present study on the removal of cadmium from aqueous solutions using adsorption technique:

1. The equilibrium contact time for the adsorption of cadmium onto activated carbon of *Bauhinia purpurea* leaves adsorbent was 50 min. Short equilibrium times indicate that the rate of adsorption is very fast for the cadmium.
2. It was observed that the maximum rate of adsorption was obtained at pH 6.5 for cadmium using activated carbon prepared from *Bauhinia purpurea* leaves. Further increase in solution pH showed that the % removal of cadmium was decreased.
3. The experimental results showed that % removal of cadmium was decreased with an increase in the initial concentration of the solution, but the actual amount of metal accumulated on the adsorbent surface per unit mass of adsorbent was decreased with an increase in the initial concentration of metal solution by using activated carbon of *Bauhinia purpurea* leaves.
4. The percent removal of cadmium was increased and metal uptake decreased with an increase in adsorbent dosage.
5. It was observed that the % removal and metal uptake of cadmium was decreased with an increase of average particle size of the adsorbent.
6. The percent removal and adsorption capacity of cadmium was increased with an increase of solution tem-

perature to indicate the endothermic nature of the adsorption process.

- The calculated thermodynamic energy parameters (ΔH° , ΔG° and ΔS°) of cadmium adsorption for the same adsorbent with solution temperatures described that the adsorption process is endothermic, spontaneous at high temperatures and non-spontaneous at low temperatures. The positive value of ΔS° , reflecting the high degree of disorder in the solid/solution interface between adsorbate and adsorbent.

REFERENCES

- Akunwa, N.K., Muhammad, M.N. and Akunna, J.C. 2014. Treatment of metal-contaminated wastewater: A comparison of low-cost biosorbents. *J. Environ. Manag.*, 146: 517-523.
- Awwad, A.M., Nida and Salem, M. 2014. Kinetics and thermodynamics of Cd(II) biosorption onto loquat (*Eriobotrya japonica*) leaves. *Journal of Saudi Chemical Society*, 18: 486-493.
- Bohli, T., Ouederni, A., Fiol, N. and Villaescusa, I. 2013. Single and binary adsorption of some heavy metal ions from aqueous solutions by activated carbon derived from olive stones. *Desalination Water Treat.*, 70: 1082-1088.
- Debasree, P., Umesh, M. and Swarup, B. 2014. A comprehensive review on Cd(II) removal from aqueous solution. *Journal of Water Process Engineering*, 2: 105-128.
- Fu, F. and Wang, Q. 2011. Removal of heavy metal ions from wastewaters: A review. *J. Environ. Manag.*, 92: 407-418.
- Gercel, O. and Gercel, H.F. 2007. Adsorption of lead(II) ions from aqueous solutions by activated carbon prepared from biomass plant material of *Euphorbia rigida*. *Chem. Eng. J.*, 132: 289-297.
- Gercel, O. and Gercel, H.F. 2007. Adsorption of lead(II) ions from aqueous solutions by activated carbon prepared from the biomass plant material of *Euphorbia rigida*. *Chemical Engineering Journal*, 132: 289-297.
- Kannan, N. and Rengasamy, G. 2005. Comparison of cadmium ion adsorption on various activated carbons. *Water Air Soil Pollution*, 163: 185-201.
- Kumar, T. and Chandrasher, K.S. 2011. *Bauhinia purpurealinn*: A review of its ethnobotany, phytochemical and pharmacological profile. *Research Journal of Medicinal Plants*. 5: 420-431.
- Leandro, J.S., Fernanda, R.P., Luiz, A.A., Crispin, H. and Garcia, C. 2014. Biosorption of cadmium(II) and lead(II) from aqueous solution using exopolysaccharide and biomass produced by *Colletotrichum* sp. *Desalin. Water. Treat.*, 52: 7878-7886.
- Momodu, M.A. and Anyakora, C.A. 2010. Heavy metal contamination of ground water: The Surulere Case Study. *Res. J. Environ. Earth Sci.*, 2(1): 39-43.
- Mona, K., Ahmad, K. and Hanafy, H. 2014. Heavy metals removal using activated carbon, silica and silica activated carbon composite. *Energy Procedia.*, 50: 113-120.
- Rao, K.S., Mohapatra, M., Anand, S. and Venkateswarlu, P. 2010. Review on cadmium removal from aqueous solutions. *International Journal of Engineering, Science and Technology*, 2: 81-103.
- Safa, O.A., Sibel, T., Tamer, A. and Adnan, O. 2009. Biosorption of lead(II) ions onto waste biomass of *Phaseolus vulgaris* L.: Estimation of the equilibrium, kinetic and thermodynamic parameters. *Desalination*, 244(1-3): 188-198.
- Umar, I.G., Emmanuel, O. and Abdul, H.A. 2015. Adsorption of aqueous Cd(II) and Pb(II) on activated carbon nanopores prepared by chemical activation of doum palm shell. *Springer Plus*, 4: 458.
- Venkatesan, G. and Senthilnathan, U. 2013. Adsorption batch studies on the removal of cadmium using wood of *Derris indica* based activated carbon. *Research Journal of Chemistry and Environment*, 17(5): 19-24.
- Zakaria, Z.A. and Abdul Hisan, E.E. 2011. In vivo antiulcer activity of the aqueous extract of *Bauhinia purpurea* leaf. *Journal of Ethnopharmacology*, 137: 1047-1054.



A Study on the E-waste Collection Systems in Some Asian Countries with Special Reference to India

Dharna Tiwari[†], Lakshmi Raghupathy, Ambrina Sardar Khan and Nidhi Gauba Dhawan

Amity Institute of Environmental Sciences, Amity University Uttar Pradesh (AUUP), Sector-125, Noida-201301, U.P, India

[†]Corresponding author: Dharna Tiwari

Nat. Env. & Poll. Tech.
Website: www.neptjournal.com

Received: 01-06-2018
Accepted: 02-08-2018

Key Words:

E-waste
Collection centres
Deposit refund scheme
Informal sector
Extended producer responsibilities

ABSTRACT

Safe management of waste electrical and electronic equipments is becoming a major problem for many countries in the world. Due to the advancement in technology, increased market penetration of electrical and electronic equipment and high rate of obsolescence, there is an increased generation of electrical and electronic waste (e-waste). E-waste being a post-consumer waste needs to be collected from the various sources of its generation. Subsequently, establishment of collection centres is necessary to channelize such wastes for environmentally sound recycling. A number of methods are adopted for the collection of e-waste in different countries all over the world. This paper is an attempt (a) to study existing collection systems in some Asian countries including Bangladesh, Burma/Myanmar, China, Hong Kong, Indonesia, Japan, Malaysia, Philippines, South Korea, Taiwan and India; and (b) to formulate a sustainable model for collection systems for the developing nations.

INTRODUCTION

With the advancement in technology around the world along with the continuous up-gradation in design, the rate of obsolete electrical and electronic equipment has been significantly increased in the electronics sector. Another reason attributed to the less life of electronic items is the economic growth and market penetration. Particularly in China, 83 million units of electronic and electrical equipment (EEE) were scrapped in 2007 that reached to 227 million in 2012 with an average annual growth of 19.9% (Veenstra et al. 2010). In another instance, over 3 million computers and 15 million mobile phones reached their end-of-life in Korea during 2004 (Hyunmyung & Yong-Chul 2006). In the year 2008, around 12.9 million units of EEE were collected at the specified collection points by Japan (Ministry of Environment, Japan 2010). As per the United Nations Environment Programme (UNEP) report the waste from mobile phones would increase by 18 times by 2020.

Wastes from electronic products contain toxic substances which lead to adverse effects on health and environment when such wastes are processed in the unorganized sectors without following adequate health and safety norms. The presence of precious metals (PMs) such as gold (Au), silver (Ag), platinum (Pt), gallium (Ga), palladium (Pd), tantalum (Ta), tellurium (Te), germanium (Ge) and selenium (Se) makes recycling of e-waste attractive economically

(Raghupathy et al. 2010). The e-waste management needs segregation, collection, transportation, storage, treatment, recovery of valuable materials and final disposal of residue. However, the developing countries are facing problems not only due to the high rate of e-waste generation and collection, but also due to the imports of obsolete electronic products and e-waste. Particularly in India, the management of e-waste still remains one of the biggest tasks, not only due to rising demand of electronic products, but also due to growing imports of electrical and electronic products from developed nations. Given the gravity of the situation, this study was undertaken on the prevailing "collection systems" for e-waste in some Asian countries namely, Bangladesh, Burma/ Myanmar, China, Hong Kong, Indonesia, Japan, Malaysia, Philippines, South Korea, Taiwan and India. The outcome of this study may provide clues important for devising future studies on the subject.

METHODS

The trends in the e-waste production have been significantly changed with the changing economy of the developing countries (Robinson 2009). The consumers are one of the key stakeholders in any e-waste system as they are the buyers of the product in the first place; they are also the users and they are the ones who decide whether to store, exchange, repair, refurbish or dispose of the products after use. The outlook of the population of the less developed nations is

also one of the major factors that influence the consumers to purchase new electronic products (Skovgaard et al. 2005, Bandara et al. 2007). As post-consumer waste, the e-waste needs to be collected from the end user to be channelized for environmentally sound management, thereby requires a system for its collection. A number of methods are adopted for the collection of e-waste in different countries the world over. This study pertains to the practices prevailing in some countries in the Asian region. The information on e-waste management in Asian countries was collected from various sources such as published reports, journals, e-books and respective websites.

RESULTS AND DISCUSSION

In most of the countries taken up for study, e-waste is collected and treated majorly by the informal sector. There is a preference for the reuse of electronic equipment, only 20% to 30% are recycled while the rest is disposed of in Bangladesh (Ha et al. 2009, Ahmad 2011). However, in Myanmar, there is a tendency to carefully reserve the damaged equipment or parts so that the same can be utilized for repair (Aung & Myint 2010). In China, both formal and informal collectors are involved in e-waste collection and most of the e-wastes collected from the urban areas are sent for recycling; whereas, those collected from the rural areas are traded to the local second-hand market (Kim et al. 1996, Tong & Wang 2004, Hicks et al. 2005, Streicher-Porte & Yang 2007, Yang et al. 2007, Chi 2011, Li 2011). Hong Kong has also faced a lot of problems due to the excessive generation of e-waste; however, the government has taken some considerable steps to control the problem of e-waste like setting up recycling facility along with proper collection system (Chung et al. 2011). Additionally, Hong Kong has also proposed to setup many collection points and recycling centres across the country. At present there are approximately 100 sites that are used for storing discarded electrical and electronic items. Most of these sites are the old scheduled agricultural areas which are privately owned. In Indonesia, there are eight industries involved in the collection and dismantling of e-wastes (Gaidajis et al. 2010, Panambunan-Ferse & Breiter 2013). According to the Indonesian Ministry of Environment, e-wastes are imported under false declaration as metal and plastic scrap for recycling in countries like Indonesia (Hanafi et al. 2011 and Meidiana & Gamse 2010). The e-waste recycling is mostly carried out by the informal sector (Andarani & Goto 2012). Dumping of e-waste is a major problem in Indonesia, which includes disposal in landfills (Gaidajis et al. 2010, Hanafi et al. 2011, Meidiana & Gamse 2010, Panambunan-Ferse & Breiter 2013). In Japan, approximately 85% of e-waste is recycled and rest 15% is discarded into landfills. A large number of

collection points (500 in numbers) have been setup as a part of Extended Producer Responsibility (EPR) and Advanced Recycling Fee (ARF) (Jimlynch 2013). Malaysia has the facility for collection as well as processing unit for precious metal recovery. There are 146 e-waste recovery facilities in Malaysia with the total capacity to manage more than 24,000 metric ton of e-waste per month. Precious metals recovery is limited to only on wet chemical processes and electrolysis (Agamuthu et al. 2009, Awang 2010). Collection centres are managed by the solid waste concessionaries or local authorities and export of e-waste is not allowed because of the presence of the facilities to process and recover useful materials from e-waste in the country. Kuala Lumpur has concessionaries and in Pulau Pinang the collection involves local authority or NGO or waste generators or recyclers (Betts 2008).

Philippines has important collection, recycling and refurbishing facility for e-wastes. The two main environmental laws define the overall framework for managing e-wastes: (a) the Ecological Solid Waste Management Act of 2000 (RA 9003) and (b) the Toxic Substances & Hazardous & Nuclear Wastes Control Act of 1990 (RA 6969). The objective of RA 9003 is to follow the 3R concept; reduce, reuse and recycling prior to collection, treatment and disposal (The Philippines Government 2000, Peralta & Fontano 2006). In Philippines, the waste collection is mainly carried out by municipality, in which e-waste may be classified under RA 9003. In case e-waste is disposed along with municipal waste, then there is no provision of treating the e-waste separately (Peralta & Fontano 2006). However, the Materials Recovery Facilities (MRF) are available only at a few locations. Notably, South Korea has Producer Recycling (PR) Rule for the management of e-waste and the recycling rate for IT equipment and appliances combined is 82% which is highest in the world, with as many as 500 collection points (Jimlynch 2013). In 1998, Recycling Fund Management Committee (RFMC) system was introduced in Taiwan to encourage recycling (Kyogikai 2000). As per the RFMC procedures, the producers pay the charges for collection and recycling of e-waste. The Fee Rate Reviewing Committee (FRRC) decides the collection and recycling charges and these charges are revised annually on the basis of factors like London Metal Exchange (LME) rates (Chung & Murakami 2008). In India, the collection of e-waste is mainly done by recyclers including both formal and informal sectors, wherein 90% of e-waste is recycled in the informal sector while the formal sector is able to collect only 10% of the total share of the e-wastes. As per the published information, India has 134 authorized collection centres in 19 States by MoEF (2014-15). India has notified the e-waste Management and Handling Rules, 2011 based on EPR, wherein the producers are

responsible for establishing collection centres and organizing collection of e-waste. However, no effective collection systems have been put in place by the producers other than storing the obsolete products in their warehouses. Most of the used electronic items are refurbished and repaired a number of times and many of them are sold in the thriving secondary market. Due to the gap in collection systems, only 40% of the total e-waste is channelized for recycling while the rest 60% remains untraceable (Secretariat 2011). In many developing countries there is also a tendency for selling the used equipment from the cities to the countryside and villages because of the lack of ownership of Waste Electrical and Electronic Equipments (WEEE) in those regions. In many cases the equipments are reused and those that are beyond repair are discarded indiscriminately thereby making e-waste collection a difficult task. The findings, which have been described above are summarized in Table 1.

The details about the different systems being practiced for collection of e-waste in the Asian countries reveal that each country has adopted these practices according to their requirements. However, there is a need to evolve an efficient system for the collection of e-waste through authorized collection centres, collection point, drop boxes, door to door collection, including the take back system organized by the producers or manufacturers of particular brand in order to channelize these for environmentally sound recycling. Such establishments may be setup by anyone or stakeholders in the e-waste value chain such as manufacturers, producers, dealers, recyclers either individually or collectively in association with other stakeholders or other agencies.

Collection centres could also be an independent unit/entity as a business activity.

China, Japan, South Korea, Taiwan and India have notified e-waste policy and regulations, while all other countries in the region do not have an e-waste policy or regulations. In Bangladesh, Myanmar and Philippines, e-waste is collected by informal sector and the waste is disposed in open areas, landfills or dumped along with garbage. In Hong Kong, the majority of the WEEE is transported overseas for recycling and some remaining e-waste is disposed along with garbage. In India, the e-waste rules provide for a collection system, however, only a few authorized collection centres have been setup to date. The collection systems are essentially devised by the recyclers rather than the producers as mandated in the e-waste rules. In China, both formal and informal collectors are involved in e-waste collection (Tong & Wang 2004, Yang et al. 2007, Streicher-Porte & Yang 2007). In Malaysia, there is no direct channelization of waste, but it is managed by NGO/local authorities. In Taiwan, the producers are made responsible to pay for collection and recycling of e-waste and the charges for collection and recycling are decided by reviewing committee.

Since different operations already exist in countries taken up for study, there is bound to be a difference in the establishment of the collection system. The following discussions provide an insight in the prevailing system in different countries with a view to evolve a model. The model/system is intended to provide linkages between various stakeholders in order to facilitate the collection of e-waste.

Table 1: Summary of e-waste collection system in Asian countries.

Country	Collection system	Law/Regulations	Recycling Formal/Informal
Bangladesh	Disposed in to landfills, rivers, ponds, drains, lakes, channels and open spaces. The e-waste is mainly recycled by the informal sector located in Dhaka and Chittagong	None	Informal
Burma/ Myanmar	No Information	No information	No information
China	Old for New Rebate Program" (also known as "Old for New Program") or exchange programs	Yes	Both
Hong Kong	Presence of eight collection points and three recycling centres	None	Both
India	Collected by formal and informal sector	Yes	Both
Indonesia	Eight industries involved in collection and dismantling	None	Both
Japan	Five hundred collection points have been set up as a part of Extended Producer Responsibility (EPR) and Advanced Recycling Fee (ARF).	Yes	Both
Malaysia	146 e-waste recovery facilities. Collection centres are managed by the solid waste concessionaires/local authorities.	None	Formal
Philippines	Collection, recycling and refurbishing facility.	None	Both
South Korea	Recycling rate is 82 % along with five hundred collection points	Yes	Both
Taiwan	Under RFMC producers pay the charges for collection and recycling of e-waste.	Yes	Both

Collection of e-waste by producer: According to the EPR system, the management of e-waste generated by the end of life products goes to the producer. Essentially, the producer uses the dealers, distributors, retailers or any other agency to collect the e-waste those may be provided certain incentives. Producer may also organize a direct take back system for their brand of products from the identified consumers. Take back system may also require an agreement between the consumer and producer to ensure that the end of life product is returned to the producer. Countries including Bangladesh, Myanmar, Malaysia and Indonesia do not apply EPR, adopt various methods for collecting e-waste and these methods include repair, refurbish, reuse and/or disposal. Additionally, the repair shops and service centres also generate e-waste which may be the whole product or components which are no longer fit for use and are discarded. In such cases, these wastes would require a dedicated collection system to deposit such wastes and subsequently channelize them for recycling.

Collection of e-waste by recycler: The e-waste collection by recyclers is also very important where recyclers play a vital role in managing and reduce e-waste through the recycling and recovery operation. In fact, e-waste recycling has become a lucrative business venture which is further regulated by the policy and regulations framed in most of the countries taken up for the study. In most cases, it is purely a business venture due to the presence of valuable materials in the e-waste that can be easily recovered by recycling. According to the EPR system, producers are required to collect and channelize e-wastes for recycling and recovery. However, in view of the business interest, recyclers collect e-wastes from consumers either directly, through hawkers or through auction and subsequently recover the material to be sold in the market as a resource. In developing nations, the informal sector has a vital role to play in the e-waste recycling. They also tend to compete with the formal recyclers and in some cases, they complement the activities. The mutual support system that integrates operations in the informal and formal recycling units is ideal for developing economies and the relation between these two sectors is essential for the success of e-waste management (Raghupathy et al. 2010). The role of informal sector in e-waste recycling has been considered important not only in India, but also in other Asian countries of this region. In most of the countries taken up under this study, e-wastes are mainly treated by the recyclers in the informal sectors; however in some cases, the formal sector is also involved as prevalent in India and China. While engaging informal sector, it is essential to identify and authorize such units to be linked with the producer and the formal recyclers.

Collection of e-waste by collection centres: Consumers

using electrical and electronic equipment/appliances have to ensure that e-wastes generated by them are channelized through collection centres. Notably, the collection centres play a vital role in the collection of e-wastes from consumers. Collection centre can reach out to the consumers by organizing door-to-door collection of e-wastes and providing incentives including the certificate of receipt, discount coupons on the purchase of new products or direct cash. Collection centres may even operate through dealers or distributors or retailers or other agencies, wherein a box or a bin is provided for the e-waste. E-waste can also be collected from the service centres and re-furbishers where, the repaired or refurbished products will go back to the consumer and the discarded components and non-repaired products are sent to the collection centre or to the recycler. In India, hawkers also known as 'kabadiwalas' contribute majorly in the collection of recyclables including e-wastes from consumers in exchange of money. The e-wastes, thus, collected are sold to the informal sector without any accountability. Therefore, the kabadiwalas may be included and motivated, and informal sector to be a part of e-waste value chain by organizing them, to participate in the e-waste collection process.

The studies on the practice for e-waste collection prevalent in the countries taken up for the study revealed that e-waste is collected by the informal sector and traded into the local second-hand market (Kim et al. 1996, Tong & Wang 2004, Hicks et al. 2005, Yang et al. 2007, Streicher-Porte & Yang 2007, Li 2011, Cheng & Chang 2017). However, the mechanism of collection and transfer varies in each of these countries. In China, the formal collectors pay tax and give away the collected e-wastes to authorized recyclers for environmentally-sound treatment. In Japan, the retailers take back home appliances only upon the request of consumers and these are transported to the collection site. The manufacturer organizes the transportation of the e-wastes to the collection site in collaboration with the retailers. In South Korea, there is producer recycling (PR) rule for the management of e-wastes wherein, the consumer buys any new product by depositing the old equipment against it. In Taiwan, consumers surrender their used equipment via retailers, municipal collection, private collectors, or donations to charities who in turn, hand over WEEE to licensed recyclers. There is also introduction of RFMC, where producers pay the charges for collecting and recycling of e-waste (Cheng & Chang 2017).

Channelization of e-waste to collection centre: Collection centre can collect the e-wastes through different sources such as household, schools and educational institutions, commercial establishments, service centre and re-furbishers and also through the producer-organized system such as

take back. In case of household e-waste, the collection centre has to be from door to door. For school and educational institutions, bins could be provided and a collection drive could be organized so that the staff and students of the group can collect the e-waste from the institutions and from their household as well. Bulk consumers, who are the major generators, may establish their own collection centres or channelize the waste to designated collection centres. Such bulk consumers may also directly send their waste to authorized dismantlers or recyclers. However, the bulk consumers also dispose their e-wastes through auctions and the collection centres may participate in such auctions to channelize the e-waste for authorized recycling. On the other hand, the producers may organize the collection through the dealers or distributors or retailers under the take back program or exchange of the used products for new products and channelize the e-waste either to authorized collection centre or to the authorized recyclers. The electronic and electrical products, which come to the service centres or refurbishers, may be repaired or refurbished and handed over to the consumers. Additionally, the components or products not repaired can be collected by the collection centres or by the recyclers. An overview of the channelization of e-wastes to collection centre is presented in Fig. 1.

Role of an independent agency in the e-waste collection system: The collection of e-waste is a critical activity in the whole e-waste management system and irregularities in the collection channels need to be rectified to make the whole process effective. The product, which is no longer in working condition, is handed over to a service centre, repair shop or a refurbishment unit where the product is made functional. Those products, which are not repairable and non-usable reaching the end of life, are channelized to dismantler or recycler. The producers invariably set up such service centres or they enter into collaboration with the producer. However, the tracking of the large number of unauthorized service centres and repair shops that prevail in most of the Asian countries is difficult. The exchange schemes though enable a huge collection of the used electrical and electronic equipment, but these are not channelized due to lack of coordination between the various agencies. In such cases, an independent organization or agency may facilitate in the process. In fact, an independent agency is required to establish the linkages between various stakeholders and to carry out the transactions required for collection and channelization of e-waste. Fig. 2 provides a model/system for such centres.

The facilitation counter set up in the collection centres would provide a platform for such transaction between consumers and collection centres to help in channelizing the e-waste from different sources to the collection centres. Such

collection centres would also collect the e-waste from household consumers on the exchange rates that may be decided by the product, its quality and condition. Such transactions may be monitored to enable reliability and transparency. The independent collection agency would also indulge in conducting awareness programs to sensitize the society to understand the function of facilitation counters and also organize collection drives.

Channelization of e-waste from consumers to facilitation counter can be done by various methods such as direct collection by deposition of e-waste by consumers, or through collection points, collection bins, drop boxes, vans etc. Collection points can be from the residential areas, commercial areas, and educational and other institutions. The collection bins can also be placed in public places like restaurants, malls, offices, post offices, market places, etc. Mobile vans can also be used for door-to-door collection of e-waste. Components and defective products from service centres/re-furbishers can be transferred to the facilitation counter to channelize the waste to collection centres. Such system requires support from the Government as well as other participating agencies.

Proposed system of e-waste collection and channelization:

The approach of the study was to provide a model/system for e-waste channelization. The overall material and financial flow details have been summarized in Fig. 3. The electrical and electronic products are used by the consumers and are returned after the end-of-life. The dealers, distributors or retailers also facilitate the producers in the collection of e-waste under the take back or buy back scheme through exchange of used products when the consumer buys the new product. It is required to channelize the wastes generated during manufacture of electrical and electronic products to the authorized recyclers. E-waste can also be collected from the service centres or re-furbishers, wherein the repaired product is given to the consumer and the defective products or components are sent for recycling. Collection centres are required to channelize the e-waste to the authorized recyclers for environmentally sound process.

The transactions were involved in the e-waste collection in most of the countries considered in this study. Therefore, an understanding of the financial flow in the e-waste management system is necessary in order to facilitate the collection of e-waste. Moreover, while purchasing any product, the consumer is required to pay an amount in advance towards the "Deposit Refund Scheme" (DRS), which is refundable when the product is returned at the end-of life. The interest earned from this deposit is to be used for recycling of the product purchased. Producers may financially support the dealers or distributors or retailers to organize the take back or buy back schemes. Collection

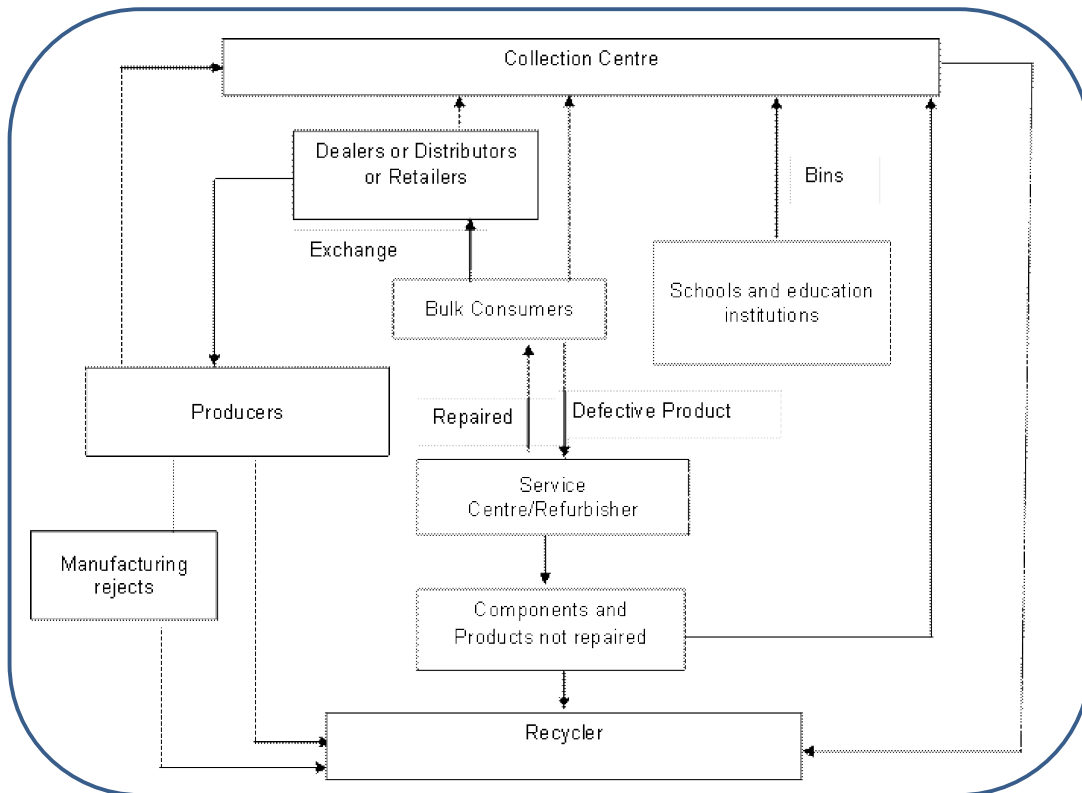


Fig. 1: E-waste collection centre.

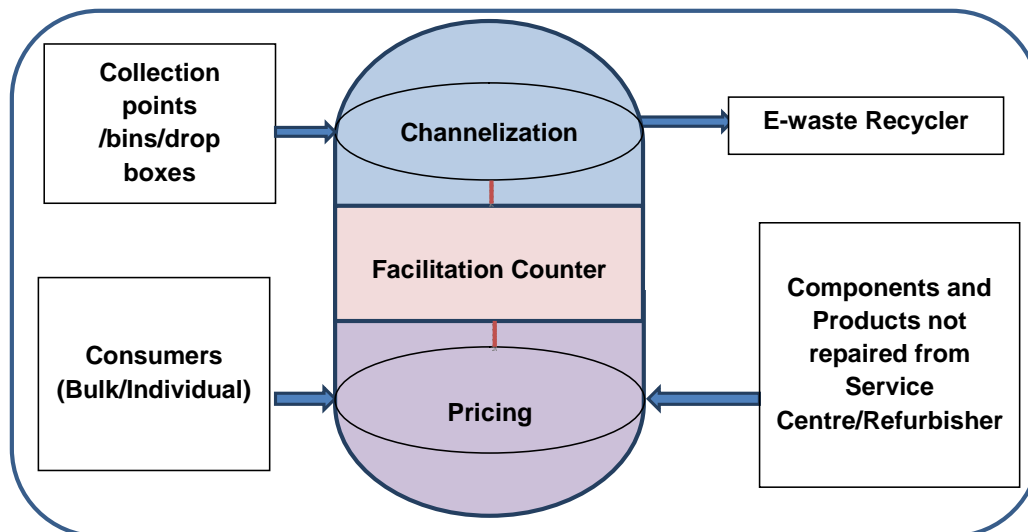


Fig. 2: E-waste collection through independent agency.

centres can facilitate e-waste collection from household consumers on the basis of e-waste exchange rates. Because collection centres provide an important link in the e-waste management system, these need to be financed by producer, government, recycler or any combination of these

stakeholders. However, there is a chance of the collection centre to be an independent entity on its own, and also create necessary linkages between the various stakeholders to channelize e-waste to authorized recyclers as well as to make it into a profitable business venture. However, effort

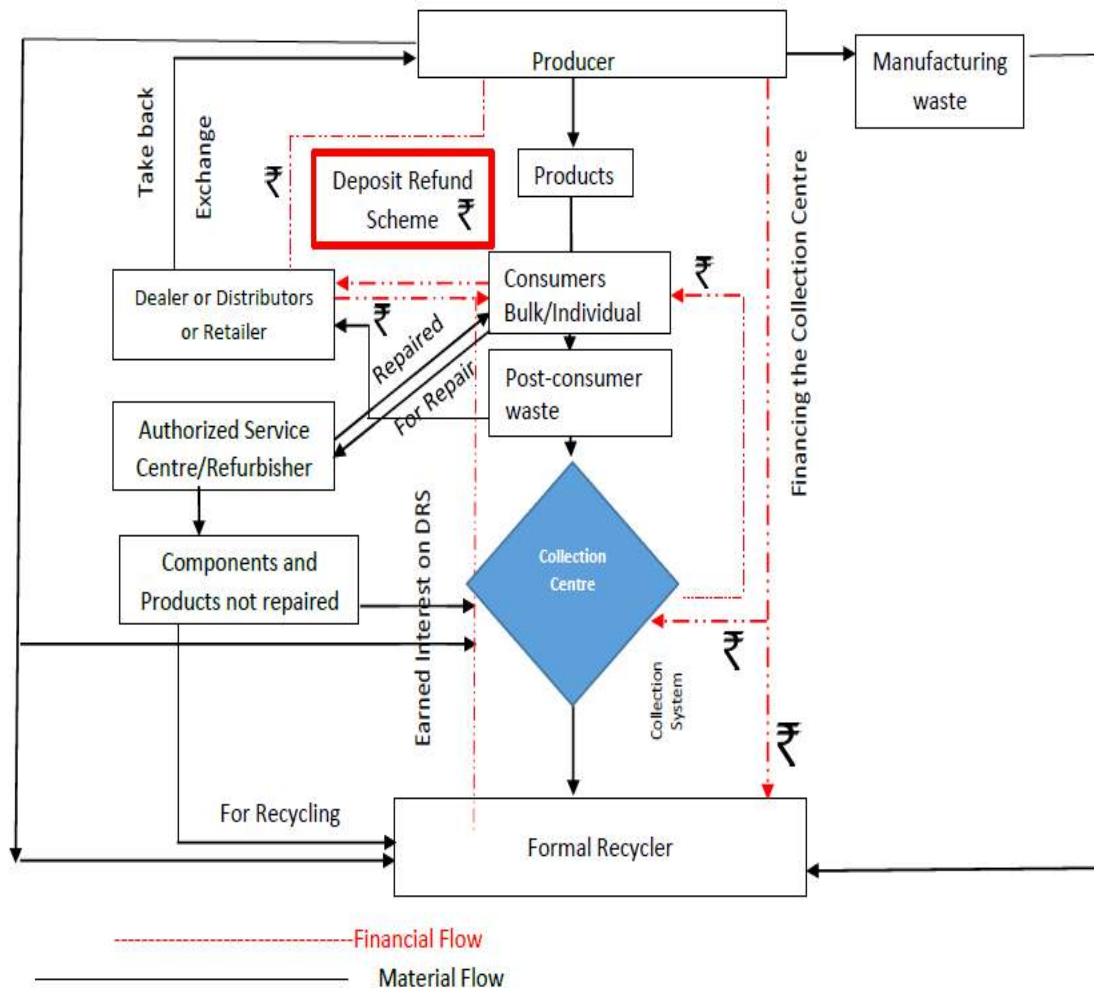


Fig. 3: The model for e-waste collection and channelization.

is required to monitor the activities and provide guidance for channelizing e-waste for environmentally sound management.

CONCLUSIONS

The study illustrated that although the Asian countries are known to recycle e-waste, however, disposal into landfills or dumping in open spaces cannot be ruled out. The need of the hour is to improve the efficiency in the collection systems. In order to start corrective actions on policy and implementation, collection and maintenance record of e-waste is of utmost importance. Formulation of standards and specifications for processing and recycling e-waste and regular assessment of e-waste generation is required for e-waste management. The authorities and the entrepreneurs are responsible agencies need to play an important role in

improving e-waste management at present as well as future. They need to increase public awareness about e-waste and the role of facilitation counter to promote the collection and channelization of e-waste. Doing this will bind them into the process through appropriate extended producer responsibilities. The proposed system provides all these in the system for effective channelization of e-waste.

ACKNOWLEDGMENTS

The authors gratefully acknowledge the Amity University for undertaking this research work.

REFERENCES

- Agamuthu, P., Fauziah, S.H. and Khidzir, K. 2009. Evolution of solid waste management in Malaysia: Impacts and implications of the solid waste bill 2007. *Journal of Material Cycles and Waste Man-*

- agement, 11: 96-103.
- Ahmad, F.R.S. 2011. E-waste management scenario in Bangladesh In: WEEE/E-waste Management Workshop on Take-Back System, 13-15 July, Osaka, Japan. Osaka, Japan: United Nations Environment Programme (UNEP)/International Environmental Technology Centre (IETC).
- Andarani, P. and Goto, N. 2012. Preliminary assessment of economic feasibility for establishing a households' e-waste treating facility in Serang, Indonesia. *International Journal of Environment Science and Development*, 3: 562-568.
- Aung, H. and Myint, O. 2010. E-waste Situation in Myanmar. Myanmar Participants.
- Awang, A.R. 2010. E-waste management in Malaysia. Department of Environment, Malaysia. Available from: [http://www.unep.or.jp/ietc/spc/news-jul10/Malaysia_\(Dr.RahmanAwang\).pdf](http://www.unep.or.jp/ietc/spc/news-jul10/Malaysia_(Dr.RahmanAwang).pdf).
- Bandara, N.J.G.J., Hettiaratchi, J.P.A., Wirasinghe, S.C. and Pilapiiya, S. 2007. Relation of waste generation and composition to socio-economic factors: A case study. *Environ. Monit. Assess.*, 135: 31-39.
- Betts, K. 2008. Producing usable materials from e-waste. *Environment Science Technology*, 42: 6782-6783.
- Cheng, Chii-Pwu and Chang, Tien-Chin 2017. The development and prospects of the waste electrical and electronic equipment recycling system in Taiwan. *Journal of Material Cycles and Waste Management*, 20(1): 667-677.
- Chi, X., Streicher-Porte, M., Wang, M.Y. and Reuter, M.A. 2011. Informal electronic waste recycling: A sector review with special focus on China. *Waste Management*, 31: 731-742.
- Chung, S., Lau, K. and Zhang, C. 2011. Generation of and control measures for e-waste in Hong Kong. *Waste Management*, 31: 544-554.
- Chung, S.W. and Murakami-Suzuki, R. 2008. A Comparative study on e-waste recycling systems in Japan, South Korea, and Taiwan from the EPR perspective. In: Kojima Michikazu (ed.) *Promoting 3Rs in Developing Countries: Lessons from the Japanese Experience*. Institute of Developing Economies.
- Gaidajis, G., Angelakoglou, K. and Aktsooglou, D. 2010. E-waste: environmental problems and current management. *Journal of Engineering Science and Technology Review*, 3(1): 193-9.
- Ha, N.N., Agusa, T., Ramu, K., Tu, N.P.C., Murata, S. and Bulbule, K.A. 2009. Contamination by trace elements at e-waste recycling sites in Bangalore, India. *Chemosphere*, 76: 9-15.
- Hanafi, J., Kristina, J.H., Jobiliong, E., Christiani, A., Halim, A.V., Santoso, D. and Melini, E. 2011. The prospects of managing WEEE in Indonesia. *Glocalized Solutions for Sustainability in Manufacturing*, pp. 492-496.
- Hicks, C., Dietmar, R. and Martin, E. 2005. The recycling and disposal of electrical and electronic waste in China-legislative and market responses. *Environmental Impact Assessment Review*, 25(5): 459.
- Hyunmyung, Y. and Yong-Chul, J. 2006. The practice and challenges of electronic waste recycling in Korea with emphasis on extended producer responsibility (EPR). *Proceedings of the IEEE International Symposium on Electronics and the Environment* 8-11 May. Washington, DC, USA: IEEE Computer Society, pp. 326-330.
- Jimlynch, 2013. Snapshot of worldwide electronics recycling. Available from: <http://ifixit.org/blog/4662/snapshot-of-worldwideelectronics-recycling-2013/>.
- Kyogikai, N.K.C. 2000. Shigen risaikuru ni kansuru seisaku fureimu no keiseini mukete (in Japanese) [Toward formation of policy framework for resource recycling], pp. 94-95.
- Li, B., Du, H.Z., Ding, H.J. and Shi, M.Y. 2011. E-waste recycling and related social issues in China. *Energy Procedia.*, 5: 2527-2531.
- Meidiana, C. and Gamse, T. 2010. Development of waste management practices in Indonesia. *European Journal of Scientific Research*, 40(2): 199-210.
- Ministry of Environment, Forests and Climate Change (MoEF) 2014-2015. Annual Report. 1-304.
- Ministry of the Environment, Japan, 2010. Establishing a sound material cycle society. Tokyo Japan: Government of Japan.
- Panambunan-Ferse, M. and Breiter, A. 2013. Assessing the side-effects of ICT development: E-waste production and management: A case study about cell phone end-of-life in Manado, Indonesia. *Technology in Society*, pp. 1-9.
- Kim, J.Y., Parnianpour, M. and Marras, W.S. 1996. Quantitative assessment of the control capability of the trunk muscles during oscillatory bending motion under a new experimental protocol. *Clinical Biomechanics*, 11(7): 385-391.
- Peralta, G.L. and Fontano, P.M. 2006. E-waste issues and measures in the Philippines. *Journal of Material Cycles and Waste Management*, 8(1): 34-39.
- Raghupathy, L., Krüger, C., Chaturvedi, A., Arora, R. and Henzler, M.P. 2010. E-waste recycling in India-bridging the gap between the informal and formal sector. In: *International Solid Waste Association, World Congress, Hamburg, Germany*.
- Robinson, B.H. 2009. E-waste: An assessment of global production and environmental impacts. *Science of Total Environment*, 408: 183-191.
- Secretariat 2011. E-waste in India. India Research Unit (Larrdis), Rajya Sabha Secretariat, New Delhi.
- Skovgaard, M., Moll, S., Møller Andersen, F. and Larsen, H. 2005. Outlook for waste and material flows: Baseline and alternative scenarios. Working paper 1. European Topic Centre on Resource and Waste Management, Copenhagen, Denmark.
- Streicher-Porte, M. and Yang, J. 2007. WEEE recycling in China. Present situation and main obstacles for improvement. *IEEE International Symposium on Electronics and Environment*. The Philippines Government, 2000. Ecological Solid Waste Management Act of 2000, RA9003.
- Tong, X. and Wang, J. 2004. Transnational flows of e-waste and spatial patterns of recycling in China. *Eurasian Geography and Economics*, 45(8): 608-62.
- Veenstra, A., Wang, C., Fan, W. and Ru, Y. 2010. An analysis of e-waste flows in China. *Intl. J. Adv. Manufact. Technol.*, 47: 449-459.
- Yang, J., Lu, B. and Xu, C. 2007. WEEE flow and mitigating measures in China. *Waste Management*, 28(9): 1589-1597.



Syzigium oleina and *Wedelia trilobata* for Phytoremediation of Lead Pollution in the Atmosphere

Fida Rachmadiarti[†], Tarzan Purnomo, Diana Nur Azizah and Ayudhiniar Fascavitri

Department of Biology, Faculty Mathematic and Natural Science, Universitas Negeri Surabaya, Surabaya, East Java, Indonesia

[†]Corresponding author: Fida Rachmadiarti

Nat. Env. & Poll. Tech.
Website: www.neptjournal.com

Received: 30-05-2018
Accepted: 02-08-2018

Key Words:

Phytoremediation
Lead
Syzigium oleina
Wedelia trilobata

ABSTRACT

Heavy metals cause pollution in the environment, including plants. In Indonesia, *Syzigium oleina* and *Wedelia trilobata* are grown on the main roads where vehicles frequently pass through; these plants are exposed to heavy metals, such as lead (Pb). The aim of this study was to evaluate how the location of plants, the plant species, and the interaction between these two variables, affect the content of Pb metal and chlorophyll in leaves. The levels of heavy metals in plant leaves were measured by using an atomic absorption spectrophotometer, and chlorophyll content by using a spectrophotometer. Data were analysed by two-way ANOVA. The results showed that the location of plant species affected the content of Pb metal and chlorophyll in the leaves, but the interaction of the location and the type of plant only affects the chlorophyll content of leaves and not the Pb metal content.

INTRODUCTION

In general, the main cause of air pollution in cities is an increasing number of motor vehicles, including in Surabaya, Indonesia (Purwatiningsih 2015). Based on the data from Surabaya Metropolitan Police, the total length of road in Surabaya is only 2,096.69 km. However, the total number of motor vehicles reaches 3,895,061 units. This has led to changes in the air quality in Surabaya (Samsuedin et al. 2015). Motor vehicles are a moving source of contaminants so that the spread of the emitted polluting material has a wide spatial dispersion pattern (Boediningsih 2011). Motorized vehicles produce emissions, which include pollutants such as lead. The accumulative Pb is mainly derived from the imperfect combustion of gasoline additives used in motor vehicles (Sunu 2001). In addition to Pb, the exhaust of motor vehicles also contains pollutant compounds such as carbon monoxide (CO), hydrocarbons (HC), sulphur oxides (SO_x), nitrogen oxides (NO_x) and particulates (Kean et al. 2000).

Lead in vehicle gasoline serves to improve octane fuel efficiency and to lubricate the valve seat of cars. Pb and gasoline are burnt in the engine (EPA 2007). About 10% of Pb emissions from a motor vehicle will contaminate locations within a radius of < 100 m, whereas 5% can contaminate locations within a radius of 20 km and 35% will be carried by the atmosphere and have a potentially very wide-reaching range (EPA 2007). It is, therefore, necessary to ad-

dress methods of reducing motor vehicle pollution, namely Pb emissions. One method of doing so is to use plants.

Plants that have the potential to absorb Pb include *Syzigium oleina* and *Wedelia trilobata*. Both of these plants are primarily grown on the main streets of cities, including Surabaya. Plants can be used as lead absorbers because they are able to absorb it in the air through passive absorption mechanisms. Pb is absorbed by the plant through leaf stomata and will stay in the leaf tissue and accumulate between the palisade tissue gaps (Santoso 2013). The plants that have the ability to be Pb-absorbent are those that can hold a large accumulation of Pb in their leaves, but will not show changes in leaf morphology such as in the stomata and chlorophyll (Fathia et al. 2015). Excessive Pb emissions in the air can affect the structure and physiology of plants. It may cause a decrease in growth and productivity, and can even cause death to plants. Excessive Pb absorption also causes a decrease in chlorophyll levels. The Pb entering the cytoplasm would hamper and inhibit the actions of the enzymes delta-aminolevulinic acid dehydratase (ALAD) and porphobilinogenase, which are both involved in the biogenesis of chlorophyll (Flanagan et al. 1980).

Plants also respond to the entry of Pb into tissue as an environmental stressor and undergo physiological changes as an adaptive response. The effects of Pb on plants include chlorosis, cell wall damage, and decreased chlorophyll biosynthesis. Changes in chlorophyll levels are another com-

mon physiological response (Novita et al. 2012). For example, a decrease in chlorophyll levels in *Swietenia macrophylla* leaves in conjunction with an increase of Pb levels has previously been described (Sembiring & Sulistyawati 2006).

The characteristics of plants that are effective Pb absorbers are that they have dense foliage that do not easily fall, that the leaves have a cuticle layer and are scaly, and that the leaf shape resembles a needle with a serrated leaf edge (NASA & ALCA 1989). *S. oleina* is characterized by dense foliage (single leaf) and lancet shaped leaves, with a shiny leaf surface. Conversely, *W. trilobata* herb characterized by oval-shaped leaves with a hairy leaf surface. Different plant habits affect the ability of the leaves to absorb Pb in the air. Herbs have a higher potential for heavy metal pollutants absorption than bushes and trees, as herbs are able to inhabit up more layers of ground cover (Landberg & Greger 1996).

In the context of the many problems of Pb air pollution, and with varying studies focusing on the potential of Pb absorption in different plants, it is necessary to determine both the Pb absorbing ability of individual plant species, and whether there are adverse effects of Pb on these plants, such as on leaf chlorophyll levels. The aim of this study is to evaluate how location, plant species, and the interaction between location and species affect the content of Pb metal and chlorophyll in the leaves of *S. oleina* and *W. trilobata* in Surabaya, Indonesia. Site selection was based on the fact that these plant species are widely grown at this location.

MATERIALS AND METHODS

Sample Collection

The samples of *S. oleina* and *W. trilobata* leaves were collected during the rainy season and taken from three different Surabaya town locations: Diponegoro Street, J.A. Suprpto Street and H.R. Muhammad Street. Of the three streets, Diponegoro Street is traversed by the most vehicles, about 154850 units a day, whereas J.A Suprpto Street is traversed by 99350 vehicles a day, and H.R. Muhammad Street is traversed by 19474 vehicles a day (Transportation Department of Surabaya Town, 2016). The leaves from both the plants were taken from the 7th position from the bud.

Analysis of Pb Content

Sample preparation: The preparation of samples was done using destructive methods. Leaves from each sample were weighed and ± 2.0 gram samples were placed into a porcelain cup or mortar. These samples were dried in an oven at 105°C for 2 hours. The samples were then cut into small pieces and put into a glass beaker, along with 10 mL of

HNO₃ 65% solution. The samples were then destroyed by using a destruction flask until red NO₂ gas appeared. The sample was then cooled and 2-4 mL of HClO₄ 70% solution was added. The sample was reheated and cooled until evaporation and reduced volume amount. The sample was then moved into a 50 mL measuring flask and diluted with distilled water until the meniscus sat on the 50 mL mark. The sample was then ready to be analysed by Atomic Absorption Spectrophotometer (AAS).

The production of standard metal solutions: Precisely 100 ppm of lead (Pb) standard solution was made from 1000 ppm of Pb main solution, then 10 mL of it was taken by drop pipette and added into 100 mL measuring flask, then diluted with distilled water until tera mark precisely, then homogenized. A 10 ppm Pb working solution was made from the 100 ppm Pb standard solution using the same method.

The production of calibration curves: The Pb standard solution was made by diluting the 10 ppm Pb solution until the desired concentration, ranging from 0-3 ppm, was reached. Then the absorbance value of each standard solution was measured with an AAS AA-700 Perkin Elmer tool using a Pb hollow cathode lamp.

The sample measurement: The measurement of the leaf samples was done according to the method generally used in tests of Pb content, in accordance with Indonesia National Standard (SNI) number 06-698945 in 2005.

The calculation of the Pb content of the leaves was obtained using the following formula:

$$Cy' = \left(Cy \times \frac{V}{W} \right) \times 1000$$

Where,

Cy' = Pb content that was absorbed in the leaves (µg/g)

Cy = Pb content that was measured by AAS (ppm or mg/L)

V = Volume of dilution solution (L)

W = Leaf biomass as dried leaf weight (g)

Analysis of Chlorophyll Content

About 1 gram sample was ground by mortar and pestle and made into an extract by mixing the leaf smear with 95% alcohol solution by as much as 100 mL, then filtering this solution with filter paper until the obtained filtrate volume was approximately 100 mL. The chlorophyll content contained in the leaf filtrate was measured using a spectrophotometer at wavelengths of 649 and 665 nm. Then the absorbance values of chlorophyll *a*, *b*, and the total chlorophyll content of the solution were calculated using

the formula of Wintermasn and de Mots as follows.

$$\text{Chlorophyll } a = 13.7 \times \text{OD } 665 - 5.76 \text{ OD } 649 \text{ (mg/L)}$$

$$\text{Chlorophyll } b = 25.8 \times \text{OD } 649 - 7.7 \text{ OD } 665 \text{ (mg/L)}$$

$$\text{Chlorophyll total} = 20.0 \times \text{OD } 649 + 6.1 \text{ OD } 665 \text{ (mg/L)}$$

Data Analysis

ANOVA analyses were carried out to assess the impact of location, plant species, and the interaction between location and species, on both the Pb and chlorophyll content of the leaves.

RESULTS

Table 1 gives the results of ANOVA on the influence of plant species, location, and the interaction between plant species and location, on Pb content. ANOVA results showed that the location and species of plants affect Pb content ($p < 0.05$), but the interaction of location and plant species did not affect the Pb content ($p > 0.05$).

The Pb content of *S. oleina* and *W. trilobata* leaves that were exposed to pollutants from motor vehicle emissions is presented in Table 2. The results of the Duncan test showed that Pb content in both the plants was highest in plants grown at station 1, second highest at station 2, and lowest at station 3. The Pb content of *W. trilobata*, in general, was higher than *S. oleina* plants.

Table 2 showed the ANOVA results investigating the influence of location and plant species as well as the interaction of location and plant species on Pb content.

Table 1: ANOVA result of location and type of plant *S. oleina* and *W. trilobata* with Pb content in the leaves.

Source	Dependent Variable	Sign
Location	Pb content	0.05
Plant	Pb bontent	0.00
Location*Plant	Pb content	0.92

Table 2: The average and standard deviation of Pb content in *W. trilobata* and *S. oleina* leaves at various locations.

Type of Plants	Station	Lead content (Pb) in the leaves (ppm)
<i>W. trilobata</i>	St. 1	0.288 ± 0.040bB
	St. 2	0.273 ± 0.016abB
	St. 3	0.258 ± 0.026aB
<i>S. oleina</i>	St. 1	0.186 ± 0.005bA
	St. 2	0.165 ± 0.010abA
	St. 3	0.146 ± 0.011aA

Notes: a, b: location; A, B: species of plant
 St. 1 Diponegoro Street, St. 2 J.A Suprpto Street and St. 3 H.R Muhammad Street.

These results show that the location and species of plants, as well as the interaction between location and the plant species, affect the Pb content ($p < 0.05$).

The chlorophyll content of *S. oleina* and *W. trilobata* leaves that were exposed to pollutants from motor vehicle emissions in the form of Pb is presented in Tables 3 and 4. The results of the Duncan test showed that chlorophyll content in both the plants was highest in plants grown at station 1, second highest at station 2, and lowest at station 3. In general, the chlorophyll content of *S. oleina* was higher than in *W. trilobata*.

DISCUSSION

In this research, *S. oleina* and *W. trilobata* grown on Diponegoro Street, J.A. Suprpto Street, and H.R. Muhamad Street in Surabaya city displayed differing levels of Pb absorption as well as different chlorophyll contents. There were no measurements of Pb content in the ambient air in this study, but the Pb content in Surabaya was assumed to be 2.664 µg/m³ (Siregar 2005). Based on the National Ambient Air Quality Standards (NAAQS), the standard of Pb content in the air was equal to 0.15 µg/m³ while the Pb content in Surabaya for particular matter (PM_{2.5-10}) was 0.27 µg/m³. However, the quality standard established by the Indonesian Government Regulation 41 in 1999 for Pb was 2 µg/m³ (24 hours) or 1 µg/m³ (12 hours), so the quality of Pb in air particulate in Surabaya from October 2012 to February 2014 has not exceeded this established quality standard. So, it can be concluded that Pb content in PM_{2.5} and PM_{2.5-10} categories has exceeded the quality standard of NAAQS from the United States Environmental Protection Agency (USEPA), but has not exceeded the quality standard of the Government Regulation 41 in 1999.

The absorption of lead (Pb) on *W. trilobata* and *S. oleina* plants: This study found that the Pb metal content of plant leaves grown in areas through which motor vehicles pass were affected by the number of vehicles that pass. *W. trilobata* and *S. oleina* leaves grown on Diponegoro Street, which, of the three streets is traversed by the most vehicles, had a higher Pb content than leaves grown on the other two streets. This indicated that the location of growth has an effect on the Pb content of leaves, both in *W. trilobata* and *S. oleina* (Samsuodin et al. 2015).

This research also found that the species of the plants affects the Pb content in leaves. The Pb content of *W. trilobata* and *S. oleina* ranged from 0.146-0.288 µg/g. The Pb content of both the plants is still within the normal range, as the accepted Pb content for many plant species range from 1.0-3.5 µg/g (Siregar 2005). However, of the two plants, *W. trilobata* had higher Pb levels than *S. oleina*. The high

Table 3: ANOVA result of location and type of plant *Wedelia trilobata* and *Oleina syzygium* with chlorophyll content in the leaves.

Source	Dependent Variable	Sign
Location	Chlorophyll content	0.00
Plant	Pb content	0.00
Location*Plant	Pb content	0.03

Table 4: The average and standard deviation of chlorophyll content in *S. oleina* and *W. trilobata* leaves at various locations.

Type of Plants	Station	Chlorophyll content in leaves (mg/L)
<i>W. trilobata</i>	St. 1	15.563 ± 1.886bA
	St. 2	12.593 ± 0.357abA
	St. 3	13.200 ± 3.346aA
<i>S. oleina</i>	St. 1	23.186 ± 0.804bB
	St. 2	16.403 ± 1.092abB
	St. 3	19.766 ± 4.570abB

Notes: a,b: location; A,B: species of plant

St. 1 Diponegoro Street, St. 2 J.A Suprpto Street and St. 3 H.R Muhammad Street.

absorption of Pb by *W. trilobata* leaves is associated with its herbaceous plant habit, as opposed to the shrubby habit of *S. oleina*. The height of a plant and the position of its leaves has an effect on its ability to absorb Pb. A lower plant height is able to absorb more Pb (Istiharoh et al. 2014). Another study stated that Pb is part of PM₁₀, particulate matter sized ≤ 10 µm, which is optimally distributed to shrub habit plants (Muzayanah et al. 2016). The level of pollutant distribution varies between altitudes from the soil surface upwards, whilst the number and distribution of plant leaves vary between canopy and stem so that higher floating pollutants can be absorbed by trees, while those floating at lower altitudes or those that fall are absorbed by ground cover plants (Inayah et al. 2010).

In addition, some studies have reported that furry leaves and rough surfaces will absorb more dust pollutants than leaves with slippery surfaces. Based on this, *W. trilobata* has a rough and wrinkled leaf surface that was effective in the absorption of Pb from the air. This was in line with the research that stated that feathered or wrinkled leaf surfaces have a high ability to absorb Pb compared with slippery and flat leaf surfaces (Nurhikmah et al. 2015). Thus, *S. oleina* plants have a low ability to absorb the Pb in the air compared with *W. trilobata*, as *S. oleina* has flat leaves, and a slippery surface in terms of leaf texture; *S. oleina* has leaves that are less effective in absorbing lead from the air. Furthermore, with the research by Gothberg (2008) that growing plants in areas with high air pollution may disturb the growth of plants susceptible to particulate Pb absorption.

The lead is deposited on the surface of the plants and can cause a decrease in the chlorophyll content of leaves (Gothberg 2008). The effectiveness of a plant's ability to absorb Pb, to a certain extent, will decrease with increasing Pb content (Kurnia 2004). Another factor that affects the mechanism of Pb absorption by plants is the opening of the leaf stomata. A Pb particle is roughly less than 2 µm in diameter, so plants with large stomata and/or large numbers of stomata can absorb more Pb into their leaf tissue during photosynthetic gas exchange than plants with small and/or few stomata. Besides these factors, the process of Pb absorption by the leaves is also influenced by temperature, light and moisture.

The mechanism of Pb absorption in *S. oleina* and *W. trilobata* leaves is through passive absorption. The Pb particles enter into the leaf through the stomatal gap and settle in the leaf tissue, accumulating between the palisade tissue gap or the spongy tissue. Because Pb particles are insoluble in water, Pb in the tissue is trapped in the cavity between the cells around the stomata. The contaminated gas enters the leaf tissue through the holes of stomata located on the upper epidermal layer. Through these holes, the pollutant dissolve in the surface water of the leaf cells (Santoso 2013). This Pb will accumulate inside the palisade tissue (Fitter & Hay 1991).

The chlorophyll content in *W. trilobata* and *S. oleina* leaves: Other research has found that location, plant species, or interaction of location and plant species affect the chlorophyll content of plant leaves. Plants that grow in areas where many motor vehicles pass through modify the chlorophyll content of their leaves. The higher number of passing vehicles lower the chlorophyll content of the leaves. The chlorophyll content in the leaves of *W. trilobata* and *S. oleina* on Diponegoro Street was lower than on JA Suprpto and HR Muhammad Street. This indicates that location affects the chlorophyll content of the leaves, both in *W. trilobata* and *S. oleina*.

W. trilobata has a higher Pb content and a lower chlorophyll content compared with *S. oleina*. *S. oleina* has a lower Pb content and a higher chlorophyll content than *W. trilobata*.

The chlorophyll content in both *S. oleina* and *W. trilobata* was still within the normal range and did not indicate a physiological response due to Pb exposure. This was supported by research that finds that plants with Pb absorbing capabilities tend to have a high accumulation of Pb in leaves but do not show any changes in leaves structure and physiology, such as in the stomata and in chlorophyll levels (Fathia et al. 2015).

S. oleina and *W. trilobata* leaves with exposure to Pb emissions on some streets in Surabaya town did not decrease the chlorophyll content of leaves, and chloroplast structure was not damaged. The formation of chloroplast structure is strongly influenced by mineral nutrients such as Mg and Fe. The entry of Pb in plants will reduce the intake of Mg and Fe, which can change the amount and volume of chloroplasts (Olivares 2003). From this description, it was evident that the accumulation of Pb in the leaves did not cause the inhibition of Mg and Fe minerals intake in the plants researched in this study. The plants did not change their absorption of mineral nutrients due to the influence of Pb and working of enzymes that were necessary for chlorophyll formation were not inhibited. These enzymes included porphobilinogen deaminase, protochlorophyllide, and a delta-aminolevulinic acid dehydratase. In terms of mechanisms that plants may use to deal with toxic concentrations, one method is through amelioration by moving ions from the circulation place with some way or become tolerant in the cytoplasm (Olivares 2003). The Pb particles that entered into the leaves will pass through the stomata, the size and number of which greatly affecting the entry of lead particles (Gunarno 2014). Plants act as absorbers because they are capable of absorbing Pb in the air through passive absorption mechanisms. Pb is absorbed by plants through leaf stomata located in the upper epidermal layer and settles in leaf tissue, accumulating between the palisade tissue gap or the spongy tissue (Santoso 2013).

The ability of plants to absorb Pb metal is also influenced by the leaf area. *W. trilobata* has wider leaves that are able to absorb more metals than *S. oleina*. This is in line with the study which concluded that *Codiaeum variegatum*, which has wide leaves, has the ability to absorb Pb in greater quantities than the leaves of *Hymenocallis speciosa* and *Cerbera manghas* leaves, which have an oval leaf shape (Sari et al. 2016). A wide leaf shape is more effective in absorbing pollutants compared to leaves with small surface areas (Dewi & Hapsari 2012).

CONCLUSION

The results showed that the location of a plant species affected the content of Pb metal and chlorophyll in leaves, but the interaction between the location and the species of plants only affects the chlorophyll content and not the Pb metal content of leaves.

ACKNOWLEDGMENTS

We would like to thank Dr. Sunu Kuntjoro and Dr. Yuliani for reviewing the article.

REFERENCES

- Boediningsih, W. 2011. The impact of traffic density on air pollution in Surabaya City. *Jurnal Fakultas Hukum*, 20(20): 119-138.
- Dewi, Y. S. and Hapsari, I. 2012. The effectiveness study of curing leaf (*Codiaeum variegatum*) and mother in-laws tongue (*Sansevieria trispasciata*) in absorbing lead in ambient air. *Satya Negara Indonesia Scientific Journal*, 5(2): 1-7
- EPA 2007. Determination of metals and trace elements in water and wastes by inductively coupled plasma-atomic emission spectrometry. https://www.epa.gov/sites/production/files/2015-08/documents/method_200-7_rev_4-4_1994.pdf.
- Fathia, L.A.N., Baskara, M. and Sitawati, S. 2015. The Analysis of plants capability at Median road in absorbing heavy metals Pb. *Journal of Plant Production*, 3(7): 528-534.
- Ferdhiani, S.L. and Proklamasingih, E. 2016. Peroxidase enzyme activity and chlorophyll content at Angsana leaves. *Biosfera*, 32(2): 126-133
- Fitter, A.H. and Hay, R.K.M. 1991. *Physiology of Plant Environment*. Yogyakarta: Gadjah Mada University Press.
- Flanagan, J. T., Wade, K. J., Currie, A. and Curtis, D. J. 1980. The deposition of leads and zinc from traffic pollution on two roadside scrubs. *Environmental Pollution*, 1: 71-78.
- Gothberg, A. 2008. Metal fate and sensitivity in the aquatic tropical vegetable *Ipomoea aquatica*. Department of Applied Environmental Science, Doctoral Thesis, Stockholm University.
- Gunarno 2014. Influence of air pollution on leaf area and number of stomata leaves of *Rhoeo discolor*. Jakarta, University of Indonesia Press.
- Inayah, S. N., Las, T. and Yunita, E. 2010. Pb content in Angsana leaf (*Pterocarpus indicus*) and mini elephant grass (*Axonopus* sp.) in Tangerang city protocol street. *Valence Chemistry Journal*, 2(1): 340-346.
- Istiharah, P.D., Martuti, N.K.T. and Bodijanto, F.P.M.H. 2014. Lead (Pb) content test by leaves based on tree location and crown position: Case study of green path Acacia mangium Jogorawi toll road. *Media Conservation*, 16(3): 101-107.
- Kean, A., Harley, R.A., Littlejohn, D. and Gery, K. 2000. On-road measurement of ammonia and other motor vehicle exhaust emissions. *Env. Sci. Technol.*, 34: 3535-353
- Kurnia, Rahma 2004. *Laporan Kegiatan Kursus Identifikasi Dampak Lingkungan*. Yogyakarta: GEGAMA.
- Landberg, T. and Greger, M. 1996. Differences in uptake and tolerance to heavy metals in *Salix* from polluted and unpolluted areas. *Applied Geochemistry*, 11: 175-180.
- Muzayanah, Ariffin, Sudarto and Yanuwadi, B. 2016. Effects of the green space proportion with cumulative concentration of particulate matter 10 (PM₁₀) in Surabaya-Indonesia. *International Journal of ChemTech Research*, 9(4): 431-436.
- NASA and ALCA 1989. Interior landscape plants for indoor air pollution abatement. National Aeronautics and Space Administration John C. Stennis Space Center Science and Technology Laboratory Stennis Space Center, MS 39529-6000.
- Novita, Yuliani and Purnomo, T. 2012. Lead metal (Pb) absorption and *Elodea canadensis* chlorophyll content on liquid waste of pulp and paper factory. *Journal of Lentera Bio.*, 1(1): 1-8.
- Nurhikmah, A., Syamsidar, H. S. and Ramadani, K. 2015. Bogenvil biosorption (*Bougainvillea spectabilis* Wild) against lead emissions (Pb) on motor vehicles. *Journal of Al Chemistry*, 3(2): 42-51
- Olivares, E. 2003. The effect of lead on phytochemistry of *Tithonia diversifolia* exposed to roadside automotive pollution or grown in pots of Pb-supplemented soil. *Brazilian Journal Plant Physiol*

- ogy, 15(3): 149-158.
- Purwatiningsih, S. 2015. Review of city development concepts: Compact city. Urban Planning Courses RP 141314. (<https://www.academia.edu/12525336/ReviewCompactCity>).
- Samsedin, I., Susidharmawan, I. W., Pratiwi and Wahyono, D. 2015. The Role of Trees in Maintaining Urban Air Quality. Forda Press, Bogor.
- Santoso, S.N. 2013. Use of plants as air pollution reduction. <http://digilib.its.ac.id/public/ITS-Undergraduate-16616-Paper-pdf.pdf>.
- Sari, F.R., Purnomo. T. and Rachmadiarti, F. 2016. Ability of betel plant (*Epipremnum aureum*) as lead (Pb) absorbent in the air. *Lentera Bio.*, 5(3): 117-124.
- Sembiring, E. and Sulistyawati, E. 2006. Pb absorption and its effect on leaf condition of *Swietenia macrophylla* King. Paper presented at the National Seminar on Environmental Research at Higher Education 2006, at Bandung Institute of Technology Campus, 17-18 July 2006.
- Siregar, E.B.M. 2005. Air pollution, plant response, and its effect on humans. Faculty of Agriculture, Forestry Study Program, University of North Sumatra, Medan.
- Sunu, P. 2001. Protecting The Environment by Applying ISO 14001. Jakarta: PT. Gramedia Widiasarana, Indonesia.



Pretreatment Comparison Between Preoxidation and Prechlorination on the Changing of Natural Organic Matter

Euis Nurul Hidayah[†], Muhammad Firdaus Kamal, Fauzul Rizqa and Mukhamad Rifki Hendianto

Department of Environmental Engineering, University of Pembangunan Nasional Veteran Jawa Timur, Surabaya, Indonesia

[†]Corresponding author: Euis Nurul Hidayah

Nat. Env. & Poll. Tech.
Website: www.neptjournal.com

Received: 06-06-2018
Accepted: 02-08-2018

Key Words:

Natural organic matter
Preoxidation
Prechlorination
Fourier-transform infrared

ABSTRACT

Surface water is mainly used as source water after treatment process to produce drinking water or clean water. The existence of natural organic matter (NOM) in surface water caused some problems in water treatment, instead of taste and aesthetic issues. Preoxidation and prechlorination are oxidation processes that have been used widely for different purposes in water treatment process. The objective of the study was to compare performance of permanganate preoxidation and prechlorination in removing NOM and to know the changing of NOM in term of its functional group properties by using Fourier-Transform Infrared (FTIR). TOC concentration and UV_{210} value were used to represent NOM parameter. The results showed that prechlorination has a higher performance to treat NOM in water than permanganate preoxidation. Further, prechlorination could be considered as pretreatment of coagulation in order to improve its performance in removing TOC concentration and aromatic compounds. FTIR could be applied to track the changing of NOM functional groups, and organic properties in prechlorination followed by alum coagulation have the lowest percentage transmittance.

INTRODUCTION

Aquatic natural organic matter (NOM) is a complex mixture of organic compounds in aquatic environment. NOM could be generated in water due to microbial activities and degradation of dead organisms, such as algae. NOM could be formed from land and soil that is transported to the water body through watershed runoff or washing out of upstream water bodies. Recently, industrial activities and its biological treatment contributed to the increasing of organic matter compounds in water bodies, or it is known as the effect of effluent organic matter (EfOM) (Shon et al. 2012). Surface water is mainly used as source water for water treatment process to produce drinking water or clean water. The existence of NOM in surface water causes some problems in water treatment, besides taste and aesthetic issues. For example, higher NOM concentration needs higher coagulant demand, incomplete NOM removal in coagulation can cause membrane fouling, and NOM will compete with the target compounds in advance process, such as ion exchange and activated carbon (Han et al. 2015). In disinfection process, NOM which is not removed by previous treatment, can react with chlorine and form disinfectant by-products (DBPs), such as trihalomethanes (THMs) and haloacetic acids (HAAs) (Reckhow & Singer 2011).

Number of treatment processes have been applied to remove NOM in source water. However, NOM removal is highly dependent on the characteristics of NOM and its

concentration. Coagulation is most widely used in water treatment processes. It has been known that coagulation could be applied to remove NOM through aggregation mechanism (Silanpaa et al. 2018, Hidayah et al. 2016). The removal mechanism of NOM will be different for specific types of NOM, because NOM has different characteristics. Aromatic and humic substances organic matter is mainly removed by coagulation through entrapment, charge neutralization and adsorption (Silanpaa et al. 2018), while aliphatic and non-humic substances can be removed by advanced treatment processes, such as membrane filtration, adsorption and ion exchange (Lamsal et al. 2012). Preoxidation has been known as pretreatment to improve coagulation process. Preoxidation could be conducted by ozone, chlorine, chlorine dioxide, permanganate, while each of preoxidant has its advantages and disadvantages. Preoxidation has various mechanisms to destroy the organic coating on the surface of particles, even preoxidant permanganate generated manganese dioxides in-situ to support organic settling. However, the higher dosage of permanganate could cause colour problems in the treated water (Ma et al. 2001, Hidayah & Yeh 2018). Prechlorination, which has high oxidation potential, is a strongest oxidant and has been applied in water treatment process, especially in post chlorination to remove pathogens. However, disinfectant by-products (DBPs) will be formed in the treated water due to chlorine is very reactive and easy to react with NOM (Kristiana et al. 2014).

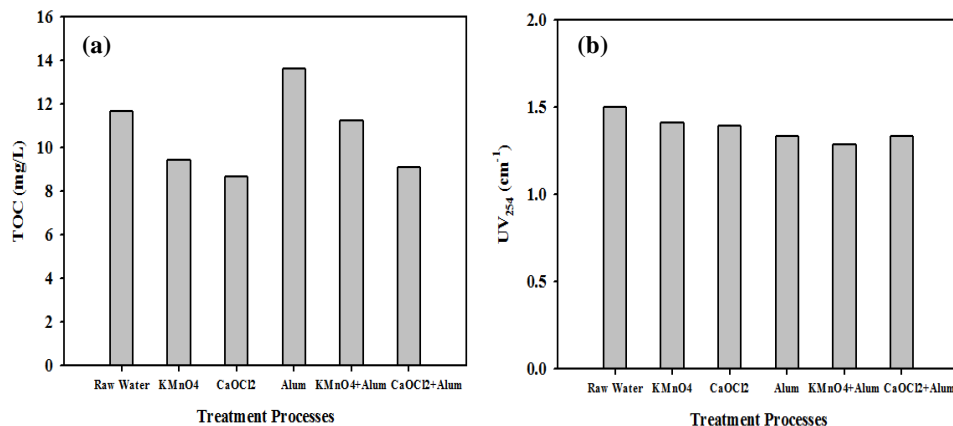


Fig. 1: NOM concentration in terms of (a) TOC concentration and (b) UV₂₁₀ value under different treatment processes.

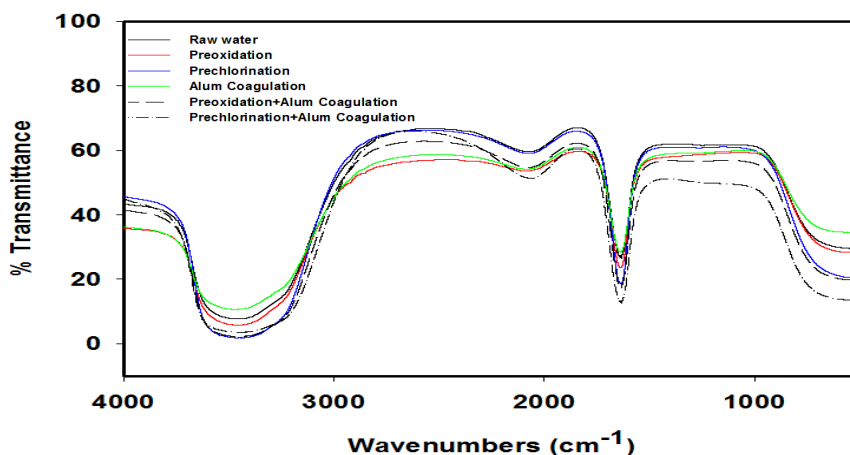


Fig. 2: Spectrum FTIR of the source water and treated water from different treatment process.

According to organic matter properties, it has been found that permanganate causes a reduction of high molecular weight biopolymers (Xie et al. 2016, Hidayah et al. 2017), while chlorine reduces high molecular and humic substance-like compounds (Hua & Reckhow 2007). However, few studies have investigated the changing of organic matter properties, in terms of its functional groups, in both preoxidation and prechlorination followed by coagulation. This study compared the performance of preoxidation and prechlorination in removing NOM and looked into the changing of NOM in terms of its functional group properties by using Fourier-Transform Infrared (FTIR). Surface water was treated by permanganate preoxidation and prechlorination followed by alum coagulation.

MATERIALS AND METHODS

The sample was collected from Jagir River, a main surface water source for water treatment plant in Surabaya, during

dry season. The experiment was conducted by using jar test apparatus (Phipps & Bird, Richmond, VA, USA). A litre of source water sample was placed in the six stirrers at a time under different treatments, including: raw water only, 0.8 mg/L KMnO₄ (Merck, Germany) preoxidation, 25 mg/L CaOCl₂ (Merck, Germany) prechlorination, 35 mg/L (Al₂(SO₄)₃·18H₂O (Merck, Germany), 0.8 mg/L KMnO₄ followed by 35 mg/L alum, 25 mg/L CaOCl₂ followed by 35 mg/L alum. Dosage was obtained from preliminary experiment. The contact time for preoxidation and prechlorination was 60 minute under slow mixing at 35 rpm. Alum coagulation was setup under 100 rpm flash mixing for 3 min, followed by 35 rpm slow mixing for 15 min, and settling for 30 min. Sample was filtered through 0.45 μm (cellulose acetate, Toyo Roshi, Japan) before further measurement.

The sample was analysed for TOC by using total organic carbon analyser (Model TOC-500, Shimadzu, Kyoto, Japan). UV₂₁₀ was measured using UV/vis spectrophotom-

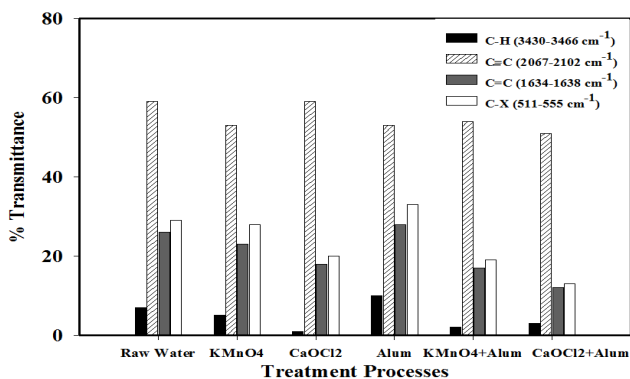


Fig. 3: Percentage transmittance of spectrum from FTIR analysis of the source water and treated water.

eter (Model U-2001, Hitachi, Japan) with a 1 cm quartz cell (APHA 2012). The powder of raw water and treated sample obtained via freeze-drying method was analysed for the structural and organic characteristics by FTIR. Briefly, KBr pellets were prepared by grinding the samples with spectrographic grade KBr in an agate mortar utilizing a fixed amount of sample (1%, wt%). FTIR spectroscopy (Thermo Nicolet NEXUS 670) was used to identify the functional groups, scanning from 4000 cm⁻¹ to 400 cm⁻¹.

RESULTS AND DISCUSSION

Effect of preoxidation and prechlorination as coagulation pretreatment on NOM concentration: Figs. 1a & 1b showed NOM concentration in terms of TOC concentration and UV₂₁₀ value under different treatment processes, respectively. First, source water has a high TOC concentration of 11.67 mg/L and contain aromatic compounds with conjugated C=C double bond, as indicated by UV₂₁₀ value. The high NOM concentration is probably due to human activities like discharge of domestic wastewater into Jagir River. According to the sampling site, area around Jagir River is indicated with high density population, and domestic wastewater discharged directly to the river. In addition, an industrial park has been settled down at the upstream of Jagir River and its effluents are discharged to the river. It has been well known that wastewater treatment from industrial activities might contribute to the quantity and quality of organic matter in the river bodies, or it is known as effluent organic matter (Shon et al. 2012). Second, all treatments could remove the organic matter concentration, except alum coagulation. Decrease of TOC concentration seems less than 50%, which indicates that source water contain mainly non-aromatic compounds. Meanwhile, increased TOC concentration during alum coagulation is probably due to the formed floc which may contain organic matter. Preoxidation, prechlorination, and pretreatment followed by alum coagulation has a high reduction of NOM. Third, prechlorination

showed a higher performance in removing TOC concentration than the other methods. It is probably due to hypochlorite, a hydrolysis product of chlorine in water, oxidized the coating organic matter into lower molecular weight or transformed aromatic or high molecular weight of organic into different compounds (Xie et al. 2016, Hidayah et al. 2017, Cahyonugroho & Hidayah, 2018). This suggestion is supported by UV₂₁₀ value, which showed decreasing concentration in all treatment processes. UV₂₁₀ detected aromatic compounds, therefore decreasing UV₂₁₀ value indicated that aromatic compounds have been reduced. It has been well established that aromatic and humic substances are easy to be degraded by coagulation only, preoxidation, and combination of water treatment processes (Edzwald & Tobiason 2011).

Effect of preoxidation and prechlorination as coagulation pretreatment on the changing of NOM: Fig. 2 showed the spectrum from FTIR analysis of the source water and treated water from different treatment processes, and the percentage transmittance of FTIR spectrum is described in the histogram graph as shown in Fig. 3. First, the results indicate that source water contains four peaks, which identify the four major functional groups including: C-H compounds at wavelength 3430-3466 cm⁻¹, triple bond C≡C compounds at wavelength 2067-2102 cm⁻¹, double bond C=C compounds at wavelength 1634-1638 cm⁻¹, and C-X compounds at wavelength 511-555 cm⁻¹. Second, source water mainly contains of group triple bond C≡C compounds. It is consistent with the TOC concentration and UV₂₁₀ value, as compared with Fig. 1a & Fig. 1b, which showed less than 50% decreasing value of NOM concentration.

Third, all treatment processes identify the decreasing of functional group compounds, except in alum coagulation process. This result is consistent with the TOC concentration and UV₂₁₀ value. Alum coagulation performed increasing percentage transmittance of all functional groups, except triple bond C≡C compounds. It seems that three functional groups C-H, C=C, and C-X compounds represented a group of compounds that is related to increasing TOC concentration in alum coagulation. Fourth, prechlorination followed by alum coagulation showed a higher reduction of percentage transmittance of organic matter, it means that prechlorination-alum coagulation could be considered as an alternative process to remove NOM in water.

CONCLUSION

Source water of Jagir River contains high TOC concentration, aromatic compounds and mainly composed of single and triple bond organic matter. This study concluded that alum coagulation only removes aromatic organic com-

pounds in source water. Therefore, alum coagulation needed a pretreatment to improve coagulation efficiencies in removing NOM. Preoxidation and prechlorination could be considered as pretreatment of coagulation process. Prechlorination followed by alum coagulation performed a higher reduction than preoxidation-alum coagulation. However, prechlorination-alum coagulation need a further process to remove nonaromatic compounds, such as triple bond $C\equiv C$ compounds.

REFERENCES

- APHA, AWWA and WEF 2012. Standard Methods for the Examination of Water and Wastewaters. 21th eds., American Public Health Association, Washington, D.C.
- Cahyunugroho, O.H and Hidayah, E.N. 2018. Characteristics of natural organic matter (NOM) surrogates under different disinfection. *Journal of Engineering and Applied Science*, 13 (20): 8372-8376
- Edzwald, J.K. and Tobiasson, J.E. 2011. Chemical principles, source water composition, and watershed protection. In: Edzwald, J.K. (eds.) *Water Quality & Treatment: A Handbook on Drinking Water*. AWWA McGraw-Hill, New York.
- Han, Q., Yan, H., Zhang, F., Xue, N., Wang, Y., Chu, Y. and Gao, B. 2015. Trihalomethanes (THMs) precursor fractions removal by coagulation and adsorption for bio-treated municipal wastewater: Molecular weight, hydrophobicity/hydrophilicity and fluorescence. *Journal of Hazardous Materials*, 297: 119-126.
- Hidayah, E.N., Chou, Y.C. and Yeh, H.H. 2016. Using HPSEC to identify NOM fraction removal and the correlation with disinfection by-product precursors. *Water Science and Technology*, 16(2): 305-313.
- Hidayah, E.N., Chou, Y.C. and Yeh, H.H. 2017. Comparison between HPSEC-OCD and F-EEMs for assessing DBPs formation in water. *Journal of Environmental Science and Health, Part A*, 52(4): 391-402.
- Hidayah, E.N. and Yeh, H.H. 2018. Effect of permanganate preoxidation to natural organic matter and disinfection by-products formation potential removal. *Journal of Physics: Conference Series*, 953(1): 012218.
- Hua, G. and Reckhow, D.A. 2007. Characterization of disinfection byproduct precursors based on hydrophobicity and molecular size. *Environmental Science and Technology*, 41(9): 3309-3315.
- Kristiana, I., Tan, J., McDonald, S., Joll, C.A. and Heitz, A. 2014. Characterization of the molecular weight and reactivity of natural organic matter in surface waters. In: Rosario-Ortiz, F.L. (eds.) *Advances in the Physicochemical Characterization of Organic Matter*. American Chemical Society: Washington DC, 209-233.
- Lamsal, R., Montreuil, K.R., Kent, F.C., Walsh, M.E. and Gagnon, G.A. 2012. Characterization and removal of natural organic matter by an integrated membrane system. *Desalination*, 303: 12-16.
- Ma, J., Li, G., Chen, Z., Xu, G. and Cai, G. 2001. Enhanced coagulation of surface waters with high organic content by permanganate preoxidation. *Water Science and Technology: Water Supply*, 1 (1): 51-61.
- Reckhow, D. and Singer, P.L. 2011. Formation and control of disinfection by-products. In: Edzwald, J.K. (eds.), *Water Quality & Treatment: A Handbook on Drinking Water*. AWWA McGraw-Hill: New York, pp. 1-59.
- Shon, H.K., Vigneswaran, S. and Snyder, S.A. 2012. Effluent organic matter (EfOM) in wastewater: Constituents, effect, and treatment. *Critical Reviews in Environmental Science and Technology*, 36(4): 327-374.
- Sillanpaa, M., Ncibi, M.C., Matilainen, A. and Vepsäläinen, M. 2018. Removal of natural organic matter in drinking water treatment by coagulation: A comprehensive review. *Chemosphere*, 190: 54-71.
- Xie, P., Chen, Y., Ma, J., Zhang, X., Zou, J. and Wang Z. 2016. A mini review of peroxidation to improve coagulation. *Chemosphere*, 155: 550-563. and Hidayah, E.N. 2018. Characteristics of natural organic matter (NOM) surrogates under different disinfection. *Journal of Engineering and Applied Science*, 13 (20): 8372-8376



Bioflocculation of Two Species of Microalgae by Exopolysaccharide of *Bacillus subtilis*

Musthofa Lutfi*†, Wahyunanto A. Nugroho*, Winny P. Fridayestu*, Bambang Susilo*, Chusak Pulmar** and Sandra Sandra*

*Department of Agricultural Engineering, Brawijaya University, Veteran St. 1, Malang, East Java, 65145, Indonesia

**Faculty of Agriculture and Agro-Industry Technology, Rajamangala University of Technology, Suwanabhumi, Ayuthaya 13000 Thailand

†Corresponding author: Musthofa Lutfi

Nat. Env. & Poll. Tech.
Website: www.neptjournal.com

Received: 30-05-2018
Accepted: 02-08-2018

Key Words:

Microalgae
Bioflocculation
Exopolysaccharide
Bacillus subtilis

ABSTRACT

Harvesting is ultimately an important step on microalgae production since a successful harvesting will increase the performance of the system totally as well as increasing the revenue. Bioflocculation is such type of the harvesting technique that offers high recovery performance, while at the same time it costs less and is more environment friendly. Exopolysaccharide (EPS) is actually the key of the performance. The objective of this research is to observe the performance of EPS produced by the *Bacillus subtilis* for microalgae harvesting. The bacterial growth medium where the EPS has been produced was induced directly to the microalgae. Two different species of microalgae, which were *Nannochloropsis oculata* and *Botryococcus braunii*, were used to compare the influence of microalgae type to the performance. Different concentration of EPS was employed to study how it affects the recovery performance. These various concentrations were 5% v/v, 10% v/v and 15% v/v. The result shows that the highest performance was presented when 5% EPS was induced to both the species, which was about 90%, while the lowest was presented by 15% EPS, which was about 70%. The same trend was applied for initial floc forming time of each treatment.

INTRODUCTION

Microalgae have been proposed as a nature provider for various chemicals ranging from low value to high value chemicals. While in production of some high value chemicals the cost might be an insignificant issue, the production of lower value chemicals such as fuel, the lowest possible cost should be taken into account. Otherwise, it will never be able to compete with conventional source of fuel.

The production of biofuel from microalgae is becoming an attractive option since it offers ease of cultivation (Sing et al. 2013), high oil productivity per dry mass basis (Rodolfi et al. 2009, Griffiths et al. 2009) and sustainable production (Ahmad et al. 2011, Pittman et al. 2011). *Nannochloropsis* sp and *Botryococcus braunii* are among the prospective microalgae due to their high oil content and biomass rate (Moazami et al. 2012, Biondi et al. 2013, Metzger et al. 2005). Another benefit of cultivating *Nannochloropsis* is its robustness, and easy growth in a wide range of environments (Sukenic et al. 2009, Kilian et al. 2011). In regard to *Botryococcus brauni*, it also synthesizes numerous hydrocarbons for wider purposes (Wijffels et al. 2010, Khatri et al. 2013).

The total production cost for biofuel from microalgae is,

in fact, a function of several variables such as labour cost, cultivation system, harvesting and refining cost. Such actions have been applied to suppress the constraints: reusing nutrient from wastewater mainly in open pond reactor (Park et al. 2011, Matamoros et al. 2015, Bohutskyi et al. 2015), improving gas transfer to increase the growth rate (Zimmerman et al. 2011, Ying et al. 2013), updating the harvesting technique (Milledge et al. 2013, Barros et al. 2015, Wang et al. 2015), and increasing the efficiency of oil refinery (Halim et al. 2012, Mubarak et al. 2015).

Cell harvesting is a step prior to the refining process of microalgae oil. The uneconomical conventional technique of harvesting could exceed half the cost of total oil production (Richmond et al. 2008). A successful technique for harvesting will not only significantly affect the total performance of the system, but also reduce the total cost. Efficiency of oil recovery in refinery is also affected by the harvesting step (Patil et al. 2015). Innovations have been made in harvesting technique with consideration of high biomass recovery, refining efficiency and low cost.

Chemical flocculation has been applied so far for microalgae harvesting. It is considered as one of the economical techniques since it achieves a good performance

with relatively low flocculant dosage and results in low harvesting cost (Bilanovic et al. 2008, Vandamme et al. 2013, Wan et al. 2015). In general principle, a particle has electrostatic charge that makes them relatively stable solutes in water, besides their small size that makes them suspend easily in the water. Chemical flocculants have opposite charge that attract particles to form a flock. When the bigger flocks are formed, they become unstable. An unstable flock either will settle down or float up, depending on its density and hydrophobicity.

Chemical flocculation has been successful to be applied for water treatment. To apply such technique for microalgae harvesting, some consideration needs to be taken. Besides its several benefits, chemical flocculation has several drawbacks when it is used in full scale microalgae production. The presence of sediment caused by the cationic substance needs more efforts to remove. Chemical flocculation will change the pH medium, temperature, dissolved oxygen as well as nutrient depletion that occur during the process. These adjusted conditions could lead to change of the composition of the harvested cells (Benemann et al. 1996). Hence, more sustainable flocculation method is important to be applied.

Bioflocculation could be an alternative for a cheaper harvesting cost, since it reduces the use of chemical coagulant, hence reducing the following treatment to dispose sediment from the site. Bioflocculation is a term to address any flocculation enhanced by exopolysaccharide (EPS) secreted by microorganisms (Christenson & Sims 2011). It is considered as a biodegradable substance and more environmental friendly than any chemical polymer used in non-biocoagulation process (Kim et al. 2011).

EPS is a major component in microbial biofilm. Several factors affect the composition of EPS as well as its formation. Microbial genetics and the physico-chemical conditions of the growth medium are among the two factors affecting the EPS composition (Castro et al. 2014). Such environmental conditions also affect the character of the EPS in terms of its porosity, density, moisture content, hydrophobicity and mechanical stability (Wingender et al. 2012). According to Pham et al. (2000), EPS itself is produced during the final session of stationary phase of microbial life cycle when it begins to experience a nutrient shortage. However, after any particular time, the number of EPS could decrease, as it will be consumed by microbes itself as a carbon source if more nutrient is not added in the medium. Hence, it is essential to decide the best time to harvest the EPS for further utilization as bioflocculant.

Aggregation of algae occurs as an effect of bridging done by the EPS. As the aggregate becoming larger, its

stabilization in the medium becomes weaker and results in settlement or floating of the floc, depending on its density and any other treatment combined with the flocculation process. The recovery performance is affected by several parameters, including EPS dosage, EPS characteristics, morphology of the microalgae and culture density (Manheim & Nelson 2013). Research by Patil et al. (2010) revealed that the flocculation performance increased along with the increasing EPS dosage until it achieved the critical flocculation performance, which was 72% and 500 mg/L for the flocculation performance and dosage of EPS respectively. The study showed that there was no increase in the flocculation performance if the EPS added into the medium exceeded 500 mg/L. The highest performance in the report was 98% recovery when higher concentration of pure γ -PGA from *Bacillus licheniformis* was employed for the harvesting (Ndikubwimana et al. 2016).

Microalgae morphology is linked to the culture density, where the smaller individual microalgae size lead to the denser floc formation resulted in the higher settling performance (Manheim & Nelson 2013). This morphological effect was also applied for the bioflocculant type produced by different species of the bacteria.

This research was to observe the effect of bioflocculants dosage in the recovery performance as well as its settling time. *Nannochloropsis* and *Botryococcus brauni* were the strains used in this experiment to compare their behaviour during floc formation as they are morphologically different. *Bacillus subtilis* was applied as the EPS producer. This type of bacteria has presented to produce biopolymer γ -PGA that was successful in harvesting microalgae by employing the pure polymer in the medium (Zheng et al. 2012). In this study, the *Bacillus subtilis* culture medium with EPS produced in it was directly employed.

MATERIAL AND METHODS

Microorganisms and its Culture

Nannochloropsis oculata and *Botryococcus brauni* were two microalgae strains used in this study. The microalgae were collected from the Institute of Brackish Water Aquaculture (BBAP) Situbondo, East Java, Indonesia. Each strain of microalgae was cultured in a standard Bold's Basal Medium (BBM) in a 5-litre fibreglass tube reactor with conventional agitation to prevent sedimentation. The sparger was placed in the bottom of the reactor to induce carbon dioxide from ambient air. Lighting was provided using fluorescent lamps with intensity of 3000 lux, 24 hours a day for 15 days.

As an EPS producer, *Bacillus subtilis* was employed. The isolate was obtained by the Department of Postharvest

Technology, Brawijaya University, Indonesia. To produce the EPS, 1 dose of isolated bacteria was put into 20 mL of 0.9% NaCl. The inoculate was then cultivated in 980 mL of sterilized nutrient broth. The nutrient broth was prepared by dissolving 8 gram of nutrient broth Merck 105443 into 1 litre of deionized water and stirred at 50°C until perfectly dissolved. The culture was homogenized using a stirrer at 100 rpm for 72 hours at room temperature of 25-30°C. Seventy-two hour was the determined time resulted from the preliminary experiment as the time for the bacteria to achieve late stationary phase in a batch medium.

Exopolysaccharide (EPS)

The total EPS was tested gravimetrically by means of putting 25 mL culture of bacterial broth medium into 50 mL centrifuge tubes. It was then centrifuged at a temperature of 4°C, 6000 rpm for 20 minutes. The supernatant was taken, twice as much as cold ethanol (96%) was added and it was allowed to stand for overnight. The second cold centrifugation was carried out at another 4°C, 5000 rpm for 25 minutes. The remaining solid was dried at a 105°C and weighed. The productivity of the bacteria to produce EPS per litre of culture was calculated using the following formula:

$$EPS_{tot} = \frac{W_e}{V_o} \times 100\% \quad \dots(1)$$

Where, W_e is the dry weight of the EPS (gram) and V_o is the sample volume (litre).

Microalgae Harvesting

Microalgae was transferred from the glass tube bioreactor into 1 litre of glass beaker with 300 mL of working volume each. The pH of the culture was increased by adding 0.1M NaOH until it reached pH 10. The *Bacillus subtilis* was then added into the beaker. To study the effect of bioflocculant concentration, different volumes of bacterium-EPS inoculum were added ranging from 5% (v/v), 10% (v/v) and 15% (v/v). In this study, undried bacterium-EPS inoculum was added instead of dried mass of EPS since it uses less energy by skipping the separation process for EPS itself from the growth medium. A volume to dry weight conversion was carried out to ease the comparison of the results of this study to others if necessary. As the control of each strain, no bacterial inoculum was added to the beaker. Each treatment was done in triplicate.

The observation of macrofloc formation was carried out using 10x magnifying glass. The time of macrofloc formation was determined when the macrofloc started to be appearing in each beaker. Measurement of the harvesting performance was carried out by calculating the initial cell density of microalgae and the left microalgae suspended in the medium. The cell density was observed with haemocytom-

eter under a microscope. The performance was determined using this formula:

$$Performance = \frac{X_0 - X_1}{X_0} \times 100\% \quad \dots(2)$$

Where, X_0 is the initial cell density (cell/mL) and X_1 is the left microalgae (cell/mL).

RESULTS AND DISCUSSION

EPS Production

Bacillus subtilis is one of the biopolymer producer used for bioflocculation. To produce the EPS, the bacteria needs to be cultured in a growth medium until it reached an optimum production of EPS. As reported by Pham et al. (2000), the optimum EPS production occurs in the late stationary phase just before the death phase. A fall number of EPS will occur in the medium during death phase as it is used by the bacteria for its carbon source. It makes, determining the best harvesting time for the bacterial culture, as essential.

To determine the harvesting time, a preliminary experiment was carried out to observe the growth curve of the bacteria in the prepared growth medium. The growth was observed by counting the number of colonies using a haemocytometer under microscope every 12 hours until it reached the death phase. The time of the bacteria to reach the late stationary phase was then determined as the time when the culture was ready to use for the microalgae harvesting.

Fig. 1 shows the growth curve of the bacterial culture carried out in the preliminary experiment. The first count was done after 12 hours since the culture started. It logarithmically increased for the next 36 hours to reach the point of inflection. From the curve, it can be determined that the death phase occurred after 72 hours of the cultivation. According to these data, the bacterial culture would be best used for microalgae harvesting when its age is 72 hours within the same growth medium type. Different media type, concentration and bacterial species might differ the growth curve. The growth rate could be higher when more nutrients were provided. A higher population (8×10^8 cfu/L) and longer stationary phase (more than 72 hours) has been achieved when the *Bacillus subtilis* was cultured under more optimized conditions (Ghribi et al. 2011).

The EPS production by the *Bacillus subtilis* is presented in Fig. 2. About 50 mL of samples was taken from the culture medium per day in three days of culture. Each sample was dried sequentially to analyse the dried EPS produced. After one day of culture, the bacteria produced only less EPS. The production increased to several folds on the following day. The rate of EPS production was decreased on the third day; while on another side, it reached the highest

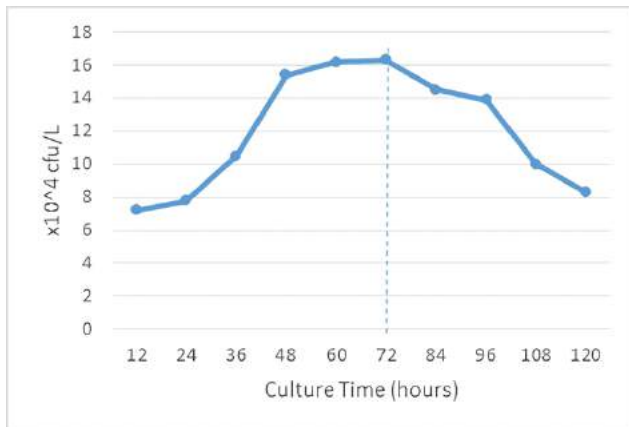


Fig. 1: Kinetics of *Bacillus subtilis* in nutrient broth carried out in the preliminary experiment.

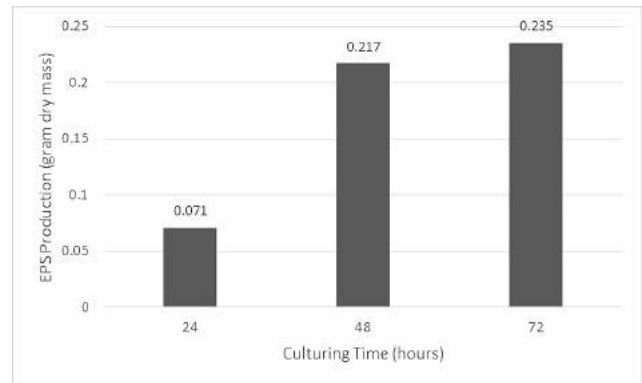


Fig. 2: Dried EPS produced by *Bacillus subtilis* from 50 mL sample.

production number, which was 0.235 gram. Given that the EPS tends to decrease as it passes the stationary phase, no observation of EPS production was carried out.

By converting the result of the last day into gram per litre basis, it can be presented that it was equal to 4.70 gram of dried EPS produced by the bacteria per litre growth medium. Type of medium has revealed to have an effect to the amount of EPS produced by the bacteria, besides the type of bacteria itself. A slightly higher production of EPS by *Bacillus subtilis* has been reported in 48 hours of culture time, which was 4.86 gram/L (Razack et al. 2013). This result was achieved by adding cane molasses into the growth medium, which increased the amount by 2% of the total volume. Molasses does not only provide carbon source for the bacteria, but it also provides some minerals and growth precursors (Liu et al. 2011). The highest reported productivity of microbial exopolysaccharide was probably by the fungus *Phoma herbarum* (13,6 gram/L) with the sorbitol used as the main carbon source, which was 60 g/L.

Microalgae recovery: Given that the harvesting step could enhance the overall performance of microalgae production, it is essential to determine the harvesting method that could recover more microalgae with less cost. Bioflocculation has been proposed as a promising method since such successful method could recover about 90% or more of the total cultured biomass. The less cost when employing this method is attributed by its biodegradability, hence no post treatment is needed to recover the flocculants.

In this study, dried EPS was not employed. Instead, the *Bacillus subtilis* culture medium with the EPS excreted in it was directly used as a flocculant. About 5%, 10% and 15% by volume of EPS was added for microalgae harvesting. By converting this percentage into milligram per litre, these numbers are equal to 220 mg/L, 420 mg/L and 620 mg/L for the 5%, 10% and 15% respectively. It is necessary to highlight that this practice, which was using EPS directly from the bacteria growth medium, is only practical when the EPS is produced in the same site as those of the

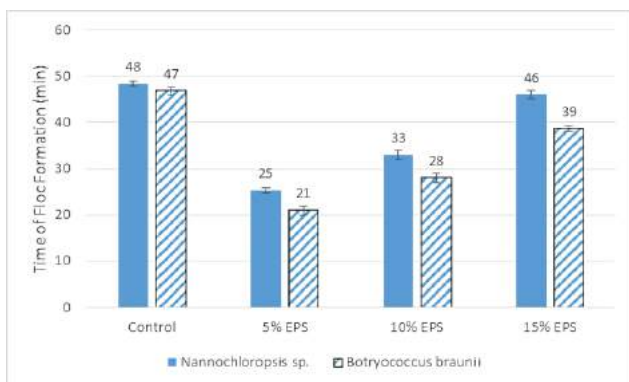


Fig. 3: Time to achieve first floc of EPS-microalgae.

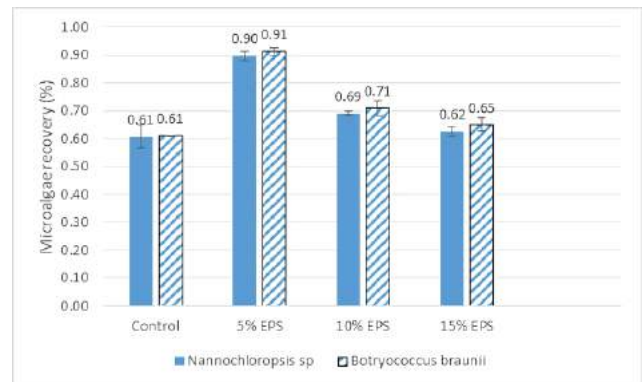


Fig. 4: EPS performance on microalgae recovery.

microalgae cultivation. For any different condition, such as the EPS produced by different producer, the use of commercially dried EPS might be preferable.

The microalgae harvesting started with the addition of the EPS to the microalgae culture. The culture was then homogenized in a magnetic stirrer with faster mixing (100 rpm) for 2 minutes followed by slower mixing (40 rpm) for 8 minutes. This step was followed by letting the samples to settle down for about 2 hours. The time of initial floc formation was observed (Fig. 3). The indicator of macrofloc formation is when the particles began to randomly moving and attach to each other or attach to a closest polymer. In both the microalgal species, the addition of 5% v/v of EPS was the best time to initially forming macrofloc, which was 25 minutes, and 21 minutes for *Nannochloropsis oculata* and *Botryococcus brauni*, respectively. Other than the control, the most unfavourable concentration among all treatment was 15% v/v for both the microalgae species.

To evaluate the recovery performance, the sample of the microalgae growth medium before and after addition of the EPS was taken and was analysed under microscope. It was carried out to see the microalgal cell number initially as well as the left cell suspended in the medium. The same trend also occurred in the EPS performance on harvesting the microalgae with 5% v/v was the most favourable concentration for the treatment with around 90% achievement for both the microalgal species, while the highest concentration shows the lowest performance (Fig. 4). A direct EPS producer bacteria induction to the microalgae medium was

also carried to harvest *Clamydomonas* sp. and *Picochlorum* sp. where the recovery performance ranged from 75% to 90% (Díaz et al. 2015). As has been reported by Patil et al. (2010), a concentration did not always linearly affect the harvesting performance. It was suggested that no significant performance increase could happen when the optimum flocculation performance has been achieved. This study was even more interesting when the increase of concentration was inversely proportional to the performance of recovery. An inverse condition was also reported by Ndikubimana et al. (2016), where the peak performance was achieved with addition of 20% γ -PGA. Beyond this point, the flocculation efficiency has been decreased.

However, it cannot be justified that less the concentration of EPS, the better is the performance. It was probably because the optimum concentration has been achieved by the lowest one, or even lower, while increasing the concentration would only distract the performance. It is hypothesized that when the optimum flocculation has happened, an additional flocculant likely will destabilize some macroflocs those have been formed by other biopolymers. A repulsive force between the same charges of the flocculants probably could be the reason of this destabilization. Avoiding more free surface of flocculant probably could be done by optimizing the flocculant-microalgae ratio.

Analysing the form of the floc microscopically is essential to understand the interaction between the microalgae and the EPS. Furthermore, it is necessary to ensure that the formation of the floc was due to the attraction of the EPS to the targeted microalgae, and was not due to any interaction with other substances. According to Salim et al. (2011), there are two ways for the polymer to form the flocs. Bridging occurs when the polymer is partially binding the microalgae on its surface. It normally occurs when the polymer is long enough. On the other side, when the polymer is short, it tends to adsorb the microalgae through its surface. The last sub-mechanism was named as patching. In this study, patching can be concluded as the way of macrofloc formation, as shown in Fig. 5 for all the treatments.

An ANOVA analysis was done using 5% confidential intervals. From the result, it could be concluded that the addition of EPS in the medium has significantly affected the harvesting performance while the type did not affect the performance of those two species employed (Table 1). A significant inverse effect was shown for the EPS concentration employed for the harvesting. While it was hypothesized that a species could affect the performance, this study did not show the effect significantly to such phenomenon. In earlier study, species might affect the harvesting performance mainly due to its density, morphology and microbial

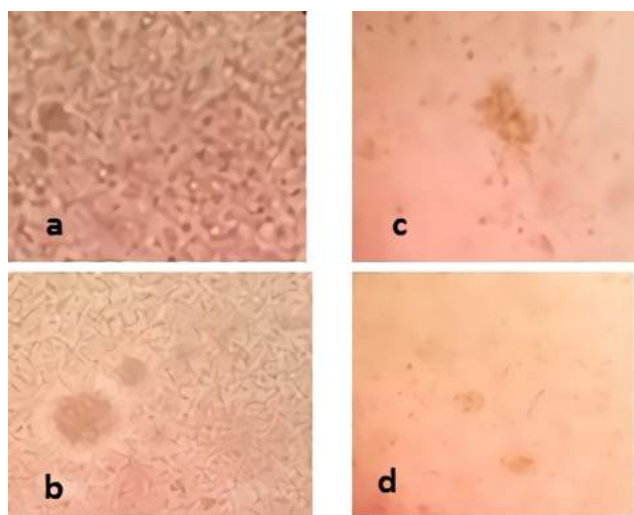


Fig. 5: Microscopic picture of first macrofloc formation of both microalgae in 100x magnitude. *Nannochloropsis oculata* with 5% EPS and 10% EPS (a and b respectively). *Botryococcus brauni* with 5% EPS and 10% EPS (c and d respectively).

Table 1: Statistical test of the harvesting performance.

Dependent Variable: Recovery

Source	Type III Sum of Squares	df	Mean Square	F	Sig.	Partial Eta Squared
Corrected Model	0.323 ^a	7	0.046	127.235	0.000	0.982
Intercept	12.191	1	12.191	33613.068	0.000	1.000
Microalga species	0.001	1	0.001	3.031	0.101	0.159
EPS Conc.	0.322	3	0.107	295.658	0.000	0.982
Microalga species * EPS Concentration	0.000	3	7.749E-5	0.214	0.885	0.039
Error	0.006	16	0.000			
Total	12.520	24				
Corrected Total	0.329	23				

a. R Squared = .982 (Adjusted R Squared = .975)

community structure (Pham et al. 2000, Díaz-Santos et al. 2015). The two microalgae have clearly different morphology and microbial community structure. While densities of these two algae might not be significantly different, which is close to water density, it probably made those two different microalgae to not show significant recovery performance for the same EPS concentration added.

CONCLUSIONS

In this work, an induction of EPS to the microalgae medium has significantly affected the recovery performance as well as decreasing the harvesting time. Instead of increasing the harvesting performance, an inverse trend was shown when the EPS concentration increased. It is predicted that repulsive force of free surface of the flocculant negatively impacted the recovery performance. To avoid such repulsive force, a study to optimize the EPS-microalgae concentration ratio is suggested for future research.

REFERENCES

- Ahmad, A.L., Yasin, N.M., Derek, C.J.C. and Lim, J.K. 2011. Microalgae as a sustainable energy source for biodiesel production: A review. *Renewable and Sustainable Energy Reviews*, 15(1): 584-593.
- Barros, A.I., Gonçalves, A.L., Simões, M. and Pires, J.C. 2015. Harvesting techniques applied to microalgae: A review. *Renewable and Sustainable Energy Reviews*, 41: 1489-1500.
- Benemann, J.R. and Oswald, W.J. 1996. Systems and economic analysis of microalgae ponds for conversion of CO₂ to biomass. Final report. California Univ., Berkeley, CA (United States). Dept. of Civil Engineering, pp. 214.
- Bilanovic, D., Shelef, G. and Sukenik, A. 1988. Flocculation of microalgae with cationic polymers - effects of medium salinity. *Biomass*, 17(1): 65-76.
- Biondi, N., Bassi, N., Chini Zittelli, G., De Faveri, D., Giovannini, A., Rodolfi, L., Allevi, C., Macrì, C. and Tredici, M.R. 2013. *Nannochloropsis* sp. F&M-M24: Oil production, effect of mixing on productivity and growth in an industrial wastewater. *Environmental Progress & Sustainable Energy*, 32(3): 846-853.
- Bohutskyi, P., Liu, K., Nasr, L.K., Byers, N., Rosenberg, J.N., Oyler, G.A., Betenbaugh, M.J. and Bouwer, E.J. 2015. Bioprospecting of microalgae for integrated biomass production and phytoremediation of unsterilized wastewater and anaerobic digestion centrate. *Applied Microbiology and Biotechnology*, 99(14): 6139-6154.
- Castro, L., Zhang, R., Muñoz, J.A., González, F., Blázquez, M.L., Sand, W. and Ballester, A. 2014. Characterization of exopolymeric substances (EPS) produced by *Aeromonas hydrophila* under reducing conditions. *Biofouling*, 30(4): 501-511.
- Christenson, L. and Sims, R. 2011. Production and harvesting of microalgae for wastewater treatment, biofuels, and bioproducts. *Biotechnology Advances*, 29(6): 686-702.
- Díaz-Santos, E., Vila, M., de la Vega, M., León, R. and Vigarà, J. 2015. Study of bioflocculation induced by *Saccharomyces bayanus* var. *uvarum* and flocculating protein factors in microalgae. *Algal Research*, 8: 23-29.
- Ghribi, D. and Ellouze-Chaabouni, S. 2011. Enhancement of *Bacillus subtilis* lipopeptide biosurfactants production through optimization of medium composition and adequate control of aeration. *Biotechnology Research International*, Article ID 653654.
- Griffiths, M.J. and Harrison, S.T. 2009. Lipid productivity as a key characteristic for choosing algal species for biodiesel production. *Journal of Applied Phycology*, 21(5): 493-507.
- Halim, R., Danquah, M.K. and Webley, P.A. 2012. Extraction of oil from microalgae for biodiesel production: A review. *Biotechnology Advances*, 30(3): 709-732.
- Khatri, W., Hendrix, R., Niehaus, T., Chappell, J. and Curtis, W.R. 2014. Hydrocarbon production in high density *Botryococcus braunii* race B continuous culture. *Biotechnology and Bioengineering*, 111(3): 493-503.
- Kilian, O., Benemann, C.S., Niyogi, K.K. and Vick, B. 2011. High-efficiency homologous recombination in the oil-producing alga *Nannochloropsis* sp. *Proceedings of the National Academy of Sciences*, 108(52): 21265-21269.
- Kim, D.G., La, H.J., Ahn, C.Y., Park, Y.H. and Oh, H.M. 2011. Harvest of *Scenedesmus* sp. with bioflocculant and reuse of culture medium for subsequent high-density cultures. *Bioresource Technology*, 102(3): 3163-3168.
- Liu, C.T., Chu, F.J., Chou, C.C. and Yu, R.C. 2011. Antiproliferative and anticytotoxic effects of cell fractions and exopolysaccharides from *Lactobacillus casei* 01. *Mutation Research/Genetic Toxicology and Environmental Mutagenesis*, 721(2): 157-162.
- Manheim, D. and Nelson, Y. 2013. Settling and bioflocculation of

- two species of algae used in wastewater treatment and algae biomass production. *Environmental Progress & Sustainable Energy*, 32(4): 946-954.
- Matamoros, V., Gutiérrez, R., Ferrer, I., García, J. and Bayona, J.M. 2015. Capability of microalgae-based wastewater treatment systems to remove emerging organic contaminants: A pilot-scale study. *Journal of Hazardous Materials*, 288: 34-42.
- Metzger, P. and Largeau, C. 2005. *Botryococcus braunii*: A rich source for hydrocarbons and related ether lipids. *Applied Microbiology and Biotechnology*, 66(5): 486-496.
- Milledge, J.J. and Heaven, S. 2013. A review of the harvesting of microalgae for biofuel production. *Reviews in Environmental Science and Biotechnology*, 12(2): 165-178.
- Moazami, N., Ashori, A., Ranjbar, R., Tangestani, M., Eghtesadi, R. and Nejad, A.S. 2012. Large-scale biodiesel production using microalgae biomass of *Nannochloropsis*. *Biomass and Bioenergy*, 39: 449-453.
- Mubarak, M., Shaija, A. and Suchithra, T.V. 2015. A review on the extraction of lipid from microalgae for biodiesel production. *Algal Research*, 7: 117-123.
- Ndikubwimana, T., Zeng, X., Murwanashyaka, T., Manirafasha, E., He, N., Shao, W. and Lu, Y. 2016. Harvesting of freshwater microalgae with microbial bioflocculant: A pilot-scale study. *Biotechnology for Biofuels*, 9(1): 47.
- Park, J.B.K., Craggs, R.J. and Shilton, A.N. 2011. Wastewater treatment high rate algal ponds for biofuel production. *Bioresource Technology*, 102(1): 35-42.
- Park, J.Y., Park, M.S., Lee, Y.C. and Yang, J.W. 2015. Advances in direct transesterification of algal oils from wet biomass. *Bioresource Technology*, 184: 267-275.
- Patil, S.V., Salunkhe, R.B., Patil, C.D., Patil, D.M. and Salunke, B.K. 2010. Bioflocculant exopolysaccharide production by *Azotobacter indicus* using flower extract of *Madhuca latifolia* L. *Applied Biochemistry and Biotechnology*, 162(4): 1095-1108.
- Pham, P.L., Dupont, I., Roy, D., Lapointe, G. and Cerning, J. 2000. Production of exopolysaccharide by *Lactobacillus rhamnosus* R and analysis of its enzymatic degradation during prolonged fermentation. *Applied and Environmental Microbiology*, 66(6): 2302-2310.
- Pittman, J.K., Dean, A.P. and Osundeko, O. 2011. The potential of sustainable algal biofuel production using wastewater resources. *Bioresource Technology*, 102(1): 17-25.
- Razack, S.A., Velayutham, V. and Thangavelu, V. 2013. Medium optimization for the production of exopolysaccharide by *Bacillus subtilis* using synthetic sources and agro wastes. *Turkish Journal of Biology*, 37(3): 280-288.
- Richmond, A. and Q. Hu 2008. *Handbook of Microalgal Culture: Biotechnology and Applied Phycology*. 1st ed., John Wiley and Sons Ltd: United Kingdom.
- Rodolfi, L., Chini Zittelli, G., Bassi, N., Padovani, G., Biondi, N., Bonini, G. and Tredici, M.R. 2009. Microalgae for oil: Strain selection, induction of lipid synthesis and outdoor mass cultivation in a low-cost photobioreactor. *Biotechnology and Bioengineering*, 102(1): 100-112.
- Salim, S., Bosma, R., Vermuë, M.H. and Wijffels, R.H. 2011. Harvesting of microalgae by bio-flocculation. *Journal of Applied Phycology*, 23(5): 849-855.
- Sing, S.F., Isdepsky, A., Borowitzka, M.A. and Moheimani, N.R. 2013. Production of biofuels from microalgae. *Mitigation and Adaptation Strategies for Global Change*, 18(1): 47-72.
- Sukenik, A., Beardall, J., Kromkamp, J.C., Kopecký, J., Masojídek, J., van Bergeijk, S., Gabai, S., Shaham, E. and Yamshon, A. 2009. Photosynthetic performance of outdoor *Nannochloropsis* mass cultures under a wide range of environmental conditions. *Aquatic Microbial Ecology*, 56(2-3): 297-308.
- Vandamme, D., Foubert, I. and Muylaert, K. 2013. Flocculation as a low-cost method for harvesting microalgae for bulk biomass production. *Trends in Biotechnology*, 31(4): 233-239.
- Wan, C., Alam, M.A., Zhao, X.Q., Zhang, X.Y., Guo, S.L., Ho, S.H., Chang, J.S. and Bai, F.W. 2015. Current progress and future prospect of microalgal biomass harvest using various flocculation technologies. *Bioresource Technology*, 184: 251-257.
- Wang, S.K., Stiles, A.R., Guo, C. and Liu, C.Z. 2015. Harvesting microalgae by magnetic separation: A review. *Algal Research*, 9: 178-185.
- Wijffels, R.H., Barbosa, M.J. and Eppink, M.H. 2010. Microalgae for the production of bulk chemicals and biofuels. *Biofuels, Bioproducts and Biorefining: Innovation for a Sustainable Economy*, 4(3): 287-295.
- Wingender, J., Neu, T.R. and Flemming, H.C. 2012. *Microbial Extracellular Polymeric Substances: Characterization, Structure and Function*. Springer Berlin Heidelberg.
- Ying, K., Gilmour, D.J., Shi, Y. and Zimmerman, W.B. 2013. Growth enhancement of *Dunaliella salina* by microbubble induced airlift loop bioreactor (ALB) - the relation between mass transfer and growth rate. *Journal of Biomaterials and Nanobiotechnology*, 4(2A): 1-9.
- Zheng, H., Gao, Z., Yin, J., Tang, X., Ji, X. and Huang, H. 2012. Harvesting of microalgae by flocculation with poly (γ -glutamic acid). *Bioresource Technology*, 112: 212-220.
- Zimmerman, W.B., Zandi, M., Bandulasena, H.H., Tesar, V., Gilmour, D.J. and Ying, K. 2011. Design of an airlift loop bioreactor and pilot scales studies with fluidic oscillator induced microbubbles for growth of a microalgae *Dunaliella salina*. *Applied Energy*, 88(10): 3357-3369.



Regional Environmental Performance Evaluation and Its Influencing Factors: A Case Study of Shandong Province, China

Junjie Cao

Shandong Women's University, Jinan, 250300, China

Nat. Env. & Poll. Tech.
Website: www.neptjournal.com

Received: 14-01-2019
Accepted: 16-02-2019

Key Words:

Regional environment
Environmental performance
Influencing factors
Shandong province

ABSTRACT

In recent years, all provinces in China have exhibited unprecedented economic development with high growth rates. However, the economic development of particular provinces is extensive, but unsustainable, and pollution problems have become increasingly prominent. Moreover, the rapid growth of productivity at the expense of resources and the environment outweighs the gain. Regional environmental performance evaluation and exploration of environmental performance factors are helpful to quantitatively analyse the impact of government management and economic and social factors on environmental efficiency. Taking Shandong Province in China as an example, this study summarizes the literature on existing regional environmental performance evaluation and constructs an analytical framework that combines data envelopment analysis - Malmquist and Tobit models. On the basis of panel data on 17 prefecture-level cities of Shandong Province from 2011 to 2016, regions are divided into those with high and low environmental efficiency, and the factors that influence the different environmental efficiencies are measured. Results show that environmental performance evaluation gradually expands from the environmental performance evaluation of an enterprise to the regional environment, specific industries, and influencing factors. The 17 prefecture-level cities under the jurisdiction of Shandong Province exhibit an increase in total factor productivity within the time frame of the investigation. Numerous factors, such as endowment structure, economic development, industrial structure, ownership structure, foreign investment, and government environmental management capabilities, have different impacts on the regional environmental performance of Shandong Province. The study results provide a positive reference for scientific and reasonable evaluations of regional environmental performance in different cities, identification of the effectiveness and shortcomings of regional environmental performance management, understanding the performance characteristics and distribution of regional environmental performance, and promoting environmental management in China.

INTRODUCTION

China's economic development models of "high input and low output" and "high pollution and high consumption" have inevitably caused serious environmental pollution problems. Although many provinces continuously increase their environmental investment, the environmental management effects remain unremarkable. Accelerating the construction of a performance-oriented government environmental management system is necessary to form a long-term and dynamic monitoring and evaluation system for environmental policy effects, and the most important part of such a system is environmental performance evaluation because it can promote environmental management in China. Environmental performance refers to a comparison of economic activities with environmental pollution or environmental resource consumption. If production activities can produce numerous goods and services under certain environmental resource consumption, the environmental economic performance will improve. Environmental economic

performance is improved when minimal pollutant emissions and environmental damage are observed during the production of the same amount of goods and services.

As shown in Fig. 1, the economies of various regions of Shandong Province have recently achieved rapid development with high growth rates. However, several urban economies have developed in an extensive, but unsustainable manner, and environmental protection issues have become increasingly prominent. Improper handling of environmental resource constraints seriously weakens the sustainable development of the economy in various regions of Shandong Province. As a resource-rich province, Shandong has abundant natural resources, but its environmental sustainability is poor. The rapid growth of productivity at the expense of resources and the environment is not worth the loss. Therefore, measuring the environmental performance values of cities in Shandong Province and quantitatively analysing the relationship between environmental performance and its influencing factors are valuable in further increasing the

governance, protection, and management of environmental pollution and in updating environmental protection concepts in order to avoid the “pollution first, treatment later” model.

EARLIER STUDIES

Environmental performance evaluation refers to the measurement and evaluation of environmental management effectiveness by using appropriate indicators in a continuous, phased, quantitative manner. Environmental performance evaluation began when environmental information was released by enterprises in the late 1980s. It mainly pertains to an environmental performance evaluation of enterprises that focuses on how to improve such performance. Subsequently, relevant investigations have gradually increased, with focus on the exploration and application of environmental performance evaluation motivation, evaluation mode, and methods. Charnes et al. (1978) proposed an endogenous weighting system that did not consider direct production inputs and outputs, but focused on the weighting between value creation and its adverse side effects on the environment. Fare et al. (1994) divided the environmental performance index into two factors, namely, environmental technology change and relative eco-efficiency change. Fare et al. (1994) also decomposed the environmental technology change factor into quantity and environmental bias indices. The advantage of this approach was that the price

information of emissions or environmental pressure was not required at any stage of the analysis. Sarkis & Talluri (2004) proposed to evaluate environmental performance by using the data envelopment analysis (DEA) method, studied the construction and application of the DEA model, and put forward many ecological assessment indicators. Nakashima et al. (2006) constructed a loop management system and used the DEA method to compare the environmental performance of different types of enterprises in a certain industry (Nakashima et al. 2006). Kortelainen (2008) proposed a general framework for analysing dynamic eco-efficiency by introducing the Malmquist index (Kortelainen 2008). Henri et al. (2008) indicated that environmental performance indicators contain key quantitative information for environmental management issues, which should include environmental management regulations, environmental management objectives, and public subsidies (Henri et al. 2008). Hindorff et al. (2009) constructed a set of environmental performance indicators for the public sector and applied it to the policy of the defence sector. Martinez (2012) combined economic benefits and environmental responsibility to study corporate environmental performance evaluation and believed that environmental management should be strategically placed in the production and operation of enterprises. Wang et al. (2013) proposed the use of the DEA window analysis method in the calculation of the energy and environmental efficiency of China’s provinces. Adeel-

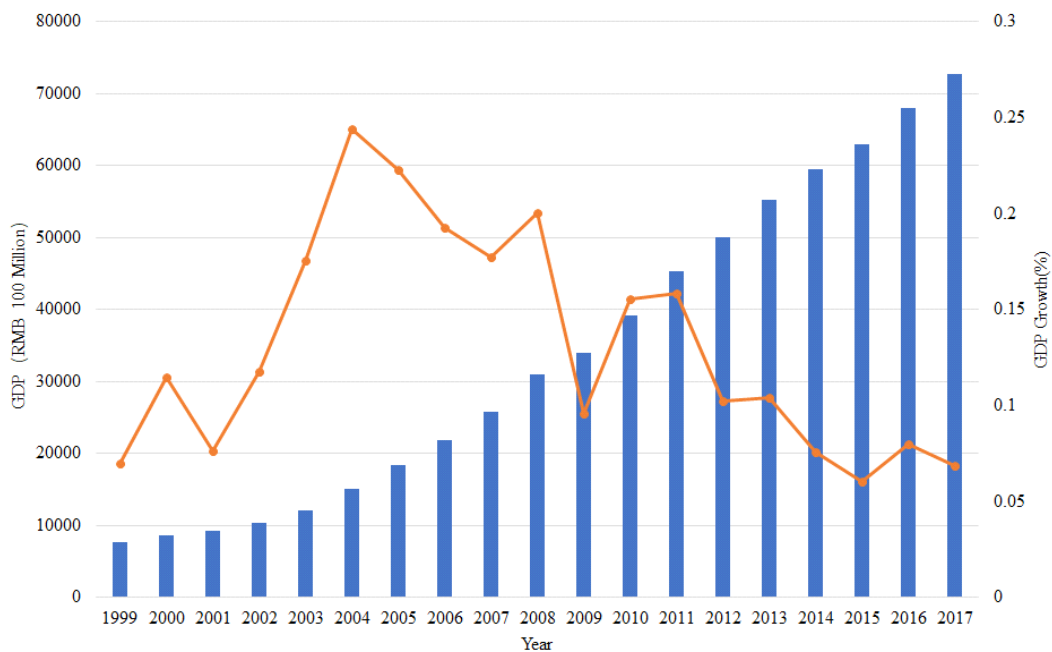


Fig. 1: GDP and GDP growth rate of Shandong Province from 1999 to 2017.
[Data from the EPS platform (<http://olap.epsnet.com.cn/>)]

Farooq et al. (2017) surveyed nine Asian developing countries and examined the impacts on their environmental performance in the aspects of green field investment, energy consumption, economic growth, and urbanization from 2003-2014. Pilouk & Koottatep (2017) assessed the sustainable development of eco-industrial real estate or industrial parks and showed that environmental performance was the key to the success of eco-industrial parks. Halkos & Zisiadou (2018) constructed an environmental performance index and compared Greece with the Mediterranean and other countries in Northern Europe. Xiao et al. (2018) tested green technology and environmental spillover performance through a panel data model and analysed the mechanism of green technology spillovers on environmental performance from a regional perspective. The results showed that external green technology spillovers had improved the internal environmental performance of enterprises and were driven by the weakening of internal environmental performance. Peiró-Palomino & Picazo-Tadeo (2018) analysed the relationship between social capital and the environmental performance of the European Union (EU) and found that the main driving force of environmental performance was economic development and per capita of GDP.

In summary, many studies have been conducted on environmental performance evaluation. The DEA method, which can reflect the advantages and characteristics of a certain method in performance evaluation applications, is widely used and provides references for the current research. On the basis of existing research, this study adopts a combination of DEA-Malmquist and Tobit models and uses Shandong Province of China as an example to study the changes and influencing factors of environmental performance at the municipal level. Corresponding counter-measures are presented.

INTRODUCTION TO THE MODEL

Introduction to the DEA-Malmquist Model

The DEM-based Malmquist index is generally used to determine total factor productivity (TFP) and its analysis factors. According to Fare et al. (1994), the Malmquist index, in reference to variable returns, outputs, t-time, and t+1 time, can be defined as:

$$M_{t,t+1} = \frac{D_{t+1}^v(x_{t+1}, y_{t+1})}{D_t^v(x_t, y_t)} \times \left[\frac{D_t^c(x_t, y_t)}{D_t^c(x_t, y_t)} \div \frac{D_{t+1}^c(x_{t+1}, y_{t+1})}{D_{t+1}^c(x_{t+1}, y_{t+1})} \right] \times \left[\frac{D_t^v(x_t, y_t)}{D_t^v(x_t, y_t)} \times \frac{D_{t+1}^v(x_{t+1}, y_{t+1})}{D_{t+1}^v(x_{t+1}, y_{t+1})} \right]^{\frac{1}{2}} \dots(1)$$

Where, $D^c(x, y)$ is the distance function under a constant return of scale, and $D^v(x, y)$ is the distance function under a variable return of scale. $\frac{D_{t+1}^v(x_{t+1}, y_{t+1})}{D_t^v(x_t, y_t)}$ denotes the

pure technical efficiency changes, $\frac{D_t^v(x_t, y_t)}{D_t^c(x_t, y_t)} \div \frac{D_{t+1}^v(x_{t+1}, y_{t+1})}{D_{t+1}^c(x_{t+1}, y_{t+1})}$

is the scale efficiency change, $\left[\frac{D_t^c(x_t, y_t)}{D_{t+1}^c(x_{t+1}, y_{t+1})} \times \frac{D_{t+1}^v(x_{t+1}, y_{t+1})}{D_t^v(x_t, y_t)} \right]^{\frac{1}{2}}$ is

for technological progress, and

$\frac{D_{t+1}^v(x_{t+1}, y_{t+1})}{D_t^v(x_t, y_t)} \times \left[\frac{D_t^v(x_t, y_t)}{D_t^c(x_t, y_t)} \div \frac{D_{t+1}^v(x_{t+1}, y_{t+1})}{D_{t+1}^c(x_{t+1}, y_{t+1})} \right]$ is the product of the first two representing the technological efficiency change.

When $M_{t,t+1} > 1$, TFP progresses. When $M_{t,t+1} < 1$, TFP regresses. When $M_{t,t+1} = 1$, TFP does not change. When technical efficiency, pure technical efficiency, scale efficiency, or the technical level change is greater than 1, it is the source of TFP growth; otherwise, it is the source of TFP reduction. In a specific study on regional environmental performance measurement, TFP refers to the ratio of the total output to the weighted average of various input factors in the production activities of the entire regional socio-economic system. Technological progress (TECH) refers to the productivity improvement of the entire regional socio-economic system through scientific research, invention, technological improvement, and the spread of high technology. Technical efficiency (TE) is determined by two factors, namely, scale efficiency (SE) and pure technology efficiency (PECH). SE refers to the extent to which the entire regional socio-economic system deviates from the optimal scale in the production process. PECH originates from the entire regional socio-economic system through management methods, such as regional energy conservation, emission reduction, and social environmental governance. In this study, the TFP index that considers pollutant emissions is defined as the regional environmental efficiency, and the environmental performance of economic development in various regions of Shandong Province is studied geographically from the municipal level.

Tobit Model

The Tobit model is an econometric model proposed by the economist Tobin in 1958 when studying the demand for durable consumer goods. The standard Tobit model is shown in the following formula.

$$\begin{aligned} y_i^* &= \beta x_i + u_i \\ y_i^* &= y_i (y_i^* > 0) \\ y_i^* &= 0 (y_i^* \leq 0) \end{aligned} \dots(2)$$

Where y_i^* is a latent dependent variable. When this latent variable is greater than 0, $y_i^* = y_i$; when the latent variable is less than or equal to 0, $y_i^* = 0$. x_i represents the independent variable vector, β represents the coefficient vector, and the error term u_i is independent and obeys the nor-

mal distribution $u_i \sim N(0, \sigma^2)$. The maximum likelihood estimation method is generally used to estimate the regression coefficient.

EMPIRICAL RESEARCH

Indicator Selection and Data Processing

In environmental performance measurement, according to the basic principles of the typical production function and by considering scientific and systematic data, this study selects industrial wastewater discharge, industrial waste gas emissions, industrial solid waste, industrial sulphur dioxide, and industrial chemical oxygen demand as input variables. The industrial added value is used as the output variable, and the annual industrial added value is converted by an annual GDP deflator. Panel data on the following 17 prefecture-level cities from 2011 to 2016 are calculated: Jinan, Dezhou, Liaocheng, Heze, Tai'an, Laiwu, Jining, Zaozhuang, Linyi, Rizhao, Qingdao, Weihai, Yantai, Weifang, Zibo, Dongying, and Binzhou. All data are obtained from the Shandong Statistical Yearbook and China Environment Yearbook.

In the analysis of the factors that affect environmental performance, this study divides the factors affecting the overall environmental efficiency of Shandong Province into endowment structure, economic development, industrial structure, ownership structure, foreign investment, and government environmental management capabilities on the basis of existing literature. The specific influencing factors are shown in Table 1. Areas with TFP larger than or equal to 1 are defined as having high environmental performance, and regions with TFP less than 1 have low environmental performance.

Regional Environmental Performance Results

Table 2 shows that the 17 cities under the jurisdiction of Shandong Province exhibit TFP growth within the time frame of the investigation. The TFP of Tai'an, Zaozhuang,

Weihai, and Dongying is relatively high, whereas the TFP of Jinan, Dezhou, Liaocheng, Heze, and Binzhou is the lowest and does not exhibit growth. The five cities also suffer from serious environmental pollution. A considerable amount of heavy industry pollution leads to low environmental performance. The rest of the cities demonstrate low levels of pollution emission and energy use through improvements in environmental technology and continuous reductions in energy consumption per unit of GDP, thereby increasing the environmental TFP. The technical efficiency of Liaocheng, Heze, Zibo, and Dongying is low due to the ineffective implementation of environmental pollution control and the low efficiency of the input and output of environmental pollution control. Most cities in Shandong Province have not achieved growth in terms of technological progress. Given that Shandong is a large industrial province, the pillar industries are still non-ferrous metals, steel processing, petroleum smelting, and other enterprises that are highly resource-dependent with a large amount of pollutants. Moreover, the lack of gathered talents and funds and weak innovation awareness lead to a relatively backward development in terms of environmental protection. In terms of scale efficiency, Jinan, Laiwu, Jining, Zaozhuang, Qingdao, and Yantai exhibit more development than the rest of the cities. Several cities have not achieved scale efficiency growth probably due to their heavy reliance on industries to realize a prosperous local economy. However, the environmental quality in the production process deteriorates with economic growth, thus bringing increased external costs to the entire economy. The decline in efficiency in these cities constrained by resources and the environment indicates that environmental quality and productivity have not achieved a simultaneous win-win development.

Analysis of Factors that Affect Environmental Performance

Considering that environmental performance is a constrained dependent variable, traditional estimation meth-

Table 1: Factors that affect environmental performance.

Factor	Index	Variable symbol
Endowment structure	Logarithm of the ratio of capital to labor	K/L
Economic development	Actual per capita GDP	PGDP
Industrial structure	Added value of the secondary industry that accounts for the proportion of regional GDP	GYH
Ownership structure	Proportion of the total output value of state-owned holding enterprises to the total industrial output value	GYHBZ
Foreign investment	Foreign direct investment that accounts for the proportion of regional GDP	FDI
Government environmental management capacity	Amounts of environmental governance investment	ZFGL

Table 2: Environmental performance measurement results.

	Technical Efficiency	Technological Progress	Pure Technical Efficiency	Scale Efficiency	Total Factor Productivity
Jinan	1.005	0.994	1.000	1.005	0.999
Dezhou	0.953	0.953	0.987	0.966	0.908
Liaocheng	0.967	1.023	0.969	0.998	0.989
Heze	0.984	1.000	0.986	0.998	0.984
Tai'an	1.121	0.984	1.123	0.998	1.103
Laiwu	1.046	0.963	1.024	1.021	1.007
Jining	1.004	0.998	0.998	1.006	1.002
Zaozhuang	1.040	0.989	0.967	1.075	1.028
Linyi	1.101	0.913	1.105	0.996	1.005
Rizhao	1.004	0.999	1.005	0.999	1.003
Qingdao	1.019	0.999	0.996	1.023	1.018
Weihai	1.033	0.996	1.035	0.998	1.029
Yantai	1.037	0.999	1.002	1.035	1.036
Weifang	0.980	0.993	0.996	0.984	0.973
Zibo	0.998	1.012	0.998	1.000	1.010
Dongying	0.990	1.035	1.034	0.957	1.024
Binzhou	0.902	1.065	0.954	0.945	0.960
Mean value	1.011	0.995	1.011	1.000	1.005

Table 3: Factors that affect environmental performance.

Index	Shandong Province as a whole	Areas with high environmental performance	Areas with low environmental performance
C	1.314***	1.635***	0.564***
K/L	-0.006***	-0.675	-0.125***
PGDP	-0.352**	-0.654**	-1.254**
GYH	-0.163***	-0.478***	-0.204***
GYHBZ	0.145**	0.098**	0.258*
FDI	0.965***	1.685***	2.576
ZFGL	-0.896	-0.854	-0.653**

(Note: *, ** and *** indicate the significance level at 10%, 5% and 1%, respectively)

ods (e.g., least-squares regression) can result in bias in the estimation results. Therefore, this study uses the Tobit model proposed by Tobin (1958) to estimate the overall environmental efficiency impact factor model of Shandong Province. The results estimated by Eviews7 software are shown in Table 3.

Table 3 shows that the endowment structure (K/L) has a substantial negative effect on environmentally inefficient areas, but does not considerably affect the whole Shandong Province and environmentally efficient areas. Therefore, environmentally efficient areas should focus on developing capital and knowledge-intensive industries to increase their environmental efficiency. The actual per capita GDP has substantial negative effects on the improvement of environmental efficiency because Shandong Province is still in the stage of rapid economic development. Improving economic development is the primary task, and the conser-

vation of resources and protection of the environment are neglected; therefore, the resource utilization efficiency is declining. The industrial structure (GYH) has substantial negative impacts on the environmental inefficiency of Shandong Province and environmentally inefficient areas. If the proportion of the industrial added value of these areas that accounts for the regional GDP increases by one unit, then Shandong Province and environmentally inefficient areas will increase by 0.163 and 0.204 units, respectively. This scenario indicates the strong dependence of Shandong Province on the secondary industry. However, the development of the tertiary industry is insufficient, and the industrial structure is unreasonable and relatively simple. Therefore, environment-friendly industries should be regarded as the priority development industry, thus minimizing the impact of pollution from industrial development on environmental efficiency. The ownership structure (GYHBZ) has

important positive impacts on the environmental efficiency values of Shandong Province and environmentally inefficient and efficient regions of the province. As a large industrial province, Shandong's state-owned enterprises have higher financial strength and more evident talent convergence effects than non-state-owned enterprises. Thus, state-owned enterprises are capable and aware of developing high-tech environmental protection technologies to improve environmental performance in the region. Foreign investment (FDI) has substantial positive impacts on the environmentally efficient regions and Shandong Province. In recent years, this province focused on the introduction of technology and capital-based foreign-invested enterprises. The advanced management experience and technology brought by these enterprises can offset the negative impact on the environmental efficiency, thereby increasing the overall environmental efficiency. Government environmental management capability (ZFGL) has remarkable negative impacts only on the environmentally inefficient areas of Shandong Province. The environmentally inefficient areas have weak economic strength, and the environmental management funds invested by the government cannot effectively improve the environmental performance. This finding shows that the government still needs to modify or even reform existing environmental regulations, incentives and punishment mechanism, and strengthen its ability to control environmental pollution.

POLICY RECOMMENDATIONS

Reasonable Adjustment of Industrial Structure and Control of Industry with Heavy Environmental Pollution

Adherence to the development of resource-saving and environment-friendly industries requires precise and careful work. The government conducts effective environmental supervision of enterprises in the process of industrialization. State-owned enterprises should take the lead in transforming production methods, actively exploring advanced environmental protection technologies, and developing other industries with high environmental efficiency and high added value to find new motivation for economic growth. Under the premise of strict screening of foreign environmental standards, we must endeavour to absorb and digest advanced foreign pollution control technologies and management concepts and produce products with high environmental efficiency and added value as much as possible to reduce pollution emissions and improve environmental efficiency. Optimizing the industrial structure, reducing industrial pollution, and focusing on developing strategic emerging, green, and low-carbon industries are required.

We will follow a new path of industrialization that conforms to the trend of "Internet Plus", and integrate information and industrialization into the main line, and improve the level of technology and product quality, and promote smart green manufacturing, and reduce the impact of industrialization on the environment. The tertiary industry should be vigorously developed by promoting the advanced industrial structure and accelerating the formation of industrial systems conducive to environmental protection and resource conservation.

Strengthen Environmental Performance and Scientific Work and Establish an Environmental Performance Assessment Mechanism

The long-standing extensive economic development model has little influence on ecological environment governance, and economic costs cannot be used in exchange for environmental improvements. In addition to several surface approaches adopted in the past to mitigate the ecological crisis by reducing the emission of harmful substances, starting from the source of pollutants, is necessary. That is, the technical level must be improved to achieve clean combustion and reduce pollutant emissions, thereby effectively improving the environment to obtain good economic benefits. Developing new energy to replace the old one is required to efficiently use energy without generating harmful gases and eventually realize economic and environmental benefits. The ecological environment awareness of economic entities should be strengthened, and relevant national laws and regulations should be improved to ensure and supervise the implementation of government policies by forming a unified goal from the individual to the government and even to the country. An improved living environment for the people can then be achieved.

Strengthen government Environmental Regulation and Implement Regional and Enterprise Subsidy Policies on High Environmental Performance

The government's environmental regulation has remarkable effects on the improvement of environmental efficiency. In the formulation of environmental policies, administrative orders, such as mandatory closure and improvement of environmental penalties, can achieve good results to a certain extent. However, the formulation of environmental regulation policies must fully consider and integrate market economic mechanisms. Economic measures, such as the market trading system represented by pollution tax, are implemented to internalize environmental costs and encourage the micro-subjects of enterprises to maximize environmental efficiency, thus transforming the production concept of the enterprise from "dare not to pollute" to "cannot pol-

lute” and even to “be unwilling to pollute.” Various factors cause uncertainty in terms of companies’ attitude towards energy conservation, emission reduction, and development of environmental technologies. Therefore, the government must apply further measures to encourage enterprises to develop advanced environmental protection technologies and continue to maintain high environmental efficiency. These measures include encouraging enterprises to undertake efforts to absorb and digest advanced pollution control technology and management experience in developed areas and providing certain subsidies to enterprises that adopt environmental protection technologies on the premise of local financial affordability.

Improve Public Environmental Awareness and Change the Concept of Environmental Protection

Strengthening the construction of ecological civilization requires the public to change their awareness; it is not a sole task of the government to protect the environment. Achieving the desired effect of protecting the ecological environment by the government alone is difficult because ecological environmental protection is a typical public participation task. Only by working together we can fundamentally repair the polluted environment and continue to protect the unpolluted environment, thus maintaining and continuously improving the quality of the ecological environment. Performing relevant activities and strengthening publicity are necessary to raise public awareness of environmental protection. In addition to the implementation of national policies and the active cooperation of enterprises, the multi-participation of families and individuals also plays a pivotal role in the process of ecological governance. As an independent economic entity, families and individuals can propose reasonable suggestions through a government-guided ecological governance program or actively participate in the environmental governance process by starting from the small things around them, such as advocating green travel.

CONCLUSIONS

As a developing country, China is currently in the stage of rapid industrialization, and ecological and environmental problems are inevitably encountered during economic development. In the various provinces of China, long-term high energy consumption, severe pollution problems, and other issues exist. In addition, the development of environmental performance is different, and the influencing factors are complicated. In this study, the DEA-Malmquist model is adopted to measure the environmental performance of 17 prefecture-level cities in Shandong Province. The Tobit model is used to analyse the influencing factors of environ-

mental performance in each region. The research structure shows that the 17 prefecture-level cities under the jurisdiction of Shandong Province achieved TFP growth within the time frame of investigation. The influencing factors include the endowment structure, economic development, industrial structure, ownership structure, foreign investment, and government environmental management capacity, all of which exert different impacts on the regional environmental performance of Shandong Province. Comprehensive investigations, including enriching the regional environmental performance evaluation index system, expanding the regional environmental performance influencing factors, spatial econometric analyses of regional environmental performance, and consideration of the impacts of micro-factors, such as enterprises, on environmental performance, could be conducted in the future.

REFERENCES

- Adeel-Farooq, R.M., Abu Bakar, N.A. and Olajide Raji, J. 2017. Green field investment and environmental performance: A case of selected nine developing countries of Asia. *Environmental Progress & Sustainable Energy*, 37(3): 1085-1092.
- Charnes, A., Cooper, W. W. and Rhodes, E. 1978. Measuring the efficiency of decision making units. *European Journal of Operational Research*, 2(6): 429-444.
- Fare, R., Grosskopf, S. and Norris, M. 1994. Productivity growth, technical progress, and efficiency change in industrialized countries. *The American Economic Review*, 84(1): 66-83.
- Fare, R., Grifellatje, E. and Grosskopf, S. 1997. Biased technical change and the Malmquist productivity index. *The Scandinavian Journal of Economics*, 99(1): 119-127.
- Halkos, G. and Zisiadou, A. 2018. Relating environmental performance with socioeconomic and cultural factors. *Environmental Economics & Policy Studies*, 20(1): 1-20.
- Henri, J.F. and Journeault, M. 2008. Environmental performance indicators: An empirical study of Canadian manufacturing firms. *Journal of Environmental Management*, 87(1): 165-176.
- Hindorf, L. A., Sethupathy, P. and Junkins, H. A. 2009. Potential etiologic and functional implications of genome-wide association loci for human diseases and traits. *Proceedings of the National Academy of Sciences of the United States of America*, 106(23): 9362-9367.
- Kortelainen, M. 2008. Dynamic environmental performance analysis: A Malmquist index approach. *Ecological Economics*, 64(4): 701-715.
- Martinez, F. 2012. The syncretism of environmental and social responsibility with business economic performance. *Management of Environmental Quality: An International Journal*, 23(6): 597-614.
- Nakashima, K., Nose, T. and Kuriyama, S. 2006. A new approach to environmental performance evaluation. *International Journal of Production Research*, 44(1819): 4137-4143.
- Peiró-Palomino, J. and Picazo-Tadeo, A. J. 2018. Is social capital green? Cultural features and environmental performance in the European Union. *Environmental & Resource Economics*, 1: 1-28.
- Pilouk, S. and Koottatep, T. 2017. Environmental performance indicators as the key for eco-industrial parks in Thailand. *Journal of Cleaner Production*, 156: 614-623.
- Sarkis, J. and Talluri, S. 2004. Performance based clustering for

- benchmarking of US airports. *Transportation Research, Part A (Policy and Practice)*, 38(5): 329-346.
- Wang, K., Yu, S. and Zhang, W. 2013. China's regional energy and environmental efficiency: A DEA window analysis based dynamic evaluation. *Mathematical and Computer Modelling*, 58(56): 1117-1127.
- Xiao, H., Han, B. and Chen, Y. 2018. A regional analysis on environmental performance, green technology spillover and environmental spillover in China. *Science and Technology Management Research*, 38(1): 233-238.



Identification of Artificial Recharges Structures Using Remote Sensing and GIS for Arid and Semi-arid Areas

R. Chandramohan*†, T.E. Kanchanabhan** and N. Siva Vignesh***

*Department of Civil Engineering, Vignan's Lara Institute of Technology and Science, Guntur-522213, India

**Department of Civil Engineering, Bharath University, Chennai-600073, India

***Department of Civil Engineering, Anna University, Chennai-600025, India

†Corresponding author: R. Chandramohan

Nat. Env. & Poll. Tech.
Website: www.neptjournal.com

Received: 15-05-2018
Accepted: 02-08-2018

Key Words:

Artificial recharge structure
Groundwater recharge
Remote sensing
GIS
Hydrology

ABSTRACT

Extensive and poorly regulated groundwater extraction to cater to agricultural, industrial, and domestic needs has severely depleted natural groundwater levels in arid and semi-arid areas. Suitable artificial recharge structures can serve as viable options for increasing groundwater levels in areas dependent on aquifers as their water source. Potential sites and suitable artificial recharge structures were suggested to recharge the groundwater level of the study area. The paper's aim is to facilitate an increase in aquifer recharge during non-rainfall days in the study area and contribute to sustainable groundwater conservation during periods of poor water availability by using remote sensing and GIS.

INTRODUCTION

Groundwater is essential for daily human sustenance. However, significant quantities of groundwater are being extracted in a poorly regulated manner for irrigation, domestic, and industrial needs (Chandramohan et al. 2017a). In India, especially in Tamil Nadu, farmers mainly depend on aquifers during non-monsoon periods. Natural recharge of the underground water basin is limited to 10 to 100 rainfall days in most arid or semi-arid areas. Moreover, most rainwater is lost through outflow during the monsoon periods. Artificial refilling techniques are frequently employed to transfer the surface water to underground water storage and aquifers during excess surface water availability. Artificial recharge structures can help conserve and store excess surface water for future use and can potentially improve the sustainable water yield in zones where aquifers have been depleted due to excessive extraction.

In light of high demand of water for urban and irrigation needs during the post-monsoon periods, technologies such as Remote Sensing (RS) and Geographical Information System (GIS) are frequently employed to identify spatial patterns in water demand and availability. These tools are very useful in identifying proper sites for artificial recharge structures. Also, artificial recharging in specific sites and replication techniques are based on local environmental and hydrological conditions (CGWB 2000).

Artificial groundwater recharge has usually been conducted in the following areas: Regions where groundwater levels shrink regularly, regions where several aquifers have already been desaturated, regions where the availability of groundwater is insufficient in the months of scarcity, and regions where salinity has increased. Some of the researchers have used Rain Water Harvesting (RWH) as an artificial recharge to reload underground water. However, much of the literature considers RWH as a part of the "aquarium managed recharge", which also includes artificial recharge, landfill, water activity, and sustainable underground storage (Gale et al. 2005).

Ramireddy et al. (2015), used thematic maps including slope, drainage, drainage density, and lineament density maps to identify sites for suitable artificial recharge structures such as desiltation of tanks, flooding and furrowing, percolation ponds, check dam, pitting and batteries of wells, en-echelon dam, and hydrofracturing to increase the groundwater level.

The researchers Anbazhagan (1994), Anbazhagan & Ramasamy (1993) and Missimer et al. (2012) have focussed on the application of remote sensing and GIS in the selection of artificial recharge zones. Combination of thematic layers (water level, rainfall, lineament, and others) is implemented by Samson & Elangovan (2015) to find suitable artificial recharge zones. Rokade et al. (2004) mentioned

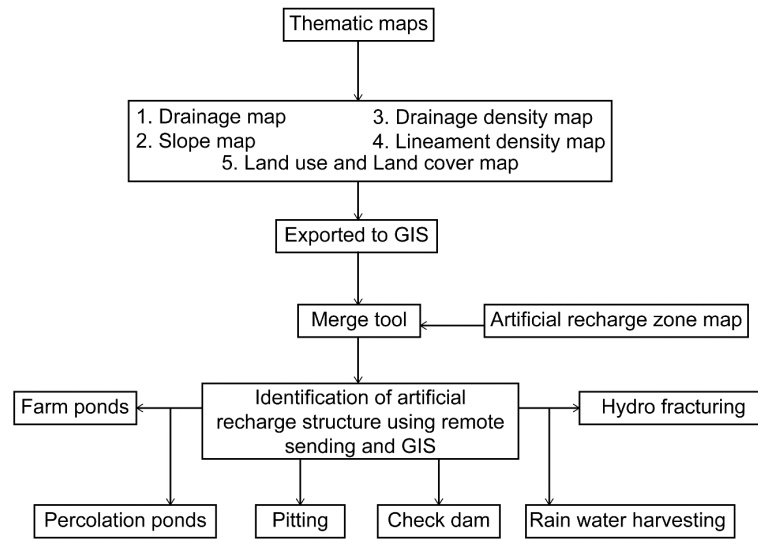


Fig. 1: Methodology for identification of artificial recharge structure using remote sensing and GIS.

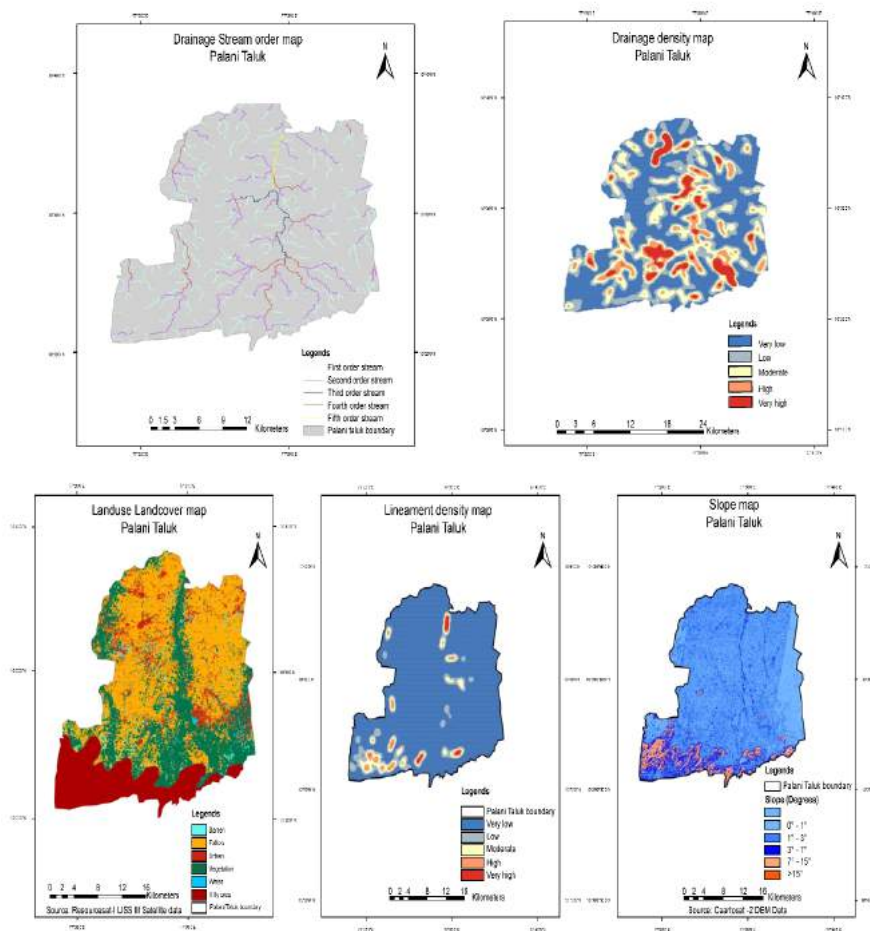


Fig. 2: Thematic maps used to identify artificial recharge structures (Source: Chandramohan et al. 2017b).

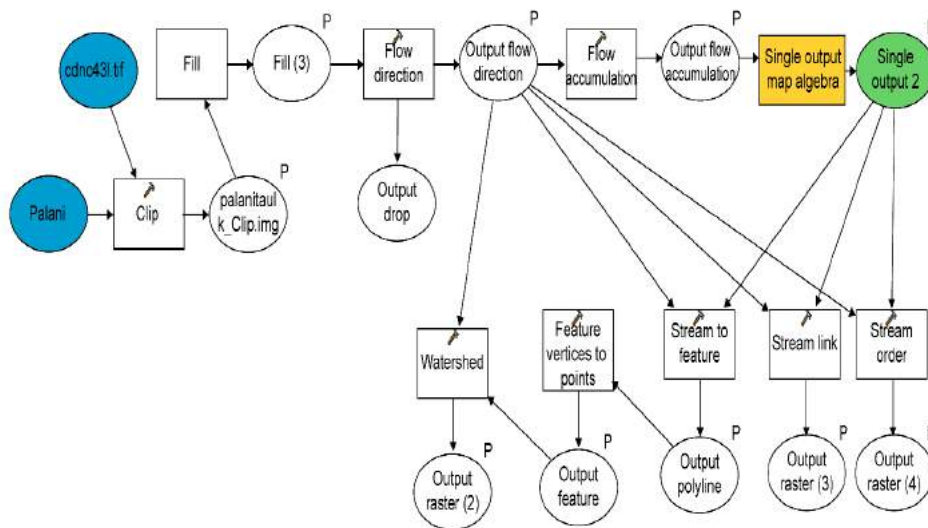


Fig. 3. Drainage catchment area delineation using GIS model.

Table 1: Thematic map combinations used to generate artificial recharge structures.

S.No	Artificial recharge structure	Thematic map combinations
1.	Check Dam	Drainage map (convergence points)
2.	Farm Ponds	Drainage map (first stream order)
3.	Percolation Ponds	Micro watershed and slope map
4.	Rain Water Harvesting	Land use land cover map
5.	Pitting	Drainage density map
6.	Hydro Fracturing	Lineament density and drainage density map
7.	Flooding and furrowing	Slope map (0° to 1°) and low drainage density map

that groundwater has become crucial and it becomes mandatory to identify potential groundwater zones and monitor and conserve this important resource.

Currently, groundwater level of the Palani Taluk in Dindigul District is very poor and artificial recharge structures are urgently required to address the rapidly depleting groundwater levels. This paper uses remote sensing and GIS to identify potential sites in the study area that will benefit from the implementation of artificial recharge structures. Further, a series of thematic maps and GIS tools are employed to suggest the type of artificial recharge structures best suited to the particular sub-regions.

MATERIALS AND METHODS

The study area included the Palani Taluk in Dindigul District in Tamil Nadu, India, which is expanded over an area of 766.83 km². The latitudes of the study area are between 10°20'2" N to 10°38'24" N and longitudes are between 77°18'6" to 77°35'41". Topography includes mountains,

which cover an area of 116.85 km² (Chandramohan et al. 2017a, 2017b). The principal source of groundwater is precipitation. The average rainfall during the 33 years (1980 - 2013) was 690 mm. The depth of groundwater varies between 4 m and 11.7 m in Palani Taluk.

Thematic maps combinations that were used to identify various artificial recharge structures are listed in Table 1. Sites that were appropriate for the implementation of artificial recharge structures were identified following the methodology described by Chandramohan et al. (2017b). The methodology employed for identifying artificial recharge structures using remote sensing and GIS is illustrated in Fig. 1.

Palani Taluk maps were primed from Dindigul TWAD (Tamil Nadu Water Supply and Drainage) Board and georeferenced by using Geological Survey of India Toposheet No. 58 F¹⁰. Thematic layers of drainage maps and slope maps were primed from Cartosat-I, DEM data.

The lineament map and land use and land cover map were generated using Resourcesat-I, LISS III Image. The the-

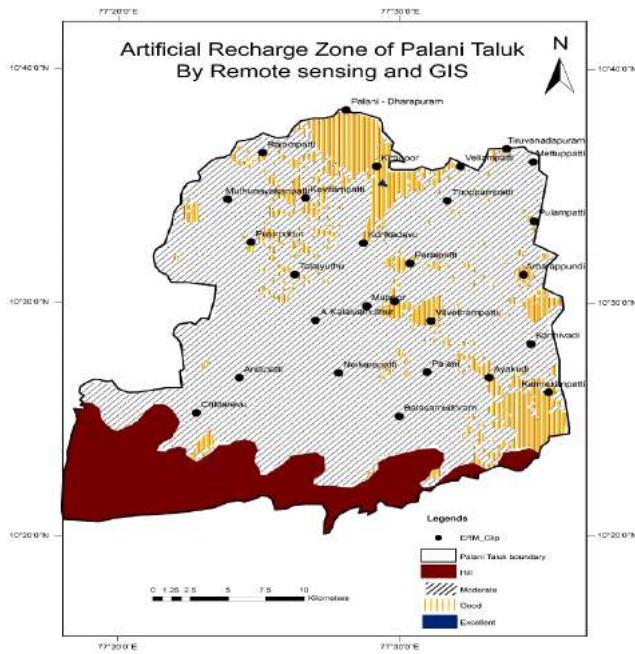


Fig. 4: Artificial recharge zone map of Palani taluk (Chandramohan et al. 2017b).

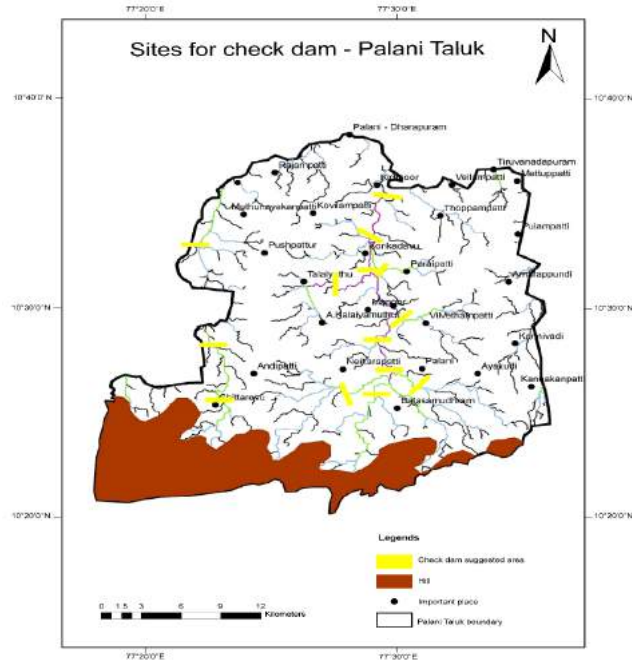


Fig. 5: Potential sites for check dams.

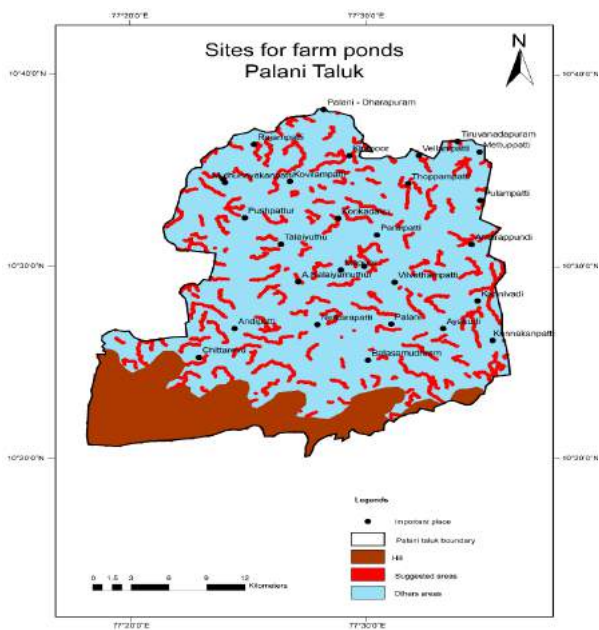


Fig. 6: Potential sites for farm ponds.

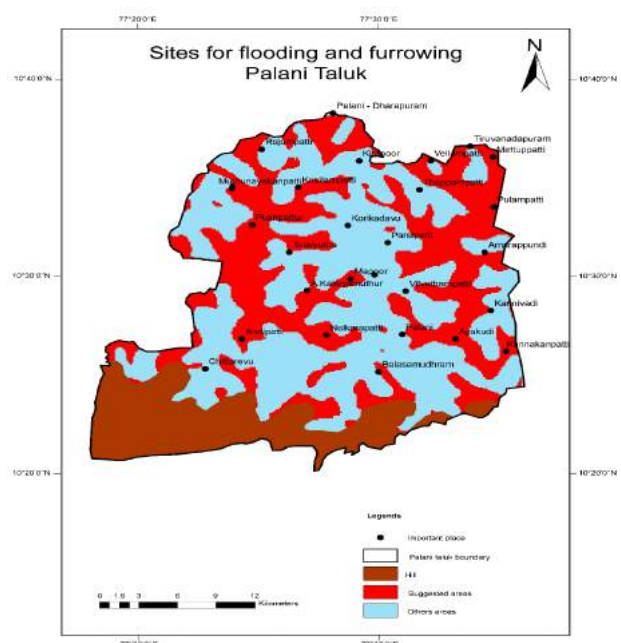


Fig. 7: Potential sites for flooding and furrowing.

matic maps (Fig. 2) and artificial recharge zone map (Fig. 4) were exported to GIS for further analysis using the merge tool.

The artificial recharge map (Fig. 4) generated by the

study, revealed that the study area comprised of moderate to excellent artificial recharge regions. Most of the area in the Palani taluk falls under moderate artificial recharge zones, (Chandramohan et al. 2017b). Few regions on the northern

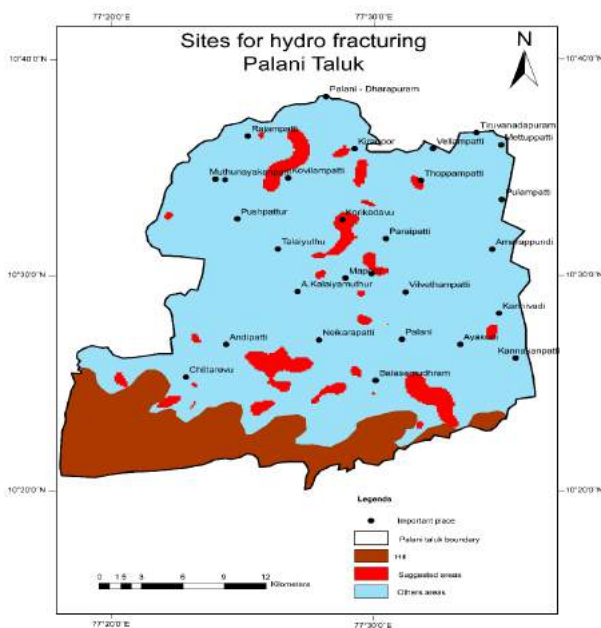


Fig. 8: Potential sites for hydro-fracturing.

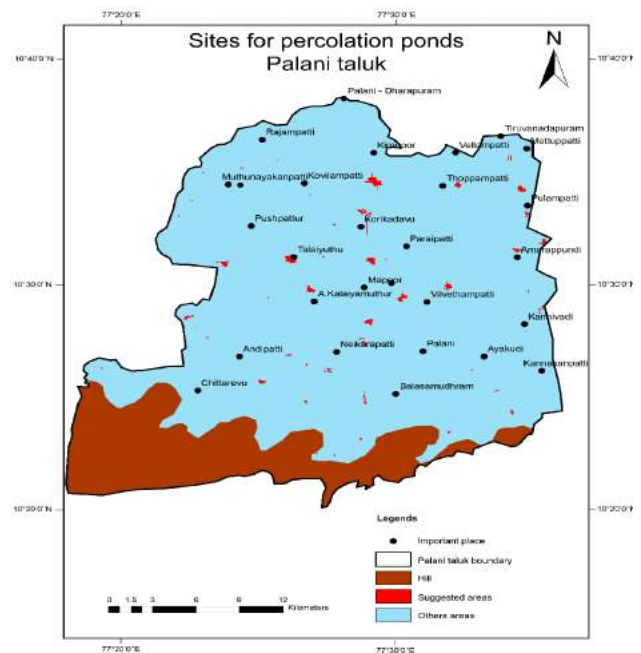


Fig. 9: Potential sites for percolation ponds.

and south-eastern parts can be categorized as good artificial recharge zones. A small area in the northern side exhibits excellent artificial recharge zone. Nearly, 71.37% of the total area is represented by moderate artificial zones; excellent artificial recharge zones account for only 0.04% of the total area, and good artificial recharge zones account for 13.29% of the total area.

RESULTS AND DISCUSSION

Check dams: The drainage map was prepared from Cartosat-I DEM image utilizing remote sensing and GIS software. The drainage convergence point areas in the drainage map were sorted using GIS software and integrated with artificial recharge zones (Fig. 4), which were categorized as good, moderate, or excellent. The check dam areas suggested for the Palani taluk are shown in Fig. 5. Most of the areas suitable for check dams are important drainage regions. The major drainage regions in the Palani taluk hilly area are situated in the southern part and flow towards the Thiruppur district located on the north side of the taluk. This drainage is a major sub-basin of the Amarathi River, which later joins the Cauvery River.

Farm ponds: Farm ponds suggestions for the area were also identified from the drainage map. The existing drainage map was demarcated based on the stream orders using the GIS model. First to fifth order drainage can be observed in the Palani taluk, as shown in Fig. 2. First stream order drainages need to be selected for farm pond sites. GIS tools

were used to the selected first-order drainage maps from the other stream order drainage maps and were integrated with artificial recharge zones (Fig. 4) categorized as good, moderate, or excellent. Farm pond suggestions were located throughout the Palani taluk, as indicated in Fig. 6. Rajanpatti, Kiranoor, Thoppampatti, Vellampatti, and A. Kaliyamuthur locations were the most suitable for farm ponds artificial structures.

Flooding and furrowing: Lineament density and slope maps were required to identify areas suitable for flooding and furrowing artificial recharge methods. Low drainage density areas were selected and integrated with flat surface areas (0° to 1° slope) to generate areas suitable for flooding and furrowing; these were integrated with artificial recharge zones (Fig. 4) categorized as good, moderate, or excellent. Areas suggested for flooding and furrowing are shown in Fig. 7. Most of the prominent locations in the Palani taluk were suitable for flooding and furrowing artificial structures. The important locations included Ayakudi, Kannivadi, Kannakanpatti, Palani, Amarapundi, Pulaampatti, Mettupatti, Tiruvanadapuram, Vellampatti, Kovillampatti, Muthunayakanpatti, Pushpathur, Talaiyuthu, Andipatti, A. Kalaiyamuthur, Mapoor, Neikarapatti, and Balasamudhram.

Hydrofracturing: Lineament density and drainage density maps were used to identify areas suitable for hydrofracturing. High drainage density regions were filtered from the drainage map; very high lineament density maps were filtered from the lineament density map in the GIS environment and

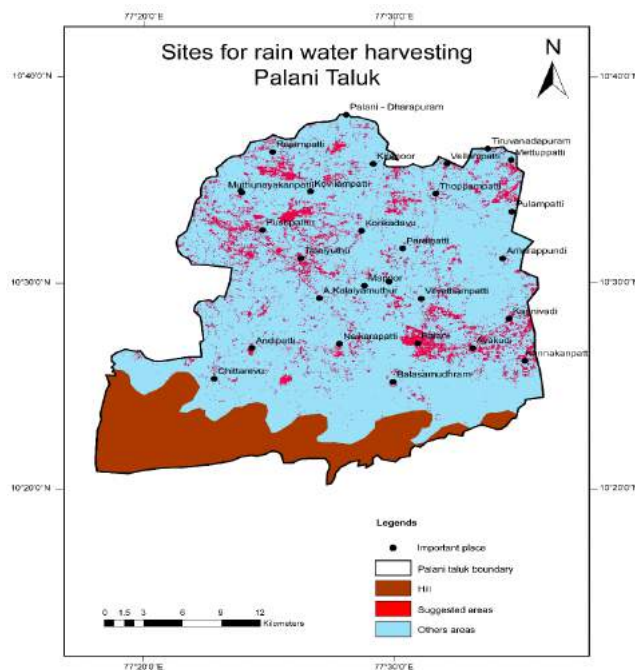


Fig. 10: Potential sites for rainwater harvesting.

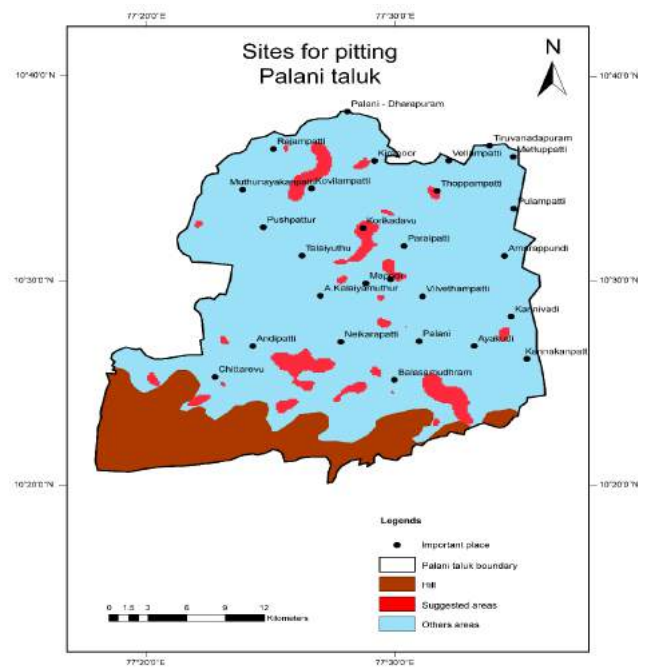


Fig. 11: Potential sites for pitting.

were integrated with artificial recharge zones (Fig. 4) categorized as good, moderate, or excellent. The very high drainage density maps were incorporated into very high lineament density maps using the GIS integrated tool to identify areas suitable for hydrofracturing in the study region, as shown in Fig. 8. Korikadavu and Thoppampatti locations in Palani taluk were well-suited for hydrofracturing artificial structures.

Percolation ponds: Area suggestions for percolation ponds were primed from slope maps and drainage catchment area maps. Drainage catchment area map prepared using the GIS model is shown in Fig. 3. Percolation pond areas should have a shallow slope region and micro drainage catchment. Suggested areas for percolation ponds were generated from micro drainage catchment areas that were selected from the drainage catchment map using GIS and were superimposed with shallow slope regions of the study area. Selected areas were integrated with artificial recharge zones (Fig. 4) categorized as good, moderate, or excellent. The results are illustrated in Fig. 9. Talaiyuthu was the most suitable location for the percolation pond artificial structure.

Rainwater harvesting: Suggested areas for rainwater harvesting were selected from land use and land cover maps of the study area. Land use and land cover map were primed from Resourcesat-I, LISS III satellite imagery. Classification tool of the remote sensing software was used to categorize the satellite images into various land use and land cover

types, which were integrated with artificial recharge zones (Fig. 4) categorized as good, moderate, or excellent. Areas suggested for rainwater harvesting are shown in Fig. 10. Palani, Ayakudi, Kannivadi, Kanakkanpatti, Talaiyuthu, Pushpathur, and Thoppampatti regions are well-suited for rainwater harvesting artificial structures.

Pitting: The drainage density map generated using GIS density tool was used to locate suitable sites for pitting in the study area. Areas with very high drainage density were identified and were integrated with artificial recharge zones (Fig. 4) categorized as good, moderate, or excellent. Suggested areas for pitting in Palani are shown in Fig. 11. Most of the pitting areas fall in the southern part of the Palani taluk, which is near the hilly regions. Korikadavu and Thoppampatti locations were suitable for pitting artificial structures.

CONCLUSIONS

In this study, de-saturated aquifers and locations that could potentially benefit from artificial recharge techniques were assessed in the Palani taluk in Tamil Nadu, India. Suitable sites for implementing artificial recharge structures were identified using land use and land cover maps, slope, lineament density, drainage, drainage density, and micro-drainage catchment area maps of the study area. Artificial recharge zones that were identified as good, moderate, or excellent were merged with various thematic layers using GIS

software and one or more appropriate artificial structures for a particular location were identified. Construction of artificial recharge sites will improve groundwater level and quality in and around the artificial recharge structure area. Temporal and seasonal variation in water demand can be monitored and appropriate recharge structures can be implemented to minimize water scarcity for irrigation and urban uses during non-rainfall periods. Thus, the artificial recharge structure maps generated using GIS in this study can be used for the construction of suitable recharge structures that will increase the groundwater level and groundwater quality and offer a long-term solution for seasonal water scarcity in the region.

REFERENCES

- Anbazhagan, S. 1994. Remote sensing based integrated terrain analysis for artificial recharge in Ayyar Basin, central Tamil Nadu, India. PhD thesis. School of Earth Sciences, Bharathidasan University, Tiruchirappalli.
- Anbazhagan, S. and Ramasamy, S.M. 1993. The role of remote sensing in the geomorphic analysis for water harvesting structures. Proceedings of the National Seminar on Water Harvesting, June 25-26 at Dept. Of Civil Engg., Regional Engineering College, Tiruchirappalli.
- Centre Ground Water Board (CGWB). 2000. Guide on Artificial Recharge to Ground Water. The Government of India - Ministry of Water Resource.
- Chandramohan, R., Kanchanabhan, T.E., Siva Vignesh, N. and Krishnamorthy, R. 2017a. Groundwater fluctuation in Palani Taluk, Dindigul district, Tamilnadu, India. *International Journal of Civil Engineering and Technology*, 8(7): 1041-1049.
- Chandramohan, R., Kanchanabhan, T.E., Siva Vignesh, N. and Krishnamorthy, R. 2017b. Remote sensing and GIS based approach for delineation of artificial recharge sites in Palani Taluk, Dindigul District, Tamilnadu, India. *International Journal of Civil Engineering and Technology*, 8(8): 698-706.
- Gale, I. and Dillon, P. 2006. Strategies for managed aquifer recharge (MAR) in semi-arid areas. United Nations Environment Programme, Division of Technology, Industry and Economics, UNESCO IHP.
- Missimer, T.M., Drewes, J.E., Amy, G., Maliva, R.G. and Kel, S. 2012. Restoration of Wadi aquifers by artificial recharge with treated waste water. *Groundwater*, 50(4): 514-527.
- Ramireddy, P.V., Padma, G.V. and Reddy, N.B. 2015. Identification of groundwater recharge zones and artificial recharge structures for part of Tamilnadu, India - a geospatial approach. *International Journal of Engineering Sciences & Research Technology*, 4(7): 999-1009.
- Samson, S. and Elangovan, K. 2015. Delineation of groundwater recharge potential zone in Namakkal district, Tamilnadu, India, using remote sensing and GIS. *Journal of the Indian Society of Remote Sensing*, 43(4): 769-778.
- Rokade, V.M., Kundal, P. and Joshi, A.K. 2004. Water resources development action plan for Sasti watershed, Chadrapur district, Maharashtra using remote sensing and geographic information system. *Journal of the Indian Society of Remote Sensing*, 32(4): 359-368.



The Use of Cobalt-Doped Tin(IV) Oxide as a Catalyst for the Photodegradation of Methyl Orange

Anti Kolonial Prodjosantoso[†] and Cahyorini Kusumawardani

Department of Chemistry, Yogyakarta State University, Yogyakarta, 55281, Indonesia

[†]Corresponding author: Anti Kolonial Prodjosantoso

Nat. Env. & Poll. Tech.
Website: www.neptjournal.com

Received: 05-04-2018

Accepted: 02-08-2018

Key Words:

Tin oxide
Cobalt oxides
Methyl orange degradation
Photocatalysis

ABSTRACT

Textile industries are always deal with water pollution caused by pigments, one of which is organic compounds. Efforts have been made to treat the polluted water, however the methods still need to be improved. Cobalt-doped tin(IV) oxide ($\text{Sn}_{1-x}\text{Co}_x\text{O}_2$, $x = 0, 0.0025$ and 0.005) prepared by a solid state reaction of SnO_2 powder and cobalt nitrate salt has been introduced to catalysis of methyl orange photodegradation. The catalysts have band gap energy (E_g) varied between 1.813 and 3.944 eV, and indicates good responses in both visible and ultraviolet lights, having high potent as photocatalysts on methyl orange degradation. The test indicates the applicability of Langmuir adsorption isotherm for the systems.

INTRODUCTION

The biggest problem with textile industries, for example, is dyes (Carmen & Daniel 2012). The dyes may poison water organisms, and block sunlight to penetrate water, disturbing the process of photosynthesis. The textile dyes are hardly decomposed causing disruption of water ecosystems for a long period of time (Ito et al. 2016).

The polluted water recovery process is very complicated, high cost and time consuming. The problem is more complex if the dyes settled in the water are toxic, carcinogenic, and mutagenic (Alves de Lima et al. 2007, Jäger et al. 2006). Many dyes are azo compounds which are nondegradable, and endanger living organisms (Cisneros et al. 2002, Ozdemir et al. 2013, Ribeiro & Umbuzeiro 2014). One of the azo dyes used in colouring textile is methyl orange (MO) which is a cationic heterocyclic aromatic compound (Li et al. 2013).

Dye removal from water includes conventional methods such as adsorption using activated carbon or zeolites, and modern methods, such as biodegradation, ozonization, chlorination, ionizing radiation and plasma technology. The conventional methods are less applicable and ineffective to use, while modern methods are usually expensive (Ozdemir et al. 2013, Robinson et al. 2002, Samad et al. 2016, Vidal et al. 2016).

Photodegradation, the environmental friendly and low cost method, may be applied to decompose the dyestuff wastes. Photodegradation may be facilitated by using

photocatalysts. Photocatalysis combines photochemical processes and catalysis. This process includes chemical transformation process using photons as energy sources and catalysts accelerating the rate of transformation. The process is based on the dual capability of a semiconductor material (such as TiO_2 , ZnO , Fe_2O_3 , CdS , ZnS) to absorb photons and simultaneously transform the material interface (Banerjee et al. 2014, Ohtani 2011). The use of this photocatalyst has the advantage of being able to totally mineralize the organic pollutants including textile waste (azo compounds), the operational cost is inexpensive with a relatively fast, non-toxic and long-term use, and environmental friendly and reusable (Ohtani 2010). Photocatalyst that is widely used is TiO_2 due to its high activity and band gap energy of 3.2 eV. The use of SnO_2 instead of TiO_2 is of interest (Zheng et al. 2016). The tin oxide photocatalyst having band gap energy of 3.6 eV is enhanced by cobalt oxide so that the catalysts may also work well under visible light (Barakat et al. 2008, Patil 1996, Prodjosantoso et al. 2017a). This stable catalyst may be prepared using arrange of methods, but the high temperature reaction is the simplest and cheapest method (De Almeida et al. 2014).

We are reporting the use of $\text{Sn}_{1-x}\text{Co}_x\text{O}_2$ ($x = 0, 0.0025$ and 0.005) to catalyse the degradation of methyl orange (MO) solution under UV and visible light radiations.

MATERIALS AND METHODS

Materials: SnO_2 (Merck), $\text{Co}(\text{NO}_3)_2 \cdot 6\text{H}_2\text{O}$ (Merck), and MO

(Sigma-Aldrich) were used as received without any further purification.

Methods: A total of 1.5071 grams of SnO₂ was thoroughly mixed with 0.00728 gram (2.5 × 10⁻⁵ mol) Co(NO₃)₂·6H₂O, and followed by calcination at 900°C for 4 hours. The work was repeated using 0.01455 g (5 × 10⁻⁵ mol) Co(NO₃)₂·6H₂O. The resulting catalysts were then characterized using UV-Vis Spectroscopy (UV-2450PC Pharmaspec Spectrophotometer) method.

The adsorption behaviour of Sn_{1-x}Co_xO₂ (x = 0, 0.0025 and 0.005) was determined as follows: a set of adsorption test was performed in the dark, in which 10 mL of MO solutions with different initial concentrations were added with 0.1 g of Sn_{1-x}Co_xO₂ (x = 0, 0.0025 and 0.005) powders, and shaken for 24 hours. The MO concentration in the suspensions before and after the adsorption were analysed to determine the amount of MO adsorbed by the catalyst.

The photocatalytic activity of Sn_{1-x}Co_xO₂ (x = 0, 0.0025 and 0.005) was determined by measuring the undecomposed MO after being exposed under visible or UV-light. The initial concentration of MO was 1 × 10⁻⁵ M. The undecomposed MO at given time intervals was measured using a spectrometry at the absorbance of 462 nm.

RESULTS AND DISCUSSION

UV-Vis spectroscopy method was used to determine the band gap energy of the material, and the absorbances. Prior to the measurements, the Sn_{1-x}Co_xO₂ (x = 0, 0.0025 and 0.005) was dissolved in a mixture of triton-x and acetylacetonate to form a paste, which was then layered on the preparatory glass. Furthermore, the glass was dried in a furnace at a temperature of 450°C for 2 hours to evaporate the solvent.

In this study, measurements were carried out at wavelengths of 200-800 nm. Each sample has absorbed energy at certain wavelength(s) (Table 1).

Table 1: Absorbances of Sn_{1-x}Co_xO₂.

Sn _{1-x} Co _x O ₂ , x =	λ (nm)	
	Visible	UV
0	-	317
0.0025	405	275 and 315
0.005	395	295

Table 2: The band gap energy of Sn_{1-x}Co_xO₂.

Sn _{1-x} Co _x O ₂ , x =	Band Gap Energy (eV)		
	E _g ¹	E _g ²	E _g ³
0	3.944	-	-
0.0025	3.819	2.588	1.829
0.005	3.931	2.236	1.813

The Kubelka-Munk equation was used to calculate the band gap energy (E_g) of catalysts (Yang & Kruse 2004). Table 2 lists the band gap energies of Sn_{1-x}Co_xO₂ (x = 0, 0.0025 and 0.005). The cobalt, which is doped onto SnO₂, decreases the band gap energy of SnO₂ (3.944 eV) (Prodjosantoso et al. 2017b, Reimann & Steube 1998, Viter et al. 2014). In general, the more cobalt additions provide the lower band gap energy of Sn_{1-x}Co_xO₂ (x = 0, 0.0025 and 0.005).

The Sn_{1-x}Co_xO₂ (x = 0, 0.0025 and 0.005) photocatalyst adsorption test was performed in the dark environment. Prior to adsorption, the measurement of MO absorbance at a wavelength of 462 nm was performed, to obtain a MO standard curve. The adsorption process used 0.05 grams of catalyst of Sn_{1-x}Co_xO₂ (x = 0, 0.0025 and 0.005), and the concentrations of MO were 2, 4, 6, 8 and 10 (×10⁻⁶ mol/L). The adsorption of MO by the catalyst was carried out for 24 hours in a closed shaker to obtain a state of equilibrium. Furthermore, the mixture of the degraded solution was centrifuged at a rate of 1500 rpm for 10 minutes to separate the liquid phase from the precipitate. The filtrate was analysed at wavelength of 462 nm to determine the concentration of MO.

The calculation of catalyst adsorption capacity was performed using Langmuir and Freundlich equations (LeVan & Vermeulen 1981). The Langmuir isotherm pattern was determined by correlating the MO concentration adsorbed on every 1 gram of catalyst (c/m) with MO concentration after 24 h (c). The calculation of the adsorption capacity value (b) on the Langmuir isotherm was undertaken using the equation as follows:

$$\frac{c}{m} = \frac{c}{b} + \frac{1}{K_f b} \quad \dots(1)$$

Freundlich isotherm pattern is determined by plotting the log value of the amount of MO adsorbed on every 1 gram of catalyst (log x/m) with the log of MO concentration after 24 hours (log c). The calculation of the adsorption capacity (k) of the Freundlich isotherm was undertaken using equation as follows:

$$\log \frac{x}{m} = \log k + \frac{1}{n} \log c \quad \dots(2)$$

The equations of Langmuir and Freundlich isotherms are presented in Table 3.

The R² values of the Langmuir adsorption isotherm pattern are higher than that of the Freundlich. Thus, we can conclude that adsorption on MO degradation by Sn_{1-x}Co_xO₂ catalysts follows Langmuir isotherm pattern. This pattern assumes the monolayer formation of adsorbate on the homogenous adsorbent surface. There is no interaction

Table 3: Equations of Langmuir and Freundlich isotherm patterns of Sn_{1-x}Co_xO₂.

Sn _{1-x} Co _x O ₂ , x =	Langmuir	Freundlich
0	y = 0.77253x - 1.29567R ² = 0.98349	y = -0.90112x - 12.05405R ² = 0.93153
0.0025	y = 0.60214x - 1.25004R ² = 0.96149	y = -1.01961x - 12.62908R ² = 0.81312
0.005	y = 0.33124x - 0.55717R ² = 0.98578	y = -2.34525x - 20.64722R ² = 0.85533

among the adsorbed molecules, i.e. MO.

The adsorption capacity can be calculated using Langmuir isotherm equation, that is the 1/slope of the line equation. The adsorption capacities of the sample is presented in Table 4. The SnO₂ indicates the lowest adsorption capacity. This is due to SnO₂- supported cobalt oxide having a larger surface and a greater ability to adsorb MO than pure SnO₂.

The photodegradation was performed using 0.05 gram Sn_{1-x}Co_xO₂ for every 10 mL of 15.63 ppm MO solution. The mixtures were placed in a shaker covered by a closed box equipped with Evaco 20 Watt fluorescent light. Measurements were undertaken at variations of time i.e., 4, 8, 12, 16, 20 and 30 minutes. The absorbances were measured at a wavelength of 462 nm. The absorbances were then referred into the standard MO curve equation to obtain the MO concentration (Fig. 1).

Fig. 1. shows that the concentration of MO decreases with increasing exposed time to UV light. This proves that MO degradation is effectively performed by using Sn_{1-x}Co_xO₂ catalysts, under UV light. Fig. 1 also indicates that the SnO₂ catalysed more effectively in degrading the MO compared to Sn_{1-x}Co_xO₂ with x = 0.0025 and 0.005, which is similar to results performed by cobalt(II) oxide supported onto tin(IV) oxide catalysts (Cerri et al. 2005).

Fig. 1., however, also shows that the little MO increase after photodegradation for 80 and 120 minutes. It might be a photolysis product appearing which absorbs at the wavelength where the MO concentration is measured, or it might be a simple error in the measurement. In principle, it also might be the consequence of the liberation of adsorbed MO due to co-adsorption of decomposition products, but the increase in the concentration is well enough.

Photodegradation of MO under visible light was undertaken using the same procedure for MO photodegradation

Table 4: Adsorption Capacity of Sn_{1-x}Co_xO₂.

Sn _{1-x} Co _x O ₂ , x=	Adsorption Capacity (mole/gram)
0	1.29444811
0.0025	1.660743349
0.005	3.018959063

under UV light, but the light source used was Philips ML 100W/220-230E27. The absorbances observed were then referred into the standard MO curve equation to obtain the MO concentration (Fig. 2).

Fig. 2 indicates that the concentration of MO solution is inversely proportional to the exposure time of visible light. The catalysts show a good performance under visible light. The performance of Sn_{1-x}Co_xO₂ with x = 0.005 in degrading MO is better compared to the SnO₂ and Sn_{1-x}Co_xO₂ with x = 0.0025 catalysts.

The reaction order was determined to study the reaction rate kinetics of the MO photodegradation. The largest value of R² was used to determine the order of reactions. The zero-order reaction was determined by integrating the equation of the reaction rate, as follows:

$$C_t = -kt + C_0 \quad \dots(3)$$

Where, C_t is the concentration of MO at time t, k is the rate constant, t is time and C₀ is the initial concentration of MO. By plotting C_t vs. t, we obtain the equation of the line for the zero-order reaction, and the R² value can be determined.

The first-order reaction was determined by integrating the rate of reaction to obtain the equation of the reaction, as follows:

$$\ln(C_t/C_0) = -kt \quad \dots(4)$$

$$\ln C_t = -kt + \ln C_0 \quad \dots(5)$$

By plotting ln C_t vs. t, we obtain the equation of the line for the first-order reaction, and the R² value can be determined.

The second-order reaction was determined by integrating the rate of reaction to obtain the equation of the reaction, as follows:

$$\frac{1}{C_t} = kt + \frac{1}{C_0} \quad \dots(6)$$

By plotting 1/C_t vs. t, we obtain the equation of the line for the second-order reaction.

By comparing the values of R² of the three reaction orders (Table 5), the rate of MO photodegradation reaction using catalysts Sn_{1-x}Co_xO₂ under UV light and visible light is

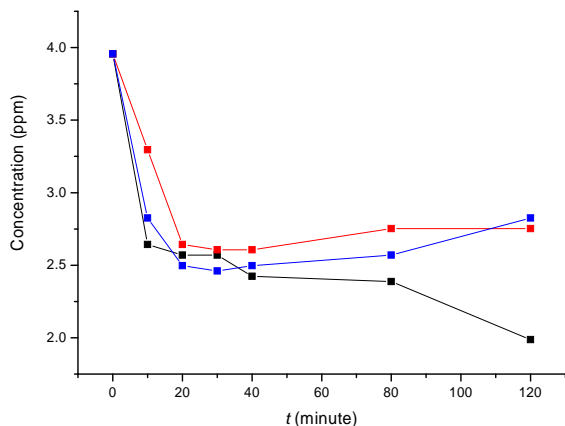


Fig. 1: Photoactivity of Sn_{1-x}Co_xO₂ with x = 0 (black), 0.0025 (red) and 0.005 (blue) on MO photodegradation under UV light.

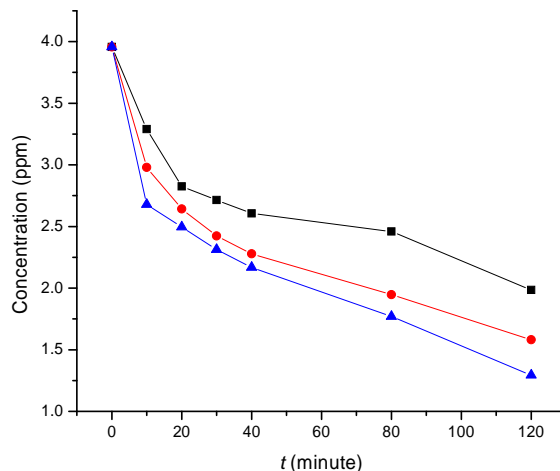


Fig. 2: Photoactivity of Sn_{1-x}Co_xO₂ with x = 0 (black), 0.0025 (red) and 0.005 (blue) on MO photodegradation under visible light.

determined. As the second-order kinetics curve has the highest R² value than that of zero and first-order, so the order of the reaction is confirmed to be second-order reaction.

The decrease of the concentration of MO in the degradation process using Sn_{1-x}Co_xO₂, under UV light and visible light can be seen in Fig. 3.

In the MO degradation experiment using UV irradiation, SnO₂ catalysis is more effective than other catalysts. But, the Sn_{1-x}Co_xO₂ performs conversely, and the Sn_{1-x}Co_xO₂ with x = 0.005 indicates the most effective catalysis compared to the rest of catalysts. This is because the undoped SnO₂ has a band gap energy working only on UV light, while Sn_{1-x}Co_xO₂ works on both UV and visible light.

The photocatalytic reaction takes place in a heterogeneous system and the reaction rate is affected by the adsorbance of the reactants on the surface of the catalyst. Reaction rate can be formulated as follows:

$$r = -\frac{dC}{dt} = \frac{k_{obs} \cdot K \cdot C}{1 + K \cdot C} \quad \dots(7)$$

The reaction rate equation can be simplified into second-order kinetics as follows:

$$\frac{1}{C} = -k_{obs}t + \frac{1}{C_0} \quad \dots(8)$$

Where, k_{obs} is the total reaction rate constant (min⁻¹), K is the adsorption constant of the reactant and C is the concentration of the reactant at any time. Kinetic constant k_{obs} is the rate constant of the reaction, which does not take into account the role of adsorption, so that when the adsorption process becomes the part affecting the photodegradation reaction, it is necessary to determine the actual reaction rate constant (k) that has corrected the k_{obs} with the adsorption constant (K), where $k_{obs} = kKL$.

Kinetics parameter k_{obs} was determined by plotting $1/C_t$ vs t followed by the calculation based on the second-order reaction. The reaction rate constant (k) is determined based on the k_{obs} and the results can be seen in Table 6.

Table 6 shows that for the Sn_{1-x}Co_xO₂ with x = 0 catalyst the magnitude of the reaction rates of MO photodegradation

Table 5: Kinetical data of MO photodegradation reaction order.

Sn _{1-x} Co _x O ₂ , x =	Reaction Order	UV light		Visible light	
		k	R ²	k	R ²
0	0	0.00683	0.57239	0.01075	0.83697
	1	0.00481	0.63375	0.00927	0.93244
	2	0.00366	0.70187	0.00913	0.95211
0.0025	0	0.00655	0.52151	0.01504	0.85657
	1	0.00466	0.57094	0.01750	0.96809
	2	0.00366	0.63328	0.02735	0.99514
0.005	0	0.00786	0.62716	0.01307	0.81567
	1	0.00607	0.72654	0.01687	0.96418
	2	0.00518	0.83113	0.03153	0.98390

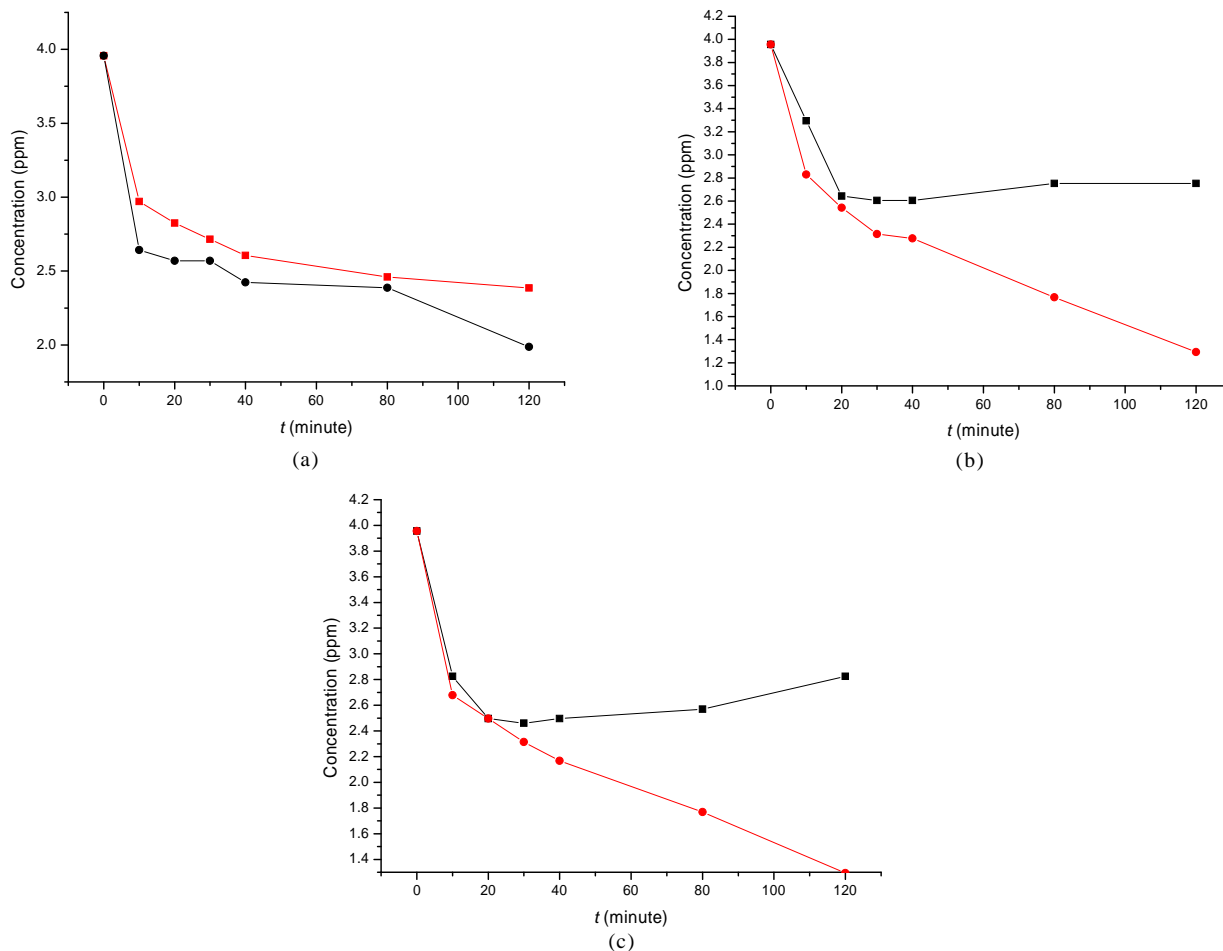


Fig. 3: The plot of the time of irradiation vs. MO concentration after the degradation under UV light (black line) and visible light (red line) using the catalysts of $\text{Sn}_{1-x}\text{Co}_x\text{O}_2$ with $x = 0$ (a), 0.0025 (b) and 0.005 (c).

Table 6: MO photodegradation kinetics with $\text{Sn}_{1-x}\text{Co}_x\text{O}_2$ catalysts under UV and visible light.

Light source	$\text{Sn}_{1-x}\text{Co}_x\text{O}_2$, $x =$	k_{obs} (minute ⁻¹)	k (minute ⁻¹)
UV	0	0.00366	0.004738
	0.0025	0.00366	0.006078
	0.005	0.00518	0.015638
Visible	0	0.00913	0.011818
	0.0025	0.02735	0.034169
	0.005	0.01687	0.050930

Table 7: Reaction rate of MO photodegradation using $\text{Sn}_{1-x}\text{Co}_x\text{O}_2$ under UV and visible lights.

$\text{Sn}_{1-x}\text{Co}_x\text{O}_2$, $x =$	Reaction rate (ppm ² .minute ⁻¹)	
	UV light	Visible light
0	$7.4157 \cdot 10^{-2}$	$1.8497 \cdot 10^{-1}$
0.0025	$9.5130 \cdot 10^{-2}$	$5.3480 \cdot 10^{-1}$
0.005	$24.4758 \cdot 10^{-2}$	$7.9713 \cdot 10^{-1}$

under UV and visible light are relatively similar. However, for $\text{Sn}_{1-x}\text{Co}_x\text{O}_2$ with $x = 0.0025$ and 0.005 catalysts the reaction rates are significantly different. The photodegradation rate constant in visible light has a greater value than that of UV light. This means that the $\text{Sn}_{1-x}\text{Co}_x\text{O}_2$ catalysis is effectively working under visible light. The rate of reaction is determined using equation as follows:

$$r = kC^n \quad \dots(9)$$

Where, r is the photodegradation reaction rate, k is the photodegradation rate constant, C is the initial concentration of MO, and n is the photodegradation reaction order. The reaction rate of MO photodegradation is listed in Table 7. The reaction rate of MO degradation under visible light is almost three time faster than that of under UV light.

CONCLUSIONS

The $\text{Sn}_{1-x}\text{Co}_x\text{O}_2$ photocatalysts have been prepared by impregnation method. The cobalt may be recognized by means of the larger lattice parameters of the $\text{Sn}_{1-x}\text{Co}_x\text{O}_2$ with the increase of cobalt. Optical absorption studies clearly indicate the visible light response with the existence of cobalt. A higher photocatalytic activity for the decomposition of MO in the visible region has been confirmed for the prepared $\text{Sn}_{1-x}\text{Co}_x\text{O}_2$ sample compared to the pure SnO_2 .

ACKNOWLEDGEMENT

This work was partially supported by the Yogyakarta State University, Indonesia. We thank Yoga Nur Rizqi for his assistance with these measurements.

REFERENCES

- Alves de Lima, R. O., Bazo, A. P., Salvadori, D.M.F., Rech, C.M., de Palma Oliveira, D. and de Arago Umbuzeiro, G. 2007. Mutagenic and carcinogenic potential of a textile azo dye processing plant effluent that impacts a drinking water source. *Mutation Research-Genetic Toxicology and Environmental Mutagenesis*, 626(1-2): 53-60.
- Banerjee, S., Pillai, S.C., Falaras, P., O'Shea, K.E., Byrne, J.A. and Dionysiou, D.D. 2014. New insights into the mechanism of visible light photocatalysis. *The Journal of Physical Chemistry Letters*, 5(15): 2543-2554.
- Barakat, N.A., Khil, M.S., Sheikh, F.A. and Kim, H.Y. 2008. Synthesis and optical properties of two cobalt oxides (CoO and Co_3O_4) nanofibers produced by electrospinning process. *The Journal of Physical Chemistry C*, 112(32): 12225-12233.
- Carmen, Z. and Daniel, S. 2012. Textile organic dyes-characteristics, polluting effects and separation/elimination procedures from industrial effluents - a critical overview. In: *Organic Pollutants Ten Years After the Stockholm Convention - Environmental and Analytical Update*.
- Cerri, J.A., Leite, E.R., Gouvêa, D., Longo, E. and Varela, J.A. 2005. Effect of cobalt(II) oxide and manganese(IV) oxide on sintering of tin(IV) oxide. *Journal of the American Ceramic Society*, 79(3): 799-804.
- Cisneros, R.L., Espinoza, A.G. and Litter, M.I. 2002. Photodegradation of an azo dye of the textile industry. *Chemosphere*, 48(4): 393-399.
- De Almeida, R.M., Souza, F.T.C., Júnior, M.A.C., Albuquerque, N.J. A., Meneghetti, S.M.P. and Meneghetti, M.R. 2014. Improvements in acidity for TiO_2 and SnO_2 via impregnation with MoO_3 for the esterification of fatty acids. *Catalysis Communications*, 46: 179-182.
- Ito, T., Adachi, Y., Yamanashi, Y. and Shimada, Y. 2016. Long term natural remediation process in textile dye polluted river sediment driven by bacterial community changes. *Water Research*, 100: 458-465.
- Jäger, I., Hafner, C., Welsch, C., Schneider, K., Iznaguen, H. and Westendorf, J. 2006. The mutagenic potential of madder root in dyeing processes in the textile industry. *Mutation Research - Genetic Toxicology and Environmental Mutagenesis*, 605(1-2): 22-29.
- LeVan, M.D. and Vermeulen, T. 1981. Binary Langmuir and Freundlich isotherms for ideal adsorbed solutions. *Journal of Physical Chemistry*, 85(22): 3247-3250.
- Li, Y.Z., Sun, C.F. and Yang, L.P. 2013. Structures and spectroscopic properties of three aromatic heterocyclic dye photosensitizers. *Journal of Theoretical & Computational Chemistry*, 12(6): 1-12.
- Ohtani, B. 2010. Photocatalysis A to Z - what we know and what we do not know in a scientific sense. *Journal of Photochemistry and Photobiology C: Photochemistry Reviews*, 11(4): 157-178.
- Ohtani, B. 2011. Photocatalysis by inorganic solid materials: Revisiting its definition, concepts, and experimental procedures. *Advances in Inorganic Chemistry*, 63: 395-430.
- Ozdemir, S., Cirik, K., Akman, D., Sahinkaya, E. and Cinar, O. 2013. Treatment of azo dye-containing synthetic textile dye effluent using sulfidogenic anaerobic baffled reactor. *Bioresource Technology*, 146: 135-143.
- Patil, P.S., Kadam, L.D. and Lokhande, C.D. 1996. Preparation and characterization of spray pyrolysed cobalt oxide thin films. *Thin Solid Films*, 272(1): 29-32.
- Prodjosantoso, A.K., Kusumawardani, K., Pranjoto, U. and Handoko, C.T. 2017a. Synthesized and characterization of $\text{Ca}_{1-x}\text{Co}_x\text{TiO}_3$ and its photocatalytic activity on photodegradation of methylene blue. *Asian J. Chem.*, 29(6): 1270-1274.
- Prodjosantoso, A.K., Rahmawati, T. and Kusumawardani, C. 2017b. Tin(IV) oxide-supported cobalt oxides catalysts for methylene blue photodegradation. *Research Journal of Chemistry and Environment*, 21(12): 12-20.
- Reimann, K. and Steube, M. 1998. Experimental determination of the electronic band structure of SnO_2 . *Solid State Communications*, 105(10): 649-652.
- Ribeiro, A.R. and Umbuzeiro, G. de A. 2014. Effects of a textile azo dye on mortality, regeneration, and reproductive performance of the planarian, *Girardia tigrina*. *Environmental Sciences Europe*, 26(1): 22.
- Robinson, T., Chandran, B. and Nigam, P. 2002. Removal of dyes from a synthetic textile dye effluent by biosorption on apple pomace and wheat straw. *Water Research*, 36(11): 2824-2830.
- Samad, A., Furukawa, M., Katsumata, H., Suzuki, T. and Kaneco, S. 2016. Photocatalytic oxidation and simultaneous removal of arsenite with CuO/ZnO photocatalyst. *Journal of Photochemistry and Photobiology A: Chemistry*, 325: 97-103.
- Vidal, J., Villegas, L., Peralta-Hernández, J.M. and Salazar González, R. 2016. Removal of Acid Black 194 dye from water by electrocoagulation with aluminum anode. *Journal of Environmental Science and Health, Part A*, 51(4): 289-296.
- Viter, R., Katoch, A. and Kim, S.S. 2014. Grain size dependent bandgap shift of SnO_2 nanofibers. *Metals and Materials International*, 20(1): 163-167.
- Yang, L. and Kruse, B. 2004. Revised Kubelka Munk theory. I. Theory and application. *Journal of the Optical Society of America*, 21(10): 1933-1941.
- Zheng, Y., Luo, C., Liu, L., Yang, Z., Ren, S., Cai, Y. and Xiong, J. 2016. Synthesis of hierarchical $\text{TiO}_2/\text{SnO}_2$ photocatalysts with different morphologies and their application for photocatalytic reduction of Cr(VI) . *Materials Letters*, 181: 169-172.



Degradation of Azo Dye Acid Orange 7 by Zero Valent Iron Activated with Potassium Persulphate

Muqing Qiu

College of Life Science, Shaoxing University, Shaoxing, 312000, P.R. China

Nat. Env. & Poll. Tech.
Website: www.neptjournal.com

Received: 22-03-2018
Accepted: 04-06-2018

Key Words:

Degradation
Acid Orange 7
Azo dye
Activated zero valent iron

ABSTRACT

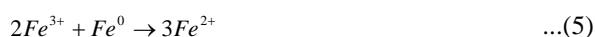
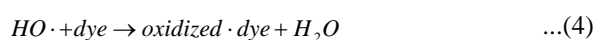
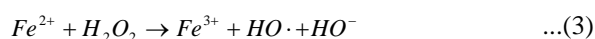
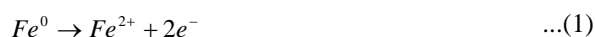
The zero valent iron has the advantage that the small particle size results in a large specific surface area and great intrinsic reactivity of surface sites. However, the zero valent iron particles tend to either react with surrounding media or agglomerate, resulting in significant loss of reactivity. The synthetic zero valent iron was activated by potassium persulphate. The degradation of azo dye Acid Orange 7 by zero valent iron activated with potassium persulphate was carried out. The effect of several parameters, such as the pH in solution, the reaction time, reaction temperature, the activated zero valent iron amount and the initial concentration of dye on the removal process was investigated. The results showed that the degradation rate of azo dye Acid Orange 7 by the activated zero valent iron was high. The operation parameters had an important effect on the degradation of azo dye Acid Orange 7 in aqueous solution.

INTRODUCTION

Dyes have been widely used in many industries, like textiles, printing, leather, paper, cosmetics and plastics. Discharge of sewage from those industries is an important threat to the environment (Cundy et al. 2008). The dye contaminated wastes can inhibit the sunlight from reaching the deep water, and resulting in the negative effect on growth of aquatic organisms (Sun et al. 2006). In particular, the accumulation of dyes in water environment is hazardous to the health of human health and other creatures because of its potential toxicity, carcinogenicity and teratogenicity (Djurđja et al. 2014). Azo pigments are applied into the industries widely. Azo groups are usually conjunct to convoluted aromatic systems and the stability of aromatic structures is dangerous for environment. Therefore, the degradation of dyes in solution is essentially necessary before they are discharged into the environment (Kanel et al. 2005).

Among the numerous dye removal techniques, adsorption is now the preferred method, which gives the best results in removing various types of colouring materials (Xiong et al. 2007). Nonetheless, there are some disadvantages associated with these techniques (Wang et al. 1998). For example, activated carbon adsorption only transfers the dyes from the liquid phase to solid phase. The biological process is difficult to start up and be controlled and also the organic compounds in the wastewater cannot be degraded completely by biological processes (Huang et al. 1998). Therefore, as a result, the total treatment cost can increase because of the need for further treatment. In the last decade,

zero valent iron was used to destroy organic pollutants in water. This method has been proved to be a cost effective treatment approach and was widely used to treat wastewater containing chlorinated aliphatics, chlorinated aromatics and organic dyes (Devlin et al. 1998). A great deal of interest has developed in the degradation of dyes wastewater by zero valent iron particles, as they are inexpensive, environment friendly, easy to operate, and low iron concentration in effluent results in no further treatment demand (Gavaskar 1999). In most studies, the sole zero valent iron or supported zero valent iron was used for the effluent treatment (Linsebigler et al. 1995). The main mechanism of degradation of dye wastewater by zero valent iron was the reductive degradation of dye molecule (Eq. 1). The more recently zero valent iron particles are widely applied for wastewater treatment and organic compounds degradation in Fenton system (Papic et al. 2004). In acidic conditions, the surface of the zero valent iron particles corrodes and generates *in situ* ferrous ions, which leads to Fenton reactions in the presence of hydrogen peroxide (Eqs. 2-4). The zero valent iron particle surface can reduce the ferric ions down to ferrous ions, and then faster recycling of ferric iron at the iron surface occurs through Eq. 5 (Deng et al. 2000).



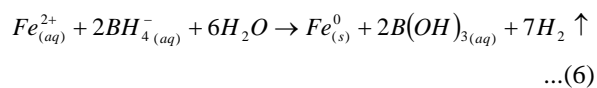
The zero valent iron has the advantage that the small particle size results in a large specific surface area and great intrinsic reactivity of surface sites (Fu et al. 2014). However, the zero valent iron particles tend to either react with surrounding media or agglomerate, resulting in significant loss of reactivity (Sun et al. 2006). To prevent particle aggregation, a wide variety of stabilizers have been proposed to modify the zero valent iron particle surface characteristics (Shu et al. 2009).

In this study, the dye Acid Orange 7 was chosen in the experiment, because it is an extensively used dye in the textile industry. The synthetic zero valent iron was activated by potassium persulphate. The degradation of azo dye Acid Orange 7 by potassium persulphate activated using zero valent iron was carried out. The effect of several parameters, such as the pH in solution, reaction temperature, the reaction time, the activated zero valent iron amount and the initial concentration of dye on the removal process was discussed in detail.

MATERIALS AND METHODS

Dyes and chemicals: The dye Acid Orange 7 was chosen as an object in this experiment to be removed from water. It was purchased from Shanghai Chemical Co. Ltd. in China. Its molecular formula is $C_{16}H_{11}O_4N_2SNa$. The chemical structure of the dye Acid Orange 7 is shown in Fig. 1.

Preparation of the activated zero valent iron by potassium persulphate: The nanoscale zero valent iron was synthesized in the laboratory using a modified method from previous liquid phase method by adding the macromolecule stabilizer. The basic principle of the synthesis process was that ferrous ion was rapidly reduced to the nanoscale zero valent iron by borohydride solution following the equation below:



The concentration of 100 mL 0.02 M ferrous chloride solution was prepared and then 4 g PVP was added into the ferrous chloride solution in a beaker, and with vigorous stirring PVP was completely dissolved. The 100 mL 0.06 M potassium borohydride solution was swiftly added into the

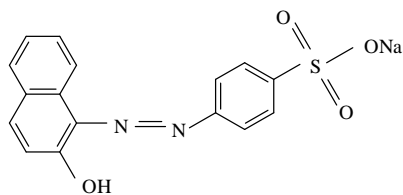


Fig. 1: The chemical structure of the dye Acid Orange 7.

above solution and the mixture was agitated in a water bath shaker with a shaking rate of 120 rpm at 15°C until the solution turned into black without rising bubbles. The nanoscale zero valent iron was washed with propanone three times in order to clean up the residual reagent, and then they were soaked with 100 mL of 2 mmol/L potassium persulphate in the beaker for 50 min at room temperature. They were then washed twice by the deionized distilled water, and dried in the oven at 105°C for 4 hours. The dry activated zero valent iron particles with potassium persulphate were gained and used for the further experiments.

Experimental procedure: Bath experiments were conducted by mixing 100 mL of dye solution and the activated zero valent iron particles in 250 mL Erlenmeyer flasks. The flasks were shaken at 150 rpm and in a contact temperature. All the degradation tests were performed twice, and the average values were used.

Analytical methods: The structures and sizes of the activated zero valent iron particles were characterized by the scanning electron microscopy. The value of pH was measured with a pH probe according to APHA standard method. The concentration of dye Acid Orange 7 was measured with a UV-1600 spectrophotometer at 485 nm.

The degradation rate of dye Acid Orange 7 was calculated as following:

$$Q = \frac{C_0 - C_t}{C_0} \times 100\% \quad \dots(7)$$

Where, C_0 and C_t (mg/L) are the initial and equilibrium concentrations of dye Acid Orange 7 in the solution respectively. Q is the degradation rate of dye Acid Orange 7.

Statistical analyses of data: All the experiments were repeated in duplicate and the data of results were the mean and the standard deviation (SD). The value of the SD was calculated by Excel software. All error estimates given in the text and error bars in figures are standard deviation of means (mean \pm SD). All statistical significance was noted at $\alpha=0.05$ unless otherwise noted.

RESULTS AND DISCUSSION

The structure of the activated zero valent iron particles: The structures and sizes of the activated zero valent iron particles were characterized by the scanning electron microscopy. The image is shown in Fig. 2.

The image indicated that there were many modular protrusions over the surface. These nodules were the *in-situ* prepared zero valent iron particles. They were spherical in

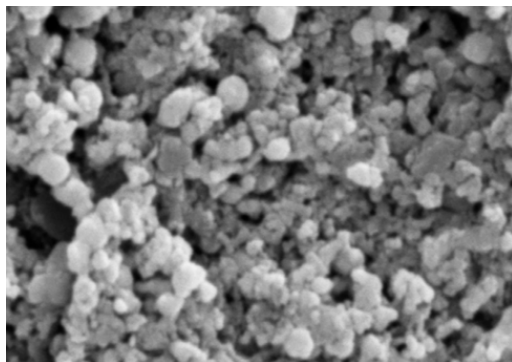


Fig. 2: SEM image of the activated zero valent iron particles.

shape, and distributed throughout the surface of the clays without noticeable aggregation.

The effect of reaction time: The reaction time is an important parameter in the process of reaction. In order to investigate the effect of reaction time on the degradation of azo dye Acid Orange 7 by the activated zero valent iron, the effect of reaction time was studied in a series of experiments. Bath experiments were conducted by mixing 100 mL of 200 mg/L azo dye Acid Orange 7 in aqueous solution, pH 2.0 in aqueous solution and 3 g of the activated zero valent iron particles in 250 mL Erlenmeyer flasks. The flasks were shaken at 150 rpm and in a contact temperature of 303 K. The results of the experiments are shown in Fig. 3.

As shown in Fig. 3, it indicated that the reaction time had an important role in the reaction process of degradation. As the reaction time increased, the degradation rate of azo dye Acid Orange 7 also increased. In the first stage of reaction process, the reaction rate was very quick. Then, the reaction rate of degradation began to increase slowly. The reaction process reached equilibrium in about 10 min. So,

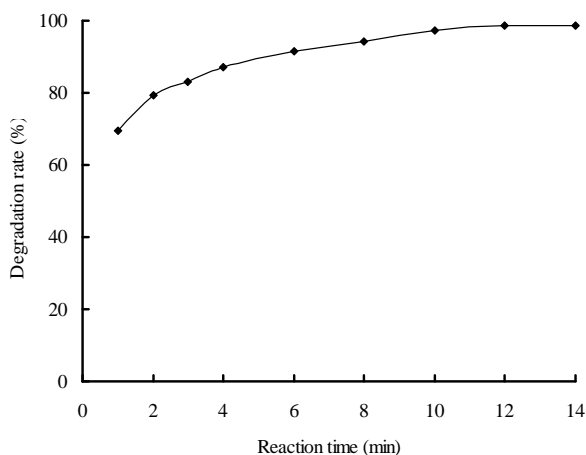


Fig. 3: The effect of reaction time on the degradation rate.

the reaction time of 10 min was thought to be optimum. In the following experiments, the reaction time of 10 min is chosen.

The effect of the activated zero valent iron dosage: The reaction parameter of the activated zero valent iron dosage is very important for the reaction rate. In order to investigate the effect of the activated zero valent iron dosage, a series of experiments were carried out. Bath experiments were conducted by mixing 100 mL of 200 mg/L azo dye Acid Orange 7 in aqueous solution, with reaction time of 10 min and pH 2.0 in 250 mL Erlenmeyer flasks. The flasks were shaken at 150 rpm and in a contact temperature of 303 K. The activated zero valent iron dosage ranged from 1 g to 5 g. The experimental results are shown in Fig. 4. It was found that the degradation rate of azo dye Acid Orange 7 in aqueous solution increased with the increasing of the activated zero valent iron particles. This is because more $\cdot\text{OH}$ radicals are produced with the increase in the activated zero valent iron particles due to Fenton's reaction (Wang et al. 2015).

The effect of pH in solution: The value of pH in aqueous solution is an important parameter affecting azo dye removal no matter what kind of azo dyes they were. The actual dye containing wastewater has a wide range of pH value in aqueous solution, so it is very necessary to investigate the influence of pH in aqueous solution on degradation process. Bath experiments were conducted by mixing 100 mL of 200 mg/L azo dye Acid Orange 7 in aqueous solution, with reaction time of 10 min and 3 g of the activated zero valent iron particles in 250 mL Erlenmeyer flasks. The flasks were shaken at 150 rpm and in a contact temperature of 303 K. The pH in solution ranged from 2.0 to 6.0. The effect of pH in solution on the degradation rate of azo dye Acid Orange 7 is shown in Fig. 5.

It can be seen from the results that the degradation rate of azo dye Acid Orange 7 decreased with an increase in the initial pH from 2.0 to 6.0. These experimental observations can be explained by the effects of pH value in solution on chemistry and Fenton reaction. It was widely reported that higher degradation rates were observed at lower pH value in solution for dye (Chen et al. 2011).

The effect of the reaction temperature: Temperature is one of the important parameters in chemical reactions. It has an important effect on the rate of the reactions. Bath experiments were conducted by mixing 100 mL of 200 mg/L azo dye Acid Orange 7 in aqueous solution, reaction time of 10 min, pH 2.0 in solution and 3 g of the activated zero valent iron particles in 250 mL Erlenmeyer flasks. The flasks were shaken at 150 rpm in the contact temperature. The reaction

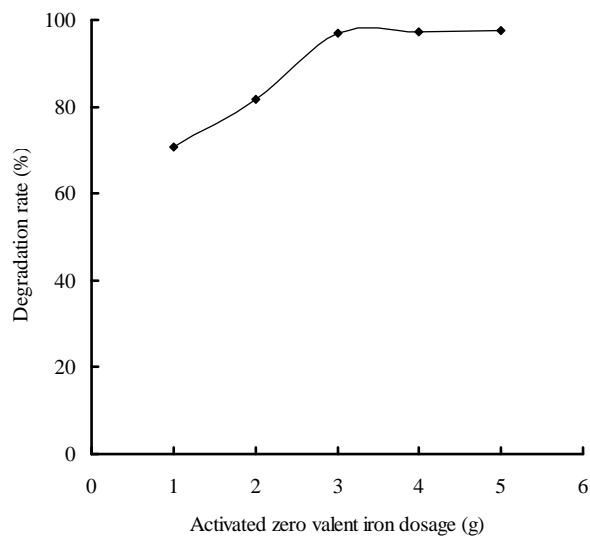


Fig. 4: The effect of activated zero valent iron dosage on the degradation rate.

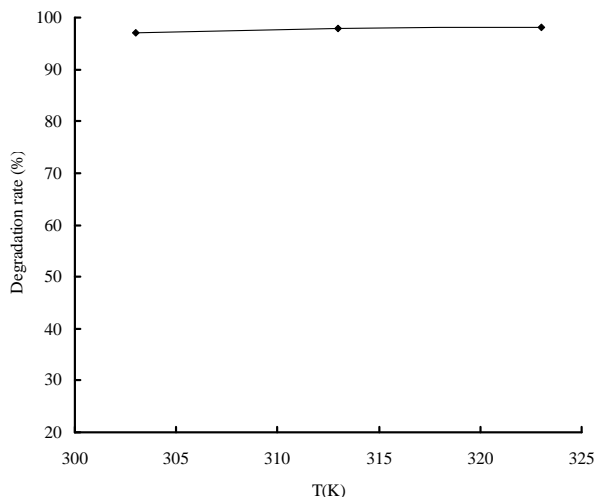


Fig. 6: The effect of reaction temperature on the degradation rate.

temperature ranged from 303 K to 323K. The effect of the reaction temperature is shown in Fig. 6.

From Fig. 6, the experimental results indicated that the degradation rate is affected by the temperature. The degradation rate of azo dye Acid Orange 7 increased with increase in temperature. It also indicated that the degradation process was an endothermic reaction. Mielczarski et al. (2005) have studied the decomposition of azo dye in water in the presence the zero valent iron at pH 4 and 5 over the temperature range from 20 to 50. They claimed that the acceleration of decolorization by raising temperature resulted from the different types of corrosion products on the

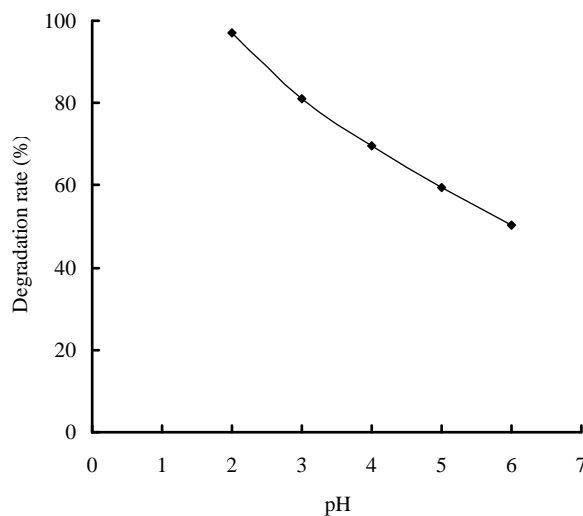


Fig. 5: The effect of pH in aqueous solution on the degradation rate.

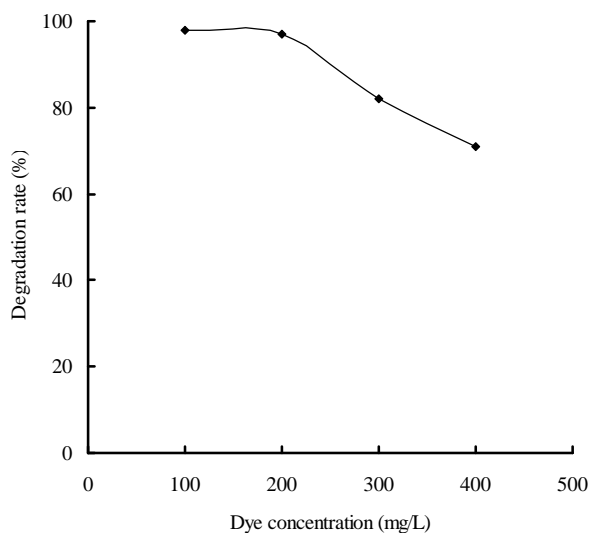


Fig. 7: The effect of dye concentration on the degradation rate.

surface of zero valent iron. Corrosion of zero valent iron could increase the surface area significantly. They reported that the decolorization reaction was controlled by the kinetics of surface process. Based on the above results, it is concluded that surface reactions, including sorption and chemical reaction, controlled the rate.

The effect of the initial concentration of azo dye: The effect of the initial concentration of azo dye Acid Orange 7 in aqueous solution on the degradation rate was evaluated at a concentration range from 100 mg/L to 400 mg/L. Batch experiments were conducted by mixing 100 mL of azo dye Acid Orange 7 in aqueous solution, reaction time of 10

min, pH 2.0 and 3 g of the activated zero valent iron particles in 250 mL Erlenmeyer flasks. The flasks were shaken at 150 rpm in a contact temperature of 303 K. The initial concentration of azo dye ranged from 100 mg/L to 400 mg/L.

Fig. 7 showed that the degradation rate of azo dye Acid Orange 7 was affected by the initial dye concentration. It can be seen that the degradation rate of azo dye Acid Orange 7 decreased with the increasing of the initial concentration of azo dye.

CONCLUSIONS

In this study, the synthetic zero valent iron was activated by potassium persulphate. The degradation of azo dye Acid Orange 7 by potassium persulphate activated using zero valent iron was carried out. The effect of several parameters, such as the pH in solution, the reaction time, reaction temperature, the activated zero valent iron amount and the initial concentration of dye on the removal process was investigated. The results showed that the degradation rate of azo dye Acid Orange 7 by the activated zero valent iron was high. The operation parameters had an important effect on the degradation of azo dye Acid Orange 7 in aqueous solution.

ACKNOWLEDGEMENTS

This study was financially supported by the project of Science and Technology Plan in Shaoxing City (2017B70058).

REFERENCES

- Chen, B., Wang, X.K., Wang, C., Jiang, W.Q. and Li, S.P. 2011. Degradation of azo dye direct sky blue 5B by sonication combined with zero-valent iron. *Ultrasonics Sonochem.*, 18: 1091-1096.
- Cundy, A.B., Hopkinson, L. and Whitby, R.L.D. 2008. Use of iron-based technologies in contaminated land and groundwater remediation: a review. *Sci. Total Environ.*, 400: 42-51.
- Deng, N., Luo, F., Wu, F., Xiao, M. and Wu, X. 2000. Discoloration of aqueous reactive dye solutions in the UV/Fe⁰ system. *Water Res.*, 34: 2408-2411.
- Devlin, J., Klausen, F. J. and Schwarzenbach, R.P. 1998. Kinetics of nitroaromatic reduction on granular iron in recirculating batch experiments. *Environ. Sci. Technol.*, 32: 1941-1947.
- Djurđja, V.K., Dragana, D.T., Gábor, K., Milena, R.B.T., Miljana, D.P., Srdjan, D.R., Ákos, K. and Božo, D.D. 2014. Three different clay-supported nanoscale zero-valent iron materials for industrial azo dye degradation: a comparative study. *J. Tai. Instit. Chem. Eng.*, 45: 2451-2461.
- Fu, F., Dionysiou, D.D. and Liu, H. 2014. The use of zero-valent iron for groundwater remediation and wastewater treatment: a review. *J. Hazard. Mater.*, 267: 194-205.
- Gavaskar, A.R. 1999. Design and construction techniques for permeable reactive barriers. *J. Hazard. Mater.*, 68: 41-71.
- Huang, C.P., Wang, H.W. and Chiu, P.C. 1998. Nitrate reduction by metallic iron. *Water Res.*, 32: 2257-2264.
- Kanel, S.R., Manning, B., Charlet, L. and Choi, H. 2005. Removal of arsenic(III) from groundwater by nanoscale zero-valent iron. *Environ. Sci. Technol.*, 39: 1291-1298.
- Linsebigler, A.L., Lu, G. and Yates, J.T. 1995. Photocatalysis on TiO₂ surfaces: principles, mechanisms, and selected results. *Chem. Rev.*, 95: 735-758.
- Mielczarski, J.A., Atenas, G.M. and Michczarski, E. 2005. Role of iron surface oxidation layers in decomposition of azo dye water pollutants in weak acidic solutions. *Appl. Catal. B: Environ.*, 56: 289-303.
- Papic, S., Koprivanac, N., Bozic, A.L. and Metes, A. 2004. Removal of some reactive dyes from synthetic wastewater by combined Al(III) coagulation/carbon adsorption process. *Dyes Pigments*, 62: 291-298.
- Shu, H.Y., Chang, M.C. and Chang, C.C. 2009. Integration of nanosized zero-valent iron particles addition with UV/H₂O₂ process for purification of azo dye acid black 24 solution. *J. Hazard. Mater.*, 167: 1178-1184.
- Sun, Y.P., Li, X.Q., Cao, J.S., Zhang, W.X. and Wang, H.P. 2006. Characterization of zero-valent iron nanoparticles. *Adv. Colloid Interf.*, 120: 47-56.
- Wang, J.M., Huang, C.P., Allen, H.E., Cha, D.K. and Kim, D.W. 1998. Adsorption characteristics of dye onto sludge particulates. *J. Colloid Interf. Sci.*, 208: 518-528.
- Wang, W., Cheng, Y., Kong, T. and Cheng, G. 2015. Iron nanoparticles decoration onto three-dimensional graphene for rapid and efficient degradation of azo dye. *J. Hazard. Mater.*, 299: 50-58.
- Xiong, Z., Zhao, D.Y. and Pan, G. 2007. Rapid and complete destruction of perchlorate in water and ion-exchange brine using stabilized zero-valent iron nanoparticles. *Water Res.*, 41: 3497-3505.



Prevalence of Skin and Respiratory Diseases in the Workers of Bird Markets

Syeda Amber Fatima[†] and Tayyaba Ishaq

Environmental Sciences Department, Kinnaird College for Women, Lahore, Pakistan

[†]Corresponding author: Syeda Amber Fatima

Nat. Env. & Poll. Tech.
Website: www.neptjournal.com

Received: 01-03-2018

Accepted: 04-06-2018

Key Words:

Bird market workers
Respiratory diseases
Skin diseases
Occupational diseases

ABSTRACT

Occupational health and safety is concerned with the safety, health and welfare of people engaged in work or employment. The majority of workers are facing occupational health problems in developing as well as in developed countries. Workers of bird markets are at higher risk of suffering from occupational skin and respiratory diseases. The present study was conducted to find out the prevalence of skin and respiratory diseases in the workers of bird markets. Study was based on survey, data collection through questionnaire and checklist, measurement of environmental parameters and also of lung function test of workers. Physical hazards, chemical hazards and ergonomic hazards were also observed. About 80% workers reported skin, and 77.7% reported respiratory diseases. Lung function test values (Mean FEV1% in summer: 57.9%, Mean FEV1/ FVC (%) in summer: 76.3%) (Mean FEV1% in winter: 53.2%, Mean FEV1/ FVC (%) in winter: 68.6%) were lower as compared to standard values. Majority of the workers were identified with restrictive defects which indicated prevalence of respiratory hazards in the bird markets. Workers health worsens during winter as they did not use the personal protective equipment. The present study may provide a baseline for further studies in this field.

INTRODUCTION

Occupational health and safety is concerned with the health, welfare and safety of people who are involved in work or employment. This involves protection of workers from diseases, injuries, illnesses and deaths. Proper working conditions and proper working environment should be provided to the workers so that the risk of diseases can be minimized. All work activities should be safe at the workplace which may include safe handling, storage and transportation of materials, and also provide adequate education, training and supervision in those activities (Baksh et al. 2015).

Work-related diseases have multiple causes, where factors in the work environment may play a role, together with other risk factors, in the development of such diseases (Elsby et al. 2008). For example, workers of bird markets are exposed to many airborne contaminants which are present in the bird markets. The dust in the air is comprised of many components which include skin debris, broken feathers, insect parts, aerosolised feed and faeces. Different types of bacteria and their endotoxins are also found in the organic dust. Rylander introduced the different types of respiratory diseases which are caused by this type of organic dust, i.e. toxic pneumonitis, irritation of mucous membrane, bronchitis, granulomatous pneumonitis, rhinitis and asthma (Hnizdo & Vallyathan 2003).

The skin is exposed to organic dust and other many pathogens in the bird markets which may cause different types of irritation and also may cause severe skin diseases.

These skin diseases include skin allergies, acne, contact dermatitis, eczema, wart and onychomycosis (Slominski et al. 2008).

Poultry dust is a mixture of bird feed, bedding material e.g. wood shavings/shreds or straw, bird droppings, feathers and dander (dead skin), dust mites and storage mites, and microorganisms such as bacteria, fungi (moulds) and endotoxins (cell wall components of bacteria). This dust causes skin problems among workers of bird markets. External agents tend mostly to come into contact with the hands and forearms, so around 95% of work-related skin diseases occur in this area. The majority of the remainder are on the face. Most work-related skin diseases are contact dermatitis. External agents are involved in an important minority of other work-related skin diseases (Gibbs 1996).

It has previously been shown that workers on poultry farms and bird markets are exposed to high levels of organic airborne dust contaminated with endotoxins, experienced symptoms of airway irritation and also a slight diurnal decrease of FEV 1. Exposure to poultry dust also occurs at poultry slaughter-houses (Hagmar et al. 1990).

Pet birds can also cause many respiratory diseases due to the biological contaminants present in their droppings. So the diseases are transferred from birds to human and then also from human to human (Hagmar et al. 1990). A virus which causes avian influenza found in the droppings of birds, which is a severe respiratory disease. Avian influenza virus affects the health of birds and humans by cough, fever,

upper respiratory tract infection and symptoms of gastro intestine, which may lead to death (Krauss et al. 2003). Influenza A viruses that reside naturally in wild bird species comprise all known subtypes and provide viral genes from which influenza viruses that infect both domestic poultry and mammalian species, including humans, arise (Harris 1991).

Histoplasma capsulatum is a fungus which causes histoplasmosis. *Histoplasma capsulatum* inhabits the digestive tract of birds, pollutes the soil through bird droppings, and mainly affect human lungs (Swayne & King 2003). Human infection most often results in conjunctivitis. Chills, fever, and lethargy are exceptionally rare (Deepe et al. 2005).

Another important respiratory disease which is caused by the organic poultry dust or poultry products is Salmonellosis. This disease caused by non-typhoidal bacteria known as *Salmonella* which is found in the bird markets (Capua 2004). A parasite which is known as *Giardia* is also found in the droppings of birds and causes the Giardiasis which is a protozoal infection of intestine. This infection can cause diarrhoea, abdominal pain, bloating, belching, nausea, and vomiting in humans. Cryptococcosis pulmonary disease is another disease caused by birds to humans, which is a severe respiratory disease. *C. neoformans* fungus which is found in dropping of pigeons triggered this respiratory disease (Hohmann 2005).

STUDY AREA

Three bird markets of Lahore city were selected for the study, these are Tollinton bird market, Dharampura bird market and Sammanabad bird market.

MATERIALS AND METHODS

Data collection: The present study was conducted for the assessment of prevalence of skin and respiratory diseases among the workers of bird market. It is based on risk factor identification, evaluation of general health profile and assessment of skin and respiratory diseases in workers of bird market. Questionnaires, checklist and spirometer were used for the collection of primary data. The study was conducted in the bird markets located in Lahore in the month of August and November 2016. The workers who are directly or indirectly exposed to multiple hazards on a daily basis were selected as a target group.

Survey: Questionnaires were filled from 45 workers of bird market and 5 workers of control group. Face to face interviews were held and questionnaires were administered. For the convenience of the workers, questions were asked in Urdu and Punjabi.

Measurement of lung function: Spirometry tests were performed to assess lung function and respiratory health of poultry farm workers. Spirometry test involved measurement of volume and flow of pulmonary inhalation and exhalation. The results of spirometry tests show normal, obstructive patterns, restrictive patterns and a combination of both obstructive and restrictive patterns. The normal spirometry readings result vary with weight, height and age.

All the tests were performed on standing worker as per standard procedure (Spirometry User Manual Version 2014). Nose clips were used by workers during the test. The workers were given some instructions to ensure the accuracy of the test results. Some of the instructions include taking a deep breath prior to the test; mouthpiece of spirometer should be closed properly by putting in mouth to obtain the correct values.

The lung function test was measured with the help of Geratherm Blue Cherry USB spirometer which is highly intuitive Windows-based software. This software was installed in the laptop through a CD. It is easy to handle and low in power consumption. It contains USB like structure which is known as Spirostick which is connected to a laptop or computer. SVC (slow vital capacity) test and the FVC (forced vital capacity test) test were conducted with the help of a spirometer which was displayed on the laptop screen. In FVC (forced vital capacity test), it displayed further values of forced expired volume in one second (FEV1%) and the ratio of forced expired volume in one second (FEV1%) to the forced vital capacity (FEV1/FVC%).

Measurement of temperature and humidity level: For the determination of the effects of temperature and humidity change on skin diseases and lung functions of workers, ambient air temperature and humidity were also measured in the bird market. Worker's health is directly affected due to changes in temperature and humidity. Indoor temperature and humidity were measured by digital temperature/humidity/clock that give accurate reading.

RESULTS

Results of checklist: A wide range of hazards was examined in the bird markets which include physical, chemical and ergonomic hazards. Poor waste management was also a big issue that was present in the workplace. Waste related to birds include droppings of birds, feathers, dander, slaughter waste, etc. So that is why poor waste management leads to growth of flies and insects on the waste and ultimately causing many diseases in the workers. In the backyard, heaps of waste were found, which causes bad smell.

High noise level was also observed in some areas of bird market, which is a physical hazard. Slippery floors,

Table 1: Lung function measurement of the workers of bird market and control group in summers (August) and winters (November).

Name	Age	BMI	Smoker	FEV ₁ FVC (%)	August FEV ₁ / Pattern	Lung Function	FEV ₁ FVC (%)	November FEV ₁ / Pattern	Lung Function
Worker 1	45	25.7	No	77	89	Restrictive	74	81	Restrictive
Worker 2	13	21.8	No	81	88	Normal	79	80	Restrictive
Worker 3	13	24.5	No	84	112	Normal	71	68	Obstructive
Worker 4	19	23.0	No	75	84	Restrictive	74	81	Restrictive
Worker 5	17	17.4	No	77	81	Restrictive	73	81	Restrictive
Worker 6	23	23.5	No	38	73	Restrictive	28	63	Obstructive
Worker 7	21	23.2	No	81	111	Normal	79	92	Restrictive
Worker 8	54	22.3	Yes	42	77	Restrictive	38	71	Restrictive
Worker 9	51	19.6	Yes	56	73	Restrictive	54	68	Restrictive
Worker 10	54	21.7	Yes	36	59	Obstructive	34	55	Obstructive
Worker 11	16	19.6	No	99	112	Normal	81	81	Normal
Worker 12	33	28.4	No	37	58	Obstructive	36	53	Obstructive
Worker 13	35	23.8	Yes	44	74	Restrictive	42	71	Restrictive
Worker 14	55	23.7	No	56	75	Restrictive	55	73	Restrictive
Worker 15	23	21.7	Yes	26	38	Obstructive	24	37	Obstructive
Worker 16	19	21.8	No	67	109	Restrictive	28	69	Obstructive
Worker 17	23	22.3	No	51	69	Obstructive	33	70	Restrictive
Worker 18	26	23.3	No	52	59	Obstructive	27	53	Obstructive
Worker 19	33	24.4	No	34	58	Obstructive	31	54	Obstructive
Worker 20	26	26.6	No	36	57	Obstructive	33	54	Obstructive
Worker 21	31	20.8	Yes	27	39	Obstructive	28	37	Obstructive
Worker 22	31	23.2	Yes	19	33	Obstructive	17	34	Obstructive
Worker 23	37	22.5	No	74	78	Restrictive	65	74	Restrictive
Worker 24	39	21.6	No	34	55	Obstructive	32	52	Obstructive
Worker 25	31	22.7	No	64	78	Restrictive	61	71	Restrictive
Worker 26	19	21.3	No	81	112	Normal	81	92	Normal
Worker 27	54	22.6	Yes	36	54	Obstructive	35	52	Obstructive
Worker 28	41	21.5	No	52	67	Obstructive	50	61	Obstructive
Worker 29	35	22.4	No	65	77	Restrictive	63	72	Restrictive
Worker 30	37	23.5	No	58	70	Restrictive	50	65	Obstructive
Worker 31	13	20.3	No	86	119	Normal	84	109	Normal
Worker 32	31	24.2	No	44	78	Restrictive	39	67	Obstructive
Worker 33	45	25.6	No	74	86	Restrictive	70	81	Restrictive
Worker 34	28	23.7	No	52	66	Obstructive	53	61	Obstructive
Worker 35	28	22.6	No	64	78	Restrictive	60	74	Restrictive
Worker 36	21	23.2	No	84	110	Normal	81	93	Normal
Worker 37	26	22.5	No	54	73	Restrictive	52	67	Obstructive
Worker 38	54	21.8	Yes	35	59	Obstructive	33	57	Obstructive
Worker 39	35	22.5	No	60	76	Restrictive	61	74	Restrictive
Worker 40	19	20.4	No	84	87	Normal	80	87	Normal
Worker 41	13	24.3	No	76	81	Normal	71	67	Normal
Worker 42	42	23.5	No	54	68	Obstructive	52	66	Obstructive
Worker 43	26	26.5	No	61	78	Restrictive	61	72	Restrictive
Worker 44	12	22.6	No	90	99	Normal	87	96	Normal
Worker 45	31	24.3	No	38	57	Obstructive	34	54	Obstructive
Control Group	27	18.4	No	82	111	Normal	81	101	Normal
Control Group	34	22.3	No	80	86	Normal	78	85	Normal
Control Group	34	21.6	No	83	84	Normal	81	82	Normal
Control Group	32	24.5	No	85	99	Normal	81	99	Normal
Control Group	39	28.6	No	92	114	Normal	90	110	Normal
Standard Value				80	70.0		80	70.0	

FEV₁: Forced expiratory volume (1st second)FEV₁/FVC: Ratio of forced expiratory volume (1st second) and forced vital capacity

Table 2: Lung function measurements (mean) of workers of bird market and control group in summers and winters.

	Season 1 (August)		Season 2 (November)	
	Mean of FEV1%	Mean of FEV1/FVC (%)	Mean of FEV1%	Mean of FEV1/FVC (%)
Target Group	57.9<80	76.3>70	53.2<80	68.6<70
Control Group	84.4>80	98.8>70	82.2>80	95.4>70

Table 3: Lung function patterns in the workers of bird market.

Frequency of workers	August	Lung function pattern	Frequency of workers	November
				Lung function pattern
19		Restrictive defect	16	Restrictive defect
16		Obstructive defect	22	Obstructive defect
10		Normal variant	7	Normal variant

poor hygiene and other safety problems were also found in the workplace. Some of the shops in market use the chemicals as cleaning detergents, therefore, chemical hazards were less. Other workers washed their shops with water only, and they did not use any chemicals. Majority of workers were not using the personal protective equipment, as they were not aware about the use of PPE's.

Results of questionnaire: Workers of bird market also filled the questionnaires which comprised of demographics, general health status of workers, assessment of skin and respiratory diseases and also information regarding personal protective equipment and safety measures (Table 1).

Demographic data of workers of birds market: The results of demographic data showed that the 60% of workers were in the age between 20-40 years, while 22.3% were below 20 and 17.7% were above 40. Next question in this section was about their marital status. Most of the workers (60%) were married while 40% were unmarried. According

Table 4: Correlations of different variables.

Sr. No.	Correlations	Pearson's Coefficient	Significance (<i>p</i> value)
1.	Correlation between working hours and respiratory problems.	0.51	0.04
2.	Correlation between work experience and respiratory problem	0.77	0.02
3.	Correlation between use of personal protective equipment and respiratory problems.	0.62	0.03
4.	Correlation between smoking and respiratory problems.	0.87	0.01
5.	Correlation between use of personal protective equipment and skin problems.	0.61	0.02

to the education level, 35.6% respondents were illiterate. Only 6.7% respondents have done intermediate, while 20% workers have done 10th class..

As we know that daily working hours and work experience play a crucial part in the incidence and severity of disease, so these questions were also asked from the workers of bird market which showed that majority of the workers (40%) working in bird market were from 5-10 years. While 6.6% respondents had the working experience of above 20 years, 28.8% had the experience of 11-20 years and 24.4% workers were working here for less than five years.

Results of monthly income showed that the monthly income of 11.1% workers was below Rs. 10,000, 13.3% workers were having income between 10,000-20,000, 62.2% workers earned rupees 21,000-40,000 and the income of 17.7% workers was above Rs 40,000. The results of working hours revealed that majority of workers (51.1%) spent more than 8 hours in the bird market. 33.3% of workers worked more than 8 hours, while only 13.3% workers spent less than 8 hours in their working area.

General health status: Body mass index (BMI) of workers of the bird market was also calculated. Results revealed that the BMI of most of the workers (75.6%) was between 18-24 kg/m². 4.4% and 24.4% were having the BMI below 18 kg/m² and above 24 kg/m² respectively. Smoking habit of workers of bird market was also asked. The results found that 84.4% workers were nonsmoker while 15.6% workers were smoker. Question related to experience of vaccination was also asked from the workers which showed that only 8.8% respondents had the experience of vaccination, while others (91.2%) had not.

Skin disease assessment: Question related to skin diseases were also asked. Results revealed that 80% respondents said that they have skin diseases and 20% respondents said that

they do not have any skin disease symptoms. Out of 80% workers having skin diseases, 39% were having eye irritation, 66.6% were having skin allergy, 68.8% had acne, only 20% were having symptoms of wart and 15.6% respondents were having the symptoms of eczema.

Among 80% of workers, only 6.6% workers knew the reason of skin problem, while others (73.4%) did not know the reason. Only 17.7% workers used medicine for their skin problems. Among 80% workers, 22.2% workers said that their job is responsible for skin problems, while 57.8% said no. Family history regarding skin diseases was also asked. Results revealed that only 4.4% worker's families were also suffering from skin diseases. Majority of workers (74.6%) said that they face the skin problems in summers more as compared to winters.

Respiratory disease assessment: Respiratory diseases are also very common in the workers of bird market. So the questionnaire also contained the question regarding respiratory diseases which were asked from the workers. 77.7% workers said that they have respiratory diseases while 22.2% workers said they did not have respiratory disease. Among 77.7% workers having respiratory diseases, the percentage of workers facing the problem of breathing, cough, chest tightness, asthma, wheezing and nasal problem was 73.4%, 71.1%, 51.1%, 33.3%, 51.1% and 28.9% respectively.

Results about the family history of workers regarding respiratory diseases showed that only 6.6% worker's families were suffering from respiratory diseases. 71.1% workers said that they feel more respiratory problems when they work in their workplace, and when they move away or go home, they feel better. 11.1% respondent said that the reason behind their respiratory diseases is seasonal changes while others (66.6%) said it is due to dust allergy that is present in the bird market. Majority of respondents (53.3%) said that these respiratory diseases become more severe in winters, 17.7% workers said that respiratory problems become more severe in summer, while others (6.6%) said that they face these problems all over the year.

Safety measures: Safety measures play an important role in the incidence and severity of work-related diseases. Question regarding safety measures were asked from the workers of bird market. Results revealed that most of the workers (80%) were not using the personal protective equipment; only 20% respondent said that they used the personal protective equipment. Results also showed that all the workers among the 45 workers of birds market, washed their hands after completing their work. For good health, regular bath is very important for workers. Questions regarding regular bath were also asked which showed that only 37.8% workers

took bath regularly. Cleanliness of workplace is also very important as the disease incidence can increase if the workplace is not cleaned. So the results showed that 48.9% workers of bird markets said that they cleaned their working area while 51.1% respondents said no.

Temperature and humidity: Temperature and humidity were also measured during survey in both the seasons for the determination of effect of different seasons on lung functions of bird market workers. First of all, monitoring was done in August and later in November. In the month of August, average temperature was 32°C while in the month of November it was 27°C. Average humidity in August was 89% while in November it was 77%.

Results of spirometer: The results of spirometer were also obtained through Blue Cherry USB spirometer, which displayed the forced expired volume in one second (FEV1%), and the ratio of forced expired volume in one second (FEV1%) and forced vital capacity (FEV1/FVC %). It was found that the percentages of FEV1 and FEV1/FVC were lower in the workers of bird markets as compared to control group and standard values. According to mean of the pulmonary function test data obtained from spirometer, respiratory function of workers of bird market (FEV1%: 57.9%, FEV1/FVC (%): 76.3%) was not in acceptable limit as compared to the control group (FEV1%: 84.4%, FEV1/FVC (%): 82.2%). According to average pulmonary function test data of two seasons (summers and winters), the respiratory function of the workers of birds market in summers (FEV1%: 53.2%, FEV1/FVC (%): 76.3%) was better than in winters (FEV1%: 57.9%, FEV1/FVC (%): 68.6%) (Table 2 & 3 and Figs. 1-3). One of the studies was carried out in Egypt to assess the effect of exposure to organic dust on respiratory symptoms and lung function of exposed workers. It showed that respiratory symptoms such as cough, expectoration, wheezing, and shortness of breath were significantly higher among exposed workers as compared to unexposed. Moreover, the results of spirometer showed that FEV1%, FVC% and FEV1/FVC% parameters were also declined in the exposed workers (Siddique et al. 2012).

Correlations: Bivariate Pearson's correlation was run to check the correlation between different variables.

So the results revealed that *p* values of correlations between working hours and respiratory problems, work experience and respiratory problems, use of personal protective equipment and respiratory problems, smoking habit of workers and respiratory problems and use of PPE and skin problems are 0.04, 0.02, 0.03, 0.01 and 0.02 respectively (Table 4).

According to the results, workers were facing more respiratory problems in winters as compared to summers as the

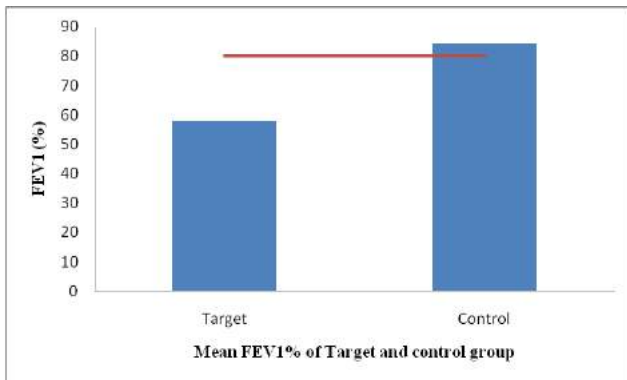


Fig. 1: Comparison between workers (target group) and control group about the mean of FEV1% in summers.

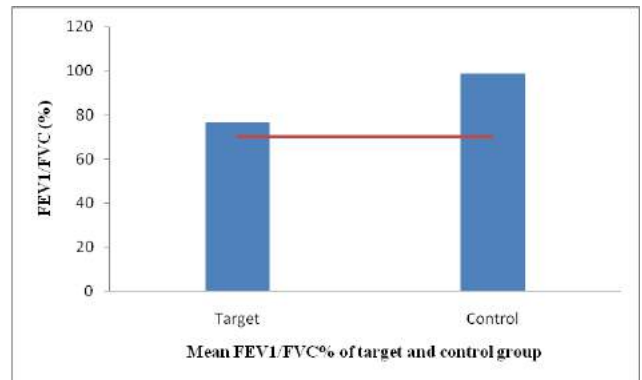


Fig. 2: Comparison between workers (target group) and control group about the mean of FEV1/FVC% in summers.

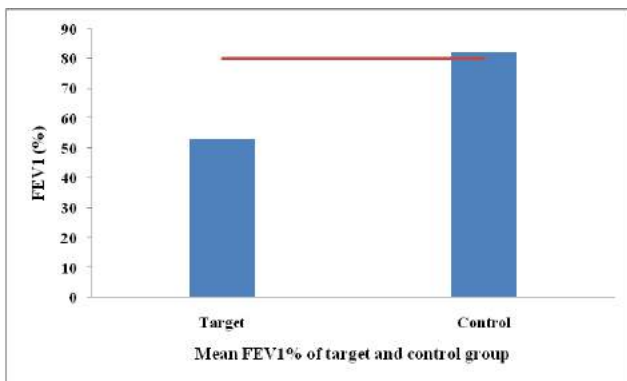


Fig. 3: Comparison between workers (target group) and control group about the mean of FEV1% in winters.

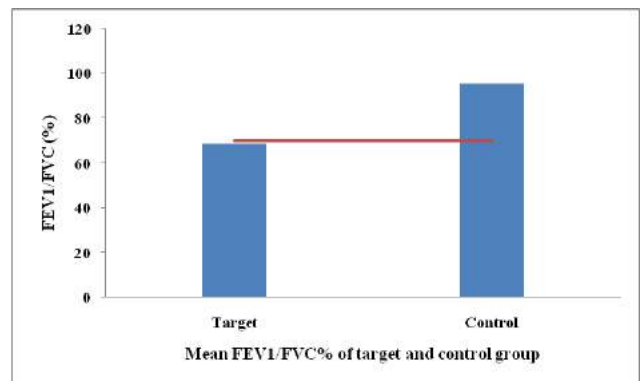


Fig. 4: Comparison between workers (target group) and control group about the mean of FEV1/FVC% in winter.

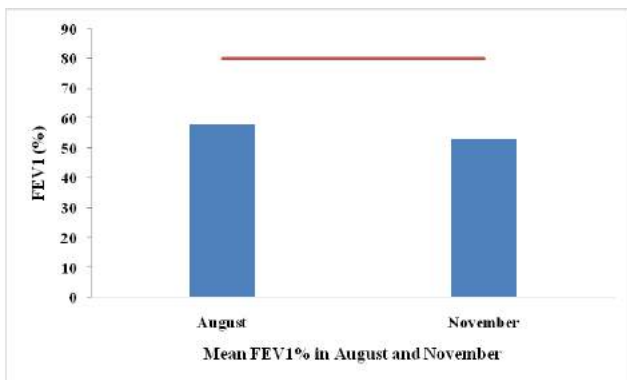


Fig. 5: Comparison of mean FEV1% in August and November.

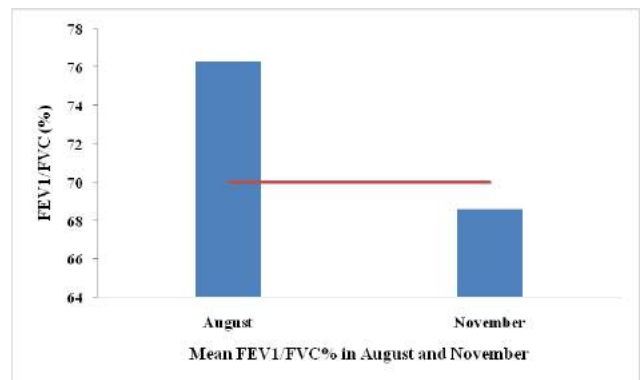


Fig. 6: Comparison of mean FEV1/FVC% in August and November.

FEV1% and FEV1/FVC% values were lower in the workers in winter as compared to summers. According to average pulmonary function test data of the two seasons (summers and winters), the respiratory function of the workers of bird market in summers (FEV1%: 57.9%, FEV1/ FVC (%): 76.3%) was better than in winters (FEV1%: 53.2%, FEV1/ FVC (%):

68.6 %) (Figs. 4-6). These results are supported by a study which confirmed that there were more moderate negative effects on lung function and the immune system during winter than during summers in bird market workers. In winter, concentrations for inhalable endotoxin for all animal types were usually higher than in spring or summer.

REFERENCES

- Baksh, K., Ganpat, W. and Narine, L. 2015. Farmer's knowledge, attitudes and perceptions of occupational health and safety hazards in Trinidad, West Indies and implications for the agriculture sector. *Journal of Agricultural Extension and Rural Development*, 7(7): 221-228.
- Capua, I. and Alexander, D.J. 2004. Avian influenza: recent developments. *Avian Pathology*, 33(4): 393-404.
- Deepe, G.S., Wüthrich, M. and Klein, B. S. 2005 Progress in vaccination for histoplasmosis and blastomycosis: Coping with cellular immunity. *Medical Mycology*, 43(5): 381-9.
- Elsby, M., Hobijn, B. and Sahin, A. 2008. Unemployment dynamics in the OECD. National Bureau of Economic Research.
- Gibbs, S.A. 1996. Skin disease and socioeconomic conditions in rural Africa: Tanzania. *International Journal of Dermatology*, 35(9): 633-639.
- Hagmar, L., Schütz, A., Hallberg, T. and Sjöholm, A. 1990. Health effects of exposure to endotoxins and organic dust in poultry slaughter-house workers. *International Archives of Occupational and Environmental Health*, 62(2): 159-164.
- Harris, D.R., Lemeshow, S., Lwanga, S.K., Chin, J. and Duchesneau, R. 1991. Evaluation of a standardized survey design proposed for use in epidemiological research on skin diseases. *International Journal of Epidemiology*, 20(4): 1048-1056.
- Hnizdo, E. and Vallyathan, V. 2003. Chronic obstructive pulmonary disease due to occupational exposure to silica dust: A review of epidemiological and pathological evidence. *Occupational and Environmental Medicine*, 60(4): 237-243.
- Hohmann, A.G., Suplita, R.L., Bolton, N.M., Neely, M.H., Fegley, D., Mangieri, R., Krey, J.F., Walker, J.M., Holmes, P.V., Crystal, J.D. and Duranti, A. 2005 An endocannabinoid mechanism for stress-induced analgesia. *Nature*, 435(7045): 1108-1112.
- Krauss, H., Schieffer, H.G. and Slenczka, W.Z. 2003. Zoonoses: Infectious Diseases Transmissible from Animals to Humans. American Society for Microbiology.
- Siddique, A.B., Rahman, S.U., Hussain, I. and Muhammad, G. 2012. Frequency distribution of opportunistic avian pathogens in respiratory distress cases of poultry. *Pak. Vet. J.*, 32(3): 386-389.
- Slominski, A., Wortsman, J., Paus, R., Elias, P.M., Tobin, D.J. and Feingold, K.R. 2008. Skin as an endocrine organ: Implications for its function. *Drug Discovery Today: Disease Mechanisms*, 5(2): e137-144.
- Spirometry User Manual 2014. Version 1.2.2. 1st ed., Geratherm Respiratory.
- Swayne, D.E. and King, D.J. 2003 Avian influenza and Newcastle disease. *Journal of the American Veterinary Medical Association*, 222(11): 1534-1540.



Influence of Environmental Pollution on Residents' Health: Evidence from Hubei, China

Lulu Hao and Jing Gao†

Research Center of Cultural and Tourism Industries, Wuhan Business University, Wuhan, 430056 China

†Corresponding author: Jing Gao

Nat. Env. & Poll. Tech.
Website: www.neptjournal.com

Received: 16-01-2019

Accepted: 18-02-2019

Key Words:

Environmental pollution

Public health

Health influencing factors

ABSTRACT

To maintain the rapid development of China's economy and simultaneously maximize the existing natural resources, China discharges a large amount of waste from its life and production activities into the environment. Environmental pollution is also becoming increasingly serious. The continuous reduction and deterioration of environmental quality has substantially affected the balance of the ecosystem and caused increasingly serious harm to public health. This study organized the research status quo and research hotspots on residents' health loss caused by environmental pollution to further analyse the influence of environmental pollution on residents' health. The quantitative relationship between environmental pollution and public health level was calculated using the expanded Grossman health production function and the data of 13 prefecture-level cities in Hubei, China from 2005 to 2017. Results show that residents' health is closely related to environmental pollution and a few macroeconomic factors. The population mortality rate has a significant positive correlation with the three influencing factors of industrial sulphur dioxide emissions, industrial smoke dust emissions, and GDP per capita. A significant negative correlation exists between the death rate of the population and number of years of education per capita and the investment in environmental protection. The number of doctors per 10,000 population and urbanization rate have no evident impact on the mortality rate of the population. The conclusions have certain reference value for analysing the severity of public health value loss and reducing public health value loss caused by environmental pollution.

INTRODUCTION

Given the rapid development of China's economy, the ecological environment has been seriously damaged, while public health has been increasingly harmed by environmental pollution. The environmental pollution problem has posed a threat to people's basic life and survival. Accordingly, the public health risk caused by environmental pollution has become a worldwide topic. In particular, the health risks caused by environmental pollution are considerably severe in a few countries and regions where public services are relatively insufficient. Environmental pollution is depleting environmental resources, on which China's economic and social development depends. The sustainable development of the social economy has been facing unprecedented pressure, while environmental pollution has posed a growing threat to public health. While seeking economic development, exploiting and utilizing the existing natural resources, and creating a new living environment, humans also discharge a large amount of wastes generated from living and production activities, thereby leading to environmental pollution. The rapid economic growth has resulted in an increase in wastes produced and discharged, thereby wors-

ening environmental pollution.

The economy of Hubei Province in China remains in the industrialization development stage. Fig. 1 shows that the secondary industry accounts for a large proportion of the economy. Under such an industrialization development mode of "high pollution, high energy consumption, and low output," the environmental quality in Hubei shows a deteriorating trend, while the public health level of the province is also seriously affected. Given the continuous improvement of public living standards, the spread of environmental protection and health knowledge, popularization of mass education, and frequent exposure to environmental pollution incidents have led the public to consciously focus on the environmental problems. The awareness on environmental protection was also strengthened. Under such circumstances, actively exploring and understanding the current situation of environmental pollution and how it causes the loss of public health value have immense theoretical and practical significance. In particular, such endeavour will enable stakeholders to solve the current problems faced by Hubei, recommend policies and measures to protect the environment, and improve environmental quality.



Fig. 1. Proportion of the three industries in Hubei from 2005 to 2017.

EARLIER STUDIES

The research on the impact of environmental pollution on residents' public health has long been the concern of scholars. Numerous studies have analysed the impact of air pollution on public health. Foreign scholars have studied environmental pollution and public health earlier than Chinese scholars. The environmental impact on health mainly depends on the concentration of pollutants, exposure response coefficient, and the number of exposed urban population. Analytical methods based on exposure response and dose effect principle mainly focuses on the research of environmental pollution on residents' health loss. Grossman (1972) first proposed that health should be regarded as a type of consumer good that can bring utility and income. The classic health production function was eventually obtained by introducing health into the utility function and maximizing the utility of an individual's entire life. This function shows that personal lifestyle, heredity, health care, and age are among the main factors that affect the formation of health. Pope et al. (2002) studied the causes of death of 500,000 residents in the US and determined that, in addition to controlling risk factors, such as smoking and diet, fine particulate matter, sulphur dioxide, and other related pollutants are related to the total mortality involving pulmonary heart disease and lung cancer. Wang et al. (2006) proved how the use of advanced coal gasification technology can provide substantial public health benefits in Eastern China. However, if such a control technology remains lacking, the impact of air pollution on public health will substantially increase in 2020. Mestl et al. (2006) proposed that indoor air pollution caused by the use of solid fuels has a serious impact on health and suggested that the impact of such pollution on residents' health should be avoided by switching to clean fuels. Wang (2010) analysed the impact of economic growth, population, and technological progress on energy consumption and the environment in China and predicted that the emission of PM10 and sulphur dioxide and their detrimental effects on health will increase substantially in the next 12 years. Gohlke et al. (2011) used time series data sets from 1965 to 2005 from 41 countries with

different development paths to analyse the relationship among electricity consumption, coal consumption, and mortality. The results proved that an increase in coal consumption leads to a considerable increase in mortality. Matus et al. (2012) performed policy prediction model analysis to show that China's health economic losses caused by air pollution emissions have brought substantial burden to the country's economy, with the loss of residents' welfare caused by air pollution reaching 112 billion dollars in 2005. Kan et al. (2012) explained that the decline in air quality causes and aggravates acute deaths related to various health hazards, including respiratory diseases, cardiovascular diseases, lung cancer, and even sensitive populations, thereby posing as an immense threat to public health. Chen et al. (2013) used the model of synergistic effect of atmospheric resources and studied that the change of atmospheric pollutant concentration in Taiwan has an impact on the potential loss of life. Sram et al. (2013) tracked the health status of 1,492 children in the Czech Republic and showed that air pollution seriously affects children's health and easily leads to an increase in the incidence rate of respiratory diseases among children. Voorhees et al. (2014) analysed the loss of public health caused by PM2.5 in Shanghai and showed that if the air quality in Shanghai meets the national level two standard, then the monetary value for avoiding all deaths is 1.7 to 12 billion RMB. Jiang et al. (2016) analysed the correlation mechanism between traffic-related air pollution and cardiac metabolic risks. Accordingly, long-term exposure to traffic-related air pollution may lead to the development or aggravation of cardiac metabolic disorders. Costa et al. (2017) substantiated that particular matter, nitrogen dioxide, and carbon monoxide have an impact on the increase in mortality by using the mortality rate of elderly residents in Sao Paulo, Brazil from 2000 to 2011. Yang (2017) analysed the relationship between residents' exposure to air pollution and health status and showed that air pollution had a certain correlation with health damage. Chen et al. (2018) conducted a survey among 8,497 Taipei residents over 65 years old in Taipei and confirmed that chronic exposure to traffic-related air pollution will increase the risk of chronic kidney disease. Shen et al. (2018) held that the migration of migrant workers has led to the size and spatial pattern of pollutant emissions. This research showed that large-scale interprovincial migration will lead to an increase of PM2.5 level. This result suggests that policies should be formulated to guide the migration direction reasonably to prevent the deterioration of environmental air quality in large cities. The existing literature has shown the extensive research results on the impact of environmental pollution on health, thereby enabling the public to acquire a profound understanding of the harm of environmental

pollution. However, additional practical and feasible measures are necessary, apart from formulating measures against environmental pollution, to help people improve their health. The current study uses panel data of 13 prefecture-level cities subordinate to Hubei from 2005 to 2017. On the basis of Grossman's health demand function, this study constructs a macro health production function and analyses the factors that influence the health of residents in China, including environmental pollution, public services, GDP per capita, and other related factors. To improve the residents' health level, all regions of Hubei should adopt different education, health care, environmental protection, and other related public policies on the basis of the adverse effects of environmental pollution on residents' health and the effects of different types of public services on improving their health.

MATERIALS AND METHODS

Modelling

This study draws on Grossman's theory of health production function, which holds that health is a commodity produced by a series of investments, including lifestyle, living environment, education, personal income, and medical and health services. The environmental pollution variable is added to the model, which is eventually built as follows:

$$H_{it} = \beta_1 E_{it} + x_{it} \beta_i + \mu_i + \varepsilon_{it} \quad \dots(1)$$

Where, H_{it} represents the residents' health level of city i in t year, E_{it} represents the environmental pollution situation of city i in t year, x_{it} represents the other control variables, μ_i represents the regional effects related to regional development and mainly reflects the influence of a few unobservable regional variables, ε_{it} represents random disturbance terms varying with time, and β_1 represents the parameters to be estimated and reflects the impact degree of environmental pollution on residents' health level. In this case, ε_{it} is assumed to be independent and identically distributed and unrelated to μ_i . In the estimation methods commonly used for panel data, scholars often assume that the slope of individual regression equation is the same, but the intercept terms are different, thereby determining individual heterogeneity. When μ_i is related to an explanatory variable, the fixed effect model can be selected for estimation to eliminate the estimation deviation caused by the unobservable fixed effect. However, the random effect model should be used for estimation once μ_i is not correlated with all the explanatory variables. The two estimation methods will be selected using the Hausman test.

Variable Selection

- (1) **Dependent variable:** Given that the health is a multi-dimensional and complex concept, a unified index is currently lacking to measure this concept. Hence, health can only be measured by a few approximate indicators, such as life expectancy and mortality per capita. Therefore, the current study chooses population mortality (death) as a measure of health.
- (2) **Independent variable:** To measure environmental pollution, the majority of scholars believe that solid particles, such as PM2.5 and PM10, are the main pollution sources that affect environmental quality and harm human health. However, such data are not easily available. This study refers to the industrial sulphur dioxide emissions (ECO1) and industrial soot emissions (ECO2) from different cities selected in previous studies to characterize the environmental quality of a certain region. These two indicators of environmental quality are also verified and approved by many scholars.
- (3) **Control variable:** Many reasons are cited for the considerable uncertainty in the relationship among various social and economic factors that affect health and various public policies. Therefore, this study also introduces other control variables. Per capita years of education (X_1), which is a comprehensive index that can reflect the education level of citizens in the region, is used as an index to measure the public service of education. The number of doctors per 10,000 populations (X_2) is used as an indicator to measure the provision of health care in the region. Environmental protection investment (X_3) mainly covers investment in urban environmental infrastructure construction, investment in industrial pollution source control, and environmental protection investment in environmental protection acceptance projects completed that year. Per capita GDP (X_4), it reflects the impact of per capita economic level on health, shows completely different situations in different periods when the per capita GDP increases. Urbanization rate's (X_5) impact on residents' health is uncertain.
- (4) **Data source:** The data used in this study are from the Statistical Yearbook of Hubei and China Environmental Statistics Yearbook from 2005 to 2017 and involved 13 prefecture-level cities in Hubei (i.e., 12 prefecture-level cities and 1 autonomous prefecture). To eliminate the sequence correlation, transform the possible non-linear relationship into linear relationship, and reduce the abnormal value, non-normal distribution, and heteroscedasticity of variables, this study uses logarithm processing on the industrial sulphur dioxide emissions (EOC1), industrial smoke emissions

(EOC2), per capita education years (X_1), number of doctors per 10,000 population (X_2), investment in environmental protection (X_3), per capita GDP (X_4), and urbanization rate (X_5).

RESULT ANALYSIS

This study selects “cross-section weight” as the weight item to allow heteroscedasticity in the different sections when performing regression analysis on the panel data model. In the estimation method, the panel corrected standard errors method is used to effectively deal with complex panel error structures. From the perspective of the overall effect of regression, the P value of the F value of the regression results at the national and regional levels is 0.001; thereby indicating that the model passed the F test and the overall regression effect is good. Table 1 shows the specific regression results.

Table 1 shows the following results:

- (1) The Hausman test results show that the corresponding *p*-value is 0.001, thereby indicating that the fixed effect model is suitable for analysis.
- (2) From the explanatory variables, industrial sulphur dioxide emissions (ECO1) have a significant positive correlation with population mortality. This result indicates that an increase in environmental pollution will significantly reduce the health level of the residents. The emission of industrial smoke dust (ECO2) is significantly positively correlated with the mortality rate of the population. This result indicates that the emission of industrial smoke dust is evidently unfavourable to the health status of residents. Thus, this effect is significant. Given that Hubei mainly relies on industrial manufacturing, substantial industrial pollution will inevitably occur while the economy grows rapidly. The emission of major pollutants in waste

gas and waste has exceeded the ecological environment tolerance level, thereby substantially affecting the health level of the residents.

- (3) From the perspective of control variables, per capita education years (X_1) has a significant negative correlation with population mortality. This result indicates that the provision of public education services has a positive and significant impact on residents’ health. The improvement of residents’ education level has significantly increased the life expectancy per capita, while the residents’ receiving education level and health awareness has also been significantly enhanced, thereby resulting in new lifestyles and behaviour habits. A negative correlation exists between the number of doctors per 10,000 populations (X_2) and mortality rate of the population. However, this result is not significant, thereby showing that although the number of doctors per 10,000 populations has a certain positive effect on the reduction of mortality rate, such a variable has a weak impact on health. Although the government’s investment in medical and health resources in Hubei has increased in recent years, thereby easing the total amount on the supply side, the medical and health resources allocation structure is unreasonable and the medical needs of the relatively poor and backward areas have not been relatively met. In addition, the top-level design of the government is ideal, thereby relatively verifying the underutilization of health care resources in Hubei. The significant negative correlation between investment in environmental protection (X_3) and population mortality shows that public services in this area are beneficial to residents’ health. Per capita GDP (X_4) shows a significant positive correlation with the mortality rate of the population. Given that Hubei is currently in a stage of rapid economic development, industrial output plays an important role in economic development. Meanwhile, the industrial energy consumption structure in Hubei is dominated by coal, thereby producing environmental pollution that has a relatively adverse impact on residents’ health. Urbanization rate (X_5) has a negative correlation with the population mortality rate, but is not significant. This result shows that with the acceleration of urbanization in Hubei, numerous population clusters do not use residents’ health. Meanwhile, the negative impact on residents’ health in urbanization is greater than the positive impact, thereby showing a negative impact on health in terms of net effect.

Table 1: Regression results.

Variables	Death	
	RE	FE
Constant	6.214	8.654
ECO1	0.145**	0.241**
ECO2	0.014**	0.009***
X1	-0.341	-0.274**
X2	0.015*	-0.004
X3	-1.864*	-0.687***
X4	0.541***	0.689***
X5	-0.087	-0.287
Hausman Test	8.974 (0.001)	

Note: FE and RE represent the fixed and random effect models, respectively; *, **, *** are significant at the 10%, 5% and 1% statistical levels, respectively.

POLICY RECOMMENDATIONS

Adjusting Industrial Structure and Strengthening Environmental Pollution Control

In recent years, the environmental pollution level in Hubei has increased annually. The level of environmental quality has continuously decreased, along with the degree of deterioration accelerating. The speed of industrialization and the economy in general are developing at a rapid pace. The high-intensity consumption of various resources and discharge of a large amount of smoke, waste gas, and wastewater have substantially polluted the environment. At present, Hubei remains dominated by the secondary industry, which intensively consumes non-renewable resources. The limitation of technology level makes it impossible for the secondary industry to discharge a large amount of waste while consuming energy to adopt better treatment methods in time, thereby resulting in the aggravation of environmental pollution. Therefore, the government should formulate the corresponding policies to provide guidance; vigorously develop clean tertiary industries, such as green environmental protection, service, and high and new technology industries; strictly control the emission of industrial waste; make industrial development change from resource-intensive to technology-intensive; reduce energy consumption and emission; strictly supervise and control the emission of pollutants from existing enterprises; and improve the quality of atmospheric environment and water environment.

Developing Clean Energy and Optimizing Energy Consumption Structure

The regional environmental pollution in Hubei is unbalanced and the task of environmental protection remains arduous. Hubei's overall energy consumption is dominated by coal, thereby easily producing a large amount of sulphur dioxide, smoke dust, and other pollutants. Therefore, the top priorities in China include improving the efficiency of energy utilization, vigorously developing clean energy technologies with minimal pollution, seeking alternative energy sources, enabling the country to realize energy transformation, and controlling environmental pollution from the source. Moreover, the single energy structure dominated by coal should be changed. Under the established economic conditions, particularly through energy transformation, the proportion and types of clean energy consumption should be increased, while the quantity and types of clean energy should be coordinated. Moreover, a potential clean energy should be developed and maximized, while the consumption of traditional energy, such as coal, should be considerably reduced to reduce pollutant emis-

sion, thereby reducing the loss of public health of residents.

Increase Investment in Environmental Health to Improve Public Health

The level of public health is closely related to environmental pollutants, medical research investment, number of health departments, number of health personnel, and other factors. To strengthen the research on the relationship between environmental pollution and public health, clarifying the health effects of environmental factors, comprehensively developing the evaluation and identification technology of environmental pollution's impact on public health, and proposing control methods to block and reduce the harm of pollutants to public health can provide scientific basis for the prevention and treatment of diseases caused by environmental pollution. Accordingly, the impact of environmental pollution on public health will be mitigated and the level of public health will be improved. At present, basic research in the fields of environment and health in Hubei is weak, while the mechanism of action of the relevant environmental pollutants is unclear, thereby resulting in difficulty to formulate and perfect the pertinent technical standards, quantify losses, and identify compensation, among others. Accordingly, we should maximize state-supported large-scale scientific research programs to implement such projects as risk assessment and model research of public health damage caused by different environmental pollutants, pollutant source tracking methods, and control technologies. When undertaking large-scale national projects, research institutes should maximize their project resources, forge teams, cultivate scientific research talents, and form high-quality scientific research teams.

Increasing Investments in Scientific Research in Environmental Health and Providing Policy Support

For the relevant research in the field of environmental pollution and public health impact, priority should be given to evaluate and increase the allocation of research funds in this field. Moreover, the relevant government departments and enterprises at all levels should strongly support and cooperate with the research process. To jointly address key problems, we will organize specialized environmental and health research institutions and laboratories and collaborate with scientists from such fields as environmental protection, epidemiology, biology, medicine, chemistry, and other related disciplines. Moreover, we will positively pursue regional and international cooperation and maximize all available and effective resources. Local governments should engage in public health promotion activities to raise public awareness of environmental protection and health. Through

various mass media, such as news, radio, television, and the internet, publicity and education activities related to the impact of environmental pollution on the loss of public health value can be implemented, environmental and health-related laws and regulations can be publicized, public legal awareness and environmental protection awareness can be improved. Engagements in these activities will enable the public to realize the extent of the impact of environmental pollution on public health. Moreover, the concepts of environment and health can be integrated into public concepts, thereby guiding practice to enhance public awareness of self-prevention and protection and actively contribute to national environmental and health undertakings. Thus, people will consciously adopt measures to prevent environmental pollution from negatively affecting public health.

CONCLUSION

Environmental pollution is posing an increasing threat to public health. While seeking economic development, exploiting and utilizing the existing natural resources, and creating a new living environment, humans also discharge a large amount of wastes generated from living and production activities, thereby contaminating the environment. This study takes Hubei as the research object and uses the expanded Grossman health production function to calculate the quantitative relationship between environmental pollution and public health level in this province. Lastly, this research presents a few suggestions and measures to protect the environment and improve the public health level. The results show that the population mortality rate is significantly positively correlated with the three influencing factors of industrial sulphur dioxide emissions, industrial smoke dust emissions, and GDP per capita. A significant negative correlation exists between the death rate of the population and number of years of education per capita and investment in environmental protection. The number of doctors per 10,000 population and urbanization rate has no evident impact on the mortality rate of the population. In-depth research can be conducted on the following aspects: (1) formation of a perfect and systematic evaluation system of residents' health loss caused by environmental pollution, (2) whether substantial differences exist on the impact of the different types of environmental pollution on residents' health in different regions, (3) enhancement of environmental pollution indicators, (4) government's investment in public health services, and (5) improvement of residents' health.

ACKNOWLEDGEMENT

This work is supported by the Research Fund for Doctor of Wuhan Business University, "Research on the institutional

change and system optimization of informal financial supervision in China" (2017KB014).

REFERENCES

- Chen, S. Y., Chu, D. C., Lee, J. H., Yang, Y. R. and Chan, C. C. 2018. Traffic-related air pollution associated with chronic kidney disease among elderly residents in Taipei City. *Environmental Pollution*, 234: 838-845.
- Chen, Y. L., Shih, Y. H., Tseng, C. H., Kang, S. Y. and Wang, H. C. 2013. Economic and health benefits of the co-reduction of air pollutants and greenhouse gases. *Mitigation and Adaptation Strategies for Global Change*, 18(8): 1125-1139.
- Costa, A. F., Hoek, G., Brunekreef, B. and Ponce de Leon, A.C.M. 2016. Air pollution and deaths among elderly residents of Sao Paulo, Brazil: An analysis of mortality displacement. *Environmental Health Perspectives*, 125(3): 349-354.
- Gohlke, J. M., Thomas, R., Woodward, A., Campbell-Lendrum, D. and Prüss-Üstün, A., Hales, S. 2011. Estimating the global public health implications of electricity and coal consumption. *Environmental Health Perspectives*, 119(6): 821-826.
- Grossman, M. 1972. On the concept of health capital and the demand for health. *Journal of Political Economy*, 80(2): 223-255.
- Jiang, S., Bo, L., Gong, C., Du, X. H., Kan, H. D., Xie, Y. Q., Song, W. M. and Zhao, J. Z. 2016. Traffic-related air pollution is associated with cardio-metabolic biomarkers in general residents. *International Archives of Occupational and Environmental Health*, 89(6): 911-921.
- Kan, H., Chen, R. and Tong, S. 2012. Ambient air pollution, climate change, and population health in China. *Environment International*, 42: 10-19.
- Matus, K., Nam, K. M., Selin, N. E., Lamsal, L. N., Reilly, J. M. and Paltsev, S. 2012. Health damages from air pollution in China. *Global Environmental Change*, 22(1): 55-66.
- Mestl, H.E.S., Aunan, K. and Seip, H.M. 2006. Potential health benefit of reducing household solid fuel use in Shanxi province, China. *Science of the Total Environment*, 372(1): 120-132.
- Pope, C. A., Burnett, R. T., Thun, M. J., Calle, E. E., Krewski, D., Ito, K. and Thurston, G. D. 2002. Lung cancer, cardiopulmonary mortality, and long-term exposure to fine particulate air pollution. *Jama*, 287(9): 1132-1141.
- Shen, H., Chen, Y., Russell, A. G., Hu, Y. and Tao, S. 2018. Impacts of rural worker migration on ambient air quality and health in China: From the perspective of upgrading residential energy consumption. *Environment International*, 113: 290-299.
- Sram, R. J., Binkova, B., Dostal, M., Merkerova-Dostalova, M., Libalova, H., Milcova, A., Rossner Jr, P., Rossnerova, A., Schmutzerova, G., Svecova, V., Topinka, J. and Votavova, H. 2013. Health impact of air pollution to children. *International Journal of Hygiene and Environmental Health*, 216(5): 533-540.
- Voorhees, A. S., Wang, J., Wang, C., Zhao, B., Wang, S. X. and Kan, H. D. 2014. Public health benefits of reducing air pollution in Shanghai: a proof-of-concept methodology with application to BenMAP. *Science of the Total Environment*, 485: 396-405.
- Wang, X. and Mauzerall, D.L. 2006. Evaluating impacts of air pollution in China on public health: implications for future air pollution and energy policies. *Atmospheric Environment*, 40(9): 1706-1721.
- Wang, Y. 2010. The analysis of the impacts of energy consumption on environment and public health in China. *Energy*, 35(11): 4473-4479.
- Yang, X., Zheng, Y., Geng, G., Liu, H., Man, H., Lv, Z., He, K. and De Hoogh, K. 2017. Development of PM_{2.5} and NO₂ models in a LUR framework incorporating satellite remote sensing and air quality model data in Pearl River Delta region, China. *Environmental Pollution*, 226: 143-153.



Aquatic Ecotoxicology and Water Quality Criteria of Three Organotin Compounds: A Review

Zhifei Li, Deguang Yu, Gong Wangbao, Wang Guangjun, Yu Ermeng and Xie Jun[†]

Key Laboratory of Tropical & Subtropical Fishery Resource Application & Cultivation, Ministry of Agriculture, Pearl River Fisheries Research Institute of CAFS, Guangzhou Guangdong 510380, Peoples's Republic of China

[†]Corresponding author: Xie Jun

Nat. Env. & Poll. Tech.
Website: www.neptjournal.com

Received: 08-06-2018
Accepted: 02-08-2018

Key Words:

Organotin compounds
Toxicology
Environmental behavior
Water quality criteria
Pollution control

ABSTRACT

Organotin compounds (OTCs) are metal-organic compounds, such as triphenyltin (TPT), tributyltin (TBT) and trimethyltin (TMT), containing at least one Sn-C covalent bond. They can be used as polyvinyl chloride (PVC) stabilizers, wood preservatives, pesticides, anti-corrosion coatings, and molluscicide agents. OTCs are frequently detected in water bodies and have a long half-life. Their ecotoxicological behaviour in the aquatic environment has long been a cause of concern. In this paper, we briefly summarize the physicochemical characteristics, fate in the aquatic environment, biodegradation/bioconcentration, metabolism, and toxicity for aquatic organisms of three organotin compounds. Furthermore, we discuss the water quality criteria of the three compounds for aquatic ecosystems, which could provide important indications for future application, management, risk assessment, as well as pollution control associated with OTCs.

INTRODUCTION

Organotin compounds (OTCs) are metal-organic compounds containing at least one Sn-C covalent bond. They are widely used as pesticides, bactericides, polyvinyl chloride (PVC) stabilizers, as well as wood preservatives, anti-corrosion coatings, and molluscicide agents (Fang et al. 2017, Sousa et al. 2014). However, they have high toxicity and can cause serious damage to the environment. As the only metallic compounds among the known endocrine disruptors, OTCs can lead to developmental malformations in oyster shells (*Crassostrea gigas*), death of shellfish larvae, and deformation of gastropods in ng/L concentrations. In addition, various organisms (especially fish and shellfish) are strong OTC accumulators that has indirect adverse effects on human health (Pagliarani et al. 2013, Anastasiou et al. 2016, Ho et al. 2014). Therefore, the toxicity of OTCs including triphenyltin (TPT), tributyltin (TBT), and trimethyltin (TMT) has become a hotspot of current research.

Many studies of the sources, distribution, environmental fate, and toxicity mechanism of OTCs have been published (Laranjeiro et al. 2018). In this paper, we review the aquatic ecotoxicological behaviour and data of the three OTCs mentioned above, to systematically understand their aquatic ecotoxicology and quality criteria, and provide a key reference for future water ecotoxicology studies.

SOURCE AND FATE OF OTCS IN AQUATIC ENVIRONMENTS

Aquatic OTCs mainly originate from PVC plastics, anti-fouling coatings, and pesticides. In particular, TPT and TBT are used in marine anti-fouling coatings, bactericides, pesticides, and plastic stabilizers, which can directly release them into the aquatic environment. They are detected in high levels, especially in harbour and wharf environments (Laranjeiro et al. 2018, Okoro et al. 2016). TPT and TBT have been found even in Antarctic waters (He et al. 2018). Wastewater and waste gas produced during the synthesis of plastic stabilizers contain TMT, which reaches the water environment through wastewater, surface runoff and other channels (Ashraf et al. 2017). In addition to artificial introduction, the biomethylation process can also form OTCs in aqueous environments. For instance, Chen et al. (2007) reported that some *Pseudomonas* bacteria can form various methylated OTCs; moreover, methylated iodide produced by some seaweed species can methylate inorganic Sn(II) salts, and diosmin can convert inorganic Sn(IV) salts into methylated Sn compounds in the presence of trivalent iron.

The migration mechanism of OTCs in aquatic environments (Fig. 1) is mainly controlled by adsorption processes. The water solubility and migration rate of aquatic OTCs are generally low, especially in the case of TPT and TBT, which

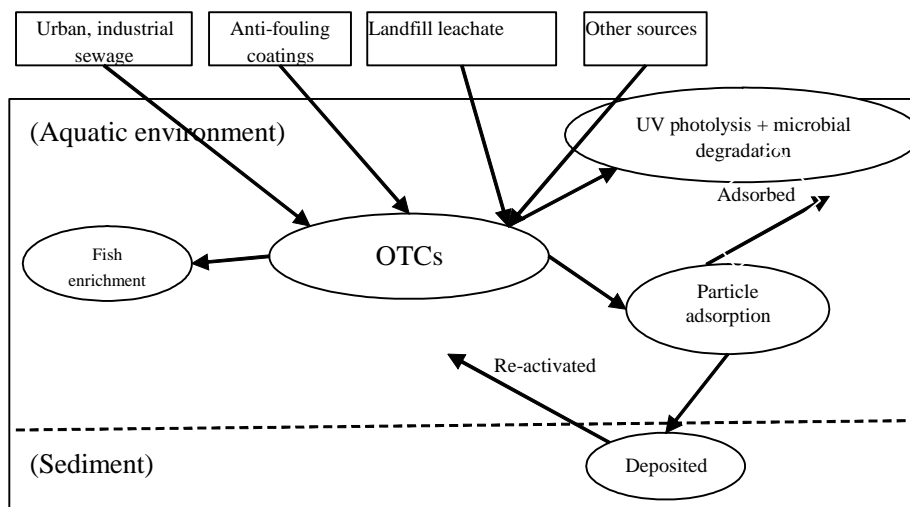


Fig. 1: Fate of organotin compounds in aquatic environments.

are easily adsorbed on suspended particles in water. TBT fractions between 57% and 95% exist in adsorbed form under simulated estuarine conditions (Laranjeiro et al. 2018). Chen et al. (2001) found that, upon entering the water environment, TBT is distributed between microlayers, water bodies, sediments, algae, and other suspended matter, as well as fish. The system reaches a steady state at certain time after TBT has entered the aqueous environment. TBT is strongly adsorbed on suspended matter (such as algae and organic compounds) and sediments, whereas the surface of microlayers is less enriched in TBT. This adsorption behaviour plays a key role in the migration process of OTCs and in their bioavailability. Dissolved OTCs are prone to enter the sea or the food chain through bioaccumulation. However, TMT has strong hydrophilic and lipophilic groups that mainly exist in ionic form in water, and is easily accumulated in aquatic organisms (Wei et al. 2013). In addition to adsorption, the interaction of OTCs with dissolved organic matter also depends on the pH value and the nature of the organic species in the water environment. The maximum adsorption of organic matter to TBT is observed at pH 8.0 (Fang et al. 2017).

OTCs are widely found in aquatic environments (including drinking water), sediments, soil, and organisms. At present, the areas contaminated with OTCs are mainly found in ports, wharfs and berths. For example, the average TBT concentrations in waters and sediments around the Cape Town harbour in South Africa, are 0.067-111.290 and 0.010-0.829 $\mu\text{g/L}$, respectively, whereas those of TPT are 0-23008.0 and 0-0.691 $\mu\text{g/L}$, respectively (Okoro et al. 2016). The TBT and TPT concentrations in the Saudi coastal water are 0.14-

1.9 and 0.12-0.70 $\mu\text{g/L}$, respectively (Al-Shatri et al. 2015). The net weight of TBT per gram sediment reaches 10000 ng in many sites, such as Port Camargue in France (Briant et al. 2013) and the Elbe river in Germany (Becker et al. 1992). TPT has also been detected in aquatic animals, sediments, soils and water (Shim et al. 2005, Harino et al. 2000). The concentration of TMT in the North Sea and in the Elbe River in Germany reaches 2-11 ng/L (Shawky et al. 1998).

Similar to other countries, studies of OTCs in China also focus on ports, wharves, and related areas. Jiang et al. (2001) measured the OTCs concentration in ports located in Dalian, Tianjin, Qingdao, Beihai, Jinan, Peking, Qinghuangdao, Yantai, the Yangtze, the Yellow River, Baiyangdian and Taihu. Every tested sample presented organotin pollution, without exception. In particular, the average concentration of TBT was 93.8 ng/L, which is much higher than the accepted limits of the Western countries. Huang et al. (2005) detected OTCs in water, sediments, and animals around the ports of Xiamen, Shantou, and Huiyang, in the southeastern coast of China. Liu et al. (2003) measured TMT concentrations of up to 360 ng/L in the Beijing Guanting reservoir and Yongding River. Qiu et al. (2008) analysed the subterranean water resources of industrial areas in Zhujiang and found TMT contents of up to 1.07×10^5 ng/L. These data highlight the presence of different degrees of organotin pollution in different countries; however, there are some similarities in the distributions of OTCs. Although the concentration levels of different areas show large variations, the contribution focus on the crowded water. Moreover, even though different locations have been studied, the maximum concentrations are found within 2 cm from the surface of

sediments; the concentrations decrease with increasing depth (Briant et al. 2013, Anna et al. 2014).

The degradation of OTCs in the aquatic environment involves the continuous removal of the organic groups bonded to the tin atom. In nature, this process is often the overall result of photodegradation, biodegradation and chemical degradation. Photodegradation in water is the fastest degradation route. Since the light intensity decreases with increasing water depth, the OTCs degrade slowly in deep-water sediments and soils.

The half-life of the OTCs show significant variations with the environmental conditions. Various studies indicated that the half-life of TBT in water ranges from days to months, whereas that in sediments is longer. Briant et al. (2016) measured the half-life of TBT in sediments as 360-775 days.

Turning to the biodegradation route, not many microorganisms able to induce degradation of organotin compounds have been identified. Bacteria (pseudomonads, *Alcaligenes faecalis*, *Shewanella putrefaciens*) and phytoplankton (*Skeletonema costatum*, *Chlorella vulgaris*, *Scenedesmus dimorphus*) degrade OTCs in aquatic systems (Briant et al. 2013). Ultraviolet light can promote TPT degradation (Hoch 2001), the photodegradation rate can reach 89.4% after exposure to ultraviolet light for 75 min (He et al. 2008). On the other hand, biodegradation of TPT in soil and sediments proceeds slowly, with only 5% degradation in 14 days (Kannan & Richard 1996). Our present understanding of the photodegradation and biodegradation processes of TMT is still limited, and further studies are needed.

QUANTITATIVE STRUCTURE-ACTIVITY-PROPERTY RELATIONSHIPS

The physicochemical properties of TPT, TBT and TMT are given in Table 1. The three OTCs contain one chlorine atom and different alkyl groups. Their molecular structure (type of substituents and positions of functional groups), average molecular polarizability, molecular weight and electron distribution directly affect the octanol-water partition coefficient (K_{ow}), solubility and biological activity (Eng 2017). OTCs are highly toxic to aquatic organisms including molluscs, fish and algae, and their toxicity is related to electronic effects. Liu et al. (2008) studied the quantitative structure-activity relationship (QSAR) of 13 OTCs based on their highest occupied orbital energy (E_H) and molecular hydration energy (E_w), and developed an effective model to predict the acute toxicity of these compounds. It shows that there is an electron supply and accepts the relationship between organic tin molecules and large target molecules *in vivo*. In addition, both E_H and E_w are positively correlated

with the biological toxicity.

The K_{ow} of organic pollutants is considered an important parameter for predicting the migration rate of these compounds in various phases of the environment, but it does not exactly match the ionic organic pollutants and metal-organic compounds. Li et al. (2002) explored the accumulation and distribution of TBT in tilapia. Their results show that a more accurate prediction of the concentration and distribution of OTCs can be obtained using an artificial biofilm-water system instead of K_{ow} . This may be due to the ionic character of the OTCs, which host the tin atom inside the molecule; therefore, their accumulation is controlled not only by the lipophilic partitioning of their simple non-polar components, but also by the bioenrichment mechanisms that rule the heavy metal ions.

BIOACCUMULATION AND METABOLISM OF OTCs

The OTCs, and especially TBT, TMT and TPT are liposoluble and easily bind to glutathione and α -keratin in organisms, which leads to their accumulation. In addition to accumulation, OTCs can also lead to food chain amplification. OTC accumulation has been detected in marine organisms ranging from lower plants, to plankton, to endothermic vertebrates and birds (Laranjeiro et al. 2018, Nsengimana et al. 2015). In addition, they have long lifetimes in organisms, after four years of restricted use of OTCs as anti-fouling coatings in Italy, TBT was still detected in 46% of fish (Amodio-Cocchieri et al. 2000).

The extent of bioenrichment of OTCs is generally measured by the bioconcentration factor (BCF). Many studies have shown that organotin compounds are easily accumulated in molluscs and fish. The bioenriched concentration of TBT in conchs is 1000 times higher than that of the surrounding water environment (Gibbs & Bryan 1986), whereas the BCF of TBT in oyster tissue in water is as high as 50000. Mussels exhibit the highest accumulation rate of OTCs from water and planktons (Zhou et al. 1994). Quintas et al. (2017) found that the concentration of TBT in mussels from different water bodies worldwide was in the range of 1-6434 ng/g; for example, the concentration of TBT in mussels from the northern Adriatic Sea was up to 6434 ng/g. Yamada et al. (1997) measured the OTC concentration in the liver of eels from the Sea of Japan and Hokkaido, and found that the BCF of TPT reached 500000, much higher than that of TBT. Organotin compounds are also easily accumulated in fish. Marine environmental surveys showed high OTC concentrations in marine fish populations worldwide. For example, the TBT and TPT concentrations in fish from the Arabian Gulf were 126.4-228.4 ng/g (dry weight) and 64.9-281.7 ng/g (Ashraf et al. 2017), respectively. The TMT ac-

Table 1: Physico-chemical properties of the three organotin compounds investigated in this study.

Indicators	TPT	TBT	TMT
International designation	66183	3535715	71166
CAS No.	639-58-7	1461-22-9	1066-45-1
Name	Triphenyltin chloride	Tributyltin chloride	Trimethyltin chloride
Chemical formula	(C ₆ H ₅) ₃ SnCl	C ₁₂ H ₂₇ ClSn	C ₃ H ₉ ClSn
State	White powder	Colorless or yellowish oily liquid	White crystal
Relative molecular weight	385.5	325.5	199
Fusion point (101.3kPa)	103-109°C	-9°C	37-39°C
Boiling point (101.3kPa)	240°C	171-173°C	148°C
Density (g/cm ³)	1.49	1.2	0.988
Flashing point	70°C	>112°C	97°C
pka	5.2	6.99	6.6
logK _{ow} (Eng. 2017)	2.65	2.6	2.3
Hazard level*	T, N, C	T,N	T+, N
Solubility in various solvents	Insoluble in water, soluble in organic solvents. Colorless after dissolution. Stable at room temperature.	Soluble in ethanol, heptane, benzene and toluene. Insoluble in cold water. Soluble in hot water.	Soluble in water, Volatile.
Applications	Anti-fouling coating of marine boats, bactericides.	Wood antiseptis, varnishes of boats.	Plastics processing, insecticides, bactericides.

*T = poisonous, N = harmful to the environment, C = corrosive

cumulation is significantly lower than that of TPT and TBT. Hadjispyrou et al. (2001) reported that the TMT content in *Artemia* was 75 times higher than that in the aquatic environment. Moreover, Nsengimana et al. (2015) found efficient accumulation of OTCs in phytoplankton algae.

The accumulation of OTCs in aquatic organisms varies with the type of organism, survival environment, size and organs. TPT and TBT accumulation is obviously lower in fish muscle than in molluscs such as oysters. Morcillo et al. (1997) also found that the TBT concentration in molluscs was higher than in other aquatic animals, and reached a maximum of 514 µg Sn/g in shellfish. This result may be related to the enzymatic metabolism, as fish can degrade TBT *in vivo*, its corresponding accumulated content is relatively low. TBT and its metabolites exhibit a heterogeneous distribution in different tissues and organs. The content of TBT in metabolic active sites such as liver, kidney, spleen, and bladder is low, which may be due to the presence of cytochrome P450 reductase that degrades TBT into dibutyltin and monobutyltin (Briant et al. 2013).

TOXICITY OF OTCs TO AQUATIC ORGANISMS

When the concentration of organotin compounds in the water environment reaches nanogram per litre levels, toxic effects can be produced on oysters, shellfish and gastropods (Sousa et al. 2014). Numerous studies have focused on the acute aquatic toxicity of common OTCs, especially of TBT and TPT on different aquatic organisms. The acute toxicity value (LC₅₀) of TBT is in the range of 0.14-282.20 µg/L, with a

median value of about 4.0 µg/L; TBT has acute toxicity to some algae, copepods and shellfish, as well as aquatic crustaceans. The LC₅₀/EC₅₀ values of TBT to *S. costatum* (Walsh et al. 1985), *Platymonas* sp. (Huang et al. 1996), as well as *U. Intestinalis* and *F. spiralis* germlings (Girling et al. 2015) at 96 h are 0.36, 0.31, 0.007 and 0.0045 µg/L, respectively. On the other hand, the LC₅₀/EC₅₀ values of TBT to *E. affinis* (Bushong et al. 1988) and *A. tonsa* (Kusk & Petersen 1997) are 1.98 and 0.87 µg/L, respectively, whereas the corresponding values for *M. edulis* (Thain 1983), *R. abronius* and *H. nudus* are 2.38, 108.00 and 83.28 µg/L, respectively (Bushong et al. 1988). According to previous studies, TPT is more toxic to aquatic plants, with LC₅₀ to *N. closterium*, *Platymonas* sp., *P. tricorutum* and *I. galbana* of 6.21, 4.55, 0.93 and 1.32 µg/L, respectively (Li et al. 1996, Zhao et al. 1990). However, TPT shows low acute toxicity to fish, for example, the LC₅₀ to carp at 96 h is 134.46 µg/L (Han et al. 2008).

Studies on the chronic toxicity of the three OTCs considered in this review have focused on reproductive toxicity and chronic death. TBT has a chronic toxicity (LD₅₀) in the range of 0.01-1.50 µg/L, with a median value of approximately 0.11 µg/L (Mu et al. 2010), the LD₅₀ of TBT against *D. magna*, *B. calyciflorus* and *S. macrocephalus* are 0.14, 0.31 and 0.54 µg/L, respectively (Zhu et al. 2009, Mu et al. 2010). Alfred et al. (1988) studied the 30-day LD₅₀ of TPT hydride against fathead minnows and found a significantly decreased survival rate at 2 µg/L. This result demonstrated that TPT in concentrations higher than 1 µg/L has

some inhibitory effects on the survival and reproduction of *Daphnia magna*. A TPT concentration of 2 µg/L prolongs the culture cycle of *N. awatschensis*, increases the mortality rate of broodstock in the incubation period, and decreases the production of shrimp, leading to the conclusion that breeding water containing 1 µg/L TPT can suppress the reproduction of *N. awatschensis*. The results of chronic toxicity tests of TMT are not clear at present, and further studies are needed.

OTCs are the only metal compounds with endocrine disrupting effects. The main manifestations of their toxicity are abnormal embryonic development, increased testosterone levels, malformations and loss of immune function in aquatic organisms. Anastasiou et al. (2016) found that TBT concentrations below 1 ng/L can cause malformations in *H. trunculus*, a biologically sensitive species. Mcallister et al. (2003) found higher male numbers of newborn zebrafish upon exposure to 0.1 µg/L TBT for 70 days, and all sperm lacked flagella upon exposure to 10 µg/L TMT. When the mass concentration of TBT and TPT reaches 1 µg/L, they cause sexual alterations in gastropods, leading to increased male characteristics and decreased fertility (Abidli et al. 2013, Anastasiou et al. 2016). Laranjeiro et al. (2016) reported that TPT can cause *Nucella lapillus* distortion through a phallic route. TBT has an inhibitory effect on the immune system of fishes and mammals. The accumulation of OTCs in the animals affects the activity of phagocytic cells and suppresses the immune system of animals. TBT can inhibit the Na⁺/H⁺ exchange pump, which induces unfavourable stress conditions in fish, especially hypoxic stress. TBT and TPT have highly toxic effects on algae, which can destroy the reticular structure of chloroplast photosynthetic sheets and hinder the growth of sensitive sea algae and plankton. When heavily concentrated in animal brains, TBT and TPT disrupt the normal activity of the neuroendocrine system and inhibit the release of neuroendocrine factors from the thoracic ganglion (Lu et al. 2017). The effect of endocrine-disrupting chemicals is often not isolated, and can often affect the endocrine function of the body through multiple pathways involving the neurological, immune, and endocrine systems (Lu et al. 2017).

HEALTH EFFECTS OF OTCs

A limited number of experimental studies showed that the three OTCs may be human carcinogens (B2 grade), with clear animal carcinogenicity. However, it is hard to assess the human health risks associated with exposure to low concentrations of OTCs (Gueguen et al. 2011), despite the continuous occurrence of human poisoning cases under different work environments (Lee et al. 2016). The main

OTC intake channel for humans is through ingestion of polluted marine fish, especially the blood of contaminated fish, which has the highest levels of OTCs (Ho et al. 2014). Although OTCs exhibit genetic toxicity, causing gene mutations, chromosome aberrations and DNA damage, their toxicity to humans has not been extensively investigated. In bacterial susceptibility experiments, Paredescervantes et al. (2017) used 28 bacterial strains to test their sensitivity to TBT and TPT without being metabolically activated. They found that only 12 of the 28 tested strains were inhibited at TBT or TPT concentrations of 1 mM, and the bacteria were essentially not affected by TBT or TPT during 48 h of *in vitro* culture growth. In SOS colour tests, we found that all dibutyltin compounds have genetic toxicity. TBT concentrations of 20-90 µg/L were found to produce genetic toxicity. Comet assays showed that TBT can induce oxidative and DNA damage in rats (Liu et al. 2006) and also cause nuclear DNA damage in nucleated red blood cells of rainbow trout (Luca et al. 2001). TPT can cause micronuclei and sister-chromatid exchange in Chinese hamster cells (Chao et al. 1999). *In vitro* assays showed that TMT increases the chromosomal aberration rate in human peripheral blood lymphocytes, and the sister chromatid exchange and positive micronucleus test. *In vivo* tests revealed that TMT causes malformations in chromosomes of rat bone marrow cells (Tang & Li 1999).

ECOLOGICAL EFFECTS OF OTCs

The water quality criteria indicate the maximum dose or concentration of pollutants in aquatic ecosystems that do not adversely affect humans or other organisms. The purpose of establishing these criteria is to prevent unacceptable long- and short-term effects of pollutants on commercial and recreational aquatic organisms, as well as other species such as fish, benthic invertebrates, and plankton in rivers and lakes. Statistical extrapolation methods based on risk statistics are generally used in the international derivation of pollutant reference values; among these, two methods are the most widely used. The first is the toxicity percentile rank method based on acute/chronic toxicity ratios, developed by the United States Environmental Protection Agency (EPA) (Stephan 1985); this method is also used in South Africa. The other one is the species sensitivity distribution (SSD) method, also known as A&S method, by Aldenberg & Slob (1993). It is based on Monte Carlo simulations and adopted by the OECD, the Netherlands, Australia and New Zealand.

At present, the development of water quality criteria for organotin compounds is still in its infancy, and the relevant data are limited, as only the TBT criteria have been published. In particular, the U.S. EPA published the TBT

water quality criteria in 2003. Based on these criteria, and taking Monte Carlo data into account, the SSD curve was established to predict the maximum concentration (CMC) and final chronic value (FCV) of TBT compounds to aquatic organisms in fresh and marine water. Based on the EPA standard method and acute/chronic toxicity ratios, the CMC values of TBT in freshwater and seawater are 0.4589 and 0.4175 µg/L, respectively, while the corresponding FCV values are 0.0723 and 0.0658 µg/L, respectively. Based on the water quality criteria adopted in European Union countries, Mu et al. (2010) introduced some improvements to the setting method of datum value, the application of the model, and the determination of the evaluation factor. They proposed to establish the datum of seawater quality of our country by using the data requirement method of “the value of double value datum”. They used TBT as an example to develop China’s high value water quality criteria (HSWC) and to determine the upper and lower TBT concentration limits in seawater as 0.43 and 0.002 µg/L, respectively. Although the criteria for TBT have been established, they only apply to a specific ecosystem, and do not take geographical and human health effects into account.

At present, large amounts of data on the acute and chronic toxicity of TPT are available. Related toxicity studies have been carried out for zooplankton, plants, arthropods and vertebrates; however, the data on the acute and chronic toxicity of TPT are incomplete. In particular, no specific data on its chronic toxicity are available (Alfred et al. 1988, Sun et al. 2000), and the corresponding water quality criteria has not been reported. Only acute toxicity data to *Chlorella pyrenoidesa*, *Daphnia magna*, *Oryzias latipes*, *Artemia* and zebrafish were reported (Nagase et al. 2010, Hadjispyrou et al. 2001, Li et al. 2011). In addition, there are insufficient data to complete the development of water quality criteria for TMT.

PERSPECTIVES

Organotin compounds, as typical representatives of environmental endocrine disruptors, cause global pollution of the water environment, posing a direct threat to aquatic organisms and human health. This reflects the current interest in the transfer processes of OTCs into water and in the environmental effects of their toxicity. Many systematic studies have focused on the presence of OTCs in the water environment, their transfer and deposition in water, as well as their adsorption characteristics, ecological toxicity and toxicity mechanism in sediments. However, these investigations are mainly focused on dibutyltin and phenyltin compounds and are limited to individual and population levels, whereas studies on other OTCs are still scarce. In addition,

our understanding of the mechanisms of organotin toxicity and detoxification is only superficial, and most studies are still at a speculative level. Therefore, we need to improve our understanding of the toxicity and detoxification mechanisms of OTCs and their influence on the biological and marine ecosystems.

The similarities in the migration mechanisms of different OTCs highlight the important role of their deposition in the sediment; the sediment microorganisms are not only the main disintegrators, but also the producers of some substances with a very important role in the biological chain. However, the effect of the OTCs on the microbial population of the sediment is still unclear, while at the same time the fraction of bacteria that can be separated and culture directly from the sediment is only 1% of the total bacteria in the bottom sediments. The study of the relationship between OTCs and microorganisms in sediment, as well as the degradation of OTCs by sediment microorganisms, are still the limitation of organotin in aquatic ecological cycling.

In terms of management and monitoring of OTC pollution, only the water quality criteria for TBT are currently available; therefore, it is essential to complete the development of water quality criteria for OTCs, especially in freshwater, in order to deal with serious water pollution issues worldwide.

ACKNOWLEDGEMENTS

This work was supported by the Modern Agro-industry Technology Research System (grant number CARS-45-21).

REFERENCES

- Abidli, S., Castro, L. F., Lahbib, Y., Reis-Henriques, M. A., Trigui, E. M. N. and Santos, M. M. 2013. Impossex development in *Hexaplex trunculus* (Gastropoda: Caenogastropoda) involves changes in the transcription levels of the retinoid X receptor (RXR). *Chemosphere*, 93(6): 1161-1167.
- Aldenberg, T. and Slob, W. 1993. Confidence limits for hazardous concentrations based on logistically distributed NOEC toxicity data. *Ecotoxicol. Environ. Saf.*, 25(1): 48-63.
- Alfred, W. J., Danny, K. T., Edward, R. K. and Michael, L. Knuth 1988. Acute and chronic toxicity of triphenyltin hydroxide to fathead minnows (*Pimephales promelas*) following brief or continuous exposure. *Environ. Pollut.*, 52(4): 289-301.
- Al-Shatri, M. A., Nuhu, A. A., Basheer, C., Al-Arfaj, A. and Al-Tawabini, B. 2015. Assessment of tributyltin and triphenyltin compounds and their main degradation products in Saudi coastal waters. *Arab. J. Sci. Eng.*, 40(10): 2959-2967.
- Amodio-Cocchieri, R., Cirillo, T., Amorena, M., Cavaliere, M., Lucisano, A. and Prete, U. D. 2000. Alkyltins in farmed fish and shellfish. *Int. J. Food Sci. Nutr.*, 51(3): 147-151.
- Anastasiou, T. I., Chatzinikolaou, E., Mandalakis, M. and Arvanitidis, C. 2015. Impossex and organotin compounds in ports of the mediterranean and the atlantic: Is the story over?. *Sci. Total. Environ.*, 569-570: 1315-1329.

- Anna, F., Grażyna, K. and Bruno, P. 2014. Organotin compounds in surface sediments of the southern baltic coastal zone: A study on the main factors for their accumulation and degradation. *Environ. Sci. Pollut. Res. Int.*, 21(3): 2077.
- Ashraf, M. W., Salam, A. and Mian, A. 2017. Levels of organotin compounds in selected fish species from the Arabian Gulf. *B. Environ. Contam. Tox.*, 98(6): 811-816.
- Becker, E. C. and Bringezu, S. 1992. Contamination of surface water by organotin compounds - concentrations effects, quality objectives, use limitations. *Acta Hydroch. Hydrob.*, 25: 40-46
- Briant, N., Banconmontigny, C., Elbazpoulichet, F., Freydier, R., Delpoux, S. and Cossa, D. 2013. Trace elements in the sediments of a large Mediterranean marina (Port Camargue, France): levels and contamination history. *Mar. Pollut. Bull.*, 73(1): 78-85.
- Briant, N., Bancon-Montigny, C., Freydier, R., Delpoux, S. and Elbaz-Poulichet, F. 2016. Behaviour of butyltin compounds in the sediment pore waters of a contaminated marina (Port Camargue, South of France). *Chemosphere*, 150: 123-129.
- Bushong, S. J., Jr, L. W. H., Hall, W. S., Johnson, W. E. and Herman, R. L. 1988. Acute toxicity of tributyltin to selected chesapeake bay fish and invertebrates. *Water Res.*, 22(8): 1027-1032.
- Chao, J. S., Wei, L. Y., Huang, M. C., Liang, S. C. and Chen, H. H. C. 1999. Genotoxic effects of triphenyltin acetate and triphenyltin hydroxide on mammalian cells *in vitro* and *in vivo*. *Mutat. Res.*, 444(1): 167-174.
- Chen, B., Zhou, Q., Liu, J., Cao, D., Wang, T. and Jiang, G. 2007. Methylation mechanism of tin(II) by methylcobalamin in aquatic systems. *Chemosphere*, 68(3): 414-419.
- Chen, Z., Zhang B. and Huang, G. 2001. Environmental behavior of tributyltin in an estuarine microcosm. *Environ. Pollut. Contr.*, 23(5): 224-226. (in chinese)
- Eng, G. 2017. Review: Quantitative structure-activity/property relationships as related to organotin chemistry. *Appl. Organomet. Chem.*, 31(10): 3712. DOI 10.1002/aoc.3712
- Fang, L., Xu, C., Li, J., Borggaard, O. K. and Wang, D. 2017. The importance of environmental factors and matrices in the adsorption, desorption, and toxicity of butyltins: a review. *Environ. Sci. Pollut. Res. Int.*, 24(10): 9159-9173.
- Gibbs, P. E. and Bryan, G. W. 1986. Reproductive failure in populations of the dogwhelk, *Nucella lapillus*, caused by imposex induced by tributyltin from antifouling paints. *J. Mar. Biol. Ass.*, 66: 767-777.
- Girling, J. A., Thomas, K. V., Brooks, S. J., Smith, D. J., Shahsavari, E. and Ball, A. S. 2015. A macroalgal germling bioassay to assess biocide concentrations in marine waters. *Mar. Pollut. Bull.*, 91(1): 82-86.
- Gueguen, M., Amiard, J. C., Arnich, N., Badot, P. M., Claisse, D., Guerin, T. and Vernoux, J. P. 2011. Shellfish and residual chemical contaminants: Hazards, monitoring, and health risk assessment along French coasts. *Rev. Environ. Contam. T.*, 213: 55-111.
- Hadjispyrou, S., Kungolos, A. and Anagnostopoulos, A. 2001. Toxicity, bioaccumulation, and interactive effects of organotin, cadmium, and chromium on *Artemia franciscana*. *Ecotox. Environ. Safe.*, 49: 179-186.
- Han, Z., Li, J. and Sun T. 2008. Study on the acute and subacute toxicities of TPTC on *Carassius auratus*. *Chin. J. Hydroecol.*, 1(2): 62-66.
- Harino, H., Fukushima, M. and Kawai, S. 2000. Accumulation of butyltin and phenyltin compounds in various fish species. *Arch. Environ. Contam. Toxicol.*, 39(1): 13-19.
- He, J., Cao, C., Gu, D., Ye, Z. and Hou, H. 2008. Photodegradation of aqueous triphenyltin chloride (TPT) using 206 nm. *Chin. Environ. Chem.*, 27(6): 712-715.
- He, Y. F., Huang, Q. H., Chen, L. and Wang F. 2018. Organotin contamination in Marine Biota from the Fildes Peninsula coast, Antarctic. *Acta Sci. Circumst.*, 38(3): 1256-1262.
- Ho, K. K. and Leung, K. M. 2014. Organotin contamination in sea-food and its implication for human health risk in Hong Kong. *Mar. Pollut. Bull.*, 85(2): 634-640.
- Hoch, M. 2001. Organotin compounds in the environment: an overview. *Appl. Geochem.*, 16: 719-743.
- Huang, C., Dong, Q., Lei, Z., Wang, Z. and Zhou, K. 2005. An investigation of organotin compound contamination in three harbors along southeast coast of China. *ACTA Oceanol. Sin.*, 27(1): 57-63.
- Huang, G., Dai, S. and Sun, H. 1996. Toxic effects of organotin species on algae. *Appl. Organomet. Chem.*, 10(5): 377-387.
- Jiang, G. 2001. Current status of organotin studied in China and abroad. *Chin. J. Hyg. Res.*, 30: 1-3.
- Kannan, K. and Richard, F. L. 1996. Triphenyltin and its degradation products in foliage and soils from sprayed pecan orchards and in fish from adjacent ponds. *Environ. Toxicol. Chem.*, 15(9): 1492-1499.
- Kusk, K. O. and Petersen, S. 1997. Acute and chronic toxicity of tributyltin and liner alkylbenzene sulfonate to the marine copepod *acartia tonsa*. *Environ. Toxicol. Chem.*, 16(8): 1629-1633.
- Laranjeiro, F., Sánchezmarín, P., Barros, A., Galanteoliveira, S., Moscosopérez, C., Fernándezgonzález, V. and Barroso, C. 2016. Triphenyltin induces imposex in *nucella lapillus* through an aphallic route. *Aquat. Toxicol.*, 175: 127-131.
- Laranjeiro, F., Sánchezmarín, P., Oliveira, I. B., Galanteoliveira, S. and Barroso, C. 2018. Fifteen years of imposex and tributyltin pollution monitoring along the Portuguese coast. *Environ. Pollut.*, 232: 411-421.
- Lee, E., Park, J. E., Iida, M., Fujie, T., Kaji, T., Ichihara, G., Weon, Y. C. and Kim, Y. 2016. Magnetic resonance imaging of leukoencephalopathy in amnesic workers exposed to organotin. *Neurotoxicology*, 57: 128-135.
- Li, S., Sun, H., Wang, Y. and Dai, S. 2002. Bioconcentration and partition behaviors of tributyltin. *Acta Sci. Circumst.*, 22(6): 726-731.
- Li, Z., Li, J., Yan, T., Teng, W. and Zhou, M. 1996. The effects of TPTC on structural variation of marine microalgae community. *Studia Mar. Sin.*, 37(10): 125-130.
- Li, Z., Xie, J., Gong, W., Yu, D., Wang, G. and Tang, X. 2011. Toxicity effect of Trimethyltin chloride on aquatic organisms. *Chin. Environ. Sci.*, 31(4): 423-430.
- Liu, H. G., Wang, Y. and Lian, L. 2006. Tributyltin induces DNA damage as well as oxidative damage in rats. *Environ. Toxicol.*, 21(2): 166-171.
- Liu, J. M., Jiang, G. B., Liu, J. Y. and Yao, Z. W. 2003. Evaluation of methyltin and butyltin pollution in beijing guanting reservoir and its downriver yongding river. *B. Environ. Contam. Tox.*, 70(2): 219-225.
- Liu, T. and Peng, Y. 2008. Study on the selected organotin compounds in QSPR and QSAR. *Comput. Appl. Chem.*, 25(1): 104-106 (in Chinese).
- Lu, J., Feng, J., Cai, S. and Chen, Z. 2017. Metabolomic responses of *Haliotis diversicolor* to organotin compounds. *Chemosphere*, 168: 860-869.
- Luca, T., Donatella, F. and Massimo, M. 2001. DNA damage induced by organotins on trout-nucleated erythrocytes. *Appl. Organomet. Chem.*, 15(7): 575-580.
- McAllister, B. G. and Kime, D. E. 2003. Early life exposure to environmental levels of the aromatase inhibitor tributyltin causes masculinisation and irreversible sperm damage in Zebrafish (*Danio rerio*). *Aquat. Toxicol.*, 65(3): 309-316.
- Morcillo, Y. 1997. Survey of organotin compounds in the western

- mediterranean using molluscs and fish as sentinel. *Arah. Environ. Contam. Toxicol.*, 32(2): 198-203.
- Mu, J., Wang, Y. and Wang J. 2010. Construction of marine water quality criterion in China: A case study of Tributyltin (TBT). *Asian J. Ecotoxicol.*, 5(6): 776-786.
- Nagase, H., Hamsaki, T., Sato, T., Kito, H., Yoshiokata, Y. and Youki, O. 2010. Structure activity relationships for organotin compounds on the red killifish *Oryzias latipes*. *Appl. Organomet. Chem.*, 5: 91-97.
- Nsengimana, H., Cukrowska, E. M., Dinsmore, A., Tessier, E. and Amouroux, D. 2009. *In situ* ethylation of organolead, organotin and organomercury species by bromomagnesium tetraethylborate prior to GC-ICP-MS analysis. *J. Sep. Sci.*, 32(14): 2426-2433.
- Okoro, H. K., Fatoki, O. S., Adekola, F. A., Ximba, B. J. and Snyman, R. G. 2016. Spatio-temporal variation of organotin compounds in seawater and sediments from cape town harbour, South Africa using gas chromatography with flame photometric detector (gc-fpd). *Arab. J. Chem.*, 9(1): 95-104.
- Pagliarani, A., Nesci, S. and Ventrella, V. 2013. Toxicity of organotin compounds: shared and unshared biochemical targets and mechanisms in animal cells. *Toxicol. In Vitro*, 27(2): 978-990.
- Paredescervantes, V., Castillovera, J., Gomezreynoso, F., Diazcedillo, F. and Aguilarantelises, M. 2017. Wastewater from Mexico city contains organotin compounds and organotin-resistant bacteria. *Cogent Environ. Sci.*, 3(1): 1347996.
- Qiu, S., Ruan, X., Hu, X., Chen, J., Bai, Y. and Tang, X. 2008. Investigation of main poisonous industrial chemical pollution of drinking-water resources in Zhuhai. *Mod. Prev. Med.*, 35(14): 216-220.
- Quintas, P. Y., Arias, A. H., Oliva, A. L., Domini, C. E., Alvarez, M. B., Garrido, M. and Marcovecchio, J.E. 2017. Organotin compounds in *Brachidontes rodriguezii* mussels from the Bahía Blanca Estuary, Argentina. *Ecotox. Environ. Safe.*, 145: 518-527.
- Shawky, S. and Emons, H. 1998. Distribution pattern of organotin compounds at different trophic levels of aquatic ecosystems. *Chemosphere*, 36(3): 523-535.
- Shim, W. J., Hong, S. H., Kim, N. S., Yim, U. H., Li, D. and Oh, J. R. 2005. Assessment of butyl and phenyltin pollution in the coastal environment of Korea using mussels and oysters. *Mar. Pollut. Bull.*, 51: 922-931.
- Sousa, A. C. A., Pastorinho, M. R., Takahashi, S. and Tanabe, S. 2014. History on organotin compounds, from snails to humans. *Environ. Chem. Lett.*, 12(1): 117-137.
- Stephan, C. E. 1985. Guidelines for deriving numerical national water quality criteria for the protection of aquatic organisms and their uses. PB85227049. Washington DC: U.S Environmental Protection Agency.
- Sun, H., Huang, G., Li, S., Dai, S., Zhang, Y. and Qiao, F. 2000. Study on toxic effects of triphenyltin and tributyltin on *Daphnia magna*. *Chin. Environ. Chem.*, 19(3): 235-239.
- Tang, X. and Li, L. 1999. Research progress on the toxicity effect of Trimethyltin chloride. *Chin. Occup. Med.*, 26(6): 46-48.
- Thain, J. E. 1983. The acute toxicity of bis(tributyltin) oxide to the adults and larvae of some marine organisms. International Council for the Exploration of the Sea, Mariculture Committee.
- Walsh, G. E., McLaughlan, L. L., Lores, E. M., Louie, M. K. and Deans, C. H. 1985. Effects of organotins on growth and survival of two marine diatoms, *Skeletonema costatum* and *Thalassiosira pseudonana*. *Chemosphere*, 14(3-4): 383-392.
- Wei, J., Zhao, L. Q., Wang, L., Cong, Y. T. and Wang, Y. 2013. Acute toxicity of trimethyltin chloride on the sea urchin (*Strongylocentrotus intermedius*) embryos and larvae. *Adv. Mater. Res.*, 864-867: 495-498.
- Wong, P. T. S., Chau, Y. K., Kramar, O. and Bengert, G. A. 1982. Structure toxicity relationship of tin compounds on aglae. *Canadian J. Fish. Aquat. Sci.*, 39: 483-488
- Yamada, H., Takayanagi, K., Tateishi, M., Tagata, H. and Ikeda, K. 1997. Organotin compounds and polychlorinated biphenyls of livers in squid collected from coastal waters and open oceans. *Environ. Pollut.*, 96(2): 217-226.
- Zhao, L., Lu, X. and Sun, B. 1990. Toxic effects of organotin on marine diatoms. *J. Ocean Univ. Qingdao*, 20(4): 125-131.
- Zhou, M., Li, Z., Yan, T. and Li, J. 1994. Organotin in marine environment and its effects on marine organisms. *Adv. Environ. Sci.*, 2(4): 67-75.
- Zhu, W., Guo, R. and Yang, J. 2009. Effect of endocrine disruptors fenvalerate and TBTC on reproduction of rotifer *Brachionus calyciflorus*. *ACTA Ecol. Sin.*, 29(7): 3605-3612.



Characterization of the Biochar Derived from Peanut Shell and Adsorption of Pb(II) from Aqueous Solutions

Chunxia Hu* and Muqing Qiu**†

*College of Pharmacy and Health, Shaoxing University Yuanpei College, Shaoxing, 312000, P.R. China

**College of Life Science, Shaoxing University, Shaoxing, 312000, P.R. China

†Corresponding author: Muqing Qiu

Nat. Env. & Poll. Tech.
Website: www.neptjournal.com

Received: 29-06-2018
Accepted: 21-09-2018

Key Words:

Industrial effluents
Pb(II)
Biochar
Peanut shell

ABSTRACT

With the rapid development of industrial activities, a large amount of industrial effluents containing heavy metals is released into the surface and underground waters. It is highly significant and urgent to develop efficient and cost-effective methods to remove heavy metals from contaminated water. Biochar has been widely used as an adsorbent for the removal of environmental pollutants. In this work, the biochar was derived from peanut shell. The research on the removal of Pb(II) ions in aqueous solution by the biochar was carried out. It can be concluded that the operational parameters, such as pH, contact time and initial concentration of the Pb(II) ions in aqueous solution, had an important effect on the removal of Pb(II) ions. The Langmuir and the Freundlich models were utilized to explain the experimental data. According to results, the adsorption process fitted to the Langmuir model. It was also suggested that the adsorption process was homogeneous adsorption. The Pb(II) in aqueous solution adsorption on the biochar was monolayer adsorption.

INTRODUCTION

With the rapid development of industrial activities, a large amount of industrial effluents containing heavy metals are released into the surface and underground waters. These industrial effluents have resulted in a number of environmental problems (Barakat 2011). Heavy metals, such as lead, copper and cadmium are toxic and non-biodegradable, they can accumulate in living organisms, and may thus pose a threat to human health (Kumar et al. 2014). Therefore, it is very important to develop effective technologies to treat heavy metal polluted wastewaters before their discharge into the natural environment (Wang et al. 2015a).

Lead is especially known to be one of the most toxic metals among heavy metals, even at low concentrations in aquatic environments (Seyda et al. 2014). Current USEPA drinking water standard for lead is 300 µg/L. When present above 0.05 mg/L in drinking water, Pb(II) is a potent neurotoxic metal (Sag et al. 1965). Acute lead poisoning in humans affect the central nervous system, the gastrointestinal system, the liver and kidneys, and it can directly or indirectly cause serious health issues, such as anaemia, hepatitis, nephritic syndrome and encephalopathy (Järup 2003, Momcilovic et al. 2011).

It is highly significant and urgent to develop efficient and cost-effective methods to remove heavy metals from

contaminated water. Heretofore, a few classical treatment technologies have been constantly applied and optimized for heavy metal removal from water, including chemical precipitation (Janyasuthiwong et al. 2015, Matthew et al. 2002), adsorption, electro coagulation (Al-Shannag et al. 2015, Elabbas et al. 2016), and membrane filtration (Wang et al. 2013, Mehdipour et al. 2015). Among these technologies, adsorption has been generally regarded as a facile, effective technique for low level heavy metal sequestration, especially for tertiary treatment. From a generic viewpoint, the design of an adsorbent with specific binding sites for heavy metal capture has significant importance. Biochar has been widely used as an adsorbent for the removal of environmental pollutants (Tan et al. 2015). Its feedstocks derived from biomass materials including food waste, sewage sludge, peanut shell, corn stalk, sawdust and other agricultural wastes, which are considered worthless waste. Particularly, modified biochars have a large surface area, fine porous structure and abundant functional groups, which were widely reported as the effective environmental remediation agent for contaminants in polluted soil or wastewater (Zhou et al. 2014).

In this study, the biochar derived from peanut shell was used as a biosorbent for the removal of Pb(II) ions in aqueous solution. In order to enhance the peanut shell, it was treated by K₂CO₃ solution. The operational parameters such

as pH, contact time and initial concentration of the Pb(II) ions in aqueous solution, were investigated. The experimental data were discussed using Langmuir and Freundlich models.

MATERIALS AND METHODS

Materials: The peanut shell was obtained from a local farm in Zhejiang province. The peanut shell was first dried for 24h at 383 K in a heating oven. Then, the dried peanut shell was milled to obtain a powder between 1 mm and 2 mm prior to use. A 40 g of peanut shell was immersed in 100 mL of 2% K_2CO_3 solution for 12 h. The mixture was dried at 353 K for 24h. Then, the mixture was put into the muffle furnace at 873 K for 3 h. It was added then into a 250 mL flask containing 7 mL of distilled water. The flask was put into the thermostat water bath and agitated for 2h at 353 K. It was dried for 9h at 383 K in the heating oven and then washed by the distilled water into pH value ranging from 7 to 9. It was dried for 5h at 383 K in the heating oven again and then ground and sifted into 100 meshes for adsorption experiment.

All the chemicals and reagents used in this work were of analytical grade and solutions were prepared using deionized water. The wastewater of Pb^{2+} ion was prepared with the $Pb(NO_3)_2$.

Experimental methods: Adsorption experiments were conducted in a set of 250 mL Erlenmeyer flasks containing the biochar and 100 mL of Pb^{2+} ion solutions with various initial concentrations. The initial pH was adjusted with 1 mol/L HCl or 1 mol/L NaOH. The flasks were placed in a shaker at a constant temperature and 200 rpm. The samples were filtered and analysed.

Analytical methods: The textural characteristics of the biochar including surface area, pore volume and pore size distribution were determined by standard N_2 -adsorption technique. Surface morphology of the samples was determined by scanning electron microscopy (SEM) equipped with an energy dispersive X-ray fluorescence spectroscopy (EDS, Oxford Instruments Link ISIS) for analysing surface elements. The biochar was also characterized by FTIR spectroscopy to identify the type of chemical bonds present in the molecules. The concentration of Pb^{2+} ion was analysed by atomic absorption spectrophotometry (AAS).

The amount of adsorbed Pb^{2+} ion q_t (mg/g) at different times, was calculated as follows:

$$q_t = \frac{(C_0 - C_t) \times V}{m} \quad \dots(1)$$

Where, C_0 and C_t (mg/L) are the initial and equilibrium liquid-phase concentrations of Pb^{2+} ion respectively. V (L)

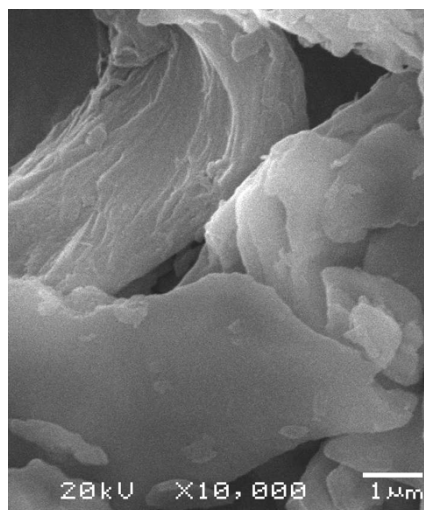


Fig.1: SEM image of the biochar.

is the solution volume and $m(g)$ is the mass of adsorbent used.

Statistical analyses of data: All the experiments were repeated in duplicate and the data of results were the mean and the standard deviation (SD). The value of the SD was calculated by Excel software. All error estimates given in the text and error bars in figures are the standard deviation of means (mean \pm SD). All statistical significances were noted at $\alpha=0.05$ unless otherwise stated.

RESULTS AND DISCUSSION

Characterization of the biochar: The SEM images of the surface morphologies of the biochar are shown in Fig. 1. They all have a fully developed and smooth structure in micron-size. As from Fig. 2, the SEM-EDS analysis confirmed the occurrence of K element on the surface of the biochar. The C, O, Al and Si contents of the biochar were 65.49%, 34.05%, 0.13% and 0.15%, respectively.

The biochar also exhibited a high BET specific surface area, total pore volume and micropore volume values. The values are 2.79 m^2/g , 0.003 cm^3/g and 0.0035 cm^3/g respectively.

The structures of the biochar were analysed with FTIR. Fig. 3 shows the FTIR spectra of the biochar in the near IR region (wave number: 4000-400 cm^{-1}).

As shown from Fig. 3, the spectra of the biochar include a band at 3900 cm^{-1} to 4000 cm^{-1} , which is mostly related to the presence of a -O-H- functional group on the surface. The broad band centered at approximately 3900 cm^{-1} . It is attributed to the -O-H- stretching vibration which indicates significant hydrogen-bonding interactions. The peak at

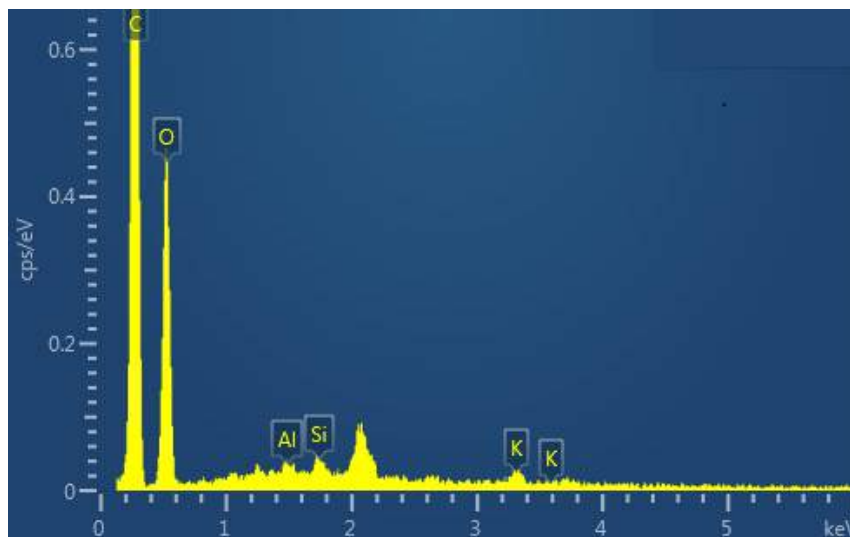


Fig. 2: EDS image of the biochar.

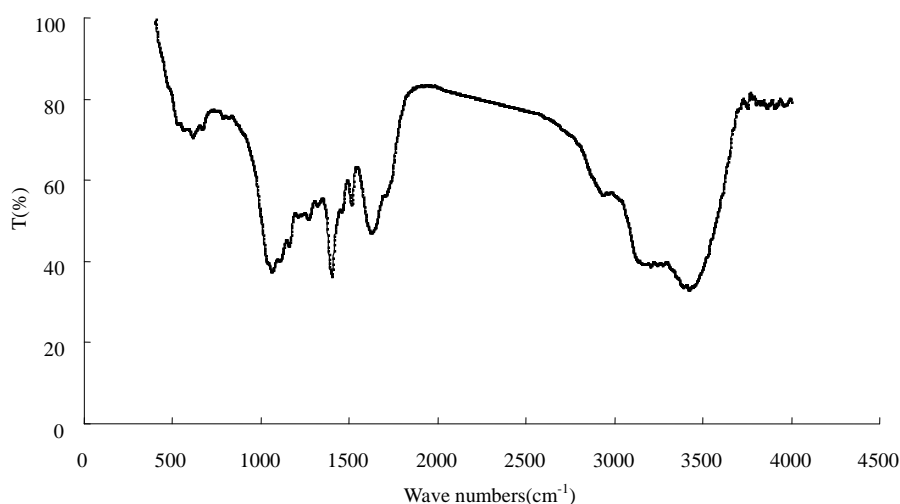


Fig. 3: FTIR spectra of the biochar.

3122 cm^{-1} is attributed to $-\text{C}=\text{C}-\text{H}$ stretching of the functional groups. The peak at 1620 cm^{-1} can be assigned to the $-\text{C}=\text{C}-$ stretching of benzene ring group. The bands at 1500 and 1060 cm^{-1} may indicate the presence of the inorganic compounds, such as carbonates and silica compounds. When the wave number is under 612 cm^{-1} , it is thought to be the fingerprint region which is related to phosphate and sulphur functional groups.

Effect of pH: It is well known that the pH of the solution is one of the most important parameters in the removal of heavy metals from aqueous solutions. In this study, the effect of pH on the biosorption of Pb(II) ions on the biochar derived from the peanut shell was investigated. These experiments

were carried out by changing the initial pH of the solution from 2.0 to 6.0. The pH dependent experiments were not conducted at a pH value higher than 6.0 to avoid the precipitation of Pb(II) ions as hydroxide. The contact time is 240 minutes. The dosage of the biochar is 0.4 g. The concentration of Pb(II) ions in solution is 200 mg/L. The effect of pH in solution on the removal of Pb(II) ions by the biochar is shown in Fig. 4.

Removal of Pb(II) ions (%): From Fig. 4, it can be concluded that the pH had an important role on the removal of Pb(II) ions by the biochar. The removal of Pb(II) ions was increased with the increasing the pH. The increase in pH would promote the removal the heavy metals. Some studies

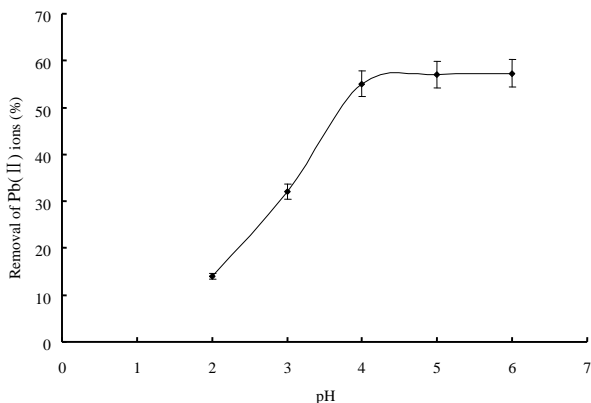


Fig. 4: Effect of pH on the removal of lead ions by the biochar.

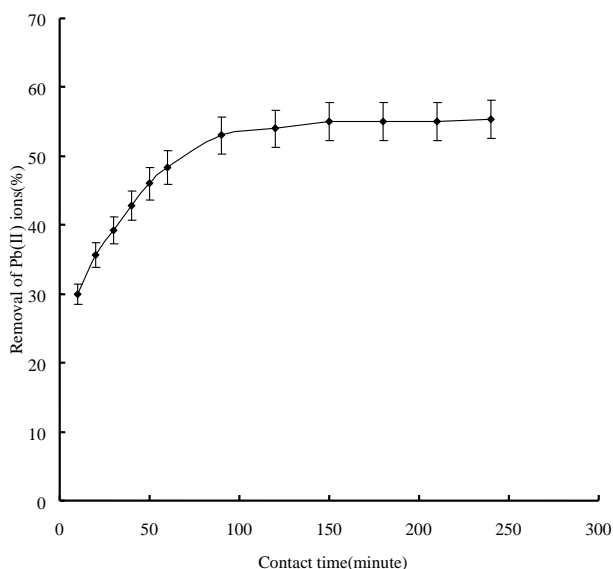


Fig. 5: Effect of contact time on the removal of lead ions by the biochar.

have shown that pH-dependent surface charges play an important role in controlling the surface adsorption of heavy metal ions through electrostatic interactions (Wang et al. 2015b). The removal of Pb(II) ions by the biochar is very low at the pH 2.0. It may be explained on the basis of electrostatic repulsion forces between positively charged H_3O^+ and Pb^{2+} ions (Ozer 2007). There are no significant differences in the removal of Pb(II) ions at the pH values between 4.0 and 6.0. When the pH value increased, the covered H_3O^+ left the biochar surface and made the sites available to Pb(II).

Effect of contact time: The contact time is one of the important parameters in the process of adsorption. The dosage of the biochar is 0.4 g and the concentration of Pb(II) ions in solution is 200 mg/L. The value of pH was adjusted to 4.0. The relationship of removal of the Pb(II) ions with contact

time is shown in Fig. 5.

From Fig. 5, it can be shown that the biosorption is relatively rapid in the initial 60 minutes, because the biosorption sites were vacant, and Pb(II) could easily interact with these sites. In addition, the biosorption efficiency increased with contact time. After 120 minutes, the biosorption efficiency was almost constant such that it could be considered the equilibrium time of the Pb(II) biosorption.

Effect of the initial concentration of the Pb(II) ions in aqueous solution: The initial concentration of the Pb(II) ions in aqueous solution had an important role on the removal of Pb(II) ions in aqueous solution by the biochar. The experiments were investigated at pH 4.0, contact time of 180 minutes and the dosage of biochar of 0.4 g. The initial concentration of Pb(II) ions in aqueous solution was ranged from 100 mg/L to 400 mg/L. The experimental results are shown in Fig. 6.

Removal of Pb(II) ions (%): The removal of Pb(II) ions in aqueous solution is decreasing with the increasing initial concentration of Pb(II) ions. This result caused lower biosorption yields at the higher concentrations due to the saturation of the biosorption sites. This increase could be due to the increase in electrostatic interactions (related to covalent interactions), involving sites of progressively lower affinity for Pb(II) ions in aqueous solution. Therefore, more Pb(II) ions in aqueous solution were left un-biosorbed in solution at higher concentration levels. These results were in agreement with the results of previous studies (Dhankhar et al. 2011, Karthika et al. 2010).

The adsorption isotherm of Pb(II) ions in aqueous solution by the biochar: It is known that the equilibrium biosorption isotherm is fundamentally important in the design of a biosorption system, because equilibrium studies of biosorption are used to determine the capacity of the biosorbent. The biosorption equilibrium is established, when the concentration of sorbate in bulk solution is in dynamic balance with that on the liquid-sorbent interface. The relationship between the initial concentration and the amount of sorbent is known as the degree of the sorbent affinity for the sorbate which determines its distribution between the solid and liquid phases. Several models are often employed to interpret the equilibrium data. In the present research, the Langmuir and the Freundlich models were utilized to explain the experimental data. The Langmuir model and Freundlich model of linear forms are as below (Liu and Zhang 2011):

$$\frac{C_e}{q_e} = \frac{1}{K_L q_{\max}} + \frac{C_e}{q_{\max}} \quad \dots(2)$$

Table 1: The adsorption parameters for Pb²⁺ ions adsorption from aqueous solution on the biochar by Langmuir adsorption isotherm and Freundlich isotherm.

Langmuir parameters			Freundlich parameters		
q_{max} (mg/g)	K_L (L/mg)	R^2	n	K_F	R^2
111.11	0.11	0.9951	909.09	82.24	0.3998

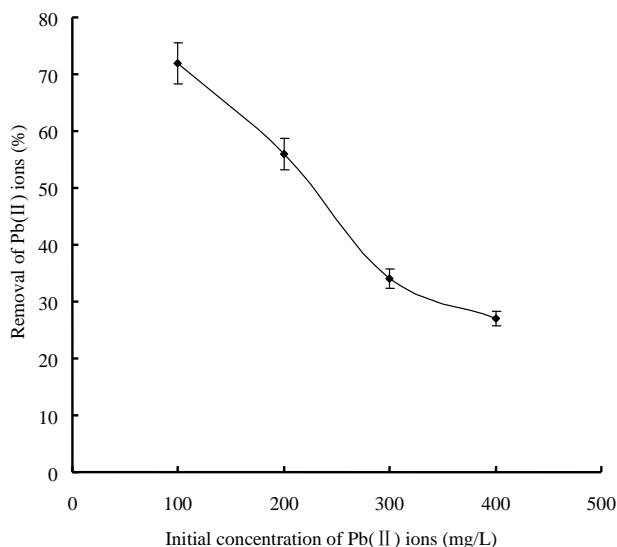


Fig. 6: Effect of initial concentration of the Pb(II) ions in aqueous solution on the removal of lead ions by the biochar.

$$\ln q_e = \ln K_F + \frac{1}{n} \ln C_e \quad \dots(3)$$

Where, C_e (mg/L) is the equilibrium concentration in the solution, q_e (mg/g) is the adsorbate adsorbed at equilibrium, q_{max} (mg/g) is the maximum adsorption capacity, n is the Freundlich constant related to adsorption intensity, K_L (L/mg) and K_F ((mg/g)^{1/n}) are the adsorption constants for Langmuir and Freundlich models respectively.

According to the experimental data, the adsorption parameters were obtained from the Langmuir adsorption isotherm and Freundlich adsorption isotherm (Table 1).

It showed that the Langmuir adsorption isotherm model is more suitable for the Pb²⁺ ion from aqueous solution than the Freundlich adsorption isotherm model. It is also suggested that the adsorption process is homogeneous adsorption. The Pb²⁺ ion from aqueous solution adsorption on the biochar is monolayer adsorption.

CONCLUSIONS

In this study, the research on the removal of Pb(II) ions in aqueous solution by the biochar derived from peanut shell

was carried out. The biochar has a fully developed and smooth structure in micron-size. According to the experimental results, the biochar showed much better adsorption ability to Pb(II) ions in aqueous solution. The adsorption of Pb(II) in aqueous solution on the biochar was monolayer adsorption. The biochar derived from peanut shell can be used to remove Pb(II) ions in aqueous solution efficiently.

ACKNOWLEDGEMENT

This study was financially supported by the project of science and technology plan in Shaoxing City (2017B70058).

REFERENCES

Al-Shannag, M., Al-Qodah, Z., Bani-Melhem, K., Qtaishat, M.R. and Alkasrawi, M. 2015. Heavy metal ions removal from metal plating wastewater using electrocoagulation: Kinetic study and process performance. *Chem. Eng. J.*, 260: 749-756.

Barakat, M.A. 2011. New trends in removing heavy metals from industrial waste water. *Arab. J. Chem.*, 4(4): 361-377.

Dhankhar, R., Hooda, A., Solanki, R. and Samger, P.A. 2011. *Saccharomyces cerevisiae*: A potential biosorbent for biosorption of uranium. *Int. J. Eng. Sci. Tech.*, 3(6): 5397-5407.

Elabbas, S., Ouazzani, N., Mandi, L., Berrekhis, F., Perdicakis, M., Pontvianne, S., Pons, M.N., Lapique, F. and Leclerc, J.P. 2016. Treatment of highly concentrated tannery wastewater using electrocoagulation: Influence of the quality of aluminium used for the electrode. *J. Hazard. Mater.*, 319: 69-77.

Järup, L. 2003. Hazards of heavy metal contamination. *Brit. Med. Bull.*, 68: 167-182.

Janyasuthiwong, S., Rene, E.R., Esposito, G. and Lens, P.N.L. 2015. Effect of pH on Cu, Ni and Zn removal by biogenic sulfide precipitation in an inverted fluidized bed bioreactor. *Hydrometallurgy*, 158: 94-100.

Karthika, T., Thirunavukkarasu, A. and Ramesh, S. 2010. Biosorption of copper from aqueous solutions using *Tridax procumbens*. *Recent Res. Sci. Tech.*, 2(3): 86-91.

Kumar, R., Rani, M., Gupta, H. and Gupta, B. 2014. Trace metal fractionation in water and sediments of an urban river stretch. *Chem. Speciation Bioavailability*, 26(4): 200-209.

Liu, Z.G. and Zhang, F.S. 2011. Removal of copper(II) and phenol from aqueous solution using porous carbons derived from hydrothermal chars. *Desalination*, 267: 101-106.

Matthew, M., Matlock, B.S.H. and David, A.A. 2002. Chemical precipitation of heavy metals from acid mine drainage. *Water Res.*, 36: 4757-4764.

Mehdipour, S., Vatanpour, V. and Kariminia, H.R. 2015. Influence of ion interaction on lead removal by a polyamide nanofiltration membrane. *Desalination*, 362: 84-92.

- Momcilovic, M., Purenovic, M., Bojic, A., Zarubica, A. and Randelovic, M. 2011. Removal of lead(II) ions from aqueous solutions by adsorption onto pine cone activated carbon. *Desalination*, 276: 53-59.
- Ozer, A. 2007. Removal of Pb(II) ions from aqueous solutions by sulphuric acid-treated wheat bran. *J. Hazard. Mater.*, 141: 753-761.
- Sag, Y., Ozer, D. and Kutsal, T. 1995. A comparative study of the biosorption of Lead(II) ions to *Z. ramigera* and *R. arrhizas*. *Process Biochem.*, 30: 169-174.
- Seyda, T., Fatih, K. and Ozer A. 2014. Biosorption of lead(II) ions from aqueous solution by peanut shells: Equilibrium, thermodynamic and kinetic studies. *J. Envir. Chem. Eng.*, 2: 1018-1026.
- Tan, X., Liu, Y., Zeng, G., Wang, X., Hu, X., Gu, Y. and Yang, Z. 2015. Application of biochar for the removal of pollutants from aqueous solutions. *Chemosphere*, 125: 70-85.
- Wang, H.Y., Gao, B., Wang, S.S., Fang, J., Xue, Y.W. and Yang, K. 2015a. Removal of Pb(II), Cu(II), and Cd(II) from aqueous solution by biochar derived from KMnO_4 treated hickory wood. *Biores. Tech.*, 197: 356-362.
- Wang, S.S., Gao, B., Zimmerman, A.R., Li, Y.C., Ma, L., Harris, W.G. and Migliaccio, K.W. 2015b. Removal of arsenic by magnetic biochar prepared from pinewood and natural hematite. *Bioresour. Technol.*, 175: 391-395.
- Wang, R., Guan, S., Sato, A., Wang, X., Wang, Z., Yang, R., Hsiao, B.S. and Chu, B. 2013. Nanofibrous microfiltration membranes capable of removing bacteria, viruses and heavy metal ions. *J. Membr. Sci.*, 446: 376-382.
- Zhou, Y., Gao, B., Zimmerman, A.R., Chen, H., Zhang, M. and Cao, X. 2014. Biochar supported zero valent iron for removal of various contaminants from aqueous solutions. *Bioresour. Technol.*, 152: 538-542.



Biodegradation of Sludge Produced from Common Effluent Treatment Plant (CETP) Using Drum Composting Technique

Seema Maheshwari*, Ajay Singh Jethoo**, Vinod Kumar Vishvakarma**, Meena Khwairakpam*** and Prashant Kriplani*

*Department of Chemistry, Govt. Women Engineering College, Ajmer-305 002, India

**Department of Civil Engineering, Malviya National Institute of Technology, Jaipur-302 017, India

***Department of Civil Engineering, National Institute of Technology, Meghalaya-793 003, India

Nat. Env. & Poll. Tech.

Website: www.neptjournal.com

Received: 30-05-2018

Accepted: 02-08-2018

Key Words:

Biodegradation
Common effluent treatment plant
Rotary drum composting
Sludge
Volatile solids

ABSTRACT

Composting of sludge is suitable waste management option as it maintains all essential physico-chemical parameters, stability parameters and maturity parameters as per standard norms. The present study was carried out to investigate the applicability of the rotary drum composting technique for the stabilization of sludge from a Common Effluent Treatment Plant (CETP). Rotary drum composting was performed in two runs i.e., winter run and summer run. During the whole composting period in the two runs, the continuous monitoring of the physico-chemical parameters like temperature, pH, electrical conductivity, volatile solids, total organic carbon, ash content, $\text{NH}_4^+\text{-N}$, $\text{NO}_3^-\text{-N}$ and phosphorus was made. All these parameters are in the agreement with recommended standards of the mature compost. It can be concluded that rotary drum composting could produce acceptable quality of compost which can be used further as fertilizer or soil amendment.

INTRODUCTION

Disposal of industrial sludge is becoming a great challenge to industries due to high cost of sludge stabilization reactors, dehydration systems and transportation of sludge to disposal site. There is no use of hazardous sludge produced in common effluent treatment plants due to presence of heavy metals, high COD and BOD, low pH, high TDS and TSS. It can only be disposed off in landfills which creates many problems in nearby soil by destroying soil fertility and changing in soil chemistry, land degradation, contaminate surface and ground water and also affect public health. During the recent years, the methodology of sludge management shifted from conventional methods such as incineration and landfill to the conversion of sludge into nutrient rich products. Composting technology seems to be a reliable alternative method for managing Industrial waste and for production of stabilized organic matter (Hajia et al. 2012). The understanding of organic matter transformation throughout the composting process and proper evaluation of the quality of compost from maturity and stability viewpoint are essential for successive utilization of compost. Mokhtari explained the method to evaluate the stability indices in municipal solid waste composting for selecting the best index in quality monitoring of the wastes (Mokhtari et al. 2011). In addition to this, physico-chemical and biological characteristics of municipal solid waste at different stages were informed by Shymala and group (Shymala et al.

2012). Dhal et al. (2012) reported composting of water hyacinth using saw dust/rice straw as a bulking agent (Dhal et al. 2012). Composting of tannery wastes in an ecofriendly method, focused mainly on the heavy metal characterization, was explained by Ahmed et al. (2007). Ashbolt et al. (1982) conducted bench scale system studies for composting of organic waste. Kalamdhad et al. (2012) studied organic matter transformation during pilot scale rotary drum composting for different C/N ratios for the mixture of grass cutting mix vegetables waste, cattle manures and saw dust. Characterization of the sludge generated from paper, sugar and agro oil industries to assess its agro potential to consider as fertilizer substitute was established by Machiraju et al. (2011). Maturity and stability parameters of compost prepared with a wide range of organic waste were explained by Bernal et al. (1997).

Due to industrialization lots of waste is produced, posing a problem for their disposal. So the purpose of the present work is the production of stabilized, matured compost by rotary drum composting technology using sludge of Common Effluent Treatment Plant (CETP) and to evaluate physico-chemical and stability parameters of industrial solid waste.

MATERIALS AND METHODS

The chemicals, used during the course of present work were purchased from E. Merck. The reactor was placed inside old

Hydraulics Lab and analysis was carried out at Environmental Engineering Lab, MNIT Jaipur and Agricultural Research Lab, Durgapura, Jaipur during winter and summer season (January to April). The main material used in the study included a rotary drum composter, CETP sludge, cow-dung and sawdust. Sludge was collected from hazardous waste storage site at common effluent treatment plant, Bhiwadi, District Alwar, Rajasthan, where effluents come from various industries such as aluminium, lead, battery, carbon black, steel bars, chemicals, sun glass, edible oils, wire and cable industries, etc. The bulking agent saw dust was collected from a wood shop and cow dung from the H-Quarters at MNIT Jaipur. The biological and physico-chemical analysis of the compost samples collected from the drum composter were carried out in PHE laboratory, Civil Engineering Department MNIT and Agricultural Research Laboratory, Durgapura. The physico-chemical and biological parameters were analysed, by the methods described in APHA, AWWA, WEF (1995). The initial parameters of different ingredients for composting of sludge with saw dust and cow dung with different combinations according to C/N ratios are given in Table 1.

The sludge, cow-dung and sawdust were mixed into the drum by means of a metal container and it can be filled up to 50 % of the total volume, but capacity of filling volume could be further increased up to 70%. Aerobic conditions were maintained by opening up both half side doors of the drum after a certain period of rotation which ensures proper mixing and aeration. Different combinations of ingredients were calculated by online calculator in Cornell University website. The study was conducted in two runs: Run 1: C/N ratio 25.1037 (in winter season) Run 2: C/N ratio 30.1 (in summer season). A good composting process requires that the temperature, oxygen and moisture levels be maintained uniform throughout the compost matrix. Therefore, the side doors of the drum were kept closed, two rotations were provided manually on a daily basis, whereas the doors were kept open for the rest of the time for aeration.

RESULTS AND DISCUSSION

Stabilized, matured compost by rotary drum composting technology was produced from sludge of a Common Effluent Treatment Plant (CETP) followed by physico-chemical analysis of various parameters. There are two distinct phases in the composting system: the active stabilisation phase and the maturation period. In this study both the phases were undertaken in the rotary drum by adjusting aeration by means of the rotation process. In context to the composting process, the key function of the rotation was to expose the composting material to air, provide oxygen and release the heat and gaseous products of decomposition.

Table 1: Initial parameters of different ingredients for composting process.

Parameter	Sludge	Cow dung	Saw dust
pH	8.44	8.3	6.95
E.C. (mS/cm)	2.73	1.01	0.83
M.C. (%)	73.25	55.75	16.75
V.S. (%)	44.47	78.23	84.1
Ash Content (%)	55.53	21.77	15.9
TOC (%)	24.9	43.8	47.09
TKN (%)	1.22	1.56	0.89
NH ₄ ⁺ -N (g/kg)	0.092	0.158	0.041
NO ₃ ⁻ -N (g/kg)	0.877	0.332	0.121
P (g/kg)	5.61	4.76	8.26

The moisture adjusted composting material was supplied to the rotating drum for fermentation. Inside the drum, the tumbling action mixed and agitated the material. The physico-chemical parameters at different stages during composting are presented in Table 2.

PHYSICO-CHEMICAL PARAMETERS DURING COMPOSTING

Temperature: The temperature observations were made at three different locations in the composter, i.e. at its centre and at two ends. Variation of temperature of the composting material with time is illustrated in Fig. 1. Actually, two runs were performed in different seasons, i.e. Run 1 in winter and Run 2 in summer, so initially temperature was 15.1°C and 22.3°C in Run 1 and Run 2 respectively.

The gradual increment in temperature showed the increase in microbial activity. The final temperature increased up to 30.1°C in Run 1 and 38.9°C in Run 2. Here, there is sharp increase in temperature in Run 2 from 15 to 27 days than Run 1. This could be because of the seasonal variation but study shows that the rate of decomposition was higher in Run 2 than Run 1.

pH: pH is a measure of acidic or alkaline nature of compost with the progress of composting. pH values varied from 6.98 to 8.39 in Run 1, and 7.76 to 8.32 in Run 2 in the first week of the experiment. At the end of the composting period, final pH values were measured as 7.03 and 7.06 in Run 1 and Run 2, respectively. The optimum pH values are 6 to 7.5 for bacterial development, while fungi prefer an environment in the range of 5.5 to 8.0 (Kapetanios et al. 1993). The pH was initially low due to the acid formation, then it increased and at the latter stage became constant. Slight increase in pH level during the composting process could be due to release of ammonia from protein degradation (Liao et al. 1996).

Electrical conductivity: Electrical conductivity value reflects the degree of salinity during the composting and in-

Table 2: Comparative study of physico-chemical parameters in Run 1 and Run 2 during composting.

Days Parameters	6 Days		12 Days		18 Days		24 Days		30 Days	
	Run 1	Run 2	Run 1	Run 2	Run 1	Run 2	Run 1	Run 2	Run 1	Run 2
Temperature (°C)	20.2	26.1	24.4	27.4	26.9	29.6	28.1	34.9	29.5	37.9
pH	8.39	8.41	7.94	8.51	8.3	8.34	7.13	7.42	7.03	7.06
EC (mS/cm)	1.8	2.47	2.27	2.5	2.08	2.28	2.36	2.04	2.46	2.98
Ash content (%)	62.24	51.99	62.46	54.55	64.99	54.78	67.81	54.56	69.96	55.02
Volatile solids (%)	37.76	48.01	37.54	45.45	35.01	45.22	32.19	45.44	30.04	44.98
Ammonia-N (g/kg)	0.056	0.123	0.055	0.071	0.044	0.063	0.038	0.059	0.018	0.048
Nitrate-N _i (g/kg)	0.066	0.118	0.093	0.165	0.117	0.188	0.136	0.256	0.178	0.308
TOC (%)	21.145	26.885	21.022	25.452	19.605	25.323	18.026	25.446	16.822	25.189
Phosphorus (%)	2.835	3.897	6.935	3.595	8.52	5.15	7.595	8.035	8.63	12.02

dicates its possible phytotoxicity effect on growth of plants if applied to the soil. Electrical conductivity is the measure of a solution’s ability to carry electrical charge, i.e. a measure of the soluble salt content of compost. The salt content of compost is due to the presence of sodium, chloride, potassium, nitrate, sulphate and ammonium salts (Brinton 2003). During the study, electrical conductivity values varied between 1.79 mS/cm and 2.46 mS/cm in Run 1 and 1.82 to 2.98 mS/cm in Run 2. As suggested by Campell, the increase in the electrical conductivity during the process of composting could be due to the effect of the concentration of salts as a consequence of degradation of organic matter (Campell et al. 1997). It was found that the increased electrical conductivity shows the availability of macronutrients and major cations in compost, which was higher in run 2 than Run 1 as shown in Fig. 2.

Total organic carbon: During the composting process organic matter is decomposed and transformed to stable humic substances (Prasad et al. 2013). The Fig. 3 shows the trend of organic matter degradation during 30 day composting process in two different runs. The content of organic matter was decreased as the decomposition progressed as from 21.36 % to 16.82 % in Run 1 and 27.87 % to 25.19 % in Run 2. So in Run 1 there was greater reduction in TOC and hence greater decomposition can be predicted. As per TOC data, observed rate of decomposition, and hence, rate of the volatilization is greater in Run 1 than in Run 2 as shown in Fig. 3.

Ammonia nitrogen: Ammonia concentration is an important indicator of compost stability and maturity. Mostly ammonia nitrogen present during aerobic composting is derived from rapidly decomposing waste. When ammonia concentration decreases and nitrate appears in composting material, it is considered ready to be used as compost. It has been noted that the absence or decrease in NH₄⁺-N is an indicator of a high-quality composting process (Hirai et al. 1983). Initially in Run 1, ammonia nitrogen concentration

was 0.085 g/kg and finally reached up to 0.018 g/kg. On the other side, ammonia nitrogen concentration was decreased from 0.134 to 0.048 in Run 2 showing the maximum limit suggested by Zucconi (Zucconi et al. 1987) for a mature compost (Fig. 4).

Nitrate-nitrogen: Nitrate-N concentration rises gradually during composting and is a limited factor in assessing compost maturity. Morisaki et al. (1989) also reported that the major decrease of ammonia nitrogen occurred after thermophilic stage leading to an increase of nitrate concentration through nitrification. In aerobic composting process, the percentage conversion of ammonia to nitrate was higher than others due to continuous aeration of compost. Haug (1993) stated that during the composting process, the appearance of appreciable quantities of nitrate could indicate the acceptable maturity of compost. Initially, nitrate concentration was 0.0325 g/kg in Run 1 and 0.1012 g/kg in Run 2. Slight variations were observed in the values of nitrate nitrogen during the study period. After 30 days, the final nitrate nitrogen was found to be 0.178 g/kg in Run 1 and 0.308 g/kg in Run 2. Net increase in nitrate concentration was observed to be 0.146 g/kg and 0.207 g/kg in Run 2. So it can be predicted that Run 2 has better quality compost with the higher nitrate-N content (Fig. 4).

Volatile solids: The content of organic matter was decreased as the decomposition progressed. The Fig. 5 shows the trend of volatilization during 30-day composting process in two different runs. The final VS were observed to be 30.04 % in Run 1 and 44.98 % in Run 2. So, there was net reduction of 7.74 % of VS in Run 1, and 4.78 % in Run 2. So, in Run 1 there was greater reduction in VS, and hence, greater decomposition or volatilization can be predicted. As per VS data, observed rate of decomposition, and hence, rate of the volatilization is greater in Run 1 than in Run 2.

Ash content: The ash content is an important indicative parameter for decomposition and mineralization of the substrate. Ash content was observed to be increasing with

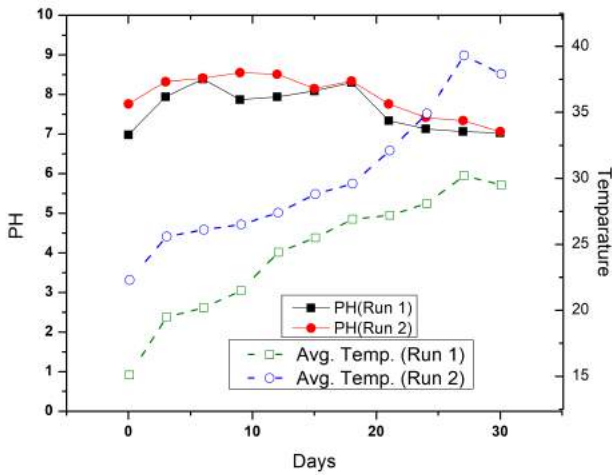


Fig. 1: Variation in pH and temperature in Run 1 and Run 2 during composting.

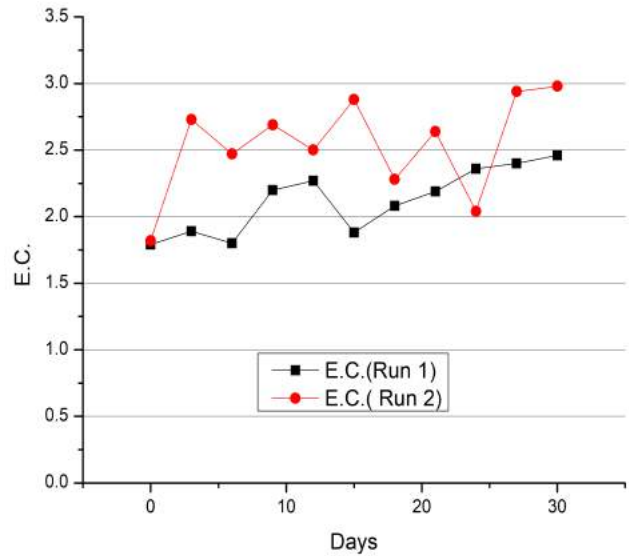


Fig. 2: Variations in E.C. in Run 1 and Run 2 during composting.

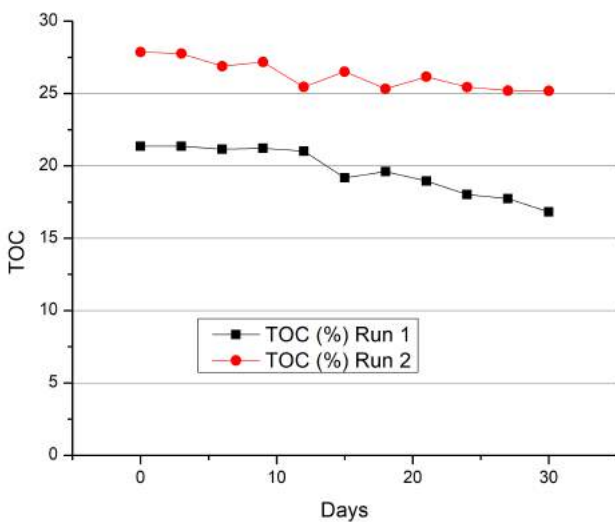


Fig. 3: Variations in TOC in Run 1 and Run 2 during composting.

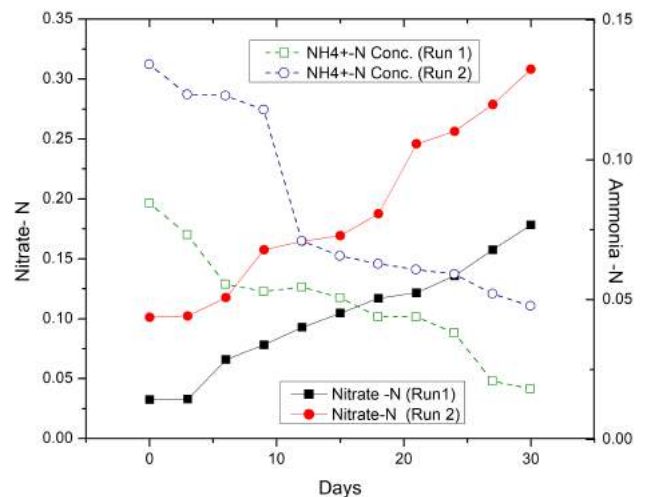


Fig. 4: Variations in Nitrate-N and Ammonia-N in Run 1 and Run 2 during composting.

increase in composting time as shown in graph (Fig. 6). There was 8.1 % increment of ash content in Run 1, and 4.78 % in Run 2. So, Run 1 showed greater rate of volatilization and simultaneous increase in ash content than Run 2. During initial to 5 days, Run 1 shows slow rate of volatilization, but after fifth day volatilization rate increases, and hence, ash content also increases. But Run 2 showed gradual increment in ash content, and hence, volatilization. Similar observations have also been reported by Singh et al. (2005).

Phosphorus: Phosphorus is a macronutrient important for plant growth and maintenance, so it is important in compost. Kalamdhad et al. (2012) suggested that phosphorus in

organic matter is released by mineralization process by the microorganisms. Inorganic phosphorus is negatively charged and after the reaction with positively charged iron (Fe), aluminium (Al) and calcium (Ca) ions forms relatively insoluble complexes. When this happens, the phosphorus is considered fixed or immobile. In this context, phosphorus does not behave like nitrate, which is also negatively charged, but does not form insoluble complexes. In Run 1, phosphorus concentration varied from 2.38 g/kg to 8.63 g/kg. In Run 2, phosphorus concentration varied from 3.59 g/kg to 12.02 g/kg. There was 37.19 % increased in phosphorus concentration in Run 1, and 59.08 % in Run 2. So, Run 2 performed

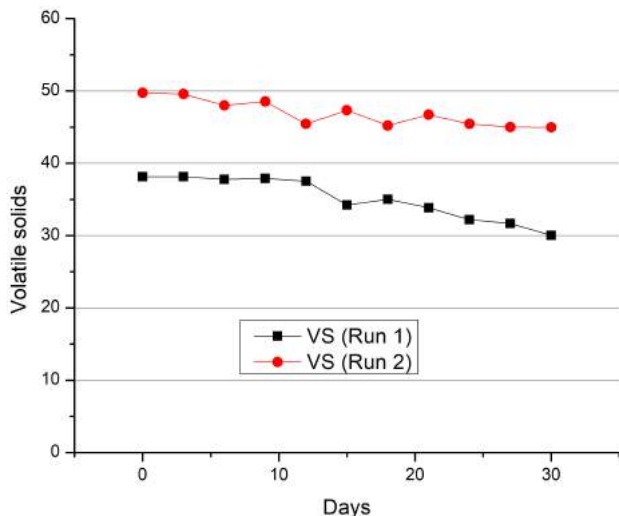


Fig. 5: Variations in volatile solids in Run 1 and Run 2 during composting.

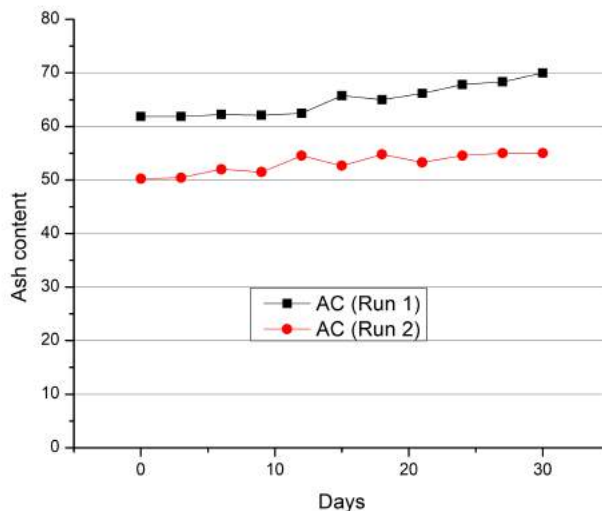


Fig. 6: Variations in ash content in Run 1 and Run 2 during composting.

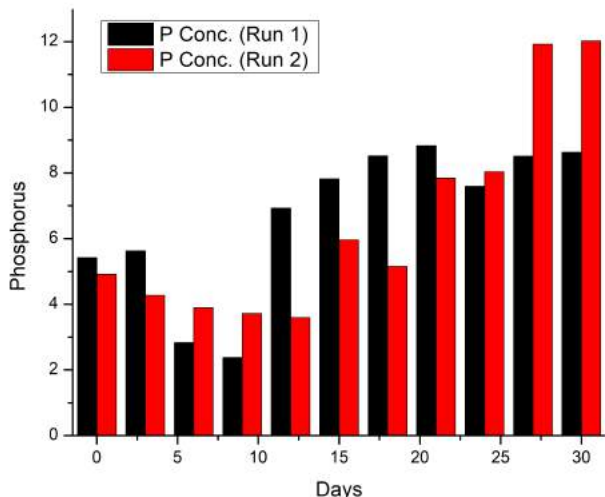


Fig. 7: Variations in phosphorus in Run 1 and Run 2 during composting.

better than Run 1 as greater increase in phosphorus was observed in Run 2, and hence, greater mineralization (Fig. 7).

CONCLUSIONS

The results of the study clearly indicate that rotary drum composting technique can transform the sludge produced from common effluent treatment plants (CETPs) into suitable compost. Physico-chemical analysis of compost from the view point of parameters like temperature, pH, ash content, volatile solids, ammonia nitrogen, nitrate nitrogen, electrical conductivity and phosphorus agreed with recom-

mended levels. The physico-chemical parameters suggest rotary drum composting method as suitable waste management option. In produced compost, level of phosphorus substantially increased, whereas the level of TOC substantially decreased. The composting of CETP sludge produced a good quality compost with pH (neutral though slightly acidic or alkaline pH), electrical conductivity (avg. 2.12 mS/cm in Run 1 and avg. 2.54 mS/cm in Run 2) and final total organic carbon of 9.02 % in Run 1 and 11.25 % in Run 2. pH and electrical conductivity were observed in suitable range, but TOC was less in both the runs as per recommendation by Official Journal of the European Community (Organic carbon 20 %). Gradual decrease in ammonia-N and simultaneously rise in nitrate-N was observed during composting suggest maturity of compost. Mineralization in terms of phosphorus content recommended the use of produced compost for plant growth. So, it was observed that based on physico-chemical parameters, nutrient and trace element analysis, and stability parameters, the performance of Run 2 (summer run) is better than Run 1 (winter run). In comparison to traditional composting, the rotary drum composting is more efficient way due to fast and mixing through rotating the drum.

ACKNOWLEDGEMENTS

Authors would like to thank Director, MNIT for providing research laboratory and necessary resources.

REFERENCES

Ahmed, M., Idris, A. and Omer, S.R.S. 2007. Physicochemical characterization of compost of the industrial tannery sludge. Journal

- of Engineering Science and Technology, 2(1): 81-94.
- Ashbolt, N.J. and Line, M.A. 1982. A Bench-Scale System to Study the Composting of Organic Wastes. *Journal of Environmental Quality*, 11(3): 405-408.
- Bernal, M.P., Paredes, C., Sanchez-Monedero, M.A. and Cegarra, J. 1997. Maturity and stability parameters of composts prepared with a wide range of organic wastes. *Bioresource Technology*, 63: 91-99.
- Biotreat, 2003. Interpretation of results report, National Food Biotechnological Centre, University College, Cork, Ireland.
- Bord na Mona 2003. Compost testing and analysis service interpretation of results, available from Bord na Mona, Newbridge, Co. Kildare.
- Brinton, W.F. 2003. Interpretation of waste and compost tests. *Journal of the Woods End Research Laboratory*, 1(4): 1-6.
- Campbell, A.G., Folk, R.L. and Tripepi, R.R. 1997. Wood ash as an amendment in municipal sludge and yard composting processes. *Compost Science and Utilization*, 5(1): 62-73.
- Dhal, G.C., Singh, W.R., Khwairakpam, M. and Kalamdhad, A.S. 2012. Composting of water hyacinth using saw dust/rice straw as a bulking agent. *International Journal of Environmental Sciences*, 2(3): 1223-1238.
- Hajia, M.S., Sadeghpour, M., Hadipour, M. and Najafpour, G. 2012. A comparison of vermi and aerobic technologies applied to manage textile industrial sludge and kitchen wastes. *World Applied Sciences Journal*, 19(6): 806-810.
- Haug, R.T. 1993. *The Practical Handbook of Compost Engineering*. Lewis publishers.
- Hirai, M.F., Chanyasak, V. and Kubota, H. 1983. A standard measurement for compost maturity. *Biocycle*, 24: 54-56.
- Kalamdhad, A.S., Khwairakpam, M. and Kazmi, A.A. 2012. Drum composting of municipal solid waste. *Environmental Technology*, 33(3): 299-306.
- Kapetanios, E.G., Loizidou, M. and Valkana, G. 1993. Compost production from Greek domestic refuse. *Bioresource Technology*, 43: 13-16.
- Liao, P.H., Jones, L., Lau, A.K., Walkemeyer, B.E. and Holbek, N. 1996. Composting of fish wastes in a full-scale in-vessel system. *Bioresource Technology*, 59: 163-168.
- Machiraju, P.V.S. and Murthy, Y.L.N. 2011. Industrial sludge as a fertilizer substitute. *International Journal of Pharma and Bio Sciences*, 2(1): B193-B199.
- Mokhtari, M., Nikaeen, M., Amin, M.M., Bina, B. and Hasanzadeh, A. 2011. Evaluation of stability parameters in in-vessel composting of municipal solid waste. *Iran. J. Environ. Health. Sci. Eng.*, 8(4): 325-332.
- Morisaki, N., Phae, C.G., Nakasaki, K., Shoda, M. and Kubota, H. 1989. Nitrogen transformation during thermophilic composting. *J of Ferment. Bioeng.*, 67: 51-61.
- Official Journal of the European Community 1998.
- Prasad, R., Singh, J. and Kalamdhad, A.S. 2013. Assessment of nutrients and stability parameters during composting of water hyacinth mixed with cattle manure and sawdust. *Research Journal of Chemical Sciences*, 3(4): 70-77.
- Shyamala, D.C. and Belagali, S.L. 2012. Studies on variations in physico-chemical and biological characteristics at different maturity stages of municipal solid waste compost. *International Journal of Environmental Sciences*, 2(4): 1984-1997.
- Singh, N.B., Khare, A.K., Bhargava, D.S. and Bhattacharya, S. 2005. Effect of initial substrate pH on vermicomposting using *Perionyx excavatus* (Perrier, 1872). *Applied Ecology and Environmental Research*, 4(1): 85-97.
- Zucconi, F. and de Bertoldi, M. 1987. Compost specifications for the production and characterization of compost from municipal solid waste. In *Compost: Production, quality and use*. Ed. M. de Bertoldi, M., Ferranti, M.P., L' Hermite, M. P. and Zucconi, F., Elsevier Applied Science, Essex, pp. 30-50.



Co-firing Municipal Solid Waste with Coal - A Case Study of Warangal City, India

Chandrasekhar Matli*†, Bhaskar Challa* and Rakesh Kadaverugu*

*National Institute of Technology, Warangal-506004, Telangana, India

†Corresponding author: Chandrasekhar Matli

Nat. Env. & Poll. Tech.
Website: www.neptjournal.com

Received: 19-06-2018

Accepted: 02-08-2018

Key Words:

Municipal solid waste
Co-firing MSW with coal
Warangal city
Cost-benefit analysis

ABSTRACT

Municipal solid waste management has become an important challenge in the developing countries. Treatment using thermal methods, especially by incineration is advantageous in comparison with biological and chemical treatments, as they require less time and space for the reduction of huge quantities of wastes and also generates energy. As the composition of municipal solid waste (MSW) and its calorific value is inconsistent for power generation, we have studied the possibility of blending MSW with an auxiliary fuel such as coal. The study was conducted in the Warangal city (in Telangana State of India) which produces around 220 tonnes of MSW per day. Various blending proportions of MSW and coal were analysed and quantified the calorific value, gaseous emissions (NO_x, SO₂ and CO₂) and also estimated the cost of production. We found that, blend of MSW and coal in the proportion of 90-80% and 10-20% respectively, is optimal in terms of waste processing and lower gaseous emissions. The cost-benefit analysis for the two scenarios consisting of either inclusion or exclusion of food wastes in the MSW validates the viability of co-firing as a better waste management practice with a minimum assured gain of Rs. 0.3 million per day.

INTRODUCTION

Solid waste management has become a daunting task for urban municipalities in India. The production of municipal solid waste (MSW) has increased tremendously with the improvement in lifestyle and growing consumerism. It is reported that India produces around 1,43,000 to 1,70,000 metric tonnes of MSW per day (Mani and Singh 2016). Nearly 40 % of the urban MSW is produced from metro cities of India (Annepu 2012). According to the Central Pollution Control Board (CPCB) report, the urban municipal authorities in India are unable to upgrade or scale up their solid waste management facilities (CPCB 2016) with the rise in population. The gap between growing urban population and waste treatment facilities is becoming wider. Further, it is reported that urban population in India is projected to reach 439 million by the year 2022 with a share of 32.5% of the country's population (MoSPI 2017), and by year 2030 the share would rise to 40.8% (UNPF 2007). Hence, scientific management of MSW takes center stage in order to make Indian cities sustainable and eco-friendly.

The MSW in urban areas is collected, transported and processed, then the remaining waste is sent to open dump sites (Singh et al. 2011). The major processes involved in the treatment of MSW are sanitary landfill disposal, incineration and composting (Atalia et al. 2015). The existing infrastructure for MSW treatment (Table 1) is insufficient

for the humongous amount of waste that India generates. Nearly 90% of the MSW in India ends up in open landfills (Kumar et al. 2017) as it involves less cost implications and the practice is prevalent in many Indian cities (Sharholly et al. 2008). Dumping causes severe problems like leachate contamination with groundwater, bad odour and fugitive emission around the dump sites (Shashidhar & Ajit Kumar 2011). In order to avoid environmental damage, the MSW is to be managed scientifically. If the current practice of open dumping of MSW is continued, the area required for the disposal of waste generated in the year 2047 (~230 million tonnes per year) would be around 1400 km² (Annepu 2012), which is equivalent to cumulative areas of three mega cities of India - Mumbai, Chennai and Hyderabad.

Waste-to-energy is becoming a best management choice for treating wastes now-a-days, as it is a two-pronged approach to address the waste volume reduction and energy generation (CPCB 2016, Yap & Nixon 2015). Especially through incineration, 70% of weight and 90% of volume of MSW can be reduced (Tian et al. 2012). Nearly 130 million tonnes of MSW is fired in over 600 waste-to-energy facilities worldwide (Xu et al. 2016). Also, producing energy from the discarded MSW is a potential energy source to lessen the dependence on fossil fuels (Kaplan et al. 2009). The energy from waste can be produced by two methods, either by direct combustion (e.g., thermo-chemical meth-

Table 1: Status of MSW processing facilities in India as of year 2015-16. Source (CPCB 2016).

Municipal solid waste processing facilities	Composting	Vermi-composting	Biogas	RDF (refuse derived fuel)	Sanitary landfills	Dump sites
Number of plants setup	209	208	82	45	-	-
Number of plants operational	168	141	67	26	175	1247

ods like incineration, pyrolysis and gasification) or by the production of combustible fuels-methane and hydrogen (e.g., biochemical methods like anaerobic digestion, biological treatments) as mentioned by Cheng & Hu (2010). Thermo-chemical methods are best suited for high calorific wastes and the time required for processing is very short. Whereas, biochemical methods are suitable for biodegradable wastes which are organic in nature, however, the time consumed is very high as compared with thermo-chemical processes. According to the Ministry of New and Renewable Energy of Indian Government, India has a potential of 1500 MW of energy from MSW, whereas only 2% is realized so far (EIA 2013). As of year 2015-16, India has 26 operational RDF (refuse derived fuel) plants (out of 45 plants installed) which are producing around 156 MW of energy (CPCB 2016).

In general, the waste-to-energy plants in India have not sustained in operation owing to multiple reasons such as, low calorific value of waste and high moisture content (Talyan et al. 2008), lack of logistic and financial planning (Kalyani & Pandey 2014), lack of expertise (Srivastava et al. 2005), and poor waste segregation (Chattopadhyay et al. 2009). Supplementary fuels like coal, cotton waste and sawdust etc. are usually added to MSW in order to improve the consistency and to make it suitable for the combustion. Furthermore, with the addition of coal as an auxiliary fuel to MSW, studies suggest that the emissions resulting from incomplete combustion of MSW can be reduced substantially (Bhuiyan et al. 2018, Narayanan & Natarajan 2007, Surroop & Juggurnath 2011). Peng et al. (2016) reported a reduction in PAHs (polycyclic aromatic hydrocarbons) emissions with co-firing MSW and coal, and Suksankraisorn et al. (2004) have studied the NO_x , SO_x and CO emissions and reported a significant reduction in CO. Co-firing biomass (including agriculture waste, forest products and MSW etc.) with coal is being encouraged worldwide as a policy decision to deliberately reduce the dependence on fossil fuels and to reduce the green house gas emissions (IRENA 2013). India is well placed in terms of biomass supplies both from MSW and agricultural wastes, which has to be utilized for solving both the waste management issues and energy deficiency (Rathnam 2013).

We have studied the MSW characteristics of Warangal

city in Telangana State of India, as the city is uniquely positioned in the country where efficient door-to-door MSW collection system is in place (CPHEEO 2014). However, at present the MSW is not been processed in a scientific manner, due to which it has become difficult to recycle and transform the solid waste. As a result, huge quantity of solid waste is getting accumulated at dumping sites at Madikonda, Shahimpet and Ramapura on the outskirts of the city (ISWM 2016, Warangal City Development Plan (CDP) 2011). Moreover, transportation of the garbage collected across the city limits to the dumping yards has become a cost intensive task. In this paper, we discuss various aspects of co-firing MSW with coal in Warangal city with broad objectives to: (1) verify the suitability of co-firing MSW with coal in incineration process for power generation, (2) derive optimum blend proportions of coal and MSW in terms of economic viability and reduction in gaseous emissions, and (3) perform the economic analysis to get viable working model of waste management.

MATERIALS AND METHODS

Study area: Warangal is the second largest city in the State of Telangana (located 17.9° N, 79.6° E) sprawling in an area of 110 km² (Warangal City Development Plan (CDP) 2011) and having 0.81 million population according to 2011 census (ISWM 2016). The city's weather is almost dry with temperature ranging from 20-48°C and the rainy season which lasts from June to September with 550 mm of average precipitation. As per 2011 census of India, Warangal is one of the cities which has seen rapid urbanization from 19% to 28%. The city generates municipal solid waste of 0.251 kg per day per capita, whereas country's average generation is 0.11 kg (CPHEEO 2014). On an average, around 200 to 300 metric tonnes of waste is produced in the city every day (Shashidhar & Ajit Kumar 2011) out of which, households, commercial establishments, street sweeping and drains contribute in 72%, 13.5%, 5.5% and 9% respectively (ISWM 2016).

Sample collection and analyses: The MSW samples were collected from Kasibugga ward of the city where a door-to-door collection system is followed and the ward is assumed to represent the social and economic strata of the city. The ward has 2,408 households with a population of 10,382

Table 2: Elemental composition of different categories of MSW and coal.

Sl. No.	Sample	C%	H%	N%	S%	O%	Ash%
1	Paper and cardboard waste	42.4	5.6	1.5	0.15	45.65	4.7
2	Plastic waste	76.4	7.5	1.2	0.2	9.5	5.2
3	Food waste	45.56	6.4	7.66	0.08	34.3	6
4	Garden waste	50.7	6.51	3.4	0.18	33.51	5.7
5	Coal	50.8	3.54	1.43	0.50	11.13	32.6

Table 3: Elemental composition of various blends of MSW and coal.

Blending proportions of MSW and Coal	Coal with MSW (including food waste)					Coal with MSW (excluding food waste)				
	C%	H%	N%	S%	O%	C%	H%	N%	S%	O%
Case-1 100% MSW + 0% Coal	49.13	6.41	5.25	0.12	37.80	54.07	6.56	2.79	0.17	30.88
Case-2 90% MSW + 10% Coal	49.23	6.23	5.01	0.14	36.17	53.77	6.29	2.67	0.20	29.09
Case-3 80% MSW + 20% Coal	49.34	6.04	4.76	0.17	34.40	53.46	6.01	2.54	0.23	27.26
Case-4 70% MSW + 30% Coal	49.47	5.83	4.48	0.20	32.46	53.15	5.72	2.41	0.26	25.39
Case-5 60% MSW + 40% Coal	49.60	5.60	4.17	0.23	30.34	52.83	5.42	2.28	0.29	23.50
Case-6 50% MSW + 50% Coal	49.75	5.34	3.83	0.26	27.99	52.51	5.12	2.15	0.33	21.57
Case-7 0% MSW + 100% Coal	50.80	3.54	1.43	0.50	11.13	50.8	3.54	1.43	0.50	11.13

persons (DCO 2011). The unsorted MSW generated from each house is collected by the municipality in a mechanical trolley and all the waste from the ward is sent to the Dry Resource Center (DRC). At DRC the waste is sorted into two categories-dry waste and wet waste. Dry waste comprises paper, cardboards, plastics, glass and metals, while wet waste comprises the organic waste-kitchen and garden waste. Representative waste samples were drawn from multiple locations of unsorted MSW pile at DRC and the samples were mixed thoroughly. In order to reduce the sample volume and to get the uniformity, cone and quarter method was followed (Choi et al. 2008). The reduced sample weighing 10 kgs was then sorted into five categories viz. food waste, paper & cardboard waste, plastic waste, garden waste and miscellaneous wastes (metals and glass). The procedure was repeated once a fortnight and a total of four such samples were analysed and the percentage compositions were averaged. The sampling campaign was done during the winter of 2017 and any effects due to seasonal variations or weekly variations on the MSW composition and waste generation trends were not investigated in the study. And, the coal samples used for co-firing the MSW in the study were obtained from the SCCL (Singareni Collieries Company Limited) coal fields situated near Ramagundam city. The coal is graded as G-10 quality having a calorific value in a range of 4301 to 4600 kCal/kg (SCCL 2017), and it is used in nearby thermal power plants in the State.

The moisture content of the waste was measured by oven drying (105°C for a duration of 24 hours) a representative sample of 50 g taken from each waste category. The sorted

wastes were shredded in order to achieve uniformity. Similarly, the ash content was determined using Muffle furnace by charring the sample at 550°C for a duration of 2 hours.

The remaining sorted samples were air dried and then powdered for elemental analysis. Two grams of the powdered sample from each waste category was fed into CHNS analyser. Total carbon, nitrogen, hydrogen and sulphur content of the samples were estimated as percentage of dry weight of the sample. Whereas, the percentage of oxygen was calculated by subtracting percentages of ash and measured elements from 100 (i.e. $100 - (C+H+N+S+Ash)$). Stoichiometric mass balance of elements viz. carbon, sulphur and nitrogen was done to estimate the gaseous emissions from the combustion processes by assuming complete oxidation ($C+O_2 \rightarrow CO_2$, $S+O_2 \rightarrow SO_2$ and $N+O_2 \rightarrow NO_2$).

MSW energy potential: Calorific value of the samples was determined by bomb calorimeter, in which the oven dried samples of 1 g were burned in the steel bomb. The difference in initial and final temperatures of the coolant was used as a measure in determining the calorific value, according to the following equation.

$$\text{Calorific value (Cal/g)} = \frac{\text{Standard factor of 1311} \times \text{Rise in Temp.}}{\text{Mass of sample}}$$

The potential of MSW in co-firing with coal was estimated based on the typical efficiency parameters of a thermal power plant (Suksankraisorn et al. 2004). The following set of equations were assumed for power calculations.

$$\text{Available Power at Furnace, E} = \text{Mass of MSW (kg/day)} \times \text{calorific value (kJ/kg)}$$

Power available at boiler = $E \times 0.85$ (kg/day)

Power available at turbine = $E \times 0.85 \times 0.95$ (kg/day)

Power produced at generator = $\frac{E \times 0.85 \times 0.95}{1000 \times 24 \times 60 \times 60}$
(Mega Watts)

Cost-benefit analysis: The cost-benefit analysis was done to estimate the benefits in production of energy from various blends of MSW and coal. We have calculated for two extreme cases- (a) case-1: using MSW alone as fuel, and (b) case-7: using coal alone as fuel. Based on the data obtained from the two cases, we have interpolated the cost-benefit data for intermediate blend proportion of coal and MSW. In intermediate cases from case-1 to 7 the MSW share was decreased, while that of coal was increased (case-2: 90% MSW + 10% coal, case-3: 80% MSW + 20% coal, case-4: 70% MSW + 30% coal, case-5: 60% MSW + 40% coal and case-6: 50% MSW + 50% coal). The data for estimating the costs incurred in various operations of power generation such as transportation of fuel, operation and maintenance of plants and cost of fuel itself were obtained from already operational industries. MSW related data were obtained from waste-to-energy plant at Bawana, New Delhi (Jain et al. 2014) and data on coal based energy plants were obtained from National Thermal Power Corporation's (NTPC) power plant at Singrauli, Uttar Pradesh, India (Mittal et al. 2012). The selling price of unit of power (in kWh) was obtained from Telangana Southern Power Distribution Company Limited (TSPDCL). The capital costs were not included in this analysis in order to simplify the calculations.

Further, we have also studied elemental compositions, gaseous emissions, energy potential and cost calculations for MSW excluding the food wastes as different scenarios. The separate analysis for MSW including and excluding food waste aids informed decision on whether the benefits of separating food waste is significant in any way. The economic aspects of utilization of segregated food waste for biometanation is also considered for cost-benefit analysis.

In order to objectively compare the best blend of MSW and coal, we have used an objective function considering three factors viz., reduction in MSW volume, emission of NO_2 and SO_2 by assuming equal weights, as shown below:

$$Score_i = \frac{MSW_i}{MSW_{max}} + \left(1 - \frac{NO_{2i}}{NO_{2max}}\right) + \left(1 - \frac{SO_{2i}}{SO_{2max}}\right)$$

MSW_i is the weight of waste consumed in the energy generation process, which is compared against the maximum possible consumption, MSW_{max} . $\text{NO}_{2,i}$ is the value of NO_2 emission for i^{th} case and $\text{NO}_{2,max}$ is the maximum emissions from all the cases considered. Similarly SO_2 values

can be calculated. Ideally, the case with score 3 (maximum possible) will be the best one with maximum waste reduction and minimum gaseous emissions. The scores were calculated for each case of the two scenarios - MSW including and excluding food wastes.

RESULTS AND DISCUSSION

Physical characterization of MSW and coal: Food wastes contribute to 51% of the MSW, followed by garden wastes (34%), plastics (8%) and others (Fig. 1). The share of food wastes in MSW of Warangal city is higher than the national average of 41% (Sharholly et al. 2008). Moisture content is maximum in food wastes to the tune of 60% and minimum in plastics and paper wastes. Ash content is around 6% for garden and food wastes. The plastic waste has highest calorific value of 38 MJ/kg and the food waste has lowest value of 5.6 MJ/kg (Fig. 2). The coal samples used in the study has calorific value of 18.6 MJ/kg, moisture content of 5.2% and ash content of 32.6%.

Elemental composition of MSW and Coal: Analysis shows that elemental carbon is highest in plastic wastes (76.4%) followed by coal (50.8%) and garden wastes (50.7%). Hydrogen is also maximum in plastic wastes (7.5%) followed by garden wastes (6.51%) as given in Table 2. It is observed that, although, MSW has comparable or some times even better elemental composition than coal, owing to its heterogeneity, the MSW cannot be directly used for combustion. It needs to be blended with auxiliary fuel-coal for consistent generation of power.

The composition of elements present in various blends for two scenarios of MSW-including and excluding the food wastes are presented in Table 3. Carbon and hydrogen contents were found to be maximum in case-1 of MSW excluding of food waste, whereas there is a significant drop in

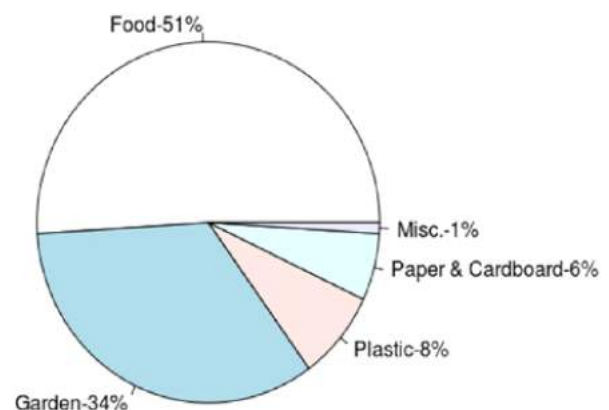


Fig. 1: Composition of municipal solid waste generated by residential area Kasibugga of Warangal city.

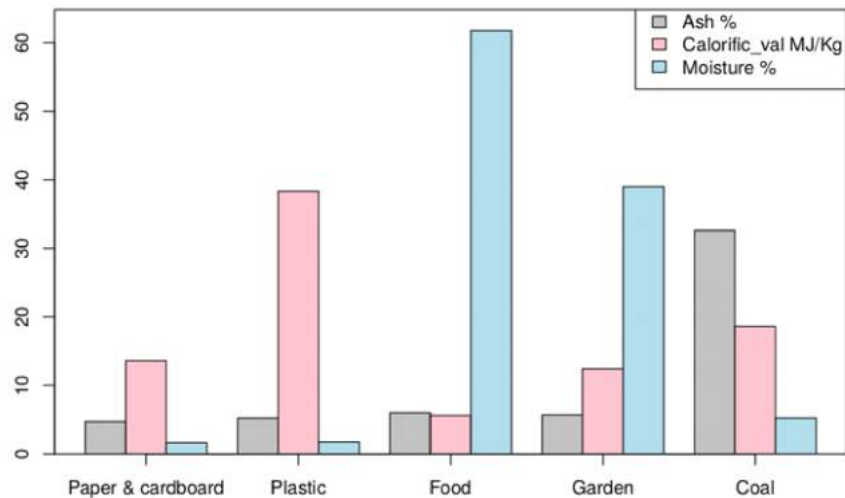


Fig. 2: Moisture, ash and calorific values of various categories of MSW and coal.

nitrogen content. The changes in elemental composition will have implications on energy potential and gaseous emissions.

Energy potential and MSW utilization: Energy potential is directly proportional to the calorific value and the rate of feed into the boiler. As Warangal city generates around 220 tonnes of MSW per day, it is assumed that the maximum available MSW for energy production is 220 tonnes/day and the same amount is considered for the rest of calculations. The maximum power possibly available at the furnace using all the MSW (case-1) would be 27.93 MW (220 times 10.97 MJ/kg). If the same amount of power is to be generated using coal alone (case-7) the quantity of coal required will be 129.81 tonnes/day. The amount of MSW and coal required for intermediate cases-2 to 6 are estimated according to the proportions of the blend (Table 4).

Further, if all the food waste from MSW is separated for being utilized in composting or bio-gasification, the MSW consisting only wastes from garden, plastics and cardboard will be fired for power generation. The maximum quantity of waste available in the scenario excluding the food waste is 105.6 tonnes/day (case-1) and maximum power possibly available at the furnace would be 20.7 MW (105.6 times 16.97 MJ/kg).

Emissions: For complete combustion, the amount of oxygen required for each blend combination is calculated based on stoichiometric equations. Nearly 25% of excess air is considered according to Mittal et al. (2012). The excess air required per day and emissions from combustion are tabulated in Table 5. The amount of excess air required for MSW excluding the food waste is more compared to MSW including food waste. The carbon, hydrogen and sulphur con-

tents are more in MSW excluding food waste. Nitrogen and oxygen are less in MSW excluding food waste. This shows that more amount of air is required for combustion of MSW excluding food waste. Although, supplying the excess air will not be a major concern, however, it may effect the operational expenditure of the energy plant. The CO₂ and SO₂ emissions from the combustion of MSW is more than MSW excluding food waste, whereas the NO_x and ash content are less. The reasons for more CO₂ and SO₂ in MSW excluding food waste is due to high carbon and sulphur content in the composition (Table 3). Co-firing of coal and MSW generated lowest amounts of total PAHs than combustion of MSW and coal alone, whereas, combustion of MSW alone generated high quantities of PAHs in the range of 111.28 µg/g - 10,047.22 µg/g (Peng et al. 2016). Suksankraisorn et al. (2004) reported a significant reduction in CO concentration in co-firing MSW with coal.

Cost-benefit analysis: If MSW including the food waste alone is considered for generation of power, the maximum possible generated power is 22.5 MW (0.67 million units). Our estimates show that the cost incurred for the power generation from collection and transport of MSW (including food waste) and operation and maintenance activities will add to Rs. 1.5 million. Profit obtained by the power generation from the MSW is estimated by subtracting the cost incurred in power production from the selling price of the electricity (Rs. 2 million, @Rs 3.8 for one kWh (TSERC 2016)), which is Rs. 0.5 million/day (Table 6). Similarly, the cost incurred for the generation of power by using only MSW excluding of food waste is estimated as Rs. 1.34 million and the profit is estimated as Rs. 0.18 million/day.

Although, firing of MSW (with or without food wastes)

Table 4: MSW energy potential and utilization at different blending ratios.

Blending proportions of MSW and Coal	MSW including food waste						MSW excluding food waste					
	MC%	Ash%	CV MJ/Kg	MSW Tonnes	Coal Tonnes	Total (MSW + Coal) Tonnes	MC%	Ash%	CV MJ/kg	MSW Tonnes	Coal Tonnes	Total (MSW+ Coal) Tonnes
Case-1 100% MSW+0% Coal	44.98	5.70	10.97	220.00	0.00	220.00	28.17	5.495	16.97	105.6	0	105.6
Case-2 90% MSW+10% Coal	42.53	7.35	11.73	198.00	12.98	210.98	26.05	7.99	17.12	95.04	9.64	104.7
Case-3 80% MSW+20% Coal	39.87	9.16	12.49	176.00	25.96	201.95	23.90	10.53	17.27	84.48	19.28	103.8
Case-4 70% MSW+30% Coal	36.95	11.13	13.26	154.00	38.94	192.93	21.71	13.12	17.42	73.92	28.91	102.8
Case-5 60% MSW+40% Coal	33.75	13.29	14.02	132.00	51.93	183.91	19.48	15.75	17.58	63.36	38.55	101.9
Case-6 50% MSW+50% Coal	30.22	15.68	14.78	110.00	64.91	174.89	17.21	18.43	17.74	52.80	48.19	101.0
Case-7 0% MSW+100% Coal	5.20	32.60	18.59	0.00	129.81	129.81	5.2	32.6	18.59	0	96.4	96.4

Table 5: Gaseous emissions estimated per tonne of MSW and coal.

Blending proportions of MSW and Coal	MSW including food waste					MSW excluding food waste				
	Excess air (tonnes/d)	CO ₂ (kg/d)	SO ₂ (kg/d)	NO _x (kg/d)	Ash (kg/d)	Excess air (tonnes/d)	CO ₂ (kg/d)	SO ₂ (kg/d)	NO _x (kg/d)	Ash (kg/d)
Case-1 100% MSW+0% Coal	7.76	1,817.8	2.40	172.7	57.0	8.91	2,000.7	3.40	92.1	55.0
Case-2 90% MSW+10% Coal	7.80	1,821.6	2.87	165.0	73.5	8.84	1,989.5	4.01	87.9	79.9
Case-3 80% MSW+20% Coal	7.85	1,825.8	3.38	156.6	91.6	8.77	1,978.2	4.63	83.7	105.3
Case-4 70% MSW+30% Coal	7.89	1,830.3	3.93	147.4	111.3	8.69	1,966.6	5.26	79.4	131.2
Case-5 60% MSW+40% Coal	7.94	1,835.3	4.55	137.2	132.9	8.62	1,954.9	5.90	75.0	157.5
Case-6 50% MSW+50% Coal	7.98	1,840.7	5.22	126.1	156.8	8.55	1,942.9	6.55	70.6	184.3
Case-7 0% MSW+100% Coal	8.20	1,879.6	10.00	47.0	326.0	8.20	1,879.6	10.00	47.0	326.0

alone is not an option for the generation of power, the calculations mentioned show the bare minimum amount of profit/gain which is expected from the business of waste-to-energy. In real life situations, MSW is to be blended with coal for getting the consistency in power generation. In any of the blending proportions, the waste-to-energy plants will have a minimum profit of Rs. 0.18 million/day (Table 6, MSW excluding food waste) and the pay back time can be estimated from the installation costs. The ash produced as a by-product will also have monetary benefits.

Furthermore, if the segregated food wastes from the MSW is used in either of biomethanation or composting, there

will be additional benefit in methane generation (for power utilities) or manure. Also, the MSW excluding food waste generates lower NO_x emissions (Table 5) than the MSW including the food wastes, and the separation also saves the hydrothermal processing costs (pre-heating and drying) associated with food wastes. The byproducts of biomethanation include biogas and nutrient rich manure. Biogas produced can be utilized for electricity generation and the manure can be used for farming. According to the experience of Pune city's Municipal Corporation, a net profit of Rs. 0.2 million per year can be obtained from 1 tonne per day of food waste (Pathak 2013). Proportionately the net profit for

Table 6: Cost-benefit analysis of power generation by using coal and MSW.

Operations	MSW including food waste		MSW excluding food waste	
	Case-7 100% Coal (Million Rupees per day)	Case-1 100% MSW (Rupees per day)	Case-7 100% Coal (Rupees per day)	Case-1 100% MSW (Rupees per day)
Cost incurred for fuel	0.39 ^a	0	0.29 ^a	0
Cost incurred for collection & transportation	0.06 ^b	0.9 ^c	0.05 ^b	0.9 ^c
Cost incurred for O&M of plant	0.13 ^d	0.6 ^e	0.1 ^d	0.44 ^e
TOTAL COST (a)	0.58	1.5	0.44	1.34
Returns from sale of power (b)	2.0 ^f	2.0 ^f	1.52 ^f	1.52 ^f
NET GAIN (b-a)	1.42	0.5	1.08	0.18

^a Cost of coal per tonne: Rs. 3,000 (Rs. 2260 + Misc. charges + 5% Tax) of grade G-10 of Singareni Collieries Company Limited (SCCL 2017)

^b Cost of transportation per tonne of coal for 160 km from mine site to Warangal city: Rs. 450 by railways (Indian Railways 2018)

^c Integrated Solid Waste Management data from Warangal city (ISWM 2016)

^d NPTC Thermal power plant data (Mittal et al. 2012)

^e Bawana Waste-to-Energy plant at Delhi (Jain et al. 2014)

^f Cost of unit power: Rs. 3.8 @ 1 kWh (TSERC 2016)

Table 7: Evaluation of different blend proportions of coal and MSW, in terms of volume reduction and air quality.

Blending proportions of MSW and Coal	MSW including food waste				MSW excluding food waste			
	Treatment of MSW or volume reduction (V) $V_i = \text{MSW}_i / \text{MSW}_{\text{max}}$	NO_2 $N_i = (1 - \text{NO}_{2i} / \text{NO}_{2\text{max}})$	SO_2 $S_i = (1 - \text{SO}_{2i} / \text{SO}_{2\text{max}})$	Score (max=3) $\text{Score}_i = V_i + N_i + S_i$	Treatment of MSW or volume reduction (V) $V_i = \text{MSW}_i / \text{MSW}_{\text{max}}$	NO_2 $N_i = (1 - \text{NO}_{2i} / \text{NO}_{2\text{max}})$	SO_2 $S_i = (1 - \text{SO}_{2i} / \text{SO}_{2\text{max}})$	Score (max=3) $\text{Score}_i = V_i + N_i + S_i$
Case-1 100% MSW+0% Coal	1.00	0.00	0.76	1.76	1.00	0.00	0.66	1.66
Case-2 90% MSW+10% Coal	0.90	0.04	0.71	1.65	0.90	0.05	0.60	1.55
Case-3 80% MSW+20% Coal	0.80	0.09	0.66	1.55	0.80	0.09	0.54	1.43
Case-4 70% MSW+30% Coal	0.70	0.15	0.61	1.46	0.70	0.14	0.47	1.31
Case-5 60% MSW+40% Coal	0.60	0.21	0.55	1.36	0.60	0.19	0.41	1.20
Case-6 50% MSW+50% Coal	0.50	0.27	0.48	1.25	0.50	0.23	0.34	1.07
Case-7 0% MSW+100% Coal	0.00	0.73	0.00	0.73	0.00	0.49	0.00	0.49

Warangal city will be added to Rs. 23 million per year (Rs. 0.063 million/day) with generation of 115 tonnes per day of food waste. Our estimates show that with the addition of added gains from biomethanation, the minimum assured profit increases to Rs. 0.24 million/day (sum of Rs. 0.18 million and 0.063 million).

Further, the scores obtained from the objective function for various blends and scenarios of MSW and coal show that, it is optimum to consider 90 to 80% of MSW (including or excluding food waste) and 10 to 20% of coal. The cases-2 and 3 in both the scenarios of MSW have the scores

in the range of 1.65 to 1.43 (out of maximum score 3), which are obtained by considering the factors of waste volume reduction and lower gaseous emissions (Table 7).

Specific to our study, the results show that co-firing MSW including food waste seems profitable by Rs. 0.26 million per day compared to MSW excluding the food waste. However, the costs involved in hydrothermal treatment of the MSW including food waste and also costs involved in segregation of food waste would actually determine the overall profitability. Further, production of manure out of food waste in opting biomethanation process will enrich

the nutritional value of wastes and it can be helpful for organic farming and thereby the dependence on chemical fertilizers can be reduced.

CONCLUSIONS

Waste-to-energy is being practiced worldwide to overcome the energy demands and to efficiently process the municipal solid wastes in urban areas. Incineration is the well known and proven thermo-chemical process for energy generation from solid wastes. Particularly, as MSW is inconsistent in composition and quantity, it needs to be blended with auxiliary fuels such as coal for making up the generation of constant amount of power. Our study characterizes the MSW of Warangal city and suggests that the waste can be suitably blended with 10-20% of coal for sustainable operation of waste-to-energy plants. Also, the cost benefit analysis shows that by operating the waste-to-energy plants a net gain of Rs. 0.18 million /day can be obtained. Urban management authorities in many Indian cities are facing a challenge of growing MSW and similar studies will help the authorities to plan a suitable technological solution for better management of the waste. Hence, the overall life cycle of MSW and its associated benefits will certainly prove its sustainability in a much wider scope of analysis. And we strongly suggest for an extension of this study with a complete life cycle assessment of waste utilization and added benefits in terms of reduction in GHGs, reduction in chemical fertilizers, waste utilization, aesthetics, improvement in health and much more.

ACKNOWLEDGEMENTS

We express our sincere thanks to National Institute of Technology, Warangal for providing every means of support.

REFERENCES

- Annepu, R. 2012. Sustainable Solid Waste Management in India. Columbia University, New York 2012: 189.
- Atalia, K.R., Buha, D.M., Bhavsar, K.A. and Shah, N.K. 2015. A review on composting of municipal solid waste. *IOSR Journal of Environmental Science, Toxicology and Food Technology*, 9: 20-29.
- Bhuiyan, A.A., Blicblau, A.S., Islam, AKMS and Naser, J. 2018. A review on thermo-chemical characteristics of coal/biomass co-firing in industrial furnace. *Journal of the Energy Institute*, 91: 1-18.
- Chattopadhyay, S., Dutta, A. and Ray, S. 2008. Municipal solid waste management in Kolkata, India- a review. *Waste Management*, 29: 1449-1458.
- Cheng, H. and Hu, Y. 2010. Municipal solid waste (MSW) as a renewable source of energy: Current and future practices in China. *Bioresource Technology*, 101: 3816-3824.
- Choi, K.I., Lee, S.H., Lee, D.H. and Osako, M. 2008. Fundamental characteristics of input waste of small MSW incinerators in Korea. *Waste Management*, 28: 2293-3300.
- CPCB 2016. Consolidated annual report on implementation of Municipal Solid Waste (Management and Handling) Rules, 2000.
- CPHEEO 2014. Municipal Solid Waste management Manual. Central Public Health and Environmental Engineering Organization.
- DCO 2011. District Census Handbook Warangal. Directorate of Census Operation.
- EIA 2013. India MSW to energy: Status, opportunities and bottlenecks. *Energy Alternatives India* 2013.
- Indian Railways 2018. Freight Calculator. https://www.fois.indianrail.gov.in/foisweb/view/qry/TQ_FrgtCalcIN.jsp (accessed February 2, 2018).
- IRENA 2013. Biomass co-firing technology brief. International Renewable Energy Agency.
- ISWM 2016. Integrated municipal solid waste management (ISWM). Project for Zone-2 of Telangana.
- Jain, P., Handa, K. and Paul, A. 2014. Studies on waste-to-energy technologies in India and a detailed study of waste-to-energy plants in Delhi. *Int. J. Adv. Res.*, 2: 109-116.
- Kalyani, K.A. and Pandey, K.K. 2014. Waste to energy status in India: A short review. *Renewable and Sustainable Energy Reviews*, b31: 113-120.
- Kaplan, P.O., DeCarolis, J. and Thorneloe, S. 2009. Is it better to burn or bury waste for clean electricity generation? *Environ. Sci. Technol.*, 43: 1711-1717.
- Mani, S. and Singh, S. 2016. Sustainable Municipal Solid Waste Management in India: A Policy Agenda. *Procedia Environmental Sciences* 35: 150-157. <https://doi.org/10.1016/j.proenv.2016.07.064>.
- Mittal, M.L., Sharma, C. and Singh, R. 2012. Estimates of emissions from coal fired thermal power plants in India. 2012 International Emission Inventory Conference, pp. 13-16.
- MoSPI 2017. Statistical Year Book India. Ministry of Statistics and Program Implementation
- Narayanan, K.V. and Natarajan, E. 2007. Experimental studies on cofiring of coal and biomass blends in India. *Renewable Energy*, 32: 2548-2558.
- Pathak, M. 2013. Biomethanation from municipal solid waste-Pune, India. Indian Council for Research on International Economic Relations. <http://icrier.org/Urbanisation/events/26-27-August-Kerala/> (accessed January 18, 2018).
- Peng, N., Li, Y., Liu, Z., Liu, T. and Gai, C. 2016. Emission, distribution and toxicity of polycyclic aromatic hydrocarbons (PAHs) during municipal solid waste (MSW) and coal co-combustion. *Science of the Total Environment*, 565: 1201-1207.
- Rathnam, R.K., Janne Karki, Matti Nieminen and Arvo Leinonen 2013. Coal and Biomass Co-firing Prospects in India. *Energetica India*.
- SCCL 2017. The Singareni Collieries Company Limited (A Government Company) 2017. <https://scclmines.com/scclnew/index.asp> (accessed January 21, 2018).
- Sharholy, M., Ahmad, K., Mahmood, G. and Trivedi, R.C. 2008. Municipal solid waste management in Indian cities - a review. *Waste Management*, 28: 459-467.
- Shashidhar, Ajit Kumar O. 2011. Municipal solid waste management of Warangal City, India. *Journal of Environmental Research and Development*, 6: 111-121.
- Singh, R.P., Tyagi, V.V., Allen, T., Ibrahim, M.H. and Kothari, R. 2011. An overview for exploring the possibilities of energy generation from municipal solid waste (MSW) in Indian scenario. *Renewable and Sustainable Energy Reviews*, 15: 4797-4808.
- Srivastava, P.K., Kulshreshtha, K., Mohanty, C.S., Pushpangadan, P. and Singh, A. 2005. Stakeholder-based SWOT analysis for successful municipal solid waste management in Lucknow, India. *Waste Management*, 25: 531-537.
- Suksankraisorn, K., Patumsawad, S., Vallikul, P., Fungtammasan, B.

- and Accary, A. 2004. Co-combustion of municipal solid waste and Thai lignite in a fluidized bed. *Energy Conversion and Management*, 45: 947-962.
- Surroop, D. and Juggurnath, A. 2011. Investigating the energy potential from co-firing coal with municipal solid waste. *University of Mauritius Research Journal*, 17(1): 109-123.
- Talyan, V., Dahiya, R.P. and Sreekrishnan, T.R. 2008. State of municipal solid waste management in Delhi, the capital of India. *Waste Management*, 28: 1276-87.
- Tian, H., Gao, J., Lu, L., Zhao, D., Cheng, K. and Qiu, P. 2012. Temporal trends and spatial variation characteristics of hazardous air pollutant emission inventory from municipal solid waste incineration in China. *Environmental Science & Technology*, 46(18): 10364-10371.
- TSERC 2016. Determination of Retail Supply Tariffs for FY 2016-17 - Tariff Order.
- UNPF 2007. Unleashing the potential of urban growth. New York, NY: United Nations Population Fund.
- Warangal City Development Plan (CDP) 2011. Warangal Municipal Corporation (WMC) 2011.
- Xu, S., He, H. and Luo, L. 2016. Status and prospects of municipal solid waste to energy technologies in China. *Recycling of Solid Waste for Biofuels and Bio-chemicals*, Springer, pp. 31-54.
- Yap, H.Y. and Nixon, J.D. 2015. A multi-criteria analysis of options for energy recovery from municipal solid waste in India and the UK. *Waste Management*, 46: 265-277.



Isotherms and Thermodynamics of CO₂ Adsorption on Thermally Treated Alum Sludge

Soleha Mohamat Yusuff*, Ong Keat Khim**†, Wan Md Zin Wan Yunus*, Mansor Ahmad***, Nor Azowa Ibrahim***, Anwar Fitrianto****, Syed Mohd Shafiq Syed Ahmad** and Chin Chuang Teoh*****

*Department of Defence Science, Faculty of Defence Science and Technology, Universiti Pertahanan Nasional Malaysia (UPNM), Kem Sungai Besi, 57000, Kuala Lumpur, Malaysia

**Department of Chemistry and Biology, Centre for Defence Foundation Studies, Universiti Pertahanan Nasional Malaysia (UPNM), Kem Sungai Besi, 57000, Kuala Lumpur, Malaysia

***Department of Chemistry, Faculty of Science, Universiti Putra Malaysia, 43400 UPM Serdang, Selangor, Malaysia

****Department for Mathematical Research, Universiti Putra Malaysia, 43400 UPM Serdang, Selangor, Malaysia

*****Engineering Research Centre, MARDI Headquarter, 50774, Kuala Lumpur, Malaysia

†Corresponding author: Ong Keat Khim

Nat. Env. & Poll. Tech.
Website: www.neptjournal.com

Received: 27-12-2017
Accepted: 03-04-2018

Key Words:

Carbon dioxide adsorption
Kinetics
Isotherms
Thermally treated alum sludge

ABSTRACT

The isotherms, and thermodynamics of adsorption of carbon dioxide (CO₂) onto thermally treated alum sludge were successfully investigated in this study. The adsorption of CO₂ was investigated using a fixed-bed column adsorption system. The equilibrium isotherms data were best described by the Freundlich multilayer isotherm model. The feasibility, spontaneity and randomness of the CO₂ adsorption process were confirmed by thermodynamic parameters (ΔG° , ΔH° , ΔS°). This study revealed that 800°C thermally treated alum sludge has a great potential as the adsorbent for CO₂.

INTRODUCTION

Large emission of greenhouse gases into the atmosphere has become a serious problem as it causes climate disasters (Upendar et al. 2012). Carbon dioxide (CO₂) gas is one of the greenhouse gases and a main contributor to the global warming (Monazam et al. 2013). About one-third of the CO₂ gas emission to the atmosphere is from fossil-fuel fired power plants (Monazam et al. 2013). Therefore, development of effective approaches to reduce atmospheric CO₂ level have received great attention and become the global research efforts (Upendar et al. 2012, Monazam et al. 2013).

For decades, CO₂ capture using solvent amine has been employed (Upendar et al. 2012). However, it has several drawbacks such as corrosion, high energy consumption and limitation on concentration of amine used (Upendar et al. 2012, Irani et al. 2016). To overcome these problems, amine-modified solid sorbents were used (Irani et al. 2016) as the adsorption of gases onto solid adsorbents. This is the promising technique (Upendar et al. 2012) due to several advantages such as higher CO₂ adsorption capacity, high selectivity, low equipment cost, easy to handle and low energy

requirement for regeneration of adsorbents (Rashidi et al. 2016).

Numerous CO₂ adsorbents were developed from waste materials. Thus, alum sludge which is a waste generated from drinking water treatment plants was used as CO₂ adsorbent in this study. The objectives of this study were to investigate isotherms and thermodynamics of CO₂ adsorption onto 800°C thermally treated alum.

MATERIALS AND METHODS

Preparation of adsorbents: The dewatered alum sludge obtained from a local drinking water treatment plant was thermally treated at 800°C for 7 hours before grinding and sieving to the particles size of 450 to 500 μm. The thermally treated alum sludge was labelled as AS800 and used as the CO₂ adsorbent.

Adsorption of CO₂: For the adsorption experiment, 1 g of AS800 was packed into a glass adsorption column (20 mm in diameter × 200 mm in length) and heated at 100°C for 30 min, before purging with purified N₂ gas at 1.5 L.min⁻¹ for 15 min. Subsequently CO₂ gas (in balance of N₂ gas)

with the desired concentration was fed into the column at a flow rate of 0.09 L.min⁻¹. The adsorption was conducted at 25°C and the concentrations of CO₂ were measured by a gas analyser (KANE100, United Kingdom) every 1 second until concentration of CO₂ at the outlet of the column similar to the concentration of CO₂ at the inlet of the column.

The adsorption capacity of AS800, q (mg.g⁻¹), was calculated by equation (1).

$$q = \frac{FC_o}{W} \int_0^t \left(1 - \frac{C_t}{C_o}\right) dt \quad \dots(1)$$

Where, F is feed volumetric flow rate (L.min⁻¹), C_o is concentration of CO₂ at the inlet of the column (mg.L⁻¹), C_t is concentration of CO₂ at the outlet of the column (mg.L⁻¹), t is adsorption time (min), and W is adsorbent dosage (g).

Adsorption isotherms: The isotherm study of CO₂ was carried out using different CO₂ concentrations of 400, 1000, 2000, 4200, 6000 and 8000 mg.L⁻¹. Subsequently, the experimental data were examined using Langmuir and Freundlich isotherm models, as shown below, respectively.

The Langmuir isotherm model is given by the equation (2):

$$\frac{C_e}{q_e} = \frac{C_e}{q_m} + \frac{1}{q_m b} \quad \dots(2)$$

Where, C_e (mg/L) is equilibrium concentration of CO₂, q_e (mg.g⁻¹) is adsorption capacity of CO₂ at equilibrium, q_m (mg.g⁻¹) is maximum monolayer adsorption capacity, and b (L.mg⁻¹) is Langmuir rate constants related to adsorption energy.

The Freundlich isotherm model is expressed as:

$$\log q_e = \log K_F + \frac{1}{n} \log C_e \quad \dots(3)$$

Where, q_e (mg.g⁻¹) is adsorption capacity of CO₂ at equilibrium, K_F (mg.g⁻¹) is the Freundlich rate constant, n is the adsorption intensity and C_e (mg.L⁻¹) is equilibrium concentration of CO₂.

For Langmuir isotherm plot, C_e/q_e was plotted against C_e , while $\log q_e$ was plotted against $\log C_e$ to obtain Freundlich isotherm model. The coefficient of determinations, R^2 , obtained from the plots, were used to determine the best fitted adsorption isotherm model.

Thermodynamics study: The thermodynamics study of CO₂ adsorption was carried out at the optimum adsorption conditions at different adsorption temperatures of 298, 308, 318, 328, 338 and 348 K. Thermodynamics parameter such as Gibbs free energy change (ΔG°), heat of adsorption, (ΔH°),

and standard entropy (ΔS°) were determined using Gibbs-Helmholtz and van't Hoff equations, as expressed in equations 4-6, respectively.

The Gibbs-Helmholtz equation:

$$\Delta G^\circ = -RT \ln K_c \quad \dots(4)$$

Where, R is the universal gas constant (8.314 J.K⁻¹.mol⁻¹), T is temperature (K), and K_c is equilibrium constant (L.mol⁻¹). The equilibrium constant, K_c (L.mol⁻¹) could be calculated using equation below (Saad et al. 2016):

$$K_c = \frac{q_e}{C_e} \times M_{w_{CO_2}} \quad \dots(5)$$

Where, q_e is equilibrium adsorption capacity (mg/g), C_e is concentration of CO₂ at equilibrium (mg/L) and $M_{w_{CO_2}}$ is molecular weight of CO₂ (g/mol).

The Van't Hoff equation:

$$\ln K_c = \frac{\Delta S^\circ}{R} - \frac{\Delta H^\circ}{RT} \quad \dots(6)$$

Where, K_c is equilibrium constant (Lmol⁻¹), ΔS° is the standard entropy (J.K⁻¹.mol⁻¹), ΔH° is the heat of adsorption (J.mol⁻¹), R is the universal gas constant (8.314 J.K⁻¹.mol⁻¹) and T is temperature (K). The standard entropy and heat of adsorption were obtained from the plot of $\ln K_c$ against $1/T$.

RESULTS AND DISCUSSION

Adsorption isotherms: The plots and parameters of the adsorption isotherms of CO₂ at 25°C are presented in Fig. 1 and Table 1, respectively. Obviously, Freundlich isotherm model can describe the isotherm adsorption better than Langmuir isotherm as indicated by higher R^2 value (0.9992). The results also indicated that the adsorption occurs via multilayer adsorption on the heterogeneous sorbent. The Langmuir adsorption model explains a monolayer adsorption on a finite number of equivalent localized sites, whereas Freundlich adsorption model describe multilayer adsorption on a heterogeneous surface (Rashidi et al. 2016).

Thermodynamics study: Table 2 shows the calculated thermodynamic parameters of the CO₂ adsorption process including the change in Gibbs free energy (ΔG°), the change in enthalpy of reaction (ΔH°), and the change in entropy of adsorbate and adsorbent interaction (ΔS°). Fig. 2 shows van't Hoff plot of the CO₂ adsorption on AS800. The negative value of ΔH° at fixed concentration of CO₂ indicated that the nature of CO₂ adsorption process was exothermic (Rashidi et al. 2016). The increase in randomness at the interface between AS800 adsorbent and CO₂ molecules and the affinity of the AS800 towards CO₂ (adsorption) was in-

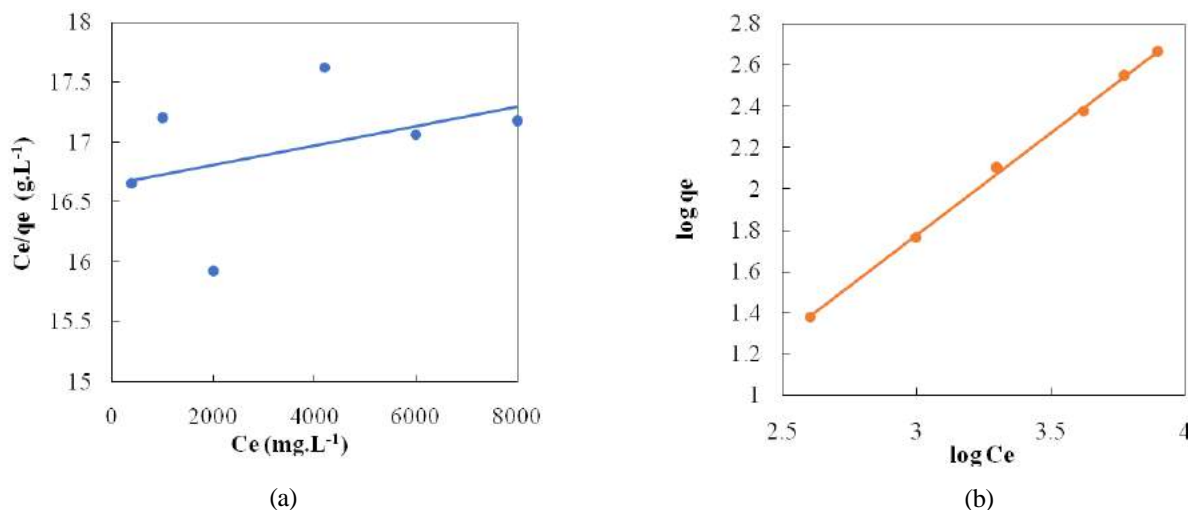


Fig. 1: (a) Langmuir and (b) Freundlich isotherm plots of CO₂ adsorption.

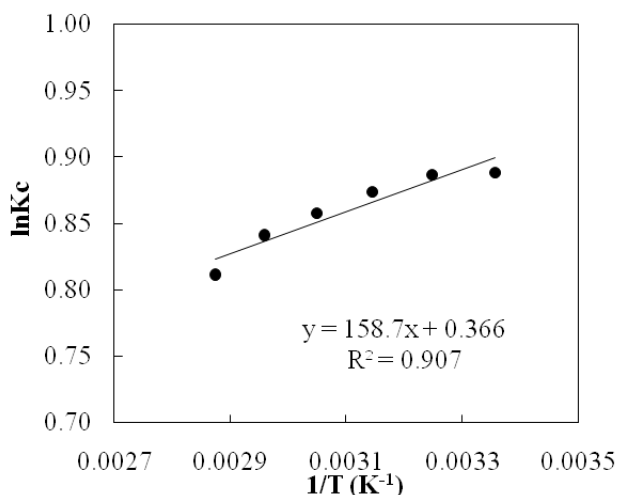


Fig. 2: Van't Hoff plot.

indicated by the positive value of ΔS° . A similar observation was found for adsorption of CO₂ gas at -10 to 40°C by Saad et al. (2016). It can be seen that increasing temperature caused increase in negative ΔG° value, thus the feasibility and spontaneity was favoured in adsorption of CO₂ onto the AS800. A similar trend was found for adsorption of CO₂ gas by RF-700 (Goel et al. 2015).

CONCLUSION

The fixed-bed adsorption of CO₂ using AS800 was investigated in order to evaluate CO₂ adsorption capacity. The adsorption isotherm of CO₂ on AS800 was best explained by Freundlich isotherms model. This indicates that the heterogeneous nature of AS800 surface participated in the CO₂

Table 1: Parameters of adsorption isotherms of CO₂ by AS800.

Isotherm model	Parameter	
Langmuir	K_L (L.mg ⁻¹)	4.80×10^{-6}
	q_m (mg.g ⁻¹)	12500
	R^2	0.167
Freundlich	K_f (mg.g ⁻¹)	0.0643
	n	1.0112
	R^2	0.999

Table 2: Thermodynamic parameters of CO₂ adsorption onto AS800.

T (K)	ΔG° (kJ.mol ⁻¹)	ΔS° (J.K ⁻¹ .mol ⁻¹)	ΔH° (kJ.mol ⁻¹)
298	-2.20	3.048	-1.320
308	-2.27	3.048	-1.320
318	-2.31	3.048	-1.320
328	-2.33	3.048	-1.320
338	-2.36	3.048	-1.320
348	-2.35	3.048	-1.320

adsorption. The thermodynamic results revealed that the CO₂ adsorption was favoured exothermically at low temperature onto AS800.

ACKNOWLEDGEMENT

This work was supported by National Defence University of Malaysia [UPNM/2014/GPJP/SG/3].

REFERENCES

Goel, C., Bhunia, H. and Bajpai, P.K. 2015. Resorcinol-formaldehyde based nanostructured carbons for CO₂ adsorption: Kinetics, isotherm and thermodynamic studies. RSC Adv., 5: 93563-93578.

- Irani, M., Gasem, K.A.M., Dutcher, B. and Fan, M. 2016. CO₂ capture using nanoporous TiO(OH)₂/tetraethylenepentamine. *Fuel*, 183: 601-608.
- Lee, C.H., Park, S.W. and Kim, S.S. 2014. Breakthrough analysis of carbon dioxide adsorption on zeolite synthesized from fly ash. *Korean J. Chem. Eng.*, 31: 179-187.
- Monazam, E.R., Spenik, J. and Shadle, L.J. 2013. Fluid bed adsorption of carbon dioxide on immobilized polyethylenimine (PEI): Kinetic analysis and breakthrough behavior. *Chem. Eng. J.*, 223: 795-805.
- Rashidi, N.A., Yusup, S. and Borhan, A. 2016. Isotherm and thermodynamic analysis of carbon dioxide on activated carbon. *Procedia Eng.*, 148, 630-637.
- Saad, M.A., Al-Marri, M.J., Yaumi, A.L., Hussein, I.A. and Shawabkeh, R. 2016. An experimental and kinetic study of the sorption of carbon dioxide onto amine-treated oil fly ash. *J. Chem.*, 2016: 1-11.
- Upendar, K., Sri Hari Kumar, A., Lingaiah, N., Rama Rao, K.S. and Sai Prasad, P.S. 2012. Low-temperature CO₂ adsorption on alkali metal titanate nanotubes. *Int. J. Greenhouse Gas Control*, 10: 191-198.



Functional Mechanism and Cointegration Relation of Environmental Regulations on Industrial Structure Upgrading in Beijing, China

Lili Zhang*(**)[†] and Gang Zong*

*School of Economics and Management, Beijing University of Technology, Beijing, 100000, China

**Beijing College of Social Administration, Beijing, 100000, China

[†]Corresponding author: Lili Zhang

Nat. Env. & Poll. Tech.
Website: www.neptjournal.com

Received: 15-01-2019
Accepted: 16-02-2019

Key Words:

Environmental regulation
Industrial structure
Functional mechanism
Cointegration relationship

ABSTRACT

In recent years, China has accelerated its urbanization and industrialization processes. The traditional extensive economic growth mode of high investments, high energy consumption, and high emissions has brought irreversible negative impacts on the ecological environment. Environmental regulation can promote necessary changes in the industrial structure and improve economic structure by eliminating the negative externalities of environmental pollution and enhancing social welfare. With time series data of Beijing from 1998 to 2017, the mechanism and impact of environmental regulations on industrial structure were analysed using cointegration analysis and Granger causality test. Results show that environmental regulations can effectively realize industrial structure upgrading by inhibiting the development of high-pollution enterprises, accelerating the development of the service industry, promoting the environmental protection of enterprise production technology, and promoting the optimization of investment structures. Thus, a long-term and positive equilibrium relationship between industrial structure upgrading and environmental regulation in Beijing can be achieved. The investment in industrial pollution control per unit can drive the growth of the tertiary industry's added value by 0.017 units. The completion of industrial pollution control investment is the one-way Granger reason for the tertiary industry's added value to the proportion of gross domestic product. The conclusions have a certain reference value for finding out the intensity of environmental regulation in promoting Beijing's industrial structure optimization and realizing the transformation of economic structure and coordinated development of ecological civilization construction.

INTRODUCTION

China's economy has rapidly grown in the past 20 years. However, ecological and environmental problems have become increasingly severe, and the contradiction between economic growth and environmental pollution has become increasingly prominent. In recent years, the smog in China has significantly worsened, gradually affecting people's daily lives and physical health. With the previous high-pollution, high-energy-consumption economic development mode, China has experienced a shortage of resources, environmental pollution, and ecological problems. Environmental destruction and other economic and social issues, ecological environmental governance, and resource conservation and utilization have become important issues that China's economic development must face. The extensive economic growth mode of high consumption, high emissions, and high investments has made China the world's largest energy consumer. This growth mode has caused serious environmental pollution and resource destruction, thereby significantly increasing China's resource and environmental constraints. It has seriously affected and restricted the sustainable development of the economy. At present,

the main challenge of China is to improve the environmental quality while pursuing sustainable economic development. The main method to overcome this challenge is to transform the economic development mode and optimize the industrial structure upgrading. The externalities of resources and the environment have made government interventions in environmental pollution necessary. Thus far, the Chinese government has implemented a series of environmental regulations, including enacting environmental protection laws, strengthening environmental supervision, increasing investments in environmental protection, and collecting sewage charges.

As a political, economic, and cultural center of China, Beijing also faces environmental problems and unreasonable industrial structure. In particular, during the period of accelerating urbanization and industrialization, Beijing has used traditional economic growth methods, such as high investments, high energy consumption, and high emissions. Such extensive methods have brought irreversible negative impacts on the ecological environment. In recent years, smog has frequently formed over Beijing, environmental pollution problems have reached serious levels in several areas,

and energy consumption has remained high. As shown in Fig. 1, although the proportion of the tertiary industry in Beijing has increased every year, industrial structure optimization remains necessary. A large number of studies and practices have shown that environmental regulation has forced the industrial structure to transform into a service economy, increase the proportion of the service industry in the three industrial structure sectors, and enable the service industry to quickly become the leading industry of the national economy. These measures can effectively reduce resource consumption and improve the environment. Therefore, an in-depth study of whether environmental regulation can promote the optimization and upgrading of the industrial structure while protecting the ecological environment will help understand the relationship between environmental regulation and industrial structure and ecological environmental protection and industrial structure of Beijing. Furthermore, upgrading presents important theoretical and practical implications.

EARLIER STUDIES

With the increasing environmental problems, countries have begun to gradually increase investments in environmental regulation since the 1930s. The impact of environmental regulation on economic development, especially how to affect the upgrading of industrial structures, has gradually attracted the attention of economists. With the continuous development of environmental regulation theory, most scholars believe that the improvement of environmental regulation levels can promote the improvement of enterprise technology innovation levels and will be transmitted to the industrial structure field, thus adjusting the industrial structure. Gray, et al. (1996) mainly studied the relationship between regulators' implementation of air pollution regulations and corporate compliance decisions. The results showed that enterprises implemented better environmental protection policies that were conducive to enterprise development. Lanjouw et al. (1996) considered the situation of the United States and Japan in 1970-1980 as examples. The study found that the industrial structure upgrade is positively correlated with the intensity of environmental regulation. Berman et al. (2001) found that the environmental regulation intensity of the petroleum industry played a significant role in promoting the total factor productivity of enterprises in the field. Lanoie et al. (2008) conducted an empirical research on Canadian manufacturing. The results showed a reverse change between industrial productivity and environmental regulation in the current period. However, a positive correlation is predicted to occur after four years, which indicates environmental regulation with a certain delay in impact. Lee (2008) estimated the cost-

limiting function of the Korean steel industry and analysed the impact of environmental regulation on its production efficiency. Christoph et al. (2010) used the German computable general equilibrium model to study the effect of carbon tax unilateral introduction. The results show that industrial structure changes are more obvious under an imperfect competition than under a perfect competition. Zhang (2010) believed that in the development process of industrialization and urbanization, the implementation of a clean production is the best choice for economic development. The industrial structure upgrading is an arduous task for the development of each region and should pay attention to environmental protection.

Relevant studies on regulatory mechanism: Lanoie (2011) used the simultaneous equation method to analyse the microdata of enterprises in seven member countries of Organization for Economic Cooperation and Development. The results also showed that environmental regulation has a significant role in promoting R & D investment. Becker et al. (2013) estimated the relationship between plant size and pollution reduction expenditures through the establishment of level data by US manufacturers. The results showed that the effect of environmental regulation varies depending on the company's size and the industry in which it belongs. Zhu et al. (2014) believed that environmental regulation is an important condition for enterprise structure adjustment. Pollution-intensive industries will accordingly adjust production and promote industrial structure upgrading through technological innovations, technology upgrading, and location layout. Wang et al. (2016) believed that environmental regulation has a significantly positive impact on a clean production industry, but a lagging effect on pollution-intensive industries. Thus, the government should formulate environmental regulation standards and industry characteristics, emphasizing flexibility rather than absolute improvements.

Relevant studies on environmental regulation level: Guo (2017) used 2011-2012 data from 30 Chinese provinces to analyse the relationship among environmental regulation, technological innovation, and regional green performance growth. The results showed that only environmental regulation driven by technological innovation produced a positive impact on regional green performance growth. On the basis of the theory of economics and industrial organization, Zhang (2018) incorporated environmental regulation policies into the traditional SCP paradigm and analysed the transmission mechanism of market structure and market behaviour to the coordinated development of environment and economy. The results of the study showed that the environment was strengthened. Supervision is an

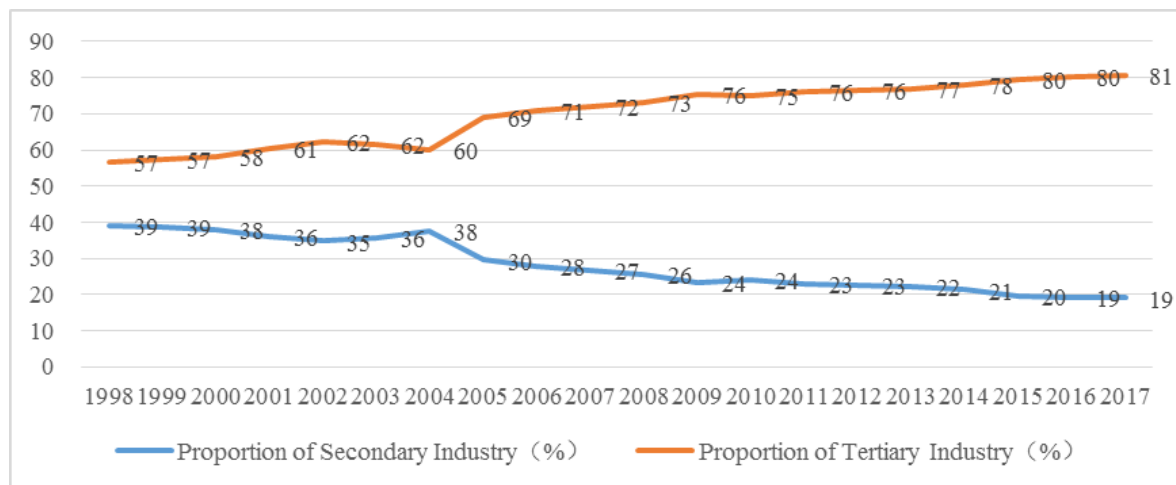


Fig. 1. Proportion of secondary and tertiary industries in Beijing, 1998–2017.

effective means of ensuring economic growth and optimizing environmental quality. Hou et al. (2018) used the 2010–2015 China's Industrial Provincial Panel Data to systematically analyse the regional structure and development trend of industrial green transformation. The study found that China's industry gradually achieved a green transformation and significantly reduced pollution emissions. The existing literature about environmental regulation focused on environmental regulation on economic growth, technological progress, international trade, and industrial restructuring. However, published works on the impact of environmental regulation on industrial structure optimization are scarce. Considering Beijing as an example, this study discusses the impact of environmental regulation on industrial structure from the mechanism of action, expounds the impact of environmental regulation on the optimization of Beijing's industrial structure, and helps the government adopt appropriate environmental regulation policy tools and economic development strategic objectives. By solving resource and environment problems, this study can effectively promote the industrial structure upgrading in various regions of Beijing and achieve sustainable economic development.

INFLUENCE MECHANISM OF ENVIRONMENTAL REGULATION ON INDUSTRIAL STRUCTURE

Environmental Regulation Inhibits the Development of High-pollution Enterprises

The improvement of the environmental regulation intensity can produce the role of survival of the fittest and promote the adjustment and upgrading of industrial structure. Strict environmental regulations will increase production costs by forcing companies to purchase sewage equipment,

reduce production to meet environmental regulations, and limit the use of specific factor inputs. Large-scale pollution-intensive industrial enterprises can reduce pollutant emissions by purchasing sewage equipment or limiting production capacity in a short period of time. Then, the combination of factors and inputs can be adjusted and more low-carbon energy-saving production technologies and service intermediate inputs can be used. These efforts will inevitably lead to faster growth of service industries, which will transform the industrial structure into a service economy. For small and medium-sized polluting industrial enterprises, rising environmental costs will affect their optimal and effective scale. Several of these enterprises are unable to obtain the economies of scale, are likewise unable to replace or upgrade production or pollution control equipment, and are eventually forced to withdraw. In the market, the scale of pollution-intensive industries is gradually shrinking, and the clean industry represented by the service industry will occupy a larger proportion. As a result, strict environmental regulations can successfully eliminate the production capacity of pollution-intensive industries, accelerate the development and expansion of the service industry, and effectively drive the adjustment and upgrading of the industrial structure. Strict environmental regulations will also increase the sunk costs and the marginal production or average costs of the polluting industrial sector, resulting in a decrease in the number of companies entering the polluting industry and increasing those entering the clean industry represented by the service industry. The green barriers to environmental regulation can inhibit the expansion of pollution-intensive industries, accelerate the development of service industries, and promote the transformation of industrial structure to higher levels.

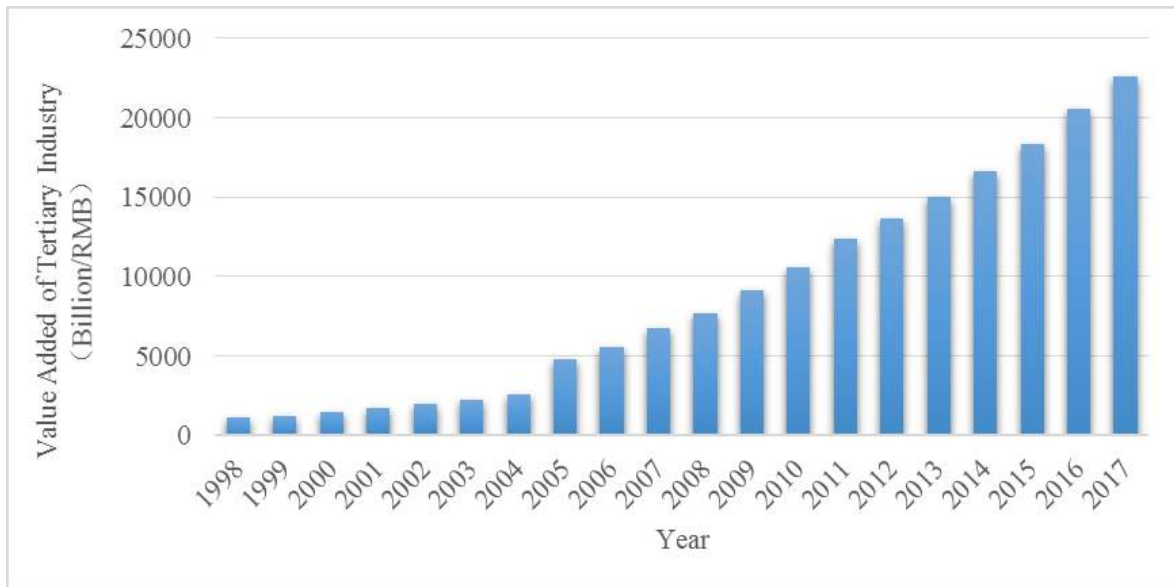


Fig. 2: Value addition of the tertiary industry in Beijing (1998-2017).

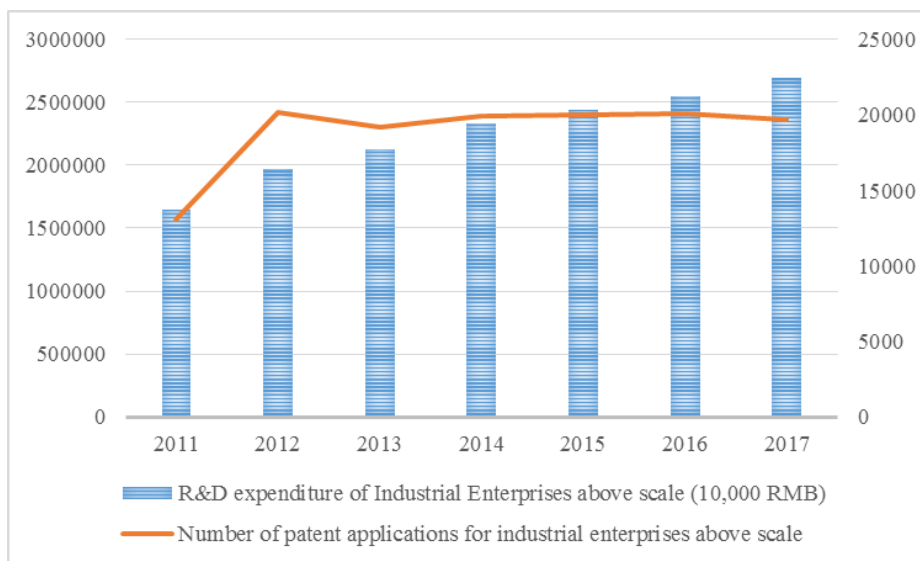


Fig. 3: R&D funds and patent applications of industrial enterprises above scale in Beijing from 2011 to 2017.

Environmental Regulation Accelerates Service Industry Development

Environmental regulation promotes the demand for green consumption. As shown in Fig. 2, the output value of Beijing’s service industry has increased every year, which in turn has driven the development of the green service industry. This development is conducive to the transformation of the industrial structure into a service economy. The direction of technology and industrial upgrading ultimately

depends on consumer or market recognition. Thus, consumers’ response to environmental regulation is the original driving mechanism for industrial restructuring. With the promotion and transmission of the concept of green consumption in the process of environmental regulation, consumer awareness of environmental protection and participation is constantly increasing. Moreover, environmental regulation is conducive to improving consumers’ understanding of product energy consumption information, eliminating the asymmetry between producers and consumers

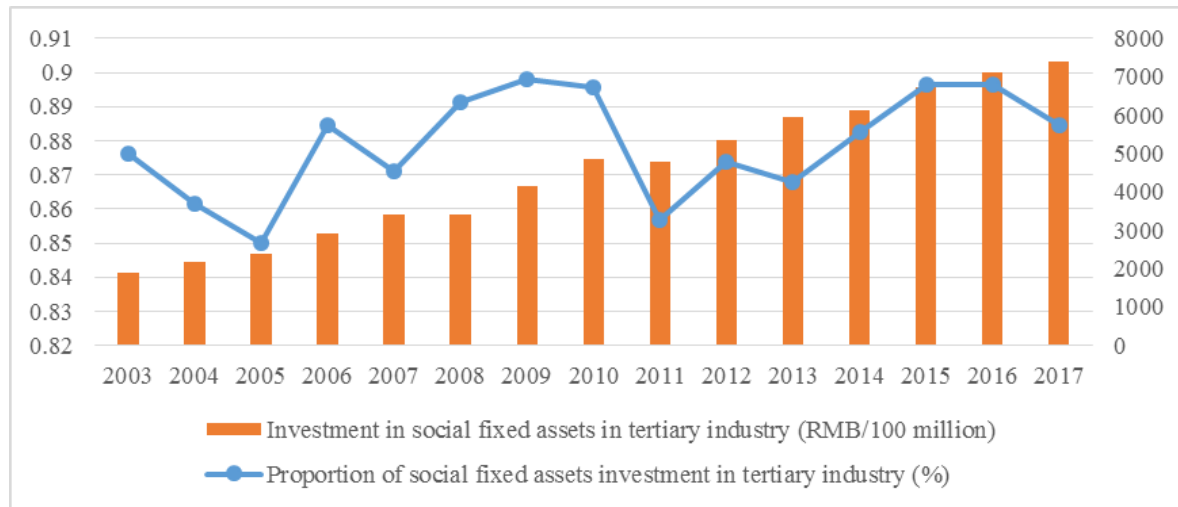


Fig. 4: Amount and proportion of social fixed asset investment in the tertiary industry in Beijing from 2003 to 2017.

about the product environmental protection information, and thus promoting green consumption. In addition, regulation is conducive to encouraging the development and application of green service products and developing and expanding the green service industry. The increase of green consumption will inevitably drive service companies to provide green products and services to consumers, while restricting the circulation of non-green products and entry of non-green services. Such market results in greater power and pressure for the green innovation of service enterprises. Consequently, the scale of green investment for service companies will be inevitably driven and increased, the share of the service industry in the national economy through the investment multiplier effect will be widened, and the industrial structure will be promoted.

Environmental Regulation Promotes More Environment Friendly Production Technology

Environmental regulation can promote the innovation and upgrading of environmental protection technologies, the rapid development of clean and environment-friendly industries represented by the service industry, and the transformation of industrial structure. Enterprises now face strict environmental regulation standards of the government. To control pollution emissions, they will improve their competitiveness by improving production processes, reducing resource input, improving efficiency, reducing production costs, and improving product quality. As shown in Fig. 3, the number of R&D funds and patent applications of industrial enterprises above the designated size in Beijing has increased each year. As a result, industrial enterprises improve their production processes or their pollution control

capabilities through technological innovation and ultimately alleviate or offset the environmental regulations implemented by the government. Environmental costs can generate innovative compensation effects, including products and production processes, to achieve a win-win situation. These R&D and innovation activities for clean production or clean products will help develop equipment and technologies that reduce pollution emissions and deal with existing pollution problems. As a result, the production technology advancement and environmental technology upgrades of the entire industry will be driven, in particular the service industry. The clean and environment-friendly industries represented by the rapid development have promoted the transformation and upgrading of the industrial structure to the service economy.

Environmental Regulation Promotes Investment Structure Optimization

The government's development of environmental regulation tools places adverse constraints on the production activities of pollution-intensive industries. As shown in Fig. 4, the amount of fixed asset investment in the tertiary industry in Beijing has increased each year. Similarly, the proportion of fixed asset investment in the tertiary industry to total industrial social fixed assets has remained at a high level of 85%. Due to the existence of environmental regulations, and driven by economic interests, investors will inevitably turn their investments toward industries with relatively low environmental protection and environmental regulations, which will affect the structure of investment demand. In an area with relatively strict environmental regulation intensity, the investment demand of capital will shift

Table 1: Unit root test.

Variable	ADF	Threshold	AIC	SC	D.W	Result
<i>LnInv</i>	-1.899	-3.029*	1.794	1.894	1.446	Unstable
<i>LnStr</i>	-1.204	-3.832*	-3.897	-3.798	2.327	Unstable
<i>DLnInv</i>	-4.991	-3.858*	1.744	1.845	1.409	Stable
<i>DLnStr</i>	-4.696	-3.857*	-3.778	-3.679	2.076	Stable

Note: * is the threshold at the 1% significance level.

to an energy-saving and clean industry. Therefore, environmental regulation will affect the investment preference of capital to a certain extent. Environmental regulation produces a certain degree of influence on the proportion of investment. For example, the low carbon economy and other related initiatives currently advocated by the policy will lead consumers to use environment-friendly products. Generally, such products have high technical content, and the increase in demand and production costs make this a type of environmental protection. Thus, the product has a higher market price than the ordinary product. However, a relatively loose environmental regulation leads to relatively lower cost of production activities of the enterprise and thereby relatively higher investment activities.

EMPIRICAL RESEARCH

Indicator Selection and Data Source

At present, China mainly uses traditional regulatory methods as environmental regulation tools. Thus, we only study the impact of command-controlled and economic-incentive environmental regulation tools on industrial structure upgrading. In view of the availability and representativeness of the data, we use Beijing's industrial pollution control completion investment (*Inv*) as indicator to measure the intensity of command-controlled environmental regulation. The industrial structure upgrade is represented by the ratio of the added value of the tertiary industry in Beijing to the gross domestic product or GDP (*Str*) in 1998-2017. The data are obtained from the China Statistical Yearbook and China Environmental Statistics Bulletin. To eliminate heteroscedasticity, the time series data are first logarithmically transformed and renamed *LnInv* and *LnStr* after the transformation.

Unit Root Test

In practical problems, when obtaining sample data that present a random time series, the first task is to judge its stationarity. Commonly used time series stationarity test methods include graphical analysis, autocorrelation function analysis, unit root test, and the commonly used ADF unit root test. The latter method is used in this study. Conversely, the non-stationary time series is directly regressed,

and a "pseudo-regression" problem may occur. The unit root test results of *LnInv* and *LnStr* are shown in Table 1.

As shown in Table 1, the ADF values of *DLnInv* and *DLnStr* are smaller than the critical values, and the DW statistics are close to 2. Thus, time series *LnInv* and *LnStr* are levelled after the first-order difference and classified to the first-order single integer.

Cointegration Test

Cointegration theory holds that although each of the two or more variables is non-stationary, some linear combinations may terminate the influence of the trend term, creating a stable combined variable. The significance of cointegration theory is its avoidance of pseudo-regression and differentiation of the long-term equilibrium relationship and short-term dynamic relationship between variables. The precondition for cointegration is that the variables must all be in the same order; otherwise, the cointegration study cannot be performed. A common method of cointegration testing is the Engle-Granger test of two variables, which is used in this study. The steps are as follows.

The equation between *LnInv* and *LnStr* is estimated using the ordinary least squares method, and the non-uniform error is calculated. The estimated equation is:

$$\text{LnStr} = 4.186 + 0.017 \text{LnInv} + 0.971 \text{AR}(1) \quad \dots(1)$$

(0.000) (0.068) (0.000)

The residuals of the regression equation (1) are named separately, denoted as Resid1, and the residuals are subjected to the ADF unit root test (the threshold are all values at the 1% significance level). The results are shown in Table 2.

As shown in Table 2, the sequence and cointegration relationship reflected by the regression model is established. A long-term equilibrium exists between the investment amount of industrial enterprise pollution control and the industrial structure upgrade, wherein the former produces a positive impact on the latter. A unit of completed industrial pollution control investment in Beijing can drive the growth of 0.017 units of added value from the tertiary industry in proportion to the GDP. This finding shows that Beijing can promote the industrial structure upgrading and rapid development of its tertiary industry by completing industrial

Table 2: ADF test results of regression equation residuals.

Variable	ADF	Threshold	AIC	SC	D.W	Result
Resid1	-4.538	-3.832*	-3.909	-3.809	2.1747	Stable

Note: * is the threshold at the 1% significance level.

Table 3: Granger test of railway freight volume and GDP.

Null hypothesis	Lag order	<i>P value</i>	Result
<i>LnStr</i> is not the Granger reason for <i>LnInv</i>	2	0.547	Acceptance
<i>LnInv</i> is not the Granger reason for <i>LnStr</i>	2	0.024	Rejection
<i>LnStr</i> is not the Granger reason for <i>LnInv</i>	3	0.478	Acceptance
<i>LnInv</i> is not the Granger reason for <i>LnStr</i>	3	0.038	Rejection

pollution control investments and implementing pollution control. In addition, as the development of real estate, catering, and tourism in the tertiary industry requires relatively high environmental quality as a guarantee, the development of these industries will promote a high degree of investment in environmental pollution control and strengthen the intensity of environmental regulation.

Granger Test

Causality refers to the dependence between variables. The resulting variable is determined by the causal variable, and changes in the causal variable leads to changes in the resulting variable. The basic premise of the Granger test is that the past cannot be predicted in the future; if the change in *Y* is caused by *X*, then the change in *X* should occur before the change in *Y*. Here, the Granger causality test is required for *LnInv* and *LnStr*. The results are shown in Table 3.

As shown in Table 3, at a significance level of 0.05, the lag periods of 2 and 3 all reject *LnInv* as the Granger reason for *LnStr*, that is, Beijing industrial pollution control completed investment is the Granger reason for the added value of the tertiary industry in proportion to GDP. At a significance level of 0.05, the lag periods of 2 and 3 accept that *LnStr* is also not the Granger reason for *LnInv*, that is, the Beijing industrial pollution control completed investment is not the Granger reason for the added value of the tertiary industry in proportion to GDP. Only a one-way Granger causality exists between *LnInv* and *LnStr*, reflecting the obvious adjustment effect of Beijing's environmental regulation on the industrial structure.

POLICY RECOMMENDATIONS

Strengthen the Implementation of Environmental Regulation Policies and Source Governance

An important means to promote the industrial structure up-

grading of the manufacturing industry and develop green manufacturing is to formulate differentiated environmental regulation policies. Specifically, thorough and in-depth investigations of different industries in different regions and understanding the actual pollution emissions in the current development of the industry are necessary before specific policy formulations to achieve large-scale production and manufacturing, optimize resource allocation, and eliminate backward production capacity. At the same time, the government can reduce the tax revenue of manufacturing enterprises and subsidize enterprises with better pollution treatments. In addition, the government needs to guide enterprises to change from "end-of-pipe governance" to "source governance" and formulate specific regulations on the use of raw materials and in the manufacturing process. These efforts will help control the emission of pollutants from the source and reduce pollutants in the production process.

Encourage Production Enterprises to Conduct Technological Innovation and Create a Good Talent Atmosphere

Active investments and improved level of technological innovation are necessary to emphasize the shift from "end governance" to "source governance". Under the increasingly strict environmental regulation policy, we should adopt active and sustainable response measures, strengthen technological innovation to promote enterprise transformation and upgrading, and remove the reliance on the "end-of-pipe" approach to passively respond to environmental regulation policies. Instead, our efforts must focus on "source governance". Technical innovation should be applied in the production, and the utilization efficiency of raw materials should be improved. The manufacturing process requires improvements and the equipment need upgrades. In addition, enterprises should actively absorb high-quality talents, create good working conditions, and hardware and software environment for technological innovation. Then,

a corporate ideology and cultural atmosphere that emphasizes and pursues technological innovation should be established.

Strengthening Environmental Regulation and Eliminating Backward Production Capacity

The monitoring and testing of pollutant emissions in the process of environmental regulation and the statistical indicators of pollutants should be improved to better detect pollutant emissions and enhance the effectiveness of environmental regulation. An increase in manpower input of the environmental protection department and further improvements of environmental regulation laws and regulations are necessary to ensure the orderly conduct of environmental regulation. As such, the technical level of some industries is lower than the industry average, partly because its production capacity is low, and the energy consumption and pollution emissions of production processes are higher than the industry average. Thus, outdated production capacity should be eliminated. The government should hasten the elimination of backward production capacity by improving market access, improving relevant laws and regulations, and increasing penalties for such industries.

Increase Investment in Technology and Develop High-tech Industries

Despite its rapid development, China's manufacturing industry has long remained in the middle and low-end manufacturing position. On the one hand, many sectors in China's manufacturing industry encounter problems of insufficient technology investment. With their low profit margins, increasing technology investments will inevitably increase their R&D investment and management costs, thereby putting pressure on their survival. On the other hand, in the current international market, the competition among high-tech industries has entered a feverish degree. However, China's high-tech industry is still in its slow development. Therefore, if China wishes to remove its low-end status in the international competition, then the government must strongly support the development of science and technology. The mandatory tasks include increasing investment in technology, prioritizing the development of high-tech industries, optimizing the investment structure, guiding the upgrading of industrial structure, and promoting the integration of "production, study, and research". We should actively seek and strengthen the training mechanism for high-tech talents, increase large-scale production in industries with high pollution control, and provide a certain level of financial support for clean enterprises. The transformation and upgrading of the traditional manufacturing indus-

try should be sped up, and the reshaping of the industrial structure and transfer to the high-tech industry should be completed.

CONCLUSION

With the continuous growth of China's economy and the continuous advancement of modernization, the contradiction between the environment and the extensive economic development growth mode of high emissions, high energy consumption, and high investment has become increasingly prominent. The emerging environmental problems have not only seriously affected people's daily lives and physical health, but also caused huge economic losses. Environmental regulation can promote the optimization and upgrading of the industrial structure while protecting the ecological environment. Considering Beijing as an example, this study first analyses the mechanism of environmental regulation that impact industrial restructuring and then uses the cointegration analysis and Granger causality test to measure the impact of environmental regulation on the industrial structure in Beijing from 1998 to 2017. The research results show that a long-term and positive equilibrium relationship exists between the industrial structure upgrading and environmental regulation in Beijing. A unit of Beijing industrial pollution control completed investment can pull the growth of 0.017 units in the tertiary industry in proportion to the GDP. This factor is determined as the one-way Granger reason for the added value. Finally, this study puts forward relevant measures in strengthening the implementation of environmental regulation policies, encouraging production enterprises to conduct technological innovation, strengthening environmental regulation, and increasing investment in high-tech industry. For future studies, relevant personnel can continue to conduct in-depth research in the following aspects. First, the path from the environmental regulation to the upgrading of the industrial structure should be determined. Second, the measurement system of environmental regulation and industrial structure upgrading should be enhanced. Third, the development model of industrial structure upgrading should be re-examined from the perspective of sustainable development. Finally, an in-depth study should be conducted on the relationship between the level of environmental regulation and the level of technological innovation of enterprises.

ACKNOWLEDGEMENT

This study was supported by the Chinese Social Science Fund (15BJY048).

REFERENCES

Becker, R.A., Pasurka, C.A. and Shadbegian, R.J. 2012. Do environ-

- mental regulations disproportionately affect small businesses? Evidence from the pollution abatement costs and expenditures survey. *Journal of Environmental Economics and Management*, 66(3): 523-538.
- Berman, E. and Bui, L.T.M. 2001. Environmental regulation and productivity: Evidence from oil refineries. *Review of Economics and Statistics*, 83(3): 498-510.
- Christoph, B., Andreas, L. and Welsch, H. 2010. Environmental taxation and induced structural change in an open economy: The role of market structure. *German Economic Review*, 9(1): 17-40.
- Gray, W.B. and Deily, M.E. 1996. Compliance and enforcement: Air pollution regulation in the U.S. steel industry. *Journal of Environmental Economics & Management*, 31(1): 96-111.
- Guo, L.L., Qu, Y. and Tseng, M.L. 2017. The interaction effects of environmental regulation and technological innovation on regional green growth performance. *Journal of Cleaner Production*, 162: 894-902.
- Hou, J., Teo, T. S. H., Zhou, F., Lim, M. K. and Chen, H. 2018. Does industrial green transformation successfully facilitate a decrease in carbon intensity in China? An environmental regulation perspective. *Journal of Cleaner Production*, 184: 1060-1071.
- Lanjouw, J.O. and Mody, A. 1996. Innovation and the international diffusion of environmentally responsive technology. *Research Policy*, 25(4): 549-571.
- Lanoie, P., Laurentlucchetti, J., Johnstone, N. and Ambec, S. 2011. Environmental policy, innovation and performance: new insights on the porter hypothesis. *Journal of Economics & Management Strategy*, 20(3): 803-842.
- Lanoie, P., Patry, M. and Lajeunesse, R. 2008. Environmental regulation and productivity: testing the porter hypothesis. *Journal of Productivity Analysis*, 30(2): 121-128.
- Lee, M. 2008. Environmental regulation and production structure for the Korean iron and steel industry. *Resource and Energy Economics*, 30(1): 1-11.
- Wang, Y. and Shen, N. 2016. Environmental regulation and environmental productivity: The case of China. *Renewable and Sustainable Energy Reviews*, 62: 758-766.
- Zhang, H., Zhu, Z. and Fan, Y. 2018. The impact of environmental regulation on the coordinated development of environment and economy in China. *Natural Hazards*, 91(2): 473-489.
- Zhang, J. F. and Deng, W. 2010. Industrial structure change and its eco-environmental influence since the establishment of municipality in Chongqing, China. *Procedia Environmental Sciences*, 2(1): 517-526.
- Zhu, S., He, C. and Liu, Y. 2014. Going green or going away: Environmental regulation, economic geography and firms' strategies in China's pollution-intensive industries. *Geoforum*, 55(55): 53-65.



Climate Change Patterns in the UAE: A Qualitative Research and Review

Manar Fawzi Bani Mfarrej

Department of Environmental Health and Safety, Department of Applied Sciences and Mathematics, College of Arts and Sciences, Abu Dhabi University, AD Campus, Abu Dhabi, UAE

Nat. Env. & Poll. Tech.
Website: www.neptjournal.com

Received: 22-07-2018

Accepted: 21-09-2018

Key Words:

Climate change
Water resources
Coastal areas
Food security
Green house gases

ABSTRACT

Climate change is an inevitable challenge for the whole world these days. United Arab Emirates (UAE) is classified among the countries with highest rate of vulnerability to the potential impacts of climate change in the world. The purpose of this qualitative research is to study the patterns of climate change in the UAE and to predict the future patterns. The methods used in the study were reviews and interviews as the data collection method. The results obtained summarized that UAE is facing many challenges related to the climate change impacts such as, water resources, coastal areas and food security. UAE's efforts and future plans in dealing with climate change have been discussed. Climate change is hard to control because the emissions of green house gases (GHG) do not respect the boards, so countries should co-operate and take actions on global level to ensure save earth.

INTRODUCTION

Climate change is one of the biggest challenges for the whole world these days. It is defined as any change in the weather caused by dynamic processes of the earth such as volcanoes, or because of human activities such as industrial activities and other activities that create greenhouse gases. (Simon-Lewis 2017).

The main cause of this phenomenon is the emissions produced from human activity; for example the green house gasses (GHG) emissions. The leading reasons of these emissions is burning of fossil fuels, cutting trees, waste incineration, and other activities that produce harmful gases which impact the level of the GHG and make it highly increased. This increase in the GHG levels will contribute directly to increase the climate change that has a lot of harmful effects such as natural disaster due to the increase in the sea level and the effect on crops (IPCC Fifth Assessment Report 2014).

The negative consequences of climate change could be mitigated by switching the dependence more on renewable energy instead of non-renewable energy. Since 1880, the statistics showed that global temperature has risen by 1.4F°. More dependency on renewable energy will reduce the harmful emissions which will prevent the global temperature from exceeding the normal (NASA 2018).

UAE is one of the pioneer countries in the Middle East that makes effort to control the phenomenon of climate change. UAE established a ministry specialized in climate change in particular and the environment, in general, under

the name of the Ministry of Climate Change and Environment. For that, UAE has future plans to depend on the renewable energy instead of fossil fuels by 2021. The ministry provides programs in order to mitigate and adapt with the effects of climate change (UAE Government 2018).

The objectives of this review are to study the patterns of climate change in the UAE's environment and their effects, to determine the effects of climate change in UAE's environment, to predict the future long term effects of the climate change especially on the UAE, and to raise awareness among UAE's population and provide them with the suitable ways to mitigate climate change.

Causes and Effects of Climate Change

One of the most known causes of climate change is carbon dioxide emissions produced by burning of fossil fuels, transportation, and solid waste incineration. These emissions can stay in the atmosphere for a long time due to the slow transfer of carbon to ocean deposits. CO₂ has the ability to absorb infrared spectrum that leads to warming and affects the composition of the atmosphere. Methane produced through the process of producing or transporting fossil fuels (oil, coal, and natural gas) and from agricultural operations; usually remains in the atmosphere for 12.4 years. Nitrous oxide is formed by burning fossil fuels, solid waste, and agricultural or industrial activity with an average age of 121 years in the atmosphere (Simon Lewis 2017)

Greenhouse gases act as a glass barrier to the atmosphere. If the level of GHG continues to grow, more heat will

be trapped in the atmosphere, because it will be able to absorb more infrared radiation, which will increase the level of climate change globally. Trees absorb CO₂ for photosynthesis, burning trees and deforestation increase carbon in the atmosphere due to the disruption of the carbon cycle, which is based on the exchange of carbon between all natural components such as atmosphere, oceans and living things. The rapid increase in carbon is linked to human activity such as industrial activity, agricultural activity and production of electricity, which are the sources of greenhouse gases leading to climate change (Simon Lewis 2017).

If the level of greenhouse gases continues to grow, this will lead to many effects such as; ocean acidification due to increase in the level of CO₂ in oceans which will harm the marine life, melting of snow due to increase of temperature, drought and rising temperatures, frequent hurricanes, increased sea level, desertification leading to food insecurity and famine, and production of agricultural crops will be also be affected (Simon Lewis 2017).

According to a report written by the Stockholm Environment Institute's US Centre, the rising sea levels will cause the United Arab Emirates to lose up to 6 percent of its developed and populated coastline by 2100. The UAE has more than 1200 kilometers of coastline, and 85 percent of its population lives in the country's low-lying coastal areas located several meters below from the sea level (Al Ittihad 2017). Additionally, up to 90 percent of the country's infrastructure based in these regions. Rising sea level poses a significant threat to the country's population, especially the increased risk of tornadoes. The escalating high temperature of the sea level will consequence in thermal contraction, and aggregating sea level (Hamza et al. 2011). The communities living close to the sea level are likely to experience changes in the movement, intensity, and frequency of storms. These vicissitudes are also likely to unpleasantly affect aquatic species movement and reproduction owing to coral bleaching (Hamza et al. 2011).

Other reasons of environmental degradation in the UAE include oil-related activities and dredging which adversely affects the marine life in addition to upsetting the sea's ecological cycle. Some plant and animal species may become extinct, and the animals that do not will probably migrate to the northern mountains. They are unlikely to adapt to these irregular cycles of the climate. Agriculture will also be adversely affected owing to the reduction of freshwater, which is ideal for farming and the increased salt water which does not support farming. Additionally, the high temperatures will also make it difficult to farm all year round, and there may be food shortages shortly (Hamza et al. 2011).

Air pollution has also reached an all-time high at an

emission of 80 tonnes per capita. These emissions are mostly the result of vehicle exhaust fumes and factory emissions. At certain levels, they are toxic to the human health. Currently, the polluted air has been found to aggravate health conditions such as asthma, bronchitis and heart disease. Continued air pollution may cause breathing health adversities especially for children and the elderly.

The GHG emissions that come from human activities are leading to continuous rise of climate change as they are now at their maximum level. Without action, the average earth surface temperature will rise to over the 20th century and it is possible to exceed 3 degree Celsius this century, with expecting some areas of the world to become warmer (Climate Change - United Nations Sustainable Development n.d.).

A study conducted by the environmental agency in Abu Dhabi, about the possible harmful effects of the climate change on the coastline, found that global warming, which is connected with the climate change, is threatening the marine habitats such as coral reefs and mangrove trees, especially in the UAE and the other parts of the Arabian Gulf. In addition, some of the marine ecosystems such as the salt marshes, grasses, and the mangroves could turn down except if they moved to the land. Also, due to the rising sea level, the coastal freshwater will be mixed with the saltwater. Coral reefs damage, less biodiversity in the subtropical and tropical water, changing rain patterns and water availability are all expected.

One more important thing the study has highlighted is the lack or limited scientific information about the negative effects of climate change on the biodiversity, especially in Asia and globally (Todorova 2014).

Climate Change in UAE

The United Arab Emirates (UAE) is identified as one of the most vulnerable countries to the impact of climate change. The stimulus of climate change is anticipated to significantly affect the country's infrastructure, the natural habitat, and the population's health. Analysts reported that social and economic vulnerabilities exacerbated by the interaction of climate change with political, economic and social variables (Hamza et al. 2011). For instance, the interaction of demographic growth and climate change will affect the quality as well as the availability of water resources in the Middle East and North African region. As the hydrological cycle accelerated, the area risks experiencing longer droughts and more intense and variable rainfall events, and these will result in increased probabilities of the extremities of desertification and flooding. As is, the country has come up with various policies under crisis management to ad-

dress the contamination and over-extraction of the land's groundwater aquifers, as well as the increasing shortage of urban water (Climate Change 2017).

According to the Gulf News report, the UAE is not safe from climate change and high carbon emissions. They predict that by 2050 a 2% increase in temperature level and 10% increase in humidity level may occur. The energy consumption will increase by 11%, construction costs will increase about \$834 million, the power required to meet the demand for additional electricity will equal 18 solar power plants, and the new demand for energy will produce CO₂ emission that is equivalent to one car making 17455 round trips to the moon, which will result in a heavy loss. As reported by the Emirates Wildlife and Wildlife Fund (EWS-WWF), climate change poses a threat to the business, economy, and society sector. The UAE certified its commitment to the United Nations Framework Convention on Climate Change (UNFCCC) to reduce the production of electricity from fossil fuel in the UAE and to start depending on the renewable energy by 2021 as 27%, as well as the commitment to the Paris Agreement that helps to keep the rise in global temperature to beneath 2 C° in the coming decades. In addition, the report stated that increasing of cooling in buildings would create a gap in energy supply, inhibit the energy security, increase the costs for consumers, and further greenhouse gas emission. Such as, the demand for air conditioning (cooling and fans) in a model of villas in the UAE might increase the greenhouse gas emissions between 10% and 35% by 2050 based on the CO₂ scenario in the future. In additional, the high temperature and humidity will reduce the productivity of workers, especially who work outside and it will increase the risk level, which is expected to cause losses of up to \$2 trillion, i.e. around Dh 7.3 trillion worldwide due to worker health effects. What might make them take longer breaks or turn their working shift to colder weather like evening and dawn. (Baldwin 2017)

Also, the coastline of the UAE is not only of commercial interest to the tourism sector, but also the Abu Dhabi Global Environment Data Initiative, that the comfort of the coastal and marine resources in Abu Dhabi is costed US \$141 million. It also mentioned the concern about the food security and the prediction in increasing the food price because of the weather events as in a previous report. UAE is one of the most important regions to export food resources which can cause increase in costs and less efficiency due to climate change leading to heat stress and flooding. Companies with a large number of the workers, who work outside, usually have special standards that workers need to follow, which have to be changed to acclimate the increasing temperature to avoid the possible risk to workers. They also stated the impacts of the climate change will not only slow down the

general sectors of the country, but will also have a huge impact on the citizen economy and enlarge the international market of commodity and services. Also, climate change will lead to drastic changes in the market and businesses in terms of costs, which increase the level of risk, especially in coastal areas and lead to reduction of the financial performance of the country (Shabeeh 2017).

In 2005, the UAE ratified the Kyoto Protocol to the UN Convention on Climate Change (UNFCCC). By 2021, UAE will generate 24% of the electricity used in the country from the clean energy instead of the current oil-electricity sources, which will make a huge positive difference on the environment and reduce the severity of many problems, especially climate change.

The Energy and Climate Change Report (2017) showed that by the end of this century, UAE might lose around 6% of its coastline because of the sea level increase. By 2050, as the raise of one meter of the sea level, 1155 square kilometres of the coast will be under water, so 9 meters raise of the sea level will make the emirate of Abu Dhabi and much of Dubai flooded. This shows us that how climate change is a serious threat on all life aspects (Energy and Climate Change 2017).

Food security is another source of concern in the UAE as 87 percent of the food supply in the UAE depends on the agricultural production. It is imported from outside the country and therefore vulnerable to the effects of climate change, which will influence the reliability and accuracy of international food market. That cause in increasing food prices, which results in depression of the households' income and making them vulnerable to food prices as a share of huge amount of their budget on food. Climate changes will affect the nation's agriculture which leads to inclusive turn down in agricultural production. According to Emirates Wildlife Society and World Wildlife Fund (EWS-WWF) report (2017), the increasing of global temperature by 2050 will lead to losses in many sectors in the UAE.

UAE was the first GCC country that accepts the Paris Convention in December 2015 which work to reduce the temperature rise of 1.5 C° by 2018 and to keep the temperature below 2 C°. As Daniel Mitchell and other researches at Oxford University confirmed that the difference between 1.5 and 2 degrees will be peripheral in the temperature rate every year, but will have a significant impact on reducing the possibility of devastating weather events such as floods, desiccation, and free wave. According to the EWS-WWF report, the changes in the air and sea temperature will lead to multiple secondary effects in different sectors of the economy. As the report stated, the direct effect of excessive weather events such as the increase in sea level will disrupt

human's daily activities. As Dubai Department of Tourism and Commerce Marketing stated, the UAE is one of the fastest growing tourism destinations in the world that welcomed more than 14.9 million passengers in 2016 and aims to reach 20 million tourists by 2020. While further research is needed to make changes in tourism due to climate as it is considered the third reason for choosing tourists a destination. If temperatures persist to be higher, the researchers expect a reduction in tourism level by 55% in the UAE by the end of the century. Many heritage and tourist resources such as coastal region attract tourists to the UAE that may be at an increased risk of flooding due to rising sea level (Shabeeh 2017).

The Interviews

In this research, interviews were used as the primary source of information. The first interview was conducted in the Ministry of Climate Change and Environment. The interview was with Mr. Qais Bader Al-Suwaidi, leading the ministry's climate change adaptation project.

A discussion meeting was held with the Environment Agency of Abu Dhabi team, Mr. Rashed Ekaabi, Mr. Marco Vinaccia, Ms. Jane Claire, Ms. Mouza Al Zaabi and Ms. Ruqaya Mohamed. This meeting provided the needed statistics about the impacts of climate change on the UAE.

The interview results are summarized and discussed in the following section.

RESULTS AND DISCUSSION

The Climate Change Effects on the Water Resources in the UAE

There is an impact of climate change on the water resources. Managing the water resources is one of the challenges UAE is facing to achieve the long-term sustainable development. Water resource management became a challenge as the industrial and the agricultural consumption of water is increasing every year along with the population growth rate. The water consumption rates differ from one emirate to another considering the size, economic growth and the population size, but it is important and urgent to manage the water sources at the national level to achieve the water conservation, better water quality, and the restoration of the aquifer systems. In addition to all above factors, climate change is contributing in water-resource management. The water-energy nexus is a framework that views water as a part of integrated water and energy system, rather than as independent source (Flores et al. 2015). In addition to the other reasons of the water-resource management challenge, this framework is important as the climate change affected the

rainfall patterns and the temperature in the whole world and unfortunately UAE and this effect will increase year by year.

Regional Atmospheric Modelling

A regional atmospheric modelling has been done by LNRCCP to evaluate the future climate changes in the UAE. Because of climate change, the average temperature in the winter and summer seasons will increase by 2°C to 3°C over the land areas. As a result of this increase in the temperature, there will be an additional demand for water in case of irrigation as the evaporation rates will be higher.

Regional Ocean Modelling

Regarding oceans, the LNRCCP also did a modelling to evaluate the effects of the climate on the Arab gulf, which UAE depends on to desalination processes. As a result of climate change the Arab gulf will become highly stressed as the temperature will increase significantly in addition to the increase in the zones of the large salinity. Due to that increase in the temperature and the salinity zones, more energy needed for the desalination activities. With the consideration of the brine discharge to the gulf, the salinity zones will increase between 1.1 and 2.6 psu in the south area of the Arab gulf.

Water System Modelling

Using the WEAP system, a water system model was built in the UAE. This model includes the surface and ground water, water demand, water quality, population growth, reuse of water, system losses and consumption. This system shows the water supply centres and the demand centres as the focus is on the flow of water abstraction to the consumption sites.

The Water Demand Scenario

- Regarding agricultural use, due to climate change between 2015 to 2060 additional 4.4 BCM is consumed which is 3.9% higher without the climate change.
- Regarding indoor uses, opposite to the agricultural uses, by applying the conservation measures, total reduction in indoor demand is about 8.8% for the same period, in other words 0.19% annually.

That means that the main impact of climate change is on the Arab gulf as the salinity zones will increase, which means more energy is needed for the desalination activities and on the agricultural uses as the evaporation processes will increase due to the increase in the temperature. These results were expected as the climate change is a real threat on the water resources, and it is contributing to the water-resource management challenge in the UAE.

The Effects of Climate Change on Al Ain Water Resources, Most Green Area with Water Resources in the UAE

All regions in UAE are affected by the climate change, but Al Ain region is the most climatically vulnerable region. As known, it is the only city in the UAE with renewable groundwater. The population of this small area increased dramatically, as in 2011 it reached 570,000. Along with this increase in the population, there was an economic development and agricultural development, the sectors which use most water with 78% consumption of the all water in the eastern region. The dependence of the irrigation in this area is on the Falaj system, which is the use of the surface water runoff from AL Hajar Mountains (Flores et al. 2016). Unfortunately, climate change is affecting the cycles and the patterns of the supplies of the water. So, how the climate change is doing that? Firstly the climate change has already affected the temperature and the rainfall patterns in the UAE including Al Ain city and the increase in the CO₂ concentration in the atmosphere could change the water and agricultural production patterns. This is in addition to the growing population demand for water. About the effect of the climate change on the water supply, the groundwater storage in Al Ain will increase slightly by 2060 because of the wetter conditions caused by the climate change, which will enhance the water recharge. Regarding the water consumption, climate change will increase the demand of water by 5% in 2060 because of the hotter conditions (Flores et al. 2016). The increase in the average groundwater storage will affect the infrastructure of Al Ain city, so there should more dependence of the groundwater than the desalinated water to keep the balance. Because of future wet conditions caused by climate change, there will be a strategic advantage to decrease the desalinated water in favour of local alluvial ground water (Flores et al. 2016). In this case there should be a huge effort to keep the balance between the water supply, the desalinated and the groundwater and the water consumption, to take the benefit of the increased groundwater storage, as an effect of climate change, and to avoid the infrastructure damage.

This impact of climate change was not predicted, but the UAE is taking huge efforts to keep the balance between the desalinated water and the increased level of the groundwater storage.

Effects of Climate Change on the Coastal and Geographic Area in the UAE

The climate change effects are already observed in the UAE's coastal and geographical area. The sea level will rise as an impact of the climate change, which is a threat to the coastal areas of all emirates of UAE, especially areas near to the

beach within one kilometre and it is approximately a home for more than 17000 people. Moreover, Dubai and Ajman will be the most emirates that will be threatened from the related hazard of the rising sea level; for example, the expectation of 2050 shows that 75% of Ajman coastal area will be in the highly exposed area while Dubai ranked second with 36% of its coastal area. However, Abu Dhabi, Sharjah and Fujairah will be the least exposed Emirates to the related hazard.

To discuss, Dubai and Ajman come at the top of the list due to the continued dependency of their economy such as tourism projects and other activities on the coastal zones. On the other hand, the decline in Abu Dhabi, Sharjah and Fujairah compared to Dubai and Ajman is because of the towering of the coastal areas, less chance of storm surge, and less exposure from local and ocean-generated waves.

Effects of Climate Change on Sea Level

New challenges will appear to the decision making on UAE due to the sea level rise. For example, more tides, waves and storms will reach inland more than before because of the rise in the sea level. This increase in the sea level will increase the chance of flooding, erosion and decay of groundwater quality. In addition, the UAE and GCC countries have a high chance to be affected more than any regions in the whole world.

To discuss globally, one of the results of the climate change is the increase in the sea level. This increase in the sea level is because of many factors such as thermal expansion when the water temperature increases so the water expands, melting glaciers and polar ice caps, and ice loss from Greenland and West Antarctica (National Geographic 2017). This rise in the sea level will have many influences as it was mentioned that more tides, waves and storms will reach inland more than before. Moreover, the chances of flooding, erosion and decay of groundwater quality will increase. However, the UAE and GCC counties are facing the risk of rising sea level more than any other region. Also, facing this high risk of rising sea level is because the Arabian Peninsula has a high concentration of population living near to the coastal zones, and the more dependency of economic activity and the tourism projects in coastal zones.

Effects of Climate Change on Food Security

The global food crisis and food goods prices, with the climate change and unsuitable water suppliers, are associated to decrease crop produce and increase food insecurity globally. Most of the imported food to the UAE will be exposed to climate change, such as rice and wheat which are imported from Brazil, India or South Africa, are considered

as unsafe food. On the other hand, beef, mutton and maize, which are imported from Canada, Egypt, New Zealand and Spain are strongly safe and secure. To discuss, around 90% of the food suppliers in the UAE are international food due to UAE desert environment where local production is limited. UAE is also considered as a major region for re-export of food, especially to GCC countries. One of the most important concern regarding food supply is increase in the price of food. For example, cereals such as rice, wheat, maize and oats are imported from India, Australia, Canada and Thailand may show huge swings. Moreover, UAE's population has been increasing around 10.3% yearly. According to the international measure, UAE is a food secure country (Dougherty 2016).

UAE's Efforts and Future Plans Regarding the Climate Change

Carbon ambassador program aims to assist UAE to achieve the economic diversification as well as increase of the awareness level. For that, the Ministry of Climate Change and environment (MOCCA) signed a Memorandum of Understanding (MOU) with Dubai Electricity and Water Authority (DEWA). Mr. Al-Suwaidi, the manager of the adaptation project in the Ministry of Climate Change and Environment, displayed the benefits of carbon ambassador program in raising awareness among the UAE population as the awareness level in UAE is still below half of the population. Also, he confirmed that UAE had a lot of efforts to control and reduce the effects of climate change by reaching the majority of the population. The carbon ambassadors program is administered by DEWA supported by the Dubai Carbon Centre of Excellence (Dubai Carbon), which aims to raise the awareness among university students and engage them in sustainable environment, low carbon growth and effective economy. There are challenges for applying the carbon ambassadors programs such as involving young people in the program and applying the program in different Emirates among the UAE. The program approach is to develop sustainable environment, reduce carbon emission, mitigation and adaptation (Carbon Ambassadors Program 2017). A Memorandum of Understanding (MOU) was signed between the MOCCA and DEWA to achieve the UAE 2021 vision as the MOCCA will be the sponsor of the program to provide training and experience for the carbon ambassador team (DEWA 2017). Carbon ambassadors program will help to raise the awareness level among UAE population and manage the greenhouse emission.

Challenges the UAE is Facing to Control the Effects of Climate Change

The challenge of climate change that UAE face is how to

increase the people's awareness of the problem, how to reduce the greenhouse gases emission, and how to manage greenhouse gases emission from other countries around the world. The United Nation Framework Convention on Climate Change is an agreement among the countries to reduce emissions as Mr. Al-Suwaidi confirmed. Climate change is a big challenge in the 21st century. One of the challenges that UAE face due to climate change is food security as it is affecting the crops growth, availability and price (World Food Programme n.d.). Other challenges are the period of time for appropriate handling to the changes of greenhouse gases concentration as the oceans have the ability to store a huge amount of the heat and applying the renewable energy to manage the GHG emissions. Also, identifying costs to manage climate change is difficult because it includes natural assets where it has no prices (National Research Council 2011). Climate change is topic that has many challenges such as people's awareness of the problem, managing the GHG emissions, and expensive cost of solving this issue.

The Future Plans that the Ministry is Aiming to Achieve to Reduce the Effects of Climate Change

Few countries around the world have a ministry under the name of The Ministry of Climate Change and Environment, which aims to achieve the government's goal and to create an Emirati society capable of dealing effectively with climate change. The National Plan for Climate Change aims to manage greenhouse gas emission, adaptation to climate change, and promote economic diversification. Also, the Energy Department's strategy aims by 2050 that 50 percent of energy production based on clean and renewable sources. In terms of sustainability, Emirates Authority for Standardization and Metrology (ESMA) stickers evaluate equipment efficiency to reduce the environment harmful impact, and the National Climate Adaptation Program aims to make the UAE one of the world's most adaptive to climate change. The Ministry of Climate Change and Environment have introduced the National Climate Adaptation Program (NCAP) and the UAE National Climate Change Plan for 2017 to the media. Engineer Fahad Al hammadi, the director of climate change department, said that UAE is mitigating the climate change phenomenon at an early stage. UAE is reducing the greenhouse gases emissions by setting and adopting a set of regulations and strategies to move to green ways of doing things including all life aspects such as energy, transportation, construction and the prevention of the environment (MOCCA 2017). Also, the UAE certified its commitment to the United Nations Framework Convention on Climate Change (UNFCCC) to reduce the production of electricity from fossil fuel in the UAE and to start to depend

on the renewable energy by 2021 as 27%. As well as, the commitment to the Paris Agreement that helps to rise the global temperature to beneath 2°C in the coming decades (Baldwin 2017). As Dr. Al Zeyoudi in the 23rd meeting of the Conference of the Parties confirmed that the UAE centennial plan objective is to depend on clean energy with 27% by 2021 and 50% by 2050. As well as build a photovoltaic station and being the first in waste to energy project (Abu Dhabi World 2017) UAE has signed an international agreement to mitigate climate change and they have national and local agreement to adapt and mitigate the climate change.

The Ministry's Advice on How Individuals can Contribute to Reduce the Climate Change Impact

Climate change requires everyone's effort as individuals, organization, government and young people on the issue. As individual they need to reduce emission by using high efficiency equipment, follow the regulations, and drink local water to reduce carbon footprint. Sustainable schools in Abu Dhabi need to provide recycling awareness to others to build green environment. Also, they can use "I drink local water" application to provide information about the places that do not buy local water. Climate change is a global issue, but it can be minimized through daily life. For example, save energy by turning off unused devices, use LED or CFL lights, and check the machine labels before buying it. Also, use renewable energy, use public transportation, and use electrical vehicles that helps in reducing the GHG emissions. The most effective way that individuals can do is to being a vegetarian, buy local food, or eat organic food, which will minimize merchandise transportation and save the body from pesticides (Greenpeace International 2016). Climate change is an international problem, everyone around the world needs to participate to minimize its harm effects. Individuals will help in handling climate change problem as they are the biggest and the main factor to change.

Is it Too Late to do Anything About Climate Change?

The Ministry of Climate Change and Environment in many countries is the first that provides a plan for climate change in terms of adaptation and mitigation. As adaptation, they consider the planning and understanding of the impact for 50 or 100 years of the climate change. As mitigation the UAE is advanced industrialized country in terms of renewable or clean energy and reduce emissions. There is no global goal for adaptation other than mitigation, which aims to not increase the temperature of more than two degrees. Mr. Al-Suwaidi said regarding the reaction of society that they need to understand the climate change term to know how to live with it. The awareness need to be increased through

schools visits, social media videos, and existing efforts with youth and agencies. The Ministry of Climate Change and Environment was established in 2016 to strengthen local efforts in all sectors related to climate change and to realize the sustainable development (United Arab Emirates Ministry of Climate Change and Environment). Climate change is one of the main objectives in the UAE to maintain sustainability growth. Globally, UAE with the US has started their first bilateral annual energy dialogue in 2014 to simplify new and current action of the global energy market. Also, government of UAE has organized awareness campaigns to raise the awareness level of the UAE population. As well as, our generation initiatives was established in November 2016 to increases the students awareness of climate change and encourage them how to reduce carbon footprint (The Office Portal of the UAE Government n.d.). UAE has signed to a global agreement to avoid the harmful impact of climate change. The UAE is not late in terms of climate change, they are the first in the world to find a radical solution of the problem.

CONCLUSION AND RECOMMENDATIONS

To conclude, climate change is a wide field to look for its causes, effects and ways of adaptation. Climate change is hard to control because the emissions of Green House Gases (GHG) do not respect the borders, so countries should cooperate and take actions on global level to ensure save the earth. However, that does not mean that working at a local level will change nothing, it should start from a narrow area spreading to the whole world. Any adaptation plan provided by the government should take its place and be a behaviour for the whole public in this particular area. On the other hand, knowing the causes of something will help a lot in eliminating the impacts. As the cause of climate change almost known, starting to mitigate the impacts is a must.

One of the reasons behind the emissions of Green House Gases is the industry manufacturing, transportation emissions, burning fossil fuels, burning waste, and cutting trees. Being focus on each aspect alone will lead directly to changing the expected numbers for the future. For transportation, nowadays countries such as UAE concentrate in depending on the renewable energy for transportation, such as cars working with solar power instead of the fossil fuel, so this will reduce both the transportation emissions as well as the fossil fuel burning. On the other side, afforestation is one of the solutions to overcome the climate change but unfortunately, the wrong practices are still going on like cutting down the trees. The continuing of cutting the trees down will lead to increase in the concentration of the carbon dioxide which is one of the green house gases.

As we have discussed, awareness level plays a major role in applying the solutions provided to reduce the effects of the climate change. The awareness level of the UAE still does not reach half of the population after all the efforts that UAE has taken. Some of the steps that UAE has taken are applying many programs as the carbon ambassadors. The carbon ambassador program looks to increase the level of awareness among students to take actions regarding the carbon emission. In addition, the ministry of climate change is depending more on researching the current situation of the UAE regarding the climate change to develop solutions that will help in mitigating or create an adaptation plan with the effects of climate change.

Adaptation plans for mitigating the effects of the climate change and encouragement of public education by concentrating on sustainability at local level as well knowing the risks of this phenomenon are recommended.

REFERENCES

- Abu Dhabi World 2017. What is the UAE doing to meet the challenge of climate change? Retrieved November 30, 2017, <http://www.adwonline.ae/uae-meet-challenge-climate-change/>
- Al Ittihad 2017. Climate Change Collaborates with DEWA to Sponsor Carbon Ambassadors Program. Retrieved October 14, 2017, from <http://www.alittihad.ae/details.php?id=58859&y=2017>
- Baldwin, Derek 2017. Climate change will hit UAE sectors. Retrieved September 23, 2017, from Gulf News: <http://m.gulfnews.com/news/uae/environment/climate-change-will-hit-uae-sectors-says-report-1.2001267>
- Carbon Ambassadors Program. (n.d.). Retrieved November 18, 2017, from Dubai Carbon <http://dce.ae/wp-content/uploads/2015/04/CAP.pdf>
- Climate Change - United Nations Sustainable Development. (n.d.). Retrieved October 17, 2017, from <http://www.un.org/sustainabledevelopment/climate-change-2/>
- Climate Change 2017. Retrieved October 17, 2017, from <https://government.ae>: <https://government.ae/en/information-and-services/environment-and-energy/climate-change/climate-change>
- DEWA 2017. Ministry of Climate Change and Environment signs MoU with DEWA to sponsor Carbon Ambassadors Programme. Retrieved November 19, 2017, from Dubai Electricity and Water Authority: <https://www.dewa.gov.ae/en/about-dewa/news-and-media/press-and-news/latest-news/2017/10/ministry-of-climate-change-and-environment-signs-mou-with-dewa-to-sponsor-carbon>
- Dougherty, B. 2016. Local, National, Regional Climate Change Programme. Abu Dhabi: Abu Dhabi Global Environmental Data Initiative .
- Energy and Climate Change 2017. Retrieved October 10, 2017, from <https://www.uae-embassy.org/about-uae/energy/energy-and-climate-change>
- Flores, Francisco, Galaitsi, Stephanie and Yates David 2016. Local, National, Regional Climate Change Programme. The Abu Dhabi Global Environmental Data Initiative. Retrieved on December 1, 2017, from https://docs.wixstatic.com/ugd/102678_3d6695caca1d4a05bd85d593d743e87f.pdf
- Flores, Francisco, Galaitsi, Stephanie and Yates, David 2015. National Water-Energy Nexus under Climate Change. The Abu Dhabi Global Environmental Data Initiative. Retrieved November 30, 2017, from https://docs.wixstatic.com/ugd/102678_d1734d69c71e40ad98765cf985151333.pdf
- Greenpeace International 2016. Individual action: What you can do about climate change. Retrieved December 1, 2017, from <http://www.greenpeace.org/international/en/campaigns/climate-change/Solutions/What-you-can-do/>
- Hamza, W., Enan, M.R., Al-Hassini, H., Stuut, J.B. and de-Ber, D. 2011. Dust storms over the Arabian Gulf: A possible indicator of climate changes consequences. *Aquatic Ecosystem Health & Management*, 14(3): 260-268.
- IPCC Fifth Assessment Report 2014. Intergovernmental Panel on Climate Change. http://ipcc.ch/pdf/assessment-report/ar5/syr/AR5_SYR_FINAL_SPM.pdf
- MOCCAE 2017. Ministry of Climate Change and Environment Organizes Media Briefing on UAE National Climate Change Plan 2017-2050. Retrieved October 18, 2017, from <https://www.moccae.gov.ae/en/media-center/news/10/10/2017/ministry-of-climate-change-and-environment-organizes-media-briefing-on-uae-national-climate-change-plan-2017-2050.aspx>
- NASA 2018. Earth Observatory - World of Change: Global Temperatures. <https://earthobservatory.nasa.gov/WorldOfChange/decadaltemp.php>
- National Geographic 2017. Sea level rise: Ocean levels are getting higher. Why is this happening, and what can we do to stem the tide? Retrieved November 27, 2017, from <https://www.nationalgeographic.com/environment/global-warming/sea-level-rise/>
- National Research Council 2011. The unique challenges of climate change. In: *America's Climate Choices*. Washington: National Academy of Sciences, pp. 30-31.
- Shabeeh, R. 2017. How climate change can impact UAE industries. *Khaleej Times*. Retrieved September 28, 2017, from <https://www.khaleejtimes.com/a-warmer-world-by-more-than-15-c-its-impact-on-industries-in-the-uae>
- Simon-Lewis, A. 2017. What is climate change? The definition, causes and effects. Retrieved October 13, 2017, from *Wired*: <http://www.wired.co.uk/article/what-is-climate-change-definition-causes-effects>
- The Office Portal of the UAE Government. (n.d.). Climate Action. UN's 2030 Agenda. Retrieved December 1, 2017 from <https://government.ae/en/about-the-uae/leaving-no-one-behind/13climateaction>
- Todorova, V. 2014. UAE 'cognisant' of climate change's threat to coastline. *The National*. Retrieved October 18, 2017, from <https://www.thenational.ae/uae/environment/uae-cognisant-of-climate-change-s-threat-to-coastline-1.281481>
- UAE Government, 2018. Climate Change. <https://government.ae/en/information-and-services/environment-and-energy/climate-change/climate-change>.
- World Food Programme. (n.d.). Climate Impacts on Food Security. Retrieved December 1, 2017 from <https://www.wfp.org/climate-change/climate-impacts>.



Adsorption Kinetics and Isotherms of Copper Ion in Aqueous Solution by Bentonite Supported Nanoscale Zero Valent Iron

Jigan Zhang and Muqing Qiu[†]

College of Life Science, Shaoxing University, Shaoxing, 312000, P. R. China

[†]Corresponding author: Muqing Qiu

Nat. Env. & Poll. Tech.
Website: www.neptjournal.com

Received: 23-07-2018

Accepted: 21-09-2018

Key Words:

Adsorption

Copper

Bentonite

Nanoscale zero valent iron

ABSTRACT

Copper ions discharged into the water can cause serious damages to the plants and living organisms in water. Therefore, it is very important to develop effective technologies to treat copper ions polluted wastewaters before their discharge into the natural environment. The main objective of this study was to evaluate copper ions removal by bentonite supported nanoscale zero valent iron (nZVI). In this work, the bentonite supported nZVI was synthesized by direct mixing of bentonite pretreated with nZVI. A range of experiments were conducted to evaluate the sorption ability of bentonite supported nZVI to copper ions in aqueous solutions. Results showed that the contact time, pH in solution and initial concentration of copper ions had an important effect on the removal of copper ions from aqueous solution by bentonite supported nZVI. The Freundlich and pseudo-second-order kinetic models can preferably describe the adsorption process.

INTRODUCTION

With the rapid development of industrial activities, a large amount of industrial effluents containing heavy metals is released into surface and underground water, which has resulted in a number of environmental problems (Aleksandra et al. 2015). Heavy metals, such as lead, copper, and cadmium, are toxic and nonbiodegradable. They can accumulate in living organisms, and may thus pose a threat to human health (Jiang et al. 2016). Copper ions have been frequently detected in waste streams and natural waters, as copper is widely used in electrical, machinery, semiconductor, and many other industries. Extensive studies have demonstrated that copper ions discharged into the water can cause serious damages to the plants and living organisms in water (Lukáš et al. 2014). Epidemiological investigation shows that excessive copper intake can result in a series of negative effects to human health, including liver cirrhosis, kidney damage, haemolysis, vomit and cramps (Jin et al. 2016). Therefore, it is very important to develop effective technologies to treat copper ion polluted wastewater before their discharge into the natural environment (Lia et al. 2013).

Several methods, such as chemical precipitation, ion exchange, solvent extraction, electrochemical treatment, reverse osmosis and the application of biological materials, have been proposed for treating copper ions (Regmi et al. 2012, Zuo et al. 2016). However, applications of these methods have been limited because of high capital costs, high

operational costs and ineffective means of disposal of the resulting sludge (Ding et al. 2016). The use of sorbents to remove and recover heavy metals from contaminated industrial effluents has emerged as a potential alternative to conventional methods (Wang et al. 2015). Development of a practical method for effective removal of toxic metal ions from water is still an urgent need and of vital significance to environmental remediation and pollution control (Park et al. 2016).

Nanoscale zero-valent iron (nZVI) is a reducing agent with a significantly large surface area and colloidal effect (Shen et al. 2015). Due to its high activity, nZVI has received increasing attention for the removal of a variety of heavy metals and chlorinated organic contaminants through chemical reduction processes (Tong et al. 2013). However, nZVI often forms aggregates and easily reacts with water and other substances in soil and groundwater environments, which leads to its instability and the rapid loss of reactivity in the subsurface (Su et al. 2016). These significant efforts have focused on the modification of aggregation alleviation of nZVI (Marcio et al. 2017). It has been demonstrated that the support of nZVI by many materials, such as clay minerals, zeolite, carbonaceous materials, biopolymers, Fe₃O₄ and resin, is effective for dispersing the nZVI and reducing its agglomeration, thus increasing the reactivity (Kerkez et al. 2014). Among these stabilizing materials, porous carbon and minerals are commonly used for nZVI. As carbon materials have a large specific surface area and, a

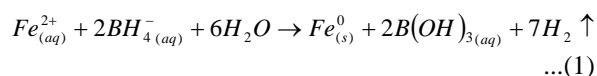
porous and stable structure, they are often used as supporting materials for nZVI (Wang et al. 2016).

The main objective of this study was to evaluate copper ions removal for bentonite supported nZVI. In this work, the bentonite supported nZVI was synthesized through direct mixing of bentonite pretreated with nZVI. A range of experiments were conducted to evaluate the sorption ability of bentonite supported nZVI to copper ions in aqueous solutions. Furthermore, the mechanisms of copper ions in aqueous solution removal by bentonite supported nZVI were explored and discussed.

METHODS AND MATERIALS

Materials: The adsorbate in this study was copper prepared by dissolving $\text{CuSO}_4 \cdot 5\text{H}_2\text{O}$ into 1000 mL of deionized water to stock solution concentrations of 1000 mg/L. The adjustment of pH in solution was achieved by adding 10% NaOH and 1 mol/L HCl.

The nZVI was synthesized in the laboratory using a modified method from previous liquid phase method by adding the macromolecule stabilizer. The basic principle of the synthesis process was that ferrous ion was rapidly reduced to the nanoscale zero valent iron by borohydride solution following the equation below:



The concentration of 100 mL 0.02 M ferrous chloride solution was prepared and then 4 g PVP was added into the ferrous chloride solution in a beaker with vigorous stirring till PVP was completely dissolved. The 5 g bentonite was swiftly added to the above solution and the mixture was agitated in a water bath shaker with a shaking rate of 120 rpm at room temperature for 20 minutes. Then the product was separated by filtration, washed with alcohol three times AND vacuum dried for 12 hr at 60°C. The dry bentonite supported nZVI was gained and used for the following experiments.

Experimental process: Adsorption experiments were conducted in a set of 250 mL Erlenmeyer flasks containing 0.1 g bentonite supported nZVI and 200 mL of Cu^{2+} ion solution with various initial concentrations (between 10 mg/L and 50 mg/L). The initial pH was adjusted to 4.0 with 1 mol/L HCl. The flasks were placed in a shaker at a constant temperature of 298 K and 200 rpm. The samples were filtered and analyzed.

Analytical methods: The BET surface area of the bentonite supported nZVI was analyzed with an ASAP2020 system. The particle size, morphology and structure of the bentonite supported nZVI were characterized by scanning electron

microscopy (SEM) and transmission electron microscopy (TEM). The concentration of Cu^{2+} ion was analyzed by atomic absorption spectrophotometry.

The amount of adsorbed Cu^{2+} ion q_t (mg/g) at different times, was calculated as follows:

$$q_t = \frac{(C_0 - C_t) \times V}{m} \quad \dots(2)$$

Where, C_0 and C_t (mg/L) are the initial and equilibrium liquid-phase concentrations of Cu^{2+} ion respectively. V (L) is the solution volume and m (g) is the mass of adsorbent used.

Statistical analyses of data: All experiments were repeated in duplicate and the data of results were the mean and the standard deviation (SD). The value of the SD was calculated by Excel Software. All error estimates given in the text and error bars in figures are standard deviation of means (mean \pm SD). All statistical significances were noted at $\alpha=0.05$ unless otherwise noted.

RESULTS AND DISCUSSION

Characterization of bentonite supported nZVI: The specific surface area is the main indicator reflecting the adsorption capacity of adsorbent. The BET surface area of the bentonite supported nZVI was analyzed with an ASAP2020 system. The specific surface area of bentonite supported nZVI was 31.15 m^2/g , which was larger than that of bentonite. The result was similar to surface areas of other supported nanoscale iron materials (Pang et al. 2014).

The morphology and particle distribution of bentonite and bentonite supported nZVI was analyzed by SEM. The results are shown in Fig. 1.

From Fig. 1, it can be concluded that the bentonite had a layered structure, and there were a lot of crevices between different layers, which provided enough space for supporting nanoscale iron particles. The bentonite supported nanoscale zero valent iron was aggregated as a chain-like clusters.

The TEM image of bentonite and bentonite supported nZVI is shown in Fig. 2. The bentonite supported nZVI has a core shell structure.

Effect of contact time: The contact time is one of the important parameters in this experiment. The effect of contact time on the removal of copper ion in aqueous solution by bentonite supported nZVI was carried out at pH 4.0, initial concentration of copper ion 40 mg/L and a constant temperature of 298 K and 200 rpm. The experimental results are shown in Fig. 3.

The efficiency of copper ions removal from the aqueous

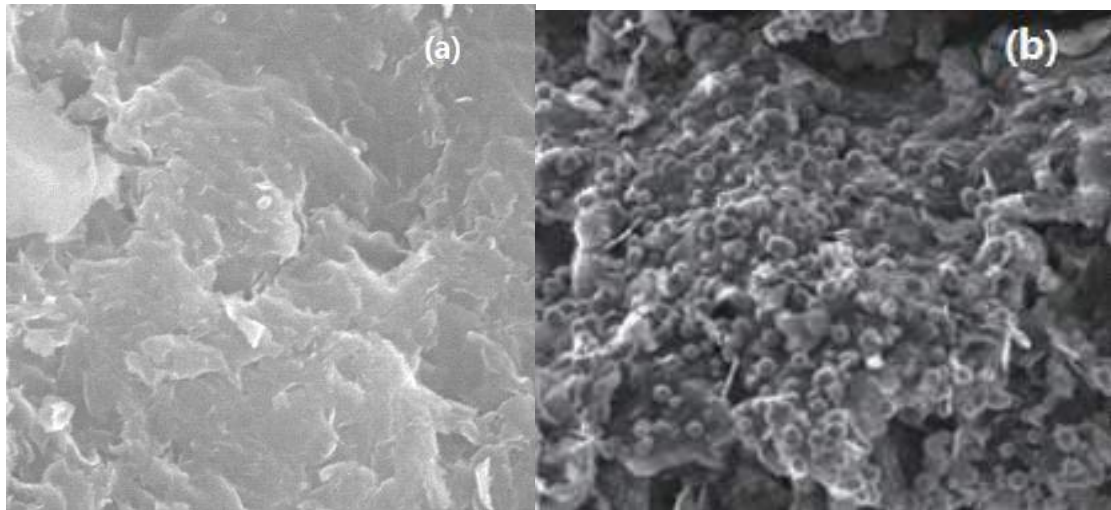


Fig. 1: SEM images of bentonite and bentonite supported nZVI, (a) bentonite and (b) bentonite supported nZVI.

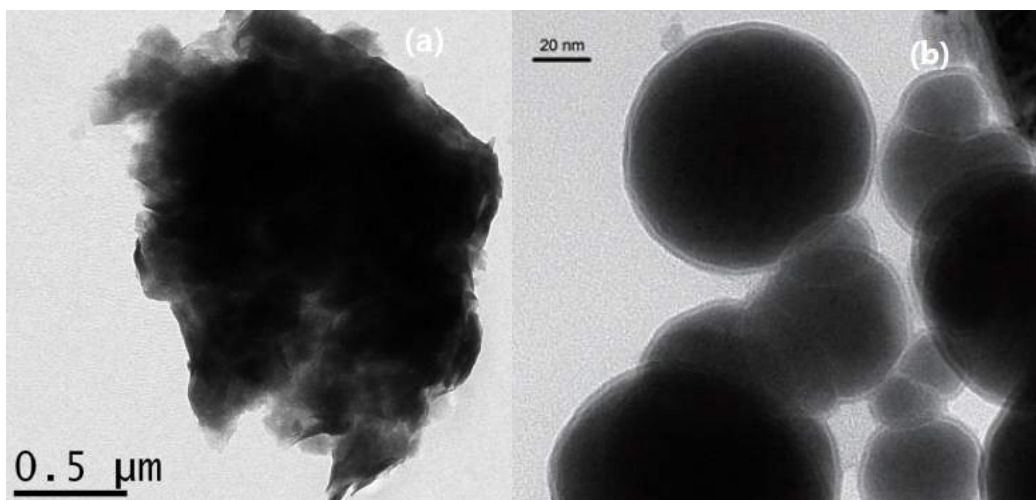


Fig. 2: TEM images of bentonite and bentonite supported nZVI, (a) bentonite and (b) bentonite supported nZVI.

solution increased rapidly as the contact time increased. At first stage, the removal process was very quick. When the contact time was 120 minutes, the efficiency of copper ions removal from aqueous solution was similar. It may be inferred that the contact time of 120 minutes was equilibrium time and adsorption process reached a saturation state.

Effect of pH: The initial pH of the electroplating effluent is a key factor determining the efficiency of copper ion in aqueous solution removal. The effect of pH on the removal of copper ion in aqueous solution by bentonite supported nZVI was carried out at a contact time of 120 minutes, initial concentration of copper ion 40 mg/L and a constant temperature of 298 K and 200 rpm. The experimental re-

sults are shown in Fig. 4.

As shown from Fig. 4, the removal rate of copper ion in aqueous solution increased significantly as the initial pH was increased. At low solution pH values, oxygen containing groups (e.g., carboxyl and hydroxyl) on the surfaces of bentonite supported nZVI might be positively or neutrally charged, which hindered the adsorption of positively charged metal ions (Liu et al. 2011). As a result, increase in pH promoted the removal the heavy metals in this work.

Effect of initial concentration of copper ions: In order to test the effect of initial concentration of copper ions, the following experiments were carried out. The initial concentration of copper ions was ranged from 10 mg/L to 50 mg/L.

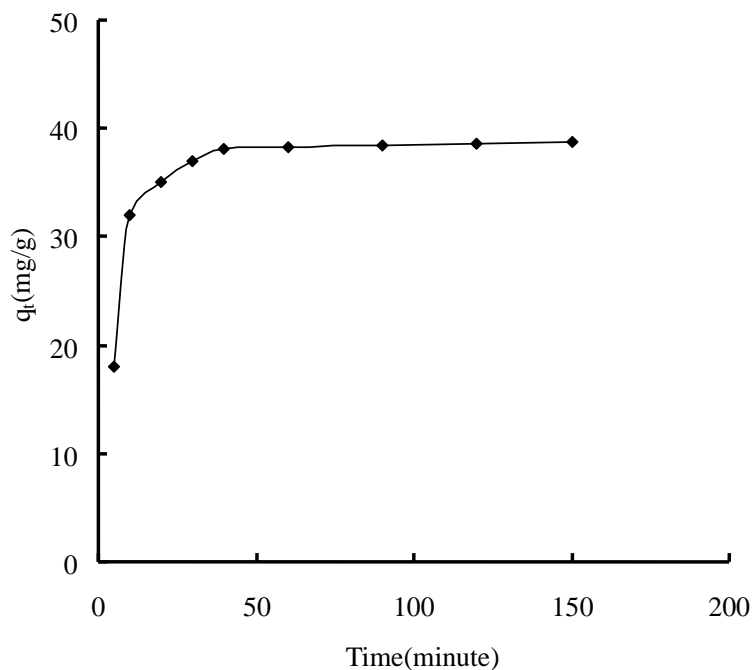


Fig. 3: Effect of contact time on the removal of copper ion in aqueous solution by bentonite supported nZVI.

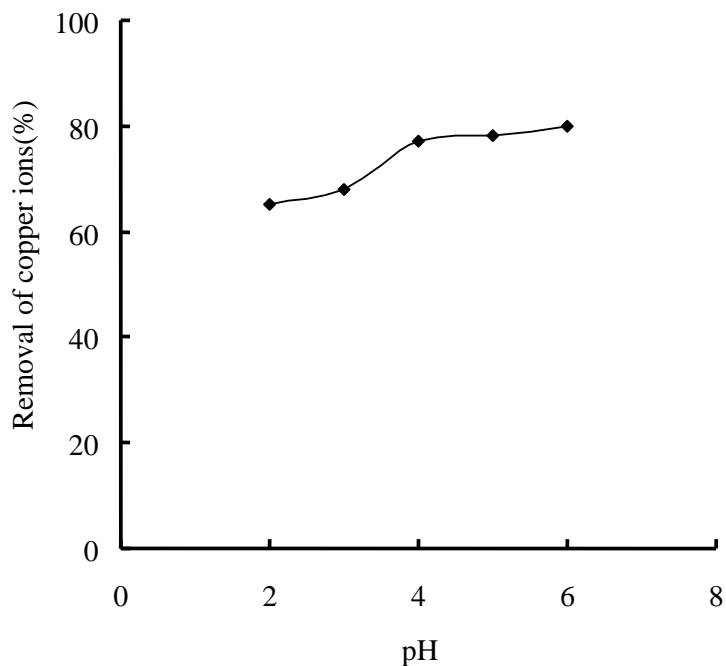


Fig. 4: Effect of pH on the removal of copper ion in aqueous solution by bentonite supported nZVI.

The other parameters were pH 4.0, contact time of 120 minutes and a constant temperature of 298 K and 200 rpm. The results are shown in Fig. 5.

The sorption of copper ions decreased with the initial

concentration of copper ions in aqueous solution.

Sorption isotherms: Langmuir and Freundlich adsorption isotherms suggested that the main adsorption mechanism usually involved the integrative effects of several kinds of

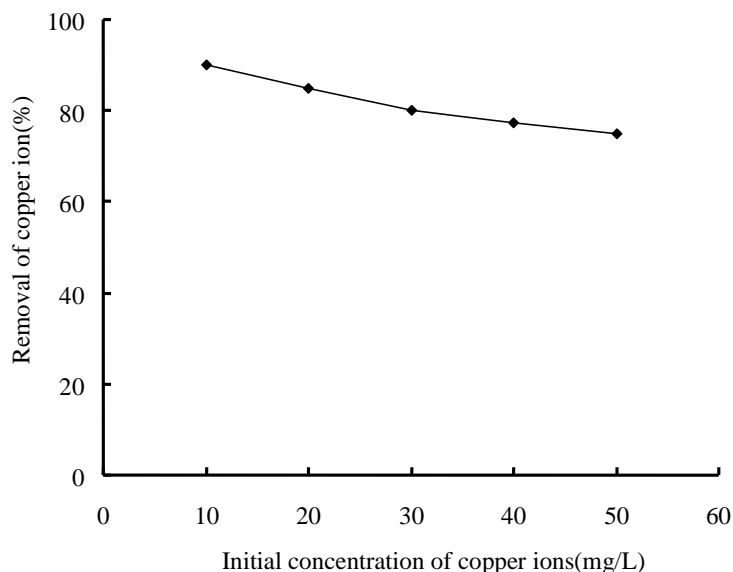


Fig. 5: Effect of initial concentration of copper ions on the removal of copper ion in aqueous solution by bentonite supported nZVI.

interactions, including electrostatic attraction, ion-exchange, physical adsorption, surface complexation and/or precipitation. The experimental data were fitted by Langmuir and Freundlich isotherms as follows.

The Langmuir model and Freundlich model of linear forms are (Liu & Zhang 2011):

$$\frac{C_e}{q_e} = \frac{1}{K_L q_{max}} + \frac{C_e}{q_{max}} \quad \dots(3)$$

$$\ln q_e = \ln K_F + \frac{1}{n} \ln C_e \quad \dots(4)$$

Where, C_e (mg/L) is the equilibrium concentration in the solution, q_e (mg/g) is the adsorbate adsorbed at equilibrium, q_{max} (mg/g) is the maximum adsorption capacity, n is the Freundlich constant related to adsorption intensity, K_L (L/mg) and K_F ((mg/g)^{1/n}) are the adsorption constants for Langmuir and Freundlich models respectively. The results are given in Table 1.

As seen from Table 1, the value of R^2 is 0.9571 according to the Langmuir isotherm model. The value of R^2 is 0.9991 according to the Freundlich isotherm model. Therefore, the adsorption process of the Cu²⁺ ion in aqueous solution by the bentonite supported nZVI fitted well with the Freundlich isotherm model. This indicated that chemisorption on heterogeneous surface played a dominating role in adsorption of copper ions.

Kinetics of copper ion adsorption: Two kinetic models, pseudo-first-order and pseudo-second-order were used to analyse the adsorption processes.

Table 1: Parameters of Langmuir isotherm model and Freundlich isotherm model for the description of Cu²⁺ ion adsorption onto the bentonite supported nZVI.

qm(mg/g)	Langmuir		Freundlich		
	K_L	R^2	K_F	n	R^2
52.63	0.17	0.9571	9.03	1.79	0.9991

The pseudo-first-order model:

$$\ln(q_e - q_t) = \ln q_e - k_1 t \quad \dots(5)$$

The pseudo-second-order model:

$$\frac{t}{q_t} = \frac{1}{k_2 q_e^2} + \frac{1}{q_e} t \quad \dots(6)$$

Where, q_t (mg/g) is the amount of copper ions adsorbed at time t , k_1 (h⁻¹) and k_2 (g/mg/h) are the pseudo-first-order reaction rate constant and the pseudo-second-order reaction rate constant, respectively. The results are presented in Table 2.

From Table 2, it can be seen that the adsorption process fits well with the pseudo-second-order kinetics model according to the value of R^2 . It implies that the predominant process is chemisorption, which involves a sharing of electrons between the adsorbate and the surface of the adsorbent.

CONCLUSIONS

In this work, the bentonite supported nanoscale zero valent iron was synthesized through direct mixing of bentonite

Table 2: Parameters of the pseudo-first-order kinetic model and the pseudo-second-order kinetic model for the description of Cu²⁺ ion adsorption onto bentonite supported nZVI.

Pseudo-first-order kinetic model			Pseudo-second-order kinetic model		
k ₁ (min)	q _e (mg/g)	R ²	k ₂ (mg/g min)	q _e (mg/g)	R ²
0.042	8.65	0.8745	0.0085	39.68	0.9994

pretreated with nZVI. A range of experiments were conducted to evaluate the sorption ability of bentonite supported nZVI to copper ions in aqueous solutions. The results showed that the contact time, pH in solution and initial concentration of copper ions had an important effect on the removal of copper ions from aqueous solution by bentonite supported nZVI. The Freundlich and pseudo-second-order kinetic model can preferably describe the adsorption process.

ACKNOWLEDGEMENTS

This study was financially supported by the project of science and technology plan in Shaoxing City (2017B70058).

REFERENCES

- Aleksandra, B., Patryk, O. and Ryszard, D. 2015. Application of laboratory prepared and commercially available biochars to adsorption of cadmium, copper and zinc ions from water. *Biores. Technol.*, 196: 540-549.
- Ding, Z.H., Hu, X., Wan, Y.S., Wang, S.S. and Gao, B. 2016. Removal of lead, copper, cadmium, zinc, and nickel from aqueous solutions by alkali-modified biochar: Batch and column tests. *J. Ind. Eng. Chem.*, 33: 239-245.
- Jiang, S.S., Huang, L.B., Tuan, A.H., Nguyen, Y.S.O., Rudolph, V., Yang, H. and Zhang, D.K. 2016. Copper and zinc adsorption by softwood and hardwood biochars under elevated sulphate-induced salinity and acidic pH conditions. *Chemosphere*, 142: 64-71.
- Jin, H.M., Muhammad, U.H., Capareda, S., Chang, Z.Z., Huang, H.Y. and Ai, Y.C. 2016. Copper(II) removal potential from aqueous solution by pyrolysis biochar derived from anaerobically digested algae-dairy-manure and effect of KOH activation, *J. Environ. Chem. Eng.*, 4: 365-372.
- Kerkez, D.V., Tomašević, D.D., Kozma, G., Becelic-Tomin, M.R., Prica, M.D., Rončević, S.D., Ákos, K., Božo, D. and Dalmacija, Z.K. 2014. Three different clay-supported nanoscale zero-valent iron materials for industrial azo dye degradation: A comparative study. *J. Taiwan Inst. Chem. Eng.*, 45: 2451-2461.
- Lia, M., Liu, Q., Guo, L.J., Zhang, Y.P., Lou, Z.J., Wang, Y. and Qian, G.R. 2013. Cu(II) removal from aqueous solution by *Spartina alterniflora* derived biochar. *Biores. Technol.*, 141: 83-88.
- Liu, Z.G. and Zhang, F.S. 2011. Removal of copper (II) and phenol from aqueous solution using porous carbons derived from hydrothermal chars. *Desalination*, 267: 101-106.
- Lukáš, T., Šigut, R., Šillerová, H., Faturíková, D. and Komárek, M. 2014. Copper removal from aqueous solution using biochar: Effect of chemical activation. *Arab. J. Chem.*, 7: 43-52.
- Marcio, B.R., Jefferson, S., Juan, A.Z. and Juan, J.R. 2017. Synthesis, characterization and application of nanoscale zero-valent iron in the degradation of the azo dye Disperse Red 1. *J. Environ. Chem. Eng.*, 5: 628-634.
- Pang, Z.H., Yan, M.Y., Jia, X.S., Wang, Z.X. and Chen, J.Y. 2014. Debromination of decabromodiphenyl ether by organomontmorillonite-supported nanoscale zero-valent iron: Preparation, characterization and influence factors. *J. Environ. Sci.*, 26: 483-491.
- Park, S.H., Cho, H.J., Ryu, C. and Park, Y.K. 2016. Removal of copper(II) in aqueous solution using pyrolytic biochars derived from red macroalga *Porphyra tenera*. *J. Indust. Eng. Chem.*, 36: 314-319.
- Regmi, P., Moscoso, J.L.G., Kumar, S., Cao, X.Y., Mao, J.D. and Schafran, G. 2012. Removal of copper and cadmium from aqueous solution using switchgrass biochar produced via hydrothermal carbonization process. *J. Environ. Manage.*, 109: 61-69.
- Shen, Z.T., Jin, F., Wang, F., McMillan, O. and Al-Tabbaa, A. 2015. Sorption of lead by Salisbury biochar produced from British broadleaf hardwood. *Biores. Technol.*, 193: 553-556.
- Su, H.J., Fang, Z.Q., Tsang, P.E., Zheng, L.C., Cheng, W., Fang, J.Z. and Zhao, D.Y. 2016. Remediation of hexavalent chromium contaminated soil by biochar-supported zero-valent iron nanoparticles. *J. Hazard. Mater.*, 318: 533-540.
- Tong, X.J. and Xu, R.K. 2013. Removal of Cu(II) from acidic electroplating effluent by biochars generated from crop straws. *J. Environ. Sci.*, 25: 652-658.
- Wang, H.Y., Gao, B., Wang, S.S., Fang, J., Xue, Y.W. and Yang, K. 2015. Removal of Pb(II), Cu(II) and Cd(II) from aqueous solutions by biochar derived from KMnO₄ treated hickory wood. *Biores. Technol.*, 197: 356-362.
- Wang, W., Hua, Y.L., Li, S.L., Yan, W.L. and Zhang, W.X. 2016. Removal of Pb(II) and Zn(II) using lime and nanoscale zero-valent iron (nZVI): A comparative study. *Chem. Eng. J.*, 304: 79-88.
- Zuo, X.J., Liu, Z.G. and Chen, M.D. 2016. Effect of H₂O₂ concentrations on copper removal using the modified hydrothermal biochar. *Biores. Technol.*, 207: 262-267.



Effect of Solution pH and Coexisting Ions on Cefradine Adsorption onto Wheat Straw

Binguo Zheng[†], Zhenmin Wan, Lizhen Liang, Qingzhao Li and Chunguang Li

School of Civil Engineering, Zhengzhou Institute of Aeronautical Industry Management, Zhengzhou 450015, PR China

[†]Corresponding author: Binguo Zheng

Nat. Env. & Poll. Tech.
Website: www.neptjournal.com

Received: 28-07-2018
Accepted: 21-09-2018

Key Words:

Wheat straw
Cefradine
Adsorption
Kinetics
Coexisting ions

ABSTRACT

Agricultural waste wheat straw was innovatively used for the adsorptive removal of cefradine. The aim of this study is to assess the adsorption behaviour of wheat straw for cefradine removal from the wastewater. Effect of solution pH and coexisting ions was investigated concurrently. Typical kinetic models including pseudo-first-order, pseudo-second-order and Elovich models were used to simulate adsorption kinetics at different pH conditions. Kinetic experiments indicated that both the linear and nonlinear pseudo-second-order kinetic models could describe the adsorption kinetics better. It can be inferred that chemisorption occurred between the cefradine molecules and the wheat straw. It is worthy to mention that most of the uptake occurred within the initial 60 min, indicating a fast removal of cefradine when wheat straw was applied in practical wastewater treatment. Ionic strength experiment demonstrated that cefradine molecules may be specifically adsorbed on the wheat straw via forming outer-sphere surface complexes. A decrease of the uptake of cefradine was observed in the presence of HCO_3^- , HPO_4^{2-} , SO_4^{2-} and SiO_3^{2-} , while the inhibiting effect was in the pecking order $\text{Na}_2\text{SiO}_3 > \text{Na}_2\text{SO}_4 > \text{Na}_2\text{HPO}_4 > \text{NaHCO}_3$. The presence of humic acid could decrease the cefradine uptake as well.

INTRODUCTION

Human activities have caused discharge of a number of pollutants into the natural water environment. As such, whether from domestic or industrial wastewater, various pollutants could be detected in the water discharge and the water bodies involved. Drugs in water environment have been globally concerned. Several hundred different antibiotic substances are widely applied in the past years and most of them eventually enter into rivers, lakes and other water bodies. Antibiotics have been considered emerging pollutants due to their continuous input and persistence in the aquatic ecosystem (Yang et al. 2011). Chemicals including antibiotics released into the environment from human activities are responsible for adverse ecological effects if the concentrations are higher than a threshold of environmental self-purification and organism tolerance (Jiang et al. 2010, Homem & Santos 2011, Chen & Guo 2012). Therefore, it will be better if antibiotics can be removed before the antibiotics containing wastewaters are discharged into the environment.

Cefradine is a first generation cephalosporin antibiotic. Some techniques such as hydrolysis, biodegradation, photolysis and adsorption of cephalosporin antibiotics were investigated. Cefradine is easy to degrade in water, but because of the large use in China, the ecological risk caused by its continuous discharge into the water cannot be ig-

nored. The potential toxicity of its degradation products also needs further study (Chen et al. 2012).

Although various water treatment technologies could be applied to the degradation and removal of cefradine, adsorption technology has been identified as one of the most practical and efficient water treatment technology. This is because adsorption has advantages such as ease of operation and high efficiency. Sludge can be used as adsorbent to adsorb cefradine in water, but the amount of adsorption is relatively small. Accordingly, searching out efficient adsorbents emerges to be a fundamental approach to achieve cefradine removal. There are many studies on the adsorption of contaminants on plant materials. Han et al. (2008) used peanut husk as an adsorbent to remove Neutral Red aqueous solutions. The plant materials have a good adsorption performance to remove the pollutants.

One potential adsorbent material can be wheat straw, which can be used for such purposes as it can also bring an unlimited number of economic and environmental benefits to the industrial wastewater treatment. Wheat straw is an agricultural waste, which is extensively cultured in North China. Most of this agricultural waste is arbitrarily discarded or set on fire. These disposals will result in environmental pollution.

Therefore, this study investigated the use of a previously untried biosorbent wheat straw for cefradine removal by

adsorption. The adsorption kinetics, effect of ionic strength, effect of coexisting ions in the experiment was investigated. The aim of the study was to develop low-cost adsorbents for an inexpensive cefradine removal technology.

MATERIALS AND METHODS

Chemicals: Cefradine was purchased from Tianjin Kermel Chemical Reagents Co., Ltd (Tianjin, China) and used without further purification. Other chemicals used were of analytical reagent grade. Deionized and doubly distilled water was used throughout this study.

Adsorbent preparation: Wheat straw was collected from farmland in Zhengzhou of Henan Province, China. The collected biomass was washed, dried, crushed and sieved using a 40 mesh sieve. Finally, the wheat straw particles were stored in a desiccator for further use.

Batch adsorption studies: Adsorption of cefradine onto the wheat straw was conducted in a series of cylindrical flasks. The stock solution of cefradine was prepared in DI water. All working solutions were prepared by diluting the stock solution with DI water to the desired concentration. The reaction temperature was controlled at a constant of 25°C. The solution pH adjustment was conducted by the addition of diluted HCl or NaOH solution.

For kinetic experiments, a desired amount of wheat straw (1000 mg) was added to a conical flask containing 1000 mL of cefradine solution with a concentration of 20 mg/L. Constant and vigorous stirring was maintained by mechanical agitation for 24 h. After adsorption, samples of 5 mL were taken from the suspension at predetermined times. To investigate the influence of ionic strength on the cefradine adsorption, experiments were carried out using 150 mL glass vessels containing 50 mL cefradine solution and 50 mg wheat straw. The ionic strength of the solutions varied from 0 to 0.1 mol/L by adding different amount of NaNO₃. The effects of coexisting ions in wastewater such as HCO₃⁻, HPO₄²⁻, SO₄²⁻ and NO₃⁻ on cefradine adsorption were investigated by adding NaHCO₃, Na₂HPO₄, Na₂SO₄ and NaNO₃ to 20 mg/L of cefradine solution, respectively. The concentration of coexisting anions ranged from 0.01 to 10 mM/L.

Analysis of cefradine: All the samples were collected and filtered through a 0.45 μm pore-size membrane before analysing. The cefradine concentration was determined by measuring the absorbance at a fixed wavelength (266 nm) using a UVmini-1240 spectrophotometer (Shimadzu, Japan) (Hu et al. 2012). The adsorption capacity was calculated using the following equation:

$$q_e = (C_0 - C_e)V/W \quad \dots(1)$$

$$q_t = (C_0 - C_t)V/W \quad \dots(2)$$

Where, q_e and q_t (mg/g) are the adsorption capacities at equilibrium and time t (min); C_0 is the initial concentration of cefradine in solution, while C_e and C_t (mg/L) are the concentrations of cefradine at equilibrium and t (min), respectively; V (L) is the volume of solution, and W (g) is the mass of adsorbent used.

RESULTS AND DISCUSSION

Adsorption kinetics: In order to assess the adsorption capability for cefradine from wastewater by wheat straw, adsorption kinetics was investigated at pH 4.0, 7.0 and 10.0, respectively. Typical kinetic models, including pseudo-first-order, pseudo-second-order and Elovich models were used to fit the experimental data (Mi et al. 2016).

The nonlinear pseudo-first-order model is expressed as (Lagergren 1898) :

$$q_t = q_e(1 - e^{-k_1 t}) \quad \dots(3)$$

The nonlinear pseudo-second-order model can be expressed as (Ho & McKay 1999)

$$q_t = \frac{k_2 q_e^2 t}{(1 + k_2 q_e t)} \quad \dots(4)$$

The Elovich model can be expressed as (Kithome et al. 1988)

$$q_t = a + k \ln t \quad \dots(5)$$

The mathematical representation of the linear models of pseudo-first-order and pseudo-second-order kinetics are given in the following equations:

$$\ln(q_e - q_t) = \ln q_e - k_1 t \quad \dots(6)$$

$$\frac{t}{q_t} = \frac{1}{k_2 q_e^2} + \frac{t}{q_e} \quad \dots(7)$$

Where, q_e and q_t are the adsorption capacities (mg/g) of the adsorbent at equilibrium and at time t (min), respectively; k_1 (/min) and k_2 (g/[mg min]) are the related adsorption rate constant for pseudo-first-order and pseudo-second-order models, respectively. Where, a (g mg/min) and k (mg/g) are constants.

From the nonlinear fitting curves presented in Fig. 1, it can be observed that about 99% of cefradine molecules were immediately adsorbed within the initial 60 min, indicating that wheat straw can be directly used for fast removal of cefradine from practical wastewater. The three nonlinear kinetic models could well describe the adsorption kinetics under all the pH conditions, while pseudo-second-order model fitted the experimental data slightly better.

Table 1: Nonlinear kinetic parameters of cefradine adsorption at different pH conditions.

Model	pH=4	pH=7	pH=10
Pseudo-first-order model			
$k_f(\text{min}^{-1})$	0.1563	0.1217	0.102
$q_e(\text{mg/g})$	12.81	12.04	10.78
R^2	0.957	0.983	0.989
Pseudo-second-order model			
$k_2(\text{g}\cdot\text{mg}/\text{min})$	0.022	0.017	0.015
$q_e(\text{mg/g})$	13.14	12.42	11.17
R^2	0.904	0.951	0.972
Elovich model			
a	8.617	6.708	5.157
k	0.703	0.902	0.954
R^2	0.794	0.836	0.864

Table 2: Linear kinetics for pseudo-first-order and pseudo-second-order simulation parameters of cefradine adsorption at different pH conditions.

	Linear pseudo-first-order model			Linear pseudo-second-order model		
	$q_e(\text{mg/g})$	$k_f(\text{min}^{-1})$	R^2	$q_e(\text{mg/g})$	$k_2(\text{mg}/(\text{g}\cdot\text{min}))$	R^2
pH=4	0.964	1.4×10^{-3}	0.133	12.731	0.058	0.999
pH=7	1.763	1.7×10^{-3}	0.278	12.126	0.027	0.999
pH=10	3.034	1.2×10^{-3}	0.611	11.010	0.017	0.999

As shown in Table 1, the correlation coefficients (R^2) of pseudo-first-order models are all above 0.957. Furthermore, only judged from the simulated curves and experimental points, the pseudo-first-order model described the experimental kinetic data are the best under their pH conditions. Accordingly, the rate determining step might be diffusive in nature for the uptake of cefradine in this case.

Meanwhile, as demonstrated in Fig. 2, the experimental data were also comparatively simulated by linear kinetic models, including pseudo-first-order and pseudo-second-order models. The linear kinetic parameters simulated for the two models are listed in Table 2. The correlation coefficient of pseudo-second-order kinetic model is 0.999, which is especially higher than the pseudo-first-order model. The calculated values are much close to the experimental values using pseudo-second-order kinetic model as well. Apparently, pseudo-second-order kinetic model fitted the experimental data better. As such, it can be inferred that chemisorption occurred between the cefradine molecules and the wheat straw.

Effect of ionic strength: The effect of ionic strength on cefradine was investigated by varying the dosage of NaNO_3 from 0 to 0.1 mol/L, as illustrated in Fig. 3. A significant decrease of cefradine uptake was observed with increasing ionic strength between pH 3.0 and 11.0. At pH 5.0, the uptake of cefradine reduced from 12.59 mg/g in the absence of

NaNO_3 to 7.58 mg/g in the presence of 0.1 mol/L NaNO_3 . It is well known that anions adsorbed by inner-sphere association either show little sensitivity to ionic strength or respond to higher ionic strength with greater adsorption. By contrast, anions adsorbed by outer-sphere association are strongly sensitive to ionic strength. The adsorption process is hindered by competition with strongly adsorbing anions such as NO_3^- since they form outer-sphere complexes through electrostatic forces (McBride 1997). Accordingly, it can be deduced that cefradine molecules may be specifically adsorbed on the wheat straw via forming outer-sphere surface complexes.

Effect of coexisting anions: As we know, adsorption selectivity is an important factor influencing removal effectiveness. Some researchers employed highly selective adsorbents to separate or remove heavy metals from aqueous systems (Lam et al. 2007). Anions such as bicarbonate (HCO_3^-), phosphate (HPO_4^{2-}), sulphate (SO_4^{2-}) and silicate (SiO_3^{2-}) commonly exist in water and wastewater, and might interfere in the adsorption of phosphate cefradine through competing for adsorptive sites on the surface of the adsorbents. The effects of these anions on cefradine adsorption at three concentration levels (0.1, 1.0 and 10 mM) were assessed and the results are shown in Fig. 4.

In general, there was an evident decrease in cefradine adsorption by wheat straw, indicating that these inorganic

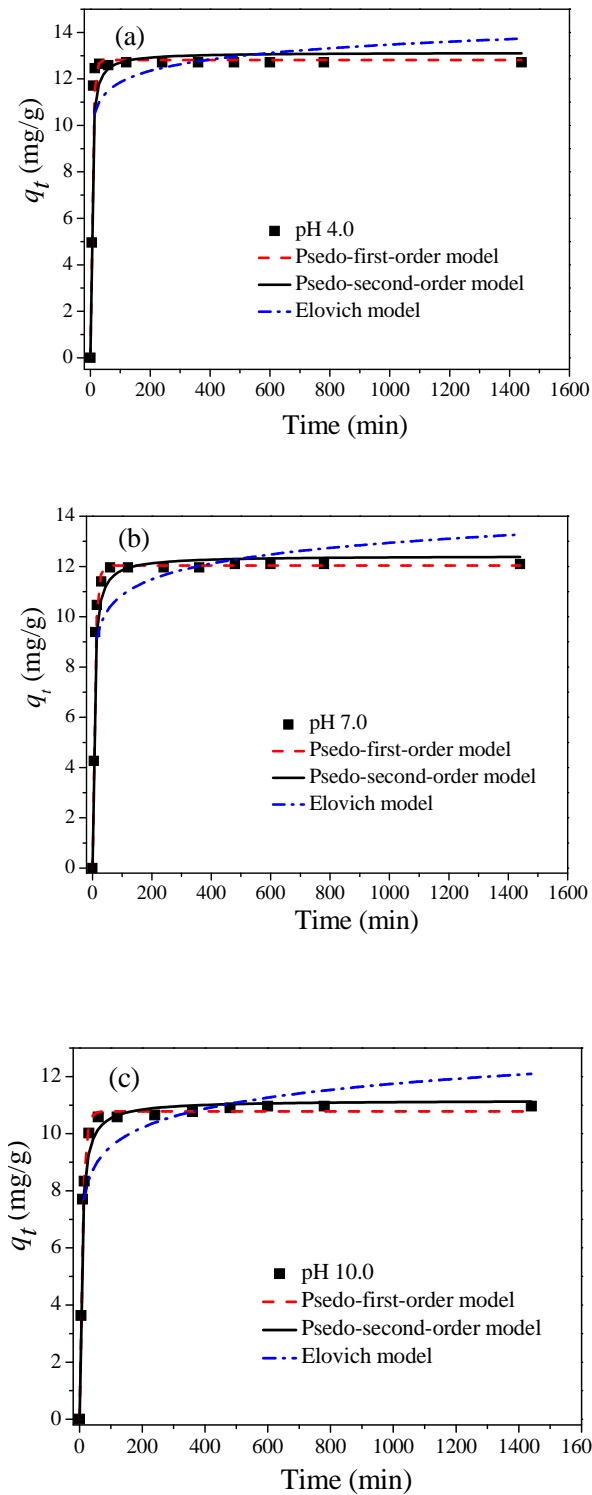


Fig.1: Non-linear kinetic simulation by pseudo-first-order, pseudo-second-order and Elovich models for cefradine adsorption at pH 4.0 (a), pH 7.0 (b) and pH 11.0 (c).

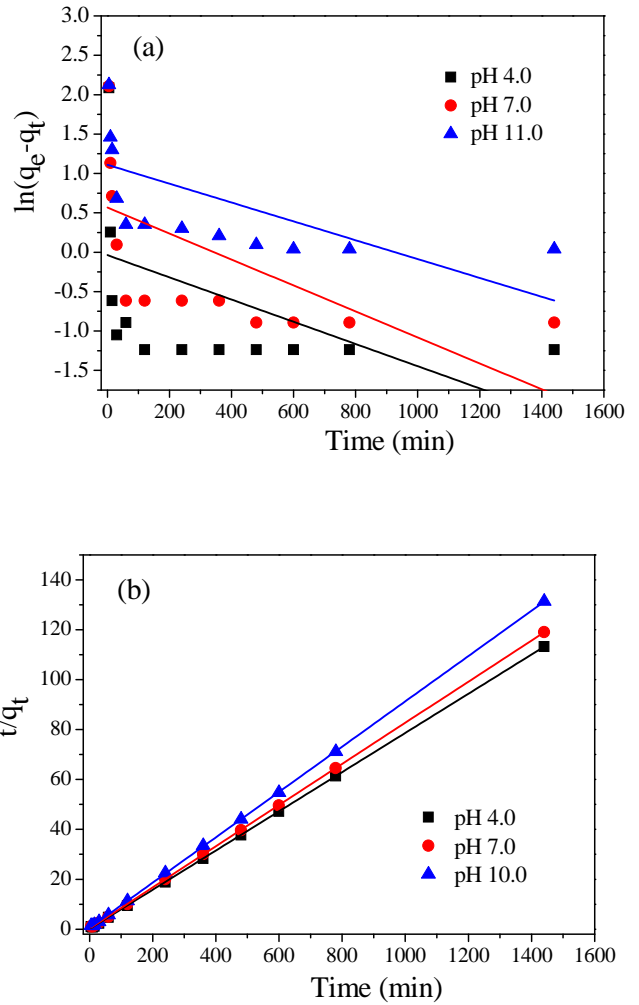


Fig.2: Linear kinetic simulation by pseudo-first-order (a) and pseudo-second-order (b) models for cefradine adsorption at different pH conditions.

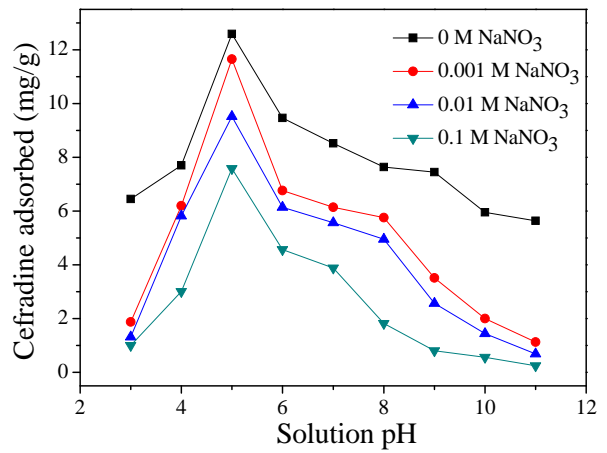


Fig.3 Effect of ionic strength on cefradine adsorption.

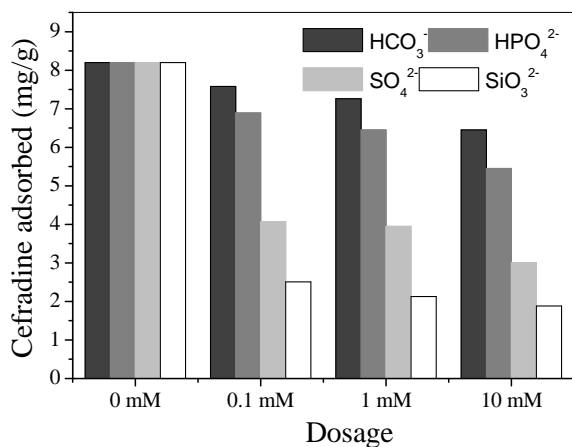


Fig. 4: Effect of coexisting ions on cefradine adsorption.

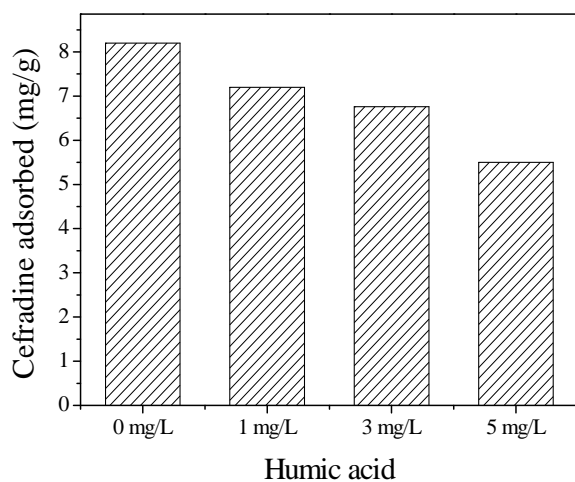


Fig. 5: Effect of humic acid on adsorption of cefradine.

anions might have competed with the cefradine molecules for the same active sites on wheat straw, due to the comparable type of the functional group that exists in the cefradine. An important and progressive decrease of cefradine uptake was observed on wheat straw with increasing dosages of anions HCO_3^- , HPO_4^{2-} , SO_4^{2-} and SiO_3^{2-} . The inhibiting effect was found in the pecking order $\text{Na}_2\text{SiO}_3 > \text{Na}_2\text{SO}_4 > \text{Na}_2\text{HPO}_4 > \text{NaHCO}_3$.

Effect of the presence of the humic acid: In nature, natural organic matter such as humic acid is a kind of macromolecule organic compound widely existing in natural water body. Humic acid has the capability of influencing adsorption and removal of pollutants in water and wastewater. The effect of humic acid was investigated and the result is presented in Fig. 5. The uptake of cefradine decreased from 8.2 mg/g without humic acid to 5.5 mg/g in the presence of 5

mg/L humic acid. The increasing dosage of humic acid could inhibit cefradine adsorption profoundly.

CONCLUSION

Wheat straw demonstrated its excellent adsorption capability for cefradine removal. Kinetic experiments indicated that most of the cefradine uptake occurred within the initial 60 min. Weakly acidic pH conditions were proved to be favourable for cefradine removal. Both, the linear and nonlinear pseudo-second-order kinetic model could describe the adsorption kinetics better, indicating that chemisorption occurred between the cefradine molecules and wheat straw. Ionic strength experiment demonstrated that cefradine molecules may be specifically adsorbed on the wheat straw via forming outer-sphere surface complexes. Inhibiting effect by coexisting anions was found to be in the pecking order $\text{Na}_2\text{SiO}_3 > \text{Na}_2\text{SO}_4 > \text{Na}_2\text{HPO}_4 > \text{NaHCO}_3$. The presence of humic acid could decrease cefradine uptake significantly as well.

ACKNOWLEDGEMENTS

The authors would like to thank the support from the National Natural Science Foundation of China (Grant No. 51409291), Henan Province science and technology attack plan project (Grant No. 182102110124) and foundation for university key teacher by Henan Province (Grant No. 2015GGJS-174).

REFERENCES

- Chen, J.Q. and Guo, R.X. 2012. Access the toxic effect of the antibiotic cefradine and its UV light degradation products on two freshwater algae. *J. Hazard. Mater.* 209-210: 520-523.
- Chen, H., Li, X.J. and Zhu, S.C. 2012. Occurrence and distribution of selected pharmaceuticals and personal care products in aquatic environments: a comparative study of regions in China with different urbanization levels. *Environ. Sci. Pollut. R.*, 19(6): 2381-2389.
- Han, R.P., Han, P., Cai, Z.H., Zhao, Z.H. and Tang, M.S. 2008. Kinetics and isotherms of Neutral Red adsorption on peanut husk. *J. Environ. Sci.*, 20: 1035-1041.
- Ho, Y.S. and McKay, G. 1999. Pseudo-second-order model for sorption process. *Process Biochem.*, 34(5): 451-65.
- Homem, V. and Santos, L. 2011. Degradation and removal methods of antibiotics from aqueous matrices a review *J. Environ. Manage.*, 92: 2304-2347.
- Hu, Z.J., Wang, N.X., Tan, J., Chen, J.Q. and Zhong, W.Y. 2012. Kinetic and equilibrium of cefradine adsorption onto peanut husk. *Desalin. Water Treat.*, 37(1-3): 160-168.
- Jiang, M.X., Wang, L.H. and Ji, R. 2010. Biotic and abiotic degradation of four cephalosporin antibiotics in a lake surface water and sediment. *Chemosphere*, 80: 1399-1405.
- Kithome, M., Paul, J.W., Lavkulich, L.M. and Bomke, A.A. 1988. Kinetics of ammonium adsorption and desorption by the natural zeolite clinoptilolite. *Soil Sci. Soc. Am. J.*, 62(3): 622-629.
- Lam, K.F., Fong, C.M. and Yeung, K.L. 2007. Separation of precious metals using selective mesoporous adsorbents. *Gold Bull.*, 40(3): 192-198.

- Lagergren, S. 1898. Zur theorie der sogenannten adsorption gelöster stoffe. Kungliga Svenska Vetenskapsakademiens. Handlinga. 24(4): 1-39.
- McBride, M.B. 1997. A critique of diffuse double layer models applied to colloid and surface chemistry. Clay & Clay Miner., 45(4): 598-608.
- Mi, X., Guo, Y.J., Zhang, C.Y., Wang, L., Zhang, S., Zou, B.B. and Li, G.T. 2016. Effect of solution pH on the kinetic adsorption of methylene blue by sugarcane bagasse biochar under a magnetic field. Nat. Env. & Poll. Tech., 15(4): 81297-81301.
- Yang, X., Flowers, R.C., Weinberg, H.S. and Singer, P.C. 2011. Occurrence and removal of pharmaceuticals and personal care products (PPCPs) in an advanced wastewater reclamation plant. Water Res., 45: 5218-5228.



Assessment of the Efficiency of Fly Ash Amended Soil for Distillery Effluent Treatment

J. S. Chauhan*† and J. P. N. Rai**

*Department of Himalayan Aquatic Biodiversity, HNBGU, Srinagar, Garhwal, Uttarakhand, India

**Department of Environmental Sciences, G. B. Pant University of Agriculture and Technology, Pantnagar-263145, India

†Corresponding author: J. S. Chauhan

Nat. Env. & Poll. Tech.
Website: www.neptjournal.com

Received: 23-05-2018
Accepted: 02-08-2018

Key Words:

Fly ash amended soil
Lysimeter
Distillery effluent
Land treatment

ABSTRACT

A lysimetric experiment was conducted to assess the effectiveness of soil amended with fly ash, to remove different contaminants of distillery effluent. Four lysimeters containing amended soil mixtures were prepared by mixing top layer of normal soil and fly ash in different ratios, i.e. S₉₅ (pure soil:fly ash, 95:5), S₉₀ (pure soil:fly ash, 90:10), S₈₅ (pure soil:fly ash, 85:15) and S₁₀₀ (pure soil). Secondly treated distillery effluent was used for irrigating the prepared lysimeter and leachate was collected to analyse the various relevant parameters, viz. pH, BOD, COD, TDS, N, P, K, Ca, Na, Mg, NO₃⁻, SO₄²⁻, Zn and Fe. The results depicted that fly ash amended soil was effective to enhance the potential of normal soil to remove the pollutants from effluent. Soil with lowest fly ash content, i.e. S₉₅ was recorded to be the best for land disposal of the effluent. With an increase in the amount of fly ash, i.e. soil S₉₀ and S₈₅, leaching of pollutants was observed indicating the possibility of contamination of groundwater.

INTRODUCTION

Effluent irrigation is one of the good methods to improve crop yield vis-a-vis save water and reduce the use of fertilizers. But, sometimes the soil capacity to retain the organic and inorganic content of effluent is low and thereby it allows the contents to percolate through soil matrix and impart changes in the quality of groundwater. Percolation of the effluent through soil column decreases the availability of N, P, K to plants, and hence the expected outcome of effluent irrigation decreases. In such case, it is required to improve the soil structure by amending it with different stabilizing agents like fly ash, cow dung, sludge, etc. Sewage sludge is used to improve soil properties and make it more suitable for agriculture (Logan & Harrison 1995). However, untreated sludge contains many toxic metals and soluble salts that become a problem later (Chaney 1983, Elseewi & Page 1984). Coal fly ash has a high amount of CaO and MgO, which makes coal fly ash a potential stabilizing material with sewage sludge (Reynolds et al. 2002, Truter 2002). Fly ash is one of the options used to improve the texture and water holding capacity of soils (Goswami & Mahanta 2007). It consists of Al, Fe, Si, O, Ca, Mg and small amounts of many plant essential trace elements, such as B, Se, Cd, Mo and As (Terman 1978, Ritchey et al. 1998). The fly ash has been effective in improving the texture, including increased air-filled porosity, decreased bulk density and improved moisture retention capacity (Bhumbla et al. 1993).

The addition of fly ash, at 70 tons/ha to soil altered the texture of sandy and clay soils to loamy soils (Jala & Goyal 2006). The addition of fly ash generally decreased the bulk density of soils, which in turn improved the soil porosity and workability and enhanced the water retention capacity (Page et al. 1979). Therefore, it is worthwhile to assess the role of land/soil and soil amendments in the treatment of pollutants present in the effluents.

MATERIALS AND METHODS

Lysimetric set-up: Lysimeter consists of galvanized sheet having 1.5 m length, 0.8 m width, and a basement and open top (Fig. 1). On one side, near basement, there is an outlet of 5 cm diameter for removal of excess water, if any. There is a 8 cm diameter pipe erected as piezometer attached on the side of this cabinet internally up to full height, i.e., 1.5 m whose base is perforated up to 30 cm. The lysimeter was filled with soil, in accordance with various soil textures required as shown in Fig. 1.

Sampling of effluent: The secondarily treated effluent was collected from the main outlet point of a distillery industry. Effluent samples at the point of discharge were collected in clean plastic containers. Immediately after collection, the samples were brought to the laboratory and stored at 4°C in a refrigerator until their further use.

Experimental layout: Lysimetric trial was conducted to assess the effectiveness of soil amended with fly ash against

distillery effluent. Four lysimeters with amended soil mixtures were prepared by mixing normal soil and fly ash in different ratios, i.e. S95 (pure soil:fly ash, 95:5), S90 (pure soil:fly ash, 90:10), S85 (pure soil: fly ash, 85:15) and S100 (pure soil). Secondly treated effluent was used for irrigating these amended soil mixtures filled in lysimeter. Leachate was collected after effluent irrigation and various relevant parameters, viz. pH, BOD, COD, TDS, N, P, K, Ca, Na, Mg, NO_3^- , SO_4^{2-} , Zn and Fe were analysed following standard methods of American Public Health Association (APHA 1995).

RESULTS AND DISCUSSION

The finding of this research marks high values of the certain parameters namely BOD, COD, N and P in the secondarily treated effluent of the distillery industry (Table 1). The Central Pollution Control Board (CBCP) has set-up general standards for discharge of effluent in the environment. These parameters are not fulfilling CBCP standard and were found above the permissible limit. Effluent used in the present study shows significantly high values of nitrogen (91.5 ppm), potassium (23.2 ppm) and phosphorus (38.3 ppm), which will be considered as pollutants, if discharged directly in an aquatic system without treatment. But, if this same effluent is reused as a water source for irrigating crops, these values of NPK will act as fertilizers, thereby enhancing the crop yield.

The effluent with a high value of BOD, COD, N and P was used in lysimeter to assess the ability of different fly ash amended soils to remove the pollutants. The results showed that all types of soil amendments were able to check the concentration of pollutants present in the effluent. By the mixing of 5, 10 and 15 percent fly ash, the rate of percolation was decreased because the pore size was decreased by mixing of fly ash, resulting in slow leaching of effluent from the soil column. Slow leaching of effluent provides proper time for the treatment of pollutants present in the effluent. Among the different soil-fly ash combinations, S_{95} soil was found efficient to reduce different parameters significantly as compared to other combinations. The trend of removal efficiency of soil was $S_{95} > S_{90} > S_{85} > S_{100}$ (Table 2). This clearly explains that fly ash influenced the soils properties like soil structure, bulk density, pore space, sorption, chemical precipitation, water retention capacity and microorganism activity (Reddy & Reddy 1999). In case of S_{95} soil, the percent reduction in TDS, BOD, COD, SO_4^{2-} , N, P, K, Ca, Mg, Na, Zn and Fe were 28.0, 51.9, 26.2, 59.2, 47.0, 45.8, 45.3, 77.3, 76.4, 82.2, 38.3 and 47.6 %, respectively. While with S_{100} soil, the corresponding values for these parameters were noticed to be only 21.0, 23.2, 15.2, 43.4, 30.9, 33.5, 27.1, 61.1, 65.2, 65.5, 13.3 and 10.9 %, respectively. For S_{90} soil, TDS, BOD, COD, SO_4^{2-} , N, P, K, Ca, Mg, Na, Zn

Table 1: Physico-chemical characteristics of secondarily treated distillery effluent.

Parameters	Effluent	Permissible limit before discharge (CPCB)
pH	7.8±0.2	5.5 to 9.0
TDS (ppm)	754±14.5	-
BOD (ppm)	46.4±5.1	30
COD (ppm)	260±10.4	250
SO_4^{2-} (ppm)	68.3±5.6	-
N-nitrate (ppm)	101.5±8.1	10
P (ppm)	68.3±5.7	5
K (ppm)	83.2±6.7	-
Ca (ppm)	31.4±2.9	-
Mg (ppm)	24.2±3.1	-
Na (ppm)	29.3±3.0	-
Zn (ppm)	2.40±0.1	3.0
Fe (ppm)	1.91±0.09	5.0

± indicates SE of mean; - not available

and Fe were reduced to 26.8, 45.6, 23.0, 52.2, 40.0, 41.1, 39.0, 70.3, 73.5, 77.4, 35.8 and 38.7 %, respectively, while with S_{85} the values were 22.5, 40.7, 15.2, 51.5, 34.3, 33.5, 28.9, 66.8, 66.5, 65.8, 17.5 and 14.1 %, respectively (Fig. 2). The lysimetric study conducted by Kumar et al. (2004) showed significant reduction of EC, colour, BOD, COD, TS, TDS, P, K, Na, Ca, Mg and lignin by normal soil after irrigation with 25% effluent of a pulp and paper mill effluent.

The different contaminants present in the effluent, when passed through the soil matrix, are offered treatment by different components of soil. The value of BOD and COD is majorly because of the organic content like cellulose present in the effluent. When the effluent passes through different layers of soil, the microorganisms present in the soil utilize them as the source of energy, and hence reduce their concentration in leachate. During percolation of industrial effluent, the cations like Na, K, Ca, and Mg get attached on



Fig. 1: Lysimeter used in the study.

Table 2: Physico-chemical characteristics of leachate collected after effluent treatment with soil S100, S95, S90 and S80.

Parameters	Effluent	After effluent treatment			
		S100	S95	S90	S85
pH	7.8±0.2	8.0±0.3	8.0±0.2	7.9±0.1	7.7±0.1
TDS (ppm)	754±14.5	595.1±14.1	542.2±9.8	551.5±14.8	584.1±11.9
BOD (ppm)	46.4±5.1	35.6±2.8	22.3±2.1	25.2±2.4	27.5±2.5
COD (ppm)	260±10.4	220.3±11.1	191.7±7.4	200.1±13.4	220.3±12.2
SO ₄ ²⁻ (ppm)	68.3±5.6	38.6±2.9	27.8±2.5	32.6±3.2	33.1±3.1
N (ppm)	101.5±8.1	70.1±6.0	53.7±4.5	60.8±8.4	66.6±4.7
P (ppm)	68.3±5.7	45.4±4.0	37.0±3.3	40.2±3.6	45.4±4.1
K (ppm)	83.2±6.7	60.6±4.2	45.5±2.5	50.7±5.2	59.1±6.1
Ca (ppm)	31.4±2.9	12.2±1.2	7.1±0.9	9.3±0.8	10.4±1.2
Mg (ppm)	24.2±3.1	8.4±0.6	5.7±0.8	6.4±0.7	8.1±0.9
Na (ppm)	29.3±3.0	10.1±0.9	5.2±0.6	6.6±0.5	10.0±1.1
Zn (ppm)	2.40±0.1	2.08±0.07	1.48±0.04	1.54±0.04	1.98±0.07
Fe (ppm)	1.91±0.09	1.70±0.03	1.0±0.01	1.17±0.02	1.64±0.02

± indicates SE of mean

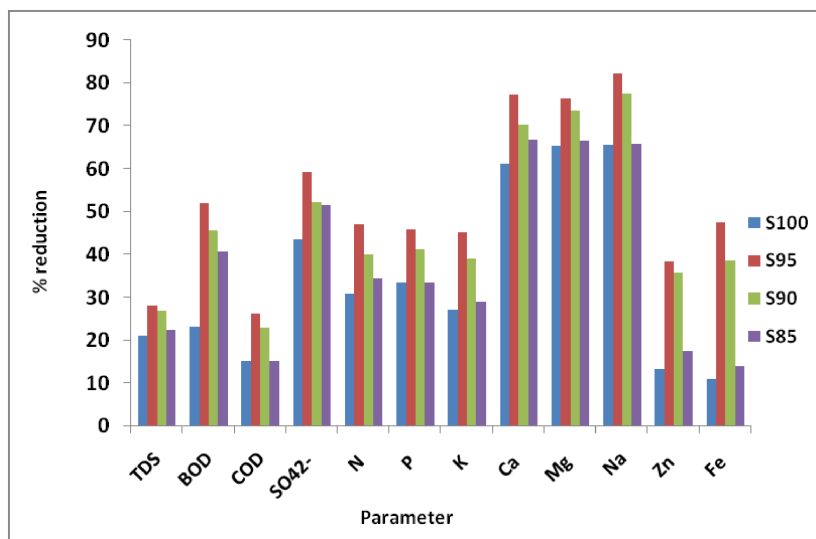


Fig. 2: Percent reduction in different physico-chemical parameters after soil treatment.

the negative binding sites of clay particles, and thus their concentration is reduced in leachate. Total solids are filtered by the soil as it acts like a sieve. Nutrients like nitrate and phosphorus are utilized by plants and microbes for different metabolic activities hence a significant reduction of nutrient content in the effluent is seen. Many of the contents of the effluent act as macro and micronutrients for plants and are involved in various metabolic activities of microorganisms present in the soil. Hence, in the due course of time, the nutrients will be uptaken by the plants and microorganisms of soil, thereby creating further space for the more. Liaghat & Prasher (1996) have also reported that a large amount of pollution load from the effluent is reduced by land treatment.

Percent increase in the removal efficiency of normal soil (S₁₀₀) with different amended soils S₉₅, S₉₀ and S₈₅ was also calculated (Fig. 3). It was recorded that when normal soil was amended with fly ash, the efficiency of soil to remove the pollutants from the effluent increased as compared to control (S₁₀₀). Among different amendments, the addition of 5% fly ash in normal soil, i.e. S95 soil gave the best results. Increase in the efficiency of reduction in normal soil with 5% fly ash in normal soil, i.e. S95 for TDS, BOD, COD, SO₄²⁻, N, P, K, Ca, Mg, Na, Zn and Fe were 9.8, 59.6, 14.9, 38.8, 30.5, 22.7, 33.1, 71.8, 47.3, 94.2, 40.5 and 70%, respectively. The fly ash acts as a stabilizing agent, and hence enhances all the physical, chemical and biological properties of soil making it more effective to treat effluent.

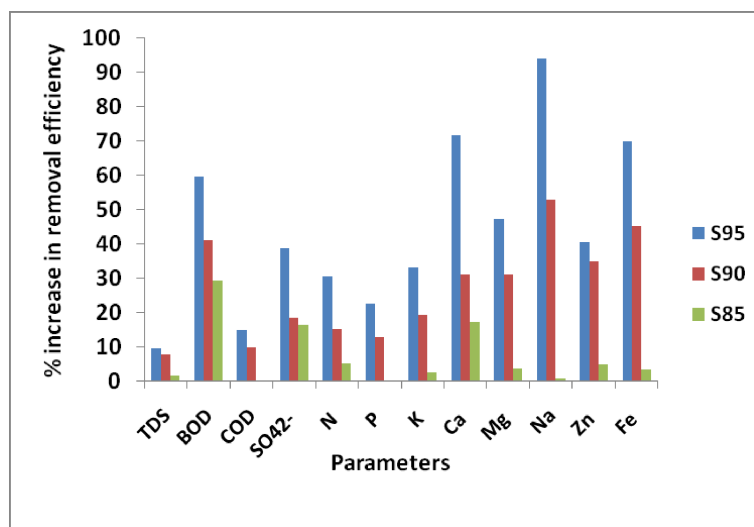


Fig. 3: Percent increase in the removal efficiency of different soil amendments over control.

CONCLUSIONS

Based on the results of this study it may be concluded that soil/land is a better option for treatment of secondarily treated effluent. Further addition of small amount of fly ash can enhance the treatment efficiency of normal soil. Fly ash helps to improve the structure of soil that further supports the removal of pollutants from the effluent. This lysimetric study reveals a significant reduction in the effluent contents that otherwise could percolate and contaminate groundwater. Land treatment of different soils has different results depending on the type of soil and effluent.

REFERENCES

- APHA 1995. Standard Methods for Examination of Water and Wastewater. 17th edition, American Public Health Association. Washington, D.C.
- Bhumbla, D.K., Keefer, R.F. and Singh, R.N. 1993. Ameliorative effect of fly ashes on acid mine soil properties. In: Proceedings 10th International Ash Use Symposium (American Coal Ash Association). Washington, DC., 3: 86.1-86.31.
- Chaney, R.L. 1983. Potential effects of waste constituents on the food chain. In: J.F. Parr (ed.) Land Treatment of Hazardous Wastes, Noyes Data Corp., pp. 50-76.
- Elseewi, A.A. and Page, A.L. 1984. Molybdenum enrichment of plants growth grown on fly ash-treated soils. *J. Environ. Qual.*, 13: 394-398.
- Goswami, R.K. and Mahanta, C. 2007. Leaching characteristics of residual lateritic soils stabilised with fly ash and lime for geotechnical applications. *Waste Management*, 27(4): 466-481.
- Jala, S. and Goyal, D. 2006. Fly ash as a soil ameliorant for improving crop production- a review. *Bioresource Technology*, 97(9): 1136-1147.
- Kumar, A., Singhal, V., Joshi, B.D. and Rai, J.P.N. 2004. Lysimetric approach for groundwater pollution control from pulp and paper mill effluent using different soil textures. *Indian J. of Scientific and Industrial Research*, 63: 429-438.
- Liaghat, A. and Prasher, S.O. 1996. A lysimeter study of grass cover and water table depth effects on pesticide residues in drainage water. *Am. Soc. Agric. Environ.*, 39: 1731-1738.
- Logan, T.J. and Harrison, B.J. 1995. Physical characteristics of alkaline stabilized sewage sludge (N-Viro soil) and their effects on soil physical properties. *J. Environ. Qual.*, 24: 153-164.
- Page, A.L., Elseewi, A.A. and Straughan, I.R. 1979. Physical and chemical properties of fly ash from coal-fired power plants with special reference to environmental impacts. *Residue Rev.* 71: 83-120.
- Reddy, T.Y. and Reddy, G.H.S. 1999. Principles of Agronomy. Kalyani Publishers, New Delhi.
- Reynolds, K.A., Kruger, R.A., Rethman, N.F.G. and Truter, W.F. 2002. The production of an artificial soil from sewage sludge and fly ash and the subsequent evaluation of growth enhancement, heavy metal translocation and leaching potential. *Proc. WISA, Durban, South Africa. Water SA Special Edition* ISBN 1-85845-946-2.
- Ritchey, K.D., Elrashidi, M.A., Clark, R.B. and Baligar, V.C. 1998. Potential for utilizing coal combustion residues in co-utilization products. In: S. Brown, J.S. Angle and L. Jacobs (eds.) *Beneficial Co-utilization of Agricultural, Municipal and Industrial By-products*, pp. 139-147.
- Terman, G.L. 1978. Solid wastes from coal-fired power plants: Use or disposal on agricultural lands. National Fertilizer Development Center. Bulletin Y (USA).
- Truter, W.F. 2002. Use of waste products to enhance plant productivity on acidic and infertile substrates. M.Sc. (Agric.) Thesis, University of Pretoria, South Africa.



Exhaust Emission Reduction in a Single Cylinder Compression Ignition Engine Fuelled With Optimized Biodiesel Blends of *Eucalyptus tereticornis*

V. Hariram[†], R. Prakash, S. Seralathan and T. Micha Premkumar

Department of Mechanical Engineering, Hindustan Institute of Technology & Science, Hindustan University, Chennai, India

[†]Corresponding author: V. Hariram

Nat. Env. & Poll. Tech.
Website: www.neptjournal.com

Received: 31-05-2018
Accepted: 02-08-2018

Key Words:

Eucalyptus tereticornis
Transesterification
Biodiesel
Compression Ignition engine
Exhaust emission

ABSTRACT

Inadequate resources, diminution in petroleum reserves, environmental pollution hazards and escalated crude oil pricing have become major points of concern for energy use. This urged the researchers to identify an alternative source of fuel energy similar to petroleum hydrocarbons to be used in internal combustion engine. In the present study, biodiesel from leaves of *Eucalyptus tereticornis* was used in the processed form in compression ignition engine. The steam distillation process yielded 4.8% of Eucalyptus bio-oil through a batch process. Single stage transesterification process using methanol and sodium hydroxide produced Eucalyptus biodiesel effectively at molar ratio of 8:1. The physico-chemical properties of Eucalyptus biodiesel were found to be comparable to commercial diesel and within ASTM limits. Eucalyptus biodiesel in straight and blended form at ratio of 50:50 with commercial diesel was used in a single cylinder compression ignition engine to understand its emission characteristics. Lower unburnt hydrocarbon and smoke emission was observed when D50EBD50 fuel blend was used at part and full load condition. EBD100 fuel emitted higher CO₂ across all loads. Oxides of nitrogen emission were found to be relatively higher at full load condition when compared with D100 and D50EBD50 fuel blends. The emission parameters of EBD100 and D50EBD50 were found to be comparable with mineral diesel.

INTRODUCTION

Fuel energy is a standout amongst other sources and has a huge contribution to the economic development of a nation. Exponential growth has been witnessed around the globe with respect to fuel energy requirements (Demirbas 2009). It is estimated that the energy requirement by the year 2022 will be around 192 metric tons, which is against the present requirement in which 78% of crude petroleum is imported from the other countries to encounter the current demand (Barnwal & Sharma 2005, Canakci & Sanli 2008). The significance of the biodiesel requirement increases day by day due to the rapid diminution of crude petroleum reserves and an increased environmental pollution hazard. Also, instability in petroleum pricing and global concerns like the greenhouse effect crafted an awareness and curiosity towards the development of non-edible vegetable based biodiesel to be used in compression ignition engines. Vegetable based bio-oils are long and short chain hydrocarbons, which are biodegradable, less toxic and principally renewable in nature. Operation of compression engine using vegetable oil was demonstrated by Rudolph's diesel in 1900 at the world exhibition in Paris. Use of biodiesel in compression ignition engine reduces dependency on non-

renewable petroleum fuel along with improved efficiency and reduced emissions in the transportation sector (Guan et al. 2009, Ma et al. 1990).

Verma et al. (2016) elaborated the potentiality of eucalyptus biodiesel using compression ignition engine. The single stage transesterification process adopted to reduce the viscosity of eucalyptus oil in order to convert it into biodiesel. The results concluded that a lower blend of Eucalyptus biodiesel with mineral diesel reduced the smoke emission considerably. Devan & Mahalakshmi (2009) amalgamated the methyl ester of eucalyptus oil with paradise oil on a volume basis and analysed its effect in a single cylinder compression ignition engine. The pressure of paradise oil methyl ester acted as an ignition improver in the fuel blend, which significantly influenced the emission formation. A higher blend of eucalyptus oil-paradise oil methyl ester reduced the concentration of hydrocarbons, carbon monoxide and smoke considerably with a marginal increase in NO_x in the exhaust emission at higher load condition. Kommana et al. (2017) investigated the effect of eucalyptus methyl ester blend in palm kernel oil at a ratio of 5, 10 and 15 by volume. The experimental studies were conducted in the VCR engine at 19:1 compression ratio and 220 bar in-

jection pressure. Senthil et al. (2016) studied the combined effect of eucalyptus biodiesel blended with Annona-oil at various ratios. The emission and performance evaluation on the test engine reveal higher NO_x when A50-Eu50 was used. Presence of oxygenate in blends of biodiesel and eucalyptus oil in a compression ignition engine show cast superior performance with reduced emission on comparison with mineral diesel. Methyl esters of eucalyptus oil and orange oil were also analysed at 20% volume ratio by Poola et al. (1994).

Lower blends of soyabean, cotton seed, rapeseed, sunflower, corn, palm and olive oil were tested in a 4S direct injection Ricardo test engine by Rakopoulos et al. (2006) and proved that exhaust emissions were greatly reduced inducing better performance. Riva et al. (2011) analysed the various possible ways for the production of biodiesel through ultrasound based transesterification. Zhang et al. (2012) developed SE-SD based oil extraction method to distillate vegetable oil from plant leaves. Higher yield of bio-oil under this optimized variable process of temperature 41°C , liquid solid ratio of 6.27 mL/s with a process time of 5 hours yielded 95% of bio-oil. Hariram et al. (2016) extracted bio-oil from seeds of *Nicotiana tabacum* using Soxhlet apparatus. Two stage transesterification process was adopted with molar ratio 1:6, reaction temperature of 60°C , and reaction time of 100 minutes yielded 92% of biodiesel when NaOH was used as catalyst.

In the present study, leaves of *Eucalyptus tereticornis* were selected as the source of bio-oil through the steam distillation process. The methyl esters of bio-oil are produced through single stage transesterification. The performance and emission characteristics of straight eucalyptus biodiesel and its blends was compared with mineral diesel in a single cylinder naturally operated compression ignition engine.

MATERIALS AND METHODS

Bio-oil extraction: In the present investigation, leaves of *Eucalyptus tereticornis* were used to extract bio-oil. The steam distillation process was adopted for separation of bio-oil. This process contains a heating container filled with water bath, a round bottomed flask, a coolant chamber and Erlenmeyer flask. Water in the bath was allowed to heat above 120°C , where it is converted into steam through an outlet tube. The superheated steam reaches a container filled with processed leaves of *Eucalyptus tereticornis*. Reaction takes place between water vapour and processed leaves fluidizing the bio-oil. The condensation tube carries the complex form of bio-oil in vapour state and directed into the cooling chamber. Liquid eucalyptus bio-oil is collected at the end of the condensation chamber in the Erlenmeyer flask

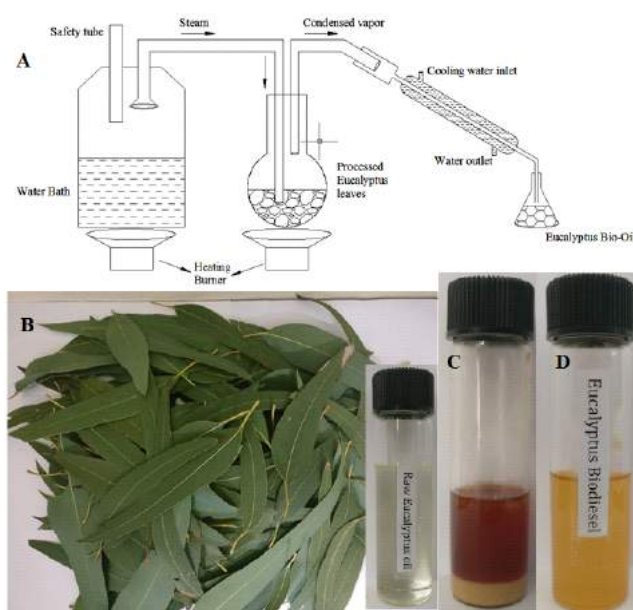


Fig. 1: Steam distillation process of Eucalyptus leaves (A), Eucalyptus leaves (B), Glycerol Separation (C) and Eucalyptus Biodiesel (D).

as shown in Fig. 1. Further, the left out eucalyptus leaves are allowed to react with *n*-hexane solvent in a closed chamber for 24 hours, which was followed by a mechanical expulsion for the removal of the remaining bio-oil. Batch process of 12 times yielded 453 mL of bio-oil from leaves of *Eucalyptus tereticornis* at an extracting efficiency of 4.8% oil (Zhang et al. 2012).

Transesterification: In the present investigation, base catalyst transesterification was adopted to esterify the derived bio-oil using sodium hydroxide and methanol solution. Transesterification process was carried out in a flat bottomed flask equipped with magnetic stirrer and a thermocouple for varying the reaction temperature. 99% pure methanol was thoroughly mixed with 1.5% by weight of sodium hydroxide to form sodium methoxide solution. 453 mL of *Eucalyptus tereticornis* oil was heated up to 70°C in a round bottom jar. An RTD type thermometer with a cut out relay was positioned to maintain the reacting environment between 55°C and 75°C . A transesterification was initiated by mixing the bio-oil with sodium-methoxide solution in a separate round bottom flask with continuous agitation at 400 to 450 rpm through a magnetic stirrer for 180 minutes. The products of the reaction were then transferred into a separating funnel and allowed to settle down for 24 hours. During this period a ring formation took place, characterizing *Eucalyptus tereticornis* biodiesel as the upper layer and glycerol as the lower layer. The glycerol was very carefully removed from the bottom layer through the knob opening.

Table 1: Physico-chemical properties of Eucalyptus oil, biodiesel and diesel.

S.No	Properties	Units	Diesel	Bio-oil	Biodiesel	D50-BD50
1	Density	kg/m ³	840	1048	905	1015
2	Viscosity	mm ² /s	2.6	3.8	2.8	2.54
3	Specific gravity	g/cm ³		0.882	0.893	0.854
4	Flash point	°C	75	116	105	47
5	Fire point	°C	78	120	108	50
6	Calorific value	kJ/kg	42500	-	41930	-
7	FFA	%	-	1.5	1.2	-

Distilled warm water was mixed with methyl esters for the removal of impurities which included the catalyst, unreacted oil and methanol in a separating funnel. Gravity separation process for 4 hours expelled the distilled water along with the impurities (Hariram & Gowtham 2016).

Physico-chemical properties: Biodiesel from *Eucalyptus tereticornis* was subjected to various analyses under ASTM standards to identify its physico-chemical properties. Mettler Toledo densitometer (ASTM-D792 and ASTM-D1963) was used to measure the density and specific gravity at 25°C and identified as 904 kg/m³ and 0.891 g/cm³ respectively. Redwood viscometer under ASTM D445 measured the kinematic viscosity at 40°C as 2.7 mm²/sec. Hamco Bomb calorimeter (ASTM D5865) measured the calorific value of *Eucalyptus tereticornis* as 40.45 MJ/kg. ASTM D3278 method was adopted to identify flash point using Abel flash point apparatus and found to be 101°C. Titration method was used along with phenolphthalein solution to measure the free fatty acid in the *Eucalyptus tereticornis* biodiesel. The acid value was drastically reduced from 2.02 mgKOH/g to 0.25 mgKOH/g by ASTM D1980 method. The Cetane number was identified as 53 by ASTM D613. The physico-chemical properties of *Eucalyptus tereticornis* oil and its biodiesel are given in Table 1.

Experimental Setup

Fig. 2 shows the schematic outline of the experimental setup. Kirloskar MMM1MET-201EL was used as the test engine. The setup consists of two fuel tanks, one for mineral diesel and the other for biodiesel blend with controller facility for fuel switching. The fuel and air consumption were measured by optical sensor and differential pressure transducer respectively, and fed into the data acquisition system. The loading of test engine is accomplished using an eddy current dynamometer as shown in the Fig. 2. AVL444 Di gas analyser measures the CO and UBHC using infrared method, and NO_x using the electro-chemical method. AVL437 smoke meter measures the smoke opacity using selenium photo cell detector. The detailed engine specifications are dis-

Table 2: Test engine specification.

Description	Specification
Make	Kirloskar TV1
Type	4 stroke, single cylinder, CI engine
No of Cylinders	One
Cubic Capacity (L)	0.661 L
Rated Speed (rpm)	1500 rpm
Bore (mm)	87.5 mm
Stroke (mm)	110 mm
Connecting rod length	234 mm
Air flow transmitter	(-) 250-0 mm WC
Power Rating (HP)	5hp (3.7 kw)
Compression Ratio	17.5:1
Start of Injection (BDTC)	23
Cooling	Water cooled
Cylinder pressure Transducer	0-345.5 bar
Sensor signal range (input for interface)	1-5 V
Dynamometer type	Eddy current

played in Table 2. Initially the experiments were conducted on the test engine with mineral diesel to identify the optimum cooling rate and further expanded with straight biodiesel and its blend by maintaining this optimum rate of engine cooling. The experiments were repeated for 3 times and mean values of the readings are recorded. The performance of the engine was evaluated in terms of brake thermal efficiency, brake specific fuel consumption, exhaust gas temperature, smoke density and the emissions of HC, CO and NO_x.

RESULTS AND DISCUSSION

Transesterification: The yield of biodiesel with sodium hydroxide as a catalyst under different operational parameters like reaction duration, reaction temperature, catalyst concentration and molar ratio were carried out. Fig. 3 illustrates the effect of reaction duration on yield of biodiesel at 55°C, 65°C and 75°C reaction temperature. In the present experimental study the reaction duration was varied from 15-100 minutes at various reacting temperatures. At 55°C reacting temperature, maximum yield of biodiesel obtained

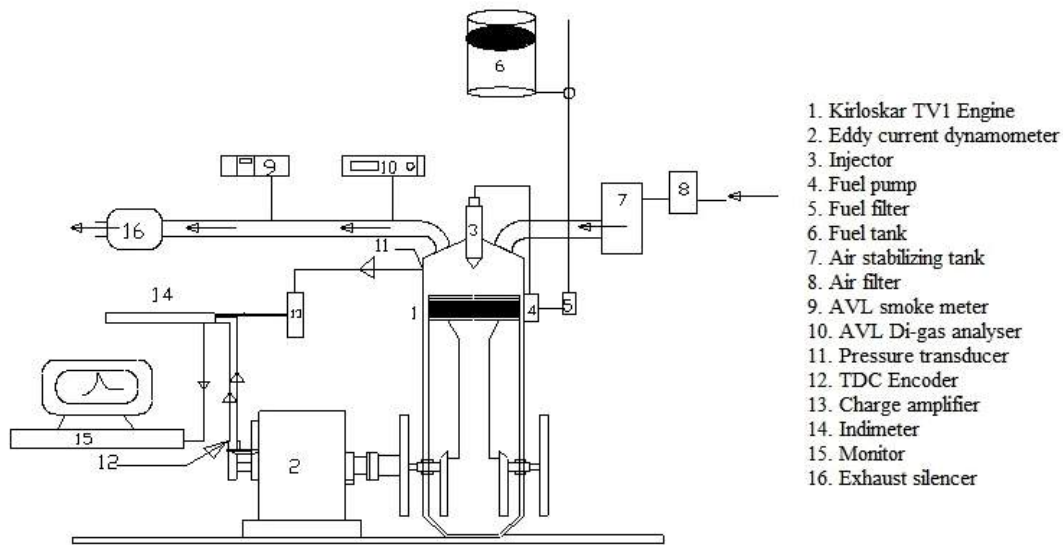


Fig. 2: Engine schematic diagram.

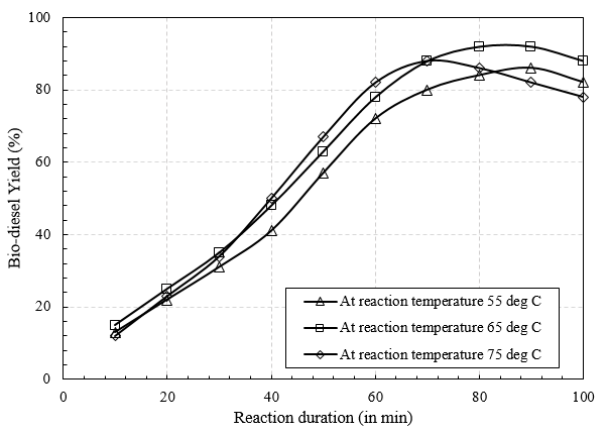


Fig. 3: Biodiesel yield versus reaction duration for different temperatures.

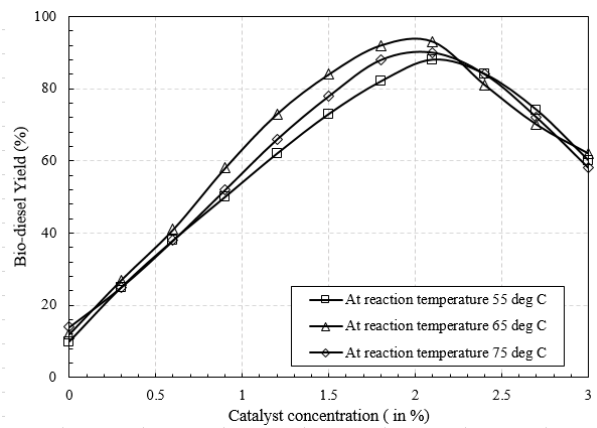


Fig. 4: Biodiesel yield versus catalyst concentration for different temperatures.

was 86% at 90 minutes reaction duration. Increase in reaction temperature up to 65°C enhanced the conversion rate of triglyceride into FAME's up to 92% at 82 minutes. Further increase in temperature up to 75°C showed a conversion efficiency of 82% at 70 minutes reaction duration, which is much earlier, but prolonging the reaction duration had a negative impact on the conversion efficiency. This may be due to higher saponification rate of the triglycerides at elevated temperature and also due to vaporization of methanol (Hariram & Gowtham 2016).

Fig. 4 depicts the effect of NaOH concentration on biodiesel yield at various reacting temperatures. It can be noticed that the catalyst concentration between 1.2% and 2.2% favoured the conversion of triglycerides into FAME's.

During this experimental study, the reaction duration of 90 minutes and agitation speed of 400-450 rpm were maintained with variations in reaction temperature between 55°C and 75°C. It can be noticed that the reaction temperature has minimal effect on the transesterification efficiency with variable catalyst concentration. However, the catalyst concentration of 1.8% by weight at 65°C yielded 93% of biodiesel; increase in concentration of NaOH beyond 1.8% showed negative impact in the transesterification process due to soapy formation. A similar trend was observed at 75°C reaction temperature during which 90% of biodiesel was obtained at 1.76% by weight of NaOH. Sludge formation was seen during this process when NaOH concentration was increased beyond 2%. At lower reaction temperature (55°C), the conversion efficiency was very similar with

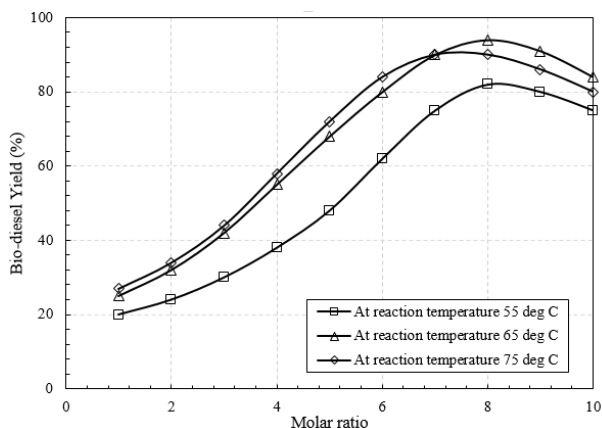


Fig. 5: Biodiesel yield versus molar ratio for different temperatures.

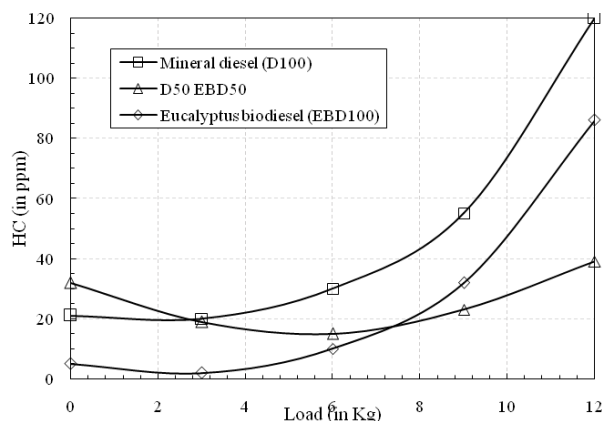


Fig. 6: Variations in hydro-carbon emission.

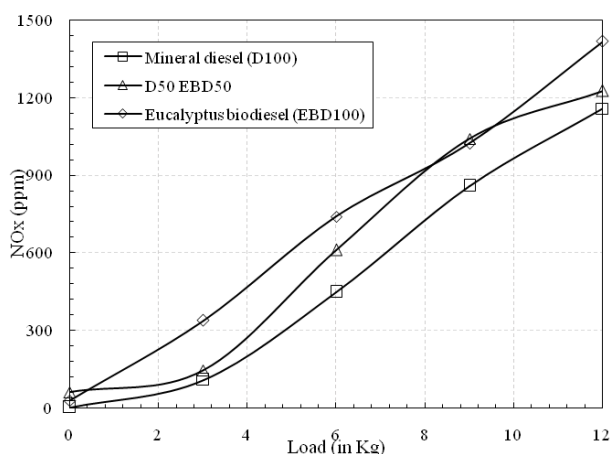


Fig. 7: Variations in NO_x emission.

biodiesel yield of 88%. Hence 1.8% of NaOH at 65°C and 450 rpm agitation speed were found to be optimum in the conversion of *Eucalyptus tereticornis* into biodiesel.

Fig. 5 illustrates the effect of molar ratio on yield of biodiesel at reaction temperatures of 55°C, 65°C and 75°C.

Molar ratio is considered to be the most influential parameter in converting the triglycerides into fatty acid methyl ester. Methanol to oil molar ratios between 2:1 and 10:1 at different reacting temperatures were investigated in the present study. At 55°C, methanol to oil molar ratio of 8:1 yielded 82% of biodiesel, increase in reaction temperature up to 65°C improved the biodiesel yield up to 94%. Further increase in reaction temperature up to 75°C exhibited a marginal decrease in the biodiesel yield as shown in Fig. 5, which may be due to evaporation of methanol at increased temperature. However, excess methanol favoured an increase in the yield of biodiesel, the catalyst concentration was very sensitive during the transesterification process. The kinematic viscosity of derived biodiesel at various molar ratios was identified and found to be within the ASTM standards.

Exhaust emissions: Fig. 6 depicts the clear plot between unburnt hydrocarbons and various engine loads of D100, D50EBD50 and EBD100. Unburnt fuel composition from the combustion chamber is termed as UBHC emission. From the graph, it was noted that in part and full load condition, higher UBHC emission was showcased and also it is notable that D50EBD50 depicted the lowest UBHC emission, which may be due to the less viscous nature of the fuel leading to better fuel atomization, which enhanced the complete combustion. At low load condition, D100, D50EBD50 and EBD100 showed 20 ppm, 32 ppm and 5 ppm respectively, whereas at part load condition resulted with 30 ppm, 15 ppm and 10 ppm respectively of UBHC emission. During the full load condition, D50EBD50 emitted lowest UBHC as 39 ppm, which may be due to higher cetane number than mineral diesel leading to shorter ignition delay thereby enhancing complete combustion (Aydin & Bayindir 2010).

Fig. 7 depicts the variation in oxides of nitrogen of mineral diesel, straight biodiesel and diesel-biodiesel blends with respect to the engine loads. Oxides of nitrogen are formed by the disintegration of nitrogen molecules due to higher temperature which then clubs with oxygen delivering oxides of nitrogen. From the plot, it is clear that NO_x increased as the load increases, which may be due to the higher temperature during high loads. From the result, it is noted that straight biodiesel detailed higher value of NO_x than diesel fuel, which may be due to higher oxygen content in biodiesel. This allows the rise in temperature during the premixed combustion phase of fuel burning. At low load condition, NO_x values for mineral diesel, D50EBD50 and EBD100 were noted as 108 ppm, 144 ppm and 337 ppm respectively, whereas at part load condition, it is 447 ppm, 609 ppm and 738 ppm respectively. During the full load condition, highest NO_x was depicted by EBD100 as 1416 ppm and lowest was depicted by mineral diesel as 1157 ppm (Kannan et al. 2011).

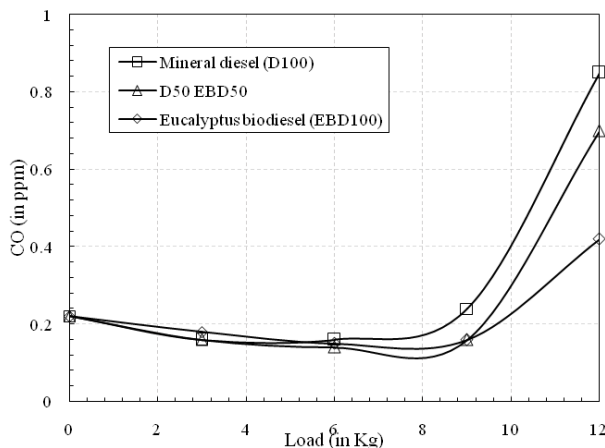


Fig. 8: Variation in CO emission.

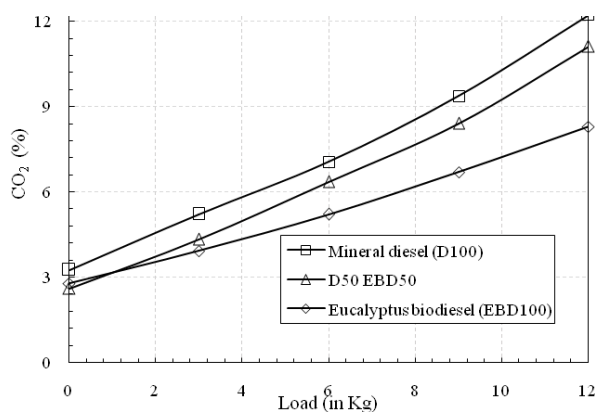


Fig. 9: Variations in carbon dioxide emission.

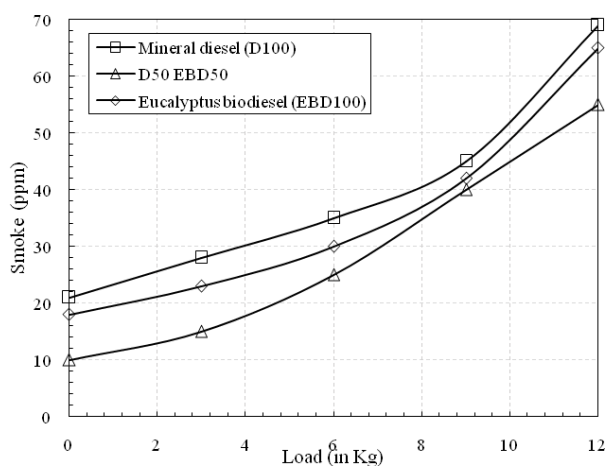


Fig. 10: Variations in smoke emission.

Fig. 8 depicts the variation in carbon monoxide emissions of mineral diesel, straight biodiesel and diesel-biodiesel blends with respect to the engine loads. CO emission portrays the incomplete combustion of the fuel. Dur-

ing low load condition, D100, D50EBD50 and EBD100 showcased almost closer percentage values of carbon monoxide. Similar pattern was noted during the part load conditions. Also it was noted that for straight biodiesel, the CO formation was reduced due to its higher cetane number, which affected the fuel atomization leading to shortened ignition delay thereby causing better premixed combustion phase. During the full load condition, CO emission was increased, which may be due to the improper latent heat of vaporization because of the lesser time duration for fuel atomization thereby promoting incomplete combustion (Tamilselvan et al. 2016, Datta et al. 2014).

Fig. 9 shows the variation in carbon dioxide emission of D100, D50EBD50 and EBD100 with respect to engine load. CO₂ emission is the oxidation of CO to CO₂ portraying the complete combustion. It can be noted from the plot that the CO₂ emission increased as the load increases. During the full load condition, it was noted that D50EBD50 shows 10.07% lower CO₂ emission than mineral diesel which may be due to higher oxygen content than diesel leading to complete burning of fuel. Also its lower viscosity promotes better fuel atomization thereby enhancing complete combustion. At part load condition, it is to be noted that EBD100 on comparison with D100 expelled lower CO₂ which may be due to higher ignition delay, which eventually affected the oxidation process through poor atomization (Hariram et al. 2017).

Smoke emission variation of D100, D50EBD50 and EBD100 with respect to engine load is shown in Fig. 10. It was noted from the graph that smoke emission increased as the load increases. Smoke formation, in general, is due to factors of kinematic viscosity, volatility and air-fuel mixture. It is to be noted at all the load conditions that D50EBD50 evidenced lowest smoke opacity percentages, which may be due to the appropriate oxygen content present in the air-fuel mixture enhancing better combustion. At low load condition, mineral diesel showed a higher smoke emission as 21%, which may be due to rich air-fuel mixture delivered for the ignition process leading to incomplete combustion. During part and full load conditions, diesel and straight biodiesel resulted with higher smoke opacity as 70% and 68%, which may be due to higher density leading to poorer atomization thereby increase in smoke emission.

CONCLUSIONS

In this experimental study, optimized biodiesel production from *Eucalyptus tereticornis* and its effect on the emission characteristics of single cylinder compression ignition engine have been evaluated and compared with commercial diesel. From this study, the following conclusions are drawn,

- Bio-oil extraction through steam distillation technique

yielded 4.8% of *Eucalyptus tereticornis* oil.

- Base catalysed transesterification using sodium hydroxide and methanol yielded 94.5% of biodiesel at molar ratio of 8:1.
- Kinematic viscosity of Eucalyptus biodiesel and its blend was found to be comparable with mineral diesel. The calorific value of EBD was also noticed to be marginally lower than mineral diesel.
- As far as exhaust emissions are concerned, it is noted that UBHC, CO and smoke emissions were abridged significantly with a marginal increase in NO_x. D50EBD50 fuel blend showed 2.4% increase on NO_x with 23.6% reduction in UBHC emission.
- From the emission analysis, it can be concluded that Eucalyptus biodiesel is one of the suitable alternative fuel for compression ignition engine. Its blend with mineral diesel at the ratio of 50:50 significantly reduced the exhaust emissions.

REFERENCES

- Aydin, H. and Bayindir, H. 2010. Performance and emission analysis of cottonseed oil methyl ester in a diesel engine. *Renew. Energy*, 35: 588-92.
- Barnwal, B.K. and Sharma, M.P. 2005. Prospects of biodiesel production from vegetable oils in India. *Renewable Sustainable Energy Rev.*, 9(4): 363-78.
- Canakci, M. and Sanli, H. 2008. Biodiesel production from various feedstocks and their effects on the fuel properties. *J. Ind. Microbiol. Biotechnol.*, 35: 431-41.
- Datta, Ambarish, Palit Samiddha and Mandal Bijan Kumar 2014. An experimental study on the performance and emission characteristics of a CI engine fuelled with *Jatropha* biodiesel and its blends with diesel. *Journal of Mechanical Science and Technology*, 28(5): 1961-1966.
- Demirbas, Ayhan 2009. Progress and recent trends in biodiesel fuels. *Energy Conservation and Management*, 50: 14-34.
- Devan, P.K. and Mahalakshmi, N.V. 2009. A study of the performance, emission and combustion characteristics of a compression ignition engine using methyl ester of paradise oil-eucalyptus oil blends. *Applied Energy*, 86: 675-680.
- Guan, Guoqing, Katsuki Kusakabe, Nozomi Sakurai and Kimiko Moriyama 2009. Transesterification of vegetable oil to biodiesel fuel using acid catalysts in the presence of dimethyl ether. *Fuel*, 88: 81-86.
- Hariram, V. and Gowtham Rajan, A. 2016. Extraction of tobacco (*Nicotiana tabacum* L.) seed oil and biodiesel preparation through two stage transesterification. *Research Journal of Pharmaceutical, Biological and Chemical Sciences*, 7(2): 978-983.
- Hariram, V., Sivamani, S., Premkumar T, M. and Tharun, P. 2017. Reduction of exhaust emissions using a nanometallic enriched lemongrass biodiesel blend. *Energy Sources, Part A: Recovery, Utilization, and Environmental Effects*, 39(21): 2065-2071.
- Kannan, G.R., Balasubramanian, K.R., Sivapirakasam, S.P. and Anand, R. 2011. Studies on biodiesel production and its effect on DI diesel engine performance, emission and combustion characteristics. *International Journal of Ambient Energy*, 32(4): 179-193.
- Ma, F. and Hanna, M.A. 1990. Biodiesel production: A review. *Biores. Technol.*, 70: 1-15.
- Kommana, S., Balu Naik, B. and Kalyani Radha, K. 2017. Impact of fuel injection pressure and compression ratio on performance and emission characteristics of VCR CI engine fueled with palm kernel oil-Eucalyptus oil blends. *Materials Today: Proceedings*, 4: 2222-2230.
- Poola, R.B., Nagalingam, B. and Gopalakrishnan, K.V. 1994. Performance studies with bio-mass derived high octane fuel additives in a two stroke spark ignition engine. *Biomass Bioenergy*, 6: 369-379.
- Rakopoulos, C.D., Antonopoulos, K.A. and Rakopoulos, D.C. 2006. Comparative performance and emission study of a direct injection diesel engine using blends of diesel fuel with vegetable oil or bio-diesel of various origins. *Energy Conservation Management*, 47: 3272-87.
- Riva, G., Toscano, G., Foppa Pedretti, E. and Duca, D. 2011. Refined soyabean oil transesterification enhanced by sonication. *Energy and Bioenergy*, 35: 2867-2873.
- Senthil, R. and Silambarasan, R. 2015. Environmental effect of anti-oxidant additives on exhaust emission reduction in compression ignition engine fuelled with *Annona* methyl ester. *Environmental Technology*, 36(16): 2079-2085.
- Tamilselvan, P., Vignesh, K. and Nallusamy, N. 2017. Experimental investigation of performance, combustion and emission characteristics of CI engine fuelled with chicha oil biodiesel. *International Journal of Ambient Energy*, 38(7): 752-758.
- Verma, P., Sharma, M.P. and Dwivedi, G. 2016. Potential use of eucalyptus biodiesel in compressed ignition engine. *Egyptian Journal of Petroleum*, 25(1): 91-95.
- Zhang, Xian Zhong, Hongjian Gao, Lifeng Zhang, Donghong Liu and Xingqian Ye 2012. Extraction of essential oil from discarded tobacco leaves by solvent extraction and steam distillation, and identification of its chemical composition. *Industrial Crops and Products*, 39: 162-169.



The Impact of Regional Economic Structural Changes on Smog Control: Empirical Evidence from Hubei, China

Ming Zhong

Academic Affairs Office, Wuhan University of Technology, Wuhan, 430070, China

Nat. Env. & Poll. Tech.
Website: www.neptjournal.com

Received: 16-01-2019

Accepted: 18-02-2019

Key Words:

Smog control
Regional economy
Structural changes
Empirical evidence

ABSTRACT

The traditional extensive production mode characterized by high energy consumption, high pollution, high resource dependence, and low efficiency has significantly increased the emission of carbon and other air pollutants. As a consequence, China is currently in the midst of a severe environmental and ecological crisis. Smog control can be realized by adjusting the industrial structure, which involves abandoning the traditional industrialization mode and pursuing the development mode of a circular economy characterized by low energy consumption and low pollution. To examine the causes of smog from the perspective of economic structure, the interactive relationship between smog control and the evolution of regional economic structure was analysed by using panel data of 13 prefecture-level cities in Hubei Province, China from 2005 to 2016. Results demonstrate that the relationship between industrial structure and degree of smog pollution shows a U-shaped curve. As such, the scale effect of economic development can reduce the emission of air pollutants. Foreign direct investment does not have a significant role in improving environmental pollution. Construction dust similarly aggravates smog pollution. These conclusions can deepen the understanding of the internal relationship between frequent smog occurrence and industrialization, as well as provide a theoretical basis and decision-making reference to effectively control smog by upgrading the regional economic structure.

INTRODUCTION

In recent years, the acceleration of China's industrialization and urbanization process has caused rapid development of the economy and the society on the one hand, but also rising environmental pollution problem on the other hand. In many northern cities, increasingly serious smog has resulted in grave threats and challenges to the local economic and social construction, as well as people's productivity, life, and health. At present, China's frequent smog weather shows a dynamic trend of entry from the Middle East to the South, spreading to the West in terms of geographical distribution. Its prominent features include a wide geographical range, long duration, and high public attention. The continuous occurrence of smog wields a serious impact on people's health and travel and, to a large extent, restricts the normal and healthy development of China's social economy. In fact, the rapid development of China's economy has led to the general improvement of people's living standards. People's demand for energy consumption is constantly increasing, driving a similar increase in energy supply. However, China's energy industry structure is dominated by coal, which has a low energy utilization rate and poor economic benefits, especially in high-energy-consuming industries. Thus, problems of energy source and structure have become prominent, and constraints of resources and environment have become increasingly severe.

Hubei Province is located in the hinterland of central China. As shown in Fig. 1, Hubei Province has experienced rapid industrial development, increased added value of industry, and high energy consumption in recent years. At the same time, it is also often affected by smog weather. Air quality shows an obvious and continuing downward trend. Smog weather directly affects the air quality of cities, causing frequent traffic accidents and threatening the health and safety of residents. Therefore, at present, Hubei Province considers severe smog weather as one of the central issues that require increased attention. Under the concept of green development, adjusting the industrial structure, energy consumption structure, and living consumption structure, as well as changing production and lifestyles are an urgent concern. Based on the current situation of smog weather control and economic development in Hubei Province, this study explores the ways to comprehensively control smog and upgrade the regional economic structure. It aims to promote green development of the regional economy and society, as well as provide a reference for smog pollution control in other provinces in the central region.

EARLIER STUDIES

Academic circles in developed countries have produced relatively mature research on the causes and countermeasures of smog formation. Many developed countries simi-

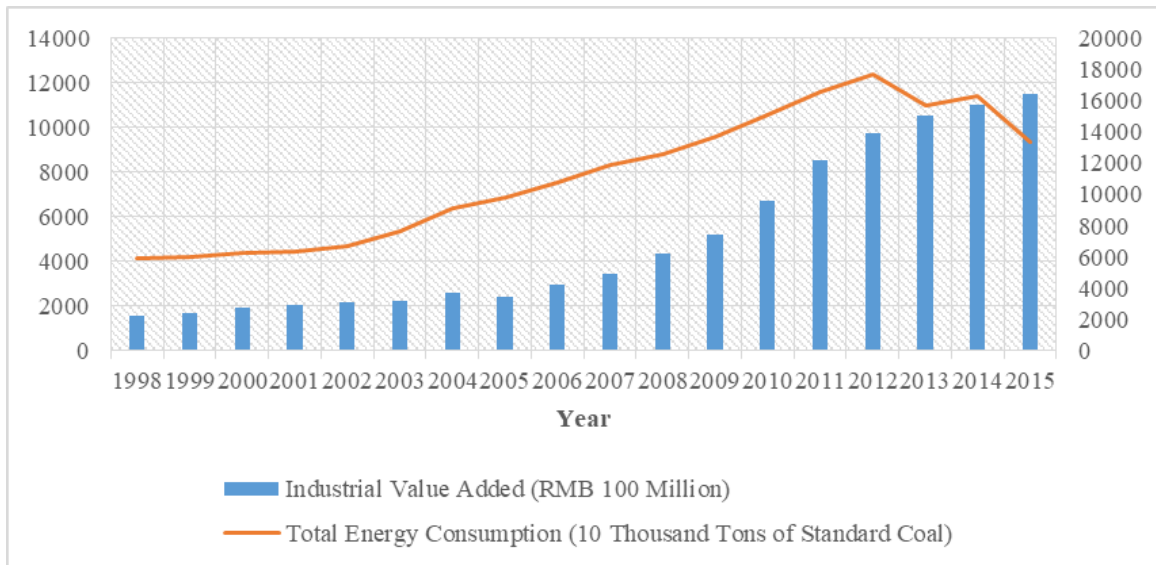


Fig. 1: Industrial value added and total energy consumption in Hubei province from 1998 to 2015.

larly suffered from air pollution in their early stages of industrialization because of their focus on economic development and neglect of environmental protection. Later, understanding the root cause of smog, successful solutions were pursued through a series of measures, including the transformation of their industrial structures. Regarding the interactive effects of environmental pollution, smog formation, industrial structure, and other socioeconomic factors, Shandra et al. (2008) used a panel regression model with lag-dependent variables for 50 samples from poor countries in 1990-2000 and found that structural adjustment and industrial exports increased water pollution. Fodha et al. (2010) studied the relationship between Tunisia's economic growth and pollutant emissions in 1961-2004. The results showed that a long-term cointegration relationship exists between per capita emissions of carbon dioxide (CO_2) and sulphur dioxide (SO_2) per capita GDP. In an empirical study, Mingsheng et al. (2011) found that the energy efficiency of Chinese iron and steel enterprises is closely related to enterprise scale. The study proposed measures to adjust the industrial organization structure to promote energy conservation and emission reduction. Brajer et al. (2011) proposed that China's industrial structure and environmental pollution do not necessarily show an inverted-U relationship. Wei et al. (2012) established an evaluation model for pollution control performance. The results showed that improving China's environmental pollution performance requires government policies that consider industrial restructuring, restrict industrial entry, and increase pollution control as well as research and development investment. Fujii et al. (2013) analysed the management of air pollutants in Chi-

na's industrial sector in 1998-2009, wherein the increase of industrial production scale led to the increase of SO_2 emissions. Tian et al. (2014) showed that regional industrial structural differences in China have a substantial impact on regional CO_2 emissions. The shift from agriculture, mining, and light industry to heavy industry in terms of resources resulted in a rapid increase in CO_2 emissions at the national level. Huo et al. (2014) considered the two important causes of air pollution in China are the high emission factors of pollution sources and the high emission intensity of the industrial structure. Finding that the service industry had the lowest emission intensity, the study proposed to further develop the service industry and thereby reduce air pollution. Huang et al. (2014) believed that in a country like China with strong industrial emissions and limited emission reduction facilities, coarser particulate matter emissions produce a great impact on health. Although urbanization reduces per capita emissions, the impact on the health of the overall population will increase due to the aggregation effect. Yuan et al. (2015) studied the impact of economic development and industrial structure on energy consumption and air pollutant emissions by comparing developed and underdeveloped regions in China. The unreasonable energy industrial structure led to an ineffective reduction of air pollutant emissions. Meng et al. (2015) showed that consumer demand for electricity and transportation highly increased the emission of air pollutants. Zhou et al. (2017) used data from 945 monitoring stations in 190 Chinese cities in 2014 to evaluate the direction and correlation intensity between socioeconomic factors and $\text{PM}_{2.5}$ pollution. The spatial regression results

showed that population density, industrial structure, industrial smoke (dust) emissions, and road density produced significant positive effects on PM2.5 concentration. Xie et al. (2018) found that population density, industrial structure, geographical features, and climate are closely related to air pollution. Yang et al. (2018) considered the iron and steel industry to be an energy-intensive industry that significantly contributed to China’s PM2.5 pollution. To achieve an effective reduction in CO₂ emissions, further technological innovation is necessary to reduce the cost threshold. Existing literature show that smog impacts the regional economy. Without smog control, the economic retrogression caused by environmental pollution in future regional socio-economic development would be fatal. Changing the traditional production methods, adjusting the industrial structure, and promoting regional cooperation could effectively control smog. However, existing literature on smog control seldom discusses the upgrading and transformation of provincial economic structures.

This study considers Hubei Province in central China for analysis. On the basis of fully understanding the smog weather and current industrial structure in Hubei Province, combined with the successful experience of foreign countries in smog control, the study presents important reference significance to realize the path towards smog control and upgrade the regional economic structures in many other regions dominated by industries.

MATERIALS AND METHODS

Model Construction

SO₂, nitrogen oxides (NOx) and inhalable particles are the main components of smog. In this study, the sum of the three indexes of smoke dust, SO₂, and nitrogen oxide emissions of cities in Hubei Province is the index considered to measure the smog situation and is expressed as explained variables. The industrial structure of each city is taken as an explanatory variable and expressed as *Str*. Simultaneously, based on data availability and existing local and international research, the economic development level, degree of

openness to the outside world, and building construction areas are introduced as control variables. The relationship between the smog pollution level in various cities and the influencing factors are shown in Formula (1).

$$\begin{aligned} \text{LnEnv}_{it} = & \beta_0 + \beta_1 \text{LnStr}_{it} + \beta_2 (\text{LnStr}_{it})^2 + \beta_3 \text{LnGdp}_{it} \\ & + \beta_4 (\text{LnGdp}_{it})^2 + \beta_5 \text{LnFdi}_{it} + \beta_6 \text{LnHou}_{it} + \varepsilon_{it} \end{aligned} \quad \dots(1)$$

Where, subscripts *i* and *t* of each variable represent city *i* and year *t*, respectively; β_0 represents the intercept term; ε_{it} represents the random error term; variable *Str* represents the industrial structure of each city; *Gdp* represents the economic development level of each city; *Fdi* represents the openness degree of each city to the outside world; and *Hou* represents the building construction area of each city.

Variables and Data

Explained variables: Given that SO₂, nitrogen oxides, and inhalable particles are the main components of smog, this study selects smoke dust, dust, SO₂, and nitrogen oxide emissions as indicators to measure smog.

Explanatory variables: In general, the development of a country’s economy from primary to mid-term stage changes the industrial structure from primary to secondary industry, and the development of heavy chemical and manufacturing industries intensifies environmental pollution. However, when a country’s economy develops from the mid-term to the high-level stage, the industrial structure gradually changes from secondary to tertiary industry. The rapid development of information, finance, and other service industries play a certain role in promoting and achieving pollution reduction. This study proposes that under industrial structure upgrades and adjustments, a nonlinear relationship may exist between the rationalization and upgrading of the industrial structure and pollution reduction. Therefore, the proportion of secondary industrial output value to GDP is used to measure the role of industrial structure in smog pollution control.

Control variables: The expansion of economic scale can

Table 1: Variable description.

Variable type	Variable symbol	Specific indicators	Unit
Explained variable	Env	Total emissions of smoke dust, SO ₂ , and nitrogen oxides	Ten thousand tons
Explanatory variable	Str	The proportion of output value of secondary industry to GDP	%
Control variables	Gdp	Per capita GDP	Ten thousand RMB
	Fdi	Proportion of foreign direct investment to GDP	%
	Hou	Building construction area	Ten thousand square meters

Table 2: Regression estimation results of influencing variables.

Variable	Model 1	Model 2	Model 3	Model 4	Model 5	Model 6
β_0	2.354***	1.541***	2.541**	3.654*	2.547***	7.214***
LnStr	-0.105**	-0.114**	-0.087	1.116**	-0.845	1.785**
LnStr ²		0.041**	0.574**	0.874	0.712***	0.965
LnGdp			-1.254	-0.741**	-1.658***	0.752
LnGdp ²				0.571**	0.054	-0.684**
LnFdi					0.024***	0.454
LnHou						0.175**

Notes: Models 1 to 6 in the table represent formulas obtained by introducing explanatory variable and control variables in sequence based on Formula (1). The upper corner marks *, **, and *** indicate significance at the 10%, 5%, and 1% levels, respectively.

reduce environmental pollution to a certain extent. Moreover, the economic scale effect of a region can reduce the pollution level of smog to a certain extent. On the premise of considering the impact of industrial restructuring on smog pollution, this study also introduces GDP per capita as a control variable. With China's low standards of environmental regulation, the introduction of foreign capital through trade liberalization is likely to increase pollution in China (i.e., the degree of openness increases environmental pollution). This study uses the ratio of foreign direct investment to GDP to measure the degree of openness and verify whether open trade is conducive to improving environmental quality. Soil dust and cement dust caused by construction activities are important components of air pollution particles and are important sources of smog pollution. In the process of urbanization in Hubei Province, the degree of smog pollution will be aggravated as the construction area and construction dust continues to expand and increase, respectively.

The specific definitions of each variable index are shown in Table 1. All variables are processed by taking the natural logarithm to reduce the heteroscedasticity of equation regression. The samples comprise panel data of 13 prefecture-level cities in Hubei Province from 2005 to 2016, obtained from the Statistical Yearbook of Hubei Province and the China Environmental Statistical Yearbook over the years.

RESULTS AND ANALYSIS

In this study, STATA14.0 software was used for quantitative analysis. An explanatory variable and other control variables are gradually introduced, and the influence of each variable on the comprehensive emission of air pollutants in various cities in Hubei Province is tested in turn. The estimated results are shown in Table 2.

Table 2 shows that the coefficient of $LnStr^2$ is significantly positive, whereas the coefficient of $LnStr$ is signifi-

cantly negative. This estimation result shows that the industrial structure and smog pollution level has a U-shaped curve relationship. With the increase in ratio of the output value of the tertiary industry to the output value of the secondary industry, the industry catch-up produces a containment effect on smog pollution emissions to a certain extent. The improvement of Hubei Province's industrial efficiency suggests that the province is far from reaching the level of active deindustrialization of developed countries. Through technological innovation, the traditional manufacturing industry still needs to move forward to the industry 4.0 with high added value. The lagging development of the high-end manufacturing industry restricts the transformation from a producer service industry to the modern service industry. The long-term, low-level development of the modern service industry in Hubei Province serves low-end industrial production more and has not changed its dependence on primary energy. The large proportion and low efficiency of the low-end service industry limit the deterrent effect of industrial upgrading on smog pollution and even aggravates smog emissions. The coefficient of variable $LnGdp$ is negative and highly significant, which indicates that the scale effect of economic development in Hubei Province can reduce the emission of air pollutants, effectively reduce the degree of smog, and improve the environmental quality. The estimated coefficient of variable $LnFdi$ is 0.024 and passed the significance test. This finding shows that for every 1% increase in the ratio of foreign direct investment to GDP, the emission of air pollutants rises by 0.024%, supporting the "pollution paradise" hypothesis. The possible reason for this finding is that the increase of foreign direct investment in various cities in Hubei Province leads to a large amount of foreign capital contributing to heavy pollution in areas that have not yet been able to fully introduce advanced clean production technology from abroad. On the contrary, it has exacerbated the smog pollution at the source. In the future, the introduction of foreign capital should include full consideration of the use of advanced manage-

ment and technology spillover effects to improve green productivity and control smog pollution, thereby reducing smog pollution levels and promoting green economic development in the province. The regression coefficient of $LnHou$ is 0.175 and is highly significant, indicating that for every 1% increase in the building construction area, the total amount of air pollutants will increase by about 0.175%. In recent years, Hubei Province has experienced rapid urbanization, accompanied by the continuous expansion of the average construction area. Consequently, the building dust generated during construction has increased and has aggravated smog pollution in various regions of Hubei Province.

POLICY RECOMMENDATIONS

Optimize and Adjust the Industrial Structure and Develop a Low-carbon Circular Economy

For its future economic development, Hubei Province should optimize its economic structure based on the circular economy mode, construct a low-carbon energy-saving industrial structure, transform low-energy consumption ecological industries to leading regional industries, improve energy utilization efficiency at the core, and ensure low-carbon ecological transformation on the leading industries in the region. We will accelerate the development and utilization of new energy sources, reduce the use of traditional resources such as coal, as well as develop and utilize new energy sources such as solar, wind, and water energies. Full development and utilization of advantageous solar energy can replace traditional energy sources on a large scale and thus reduce pollution sources. We can determine the unbalanced and coordinated development strategy as well as implement the dynamic development of dislocation and complementarity. Further study could continue to improve the scientific and technological content of enterprises, equipment manufacturing, high-tech industries, modern services, and other industries. In addition, market demand could serve as a guide to strengthen the overall low-carbon circular development of Hubei's regional industrial system. We should strengthen the control of local automobile exhaust and domestic exhaust emissions, advocate "low-carbon life", strictly limit construction dust pollution, reduce inhalable particles, and maintain ecological advantages.

Adjust the Energy Structure and Improve the Efficiency of Energy Utilization

Unreasonable energy consumption structure dominated by coal consumption is an important contributor to smog weather in Hubei Province. Realizing smog control entails optimizing and adjusting the energy structure, vigorously developing low-carbon energy, and improving the utilization

of renewable and alternative energy resources. Laws and economic policies must promote the diversification of energy consumption and coal utilization, as well as guide the adjustment of energy consumption structure to reduce the total emission of various pollutants. In addition, we must increase the transformation and upgrading of the traditional coal industry, continue to extend the industrial chain, and improve the added value. Extending the industrial chain of the coal energy industry would greatly reduce the transaction cost, thereby increasing the added value, gross production value, and profit of the energy industry. Based on material energy conservation and recycling, a series of measures have been adopted to optimize the coal industry organization, guide the establishment of an effective competitive market structure, avoid over-exploitation and waste of energy resources, improve Hubei's environmental performance, enhance the economic strength of relevant enterprises, encourage the use of sufficient funds to innovate and improve coal mining and production processes, and further promote the realization of sustainable development in Hubei Province as a whole.

Increase Investment in Smog Control and Encourage Technological Innovation in Enterprises

We propose to establish special funds for environmental protection and low-carbon technology research, as well as for new energy development and technological innovation. These funds should support relevant research and development (R&D) to improve the scientific and technological level of energy structure optimization and environmental quality protection in Hubei Province. The government could increase financial support for technological innovation, increase the proportion of R&D on low-carbon and energy-saving technologies in public financial expenditures, and increase capital investment in scientific research institutions. Clean energy technological innovations can achieve the following: effectively reduce the emission of atmospheric pollutants; encourage traditional industry enterprises to improve their energy utilization efficiency; promote clean energy technology; reduce the emission of pollutants, air pollution, and the particles that form smog; as well as promote industrial structure upgrading and economic structure adjustment. Various policies could likewise encourage industrial enterprises to actively promote and use new clean energy technologies, improve energy utilization efficiency, and pay close attention to energy-saving production.

Advocating Green Consumption Pattern and Intensifying Environmental Protection Publicity

A dynamic mechanism that includes internal interest incentives and external behaviour constraints and advocates a

green consumption view can be constructed. We should strengthen the guidance for residents' income and relevant advanced ideas to encourage people's daily routines to conform to the consumption concept of a circular economy, choose a reasonable green consumption mode, and promote a low-carbon life. Government departments have issued several relevant policies or bills to encourage people to consciously use low energy consumption resources and public transportation resources; adopt less pollution, more healthy consumption and travel methods; and, to a certain extent, inhibit the rapid expansion of high-energy consumption services. These policies promote the formation of a conservation-oriented consumption system in the whole society. The necessity and importance of controlling smog and developing a low-carbon economy should be publicized in a targeted manner through various forms, such as television, radio, newspapers, and knowledge competitions. Through the government and media guidance and the efforts of social public welfare organizations, the residents of the whole society would gradually realize that adjusting their consumption structure is the basic premise for smog control and the development of a low-carbon economy, and thus consciously establish a low-carbon life.

CONCLUSIONS

With the frequent occurrence of heavy smog pollution incidents, the contradiction between smog control, coordination of regional economic development, and air pollution has become a prominent research topic. Analysing the formation mechanism and influencing factors of smog pollution in urban agglomeration in different provinces is of high practical significance to promote the coordinated and sustainable development of energy, environment, and economy in the regions, as well as ensure the smooth progress of smog pollution control. This study explores the interactive relationship between smog control and the upgrading of the regional economic structure. The relationship between industrial structure and smog pollution degree shows a U-shaped curve, meaning that economic development can reduce the emission of air pollutants. Foreign direct investment does not produce a significant effect in improving environmental pollution. Construction dust also aggravates smog pollution. In the future, in-depth research can focus on the degree of correlation between smog and industrial development, the dynamic relationship between urbanization and smog, the temporal and spatial distribution characteristics of smog and its correlation, the adjust-

ment of industrial structure, and the improvement of green productivity.

REFERENCES

- Brajer, V., Mead, R.W. and Xiao, F. 2011. Searching for an environmental Kuznets curve in China's air pollution. *China Economic Review*, 22(3): 383-397.
- Fodha, M. and Zaghdoud, O. 2010. Economic growth and pollutant emissions in Tunisia: An empirical analysis of the environmental Kuznets curve. *Energy Policy*, 38(2): 1150-1156.
- Fujii, H., Managi, S. and Kaneko, S. 2013. Decomposition analysis of air pollution abatement in China: Empirical study for ten industrial sectors from 1998 to 2009. *Journal of Cleaner Production*, 59: 22-31.
- Huang, Y., Shen, H., Chen, H., Wang, R., Zhang, Y. Y., Su, S., Chen, Y. C., Lin, N., Zhuo, S. J., Zhong, Q. R., Wang, X. L., Liu, J. F., Li, B. G., Liu, W. X. and Tao, S. 2014. Quantification of global primary emissions of PM_{2.5}, PM₁₀, and TSP from combustion and industrial process sources. *Environmental Science & Technology*, 48(23): 13834-13843.
- Huo, H., Zhang, Q., Guan, D., Su, X., Zhao, H. and He, K. 2014. Examining air pollution in China using production-and consumption-based emissions accounting approaches. *Environmental Science & Technology*, 48(24): 14139-14147.
- Meng, J., Liu, J., Xu, Y. and Tao, S. 2015. Tracing primary PM_{2.5} emissions via Chinese supply chains. *Environmental Research Letters*, 10(5): 054005.
- Mingsheng, C. and Yulu, G. 2011. The mechanism and measures of adjustment of industrial organization structure: the perspective of energy saving and emission reduction. *Energy Procedia*, 5: 2562-2567.
- Shandra, J.M., Shor, E. and London, B. 2008. Debt, structural adjustment, and organic water pollution: a cross-national analysis. *Organization & Environment*, 21(1): 38-55.
- Tian, X., Chang, M., Shi, F. and Tanikawa, H. 2014. How does industrial structure change impact carbon dioxide emissions? A comparative analysis focusing on nine provincial regions in China. *Environmental Science & Policy*, 37: 243-254.
- Wei, J., Jia, R., Marinova, D. and Zhao, D. 2012. Modeling pollution control and performance in China's provinces. *Journal of Environmental Management*, 113: 263-270.
- Xie, Y., Zhao, L., Xue, J., Gao, H. O., Li, H., Jiang, R., Qiu, X. Y. and Zhang, S. H. 2018. Methods for defining the scopes and priorities for joint prevention and control of air pollution regions based on data-mining technologies. *Journal of Cleaner Production*, 185: 912-921.
- Yang, H., Liu, J., Jiang, K., Meng, J., Guan, D., Xu, Y. and Tao, S. 2018. Multi-objective analysis of the co-mitigation of CO₂ and PM_{2.5} pollution by China's iron and steel industry. *Journal of Cleaner Production*, 185: 331-341.
- Yuan, X., Mu, R., Zuo, J. and Wang, Q. 2015. Economic development, energy consumption, and air pollution: A critical assessment in China. *Human and Ecological Risk Assessment: An International Journal*, 21(3): 781-798.
- Zhou, C., Chen, J. and Wang, S. 2018. Examining the effects of socio-economic development on fine particulate matter (PM_{2.5}) in China's cities using spatial regression and the geographical detector technique. *Science of the Total Environment*, 619: 436-445.



Hydrogeo-Stratigraphic Model of Coastal Sediments in Kuttanad Area of Kerala, India

V. Kunhambu*, D. S. Sureshbabu** and N. Vinayachandran*

*Central Groundwater Board, Kerala Region, Thiruvananthapuram, India

**National Centre for Earth Science Studies, Akkulam, Thiruvananthapuram, India

Nat. Env. & Poll. Tech.
Website: www.neptjournal.com

Received: 27-06-2018

Accepted: 02-08-2018

Key Words:

Multi-aquifer system
Tertiary sediments
Hydrogeology
Coastal sediments

ABSTRACT

The coastal sediments of Kuttanad mainly consist of recent alluvium and Tertiary sediments unconformably underlay the Precambrian crystallines. Hydrogeologic and stratigraphic characterization of a multi-aquifer system embedded in this coastal sedimentary sequence was conducted using mapping and analysis of lithological and geophysical logs from 125 boreholes. The lateral and vertical variations in the lithostratigraphy and a conceptual model of the hydrogeology of the area could be established from the study. The isopach maps and panel diagrams of stratigraphic formations indicate thick offshore extension of the aquifer systems. The hydraulic gradients in the Tertiary aquifers are indicative of an offshore freshwater interface. The depositional history of Tertiary sediments and the marine transgressions and regressions during Pleistocene glaciations played a major role in the evolution of aquifer systems in these sediments.

INTRODUCTION

'Kuttanad' is a low-lying area in the west coast of Indian peninsula bordering the State of Kerala (Fig. 1). The Kuttanad terrain is characterised by wetlands, below mean sea level areas and the Vembanad Lake, a Ramsar site into which five rivers debouch before joining the Arabian Sea. The area comprises recent alluvium mainly consisting of sand, silt and clay, underlain by Tertiary sediments. The sediments of Kuttanad area are deposited on a sagging basin dipping towards west with a thick pile of sediments. Thus, the sediment thickness increases towards the coast which further extends offshore. The basement rocks, charnockite and migmatite complex are exposed in the east, bordering the peripheral areas of the coastal sedimentary formations. Residual laterite formations are encountered in the south-eastern parts of the study area. The area has complex hydrogeological environment evolved out of various geological and tectonic activities in the geological past. Based on the analysis of lithological and electrical logs of Tertiary sediments, four distinct stratigraphic units were deciphered in the area, viz; Alleppey, Vaikom, Quilon and Warkalai beds (CGWB 1992). Exploratory drillings in the area by Central Ground Water Board (CGWB) indicate more than 600 m thick pile of Tertiary sediments near the coast. Various litho-units in the stratigraphic sequence are given in Table 1.

Various studies on coastal Kerala sediments (GSI 1980, Nair 1987, CGWB 1992, 2002) have established an afluvi-

marine depositional environment for the Tertiary sediments.

Geological history of the area: The history of sea level changes in the Pleistocene, are partly the geological history of the region. The formation of glaciers in the northern continents by the early Pleistocene had subtracted stupendous quantities of water from the world's oceans, forcing the sea level to reach a level of about 130 m below the modern sea level. The sea level rise was not gradual; instead, it was episodic as the land rebounds due to offloading of ice (Thrivikramji et al. 2003). Curray (1961) published a sea level change curve based on ^{14}C dates of sediment particles depicting the procession of sea level during the last 40000 years before present (BP). Two events of sea level rise or transgressions are indicated here. Vaidyanathan (1981) suggested filling up a series of bays during the Holocene period with mud, which later on got covered by sand sheets moulded into sub-aerial dunes. Based on the investigations in western continental shelf (including Kerala offshore), Nair (1980) recognized four still stands demonstrated by submarine terraces at 92, 85, 75 and 55 m below the modern sea level and ranging in age from 9000 to 11000 years BP. Nair (2003) suggested that the rocks are of Holocene age and sea level was rising (transgressive phase). Kale & Raja Guru (1985) constructed a sea level rise curve and postulated a rate of 1.8 cm per year and the sea level reached the present-day position 6000 years BP. The lowest stand at 138 m below mean sea level occurred probably about 12000 years BP.

Table 1: Stratigraphy of the area.

	Age	Formation	Lithology
Quaternary	Recent	Alluvium	Sand and clays along the coast and flood plain deposits
	Sub-recent	Laterite	Laterite capping over crystalline and sedimentary formations
Tertiary	Lower Miocene	Warkalai beds	Sandstones and clays with thin bands of lignite
	Lower Miocene	Quilon beds	Limestone and clay
	Oligocene to Eocene	Vaikom beds	Sandstone, clay and thin bands of lignite
	Eocene	Alleppey beds	Carbonaceous clay with minor lenses of fine sand
		Unconformity	
	Archaean (crystalline formation)		Charnockites, Khondalites and granites

The sediment deposits along the Kerala coast during these marine transgressions and regressions and the palaeoclimate influenced the evolutionary history of groundwater in the tertiary aquifer systems.

Hydrogeology: The aquifer systems in the area are embedded in recent alluvium and Tertiary sediments. The top phreatic aquifer is spread over the entire area except in low-lying areas where the topsoil is clayey and water quality is poor or brackish. The recent alluvium is well developed near the coast where the phreatic and confined aquifer systems are very potent. Towards the east, the aquifer continuity is lost and the thickness of recent alluvium is also less. Brackish paleo-water is reported from tube wells in the low lying areas in the east (CGWB 1992, 2002).

The Tertiary sedimentary formation is classified into four beds viz; Alleppey, Vaikom, Quilon and Warkalai beds chronologically from older to younger, based on the geological, geophysical and fossil evidence (CGWB 1992). Of the four Tertiary beds, the Vaikom and Warkali beds bear potential freshwater aquifers. The Alleppey beds at the bottom contain brackish water as inferred from electrical logs, whereas, the Quilon beds are poor limestone aquifers. All the four beds are encountered in boreholes drilled in Kuttanad area.

The water table contour maps generated for Warkalai and Vaikom aquifers in previous studies (Vinayachandran 2015) suggest groundwater recharge to these aquifer systems from the southeastern part of the area (south of Alleppey) and further south from the eastern hard rock-sedimentary contact zone.

The aquifer geometry indicates a plausible hydraulic continuity of Tertiary aquifers with the deep fracture aquifer system in the east. The recharge from exposed beds of Warkalai and Vaikom formations are insignificant as the vertical flow of water is restricted by thick clay layers (Vinayachandran et al. 2013). The long-term hydrographs representing the Tertiary aquifers show a falling trend whereas, the hydrographs from the overlying phreatic aquifers are stable. This indicates a distant recharge area for the Tertiary aquifers.

Objective: The objective of the study is to develop a hydrogeo-stratigraphic model of coastal sediments in the Kuttanad area by defining the stratigraphic relation of the multi-aquifer systems, their interrelation, aquifer geometry and the hydro-chemical evolution of the aquifers.

MATERIALS AND METHODS

The lithological and electrical log data from 125 bore wells have been analysed for demarcation of various granular zones for defining the aquifer geometry, stratigraphic succession and formation thickness variations in the area. Panel diagram and cross-sections were prepared to decipher spatial and vertical changes in lithology. The study concentrates on the litho-stratigraphy and hydrology related to the three aquifer systems viz., the unconfined aquifer system in recent alluvium and the Warkalai and Vaikom aquifers in the Tertiary sediments.

The piezometric heads and water levels were collected from the monitoring wells maintained by Central Ground Water Board and State Ground Water Department for flow regime analysis. Pumping test data have been used to evaluate aquifer characteristics (transmissivity and storativity). The aquifer characteristics of deep confined aquifers in the Tertiary beds were collected from the unpublished reports of the Central Ground Water Board.

RESULTS AND DISCUSSION

The stratigraphic classification by CGWB is followed in defining the stratigraphic position of aquifer systems. The spatial variations in sediment thickness in Kuttanad area, based on 125 borehole litho-log, depicted in Fig. 2, indicate a steep gradient of basement with an increase in sediment thickness towards the coast, which further extends into the Arabian sea. The panel diagram depicting the lateral and vertical variations in litho-stratigraphy (Fig. 3) also indicates a similar pattern and here all the four stratigraphic units are well developed near the coast. Towards the east, recent alluvium unconformably rests either over the taper-

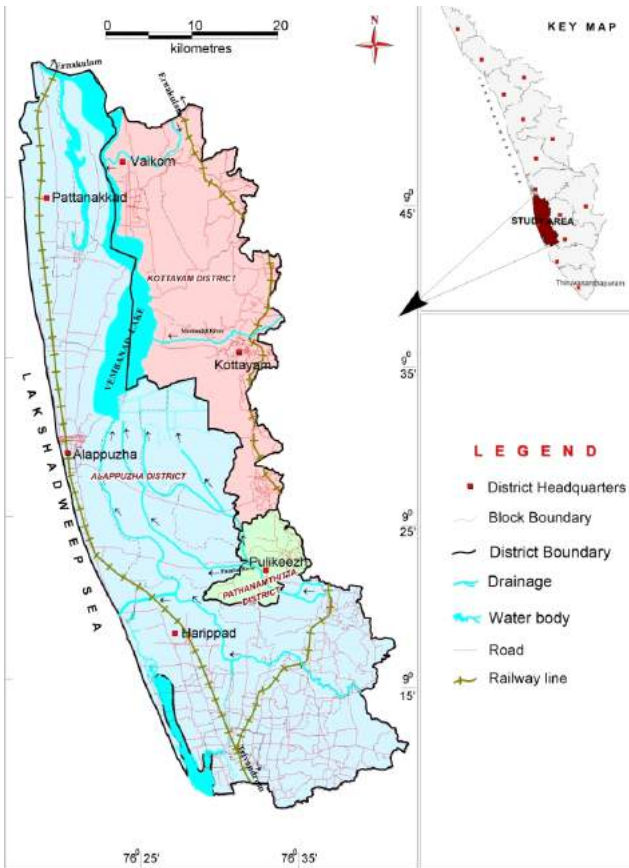


Fig.1: Location map of the area.

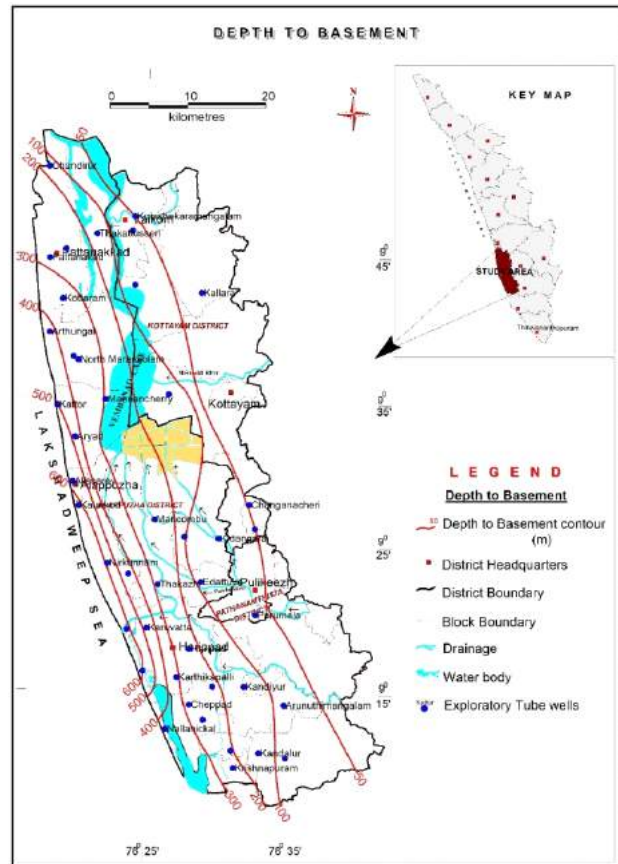


Fig. 2: Isopach of coastal sediments in Kuttanad area.

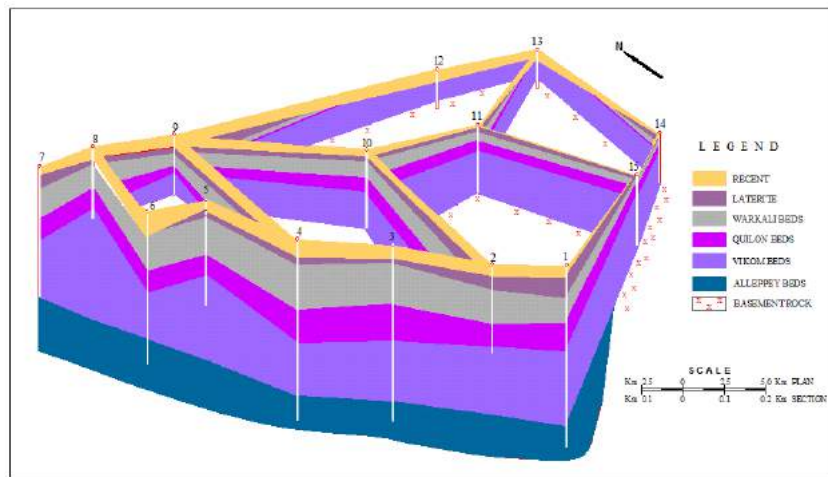


Fig. 3: Panel diagram showing lateral and vertical variations in lithology.

ing Warkali beds or directly over the Vaikom beds. Presumably, the recent alluvium was deposited over an eroded and faulted Tertiary bed. This is elaborated in the findings of the studies by ONGC in the Kerala coast.

According to seismic measurements carried out by ONGC in the sea outside Kerala, a series of mainly NNW-SSE trending faults affect the offshore sediments and basement (Fig. 4). This is completely in accordance with what

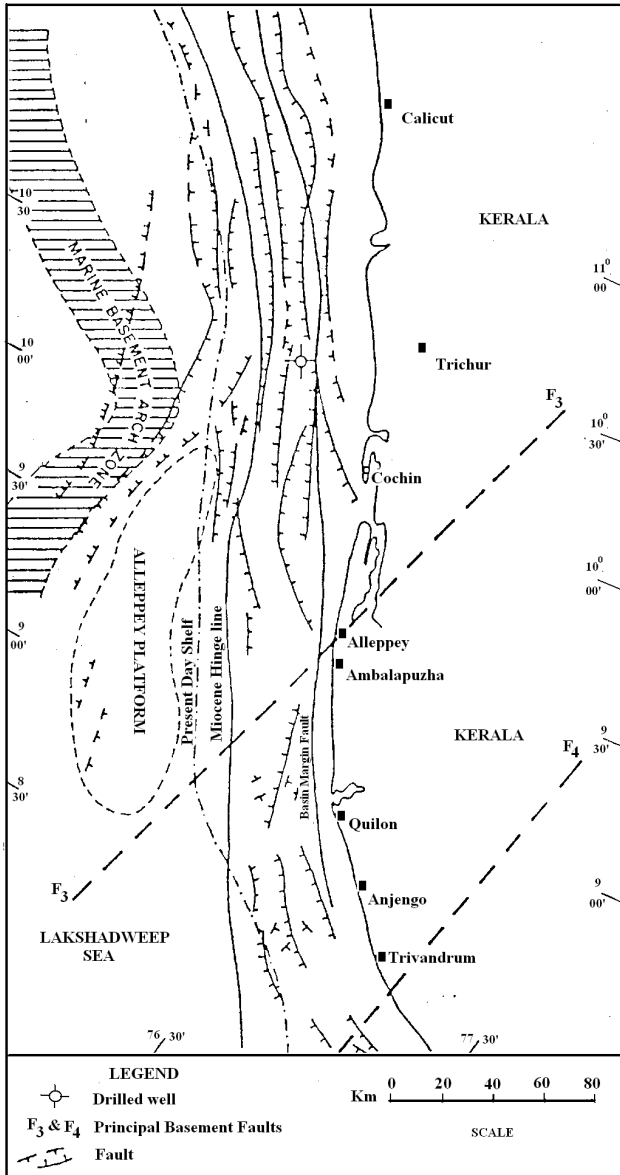


Fig 4: Tectonic map of Kerala coast and offshore (Prasada Rao 1984).

can be expected in areas with a geological history of the kind the Indian west coast has experienced in connection to rifting, separation from the African continent and following the plate tectonic events.

It can be taken as a fact that the faulting also has affected the overlying sediments that were present at the time of faulting. In this connection, it should be kept in mind that the Vaikom, Quilon and Warkali sediments today are not very consolidated. This is reflected in the caving and sometimes even total collapse of boreholes that are not cased for a few days or even a few hours after the drilling has stopped.

It is obvious that these sediments were even less consolidated at the time of faulting. The faulting probably took place over a period of time, so it is not likely that all the faults have affected all the sediments. It can also be expected that the faulting and the sedimentation to a large extent were synchronous.

With this background, it is rather unlikely that the sediments have reacted to faulting by developing clear-cut fractures, as is in the case in brittle rocks. It is more likely that they have reacted by developing monoclin folds or flexures, especially if each fault step is not too much displaced.

The isopach maps of Warkali and Vaikom beds (Fig. 5 and 6) show an increase in the thickness of sediments towards west (sea coast) where the Vaikom beds are thicker and spatially cover the entire area. A gradual increase in sediment thickness of Vaikom beds compared to that of Warkali is evident from these maps. The top elevation maps of Warkali and Vaikom beds (Fig. 7 and 8) show gradient towards the coast, and near the coast it is steeper. Compared to Vaikom the bed gradient near the coast is steeper in Warkali. Thus, the seaward extension of Vaikom beds should be much higher than the Warkali beds.

The borehole made by ONGC about 30 km off shore, just north of Cochin shows the sequence as given in Table 2, according to ONGC. The electrical log of this borehole indicates the presence of freshwater sediments between 701 and 1814 m. However, it is quite possible that the log merely indicates that the sediments originally were deposited under freshwater environment. This matter has to be checked in detail. Anyhow, the log shows that freshwater is present in these sediments and it is quite possible that parts of it have been entrapped between clayey layers at considerable depths. It is quite possible that the lower layers (701-1814 m) seem to be containing freshwater, has a hydraulic connection with the Vaikom layers that we are encountering on land.

Table 2: Sequence shown by the borehole made by ONGC about 30 km off shore, just north of Cochin.

Depth range(m)	Lithology
0-295	Shallow marginal marine sediments. Dominantly sandstone.
295-694	Shallow marine sediments. Clays with sand stone and carbonate. A layer of basalt of unspecified thickness.
674-701	Clay, sand, and carbonate. Another layer of basalt of unspecified thickness
701-1814	Continental sediments. Sandstone with clay and trap derivatives (dominantly fresh water)
	The borehole ends in Basalt.

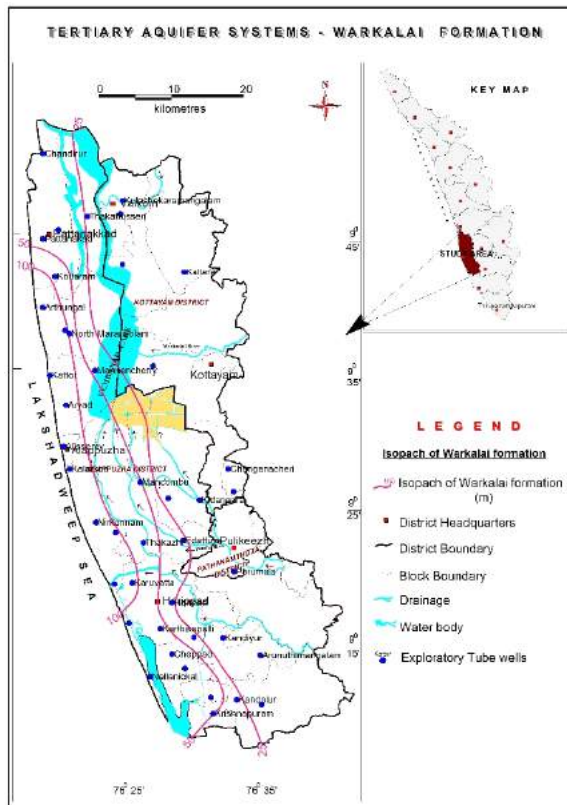


Fig. 5: Isopach of Warkali beds.

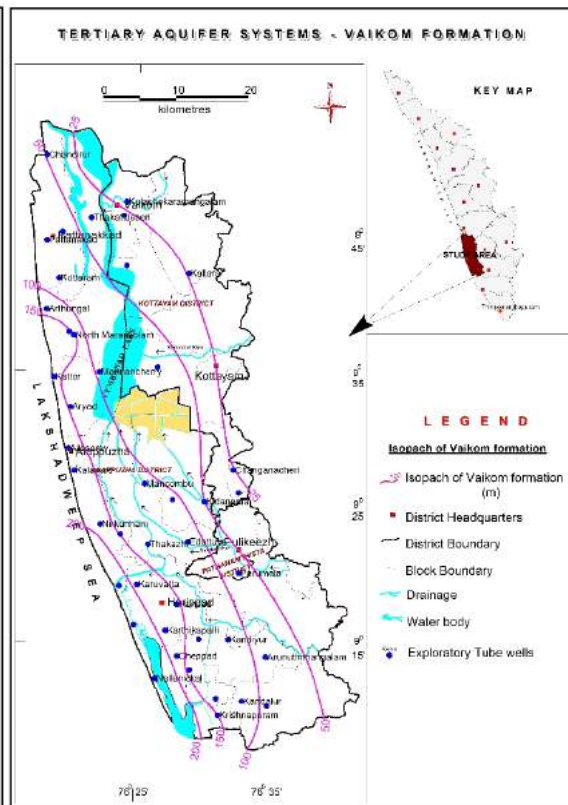


Fig. 6: Isopach of Vaikom beds.

Certainly, the presence of freshwater in a position like this is not normal. However, it is known to occur in similar positions at several different places around the world. The freshwater with lower specific density than saltwater will strive to reach higher elevations, and the easiest way under the confining clay layers and the general dip of the sedimentary formations will be to the east.

A theoretically possible, although a quite fictive picture can be drawn from the coast to the shelf slope. If the Vaikom layers are extended up to this slope, keeping their general dip as we know it on land, they will intersect the shelf slope at a depth of about 1600 m below msl. The column of 1600 m of salt sea water will hydrostatically correspond to a column of 1640 m of freshwater. This means that hypothetically and also possibly there can be a hydrostatic pressure of salt water corresponding to a piezometric freshwater head of +40 m acting on the aquifer at a distance of 130 km from the coast. This could be the force driving the (very slow) flow of fresh groundwater from the west to the east in the Vaikom aquifer, as we record it in terms of a piezometric gradient in this direction on land in the coastal area. The piezometric head observed at the time of con-

struction of piezometers in Vaikom aquifer at Karthikapally about 5 km from the beach was 6 m above msl and at Muttom and Kandiur located 9 km and 13 km further inland were 5 m and 4 m above msl respectively. That is, in this area the conditions were artesian, and the gradient suggests a flow mainly from west to east in this aquifer. Also, the flow across the hard rock contact zone may be negligible as the existing pressure head in the Tertiary aquifer system is high.

Large-scale pumping from this aquifer system created a trough around the area of extraction of water with flow from all the sides. The piezometric gradient observed at present show groundwater flow towards west (towards the sea) or towards the trough with heads below msl. The flow from offshore towards the trough could not be evidenced as there is no provision to measure the piezometric heads offshore.

The conclusion of this is that the fresh/saltwater interface, very likely is situated farther out under the sea, possibly more than 25 to 30 km. Hence, the pumping wells tapping this aquifer very close to the sea may not be affected by salt water intrusion as the seawater-freshwater interface is further off than it normally is.

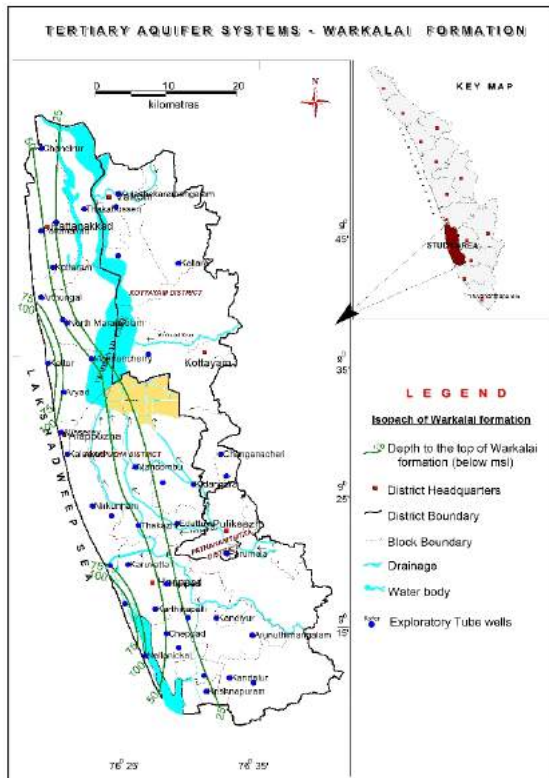


Fig. 7: Top elevation of Warkali beds.

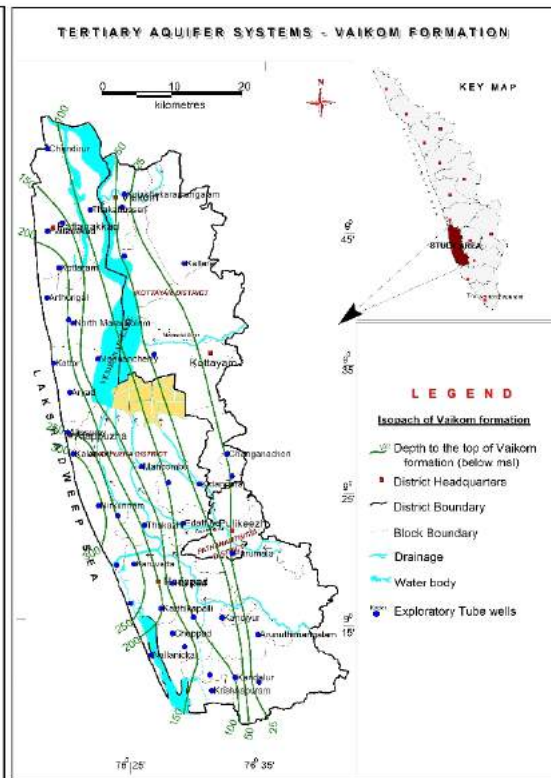


Fig. 8: Top elevation of Vaikom beds.

CONCLUSION

The hydrogeology of the area is evolved out of various sedimentation and hydraulic cycles underwent during the marine transgressions and regressions in the geological past.

During the Quaternary period, the latest 3 million years, the time span of the glaciations has been in the order of ten times longer of the inter-glaciations and the sea levels were in the order of 100 to 200 m lower during the glaciations than it is now (because large volumes of water were confined in the huge ice masses). The shoreline at the peak of this glaciation would be the shelf edge, which in this area is situated 60 to 70 km west of the present coast.

This means that the sediments that were deposited during the inter-glaciations, on the present shelf, in seawater or brackish water, during glaciations came in a position above the sea level. During such periods, the original interstitial salty water was flushed out and replaced by freshwater and under certain conditions, with overlying confining clay layers, this freshwater was trapped in the sediments when they were transgressed during the subsequent inter-glaciation. Thus, it is possible that the fresh/salt water interface in the Vaikom aquifer is situated rather far out in the shelf. Further detailed study is required to confirm this conclusion.

REFERENCES

- Central Ground Water Board 1992. SIDA assisted coastal Kerala Ground Water Project (1983-88). Unpub. Final Tech. Report, Central Ground Water Board, Ministry of Water Resources, Govt. of India, pp. 220.
- Central Ground Water Board 2002. Solute transport modeling studies in Kuttanad Alluvium, Kerala. Unpub. Report Central Ground Water Board, Ministry of Water Resources, Un. Pub. Report., Govt. of India, pp. 117.
- Curry, J.R. 1961. Late quaternary sea level: A discussion. *Geol. Soc. Am. Bull.*, 2: 1707-1712.
- Geological Survey of India 1980. *Geology and Geomorphology of Kerala*, Spl. Pub. No. 5.
- Kale, V.S. and Rajaguru, S.N. 1985. Neogene and quaternary transgressional history of the west coast of India: An overview. *Deccan College Research Institute Bulletin*, 44: 153-167.
- Nair, A.S.K. 2003. An evolutionary model for the coastal plain of Kerala using satellite remote sensing data. Unpub. Ph.D. Thesis submitted to Tamil University, Tanjavur, S. India.
- Nair, M.M. 1987. Coastal geomorphology of Kerala. *J. Geol. Soc. India*, 29(4): 450-458.
- Nair, R.R. and Hashimi, N.H. 1980. Holocene climate inferences from the sediments of the western Indian continental shelf. *Proceedings of Indian Academy of Sciences*, 89(3): 299-315.
- Prasada Rao, K. and Srivatsava, D.C., 1984. Regional seismic facies analysis of western offshore, India. *Bull. ONGC.*, 18(2): 25-26.
- Thrivikramji, K.P., Nambiar, C.G. and Krishnakumar, N. 2003. Proposed mineral sand mining in coastal Arattupuzha and Thirkun-

- apuzha Panchayats: An environmental impact study. Unpub. Report, Dept. of Industries, Govt. of Kerala, pp. 74.
- Vaidyanathan, R. 1987. Coastal geomorphology in India. *Jour. Geol. Soc. India*, 29: 373-378.
- Vinayachandran, N. 2013. Disposition of aquifer system, geo-electric characteristics and gamma-log anomaly in the Kuttanad alluvium of Kerala. *J. Geol. Soc. of India*, 81(2): 183-191.
- Vinayachandran, N. 2015. Hydrogeology and hydrochemistry of the aquifer systems of Kuttanad area, Kerala: Their role in understanding the evolution of groundwaters. Ph.D. Thesis, Department of Marine Geology and Geophysics, Cochin University of Science and Technology, 227p.



Analysis of Sea-water Treated Laminated Bamboo Composite for Structural Application

Teodoro A. Amatosa, Jr.*(**)†, Michael E. Loretero*(***), Romeo B. Santos** and Marnie B. Giduquio*

*Engineering Graduate Program, School of Engineering, University of San Carlos, Talamban Campus, Cebu City, 6000 Philippines

**College of Engineering and Technology, Northwest Samar State University, Calbayog City, Samar, 6710 Philippines

***Department of Mechanical Engineering, University of San Carlos, Talamban Campus, Cebu City, 6000 Philippines

†Corresponding author: Teodoro A. Amatosa, Jr.

Nat. Env. & Poll. Tech.
Website: www.neptjournal.com

Received: 04-06-2018

Accepted: 02-08-2018

Key Words:

Green engineering
Laminated bamboo
composite (LBC)
Epoxy resin
Structural application

ABSTRACT

Green engineering is increasingly investigated as a possibility to treat organic green material for structural applications. *Dendrocalamus asper* bamboo culms as green engineering materials were processed to produce composite materials using epoxy resin from a natural treatment by soaking with an average of pH 7.6 level of sea-water. Mechanical properties of proposed laminated bamboo composites (LBCs) have been assessed under loading conditions and standards. The study provides a comparison of the structural performance with different conventional timbers as avenue for application in engineering design and practices. Comparison of laminated bamboo with woods indicate that average value of 27.47 MPa and 52.59 MPa for compressive and bending strength respectively, obtained much higher allowable value and average strength, which are comparable to stiffness values of softwoods and hardwoods. However, even though the present study shows properties with higher and comparable to other composite materials, further research must be given better attention for characterization and standardization before acceptance in the marketplace as alternative green engineering material to timber and wood-based composites and other building materials for construction design, and structural elements as composite materials for engineering utilization.

INTRODUCTION

Evaluation of bamboo through life cycle assessment is presented in an effort to resolve the environmental implication of bamboo as a source for construction material. The results of this interpretation show that, in some applications, bamboo has marked a high “factor 20” environmental impact, which means a 20 times less load on the environment than compared to some alternatives (Van der Lugt et al. 2006). Wood and bamboo have recently been renowned in the green engineering technology industry because of their environmentally promising characteristics. They can be replaced by a natural processes, biodegradable, confine carbon from the atmosphere, low in combined energy, and create less pollution in development than concrete or steel (Falk 2009 and Mahdavi et al. 2011). Bamboo is a green material that can possibly substitute the wood for reasons that, bamboo can be cropped in 3-4 years from the time of plantation as compared to timber which takes decades (Lakkad & Patel 1980 and Amada et al. 1997). Compared with other similar composite building materials, strength-to-specific gravity ratio, bamboo is much stronger and has a greater value than that of common hardwood, softwood and even metals such

as aluminium alloy, cast iron, and structural steel (Mahdavi et al. 2011).

Bamboo has high strength fibres, and as one of the existing flowering plants and available forest resources, it plays an important economic and cultural role in tropical areas worldwide. For instance, bamboo utilization in China’s pulp industry is very significant, with the production of approximately one million tons (Zhou et al. 2010). These bamboos are characterized as a competitive material in relation to wood and other non-wood vegetal fibres to produce pulp (Correia et al. 2015) and nanofibrillated bamboo cellulose as reinforcements made without using any artificial chemicals and inorganic matrices, such as in polymeric composites (Lu et al. 2013, Guimaraes et al. 2015) and in construction building materials like cement and concrete reinforcement (Coutts & Ni 1995, Correia et al. 2014 and Xie et al. 2015).

Although bamboo is a potential wood replacement, structurally it can be used with a certain limit by the proportionate dimension of the bamboo culm and the low inflexibility of the bamboo. To address the limitation of member size and to increase the measurement consistency, capacity and

Table 1: Macroscopic characteristics of giant bamboo (*Dendrocalamus asper*).

Macroscopic characteristics	Unit	Literature			Native Bamboo*
		1	2	3	
Culm length	m	20-30	18-23	-	20-30
Internode length	cm	20-25	35	14-45	30-35
Internode Diameter	cm	8-20	9-13	1.2-9.3	8-18
Culm wall Thickness	mm	11-20	10-14	4-30	6-13

Literature: 1/ Dransfield & Widjaja (1995) 2/ Othman et al. (1995) 3/ Pakhkerree (1997) / *Present study

Table 2: Comparison of average mechanical properties of *Dendrocalamus asper* bamboo culm to other common building materials.

Building materials	Specific gravity	Compressive			Bending	
		MOR (MPa)	Standard Deviation, S.D.	MOE (GPa)	MOR (MPa)	MOR to specific gravity ratio (MPa)
<i>Dendrocalamus asper</i> *	0.54					
Freshwater treatment		45.20	12.16 ($\pm 26.93\%$)	17.658	188.05	348.24
Sea-water treatment		53.60	15.59 ($\pm 29.08\%$)	23.578	218.35	404.35
Untreated		34.10	5.00 ($\pm 14.65\%$)	7.608	71.75	132.87
Giant timber bamboo ^a	0.52	-	-	10.7	102.70	197.50
Other bamboo ^a	-	-	-	9.0-20.7	97.9-137.9	-
Hardwoods						
Beech ^b	-	50.30	-	-	103.00	-
Oak (Pin) ^b	-	41.78	-	-	71.02	-
Poplar, Balsam ^b	-	27.70	-	-	47.00	-
Mahogany ^b	-	46.70	-	-	79.30	-
Rosewood, Indian ^b	-	63.60	-	-	116.50	-
Teak ^c	-	69.50	-	-	128.00	-
Softwoods						
Cedar ^b	-	24.80	-	-	42.00	-
Redwood, young ^b	-	35.99	-	-	54.46	-
Loblolly pine ^b	0.51	36.00	-	12.3	88	172.50
Douglas-fir ^b	0.45	50.00	-	13.6	88	195.60
Metal						
Cast iron ^d	6.97	-	-	190	200	28.70
Aluminum alloy ^d	2.72	-	-	69	200	73.40
Structural steel ^d	7.85	-	-	200	400	50.90
Carbon fiber ^d	1.76	-	-	150.3	5,650	3,205.10

*Present study; ^aLee et al. 1998; ^bForest Products Laboratory 1999; ^cKrestschmann 2010; ^dRittironk & Elnieri 2007

uniformity, the bamboo culm can be dismantled into thin, slender laminae and then laminated into one group with adhesive to form genuine structural members. The composite material is called laminated bamboo (Correal 2008). Mechanical properties of the laminated bamboo composite will look closely with those of common hardwood and softwood, and so laminated bamboo structural members are better than others with commonly used building construction materials, whilst also able to be extended for another period of time (Lopez & Correal 2009, Mahdavi et al. 2012, De Flander & Rovers 2009 and Nugroho & Naoto 2001). Much research work has been carried out on wood (Verma & Chariar 2012, Verma & Chariar 2013, Verma et al. 2014 and Sulastiningsih & Nurwati 2009), but less on laminated bam-

boo lumber (Lee et al. 2012, Sulaiman et al. 2006, Paes et al. 2009, Correal & Ramirez 2010, Lee et al. 1998, Wei et al. 2011, Sinha et al. 2014, Yeh & Lin 2012, Li et al. 2013, Xiaohong 2011, Yu et al. 2003, Yu et al. 2005, Siddhaye & Sonar 2006, Richard & Harries 2012 and Li et al. 2015), so more work needs to be done on this kind of new building material.

MATERIALS AND METHODS

Materials

Three-year-old giant bamboo (*Dendrocalamus asper*) was harvested from Mandaue city, in the Philippines. Portion cut up to 3.0 m from the basal region was used for the assessment (Fig. 1). The bamboo was manually cut into a speci-

Table 3: Comparison of mechanical strength properties of LBCs *Dendrocalamus asper* with other similar composites.

Materials	Density ρ_{mean} kg/m ³	Compressive		Tension		Shear f_{mean} (MPa)	Bending f_{mean} (MPa)
		f_{\parallel} (MPa)	f_{\perp} (MPa)	f_{\parallel} (MPa)	f_{\perp} (MPa)		
Laminated Bamboo*	1,022.24	27.47	1.97	-	1.49	-	52.59
C24 - EN 338 ^a	420	21.00	-	32.00	-	4	24.00
GL 24h-EN 14080-06 ^b	420	24.00	-	14.00	-	3.5	24.00
Norway spruce ^{c,d}	-	44.00 ^b	-	19.50	-	6	48.00
Glue laminated spruce ^e	450	32.00	-	-	-	-	50.00
Thermally modified beech ^f	580	48.70 ^b	-	14.00	-	-	31.00
Caramelized bamboo ^g	686	77.00	22.00	90.00	2.00	16	77 – 83
Sitka spruce ^{i,k}	383	36.00	-	59.00	-	9	67.00
Douglas-fir LVL ^{l,m}	520	57.00	-	49.00	-	11	68.00
Sheathing-grade Plywood ⁿ	-	20.7-34.5	-	10.3-27.6	-	-	20.7-48.3
Sheathing-grade OSB ⁿ	-	10.3-17.2	-	6.9-10.3	-	-	20.7-27.6
Normal laminated wood ⁿ	-	44.10	-	153.10	-	-	140.60
Low density cement-wood ⁿ	-	0.69-5.5	-	0.69-4.1	-	-	1.7-5.5
Wood-Popypropylene ⁿ	-	38.3-72.4	-	28.5-52.3	-	-	-

*Present study; ^aCEN (2009); ^bCEN (2013); ^cSteiger & Arnold (2009); ^dJenkel et al. (2015); ^eDe Lorenzis et al. (2005); ^fWidmann et al. (2012); ^gTest not conducted in accordance with EN 408 (CEN, 2012); ^hExperimental mean; ⁱSharma et al. (2015); ^jLavers (2002); ^kKretschmann (2010); ^lKretschmann et al. (1993); ^mClouston et al. (2002); ⁿForest Products Laboratory (1999)

fied length of 300 mm and was split longitudinally at the top, middle and bottom part. During the submersion of specimens, five for each bamboo parts were immersed in salt water to protect bamboo against insect attack for 7 days cycles as traditional preservation. A setup was performed using traditional treatment to show up the specimens to wetting and drying cycle; the bamboo specimens were removed from the water and stacked vertically for air-drying for one week (Amatosa & Loretero 2017).

Production

Manufacturing of the laminated bamboo composite (LBC) from *Dendrocalamus asper* was made in the Mechanical and Manufacturing Engineering Laboratory at the University of San Carlos, Cebu City, Philippines. The culm sections of 2 m to 3 m were cut again into 1 m to 1.5 m in order to have straight pieces. Each piece was split in the longitudinal direction for a proper number of slices and the node sections were removed. The slices were vertically placed for air-drying to an average of 6% to 8% moisture content. Each slice is manually cut off, the inner and outer faces containing wax and silica that weaken adhesive bonding are not included to form LBC with a thickness from 3 mm to 5 mm. All laminas were impregnated with epoxy resin and staked to form laminated bamboo. Each LBC was cold pressed in a hydraulic press at a pressure of 1.5-2 MPa for 15 minutes.

RESULTS AND DISCUSSION

This paper analyses the treated giant bamboo species within one week and air-dried for another week, if it could influence the mechanical properties of the specimen, specifi-

cally compressive and bending strength together with the other properties of the laminated composite.

Mechanical Properties of Bamboo Culm/Laminated vs Woods

Table 2 gives the comparative analysis of mechanical strength properties of a full culm of *Dendrocalamus asper* bamboo to other woods and comparable materials, and Table 3 presents the variation in nature of mechanical properties of LBC as a possible substitute to woods and wood-based composites. These data provide that *Dendrocalamus asper* bamboo can be deployed for fabrication as LBCs.

Using the internode section from a full culm bamboo parallel to the grains, the mechanical properties of *Dendrocalamus asper* are given in Table 2. ASTM D 695 - 96 test procedure (ASTM 1999) has been used for the assessment of compressive strength, wherein specimens treated in sea-water got the highest average value which reached up to 53.60 MPa with S=15.6 MPa, followed by the specimens in freshwater and untreated with average strength of 45.20 MPa, S=12.5 MPa, and 34.10 MPa, S=5.00 MPa respectively. It shows that the *Dendrocalamus asper* specimens, which are treated in sea-water, have gained its strength by 62.98% and freshwater increased by 32.36% from untreated specimens. As the results prove, unlike the untreated specimens, the fresh water and sea-water treated specimen have a larger amount to withstand specified loads.

The present study went through different variations of treatment (soaking it from fresh and sea-water, and untreated as control), same with properties of some bamboo species

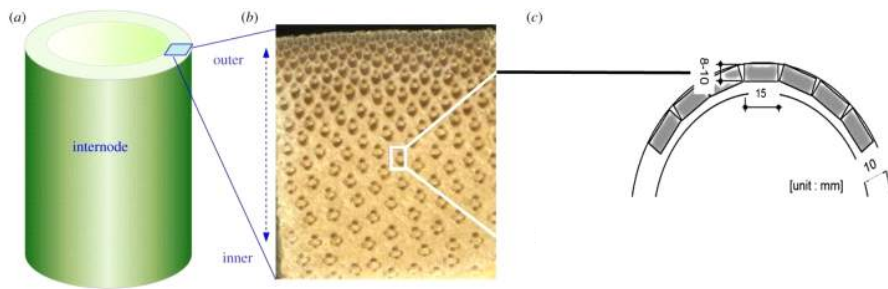


Fig. 1: Extraction of specimens (cross section of bamboo).

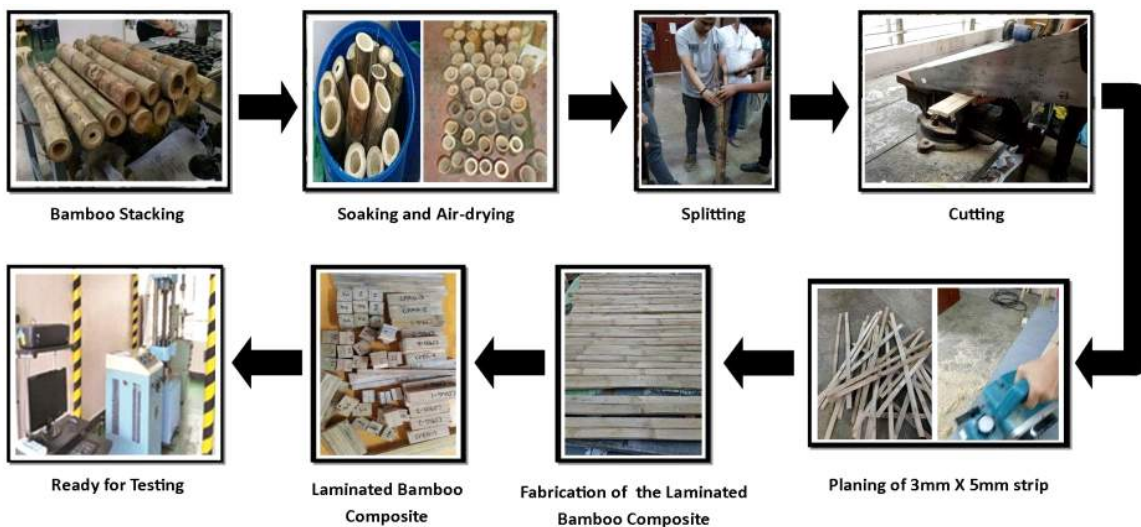


Fig. 2: Distribution flow of laminated bamboo composite.

for construction building materials; and, this wood species such as Teak or Beech for hardwood has most likely the same quality of *Dendrocalamus asper*. The information indicates that *Dendrocalamus asper* bamboo is stronger in strength for flexural rather than timber, and its strength-to-weight ratio is higher than that of all other materials indicated except for carbon fibre. Not just bamboo is fast-growing, but it is also highly effective substitute material in relation to other green construction materials for structural application.

Comparison of Strength of LBCs with Other Structural Composite Lumber Products

Different laboratory tests were conducted for mechanical properties of *Dendrocalamus asper* bamboo for laminated bamboo composite (LBC) specimens to provide a direct comparison with some commercial composite products. Specimens were produced with prescribed dimensions and

tests were performed according to ASTM D143 (ASTM 2014). Due to the higher value of properties by sea-water treated bamboo, this was used to produce LBCs for evaluation. The size of the specimen and test procedure was selected to be consistent with other LBLs to establish similarities of strong values and to prevent contrast of configuration result between size and load. Flatten specimens were tested in the horizontal lamination (joist) orientation. All tests were performed using a 600 kN capacity universal testing machine. A continuous compression load with a load rate of 0.6 mm/min was applied and distributed up to deformation equal to 5% of the specimen thickness, until it reached and the stress at that point is calculated. The relative humidity of the specimen with an average moisture content of 8%-12%, was placed in the laboratory using ambient temperature for drying.

Presenting from this research work, the mean strength values of these tests are provided for the proposed LBCs

(Table 3). This table also presents the flexural properties of LBL with those published from the Forest Products Laboratory (1999) with the consistency of specimens of 10% moisture content made using Method 3 (Lee et al. 1998). The flexural strength is most comparable data to some CEN standards and other softwood and hardwood structural composites. LBC specimens may share partly to the observed differences of the samples; flexural properties exhibit an inclination to increment with a decrease in moisture content for clear wood (Bergman et al. 2010). Data analysis indicates that mechanical properties of LBCs of *Dendrocalamus asper* are better than other structural composite materials and even comparable to one of the hardest and strongest woods such as the teak wood.

CONCLUSIONS

Laminated bamboo composite from *Dendrocalamus asper* bamboo has properties showing better performance, that it can be compared to some other structural composite wood products. The study provided a natural treatment soaking in sea-water from a full culm bamboo to justify the strength of the materials for possible structural application. Anisotropy is the one that could add up for this research to develop more flexible and unique materials that are comparable to the results of other structural composites from hardwood and softwood in relation to structural design innovation. In general, it is concluded that the LBC does have a much higher allowable and mean strength values in tensile and flexural data, which are comparable to woods stiffness values. However, further research to give attention on the characterization and standardization is needed before acceptance in the marketplace of LBC as structural composite materials for design and engineering use.

ACKNOWLEDGMENTS

This study was conceptualized by the author/s and sponsored by Engineering Research and Development for Technology under the Department of Science and Technology, the Philippines, and all experiments were carried out in the Department of Mechanical and Manufacturing Engineering Laboratory, University of San Carlos, Cebu City, Philippines.

REFERENCES

- Amada, S., Ichikawa, Y., Munekata, T., Nagase, Y., and Shimizu, K. 1997. Fiber texture and mechanical graded structure of bamboo. *Composites Part B*, 28: 13-20.
- Amatosa, T. Jr., and Loretero, M. 2017. Axial tensile strength analysis of naturally treated bamboo as possible replacement of steel reinforcement in the concrete beam (December 6, 2017). Papua New Guinea University of Technology, Global Virtual Conference in Civil Engineering (GVCCE) 2016. Available at SSRN: <https://ssrn.com/abstract=3083832>
- American Society for Testing Materials (ASTM) 1996. ASTM D695-96 Standard Test Method for Compressive Properties of Rigid Plastics. Annual Book of ASTM Standards.
- American Society for Testing Materials (ASTM) 2014. ASTM D143-14 Standard Test Methods for Small Clear Specimens of Timber, Feb 2014.
- Paes, J.B., Oliveira, A.K.F.D., Oliveira, E.D. and Lima, C.R.D. 2009. Physical-mechanical characterization of the glue laminated bamboo (*Dendrocalamus giganteus*). *Ciencia Florestal*, 19(1): 41-51.
- Bergman, R., Cai, Z., Carll, C.G., Clausen, C.A., Diertenberger, M.A., Falk, R.H., Frihart, C.R., Glass, S.V., Hunt, C.G., Ibach, R.E., Kretschmann, D.E., Rammer, D.R., Ross, R.J., Stark, N.M., Wacker, J.P., Wang, X., White, R.H., Wiedenhoef, A.C., Wiemann, M.C., and Zelinka, S.L. 2010. Wood Handbook, Wood as an Engineering Material. U.S. Department of Agriculture, Forest Service, Forest Products Laboratory, Madison, WI, pp. 508.
- CEN 2012. EN 408: Timber structures - structural timber and glued laminated timber - determination of some physical and mechanical properties. CEN, Brussels, Belgium.
- CEN 2013. EN 14080:2013-06 Timber structures. Glued laminated timber and glued solid timber. Requirements. CEN, Brussels, Belgium.
- CEN 2009. European Committee for Standardization. EN 338: Structural timber - strength classes. CEN, Brussels, Belgium.
- Clouston, P. L. and Lam, F. 2002. A stochastic plasticity approach to strength modeling of strand-based wood composites. *Composites Science and Technology*, 62(10-11): 1381-1395.
- Correal, J.F. and Ramirez, L.F. 2010. Adhesive bond performance in glue line shear and bending for glued laminated guadua bamboo. *J. Trop. for Sci.*, 22(4): 433e9.
- Correal, Juan F. 2008. Mechanical properties of Colombian glued laminated bamboo. In: *Proceedings of the 1st International Conference on Modern Bamboo Structures, ICBS-2007*, pp. 121e7.
- Correia, V.C., Curvelo, A.A.S., Marabezi, K., Almeida, A.E.F.S. and Savastano, H. Jr. 2015. Bamboo cellulosic pulp produced by the ethanol/water process for reinforcement applications. *Ciencia Florestal*, 25: 127-135.
- Correia, V.C., Santos, S.F., Marmol, G., Curvel, A.A.S. and Savastano, H. Jr. 2014. Potential of bamboo organosolv pulp as reinforcement element in fiber-cement. *Constr. Build. Mater.*, 72: 65-71.
- Coutts, R.S.P. and Ni, Y. 1995. Autoclaved bamboo pulp fiber reinforced cement. *Cem. Concr. Compos.*, 17: 99-106.
- De Flander, K. and Rovers, R. 2009. One laminated bamboo-frame house per hectare per year. *Constr. Build. Mater.*, 23(1): 210e8.
- De Lorenzis, L., Scialpi, V. and La Tegola, A. 2005. Analytical and experimental study on bonded-in CFRP in glulam timber. *Composites Part B: Engineering*, 36(4): 279-289.
- Dransfield, S. and Widjaja, E. A. 1995. *Plant Resources of South-east Asia No. 7: Bamboos*. Leiden, Netherlands.
- Falk, B. 2009. Wood as a sustainable building material. *Prod. J.*, 59(9): 6e12.
- Forest Products Laboratory 1999. *Wood Handbook: Wood as an Engineering Material*. FPL-GTR-113, U.S. Dept. of Agriculture, Forest Service, Madison, WI.
- Guimaraes, M. Jr., Botaro, V.R., Novack, K.M., Teixeira, F.G. and Tonoli, G.H.D. 2015. Starch/PVA-based nanocomposites reinforced with bamboo nanofibrils. *Ind. Crop. Prod.*, 70: 72-83.
- Jenkel, C., Leichsenring, F., Graf, W. and Kaliske, M. 2015. Stochastic modeling of uncertainty in timber engineering. *Engineering Structures*, 99(1): 296-310.
- Kretschmann, D.E., Moody, R.C., and Pellerin, R.F. 1993. Effect of various proportions of juvenile wood on laminated veneer lum-

- ber. U.S. Department of Agriculture, Forest Service, Forest Products Laboratory, Madison, WI, USA, Technical Report FPL-RP-521.
- Kretschmann, D.E. 2010. Mechanical properties of wood. In: (Chapter 5) Wood Handbook: Wood as an Engineering Material (Centennial Edition). General Technical Report FPL-GTR-190. Madison, WI: US Department of Agriculture, Forest Service, Forest Products Laboratory, 508.
- Lakkad, S.C. and Patel, J.M. 1980. Mechanical properties of bamboo, a natural composite. *Fiber Sci. Technol.*, 14: 319-22.
- Lavers, G.M. 2002. The Strength Properties of Timber, 3rd edn. Building Research Establishment (BRE), London, UK, Report Series.
- Lee, A.W.C., Bai, X.S. and Bangi, A.P. 1998. Selected properties of laboratory-made laminated bamboo lumber. *Holzforschung*, 52(2): 207e10.
- Lee, C.H., Chung, M.J., Lin, C.H. and Yang, T.H. 2012. Effects of layered structure on the physical and mechanical properties of laminated moso bamboo (*Phyllosachys edulis*) flooring. *Constr. Build. Mater.*, 28(1): 31e5.
- Li, H., Zhang, Q., Huang, D. and Deeks, A.J. 2013. Compressive performance of laminated bamboo. *Compos. Part B Eng.*, 54: 319e28.
- Li, H., Su, J., Zhang, Q. and Zhang, C. 2015. Experimental study on the mechanical performance of side pressure laminated bamboo beam. *J. Build. Struct.*, 36(3): 121e126.
- Lopez, L.F., and Correal, J.F. 2009. Exploratory study of the glued laminated bamboo *Guadua angustifolia* as a structural material. *Maderas: Cienciay Technlogia*, 11(3): 171e82.
- Lu, T., Jiang, M., Jiang, Z., Hui, D., Wang, Z. and Zhou, Z. 2013. Effect of surface modification of bamboo cellulose fibers on mechanical properties of cellulose/epoxy composites. *Compos. Part B Eng.*, 51: 28-34.
- Mahdavi, M., Clouston, P.L. and Arwade, S.R. 2012. A low-technology approach toward fabrication of laminated bamboo lumber. *Constr. Build. Mater.*, 29: 257e62.
- Mahdavi, M., Clouston, P.L. and Arwade, S.R. 2011. Development of laminated bamboo lumber: Review of processing, performance and economical considerations. *J. Mater. Civ. Eng.*, 23(7): 1036e42.
- Nugroho, N. and Naoto, A. 2001. Development of structural composite products made from bamboo. II. Fundamental properties of laminated bamboo lumber. *J. Wood Sci.*, 47(3): 237e42.
- Othman, A.R., Mohmod, A.L., Liese, W. and Haron, N. 1995. Research pamphlet No. 118: Planting and utilization of bamboo in Peninsular Malaysia. Forest Research Institute Malaysia. Kuala Lumpur, Malaysia.
- Pakhkerree, T. 1997. Physical and Mechanical Properties of *Dendrocalamus asper* Becker. M.S. Thesis, Kasetsart University, Thailand.
- Richard, M. and Harries K. 2012. Experimental buckling capacity of multiple culm bamboo columns. *Key Eng. Mater.*, 517: 51e62.
- Rittironk, S. and Elnieiri, M. 2007. Investigating laminated bamboo lumber as an alternate to wood lumber in residential construction in the United States. *Proc., 1st Int. Conf. on Modern Bamboo Structures*, Taylor & Francis, Abingdon, U.K., pp. 83-96
- Sharma, B., Gatóo, A. and Ramage, M. 2015. Engineered bamboo for structural applications. *Journal of Construction and Building Materials*, 81(1): 66-73.
- Siddhaye, V.R. and Sonar, I.P. 2006. Behavior of bamboo under axial compression. *J. Inst. Eng. India Civ. Eng. Div.*, 87(5): 3e8.
- Sinha, A., Way, D. and Mlasko, S. 2014. Structural performance of glued laminated bamboo beams. *J. Struct. Eng.*, 140(1): 04013021-1-8.
- Steiger, R. and Arnold, M. 2009. Strength grading of Norway spruce structural timber: Revisiting property relationships used in EN 338 classification system. *Wood Science and Technology*, 43(3): 259-278.
- Sulaiman, O., Hashim, R. and Wahab, R. 2006. Evaluation of shear strength of oil treated laminated bamboo. *Bioresour. Technol.*, 97(18): 2466e9.
- Sulastiningsih, I.M., and Nurwati 2009. Physical and mechanical properties of laminated bamboo board. *J. Trop. Sci.*, 21(3): 246e51.
- Van der Lugt, P., Van den Dobbelen, A.A.J.F. and Janssen, J.J.A. 2006. An environmental, economic, and practical assessment of bamboo as a building material for supporting structures. *Constr. Build. Mater*, 20(9): 648-656.
- Verma, C.S. and Chariar, V.M. 2012. Development of layered laminate bamboo composite and their mechanical properties. *Compos. Part B Eng.*, 43(3): 1063e9.
- Verma, C.S. and Chariar, V.M. 2013. Stiffness and strength analysis of four layered laminate bamboo composite at macroscopic scale. *Compos. Part B Eng.*, 45(1): 369e76.
- Verma, C.S., Sharma, N.Kr., Chariar, V.M., Maheshwari, S. and Hada, M.K. 2014. Comparative study of mechanical properties of bamboo laminae and their laminates with woods and wood-based composites. *Compos. Part B Eng.*, 60: 523e30.
- Wei, Y., Jiang, Sh. X., Lu, Q. F., Zhang, Q. Sh., Wang, L.B. and Lu, Zh. T. 2011. Flexural performance of glued laminated bamboo beams. *Adv. Mater. Res.*, 168e170: 1700e3.
- Widmann, R., Fernandez-Cabo, J.L. and Steiger, R. 2012. Mechanical properties of thermally modified beech timber. *European Journal of Wood Products*. 70(6): 775-784.
- Xiao-hong, Lv. 2011. Experimental study and finite element analysis of glulam column under axial compression. Chang-sha, China: Thesis of Hu-nan University.
- Xie, X., Zhou, Z., Jiang, M., Xu, X., Wang, Z. and Hui, D. 2015. Cellulosic fibers from rice straw and bamboo used as reinforcement of cement-based composites for remarkably improving mechanical properties. *Compos. Part B Eng.*, 78: 153-161.
- Yeh, M.C. and Lin, Y.L. 2012. Finger joint performance of structural laminated bamboo member. *J. Wood Sci.*, 58(2): 120e7.
- Yu, W.K., Chung, K.F. and Chan, S.L. 2005. Axial buckling of bamboo columns in bamboo scaffolds. *Eng. Struct.*, 27(1): 61e73.
- Yu, W.K., Chung, K.F. and Chan, S.L. 2003. Column buckling of structural bamboo. *Eng. Struct.*, 25: 755e68.
- Zhou, L., Shao, Z.P., Liu, Y.M., Wu, Z.M. and Arnaud, C.M. 2010. Differences in structures and strength between internode and node sections of Moso bamboo. *Wood Science and Technology*, 22(2): 133-138.



Effect of Probiotics on Survival Rate and Growth Performance of *Clarias gariepinus*

Muhammad Fakhri[†], Arning Wilujeng Ekawati, Nasrullah Bai Arifin, Ating Yuniarti and Anik Martinah Hariati

Department of Aquaculture, Faculty of Fisheries and Marine Science, University of Brawijaya, 65145, Indonesia

[†]Corresponding author: Muhammad Fakhri

Nat. Env. & Poll. Tech.
Website: www.neptjournal.com

Received: 05-06-2018
Accepted: 02-08-2018

Key Words:

African catfish
Feed conversion ratio
Probiotics
Growth performance
Survival rate

ABSTRACT

Influence of probiotics (mixture of *Lactobacillus* sp. and *Bacillus subtilis*) on survival rate, growth performance and feed conversion ratio of African catfish *Clarias gariepinus* fingerling was examined. Two treatments, namely with (trial) and without probiotics (control) supplementations were performed. In both the treatments, commercial feed containing 31-33% crude protein was applied twice a day for 85 days. For the trial, the probiotics mixture was supplemented in both the feeds (10^5 cells/g feed) and tank medium (10^7 cells/mL). The fish were cultured into 3 m³ tank. Each trial and control was done in duplicate. The results exhibited that the survival of African catfish was remarkably higher in probiotics treatment than the control ($P < 0.05$). The growth performance [specific growth rate (SGR) and daily gain (DG)] and feed conversion ratio (FCR) were significantly ($P < 0.05$) better in fish treated with probiotics compared with those in the control. To sum up, the supplementation of probiotics in feed and culture medium improved the survival rate, growth performance and feed conversion ratio of *C. gariepinus*.

INTRODUCTION

The *Clarias gariepinus* (African catfish) is one of the popular and essential commodities of aquaculture in Indonesia. Directorate General of Aquaculture (2015) reported that an increase in catfish production by 369% from 14,475 tons in 2009 to 679,379 tons in 2013. However, this production has not met the target set of 450% by the Ministry of Maritime Affairs and Fisheries. In order to increase the production of catfish culture, intensive aquaculture activities have been applied by the most farmers (Afrilasari et al. 2016). However, intensification of aquaculture caused some problems such as water quality degradation and enhancement of the possibility of the disease attack (Piedrahita 2003, De Schryver et al. 2008). Moreover, Fakhri & Sunarmi (2017) reported that the common problem in catfish culture is low feed digestibility that causes high feed conversion ratio.

Supplementation of probiotics in feed and rearing medium is one of the ways to overcome the obstacles faced in intensive catfish culture. The probiotics are live bacteria, yeast and fungi, which once supplied in sufficient quantities, give a beneficial effect on the host health (FAO/WHO 2002). Probiotics have been commonly applied in aquaculture in order to prevent disease outbreaks, increase immune responses, providing nutrients and enzymatic contributions, and keeping good water quality (Qi et al. 2009). In addition, a few researchers reported that the probiotics application help minimize the cost of aquaculture produc-

tion through enhancing the biomass and efficiency of feed utilization (El-Haroun 2007, Al-Dohail et al. 2009, Dennis & Uchenna 2016).

In aquaculture, probiotics supplementation not only improves the gastrointestinal health, but also improves the water quality (Gomez-Gil et al. 2000). Omenwa et al. (2015) demonstrated that the supplementation of *Lactobacillus plantarum* and *Pseudomonas fluorescens* in tank water results in the highest survival rate of *C. gariepinus* juvenile by 96.22%. The probiotics addition in intensive aquaculture to stimulate intestinal health is increasing (Ige 2013). Among probiotics bacteria, *Lactobacillus* and *Bacillus* strains have been widely used in aquaculture because of their capability to produce extracellular enzymes and high antagonism activity (Banerjee & Ray 2017). Therefore, the use of probiotics (mixture of *Bacillus subtilis* and *Lactobacillus* sp.) through, both feed and culture medium, is a relatively new approach to improve productivity in African catfish culture. This study was proposed to analyse the effect of probiotics mixture (*B. subtilis* and *Lactobacillus* sp.) supplementation in feed and rearing medium on the survival rate, daily gain, specific growth rate and feed conversion ratio of the fish *C. gariepinus*.

MATERIALS AND METHODS

Probiotics Preparation

The probiotics culture was prepared by inoculating

Table 1: The composition of medium for probiotics culture.

No.	Materials	Compositions
1.	Probiotic starter (L)	1
2.	Coconut water (L)	3
3.	Palm sugar (kg)	3
4.	Fresh milk (L)	3
5.	Bean sprouts extract (L)	3
6.	Water (L)	3

Table 2: Growth performances and feed conversion ratio of *C. gariepinus* with (trial) or without (control) supplemented with probiotics.

Group/treatment	Trial	Control
Initial weight (g)	5.18±0.20	5.16±0.17
Final weight (g)	83.28±0.52	79.34±0.88
DG (g.d ⁻¹)	0.92 ± 0.004	0.87±0.009
SGR (% d ⁻¹)	3.27 ± 0.039	3.22±0.028
FCR	0.92 ± 0.03	1.22 ± 0.02

probiotics starter containing *Bacillus subtilis* and *Lactobacillus* sp. into medium composed of organic carbon, micronutrients, and minerals for microorganisms growth (Table 1). The probiotics culture was incubated under the anaerobic condition for five days period to obtain optimal density of approximately 1×10^9 cells/mL.

Experimental Conditions

This study was conducted at intensive catfish culture in Buring Village, Kedungkandang District, Malang, Indonesia. Catfish culture was carried out for 85 days (from June 2017 to September 2017). The study consisted of two treatments, namely with (trial) and without probiotics (control) supplementations. The probiotics was supplemented in both feed and rearing medium. The study was conducted in duplicate using 3 m³ in the volume of tanks with continuous aeration. Each tank was stocked with 800 catfish fingerlings of size 7±1 cm or 5±1 g. During the study period of 85 days, catfish were fed with commercial feed containing 31-33% crude protein. For probiotics supplementation, the commercial feed was fermented with probiotics ingredients at approximately 10⁵ cells/g feed for three days in airtight plastic containers at room temperature (25-30°C) prior to the feeding. In addition to the fermented feed, probiotics (10⁷ cells/mL) were also supplemented in culture water at 5 mL/m³ along the culture periods. On the other hand, the fish of control tanks were fed without any probiotics supplementation. The fish were fed twice per day at 09:00 a.m. and 15:00 p.m. at satiation. Water quality parameters in *C. gariepinus* culture, including water temperature range (27.50°C-29.80°C), pH range (6.72-7.15) and dissolved oxygen range (4.24 mgL⁻¹ - 4.94 mgL⁻¹). At the end of the

study, several performances including survival rate, specific growth rate, daily gain and feed conversion ratio were calculated.

Survival Rate

Survival rate (SR) was calculated according to Lauzon et al. (2010) as follows:

$$SR (\%) = (\text{number of final fish} / \text{number of initial fish}) \times 100$$

Specific Growth Rate

Specific growth rate (SGR) was estimated as follows (Zhou et al. 2010):

$$SGR (\% d^{-1}) = \frac{\ln \text{ final weight (g)} - \ln \text{ initial weight (g)}}{\text{time (days)}} \times 100$$

Daily Gain

The daily gain (g.d⁻¹) (DG) was calculated based on Yanbo & Zirong (2006) as follows:

$$DG (g.d^{-1}) = \text{Final weight (g)} - \text{Initial weight (g)} / \text{time}$$

Feed Conversion Ratio

Feed conversion ratio (FCR) was determined based on Lauzon et al. (2010) as follows:

$$FCR = \text{offered feed (g)} / \text{total weight gain (g)}$$

Statistical Analysis

Data were analysed by *t*-test at *p*<0.05 significant level. Homogeneity and normality tests were performed prior to the *t*-test analysing. Data were analysed by SPSS 24.0 program.

RESULTS

Survival rates (SR) in trial and control are presented in Fig. 1. After 85 days, the survival rate of 93.89±0.4% in the treated tank was remarkably greater than in control with the survival rate of 83.33±1.6% (*P*<0.05). It indicates that probiotics (*Bacillus subtilis* and *Lactobacillus* sp.) supplementation considerably improved the survival of *C. gariepinus* culture.

Data of daily gain (DG), specific growth rate (SGR) and feed conversion ratio (FCR) were reviewed in Table 2. At the start of the study, there was no significant difference in initial weight between two treatments (*P*>0.05). Nevertheless, the mean final weight of the trial (83.28±0.52 g) was outstandingly better (*P*<0.05) than the control (79.34±0.88 g).

Daily gain (DG) and specific growth rate (SGR) values in the trial were greatly higher compared with the control (*P*<0.05). The supplementation of probiotics in feed and rearing medium also resulted in the best feed conversion

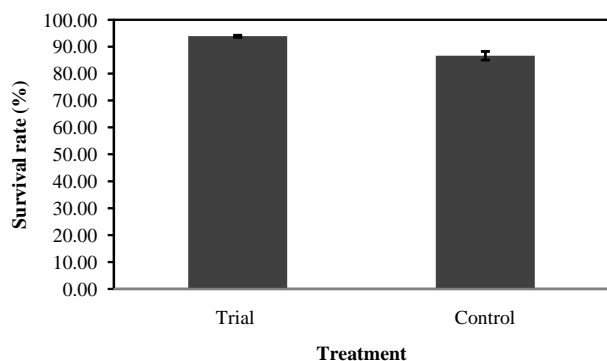


Fig. 1: The survival rate of African catfish after 85 days culture period with (trial) or without (control) supplemented with probiotics.

ratio (FCR) in comparison to the control ($P < 0.05$). It exhibited that the probiotics significantly improved the growth performances and enhanced the feed utilization of *C. gariepinus* culture.

DISCUSSION

Supplementation of probiotics (mixture of *Bacillus subtilis* and *Lactobacillus* sp.) in feed and tank medium resulted in survival rate, growth performance and feed conversion ratio greater than that of the control without addition of probiotics (Fig. 1 and Table 1), indicating that the probiotics supplementation improved the economic efficiency of African catfish culture (*C. gariepinus*). This result agreed with Yanbo & Zirong (2006) in common carp and Putra et al. (2017) in African catfish. Al et al. (2008) stated that the supplementation of *L. acidophilus* and *B. subtilis* mixture improved the growth in *Tilapia nilotica*. El-Haroun (2007) also found that the application of probiotics (Biogen) of *Bacillus* in the fish diet increased the specific growth rate and reduced the feed conversion ratio of African catfish. The lower FCR values resulted in probiotics treatment indicated that probiotics supplementation enhanced feed utilization of African catfish. Moreover, Dennis & Uchenna (2016) studied the influence of probiotics on the survival rate of *C. gariepinus* larvae and found better survival in probiotics treatment (mixture of *L. acidophilus*, *B. subtilis* and *L. bugarcicus*) compared with the control diet.

Probiotics are living microbial cell supplements which beneficially improve digestive process and health by optimizing the population and formation of microbial community inside the gastrointestinal in host (Bomba et al. 2002). The use of probiotics in aquaculture have main beneficial effects that are enhancement of animal growth (Ghosh et al. 2008, Merrifield et al. 2010), controlling of disease through improvement of immunity system (Nayak 2010, Qi et al. 2009) and exclusion of pathogen (Ibrahim 2015).

Welker & Lim (2011) explained that probiotics could trigger the digestive enzymes production or via other modifications in the intestinal environment that can boost digestion and ultimately enhanced the fish growth performance. In addition, Bomba et al. (2002) suggested that improvement of digestibility and feed utilization in fish treated with probiotics, probably caused by the ability of probiotics to promote the beneficial microorganism population, microbial enzymatic activity and improve intestinal microbial balance in the gastrointestinal system. With regard to survival rate, the higher survival was found in probiotics treatment because probiotics have the ability to suppress the cell density of pathogenic bacteria through competition for nutrients and other resources (Queiroz & Boyd 1998). Forestier et al. (2001) have reported that *Lactobacillus* strain was able to attach in intestinal mucus and produce antimicrobial peptides. Similar characteristics were also found by Cherif et al. (2001) and Cladera-Olivera et al. (2004) for *Bacillus* strains.

CONCLUSIONS

In conclusion, the addition of probiotics mixture (*Bacillus subtilis* and *Lactobacillus* sp.) in feed and rearing medium positively increased the survival rate, growth performance and improved feed efficiency in *C. gariepinus* culture. Use of *B. subtilis* and *Lactobacillus* sp. with the concentration of 10^5 cells/g feed and 10^7 cells/mL in water were effective and efficient to stimulate fish production.

ACKNOWLEDGEMENTS

This study was funded by Directorate General of Research and Community Services, Indonesia.

REFERENCES

- Afrilasari, W. and Meryandini, A. 2016. Effect of probiotic *Bacillus megaterium* PTB 1.4 on the population of intestinal microflora, digestive enzyme activity and the growth of Catfish (*Clarias* sp.). HAYATI Journal of Biosciences, 23: 168-172.
- Al-Dohail, M.A., Hashim, R. and Aliyu-Paiko, M. 2009. Effects of the probiotic, *Lactobacillus acidophilus*, on the growth performance, haematology parameters and immunoglobulin concentration in African Catfish (*Clarias gariepinus*, Burchell 1822) fingerling. Aquaculture Research, 40: 1642-1652.
- Banerjee, G. and Ray, A.K. 2017. The advancement of probiotics research and its application in fish farming industries. Research in Veterinary Science, 115: 66-77.
- Bomba, A., Nemcova, R., Gancarcikova, S., Herich, R., Guba, P. and Mudronova, D. 2002. Improvement of the probiotic effect of microorganisms by their combination with maltodextrins, fructooligosaccharides and polyunsaturated fatty acids. British Journal of Nutrition, 88: S95-S99.
- Cherif, A., Ouzari, H., Daffonchio, D., Cherif, H., Ben Slama, K., Hassen, A., Jaoua, S. and Boudabous, A. 2001. Thuricin 7: A novel bacteriocin produced by *Bacillus thuringiensis* BMG1.7, a new strain isolated from soil. Letter of Applied Microbiology, 32: 243-247.

- Cladera-Olivera, F., Caron, G.R. and Brandelli, A. 2004. Bacteriocin-like substance production by *Bacillus licheniformis* strain P40. *Letter of Applied Microbiology*, 38: 251-256.
- De Schryver, P., Crab, R., Defoirdt, T., Boon, N. and Verstraete, W. 2008. The basics of bio-flocs technology: The added value for aquaculture. *Aquaculture*, 277: 125-137.
- Dennis, E.U. and Uchenna, O.J. 2016. Use of probiotics as first feed of larval African catfish *Clarias gariepinus* (Burchell 1822). *Annual Research & Review in Biology*, 9(2): 1-9.
- Directorate General of Aquaculture 2015. Statistical data series on aquaculture production in Indonesia. Directorate General of Aquaculture. Ministry of Marine Affairs and Fisheries, Indonesia
- El-Haroun, E.R. 2007. Improved growth rate and feed utilization in farmed African catfish *Clarias gariepinus* (Burchell 1822) through a growth promoter Biogen supplementation. *Journal of Fisheries and Aquatic Science*, 2(5): 319-327.
- Fakhri, M. and Sunarmi, P. 2017. Probiotic application in the nursery and rearing of *Clarias* sp. in the Tumpang sub-district. *Journal of Innovation and Applied Technology*, 3(1): 440-444.
- FAO/WHO 2002. Working Group Report on Drafting Guidelines for the Evaluation of Probiotics in Food. London, Ontario, Canada.
- Forestier, C., De Champs, C., Vatoux, C. and Joly, B. 2001. Probiotic activities of *Lactobacillus casei* rhamnosus: in vitro adherence to intestinal cells and antimicrobial properties. *Research in Microbiology*, 152: 167-173.
- Ghosh, S., Sinha, A. and Sahu, C. 2008. Dietary probiotic supplementation in growth and health of live-bearing ornamental fishes. *Aquaculture Nutrition*, 14: 289-299.
- Gomez-Gil, B., Roque, A. and Turnbull, J.F. 2000. The use and selection of probiotic bacteria for use in the culture of larval aquatic organisms. *Aquaculture*, 191: 259-270.
- Ibrahim, M.D. 2015. Evolution of probiotics in aquatic world: Potential effects, the current status in Egypt and recent prospectives. *Journal of Advanced Research*, 6: 765-791.
- Ige, B.A. 2013. Probiotics use in intensive fish farming. *African Journal of Microbiology Research*, 7(22): 2701-2711.
- Lauzon, H.L., Gudmundsdottir, S., Steinarsson, A., Oddgeirsson, M., Martinsdottir, E. and Gudmundsdottir, B.K. 2010. Impact of probiotic intervention on microbial load and performance of Atlantic cod (*Gadus morhua* L.) juveniles. *Aquaculture*, 310: 139-144.
- Merrifield, D.L., Dimitroglou, A., Bradley, G., Baker, R.T.M. and Davies, S.J. 2010. Probiotic applications for rainbow trout (*Oncorhynchus mykiss* Walbaum) I. Effects on growth performance, feed utilization, intestinal microbiota and related health criteria. *Aquaculture Nutrition*, 16: 504-510
- Nayak, S.K. 2010. Probiotics and immunity: A fish perspective. *Fish and Shell Fish Immunology*, 29: 2-14.
- Omenwa, V.C., Mbakwem-Aniebo, C. and Ibiene, A.A. 2015. Effects of selected probiotics on the growth and survival of fry-fingerlings of *Clarias gariepinus*. *Journal of Pharmacy and Biological Sciences*, 10: 89-93.
- Piedrahita, R.H. 2003. Reducing the potential environmental impact of tank aquaculture effluents through intensification and recirculation. *Aquaculture*, 226(1-4): 35-44.
- Putra, I., Rusliadi, R., Fauzi, M., Tang, U.M. and Muchlisin, Z.A. 2017. Growth performance and feed utilization of African catfish *Clarias gariepinus* fed a commercial diet and reared in the biofloc system enhanced with probiotic. *F1000 Research*, 6: 1545
- Qi, Z., Zhang, X.H., Boon, N. and Bossier, P. 2009. Probiotics in aquaculture of China-current state, problems and prospect. *Aquaculture*, 290: 15-21.
- Queiroz, J.F. and Boyd, C.E. 1998. Effects of a bacterial inoculum in channel catfish ponds. *Journal of World Aquaculture Society*, 29: 67-73.
- Welker, T.L. and Lim, C. 2011. Use of probiotics in diets of tilapia. *Journal of Aquaculture Research and Development*, S1-14.
- Yanbo, W. and Zirong, X. 2006. Effect of probiotics for common carp (*Cyprinus carpio*) based on growth performance and digestive enzyme activities. *Animal Feed Science and Technology*, 127: 283-292.
- Zhou, X., Tian, Z., Wang, Y. and Li, W. 2010. Effect of treatment with probiotics as water additives on tilapia (*Oreochromis niloticus*) growth performance and immune response. *Fish Physiology and Biochemistry*, 36: 501-509.



Effect of Solution pH on Adsorption of Cefradine by Wheat Straw and Thermodynamic Analysis

Jianmian Deng*†, Zufeng Zhai*, Qinying Yuan* and Guoting Li*(**)*†

*Department of Environmental and Municipal Engineering, North China University of Water Resources and Electric Power, Zhengzhou 450011, China

**Henan Key Laboratory of Water Environment Simulation and Treatment, North China University of Water Resources and Electric Power, Zhengzhou 450011, China

†Corresponding authors: Jianmian Deng and Guoting Li

Nat. Env. & Poll. Tech.
Website: www.neptjournal.com

Received: 06-06-2018
Accepted: 02-08-2018

Key Words:

Adsorption
Cefradine
Wheat straw
Isotherms
Thermodynamics

ABSTRACT

As to many pollutants in aqueous solution, wheat straw is considered to be an environment friendly and low-cost adsorbent. Cefradine is a kind of broad-spectrum semisynthetic antibiotics widely used in clinical practices, which causes pollution in natural water bodies. As such, natural wheat straw was tentatively used for adsorptive removal of cefradine. Effect of solution pH on the adsorption of cefradine by wheat straw was investigated. It was found that the optimal solution pH for cefradine adsorption was pH 5.0. The typical functional groups present on raw and exhausted wheat straw after cefradine adsorption were confirmed through fourier-transform infrared spectroscopy. The isotherm data were analysed by Langmuir, Freundlich and Temkin isotherm models. It demonstrated that Freundlich model described the adsorption isotherm better. By Langmuir model, the maximal adsorption capacity for cefradine was 39.5 mg/g at 298 K. The thermodynamic analysis indicates that the cefradine adsorption process on the wheat straw was endothermic in nature and the increase of reaction temperature was beneficial to the uptake of cefradine. This demonstrates that wheat straw could be an ideal and cost-effective bio-sorbent used for effective removal of antibiotics such as cefradine from water.

INTRODUCTION

Cephalosporin is a broad-spectrum of semisynthetic antibiotics, commonly used in humans, animals and aquaculture, accounting for 60% of the total consumption of antibiotics (Kümmerer 2009). They have strong antibacterial activity, resistance to penicillinase, high clinical efficacy, less allergic reactions than penicillin, widely used in clinical practice. According to statistics, about 100000~200000 tons of antibiotics are used in medical, aquatic and livestock farming every year. The annual consumption of our country is about 25000 tons (Wise 2002). The continuous use and discharge of antibiotics has caused water pollution. However, these antibiotics do not undergo measurable biodegradation in natural water environments (Jiang et al. 2010). Up to 80 kinds of antibiotics have been detected in rivers, seawater, underground water and sewage treatment plants in Europe, the United States, Canada, Japan and China. Long-standing antibiotics may induce drug resistant bacteria, inhibit the growth of microbes, and have potential ecological risks, such as the emergence of "super resistant bacteria" (Han et al. 2010, Zuccato et al. 2010).

The treatment technologies for antibiotics wastewater

include chemical treatment, physical treatment and biological treatment (Tam et al. 2002, Stackelberg et al. 2007). Nevertheless, there are many problems such as high operating cost, energy demand, low efficiency and so on (Homem & Santos 2011, Yang et al. 2011). Comparatively speaking, adsorption technology is an important cost-effective technology for water treatment. Adsorption process is regarded as one of the most powerful, efficient and cost-effective water treatment technologies due to ease of operation, universal nature and high efficiency (Qu 2008). Therefore, it is very important to study the cheap, efficient and practical adsorption materials.

China is a large agricultural country with rich straw resources, producing about 8 million tons of crop straw per year. Wheat straw is one of the main agricultural wastes especially in north China. Improper disposal of crops such as incineration straw has a serious negative impact on the atmospheric environment (Owamah 2014). The chemical components of wheat straw are as follows: 5.71% water, 6.41% ash, 1.04% crude fat, 2.38% crude protein and 32.95% crude fibre (Yi 2003). As a comparison, these natural components are deduced to be more environment friendly. Peng et al. (2017) studied the excellent adsorption performance

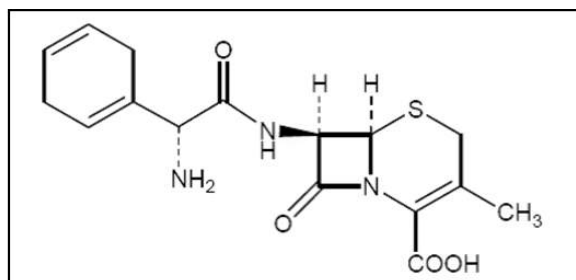


Fig. 1: The molecular structure of cefradine.

of sulfonamide antibiotics on rice straw biochar. Hu et al. (2012) have studied the thermodynamics and kinetics of the adsorption of cefradine on peanut shells. Accordingly, raw wheat straw can be selected as an efficient, inexpensive and natural adsorbent for antibiotics removal.

In this study, cefradine was selected as a target pollutant subjected for the adsorptive removal by wheat straw. Effect of solution pH was emphatically investigated as the solution pH is one of the key parameters for the uptake of various pollutants. Nonlinear simulation for adsorption isotherm and thermodynamic analysis were conducted to better understand adsorption mechanism and adsorption capability of wheat straw. This could provide a reference for practical application of raw agricultural waste.

MATERIALS AND METHODS

Chemicals: Cefradine was purchased from the Tianjin Kermal Chemical Reagent Co., Ltd. and used without further purification. The molecular structure of cefradine is shown in Fig. 1.

Preparation of wheat straw: Wheat straw was collected from farmland in Zhengzhou, Henan Province. The collected biomass was washed, dried, crushed, and sieved through a 40 mesh sieve.

Characterization before and after cefradine adsorption: The wheat straw before and after cefradine adsorption were characterized by Fourier-transform infrared spectroscopy (FTIR). FTIR spectra were collected on a transmission model. Samples for FTIR determination were prepared by grinding 1 mg of sorbents with 80 mg of spectral grade KBr in an agate mortar. All the IR measurements were carried out at room temperature.

Batch adsorption studies: Adsorptive removal of cefradine was conducted by batch experiments in a series of conical flasks. A dose of 50 mg wheat straw was added into conical flasks containing 50 mL of cefradine solution (10–200 mg/L). These mixtures were shaken at 125 rpm for 24 h to achieve equilibrium. The temperature was kept at 288, 298 and 308

K, respectively. Finally, samples were collected and filtered through a 0.45 μm pore-size membrane before analysis.

Analysis of cefradine: The concentration of cefradine was analysed using an UV mini-1240 spectrophotometer (Shimadzu) by monitoring at the wavelength of maximum absorption (266 nm) (Hu et al. 2012). The adsorption capacity (q_e) of cefradine is calculated as equation (1).

$$q_e = (C_0 - C_e)V/m \quad \dots(1)$$

Where, q_e (mg/g) is the adsorption capacity at equilibrium; C_0 is the initial concentration of cefradine in solution, and C_e (mg/L) is the concentrations of cefradine at equilibrium; V (L) is the volume of solution, and m (g) is the mass of the wheat straw.

RESULTS AND DISCUSSION

FTIR spectra of the raw and exhausted wheat straw: The FTIR spectra of the raw and exhausted wheat straw after cefradine adsorption are shown in Fig. 2. The characteristic absorbance band at 2916 cm^{-1} is ascribed to the stretching of $-\text{CH}_3$ groups. The weak absorption peaks at 1736 and 1620 cm^{-1} are ascribed to the vibrations of $-\text{OH}$ and $-\text{C}=\text{O}$, respectively. However, no characteristic absorption band of cefradine was observed on the exhausted wheat straw. This is because the limited amount of cefradine on the exhausted

Table 1: Parameters of Langmuir, Freundlich and Temkin models for the adsorption of cefradine on wheat straw.

	Nonlinear method		
	288 K	298 K	308 K
Langmuir			
q_{max} (mg/g)	36.2	39.5	46.3
k_L (L/mg)	0.0264	0.0275	0.0289
R^2	0.988	0.963	0.935
Freundlich			
k_F (mg/g)	3.457	4.189	5.152
n	0.4315	0.4131	0.4076
R^2	0.958	0.991	0.985
Temkin			
A	-7.134	-2.545	-1.446
B	7.1176	6.6031	7.4876
R^2	0.975	0.940	0.937

Table 2: Thermodynamic parameters at different reaction temperatures.

T/K	$\ln K_0$	ΔG^0 (kJ/mol)	ΔH^0 (kJ/mol)	ΔS^0 ($\text{J}\cdot\text{mol}^{-1}\cdot\text{K}^{-1}$)
288 K	7.277	-17.43	24.31	145.0
298 K	7.727	-18.50	24.31	145.0
308 K	8.488	-20.32	24.31	145.0

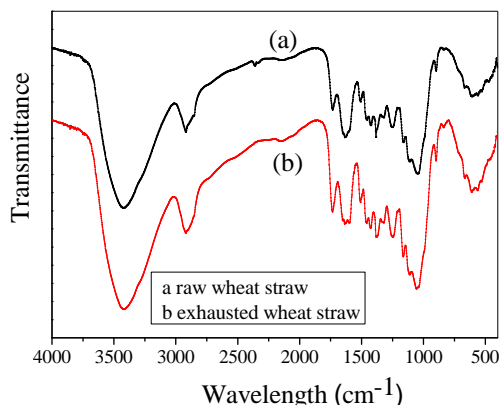


Fig. 2: FTIR spectra of the raw wheat straw and exhausted wheat straw after adsorption.

wheat straw and the influence of the strong absorption of the wheat straw.

Effect of solution pH on cefradine adsorption: Both, the surface charge properties of wheat straw and cefradine, are deduced to be significantly influenced by solution pH as the functional groups of the wheat straw and cefradine vary with changing solution pH. As such, the effect of solution pH for cefradine adsorption on wheat straw was investigated from pH 3.0 to 11.0, as presented in Fig. 3. At pH 4.0, 5.0, 6.0 and 7.0, the uptake of cefradine was of 10.70, 12.59, 9.46 and 8.52 mg/g, respectively. Apparently, the highest uptake of cefradine was achieved at pH 5.0. It can be deduced that weak acidic solution pH is especially favourable for the cefradine removal.

Adsorption isotherms: Adsorption isotherm is the basis for analysis of adsorption capacity and design of adsorption tests. The adsorption model was well established to analyse the adsorption isotherm. Three classical isotherm models including Langmuir, Freundlich and Temkin equations were used to fit the experimental data. The three equations can be expressed as follows (Langmuir 1916, Freundlich 1906, Fu et al. 1994):

$$\text{Langmuir model} \quad q_e = \frac{q_m k_L C_e}{1 + k_L C_e} \quad \dots(2)$$

$$\text{Freundlich model} \quad q_e = k_F C_e^{\frac{1}{n}} \quad \dots(3)$$

$$\text{Temkin} \quad q_e = A + B \ln C_e \quad \dots(4)$$

Where, q_e and q_m represent the amount of equilibrium adsorption capacity and the maximum adsorption capacity (mg/g) respectively, k_L (L/mg) is the Langmuir coefficient, C_e is the equilibrium concentration (mg/L), k_F is roughly an indicator of the adsorption capacity, n is the heterogeneity

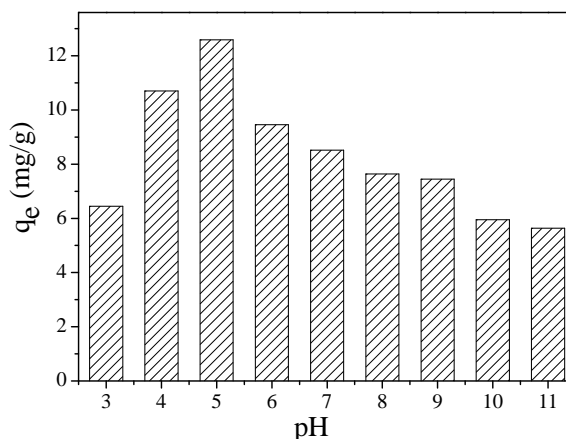


Fig. 3: Effect of solution pH on cefradine adsorption.

factor, and A and B are Temkin constants.

The fitting curves by Langmuir, Freundlich and Temkin models at 298 K are illustrated in Fig. 4. Meanwhile, the typical adsorption parameters obtained from the simulated isotherm models are listed in Table 1.

From Fig. 3, the three isotherm models well fitted the experimental data as the experimental data are much closer to the simulated curves. Even though, from Table 1, the correlation coefficients (R^2) of Freundlich model are slightly higher than those of Langmuir and Temkin model. This indicates that the surface of wheat straw is more heterogeneous in nature.

By Langmuir model, the calculated maximum adsorption capacities at 288, 298 and 308 K were 36.2 mg/g, 39.5 mg/g and 46.3 mg/g, respectively. It indicates that the adsorption capacity of cefradine on the wheat straw increases with rising reaction temperature. As a result, the adsorption process is deduced to be an endothermic process in nature. This is because the thermal motion of cefradine molecules in solution was accelerated with the increasing temperature, and adsorption activation energy decreased, promoting the adsorption reaction and increasing the adsorption amount.

Thermodynamic analysis: Thermodynamic parameters associated with the adsorption process including standard free energy change (ΔG^0), standard enthalpy change (ΔH^0) and standard entropy change (ΔS^0) were calculated using the following equations:

$$\Delta G^0 = RT \ln K_0 \quad \dots(5)$$

$$\Delta G^0 = \Delta H^0 - T \Delta S^0 \quad \dots(6)$$

$$\ln k_0 = -\frac{\Delta H^0}{RT} + \frac{\Delta S^0}{R} \quad \dots(7)$$

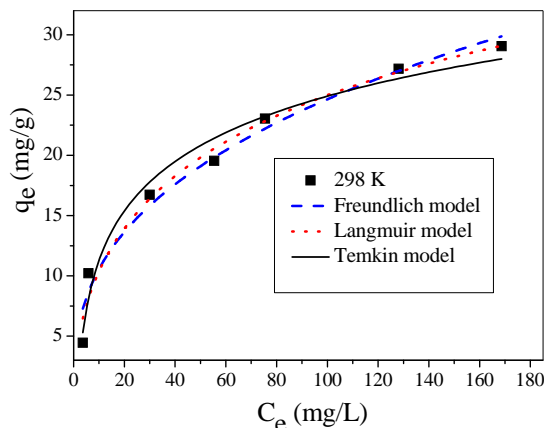


Fig. 4: Adsorption isotherms for the uptake of cefradine on wheat straw.

In these equations, T is in Kelvin; ΔH^0 is the entropy of adsorption and R is the universal gas constant ($8.314 \text{ J mol}^{-1} \text{ K}^{-1}$). The intersection with the vertical axis gives the value of $\ln k_0$ at the three different temperatures. The thermodynamic equilibrium constant k_0 for the adsorption process was determined by plotting $\ln q_e/C_e$ versus q_e and extrapolating to zero q_e using a graphical method (Yuan et al. 2009, Li et al. 2015). The values of ΔH^0 and ΔS^0 can be obtained from the slope and intercept of a plot $\ln k_0$ versus the reciprocal of absolute temperature ($1/T$) (Fig. 5).

It can be seen from Table 2 that the enthalpy and entropy of the adsorption process are $24.31 \text{ KJ mol}^{-1}$ and $145.0 \text{ J mol}^{-1} \text{ K}^{-1}$, respectively. The negative value of ΔG^0 and positive value of ΔH^0 indicate that the adsorption process is spontaneous and endothermic, which is consistent with the aforementioned results.

CONCLUSIONS

In summary, the wheat straw is a low-cost and abundantly available biomass adsorbent, which can be used for effective removal of antibiotics cefradine from water. The optimal pH adsorption of cefradine is found to be pH 5.0, and weak acidic pH conditions are especially favourable for cefradine removal. The isotherm data were analysed by Langmuir, Freundlich and Temkin isotherm models. It demonstrated that Freundlich model described the adsorption isotherm better. By Langmuir model, the maximal adsorption capacity for cefradine was 39.5 mg/g at 298 K . The thermodynamic analysis indicates that the cefradine adsorption process on the wheat straw was endothermic in nature and the increase of reaction temperature was beneficial to the uptake of cefradine.

ACKNOWLEDGEMENTS

The authors thank for the financial support from foundation

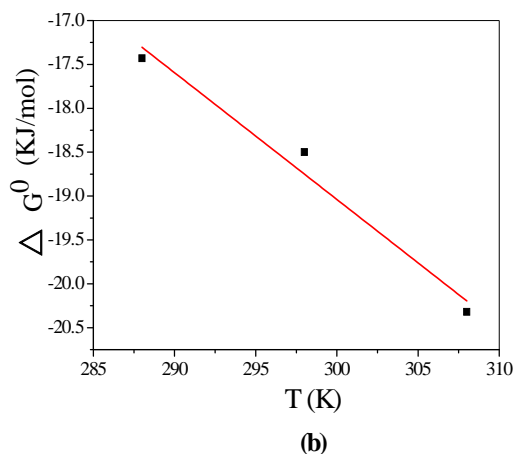
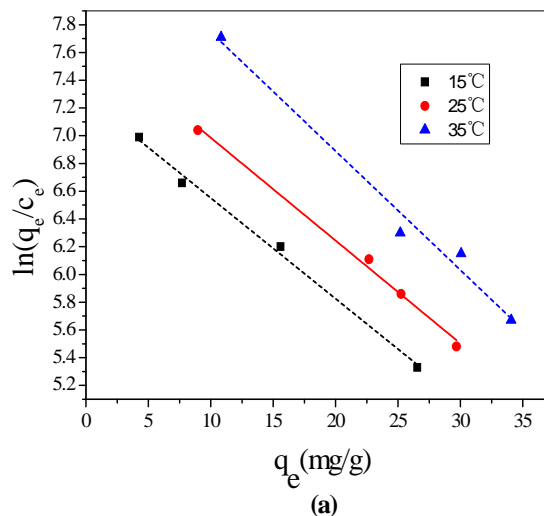


Fig. 5: Plots of $\ln q_e/C_e$ versus q_e for cefradine adsorption on wheat straw (a); changes of free energy (thermodynamic calculations) (b).

for university key youth teacher by Henan Province of China (2013GGJS-088), and innovative experimental programme of NCWU (HSCX2014054).

REFERENCES

- Freundlich, H.M.F. 1906. Über die adsorption in lasungen. *J. Phys. Chem.*, 57: 385-470.
- Fu, X.C., Shen, W.X. and Yao, T.Y. 1994. *Physical Chemistry*. 4th ed. Beijing: Higher Education Press, pp. 303-321.
- Han, Y.R., Wang, Q.J., Mo, C.H. et al. 2010. Determination of four fluoroquinolone antibiotics in tap water in Guangzhou and Macao. *Environmen. Pulluti.*, 158(7): 2350-2358.
- Homem, V. and Santos, L. 2011. Degradation and removal methods of antibiotics from aqueous matrices- A review. *J. Environ. Manage.*, 92: 2304-2347
- Hu, Z.J., Wang, N.X., Tan, J., Chen, J.Q. and Zhong, W.Y. 2012. Kinetic and equilibrium of cefradine adsorption onto peanut husk. *Desalin. Water Treat.*, 37: 160-168.
- Jiang, M., Wang, L. and Ji, R. 2010. Biotic and abiotic degradation of four cephalosporin antibiotics in a lake surface water and sediment. *Chemosphere*, 80: 1399-1405.

- Kümmerer, K., 2009. Antibiotics in the aquatic environment- A review, Part I. *Chemosphere*, 75: 417-434.
- Langmuir, I. 1916. Kinetic model for the sorption of dye aqueous solution by clay-wood sawdust mixture. *J. Am. Chem. Soc.*, 38: 2221-2295.
- Li, G.T., Feng, Y.M., Chai, X.Q. and He, X.S. 2015. Equilibrium and thermodynamic studies for adsorption of 1,4-benzoquinone by fly ash. *Nat. Env. & Poll. Tech.*, 14(4): 865-869
- Owamah, H. 2014. Biosorptive removal of Pb(II) and Cu(II) from wastewater using activated carbon from cassava peels. *J. Mater. Cycles Waste.*, 16(2): 347-358.
- Peng, N., Wang, K.F., Wu L.B., Chen, R.X. and Huang, Z.H. 2017. Sorption characteristics of sulfonamide antibiotics by rice straw biochar. *Environmen. Sci. Technol.*, 40(9): 61-67.
- Qu, J.H. 2008. Research progress of novel adsorption processes in water purification. *J. Environ. Sci.*, 20: 1-13.
- Stackelberg, P.E., Gibs, J., Furlong, E.T., Meyer, M.T., Zaugg, S.D. and Lippincott, R.L. 2007. Efficiency of conventional drinking-water-treatment processes in removal of pharmaceuticals and other organic compounds. *Sci. Total Environ.*, 377: 255-272.
- Tam, N.F.Y., Chong, A.M.Y. and Wong, Y.S. 2002. Removal of tributyltin (TBT) by live and dead microalgal cells. *Mar. Pollut. Bull.*, 45: 362-371.
- Wise, R. 2002. Antimicrobial resistance: Priorities for action. *J. Antimicrob. Chemoth.*, 49(4): 585-586.
- Yang, X., Flowers, R.C., Weinberg, H.S. and Singer, P.C. 2011. Occurrence and removal of pharmaceuticals and personal care products (PPCPs) in an advanced wastewater reclamation plant. *Water Res.*, 45: 5218-5228.
- Yi, M.H. 2003. *Development and Utilization of Biological Resources*. China Light Industry Press, Beijing.
- Yuan, X., Xing, W., Zhuo, S.P., Han, Z.H., Wang, G.Q., Gao, X.L. and Yan, Z.F. 2009. Preparation and application of mesoporous Fe/carbon composites as a drug carrier. *Micropor. Mesopor. Mat.*, 117: 678-684.
- Zuccato, E., Castiglioni, S., Bagnati, R. et al. 2010. Source, occurrence and fate of antibiotics in the Italian aquatic environment. *J. Hazard. Mater.*, 179(1-3): 1042-1048.



Macroscopic Factor Decomposition of Non-Point Source Pollution of Chemical Fertilizer: Scale, Structure and Constraint

Wenjie Yao

Research Institute of Water Culture and Resources Economy, Zhejiang University of Water Resources and Electric Power, Hangzhou, 310018, China

Nat. Env. & Poll. Tech.
Website: www.neptjournal.com

Received: 16-07-2018
Accepted: 21-09-2018

Key Words:

Chemical fertilizer
Non-point source pollution
Factor decomposition
Source control

ABSTRACT

This paper builds a factor decomposition model of non-point source pollution of chemical fertilizer from the three dimensions of scale, structure and constraint, with using the panel data covering 31 provincial regions in China during 2007-2016, aims to reveal the action mechanism of scale effect, structure effect and effect of restraint on non-point source pollution of chemical fertilizer. The research shows that the inverted U-shaped curve relationship between economic scale and non-point source pollution of chemical fertilizer is essentially an environmental negative externality in production, as well as the evolution path of the implementation of control measures. Economic structure and resource constraint, each has positive exogenous effects on non-point source pollution of chemical fertilizer, while technical constraint has negative exogenous effects on it. Thus, the ultimate effectiveness of pollution control measures depend on the balance of the two opposing forces in reality. In addition, population size and population structure both have no exogenous effect on non-point source pollution of chemical fertilizer. Therefore, implementation of the "source control" mode of pollution control, with optimizing the internal structure of agriculture, transforming agricultural production patterns, making rational use of cultivated land resources, and vigorously promoting applicable environmental technologies, etc., are particularly important.

INTRODUCTION

Chemical fertilizer application has been an important way to increase agricultural production in China. Over the past 30 years, while the amount of chemical fertilizer being used in agricultural production continued to increase, the marginal production had fallen and there was a little room for increased production. However, as the application intensity kept increasing and the utilization level was generally low, a large amount of residual nutrients in chemical fertilizer not only lead to soil compaction and air pollution, but also lead to eutrophication of water bodies through leaching. From 2007 to 2016, the amount of chemical fertilizer applied in China increased from 51.078 million tons to 59.841 million tons, an average annual increase of 1.91 percent. In 2016, the amount of chemical fertilizer applied per unit area of cultivated land in China was 443.53 kg/hm², far higher than the internationally recognized safe limit of 225 kg/hm². It can be inferred that the non-point source pollution caused by excessive use of chemical fertilizer has been very serious.

As the micro subject of agricultural production, farmers' application of chemical fertilizer will have a direct impact on environmental quality. Therefore, most of the studies are based on the field investigation to explore the influence factors of non-point source pollution of chemical fertilizer

from the perspective of farmers. In fact, the occurrence of micro-subject behaviour must be guided by the overall macroeconomic situation. At a time when industrialization was advancing rapidly, the primitive accumulation of capital had not been realized and industry was still unable to nurture agriculture. The lagging of the agricultural economic development itself is difficult to meet the growing needs of farmers for life, which has formed the idea that economic benefits precede environmental benefits, and thus agricultural production is solely dependent on the increase of inputs such as chemical fertilizers and pesticides, resulting in the increasing pollution of non-point sources. Obviously, it is the key to grasp the policy direction of environmental management accurately to analyse the internal mechanism of non-point source pollution of chemical fertilizer from the macro level.

A series of studies on the decomposition of environmental quality influencing factors were mainly carried out through IPAT model and EKC model. Ehrlich et al. (1971), based on the three aspects, population, consumption and technology, proposed the IPAT model for the relation between population and environment, believing that the combination of population and consumption will cause great environmental pressure, which must be alleviated through technological adjustment. Subsequently, the IPAT model

was improved by Yorker et al. (2002) and evolved into a STIRPAT model which could incorporate various other factors. So far, these two models have been widely used, mainly devoted to the decomposition of the factors influencing on industrial energy consumption and carbon emissions (Poumanyong & Kaneko 2010, Zhangqi 2018) and other factors affecting industrial waste gas emissions (Nan & Weiyang 2016, Ling et al. 2017), but the empirical analysis of the agricultural non-point source pollution is not much (Yuzhuo 2017).

The EKC model proposed by Grossman et al. (1991) to explain the relationship between economy and environment has always been an important tool for environmental economic analysis. However, this model has become a "black box" because it abstracts many key factors in application. For this, Grossman et al. (1995) and Islam et al. (1999) analysed the impact of economic growth on environment quality, the former revealed the economic scale effect, economic structure effect and technology progress effect; the latter revealed the scale effect, structure effect and waste reduction effect. But before that, Commoner (1972) and Angang (1993) had made a similar decomposition, and their research ideas tended to be consistent, that is, the effects of economic growth on environmental quality were analysed from three aspects: population growth effect, economic scale effect and technological progress effect. At present, although some scholars have explored the decomposition of influencing factors of agricultural non-point source pollution (Taiping et al. 2011, Liutao et al. 2013), most studies have not opened their own "black box" when applying EKC model, to further deepen their conclusions (Haipeng & Junbiao 2009, Xianghai et al. 2015).

Draw lessons from existing research, with using the panel data covering 31 provincial regions in China during 2007-2016, we built the factor decomposition model of non-point source pollution of chemical fertilizer from the three dimensions of scale, structure and constraint, designed to reveal the mechanism of scale effect, structure effect and constraint effect on non-point source pollution of chemical fertilizer, so as to increase the strength of macro-explanation beyond micro-explanation.

MATERIALS AND METHODS

We argue that, scale and structure are two important dimensions to decompose the influencing factors of non-point source pollution of chemical fertilizer, and the effect of each dimension should involve economic and demographic factors. Non-point source pollution of chemical fertilizer is a negative environmental externality problem caused by excessive application of chemical fertilizer in agricultural production. In terms of scale effect, the urban and rural popula-

tion scale of continuous expansion drives the whole society the general increase of agricultural product demand, pressing for faster agricultural production, or the scale of agricultural economy itself continues to expand, both of which will lead to an extensive use of chemical fertilizers. In terms of scale effect, the internal structure of agricultural economy, especially the proportion of the output value of the agricultural industry with a demand for chemical fertilizer in the whole agriculture, plays an important role in the direct input of chemical fertilizer; in population structure, with the increasing proportion of urban population and the transfer of agricultural labour force, intensification of agricultural production inevitably requires the concentrated investment of chemical fertilizers.

Technological factors have gradually tended to improve environmental quality in the process of changing from extensive mode to intensive mode in economic development. As a result, advances in agricultural technology are likely to reduce the amount of chemical fertilizer applied while increasing the level of output, thus reducing the degree of pollution. However, technology itself has certain applicability, if technological progress deviates from production mode, it will be difficult to give full play to its environmental protection effect. It can be seen that technical factors should be within the constraint dimension when the influencing factors of non-point source pollution of chemical fertilizers are decomposed. In addition, the area of cultivated land also belongs to the constraint dimension for defining the space range of chemical fertilizer application.

According to the three dimensions of scale, structure and constraint, as well as the establishment of economy, population, technology and resources, we construct a decomposition model of influencing factors of non-point source pollution of chemical fertilizers as follows:

$$CFP = f(E, H, S, U, T, C) \quad \dots(1)$$

Here, the dependent variable CFP indicates non-point source pollution of chemical fertilizer, and the independent variables E, H, S, U, T and C indicate respectively, the economic scale, population scale, economic structure, population structure, technical constraint and resource constraint. We introduce a quadratic term of E to verify the possible EKC curve.

Concretely, two indicators, nitrogen pollution emission and phosphorus pollution emission, are set up to represent non-point source pollution of chemical fertilizer, for nitrogen fertilizer and phosphate fertilizer are mainly used in China's agriculture for a long time, and nitrogen, phosphorus and other elements were lost in a large number with extremely low utilization rate, resulting in water eutrophication and becoming a serious pollution source.

As chemical fertilizer application is closely related to crop production, we set two indicators, crop production value and the proportion of crop production value in total agricultural output value, respectively, to represent economic scale and economic structure. The demand for agricultural products comes from the total population of urban and rural areas in a certain period, and the proportion of urban population determines the supply structure of agricultural products, so two indicators, year-end population and urban population proportion, respectively, represent population scale and population structure. In order to show the effect of agricultural technology progress on reducing non-point source pollution of chemical fertilizer and the effective space of chemical fertilizer application, we set two indicators, crop production value per unit of chemical fertilizer (nitrogen fertilizer or phosphate fertilizer) and irrigated area, respectively represent technical constraint and resource constraint (Table 1).

Based on the decomposition model of influencing factors of non-point source pollution of chemical fertilizer, two regression equations are established as follows:

$$N = \alpha_0 + \alpha_1 e + \alpha_2 e^2 + \alpha_3 h + \alpha_4 s + \alpha_5 u + \alpha_6 t_n + \alpha_7 c + \varepsilon \quad \dots(2)$$

$$P = \beta_0 + \beta_1 e + \beta_2 e^2 + \beta_3 h + \beta_4 s + \beta_5 u + \beta_6 t_p + \beta_7 c + \eta \quad \dots(3)$$

Here, N and P are respectively nitrogen pollution emission (ten thousand tons) and phosphorus pollution emission (ten thousand tons), e is crop production value (100 million RMB yuan) and e^2 is a quadratic term of e , h is year-end population (ten thousand people), s is the proportion of crop production value in total agricultural output value (%), u is urban population proportion (%), t_n and t_p are respectively crop production value per unit of nitrogen fertilizer (ten thousand RMB yuan) and crop production value per unit of phosphate fertilizer (ten thousand RMB yuan), c is irrigated area (thousands of hectares), α_i and β_i ($i=0, 1, 2, \dots, 7$) denote the corresponding coefficient, and ε and η are the random perturbation terms.

Nitrogen pollution emission and phosphorus pollution emission are calculated by multiplying the amount of fertilizer applied (ten thousand tons) by the fertilizer loss rate

(%). The fertilizer loss rate of 31 provinces in China was measured by Feng (2011). The application amount of nitrogen fertilizer and phosphate fertilizer and the relevant panel data required for each explanatory variable are related to 31 provinces in China from 2007 to 2016, all of which are from China Statistical Yearbook from 2008 to 2017.

RESULTS AND DISCUSSION

We use mixed OLS, fixed effect and random effect for regression. First, LSDV test showed that most individual virtual variables are significant at 5% level, that means, there is an individual effect, and mixed OLS regression should not be used; then Hausmann test showed that the two equations are significant at 5% level and the regression of random effect is rejected; finally, we choose the fixed effect regression estimation result of cluster robust standard deviation.

Table 2 shows the estimation results. There are significant quadratic function relationships between crop production value and nitrogen pollution emission, and between crop production value and phosphorus pollution emission, and the corresponding inverted U-shaped EKC curves are formed. The crop production values at the inflection points are respectively 491.803 billion RMB yuan and 519.931 billion RMB yuan. There are significant positive correlations between the proportion of crop production value in total agricultural output value and nitrogen pollution emission, and between the proportion of crop production value in total agricultural output value and phosphorus pollution emission, which means an increase in the proportion of 1% of crop production value would increase nitrogen pollution emission and phosphorus pollution emission by 1,040 tons and 92 tons respectively. There are significant negative correlations between crop production value per unit of nitrogen fertilizer and nitrogen pollution emission, and between crop production value per unit of phosphate fertilizer and phosphorus pollution emission, which means an increase of 10,000 RMB yuan of crop production value per unit of nitrogen fertilizer would reduce nitrogen pollution emission by 1,268 tons and an increase of 10,000 RMB

Table 1: Decomposition of the influencing factors of non-point source pollution of chemical fertilizer.

Factors	Scale	Structure	Constraint
Economic factors	Crop production value	The proportion of crop production value in total agricultural output value	-
Demographic factors	Year-end population	Urban population proportion	-
Technical factors	-	-	Crop production value per unit of chemical fertilizer
Resources factors	-	-	Irrigated area
Note: -represents default.			

Table 2: Estimation results of panel model regression.

Influencing factors	<i>N</i>		<i>P</i>	
	Coefficient	<i>t</i> -Statistic	Coefficient	<i>t</i> -Statistic
<i>E</i>	0.003 6***	3.71	0.000 3***	3.91
<i>E</i> ²	-7.32e-07***	-3.98	-5.77e-08**	-2.41
<i>H</i>	0.000 7	0.65	0.000 0	0.20
<i>S</i>	0.104 0**	2.29	0.009 2*	1.70
<i>U</i>	0.033 7	0.59	-0.008 5	-1.65
<i>T</i>	-0.126 8***	-3.29	-0.001 6*	-1.87
<i>C</i>	0.000 8*	1.96	0.000 2**	2.56
Intercept	1.448 5	0.26	0.573 9	0.72
<i>F</i> -Statistic		8.38***		20.22***
within-R ²		0.438 7		0.386 8
VIF		6.46		6.12

Note: ***, ** and * respectively indicate that the estimated results are significant at the levels of 1%, 5% and 10%, respectively.

yuan of crop production value per unit of phosphate fertilizer would reduce phosphorus pollution emission by 16 tons. There are significant positive correlations between irrigated area and nitrogen pollution emission, and between irrigated area and phosphorus pollution emission, which means an increase of 1,000 hectares of irrigated area would increase nitrogen pollution emission and phosphorus pollution emission by 8 tons and 2 tons respectively. However, there are no correlations between the year-end population and chemical fertilizer pollution emission, and between urban population proportion and chemical fertilizer pollution emission.

In terms of scale effect, the inverted U-shaped curve relationship between the economic scale and non-point source pollution of chemical fertilizer is essentially an environmental negative externality in production, as well as the evolution path of the implementation of control measures. Over the years, the application of chemical fertilizer has been subject to a variety of direct or indirect subsidy incentives, which inevitably aggravate the degree of pollution. During 2011-2015, after clearly put forward agricultural non-point source pollution control target at the policy level, measured soil fertilizer technology had been used more widely, and chemical fertilizer use efficiency had also improved, which makes the degree of non-point source pollution reduced. In terms of structural effect, economic structure has a significant positive influence on non-point source pollution of chemical fertilizer, which indicates that the increase of relative value of crop industry in agriculture is mainly caused by the increase of its absolute value. Nevertheless, we can judge that an increase in the number of urban and rural population expanded the demand of agricultural products, at the same time an increase in the proportion of urban population made the transfer of agricultural

labour force to cities, reducing the supply of agricultural products, and the demand gap generated cannot be met with by the agricultural production (including crop production), which relied more on imports. This is undoubtedly an important reason that both population size and population structure have no significant influence on non-point source pollution of chemical fertilizer. In terms of constraint effect, technical constraint has a significant negative effect on non-point source pollution of chemical fertilizer, which is consistent with the research results of Taiping et al. (2011) and Liutao et al. (2013). Due to the different calculation methods of indicators, in fact, the improvement effect of technical constraint on environmental quality is limited to the way of substitution or consumption reduction. For example, use of slow-release fertilizers instead of conventional fertilizers not only reduces dosage by 10% to 20%, but also extends fertilizer effect by 30 days. In addition, resource constraint has a significant positive effect on non-point source pollution of chemical fertilizer. The larger irrigated area, the more effective cultivated land is put into use, which means the more extensive space for pollution spread.

It is important to note that under the inverted U-shaped curve relationship between economic scale and non-point source pollution of chemical fertilizer, economic structure, technical constraint and resource constraint have exogenous effects on non-point source pollution of chemical fertilizer. Specifically, positive changes in economic structure and resource constraint will cause the entire inverted U-shaped curve to shift upward, further weakening the effect of pollution control; the positive change of technical constraint will cause the entire inverted U-shaped curve to shift downward and further enhance the effect of pollution control. The ultimate effectiveness of pollution control measures depends on the balance of the two opposing forces in reality.

CONCLUSION

Based on the existing literature, this paper builds a factor decomposition model of non-point source pollution of chemical fertilizer from the three dimensions of scale, structure and constraint, with using the panel data covering 31 provincial regions in China during 2007-2016, aims to investigate the effects of economic scale, population size, economic structure, population structure, technical constraint and resource constraint on non-point source pollution of chemical fertilizer.

The results show that the influencing factors of non-point source pollution of chemical fertilizer come from scale effect, structure effect and constraint effect. Economic size rather than population size leads to scale effect, economic structure rather than population structure leads to structure effect, and technical constraint and resource constraint jointly lead to constraint effect. The inverted U-shaped curve relationship between economic scale and non-point source pollution of chemical fertilizer is essentially an environmental negative externality in production, as well as the evolution path of the implementation of control measures. Economic structure and resource constraint have positive exogenous effects on non-point source pollution of chemical fertilizer, and technical constraint has a negative exogenous effect on non-point source pollution of chemical fertilizer. The ultimate effectiveness of pollution control measures depends on the balance of the two opposing forces in reality.

Although there are also environmental negative externalities of economic size, in terms of non-point source pollution of chemical fertilizer, the industrial point source pollution control model of "attaching importance to end management and neglecting source control" is no longer applicable, for that the high dispersion and concealment of pollution sources, and the randomness and heterogeneity of pollution emission makes it difficult to define the subject and the share of environmental responsibility, combined with the difficulty of process monitoring and the lag in end governance. It is urgent to promote the pollution control mode of "source control". Due to the formulation and implementation of environmental control policies, there is a possibility of coordination between the scale of agricultural economy and non-point source pollution of chemical fertilizer. Therefore, we should spare no effort to optimize agricultural structure, transform agricultural production mode and make rational use of cultivated land resources, at the same time, we should vigorously promote applicable environmental technologies, especially continue to increase the popularization of soil testing formula fertilization technology.

REFERENCES

- Angang, H. 1993. Population growth, economic growth and technological change in relation to the environmental change: Modern environmental change in China (1952-1990). *Chinese Journal of Environmental Engineering*, 5: 1-17.
- Commoner B. 1972. The environmental cost of economic growth. *Chem. Br.*, 8(2): 52-56.
- Ehrlich, P.R. and Holdren, J.P. 1971. Impact of population growth. *Science*, 171(3977): 1212-1217.
- Feng, Z. 2011. Study on the non-point pollution of the agricultural fertilizer input in China: Based on the aspect of farmers' fertilizer input. Nanjing Agricultural University, Nanjing.
- Grossman, G.M. and Krueger, A.B. 1991. Environmental impacts of a North American free trade agreement. *Social Science Electronic Publishing*, 8(2): 223-250.
- Grossman, G.M. and Krueger, A.B. 1995. Economic growth and the environment. *Quarterly Journal of Economics*, 110(2): 353-377.
- Haipeng, L. and Junbiao, Z. 2009. An empirical test on the EKC relationship between the agricultural non-point source pollution and economic development in China. *Resources and Environment in the Yangtze Basin*, 18(6): 585-590.
- Islam, N. and Vincent, J. 1999. Unveiling the income-environment relationship: An exploration into the determinants of environmental quality. Harvard Institute for International Development, Department of Economics, Emory University. Working Paper.
- Ling, B., Lei, J. and Yaobin, L. 2017. Spatio-temporal characteristics of environmental pressures of the urban agglomeration in the middle reaches of the Yangtze River: A case study based on industrial SO₂ emissions. *Economic Geography*, 37(3): 174-181.
- Liutao, L., Futian, Q. and Shuyi, F. 2013. Economic development and agricultural non-point source pollution: Decomposition model and empirical analysis. *Resources and Environment in the Yangtze Basin*, 22(10): 1369-1374.
- Nan, H., and Weiyang, Y. 2016. Spatial characteristics and influencing factors of industrial waste gas emission in China. *Scientia Geographica Sinica*, 36(2): 196-203.
- Poumanyong, P. and Kaneko, S. 2010. Does urbanization lead to less energy use and lower CO₂ emissions? A cross-country analysis. *Ecological Economics*, 70(2): 434-444.
- Taiping, L., Feng, Z. and Hao, H. 2011. Authentication of the Kuznets Curve in agriculture non-point source pollution and its drivers analysis. *China Population, Resources and Environment*, 21(11): 118-123.
- Xianghai, M., Haichuan, Z. and Junbiao, Z. 2015. Spatial and temporal characteristics and EKC verification for livestock pollution. *Journal of Arid Land Resources and Environment*, 29(11): 104-108.
- Yorker, R., Rosae, E.A. and Dietz, T. 2002. Bridging environmental science with environmental policy: Plasticity of population, affluence, and technology. *Social Science Quarterly*, 83(1): 18-31.
- Yuzhuo, S., Gangyi, W. and Xinhui, W. and Li, H.S. 2017. Analysis of water's nitrogen pollution caused by hog industry agglomeration: Based on the analytical framework of IPAT. *Chinese Journal of Animal Science*, 53(11): 117-122.
- Zhangqi, Z., Lei, J., Lingyun, H. and Zheng, W. and Bai Ling 2018. Global carbon emissions and its environmental impact analysis based on a consumption accounting principle. *Acta Geographica Sinica*, 73(3): 442-459.



Source Apportionment and Elemental Composition of PM_{2.5} in Chengdu, China

Ya Tang*, Youping Li*†, Hong Zhou** and Jialing Guo*

*College of Environmental Science and Engineering, China West Normal University, Nanchong 637009, China

**Sichuan Keshengxin Environment & Technology Co. Ltd., Chengdu 610100, China

†Corresponding author: Youping Li

Nat. Env. & Poll. Tech.

Website: www.neptjournal.com

Received: 17-07-2018

Accepted: 21-09-2018

Key Words:

PM_{2.5}

Elemental composition

Source apportionment

Chengdu

ABSTRACT

In order to investigate the elemental composition of PM_{2.5} and its sources, PM_{2.5} samples were collected at an urban site in Chengdu, China. The contents of 20 elements including Al, As, Ba, etc. in PM_{2.5} were analysed. Enrichment factor, correlation analysis and principal component analysis were applied to analyse the sources of PM_{2.5}. The results showed that the daily mean concentration was 49.2–425.0 µg·m⁻³ and annual mean concentration was 165.1±84.7 µg·m⁻³. The element concentrations in winter (7,575.0 ng·m⁻³) were higher than those in summer (3,326.8 ng·m⁻³). The results of source apportionment showed that the sources of PM_{2.5} were soil dust and dust storm, traffic emission, combustion of fossil fuels and coal, and metal smelting in Chengdu. The results of multiple linear regression analysis showed that wind speed and temperature had a negative correlation with most trace elements.

INTRODUCTION

In recent years, with the rapid development of economy, population and urbanization, fine particulate matter has become a major air contaminant, which severely affects human health, visibility and climate change (Yang et al. 2013). Due to its large surface area, PM_{2.5} can absorb many kinds of toxic air contaminants such as metal elements and organic compounds (Yang et al. 2015). Although elements contribute less to PM_{2.5} compared with other pollutants, some of the elements, even at extremely low contents, pose a threat to human health (Han et al. 2015). For instance, Zn can lead to arteriosclerosis, heart disease and hypertension, As and Cd have a potential teratogenic effect on the human body, and Pb and Hg have a toxic effect on the fetus (Fang et al. 2010). At present, there are several studies on the source apportionment and elemental composition of PM_{2.5} in domestic and overseas regions. In China, investigations on the source apportionment and elemental composition of PM_{2.5} have been conducted in several main cities and regions, such as Beijing, Shanghai, Guangzhou (Zhang et al. 2009). For example, the ground observation of dust aerosols was conducted in Beijing in spring to investigate the elemental composition and origin of mineral dust. The results showed that most mineral elements of particles (i.e. Mg, Si, Fe, Al and Ti) mainly come from dust events. Gu et al. (2011) studied the chemical composition of PM_{2.5} during winter in Tianjin, and the elevated PM_{2.5} was mainly attributed to combustion sources including vehicle exhaust, heating, cooking and industrial emissions, as well as low

wind speeds and high relative humidity. Aldabe et al. (2011) evaluated the PM_{2.5} concentration and its trace element levels during 2009 at three different locations (rural, urban and urban-traffic) in Navarra (North of Spain). The results indicated that 90–96% of the total trace elements present in PM_{2.5} consisted of P, Ti, Cr, Mn, Ni, Cu, Zn, Sr, Sn, Ba and Pb, and the main sources were crustal, secondary sulphate, secondary nitrate, traffic and sea-salt aerosols. However, there is limited data available on the elemental composition of PM_{2.5} in Chengdu city, which is located in the Chengdu-Chongqing Economic Zone and is densely populated with serious air pollution.

In this work, the mass concentrations of PM_{2.5} and its elements from April 19, 2009 to January 31, 2010 were determined to evaluate the levels of PM_{2.5} and its elemental components, as well as its seasonal variation characteristics. Furthermore, enrichment factor, correlation analysis and principal component analysis were applied to analyse the possible sources of PM_{2.5}. It is expected that the analysis results will provide a scientific basis to regulate and control PM_{2.5} levels in Chengdu.

MATERIALS AND METHODS

Sample collection: PM_{2.5} samples were collected on the roof of a building 15 m above the ground within the Institute of Plateau Meteorology of China, located in the western part of downtown Chengdu in a residential commercial neighbourhood. The PM_{2.5} samples for elemental analysis were collected using a low-flow air sampler (MiniVol TAC,

AirMetrics Corp., Eugene, OR, USA) with a flow rate of 5 L·min⁻¹ on 47 mm Teflon filters (Whatman PTFE). The sampling procedure was carried out based on the US EPA National Ambient Air Quality Standard for particulate matter. A total of 121 PM_{2.5} samples and 10 blank samples were collected in spring, summer, autumn in 2009 and winter in 2010. The collection period for each sample was 24 h. The filters were analyzed gravimetrically for particle mass concentrations using a Sartorius MC5 electronic microbalance with a sensitivity of ±1 µg (Sartorius, Göttingen, Germany) after 24 h equilibration at a temperature of 22±1°C and a relative humidity of 40±5%. Each filter was weighed at least three times before and after sampling, and the average weight was calculated to determine the mass concentration of PM_{2.5}. All the filters were individually placed into plastic bags and stored in a freezer (-18°C) until the subsequent analysis to limit any contamination.

Elemental analysis: In this study, Energy Dispersive X-Ray Fluorescence Spectrometry (Epsilon 5 ED-XRF, PANalytical B. V., Netherlands) was used to determine concentrations of the elements collected on the PM_{2.5} Teflon filters. In total, 20 elements (i.e. Al, As, Ba, Br, Ca, Cd, Cr, Cu, Fe, Mn, Mo, Ni, Pb, Rb, Sr, Sb, Si, Sn, Ti and Zn) were determined. In addition, quality assurance (QA) and quality control (QC) procedures were carried out, including regular instrument calibration with standard reference materials (SRM), and following the standard QA/QC requirements of the Chinese government. These standard procedures were performed routinely during the entire study. Also, an intensive QC program was implemented to maintain accuracy and precision throughout this project and the ED-XRF spectrometer was calibrated with thin-film standards obtained from MicroMatter Co. (Arlington, WA, USA).

Statistical analysis: A thorough literature survey showed that statistical methodology has been widely used to study possible pollution sources for the atmospheric environment (Lee et al. 2013). In this paper, correlation analysis (CA), principal component analysis (PCA) and enrichment factors (EF) were applied to analyse the possible sources of PM_{2.5} in Chengdu.

RESULTS AND DISCUSSION

Elemental composition of PM_{2.5}: During the period of observation, the annual average mass concentration of PM_{2.5} in Chengdu was 165.1 µg·m⁻³ (Table 1), which is 4.7 times higher than the National Ambient Air Quality Standard for annual PM_{2.5} (35 µg·m⁻³). Daily mean concentrations were 49.2~425.0 µg·m⁻³. The number of days which exceeded the second-level ambient air quality standard (75 µg·m⁻³, GB3095-2012) issued by the Ministry of Environmental

Protection of China accounted for 90.9%. In addition, the total mass concentration of the elements in this study was 6,543.3 ng·m⁻³, which accounted for 4.0% of PM_{2.5} mass concentration. The concentrations of the 20 elements are given in Table 1. It can be seen that the concentrations of the elements followed the order: Fe>Si>Al>Ca>Zn>Pb>Mn>Ti>Br>Cu>Sr>As>Ba>Sn>Cr>Mo>Sb>Cd>Rb>Ni. The concentrations of Fe, Si and Al exceeded 1,000.0 ng·m⁻³ (1,679.0, 1,093.9 and 1,053.0 ng·m⁻³, respectively), which are considered high pollution levels. Then, the concentrations of Ca, Zn, Pb, Mn and Ti were 995.2, 822.9, 320.5, 137.6 and 126.3 ng·m⁻³, respectively. The concentrations of Br, Cu, Sr, As, Ba, Sn, Cr, Mo, Sb, Cd and Rb were lower than 100.0 ng·m⁻³ (ranging from 55.5~9.5 ng·m⁻³). Finally, Ni concentration was the lowest at 5.1 ng·m⁻³. However, As (40.5 ng·m⁻³) concentration was 5.7 times the annual average concentration standard (6.0 ng·m⁻³), and Cd (9.5 ng·m⁻³) concentration was about 2 times the standard (5.0 ng·m⁻³), and they are both typical carcinogenic heavy metal elements. Moreover, the total concentration of the earth's crust elements (including Fe, Si, Al, Ca and Ti in this study) was 4,947.3 ng·m⁻³, accounting for 75.6% of the 20 elements. The results showed that the main elements in atmospheric PM_{2.5} from Chengdu were earth's crust elements and carcinogenic heavy metals, indicating that the pollution was serious.

Comparing the study data with other domestic and global cities (as presented in Table 1), it was found that the PM_{2.5} concentration in Chengdu was higher than Beijing (118.50 µg·m⁻³), Guangzhou (81.70 µg·m⁻³) and Shanghai (103.10 µg·m⁻³). In addition, Si (1,790.0, 2,200.0 ng·m⁻³), Cu (70.0, 60.0 ng·m⁻³), Cr (50.0, 190.0 ng·m⁻³), Cd (50.0, 70.0 ng·m⁻³) and Ni (20.0, 30.0 ng·m⁻³) concentrations in Beijing were higher than Chengdu, respectively. The concentrations of all elements except for Al (2,905.0 ng·m⁻³), Ca (3,008.0 ng·m⁻³) and Sr (206.0 ng·m⁻³) in Shanghai were lower than Chengdu. Also, Ti (110.0 ng·m⁻³), Cu (190.0 ng·m⁻³), As (40.0 ng·m⁻³) and Ba (70.0 ng·m⁻³) concentrations in Chengdu were higher than Guangzhou. Moreover, concentrations of elements in Navi Mumbai were lower than Chengdu, except for Ba (270 ng·m⁻³), Cr (44 ng·m⁻³), Mo (23 ng·m⁻³), Rb (11 ng·m⁻³) and Ni (6.3 ng·m⁻³). In Jeddah and Navarra, all the elemental concentrations were lower than Chengdu, except for Si (2,100 ng·m⁻³) and Ni (6 ng·m⁻³) in Jeddah, which were higher than those in Chengdu. The analysis results showed that most of the elemental concentrations in PM_{2.5} in Chengdu were higher than the other domestic and foreign cities, such as Beijing, Shanghai, Guangzhou, Jeddah and Navarra. Thus, Chengdu is suffering from a considerably severe PM_{2.5} pollution problem.

Table 1: Comparison of PM_{2.5} (µg·m⁻³) and elements (ng·m⁻³) mass concentrations at urban locations in other domestic and foreign cities.

City Year	Chengdu 2009-2010	Beijing 2005-2006	Shanghai 2009-2010	Guangzhou 2008-2009	Jeddah 2011	Navi Mumbai 2008	Navarra 2009
PM _{2.5}	165.1	118.5	103.10	81.7	-	42	15.38
Fe	1679	1130	1328	1850	590	310	-
Si	1093.9	1790	-	-	2100	840	-
Al	1053	790	2905	-	800	450	-
Ca	995.2	900	3008	-	540	310	-
Zn	822.9	530	236	1360	41	64	17.98
Pb	320.5	240	59	450	160	36	2.29
Mn	137.6	90	66	150	19	9.2	2.57
Ti	126.3	80	-	110	55	23	6.31
Br	55.5	30	-	-	9	12	-
Cu	54.1	70	15	190	6	6.2	11.98
Sr	44	-	206	-	4	14	1.16
As	40.5	20	-	40	9	7.1	0.16
Ba	38	210	-	70	34	270	12.08
Sn	18.8	-	-	-	-	-	0.94
Cr	17.9	50	9	70	2	44	2.39
Mo	10.7	-	-	-	-	23	-
Sb	11	-	-	-	-	-	0.7
Cd	9.5	50	1	20	8	-	0.05
Rb	9.9	-	-	-	1	11	0.25
Ni	5.1	20	9	-	6	6.3	1.31

The seasonal variation of PM_{2.5} concentrations is presented in Fig. 1. Clearly, the concentrations in autumn and winter were higher than those in spring and summer. Seasonal mean concentrations were 133.2±54.5 µg·m⁻³ in spring, 113.5±38.7 µg·m⁻³ in summer, 188.0±105.2 µg·m⁻³ in autumn and 225.5±71.9 µg·m⁻³ in winter, and the ranges were 60.0~300.5 µg·m⁻³, 49.2~218.9 µg·m⁻³, 57.2~425.0 µg·m⁻³ and 93.4~376.8 µg·m⁻³, respectively. Generally, PM_{2.5} levels are governed by emissions, transportation, chemical transformation and depositional processes, which are all related to meteorological conditions. The effects of meteorological factors (precipitation, wind speed, temperature and humidity) on PM_{2.5} concentrations showed negative correlation. Studies have shown that precipitation can wash away part of atmospheric particulate matter and inhibit the generation of ground dust. Accordingly, ambient air pollutants are dispersed and diluted by frequent rainfall. Wind speed has dual effects on the concentrations of pollutants. Within a certain range, wind speed is favourable to the diffusion and dilution of air pollutants. However, if it is larger than the given range, increased wind speed will lead to a significant increase in PM_{2.5} concentrations in air (Li et al. 2014). In addition, the diffusion of air pollutants in the vertical direction mainly depends on temperature. The atmosphere is unstable when the temperature is higher and the pollutants diffuse upwards under the action of thermal convection, resulting in lower concentrations of pollutants. Conversely, at low temperatures, the atmosphere is stable. Thus,

the diffusion of pollutants is restrained, and the concentrations are higher. The precipitation, temperature and humidity values in spring and summer were higher than those in autumn and winter in Chengdu. Therefore, the influence of meteorological factors on PM_{2.5} concentrations was significant. On the other hand, the reason was the local pollution sources.

The total mass concentrations of the elements were 9,911.6 ng·m⁻³ in spring, 3,326.8 ng·m⁻³ in summer, 5,611.3 ng·m⁻³ in autumn and 7,575.0 ng·m⁻³ in winter, accounting for 7.44%, 2.93%, 2.98% and 7.58% in PM_{2.5}, respectively. Seasonal variation of elemental concentrations is shown in Fig. 2. It can be clearly seen that the elemental concentrations in spring and winter were higher than those in summer and autumn. The concentrations of Fe (2,385.6, 2233.8 ng·m⁻³), Si (2,281.9, 1011.2 ng·m⁻³) and Ca (1,717.4, 1092.1 ng·m⁻³) in spring and winter, respectively, Fe (1,365.0 ng·m⁻³) in autumn and Al (2,409.1 ng·m⁻³) in spring exceeded 1,000.0 ng·m⁻³, which are high pollution levels. The total concentration of earth's crust elements was 8,987.3 ng·m⁻³ in spring, 2,019.8 ng·m⁻³ in summer, 3,752.5 ng·m⁻³ in autumn and 5,301.7 ng·m⁻³ in winter, accounting for 90.7%, 60.7%, 66.9% and 70.0% of the 20 elements, respectively. Clearly, the effects on the earth's crust elements concentrations in spring were larger compared to the other seasons. The reason for this may be remote transmission. The northern dust storm affected by wind can transfer to Chengdu. The soil dust was transported to Chengdu by northerly air-

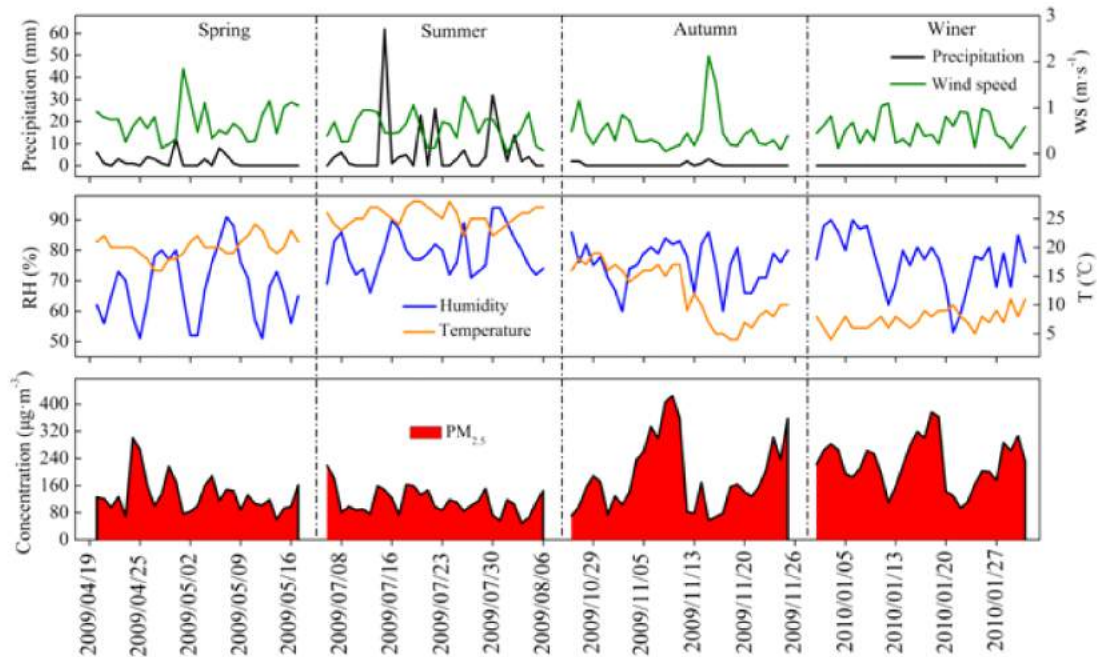


Fig. 1: The seasonal variation of PM_{2.5} concentrations and meteorological factors in Chengdu.

flow, and PM_{2.5} concentrations reached 300.5, 266.0 and 161.1 µg·m⁻³ on April 24, 25 and 26, respectively. Moreover, the concentrations of Al, Si, Ca and Fe on April 24 reached 17,690.1, 18,904.7, 11,474.4 and 14,114.1 ng·m⁻³, respectively. Therefore, the concentrations of earth's crust elements in spring were higher than those in summer, autumn and winter in this study. In addition, the concentrations of Zn, Pb and Mn (except Zn in winter (1,193.3 ng·m⁻³)) fluctuated between 100.0 to 1,000.0 ng·m⁻³ during the four seasons (Fig. 2). Also, the concentrations of Cu, As, Cr, Sb, Cd and Ni were lower than 100.0 ng·m⁻³, but As concentrations were 0.30, 4.65, 7.67 and 10.47 times that of the standard in spring, summer, autumn and winter, respectively. Cd concentrations were 0.28, 1.50, 1.58 and 0.18 times the standard, respectively. The reason for this elemental distribution is that waste gas of fired coal, automobile exhaust, rubber abrasion and smelting industry contributed to the atmospheric environment in Chengdu.

Possible sources of PM_{2.5}: The EF was calculated for each detected element to evaluate the anthropogenic contribution to atmospheric elemental levels. The EFs were calculated using the following equation:

$$EF_i = \frac{(C_i / C_j)_{PM_{2.5}}}{(C_i / C_j)_{crust}} \quad \dots(1)$$

Where, C_i is the concentration of the element considered in PM_{2.5} or crust and C_j is the concentration of the reference element in PM_{2.5} or crust. Al, Si, Ti and Fe are

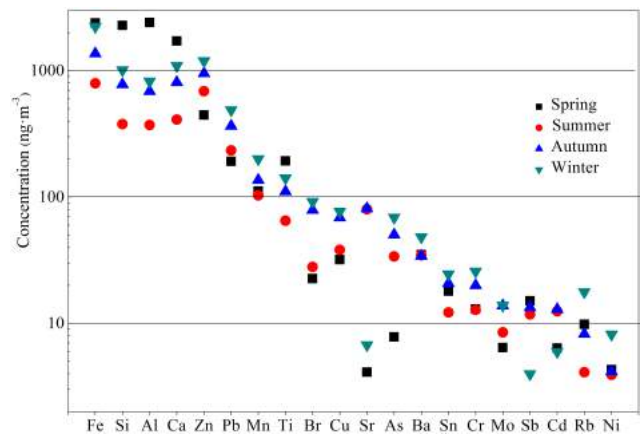


Fig. 2: The seasonal variation of elemental concentrations in Chengdu.

commonly considered as the reference elements of crustal material. In this study, Al was used as a reference element because it is relatively stable and not affected by contamination. The concentrations of elements in the crust indicate their content in the topsoil or soil in China. EF value lower than 10 is taken as an indication that the element in PM_{2.5} has a significant crustal source, while EF value greater than 10 indicates a significant anthropogenic origin.

The EFs of the elements in PM_{2.5} estimated from this study are shown in Fig. 3. Cd exhibited the highest enrichment factor (>1,000) with EF value of 6,481. Pb, Zn, Br, Sb,

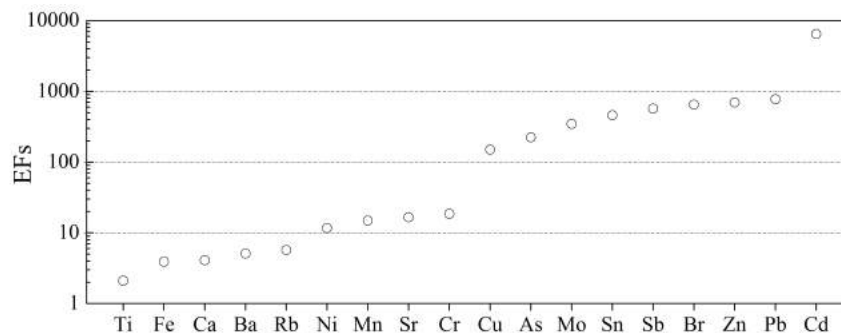


Fig. 3: Enrichment factors of elements in PM_{2.5}.

Sn, Mo, As and Cu also showed high enrichment factors (>100). Cr, Sr, Mn and Ni also appeared to be moderately enriched but to a lesser extent ($10 > EF > 100$). The high enrichment of these elements suggest that the dominant sources for these elements were non-crustal and a variety of pollution emissions contributed to their loading in the ambient air. Low EF values (in general < 10) were found for Ti, Fe, Ca, Ba and Rb, suggesting a negligible contribution from anthropogenic emissions to the ambient levels of these elements. On the other hand, the EFs of carcinogenic heavy metals such as Cd, Pb, As, Cr and Ni were 6,481.2, 776.2, 224.5, 18.6 and 11.7, respectively, indicating that these heavy metals were of anthropogenic origin. For example, Mn is a metal element present in high concentrations in fly ash from coal combustion. In addition, high-temperature processes such as metal smelting and fuel combustion are usually the source of non-crustal volatile metals (e.g. Cd, Ni, Cu) in the atmosphere. Thus, anthropogenic sources were responsible for the main contributions to PM_{2.5} in Chengdu, and natural sources such as soil dust had lesser contribution.

In order to further understand the relationship between elements in PM_{2.5} and its sources, the correlations were analyzed. The results showed that high correlations were observed for Fe, Si, Al, Ca and Ti. For these five elements, the correlation coefficient was greater than 0.9 ($P < 0.01$), indicating that these elements in PM_{2.5} were more strongly affected by crustal sources. In addition, Zn was strongly correlated with Pb, Br and Cu, with $R^2 = 0.891$, 0.854 and 0.824 , respectively, and $P < 0.01$. Zn is associated with tire wear and tailpipe emissions as a result of its use in motor oil. Pb and Br mainly come from vehicle emissions. Cu is emitted from automobile brake system (Liu et al. 2015). Therefore, motor vehicle exhaust emissions were the main contributors to Zn, Pb, Br and Cu contents in PM_{2.5}. As element showed moderate correlations with Zn, Pb, Mn, Cu and Cr, with $R^2 = 0.860$, 0.890 , 0.646 , 0.772 and 0.796 , respectively, and $P < 0.01$. Therefore, these elements in PM_{2.5} had a com-

mon source. As is an indicator element of coal (López et al. 2011). Zn can also come from combustion of fossil fuels and waste incineration, indicating that the elements were influenced by combustion of fossil fuels, coal and waste. However, there was a weak correlation for Fe with Mn, $R^2 = 0.706$, $P < 0.01$. Fe not only comes from crustal sources, but also comes from metallurgical processes, suggesting that industrial emissions partly contributed to Fe content in PM_{2.5}. Thus, the main sources of PM_{2.5} were soil dust, automobile exhaust, combustion of fossil fuels, coal and waste, and industrial emissions.

In this study, the various sources of elements in PM_{2.5} were identified by PCA (Cong et al. 2007), and the results are presented in Table 2. The four principal components with eigen values greater than 1 were extracted and they accounted for 74.7% of the total variance. Factor 1 accounting for 34.3% of total variance was dominated by Zn, Pb, Mn, Br, Cu, As, Ba, Sn, Cr, Mo, Rb and Ni. The elements Br, Cu and Pb mainly came from vehicle emissions and tire wear. The combustion of coal, fossil fuels and waste mainly contributed to Zn, Cr, Ni and As contents in PM_{2.5}. The results showed that vehicle emissions, coal combustion, burning of fossil fuels and waste incineration were the primary pollution sources. Factor 2 was characterized by Fe, Si, Al, Ca and Ti, reflecting the effect of crustal sources, and accounted for 27.8%. In addition, Ca is a characteristic element of building constructions. Thus, the secondary pollution sources were identified as soil dust and building dust. Factor 3 was represented by Cd and Sr, accounting for 7.0%. Cd content can be affected by metallurgy and mechanical manufacturing emissions, suggesting that the third pollution source may be mainly industrial emission. Factor 4 was the component of Sb, accounting for 5.6%. Sb is commonly found in brake dust. Therefore, the fourth pollution source is road traffic. The PCA results showed that soil and building dust, automobile exhaust, combustion of coal, fossil fuels and waste, industrial emission, and road traffic were contributors to PM_{2.5} in Chengdu.

Table 2: Rotated component matrix for PM_{2.5} elements.

Elements	Principal components			
	F1	F2	F3	F4
Fe		0.607		
Si		0.809		
Al		0.851		
Ca		0.780		
Zn	0.795			
Pb	0.804			
Mn	0.900			
Ti		0.694		
Br	0.733			
Cu	0.750			
Sr			0.610	
As	0.730			
Ba	0.601			
Sn	0.323			
Cr	0.839			
Mo	0.395			
Sb				0.894
Cd			0.749	
Rb	0.806			
Ni	0.580			
% of variance	34.332	27.793	7.017	5.624
Cumulative %	34.332	62.124	69.141	74.765

CONCLUSIONS

In this paper, we have investigated the elemental composition of PM_{2.5} and its possible sources in Chengdu from April 2009 to January 2010. The total mass concentration of the elements in PM_{2.5} was 6,543.3 ng·m⁻³, accounting for 4.0% of PM_{2.5} mass concentration. The concentrations of the elements followed the order of Fe>Si>Al>Ca>Zn>Pb>Mn>Ti>Br>Cu>Sr>As>Ba>Sn>Cr>Mo>Sb>Cd>Rb>Ni. The concentrations in autumn and winter were higher than those in spring and summer. The elemental concentrations in spring and winter were higher than those in summer and autumn. The elemental concentrations in the four seasons were 9,911.6, 7,575.0, 3,326.8 and 5,611.3 ng·m⁻³, accounting for 7.44%, 7.58%, 2.93%, and 2.98% of PM_{2.5}, respectively. The results of EF, CA and PCA consistently indicated that the sources of PM_{2.5} in Chengdu were mainly crustal material, construction dust, automotive exhaust emission, coal-fire, dust of fossil fuel and refuse burning, and industrial emissions. These sources contributed to the pollution due to the rapid increase in motor vehicles, total energy consumption, smelting industry and dust storm events.

ACKNOWLEDGEMENTS

The work was supported by Science & Technology Department of Sichuan Province (Grant No. 2015JY0094) and the Scientific Research Fund of Sichuan Provincial Education Department (Grant No. 13ZB0011).

REFERENCES

- Aldabe, J., Elustondo, D., Santamaría, C., Lasheras, E., Pandolfi, M., Alastuey, A., Querol, X. and Santamaría, J.M. 2011. Chemical characterisation and source apportionment of PM_{2.5} and PM₁₀ at rural, urban and traffic sites in Navarra (North of Spain). *Atmospheric Research*, 102(1-2): 191-205.
- Cong, Z., Kang, S., Liu, X. and Wang, G. 2007. Elemental composition of aerosol in the Nam Co region, Tibetan Plateau, during summer monsoon season. *Atmospheric Environment*, 41(6): 1180-1187.
- Fang, G.C., Huang, Y.L. and Huang, J.H. 2010. Study of atmospheric metallic elements pollution in Asia during 2000-2007. *Journal of Hazardous Materials*, 180(1-3): 115-121.
- Gu, J., Bai, Z., Li, W., Wu, L., Liu, A., Dong, H. and Xie, Y. 2011. Chemical composition of PM_{2.5} during winter in Tianjin, China. *Particuology*, 9(3): 215-221.
- Han, Y., Kim, H.W., Cho, S.H., Kim, P. and Kim, W. 2015. Metallic elements in PM_{2.5} in different functional areas of Korea: Concentrations and source identification. *Atmospheric Research*, 153: 416-428.
- Lee, B.K. and Hieu, N.T. 2013. Seasonal ion characteristics of fine and coarse particles from an urban residential area in a typical industrial city. *Atmospheric Research*, 122: 362-377.
- Li, W., Wang, C., Wang, H., Chen, J., Yuan, C., Li, T., Wang, W., Shen, H., Huang, Y., Wang, R., Wang, B., Zhang, Y., Chen, H., Chen, Y., Tang, J., Wang, X., Liu, J., Coveney, R.M. Jr. and Tao, S. 2014. Distribution of atmospheric particulate matter (PM) in rural field, rural village and urban areas of northern China. *Environmental Pollution*, 185: 134-140.
- Liu, G., Li, J.H., Wu, D. and Xu, H. 2015. Chemical composition and source apportionment of the ambient ambient PM_{2.5} in Hangzhou, China. *Particuology*, 18: 135-143.
- López, M.L., Ceppi, S., Palancar, G.G., Olcese, E., Tirao, G. and Tosellia, B.M. 2011. Elemental concentration and source identification of PM₁₀ and PM_{2.5} by SR-XRF in Córdoba City, Argentina. *Atmospheric Environment*, 45(31): 5450-5457.
- Yang, J., Fu, Q., Guo, X., Chu, B., Yao, Y., Teng, Y. and Wang, Y. 2015. Concentrations and seasonal variation of ambient PM_{2.5} and associated metals at a typical residential area in Beijing, China. *Bull. Environment Contamination Toxicology*, 94: 232-239.
- Yang, L., Cheng, S., Wang, X., Nie, W., Xu, P., Gao, X., Yuan, C. and Wang, W. 2013. Source identification and health impact of PM_{2.5} in a heavily polluted urban atmosphere in China. *Atmospheric Environment*, 75: 265-269.
- Zhang, R., Han, Z., Cheng, T. and Tao, J. 2009. Chemical properties and origin of dust aerosols in Beijing during springtime. *Particuology*, 7(1): 61-67.



Accuracy Assessment of Land Use Classification Using Support Vector Machine and Neural Network for Coal Mining Area of Hegang City, China

Lei Wang^{*(**)(***), Yunna Jia^{**(****), Yunlong Yao^{*****(***)†} and Dawei Xu^{*†}}}

^{*}College of Landscape Architecture, Northeast Forestry University, Harbin 150040, China

^{**}College of Architectural Engineering, Heilongjiang University of Science and Technology, Harbin 150022, China

^{***}College of Agricultural and Life Sciences, University of Wisconsin, Madison, 53706, United States

^{****}Henan Urban and Rural Planning and Design Research Institute Co. Ltd, Zhengzhou 450000, China

^{*****}College of Wildlife Resources, Northeast Forestry University, Harbin 150040, China

[†]Corresponding authors: Dawei Xu and Yunlong Yao

Nat. Env. & Poll. Tech.
Website: www.neptjournal.com

Received: 18-07-2018
Accepted: 21-09-2018

Key Words:

Coal mining area
Land use classification
Support vector machine
Neural network
Texture feature

ABSTRACT

Information of land use plays a key role in the ecological systems. Most studies focus on the land use studies in large cities or large areas, but rarely carry out a land system in vulnerable areas. In this study, the size of 1000×1000 pixels in Hegang coal mining area was used as the experimental area. Based on Landsat TM image of September 8, 2010, principal component analysis (PCA) and optimum index factor (OIF) were used to select the best band combination of images, and the texture statistics, texture features and spectral information of the homogeneity, contrast, entropy and angular second moments of the remote sensing image were extracted by using the gray level co-occurrence matrix texture feature. A sample of 600 pixels was selected, of which 400 pixels were used as training samples and 200 pixels as test samples. The results show that the support vector machine (SVM) and neural network (NN) classification technique are used to classify land use in coal mining area. The overall accuracy obtained was 92.40% and the kappa statistics 0.9126 for SVM, 90.90% and 0.8930 for NN, respectively. This study provided a comprehensive extraction of samples to improve the accuracy method. The SVM and NN classification results show that SVM classification method is superior to NN classification method, and it can effectively be utilized for Landsat TM images to identify land use types in coal mining areas.

INTRODUCTION

Information on land use/land cover (LULC) plays a key role in natural resource management (Wentz et al. 2006, Soffianian et al. 2015). LULC mapping using satellite images has become widely popular in the last decades (Sen et al. 2015). Coal city as a special urban group, land use and land cover of areas in the vicinity of mining sites are significantly affected by the corresponding mining activities and consequently change faster than other areas (Rathore et al. 1993). Remote sensing and GIS tools have been used extensively in the mining industry for various purposes such as mineral exploration, modelling and monitoring, mine planning, and environmental impact assessment (Vander Meer et al. 2012, Karan et al. 2016). Numerous researches have been published on comparison of different remote sensing image classification algorithms used for LULC mapping (Vorovencii 2014a). Although these classification methods are very effective in land-use extraction, because of the multi-scale and complexity of the objects, the phenomenon of "homologous spectrum" and "foreign matter homology" exists, which

cannot simply use spectral features or a classification method for remote sensing image classification. Support vector machine (SVM) is a recent non-parametric supervised statistical machine learning technique that aims to find an optimal hyperplane (Cortes et al. 1995), which separates the multispectral feature data into discrete predefined clusters consistent with training datasets. The classification errors in the individual images affect the final accuracy of change detection. In case of these techniques, it is very important to develop high accuracy classifications for each satellite image (Lu et al. 2004). Traditional support vector machine (SVM) has adverse effects on classification accuracy. Therefore, we use SVM classification method which is combined with texture information and spectral information to extract the information of land use in Hegang coal mining area, so as to improve land use classification accuracy and better use of remote sensing technology in the application of LULC.

MATERIALS AND METHODS

Study site: Hegang is located in the hilly region of the eastern

foot of the Little Xing'an Mountains and the plains at the junction of the Songhua River and Heilongjiang River, in Northern China (47°03'30"- 48°21'00" N and 129°39'50"- 132°31'00"), as shown in Fig. 1. The coal mining area is located in the northwestern region of Hegang, selected as a typical research area. The climate of Hegang City is affected by the temperate continental monsoon, it is cold and dry in winter and warm and rainy in summer. The average annual temperature is 1.0-4.6°C, the average annual frost-free period is about 125 days, and the average annual rainfall of about 608.5 mm. The study area as a whole showed a low trend in the south and high in the north, with the hills in the north and the plains in the south.

Remote sensing image data preprocessing: Landsat5 TM surface reflectance data of 8 September 2010 was collected from USGS Earth Explorer. The image was standardized and projected to the projection system, Universal Transverse Mercator (UTM) Zone52N Datum WGS 1984 projection using ArcGIS10.5. Image collected is based on the local climate characteristics of choice, this time period is rich in species, has bright colours, and easy to identify. Remote sensing image preprocessing includes 2% linear stretch image enhancement processing, crop cutting, noise removal and other processing to reduce the classification error. According to the land use classification criteria and the actual situation of the site, the land use types of the test area are divided into 8 categories: residential land, coal mine land, forest land, grassland, water area, cultivated land, unused land and transportation land.

METHODS

Classification methods: The performance of two classification algorithms was examined. These algorithms include neural network (NN) and support vector machine (SVM).

The landsat TM images are classified by the two classifiers using the same training dataset per case study.

Support vector machine (SVM) technique is based on statistical learning theory presented by Cortes and Vapnik in 1995s. The SVM classifier is a modern, powerful supervised classification method that can handle multiple-band imagery having high resolution and large segmented satellite data with ease when compared to other classification techniques, where attribute table management becomes difficult (Shivesh et al. 2016). It can solve some practical problems such as high dimension data, small sample, non-linearity and so on. It has high precision and stability for the classification of ground objects. Set the training sample is $\{x_i, y_i\}_{i=1}^N$, among them $x_i \in R^n$, indicates the input mode and $y_i \in \{-1,1\}$ indicates the target output. Set the optimal decision surface equation: $W^T x_i + b = 0$, the weight vector W and the offset b must satisfy the constraints:

$$y_i (W^T x_i + b) \geq 1 - \xi \quad \dots(1)$$

Where ξ is the slack variable under the linearly indivisible condition, which indicates the degree of deviation of the model from the ideal linear case. The following optimization formula can be deduced based on the principle that the average error of the training sample classification data is the smallest.

$$L(w, \xi) = \frac{1}{2} W^T W + C \sum_{i=1}^N \xi \quad \dots(2)$$

$C > 0$ is the error term penalty parameter. The SVM locates a linear separating hyperplane with the maximum margin in this higher dimensional space. By using the Lagrange multiplier method, the optimal decision surface can be transformed into the following constrained optimization problems:

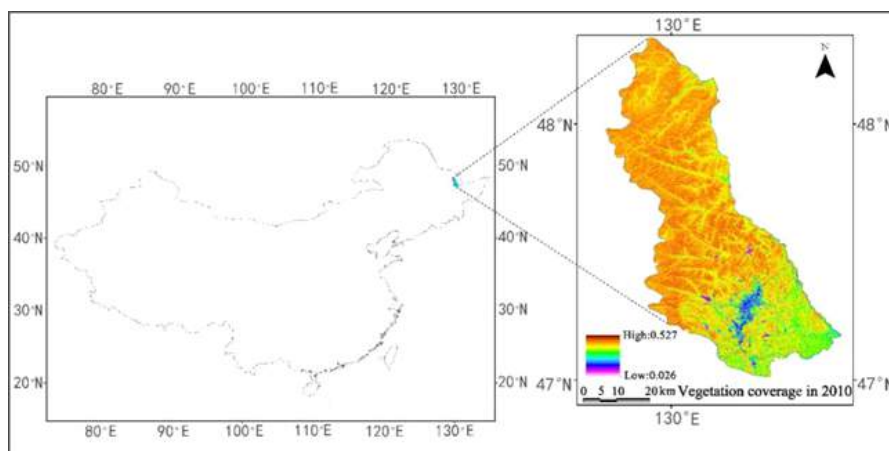


Fig. 1: Location of the study area.

$$Q(a) = \sum_{i=1}^N a_i - \frac{1}{2} \sum_{i=1}^N \sum_{j=1}^N a_i a_j y_i y_j K(x_i, y_j) \quad \dots(3)$$

Where, $\{a_i\}_{i=1}^N$ is the Lagrangian multiplier and $K(x, x_i)$ is a kernel function and satisfies the Mercer's theorem. The kernel function has many forms, including linear, radial basis function and polynomial. With different kernel function and parameter setting, its classification effect is different.

Neural network (NN) is a nonparametric algorithm that does not make any assumptions on the distribution of data (Vorovencii 2014). One challenge in using NN classifier is to decide the appropriate network architecture and training parameters. Saleh et al. (2015) have tested different combinations of network values in a neural network algorithm and determined the classification with the highest complete accuracy for each case study. The optimized network parameters include training threshold contribution, tested with three values of 0.5, 0.7 and 0.9; training rate, tested with three values of 0.1, 0.2 and 0.5; training momentum, tested with four values of 0.1, 0.2, 0.5 and 0.9; structure of hidden layers 1 and 2; and a fixed logistic activation function (Saleh et al. 2015).

Optimum band combination selection based on PCA and OIF: Principal component analysis (PCA) represents a method used in many applications for remote sensing, including land use/land cover change detection (Fung et al. 1987). Its main advantage is the capacity to reduce the size of the data with minimum information loss (Iosif 2014). All variables were submitted to PCA to reduce the data dimensionality by performing a covariance analysis between the factors. The transformed first principal component usually contains more than 80% of the total information, which can reflect the total radiation intensity of the object, and can effectively extract the linear features, thus improving the classification rate.

The combination of the best bands is an important prerequisite for the visual interpretation and feature extraction of remote sensing images. According to different uses, different bands are selected as the RGB component to synthesize the RGB colour images. The colour saturation of the synthesized images can display rich feature information or highlight a particular aspect of information, convenient and efficient identification of objects. Band selection is usually based on the combination of the maximum amount of information band and the minimum information between the relevance of the principle of selection, the use of correlation coefficient analysis of the degree of information overlap between bands. The higher the correlation coefficient, the higher the data similarity, otherwise the data redundancy is low. The PCA is used to remove the redundant information of each band. The first three components contain 92.63%

of the information in all the bands, and the first three components can be combined to help the classification of RGB, through the statistical calculation of the inter-band correlation coefficient matrix (Table 1).

From Table 1, we can know that Band4 has highest independence, Band2 and Band3 correlation is significant, the correlation coefficient is greater than 0.9, Band2 and Band3 have consistent spectrum. But as only one can be selected, Band4 and other band correlation is small, it has strong independence and high-quality information, so the choice of band Band4 as a mandatory band. Band 5, 6 and band 5, 1 correlation is low, Band7 is slightly superior to Band5, 6. According to the above analysis, the best band combination is 742 and 743, and the best band combination is quantitatively evaluated by using the best band index (OIF) to obtain the best band combination.

The OIF index takes into account the standard deviation, which reflects the degree of dispersion of the data and the correlation coefficient that reflects the correlation between the bands. Band combination of the larger standard deviation and the smaller correlation coefficient, indicate a good band combination. The result shows that the order of OIF index is Band743 > Band742. The results show that Band743 is the best band combination, and its information is the most abundant. In practice, it will be found that due to the complexity of surface features, the optimal band combination of different landforms will change accordingly, so the most good combination of bands is selected that will contribute to land-use classification.

Texture feature analysis based on gray level co-occurrence matrix: The gray level co-occurrence matrix is a commonly used method to describe the texture features, which can reflect the gray space between any two points in the image by the matrices formed by angular second moment joint probability density between the image gray values related properties (Wu et al. 2005). Texture is made up of alternating gray-scale spatial distribution, and each object has a certain spatial correlation. Therefore, we used the statistical index of gray-level co-occurrence matrix to describe the texture feature, after selecting the appropriate texture scale and indicators to optimize the classification results.

Remote sensing spectral data provide a large number of spectral features of landforms, and the use of spectral information for land use classification of remote sensing images can reduce the error of visual interpretation of classification. However, spectral information classification also has certain drawbacks. Spectral information of a single place of its classification effect is better, but the spectral confusion of the classification effect is more broken. The texture feature of each feature is different. It is effective to improve the

Table 1: Band correlation coefficient matrix.

Band	Band 1	Band 2	Band 3	Band 4	Band 5	Band 6	Band 7
Band 1	1	0.9185	0.9247	-0.1774	0.5381	0.6466	0.8140
Band 2	0.9185	1	0.9571	0.0155	0.6094	0.5448	0.7800
Band 3	0.9247	0.9571	1	-0.1509	0.5809	0.5902	0.8158
Band 4	-0.1774	0.0155	-0.1509	1	0.3378	-0.3298	-0.1144
Band 5	0.5381	0.6094	0.5809	0.3378	1	0.3898	0.8109
Band 6	0.6466	0.5448	0.5902	-0.3298	0.3898	1	0.6469
Band 7	0.8140	0.7800	0.8158	-0.1144	0.8109	0.6469	1

Table 2: Accuracy assessment using the confusion matrix based on the SVM and NN technique.

Cover	SVM		NN	
	PA(%)	UA(%)	PA(%)	UA(%)
Forest land	92.50	96.52	98.33	97.52
Grassland	86.87	66.67	80.00	72.73
Water area	97.50	100.00	100.00	100.00
Cultivated land	90.91	99.17	92.42	84.14
Residential area	100.00	100.00	94.79	98.91
Coal mine land	93.33	100.00	95.00	100.00
Unused land	89.29	82.42	86.11	67.39
Transportation land	86.90	85.88	58.55	100.00
OA(%)	92.40		90.90	
Kappa coefficient	0.9126		0.8930	

Note: UA-user's accuracy, PA-producer's accuracy, OA-overall accuracy.

classification accuracy by combining the spectral information with the image texture feature extraction. The texture feature extraction is the most widely used and the best.

Gray matrix co-occurrence matrix: Each matrix element describes the probability that the gray level j occurs with the gray level i as the starting point when the pixel distance d is separated by a certain distance in the q direction, and the probability that the gray level is j is denoted as $p(i, j, d, q)$ (Harlick et al. 1973). The results show that 17×17 is the best processing window, and the gray level is 64. According to the selection of the field and the texture index, the homogeneous, contrast, angular second moment, and entropy of the four indices were extracted for texture analysis (Fig. 2). The angular second moment image can highlight the construction land and water information, contrast can clearly identify the residents, roads and other information; information entropy can describe the spatial complexity and chaos of the study area. You can use entropy threshold to extract unused land, while the homogeneity of the extraction of water is more accurate. The four eigen values of 0° , 45° , 90° and 135° in the four directions are more accurate and the mean value of the feature values in the four directions varies with distance.

RESULTS AND DISCUSSION

Analysis of classification results: According to the field survey dataset, the land use types of the study area were divided into 8 types, which were cultivated land, forest land, grassland, water area, residential area, coal mine land, unused land and transportation land. Using the ROI separability to determine the degree of discrepancy between categories, the statistical distance between classes is based on Jeffries-Matusita distance and transformed divergence (TD) can be used to measure the separability of training samples (Mallet et al. 2011). In the sample selection, we should not only consider the spectral characteristics, the distribution of regional characteristics and radiation characteristics, but also consider the edge of the map, topographic factors such as coverage characteristics, combined with field surveys, to ensure the selected sample representative in order to obtain a higher precision. The reference datasets of each image were randomly divided into training and validation set. Training sets included 400 pixels of each land cover and used for image classification. Validation sets included 200 pixels of each land cover and were used for classification accuracy assessment.

Eight different land uses (cultivated land, forest land,

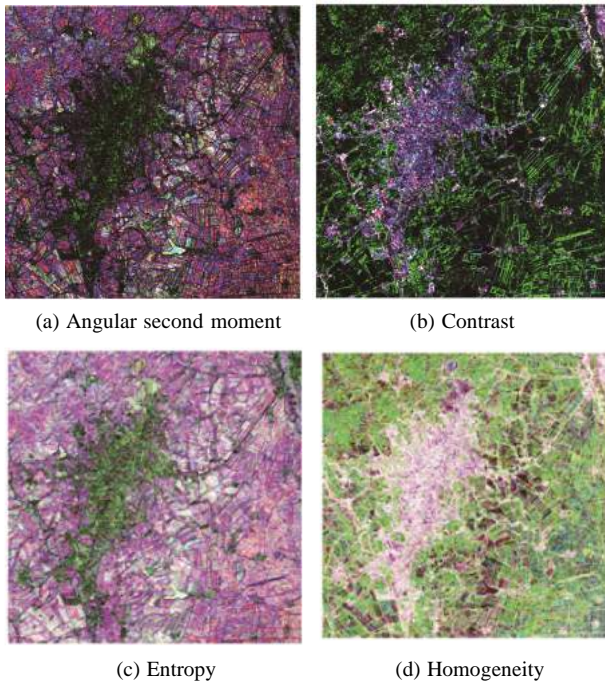


Fig. 2: The result texture analysis of gray level co-occurrence matrix.

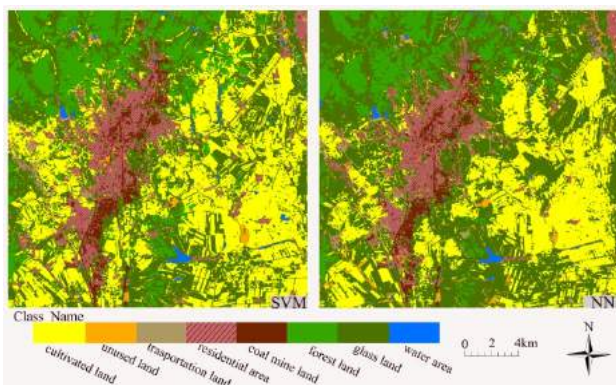


Fig. 3: The classified images of support vector machine and neural networks.

grassland, water area, residential area, coal mine land, unused land and transportation land) were successfully delineated using SVM and NN classification technique (Fig. 3). The classification results show that SVM classification and NN classification technique based on spectral information and texture features can be successful to extract the features, which can better highlight the details of the features, and the classification results are closer to the actual situation.

Accuracy assessment: After the land use classification process, it is important to assess the accuracy of the classified image, to peg and quantify mapping or classification errors

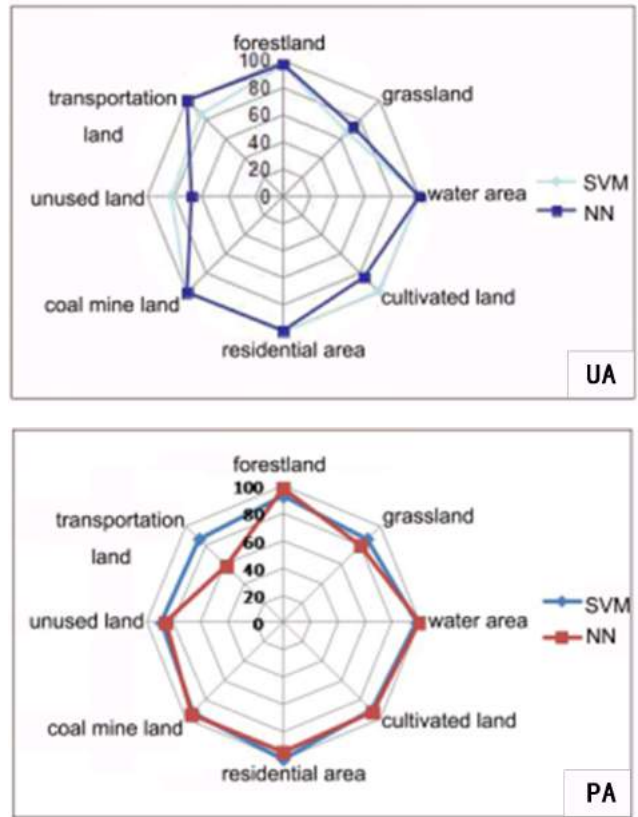


Fig. 4: Classification accuracy comparison image of SVM and NN methods.

(Koukoulas et al. 2001, Kalkhan et al. 1995). There are many precision evaluation methods available, the most commonly used technique is the confusion matrix method. In this method, a simple cross tabulation of the mapped class label against that observed in the ground or reference data is employed for a sample of cases at specified locations (Canter 1997). Classification accuracy and Kappa coefficient can reflect the accuracy of classification results of remote sensing images in the whole study area. Based on the texture and spectral information, the classification of land use in coal mining area was carried out, and the confusion matrix was used to classify and evaluate. The producer's accuracy is derived from the total number of the correct pixels of a class divided by the total number of the pixels. The user's accuracy is measured by total number of the correct pixels of a class divided by the total number of the pixels (Simitkumar et al. 2014). Table 2 presents the user's accuracy, producer's accuracy, and overall accuracy independent of class probability as our focus is classifier performance that is not site-specific.

The results revealed that the classification accuracy of ROI based on texture feature and spectral information tech-

nology is high, the overall accuracy of two classification techniques is more than 90%. Using SVM classification technology, user's accuracy of water area, residential area and coal mine land reached 100%. The classification error of forest land, cultivated land is also very small, with the accuracy of 96.52% and 99.17%, respectively. But grassland classification accuracy is low, which is related to grass growth habit, easy to be confused with other features. The producer's accuracy of grassland classification is 20.2% higher than that user accuracy in SVM. Using neural network classification technique, the overall classification accuracy is low with 1.5% support vector machine. But the classification accuracy of forest land, transportation land which used NN classification technique is higher than that of SVM classification. Unclassified user classification accuracy is only 67.39, 15.03% less than SVM classification accuracy.

The accuracy of SVM and NN classification is compared with the accuracy of the users. From Table 2 and Fig. 4, the user's accuracy of land use type is higher than that of NN classification by using SVM classification method, except for transportation land and grassland. The producer's accuracy comparison image also shows the classification advantage of SVM technology. The producer's accuracy of transportation land is low in NN classification, except for other types of land use accuracy which are about the same as SVM classification accuracy.

CONCLUSION

In this research, the training samples and test samples were selected based on the texture feature, and spectral information and different classification algorithms were examined for coal mining area LULC classification. The SVM and neural network methods performed high classification accuracy with a slight out performance of SVM (92.40%) over NN (90.90%). From the algorithmic perspective, results indicate that for coal mining area land use, SVM was superior to NN in overall classification accuracy as well as individual classification accuracy for many classes. One of the advantages of the SVM algorithm for land cover mapping is producing highly accurate classified images from small training sets (Halder et al. 2011). This advantage helps environmental and natural resource managers to provide LULC maps with accurate information quickly, thus saving them time and cost (Mountrakis et al. 2011). The setting of the NN threshold parameter is important for classification accuracy, NN of training algorithm adjusts the weights and node thresholds of the nodes in a crossed way, which can reduce the error to a minimum, and generate a good classified image.

SVM and NN were superior to other classification methods in supervised classification, but SVM classification is

more accurate than NN in land use classification of coal mining area. In our study, using the combination of PCA and OIF method to select the optimal band combination, the 743 band imaging bright colours conducive to visual interpretation of objects. Texture feature and spectral information analysis method to select the appropriate sample and land use classification were carried out using SVM and NN techniques. The above method is combined to make the classification accuracy higher, which effectively solves the problem of classification. This is the first step towards the provision of ecological services to environmentalists and policy makers, and is the key to sustaining sustainable development.

ACKNOWLEDGMENTS

The authors would like to express gratitude to the research grant support kindly provided by China Postdoctoral Science Foundation (Grant No.2017M621229), Postdoctoral Science Foundation of Heilongjiang Province (Grant No.LBH-Z17001), the National Natural Science Foundation of China for Young Scholars (Grant No.41101177, 41301081), Philosophy and social science program in Heilongjiang Province (Grant No.17GLD173, Grant No. 16GLC04), Scientific Research Foundation for the Returned Overseas Chinese Scholars, Heilongjiang Province, the University Strategic Reserve Personnel Abroad Research project funded by Heilongjiang Province, University Nursing Program for Young Scholars with Creative Talents in Heilongjiang Province (ecological environmental vulnerability and land reclamation in Coal Mining Areas of Heilongjiang Province).

REFERENCES

- Cortes, C. and Vapnik, V. 1995. Support-vector networks. *Machine Learning*, 20(3): 273-297.
- Canter, F. 1997. Evaluating the uncertainty of area estimates derived from fuzzy land cover classification. *Photogrammetric Engineering and Remote Sensing*, 63: 403-414.
- Fung, T. and Le Drew, E. 1987. Application of principal components analysis to change detection. *Photogrammetric Engineering and Remote Sensing*, 53: 1649-1657.
- Halder, A., Ghosh, A. and Ghosh, S. 2011. Supervised and unsupervised land use map generation from remotely sensed images using ant based systems. *Applied Soft Computing Journal*, 11(8): 5770-5781.
- Harlick, R.M., Shanmugam, K. and Dinstein, H. 1973. Textual features for image classification. *IEEE Transactions on Systems, Man and Cybernetics*, 3(6): 610-621.
- Iosif, V. 2014. Assessment of some remote sensing techniques used to detect land use/land cover changes in South East Transylvania, Romania. *Environmental Monitoring and Assessment*, 186: 2685-2699.
- Kalkhan, M.A., Reich, R.M. and Czaplowski, R.L. 1995. Statistical properties of five indices in assessing the accuracy of remotely sensed data using simple random sampling. *Proceedings ACSM/*

- ASPRS Annual Convention and Exposition, 2: 246-257.
- Koukoulas, S. and Blackburn, G.A. 2001. Introducing new indices for accuracy evaluation of classified images representing seminatural woodland environments. *Photogrammetric Engineering and Remote Sensing*, 67(4): 499-510.
- Karan, S.K. and Samadder, S.R. 2016. Reduction of spatial distribution of risk factors for transportation of contaminants released by coal mining activities. *Journal of Environmental Management*, 180: 280-290.
- Lu, D.S., Mausel, P. and Brondizio, E.S. and Moran, E. 2004. Change detection techniques. *International Journal of Remote Sensing*, 25(12): 2365-2401.
- Mallet, C., Bretar, F., Roux, M., Soergel, U. and Heipke, C. 2011. Relevance assessment of full-waveform lidar data for urban area classification. *ISPRS Journal of Photogrammetry and Remote Sensing*, 66(6): 71-84.
- Mountrakis, G., Im, J. and Ogole, C. 2011. Support vector machines in remote sensing: a review. *ISPRS Journal of Photogrammetry and Remote Sensing*, 66(3): 247-259.
- Rathore, C.S. and Wright, R. 1993. Monitoring the environmental impacts of surface coal mining. *International Journal of Remote Sensing*, 14(6): 1021-1042.
- Soffianian, A. and Madanian, M. 2015. Monitoring land cover changes in Isfahan Province, Iran using Landsat satellite data. *Environmental Monitoring and Assessment*, 187(8): 1-15.
- Sen, G., Bayramoglu, M.M. and Toksoy, D. 2015. Spatiotemporal changes of land use patterns in high mountain areas of Northeast Turkey: a case study in Macka. *Environmental Monitoring and Assessment*, 187(8): 1-14.
- Shivesh, K.K. and Sukha, R.S. 2016. Accuracy of land use change detection using support vector machine and maximum likelihood techniques for open-cast coal mining areas. *Environmental Monitoring and Assessment*, 188: 486.
- Simitkumar, R. and Ali, S. 2014. A monitoring framework for land use around Kaolin mining areas through Landsat TM images. *Earth Science Informatics*, 7: 153-163.
- Saleh, Y., Reza, K., Giorgos, M., Somayeh, M., Hamid Reza, P. and Mehdi, T. 2015. Accuracy assessment of land cover/land use classifiers in dry and humid areas of Iran. *Environmental Monitoring and Assessment*, 187: 641
- Vorovencii, I. 2014. A change vector analysis technique for monitoring land cover changes in Copsa Mica, Romania, in the period 1985-2011. *Environmental Monitoring and Assessment*, 186(9): 5951-5968.
- Vander Meer, F.D., Vander Werff, H.M.A., Van Ruitenbeek, F.J.A., Hecker, C.A., Bakker, W.H., Noomen, M.F., Mark van der Meijde., Carranza, E.J.M., Boudewijn de Smeth, J. and Tsehaie Woldai 2012. Multi-and hyperspectral geologic remote sensing: a review. *International Journal of Applied Earth Observation and Geoinformation*, 14(1): 112-128.
- Wentz, E.A., Stefanov, W.L., Gries, C. and Hope, D. 2006. Land use and land cover mapping from diverse data sources for an arid urban environments. *Computers, Environment and Urban Systems*, 30(3): 320-346.
- Wu, F., Wang, C. and Zhong H. 2005. Residential areas extraction in high resolution SAR image based on texture features. *Remote Sensing Technology and Application*, 20(1): 148-152.



Interactive Relations Among Environmental Pollution, Energy Consumption and Economic Growth in Jilin Province, China

Yang Fang* and Jinling Wang**†

*School of Economics, Changchun University, Changchun, 130021, China

**School of Economics, Changchun University, Changchun, 130021, China

†Corresponding author: Jinling Wang

Nat. Env. & Poll. Tech.
Website: www.neptjournal.com

Received: 16-01-2019
Accepted: 18-02-2019

Key Words:

Environmental pollution
Energy consumption
Economic growth
Jilin Province
Spatial error model

ABSTRACT

As the material base of modern civilization, energy sources influence economic development considerably. While large energy consumption facilitates rapid economic growth, it also results in increasing environmental pollution and severe disequilibrium of the ecosystem. These troublesome outcomes are caused by high energy consumption, great wastes and unreasonable demand structure. Spatial autocorrelation of environmental pollution in nine prefecture-level cities in Jilin Province of China from 2005 to 2016 was measured by Moran's index based on collected panel data firstly. Subsequently, the dynamic relationship among energy consumption, environmental pollution, and economic growth was estimated by the spatial error model. Results demonstrate that energy consumption and environmental pollution in nine prefecture-level cities in Jilin Province of China present certain characteristics of spatial agglomeration from 2005 to 2016, as well as an annual rise in COD. Besides, significant positive correlations exist between environmental pollution and regional economic growth. Such correlations are significantly stronger than the correlation between energy consumption and economic growth. The dual goals of reasonable saving and utilization of energy sources and ecological environmental protection while maintaining high economic growth rate can be realized by optimizing the industrial and energy consumption structures, establishing sustainable environmental development strategy, and implementing differentiated environmental protection policies. Research conclusions can provide Jilin Province of China with some references in formulating energy and environmental development strategies, determining of emission-reduction goal, and choosing low-carbon, high-efficiency, and sustainable development path.

INTRODUCTION

Energy consumption increases dramatically as a response to the national economic development in China. China has become the largest energy consumption country in the world. Energy sources, which are the material base of modern civilization, influence economic development in China considerably. The large energy consumption facilitates the rapid economic growth in China, but introduces serious environmental pollution problems. The high energy consumption and economic growth are accompanied with serious environmental problems, such as pollution and ecological imbalance. Although energy consumption promotes economic growth, the consumption of polluted energy sources causes environmental damages and is the primary cause of environmental pollution. Problems of unreasonable energy demand structure, such as high energy consumption, great energy waste, and serious pollution, are extremely prominent in China. The conflicts among energy consumption, economic growth, and environmental protection become increasingly prominent and have become the

bottleneck against China's sustainable development. Maintaining a harmonious development among preserving the high economic growth, saving and using energy sources reasonably, and protecting the environment has become a problem that has to be solved urgently in China.

Jilin Province, which is an economically underdeveloped region in China, is in the early stage of industrialization and has dual pressures of both economic development and environmental protection. As shown in Fig. 1, Jilin Province consumes a great amount of energy sources, and its environmental pollution caused by energy consumption is closely related to economic growth. Facilitating the sustainable development of economy, energy source, and environment, reducing energy consumption, and improving environmental quality while protecting the increasing energy demands for economic development have become major problems worldwide. Jilin Province is still applying the extensive economic growth model that focuses on the rapid growth of energy-consuming industries. The construction of high-energy consumption and high-pollution projects

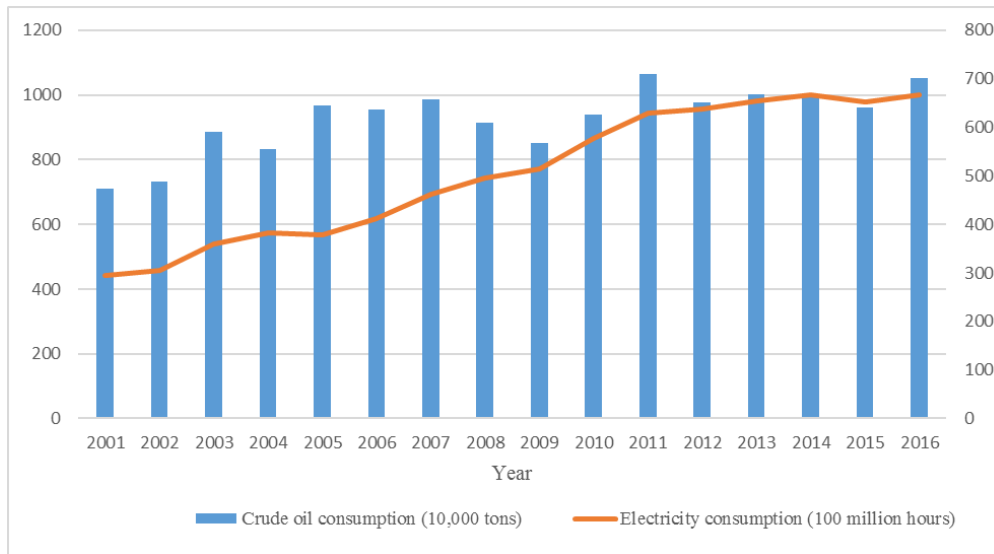


Fig. 1: Crude oil and electricity consumption in Jilin Province from 2001 to 2016.

are continuing, and this situation has brought considerable pressures to energy conservation and emission reduction. Economic growth evidently causes large energy consumption, which contributes to economic growth and environmental pollution in turn. Environmental pollution introduces substantial economic input to solve the negative effects caused by environmental pollution. Therefore, analysing interactive relations among energy sources, environmental pollution, and economic development based on relevant understanding and studies on influencing factors of energy consumption and environmental pollution in Jilin Province will provide a theoretical guidance and practical relevance to formulate economic development strategies and policies.

EARLIER STUDIES

Scholars in developed countries have been studying the relationships among environmental pollution, energy source, and economic development since 1970s. In particular, some scholars have focused on the relationship between economic growth and environmental pollution by combining endogenous economic growth model with climatic changes and sustainable development to address increasingly serious environmental pollution problems caused by energy sources. The relationships among environmental pollution, energy consumption, and economic growth have been widely explored. Kraft et al. (1978) quantitatively analysed the causal relationship between economic growth and energy consumption in America. Stern (1993) analysed the causal relationship between GDP and energy use in America from 1947 to 1990 and found a causal relationship between energy utilization

and economic growth. Hawdon et al. (1995) discussed the complicated relations among energy source, environment, and economic growth. Cheng et al. (1997) examined the long-term equilibrium relationship between energy consumption and economic growth in Taiwan and found no causal relationship between GDP and energy consumption. Asafu-Adjaye (2000) estimated the causal relationship between energy consumption and income in India, Indonesia, Philippines, and Thailand. Aqeel et al. (2001) analysed the causal relationship between economic growth and energy consumption in Pakistan and believed that economic growth causes a continuous growth of energy consumption. Hondroyannis et al. (2002) pointed out a long-term relationship among energy consumption, actual GDP, and price development in Greece. Ang (2008) explored the long-term relationships among economic growth, pollutant emission, and energy consumption in Malaysia from 1971 to 1999 and concluded positive correlations among the three variables in the short and long run. Kukla-Gryz (2009) disclosed that economic growth imposes different influences on atmospheric pollution strength in developing and developed countries. Zhang et al. (2009) studied the Granger causality among economic growth, energy consumption, and carbon emission in China. They found a one-way Granger causality between GDP and energy consumption and between energy consumption and carbon emission. Ozturk et al. (2010) investigated the long-term relationships and causal relations among economic growth, carbon emission, energy consumption, and employment rate in Turkey. Kiviyiro et al. (2014) estimated the causal relations among CO₂ emission, energy consumption, economic development, and foreign

direct investment in six sub-Saharan African countries and found significant differences in causal relations among these variables in six countries. No universal policies and suggestions can be offered. Alam et al. (2016) pointed out that CO₂ emission increases considerably with the increase in income and energy consumption in India, Indonesia, China, and Brazil. Bildirici et al. (2017) analysed the relationship among environmental pollution, economic growth, and hydroelectric energy consumption in the Group of Seven from 1961 to 2013. Analysis results supported the Grange causality between CO₂ emission and economic growth. Özokcu et al. (2017) examined the relations among financial stability, economic growth, energy consumption, and CO₂ emission of South Asian countries from 1980 to 2012. He found that financial stability is conducive to improve environmental quality, and economic growth and increase in energy consumption and population density are disadvantageous to environmental quality in the long run. Baloch (2018) studied the dynamic relationships among economic growth, energy consumption from road traffic, and environmental quality in Pakistan. He discovered that road infrastructure and urbanization hinder improvement in environmental quality, accelerate emission of SO₂ in atmosphere, and reduce negative influences of economic growth on total SO₂ emission. In summary, existing studies on the relations between energy consumption and economic growth have mainly focused on econometric analysis of relevant data, and research conclusions are highly sensitive to studying countries, studying period, and quantitative methods. In this study, the dynamic spatial correlations among environmental pollution, energy consumption, and economic growth in Jilin Province were studied to provide theoretical references for optimization of local industrial structure and reduction in environmental pollution.

BRIEF INTRODUCTION TO THE MODEL AND DATA PROCESSING

Brief Introduction of Model

Existing analysis methods of relations among environmental pollution, energy consumption, and economic growth mainly focus on time data or panel data. Different cities in Jilin Province have evident spatial differences. Traditional analysis based on total time series data may cover such evident spatial differences. Considering the spatial difference, time series regression method or panel data are unsuitable to explain the complicated relations among economic growth, energy consumption, and environmental pollution and have difficulties in reflecting practical analysis conclusions. Therefore, spatial statistical analysis method has to be introduced properly when processing regional data. On this basis, a Douglas production function model involving energy consumption and environmental pollution was con-

structed. As a result, spatial variables were introduced into this model, and a spatial econometric model was established to analyse spatial autocorrelations of energy consumption and environmental pollution and influences of agglomeration form of economic growth rate, energy consumption, and environmental pollution on regional economic growth.

Classical Douglas production function: Energy consumption and environmental pollution were considered as input elements. The production function of Jilin Province is expressed as Eq. (1):

$$Y = AK^\alpha L^\beta (Eco)^\gamma E^\theta \quad \dots(1)$$

Where, Y is the total economic output, A is the total factor productivity, K is the input of physical capital stock, L is the labour input, Eco is the environmental input, and E is the energy input. $\alpha, \beta, \gamma,$ and θ are elasticity coefficients. The logarithmic expression of Eq. (2) is

$$\ln Y_{it} = A_i + \alpha_i \ln K_{it} + \beta_i \ln L_{it} + \gamma_i \ln(Eco)_{it} + \theta_i \ln E_{it} \quad \dots(2)$$

Where, i refers to the region and t refers to time.

Construction of the spatial model: Spatial autocorrelation was verified using statistical variables in spatial statistics in this study. Through the spatial effect analysis of economic growth, the relations among economic growth, energy consumption, and environmental pollution in all cities of Jilin Province were studied by the spatial econometric model proposed by Anselin (2002). The expression of Moran's I is:

$$Moran's I = \frac{\sum_{i=1}^n \sum_{j=1}^n W_{ij} (Y_i - \bar{Y})(Y_j - \bar{Y})}{S^2 \sum_{i=1}^n \sum_{j=1}^n W_{ij}} \quad \dots(3)$$

Where, $S^2 = \frac{1}{n} \sum_{i=1}^n (Y_i - \bar{Y})^2, \bar{Y} = \frac{1}{n} \sum_{i=1}^n Y_i$, Y_i is the observation value of city i , and n is the total number of cities. W_{ij} denotes the approximate spatial weight matrix of binary system. After the spatial correlation was tested by Moran's I , Eq. (2) was expanded with the above-mentioned theoretical model with full consideration to the first-order lag variables and a new spatial error model based on panel data could be gained. It is expressed as Eq. (4):

$$\begin{aligned} \ln Y_{it} &= C + \tau \ln Y_{it-1} + \alpha_i \ln K_{it} + \beta_i \ln L_{it} + \gamma_i \ln(Eco)_{it} \\ &+ \theta_i \ln E_{it} + \mu + \psi_t \\ \psi_t &= \delta W \psi_t + \varepsilon_t \end{aligned} \quad \dots(4)$$

Where, $\ln K_{it}, \ln L_{it}, \ln (ECO)_{it},$ and $\ln E_{it}$ are explanatory variables and $\ln Y_{it}$ is explained variable. $\tau, \alpha_i, \beta_i, \gamma_i$ and θ_i are regression coefficients of variables. μ is the random

interference term. δ is the spatial autocorrelation coefficient. W is the spatial adjacent weight matrix.

Data Source

Annual data from 2005 to 2016 were applied in this study. Panel data of nine prefecture-level cities in Jilin Province (Changchun, Jilin, Siping, Liaoyuan, Tonghua, Baishan, Songyuan, Baicheng, and Yanbian Korea Autonomous Prefecture) were used as the empirical analysis samples. On the basis of the model constructed above, GDP (unit: 100 million RMB) represents the explained variable (Y), whereas capital input (unit: 100 million RMB), labour input (unit: 100 million population), environmental input (unit: 100 million tons), and energy input (unit: 10,000 tons of standard coal) represent explanatory variables (K , L , Eco , and E). Logarithms of all data were calculated first. $\ln Y$, $\ln K$, $\ln L$, $\ln Eco$, and $\ln E$ were used to express logarithms of GDP, capital stock, quantity of employment, COD, and energy consumption, respectively. The above-mentioned data were collected from Jilin Statistics Yearbook of previous years, and environmental data came from the China Environmental Statistical Yearbook.

EMPIRICAL ANALYSIS AND RESULTS

Spatial Autocorrelation Verification of Energy Consumption and Environmental Pollution

Spatial autocorrelations of energy consumption and environmental pollution in Jilin Province were verified by the global spatial correlation index *Moran's I*. It was calculated by the software of GeoDa (version 0.9.5-i). Table 1 shows that energy consumption and environmental pollution from 2005 to 2016 presented certain spatial agglomeration among nine prefecture-level cities. In other words, cities with high energy consumption and environmental pollution prefer to be adjacent to cities with high energy consumption and environmental pollution. In particular, the *Moran's I* of COD, which is an environmental pollution indicator, increased annually, thereby showing an evident agglomeration trend.

SEM Panel Analysis

Eq. (4) was estimated using Matlab2012b software and spatial module (downloaded from <https://www.paneldatatoolbox.com/>). Table 2 shows the results.

Table 2 shows that the regression coefficients of relevant statistical variables are significantly positive, which indicates that the spatial correlation of the spatial econometric model is significant and can be measured. Viewed from fitting effect, the goodness-of-fit of Model 2 is better than those of other models, and estimation coefficients of all four models pass through the significance test.

Table 1: Statistics of energy consumption and COD in Jilin Province.

Year	Moran's I of Energy consumption	Moran's I of COD
2005	0.0715	0.0314
2006	0.1021	0.0419
2007	0.0812	0.0784
2008	0.0654	0.0654
2009	0.0584	0.0845
2010	0.0521	0.1041
2011	0.0551	0.1098
2012	0.0576	0.1125
2013	0.0684	0.1254
2014	0.0754	0.1125
2015	0.0564	0.1241
2016	0.0598	0.1058

P-value of δ in all four models passes through the 10% significance test, and regression coefficients are positive. This finding reveals the significantly positive spatial correlation of economic growth among nine prefecture-level cities in Jilin Province, and economic growth of one region depends on the economic growth with similar spatial characteristics to some extent. Songyuan and Baicheng in Jilin Province bear small environmental protection pressure due to the rich energy sources. Moreover, the improvement in infrastructure further increases the economic growth rate in these regions. This situation reflects that economic growth between adjacent cities has significant overflow effect. All four input elements make different positive contributions to economic growth. The regression coefficient of capital is higher than those of other variables, which indicates the high dependence of economic growth in Jilin Province on investment pulling in recent years. The regression coefficient of COD is positive and passes through the 5% significance test. This finding fully proves the significantly positive correlation between environmental pollution input elements and regional economic growth in Jilin Province. This correlation is also stronger than the correlation between energy consumption and economic growth.

POLICY SUGGESTIONS

Optimize the Industrial Structure and Increase the Proportion of the Tertiary Industry

Jilin Province has low energy utilization and serious environmental pollution due to unreasonable industry structure. Therefore, the province must optimize industrial structure and promote industrial upgrade to achieve harmonious development of energy, environment, and economy. Optimization of industrial structure refers to the adjustment in industrial structure. Given the high proportion of heavy industry in Jilin Province, government sectors should adjust proportion distribution of light and heavy industries, de-

Table 2: Regression results of SEM panel.

Variable	Model 1		Model 2		Model 3		Model 4	
	Coefficient	p-value	Coefficient	p-value	Coefficient	p-value	Coefficient	p-value
	0.201	0.041	-	-	-	-	-	-
	0.422	0.001	0.664	0.005	0.425	0.005	0.414	0.001
	0.283	0.002	0.215	0.015	0.249	0.014	0.115	0.015
	0.144	0.011	0.048	0.044	0.170	0.042	0.083	0.356
	0.294	0.022	0.095	0.079	0.165	0.000	0.042	0.042
	0.552	0.019	0.586	0.063	0.447	0.024	0.440	0.047
	0.941	-	0.968	-	0.923	-	0.878	-
	0.024	-	0.009	-	0.035	-	0.007	-

(Note: Model 1 has no fixed effect, Model 2 only has space fixed effect, Model 3 only has time fixed effect, and Model 4 has space and time fixed effect)

velop the tertiary industry and light industry vigorously, and control the development of energy-consuming industries to reduce energy consumption. In addition, the government should encourage and guide development of the tertiary industry from multiple aspects through investment and policies, pay key attention to the development of tourism, labour-intensive and modern service industries. Moreover, the government should adjust and update the industrial structure of Jilin Province towards heavy, high-processing, and technical-intensive industries. While focusing on the pillar and advantageous industries, attention should be paid to optimize element configuration, increase input on technology, and adjust industrial structure toward industries with less pollution. Meanwhile, some industries with serious pollution issues shall be updated and reorganized continuously and increasing internal pollution management and technological reconstruction should be carried out to reduce pollutant production and emission.

Optimize the Energy Consumption Structure and Reduce Unreasonable Energy Consumption

The energy consumption pattern centered at coal in Jilin Province will not change considerably in the coming years due to the limitation of resource conditions. Coal consumption not only brings huge environmental and transportation pressure, but also is against the increase in energy utilization. In energy consumption structure, Jilin Province should increase consumption proportions of high-quality energy sources including hydropower, oil, and gas and reduce proportion of low-carbon energy sources. Meanwhile, Jilin Province should increase technological innovation and government support to develop and promote new technologies positively, such as clean coal, coal gasification, and coal liquefaction technologies. Utilization of renewable energy sources should be enhanced. Key attention should be paid to the development and utilization of solar energy, geothermal energy, hydropower, and biomass energy and

reduction in energy consumption by increasing energy utilization. The resource advantages should be developed fully to reduce consumption of raw materials and energy consumption and realize the goal of small input, high output, and low pollution. This condition is conducive to reduce and recycle waste materials, thereby realizing the harmonious unification of economic, social, and environmental benefits.

Strengthen Environmental Protection and Establish Sustainable Environmental Development Strategies

Use of clean energy sources should be increased by developing and promoting new generations of clean high-efficiency coal processing technologies. Apart from maintaining economic and social development, Jilin Province should also reduce energy consumption per unit of industry production and relieve environmental pollution caused by combustion of large quantity of coals to provide people with a good environment for living and social production. A harmonious relationship between sustainable energy development and environmental protection is recommended. Moreover, Jilin Province should accelerate structural adjustment, technical improvement, and industrial upgrade. The province should also adjust energy consumption structure and energy product structure, increase utilization of energy sources, accelerate research and development of new energy sources, and relieve environmental pressure and effects from energy consumption fluctuations on the economy. The final goal is to realize the harmonious sustainable development of social economy, energy source, and environmental protection while realizing the strategic goal of economic and social development.

Implement Differentiated Environmental Protection Policies and Improve Regional Environment

Enterprises with high pollution and energy consumption should take steps to eliminate outdated production capacity, improve protection technologies to increase output efficiency

and reduce pollution emission. The industry entry threshold should be controlled strictly, and newly enrolled enterprises should be guided to low energy consumption and low-carbon environmental protection. Accordingly, positive interaction and harmonious development among economy, energy sources, and environment protection can be realized. Regional economic growth priority should be fostered to drive peripheral economic growth and realize win-win cooperation. Considering the spatial agglomeration features of regional economic development, the government should take the following initiatives: promote industrial restructuring; accelerate the training of strategic emerging industries with regional characteristics; support technological development and innovation activities in new energy sources, energy conservation, and environmental protection; implement key energy-saving projects (e.g., energy-saving technological transformation and contract energy management); and form a new green industrial cluster.

CONCLUSIONS

Energy consumption facilitates economic development. Consumption of polluted energies causes environmental damages and is the main cause of environmental pollution. Unreasonable energy demand structural problems, such as high energy consumption, vast energy waste, and serious pollution, are extremely prominent in China. The conflict among energy consumption, economic growth, and environmental protection becomes increasingly prominent, which becomes the bottleneck against China's sustainable development. A case study based on Jilin Province of China is presented in this paper. Spatial autocorrelation of environmental pollution is estimated by the Moran's index. The dynamic relations among energy consumption, environmental pollution, and economic growth are estimated by spatial error model. The results demonstrate that energy consumption and environmental pollution in nine prefecture-level cities in Jilin Province present certain characteristics of spatial agglomeration from 2005 to 2016 and continuous annual increase in COD. Significant positive correlations exist between environmental pollution elements and regional economic growth. Such correlations are significantly stronger than the correlation between energy consumption and economic growth. Further studies should be made on estimation of spatial correlation of industrial structure and environmental pollution, environmental protection cooperation across administrative regions, quantitative relationship between energy consumption of a specific industry

and environmental pollution and influencing factors of energy consumption and environmental pollution.

REFERENCES

- Asafu-Adjaye, J. 2000. The relationship between energy consumption, energy prices and economic growth: time series evidence from Asian developing countries. *Energy Economics*, 22(6): 615-625.
- Aqeel, A. and Butt, M. S. 2001. The relationship between energy consumption and economic growth in Pakistan. *Asia-Pacific Development Journal*, 8(2): 101-110.
- Alam, M.M., Murad, M.W., Noman, A.H.M. and Ozturk, I. 2016. Relationships among carbon emissions, economic growth, energy consumption and population growth: Testing environmental Kuznets Curve hypothesis for Brazil, China, India and Indonesia. *Ecological Indicators*, 70: 466-479.
- Ang, J. B. 2008. Economic development, pollutant emissions and energy consumption in Malaysia. *Journal of Policy Modeling*, 30(2): 271-278.
- Anselin, L. 2002. Under the hood issues in the specification and interpretation of spatial regression models. *Agricultural Economics*, 27(3): 247-267.
- Baloch, M. A. 2018. Dynamic linkages between road transport energy consumption, economic growth, and environmental quality: evidence from Pakistan. *Environmental Science and Pollution Research*, 25(8): 7541-7552.
- Bildirici, M. E., and Gökmenoğlu, S. M. 2017. Environmental pollution, hydropower energy consumption and economic growth: Evidence from G7 countries. *Renewable and Sustainable Energy Reviews*, 75: 68-85.
- Cheng, B. S. and Lai, T. W. 1997. An investigation of co-integration and causality between energy consumption and economic activity in Taiwan. *Energy Economics*, 19(4): 435-444.
- Hawdon, D. and Pearson, P. 1995. Input-output simulations of energy, environment, economy interactions in the UK. *Energy Economics*, 17(1): 73-86.
- Hondroyannis, G., Lolos, S. and Papapetrou, E. 2002. Energy consumption and economic growth: Assessing the evidence from Greece. *Energy Economics*, 24(4): 319-336.
- Kraft, J. and Kraft, A. 1978. On the relationship between energy and GNP. *The Journal of Energy and Development*, pp. 401-403.
- Kukla-Gryz, A. 2009. Economic growth, international trade and air pollution: A decomposition analysis. *Ecological Economics*, 68(5): 1329-1339.
- Kiviyiro, P. and Arminen, H. 2014. Carbon dioxide emissions, energy consumption, economic growth, and foreign direct investment: Causality analysis for Sub-Saharan Africa. *Energy*, 74: 595-606.
- Ozturk, I. and Acaravci, A. 2010. CO₂ emissions, energy consumption and economic growth in Turkey. *Renewable and Sustainable Energy Reviews*, 14(9): 3220-3225.
- Özokcu, S. and Özdemir, Ö. 2017. Economic growth, energy, and environmental Kuznets curve. *Renewable and Sustainable Energy Reviews*, 72: 639-647.
- Stern, D. I. 1993. Energy and economic growth in the USA: A multivariate approach. *Energy Economics*, 15(2): 137-150.
- Zhang, X. P. and Cheng, X. M. 2009. Energy consumption, carbon emissions, and economic growth in China. *Ecological Economics*, 68(10): 2706-2712.

... Continued from inner front cover

- The text of the manuscript should run into **Abstract, Introduction, Materials & Methods, Results, Discussion, Acknowledgement** (if any) and **References** or other suitable headings in case of reviews and theoretically oriented papers. However, short communication can be submitted in running with **Abstract and References**. The references should be in full with the title of the paper.
- The figures should preferably be made on a computer with high resolution and should be capable of withstanding a reasonable reduction with the legends provided separately outside the figures. Photographs may be black and white or colour.
- Tables should be typed separately bearing a short title, preferably in vertical form. They should be of a size, which could easily be accommodated in the page of the Journal.
- References in the text should be cited by the authors' surname and year. In case of more than one reference of the same author in the same year, add suffix a,b,c,.... to the year. For example: (Thomas 1969, Mass 1973a, 1973b, Madony et al. 1990, Abasi & Soni 1991).

List of References

The references cited in the text should be arranged alphabetically by authors' surname in the following manner: (Note: The titles of the papers should be in running 'sentence case', while the titles of the books, reports, theses, journals, etc. should be in 'title case' with all words starting with CAPITAL letter.)

- Dutta, A. and Chaudhury, M. 1991. Removal of arsenic from groundwater by lime softening with powdered coal additive. *J. Water Supply Res. Techno. Aqua.*, 40(1) : 25-29.
- Hammer, D.A. (ed.) 1989. *Constructed Wetlands for Wastewater Treatment-Municipal, Industrial and Agricultural*. Lewis Publishers Inc., pp. 831.
- Haynes, R. J. 1986. Surface mining and wetland reclamation. In: Harper, J. and Plass, B. (eds.) *New Horizons for Mined Land Reclamation*. Proceedings of a National Meeting of the American Society for Surface Reclamation, Princeton, W.V.

Submission of Papers

- The paper can be submitted by e-mail as an attachment in a single WORD file at **contact@neptjournal.com**
- The paper can also be submitted online in a single WORD file through the journal's website: **www.neptjournal.com**

Attention

1. Any change in the authors' affiliation may please be notified at the earliest.
2. Please make all the correspondence by e-mail, and authors should always quote the manuscript number.

Note: In order to speed up the publication, authors are requested to send the publication charges as soon as they get the 'initial acceptance' letter, and also correct the galley proof immediately after receipt. The galley proof must be checked with utmost care, as publishers owe no responsibility for mistakes. The papers will be put on priority for publication only after receiving the processing and publication charges.

Nature Environment and Pollution Technology

(Abbreviation: Nat. Env. Poll. Tech.)

(An International Quarterly Scientific Journal)

Published by



Technoscience Publications

A-504, Bliss Avenue, Opp. SKP Campus
Balewadi, Pune-411 045, Maharashtra, India

In association with

Technoscience Knowledge Communications

Mira Road, Mumbai, India

For further details of the Journal please visit the website. All the papers published on a particular subject/topic or by any particular author in the journal can be searched and accessed by typing a keyword or name of the author in the 'Search' option on the Home page of the website. All the papers containing that keyword or author will be shown on the home page from where they can be directly downloaded.

www.neptjournal.com

©**Technoscience Publications:** The consent is hereby given that the copies of the articles published in this Journal can be made only for purely personal or internal use. The consent does not include copying for general distribution or sale of reprints.

Published for Proprietor, Printer and Publisher: Mrs. T. P. Goel, B-34, Dev Nagar, Tonk Road, Jaipur, Rajasthan, India; Editors: Dr. P. K. Goel and Prof. K. P. Sharma